17TH GENERAL MEETING

INTERNATIONAL MINERALOGICAL ASSOCIATION

AUGUST 9 – 14, 1998 TORONTO, CANADA

ABSTRACTS & PROGRAMME

17TH GENERAL MEETING OF THE INTERNATIONAL MINERALOGICAL ASSOCIATION

August 9 - 14, 1998 • Toronto, Canada

Co-Sponsors with the International Mineralogical Association:

Mineralogical Association of Canada • University of Toronto, Department of Geology • Royal Ontario Museum, Toronto • Ontario Science Centre, Toronto • International Association for Geochemistry & Cosmochemistry (IAGC) • International Association for the Genesis of Ore Deposits (IAGOD)

OFFICERS AND COUNCIL OF THE IMA

President
- S. Merlino, University of Pisa, Pisa

Past-President
- Xiande Xie, Guangzhou Branch of Academia Sinica

First Vice-President
- A. J. Naldrett, University of Toronto

Second Vice-President
- Z. Johan, BRGM, Orléans

Secretary
- S. Hafner, University of Marburg

Treasurer
- C. Klein, University of New Mexico

Councillors
- I. Parsons, University of Edinburgh
- D. H. Green, Australian National University
- S. Sueno, University of Tsukuba
- D. V. Rundqvist, Moscow State University
- W. Schreyer, University of Bochum

ORGANIZING COMMITTEE

General Chairman
- A. J. Naldrett, University of Toronto

Secretary
- Eva S. Schandl, University of Toronto

Scientific Programme
- G. S. Henderson, University of Toronto

Field Excursions
- A. R. Cruden, University of Toronto (Erindale)

Registration and Abstracts
- J. C. Rucklidge, University of Toronto

Finance
- J. A. Mandarino, Royal Ontario Museum, Toronto

Exhibits
- M. Back, Royal Ontario Museum, Toronto

Technical Services
- C. Cermignani, University of Toronto

Social Activities
- J. Brenan, University of Toronto

Publicity
- R. I. Gait, Royal Ontario Museum, Toronto

Local Arrangements
- C. Cermignani, University of Toronto
- J.A. Mandarino, Royal Ontario Museum, Toronto

Short Course Coordinator
- D. Schulze, University of Toronto (Erindale)

SCIENTIFIC PROGRAMME COMMITTEE

Chairman

G. S. Henderson
Department of Geology
University of Toronto
22 Russell Street
Toronto, Ontario
Canada M5S 3B1

Tel. +1 (416) 978-6041
Fax +1 (416) 978-3938
e-mail
henders@afm1.geology.utoronto.ca

Secretary
- F. C. Hawthorne, Canada

Members

R. H. Mitchell, Canada; T. K. Kyser, Canada; F. Seifert, Germany; G. Calas, France; S. Merlino, Italy; C. M. B. Henderson, England; S. Sunigawa, Japan; R. Ewing, USA; V. Zharikov, Russia

ADDRESS FOR CORRESPONDENCE

IMA'98
Department of Geology
University of Toronto
Earth Sciences Centre
22 Russell Street
Toronto, Ontario
Canada M5S 3B1

Tel. +1 (416) 946-3306
Fax +1 (416) 978-3938
e-mail ima98@quartz.geology.utoronto.ca.
IMA'98 Web site at:
http://www.geology.utoronto.ca/IMA98

ORGANIZING SECRETARIAT

- Irene Rucklidge, Toronto
- Shayne Hutton, Toronto

WELCOME TO IMA '98

With over 600 registrants and 585 papers, I believe this will be a great meeting. Thank you for coming and I hope you enjoy your stay in Toronto.

A.J. Naldrett
General Chairman

OPENING CEREMONY

The Opening Ceremony of the 17th General Meeting of the International Mineralogical Association will take place on **Sunday, August 9**, from 17:00 to 17:45 at **Convocation Hall** on the campus of the **University of Toronto**. The Opening Ceremony will include welcoming addresses from Prof. Tony Naldrett, (Chairman of IMA'98 Organizing Committee); Designate of the President of the University of Toronto; Prof. Jeff Fawcett (Chairman of the Department of Geology, University of Toronto); Dr. James Nicholls (President of the Mineralogical Association of Canada), and Prof. Stefano Merlino (President of the International Mineralogical Association).

This will be followed immediately by the **Ice-Breaker party** at the **Royal Ontario Museum** which will start at 18:30.

MEETING SITE

Earth Sciences Centre
Department of Geology
University of Toronto
22 Russell Street
Toronto

Tel. +1 (416) 946-3306
FAX +1 (416) 978-3938
E-mail: ima98@quartz.geology.utoronto.ca.

IMA'98 Web site at:
http://www.geology.utoronto.ca/IMA98

The University is centrally located in the city of Toronto and is easily accessible by public transportation, or on foot from most of the conference hotels.

REGISTRATION DESK

The registration desk will be located on the campus at **Wetmore Hall, New College** and will be open from Sunday, August 9 from 12:00 to 18:00, on Monday, August 10 from 07:30 to 18:00 and on Tuesday, August 11 from 07:30 to 12:00. After 12:00 on Tuesday the Registration Desk will be moved to **Room 1061** in the **Department of Geology** where it will be open until 16:00. On Wednesday, August 12 it will be open from 7:30 to 14:00 and on Thursday and Friday, August 13 and 14 it will be open from 7:30 to 16:00.

All participants are advised to collect their meeting kits, name tags, abstract books, etc., at this desk. Participants must wear their name tags at all times. Accounts may be settled and tickets for events (if available) can be obtained at the registration desk.

An official receipt will be included in the registration kits.

The nearest Post Office is in the University Bookstore at the North West corner of College and St. George Streets.

MESSAGES

Messages will be received on behalf of participants and posted in the area of the Registration Desk at:

Tel. (416) 978 3306 or
FAX (416) 978 3938

SCIENTIFIC PROGRAMME

PLENARY LECTURES

Nine plenary lectures will be given during the conference. These will take place daily between August 10-14 from 12:15-13:15.

ORAL PRESENTATIONS

Three Symposia and 24 scientific sessions will take place concurrently from 08:30-12:00 from August 10-14.

Speakers are requested to adhere strictly to their allotted time schedules.

Two slide projectors and one overhead projector will be available in each of the meeting rooms. A slide preparation room will be available in the Department of Geology (Room 1067). Speakers planning to use slides in their presentations can obtain a carousel in this room and view their slides. The carousel and slides should be handed to the projectionist of their session well in advance of their lecture. The room will be open from 07:30 to 17:00 every day.

POSTER PRESENTATIONS — WETMORE HALL

Four Poster Sessions are scheduled for August 10, 11, 13 and 14 from 14:00 to 17:00. These will match as closely as possible the daily schedule of oral presentations. Poster size must not exceed 2.4 m in width and 1.0 m in height including the title, author(s), and affiliation(s). Each poster board will be identified by the abstract title and author placed at the top of the board. Velcro tape is strongly recommended to attach your posters, however, pins can also be used.

The posters can be mounted any time after 10:00 and dismounted not later than 17:30 on the day they are to be discussed.

GENERAL OUTLINE OF THE DAYTIME SCHEDULE

08:30-12:00	Symposia & Oral Presentations. (Mid-morning coffee break)
12:15-13:15	Plenary Lectures
13:15-14:30	Lunch

(NOTE: For convenience, lunches may be purchased at the New College Cafeteria. However, there are many other restaurants and food outlets in the area.)

14:00-17:00	Poster Sessions (except Wednesday, August 12)

SCHEDULE OF IMA BUSINESS AND COUNCIL MEETINGS

(All rooms are in the Department of Geology, Earth Sciences Centre)

SUNDAY, AUGUST 9

11:30-16:30	First Council Meeting, IMA — *Rio Algom Room (1072)*
17:00-17:45	Opening Ceremony — *Convocation Hall*

MONDAY, AUGUST 10

13:00-17:00	Commission on New Minerals and Mineral Names — *Room 2111*
13:00-15:00	Commission on Crystal Growth of Minerals — *Room 2093*
15:00-17:00	Commission on Gem Materials — *Room 2100*
15:00-17:00	Commission on History and Teaching — *Room 2101*
17:00-19:00	First Business Meeting, IMA — *Convocation Hall*
17:00	IGCP Project 427 Meeting — *Room 2093*

TUESDAY, AUGUST 11

12:00-15:00	Working Group on Cosmic Mineralogy — *Room 2119*
13:00-17:00	Commission on New Minerals and Mineral Names — *Room 2093*
13:00-15:00	Commission on Applied Mineralogy — *Room 1062*
15:00-17:00	International Council on Applied Mineralogy — *Room 1062*
15:00-17:00	Commission on Gem Materials — *Room 2101*
13:00-15:00	Working Group on Mineral Equilibria — *Room 2100*
15:00-17:00	Working Group on Databases and Computer Applications — *Room 2100*

WEDNESDAY, AUGUST 12

NO MEETINGS

THURSDAY, AUGUST 13

13:00-15:00	Commission on Museums — *Room 2100*
13:00-15:00	Commission on History and Teaching — *Room 2101*
13:00-15:00	Working Group on Organic Minerals — *Room 2119*
13:00-15:00	Commission on Ore Mineralogy — *Room 1062*
13:00-15:00	Commission on Physics of Minerals — *Room 2093*
13:00-14:00	Working Group on Inclusions in Minerals — *Room 2111*

SCIENTIFIC PROGRAMME CONT'D

15:00-17:00 Second Business Meeting, IMA — *Convocation Hall*

17:00-19:00 Second Council Meeting, IMA — *Room 1072*

FRIDAY, AUGUST 14

13:00-15:00 Commission on Museums — *Room 2100*

15:00-17:00 Commission on Classification of Minerals — *Room 2111*

17:00-19:00 Closing Ceremony — *Convocation Hall*

FIELD TRIPS

The following field trips have been confirmed. Spaces are still available for some of these trips. Please enquire. [NOTE: Field Trips A3, B1, B3, and B4 have been cancelled.]

Detailed descriptions of these trips can be found in the Second Circular.

A1. Metamorphic Mineral Assemblages in the Central Gneiss Belt, Grenville Province, Ontario, with emphasis on mafic rocks and their tectonic setting.

Leader: A. Davidson
Duration: 3 days
Participants: Maximum 25
Cost: $250
Departure: Toronto, August 6, 13:00
End of Excursion: Toronto, August 8

A2. Mineralogy and Geology of the Hemlo Gold Deposit, Ontario

Leaders: Y. Pan and M. E. Fleet
Duration: 3 days
Participants: Maximum 25
Cost: $450
Departure: Toronto, August 6
End of Excursion: Toronto, August 8

A4. Mineral Specimen Collecting in the Montreal area

Leaders: R. Ramik, R. Gault
Duration: 2 days
Participants: Maximum 43
Cost: $160
Departure: Toronto, August 7, 07:00
End of excursion: Toronto, August 8, 21:30

A5. Building Stones of Toronto

Leaders: K. Kemp and E. Freeman
Duration: 1/2 day
Participants: Maximum 40
Cost: $20
Departure: Toronto, August 9, 09:00
End of excursion: Toronto, August 9, 13:00

B2. Relationships between the Sublayer, Offsets, and Main Mass of the Sudbury Igneous Complex, Ontario

Leaders: Peter Lightfoot and Gord Morrison
Duration: 2 days
Participants: Maximum 25
Cost: $150 (including field costs and luncheons for two days, but excludes travel to Sudbury, accommodation, breakfast and evening meals).
Departure: 08:00 Science North parking lot, Sudbury, August 17
End of the excursion: Science North parking lot, Sudbury, August 18, 19:00

B5. Mineralogy of Bancroft, Ontario

Leaders: C. Fouts, J. Mandarino, M. Back, V. Vertolli
Duration: 4 days
Participants: Maximum 30
Cost: $500
Departure: University of Toronto, August 15, 08:00
Return: University of Toronto, August 18, 18:00

B6. Mineralogy and Petrology of the Tanco pegmatite deposit, Manitoba

Leaders: P. Cerny, T. S. Ercit, P. J. Vanstone
Duration: 1 Day
Participants: Maximum 50
Cost: $100 (excluding breakfast and evening meal)
Departure: Winnipeg, Manitoba, August 16, 06:30
End of the field trip: Winnipeg, August 16, approx. 19:00

B7. Geology of Niagara Falls and Niagara's Vineyards and Wines

Leader: Simon Haynes
Duration: 1 day
Participants: Maximum 46
Cost: $79 (includes restaurant lunch, and wine/cheese at 3 wineries)
Departure: Toronto, Saturday, August 15 at 08:00
End of excursion: Toronto, August 15 at 19:00 to 20:00

SHORT COURSE

The following short course has been confirmed:

Pre-meeting [Mineralogical Association of Canada]: Modern Approaches to Ore and Environmental Mineralogy, August 4-7, at Ottawa, Ontario.

MINERALOGICAL SOFTWARE FAIR

A Computer Software Fair (CSF), dedicated to researchers and teachers who have designed Public Domain Mineralogical Software, will be held in the Department of Geology Room 4107. The CSF will allow exhibitors to exhibit and demonstrate their products and provide an opportunity for delegates to obtain or exchange software products and databases. Both PC- and MAC-based platforms will be available.

The fair is scheduled to run from 14:00 to 17:00 on Monday and Tuesday, August 10 and 11, but may be extended depending on the collective response from potential contributors.

For more information, please contact Andy M. McDonald at: amcdonal@nickel.laurentian.ca

EXHIBITS — WETMORE HALL

Academic Book Exhibits, *Fairfax, Virginia*

Activation Laboratories, *Ancaster, Ontario*

Beevers Miniature Models, *Edinburgh, Scotland*

European Mineralogical Union

IMA 2002, *Edinburgh, Scotland*

John Wiley & Sons, Canada Ltd., *Toronto*

Meridian Scientific Services, *Carp, Ontario*

MicroScience Enterprises Ltd., *Guelph, Ontario*

Mineralogical Association of Canada

Rigaku/USA, Inc., Danvers, *Massachussetts*

Royal Ontario Museum, *Earth Sciences Dept.*

Systematik in der Mineralogie, *Ober-Olm, Germany*

The Canadian Gemmological Association, *Toronto*

The Mineralogical Society of America, *Washington, DC*

University of Toronto, Department of Geology

SUNDAY, AUGUST 9

12:00-16:30 Exhibitors' set up

MONDAY & TUESDAY, AUGUST 10-11

09:00-10:00 Exhibits open to exhibitors only

10:00-18:00 Exhibits open to delegates

WEDNESDAY, AUGUST 12

09:00-10:00 Exhibits open to exhibitors only

10:00-13:00 Exhibits open to delegates

13:00-17:00 Exhibitors tear down

NOTE: All exhibit material must be removed from the Exhibit Area by 17:00.

CLOSING CEREMONY

The Closing Ceremony will be held on Friday, August 14 in Convocation Hall, University of Toronto from 17:00 to 17:30.

SOCIAL PROGRAMME

SUNDAY, AUGUST 9, AT 18:30

Ice-Breaker Party with cash bar at the Royal Ontario Museum, 100 Queen's Park Crescent at Bloor Street (Museum Subway). Meet old and new friends, admire the treasures of the ROM, and enjoy the music of the Amati Quartet.

TUESDAY, AUGUST 11, AT 18:00

Dinner Cruise on Lake Ontario accompanied by a live Dixieland band. $55 per person.

WEDNESDAY (AFTERNOON), AUGUST 12

Niagara Falls and the **Shaw Festival**. $100 per person.

WEDNESDAY (AFTERNOON), AUGUST 12

Baseball Game: Toronto Blue Jays vs Seattle Mariners. $30 per person.

MEETING BANQUET

The **Conference Banquet** will be held at the Ontario Science Centre on Thursday, August 13, 1998. All the exhibits will be open to delegates. Buses will depart between 19:00 and 19:30 from the Geology Department. **$65 per person.**

Please ask at the registration desk for tickets to these events.

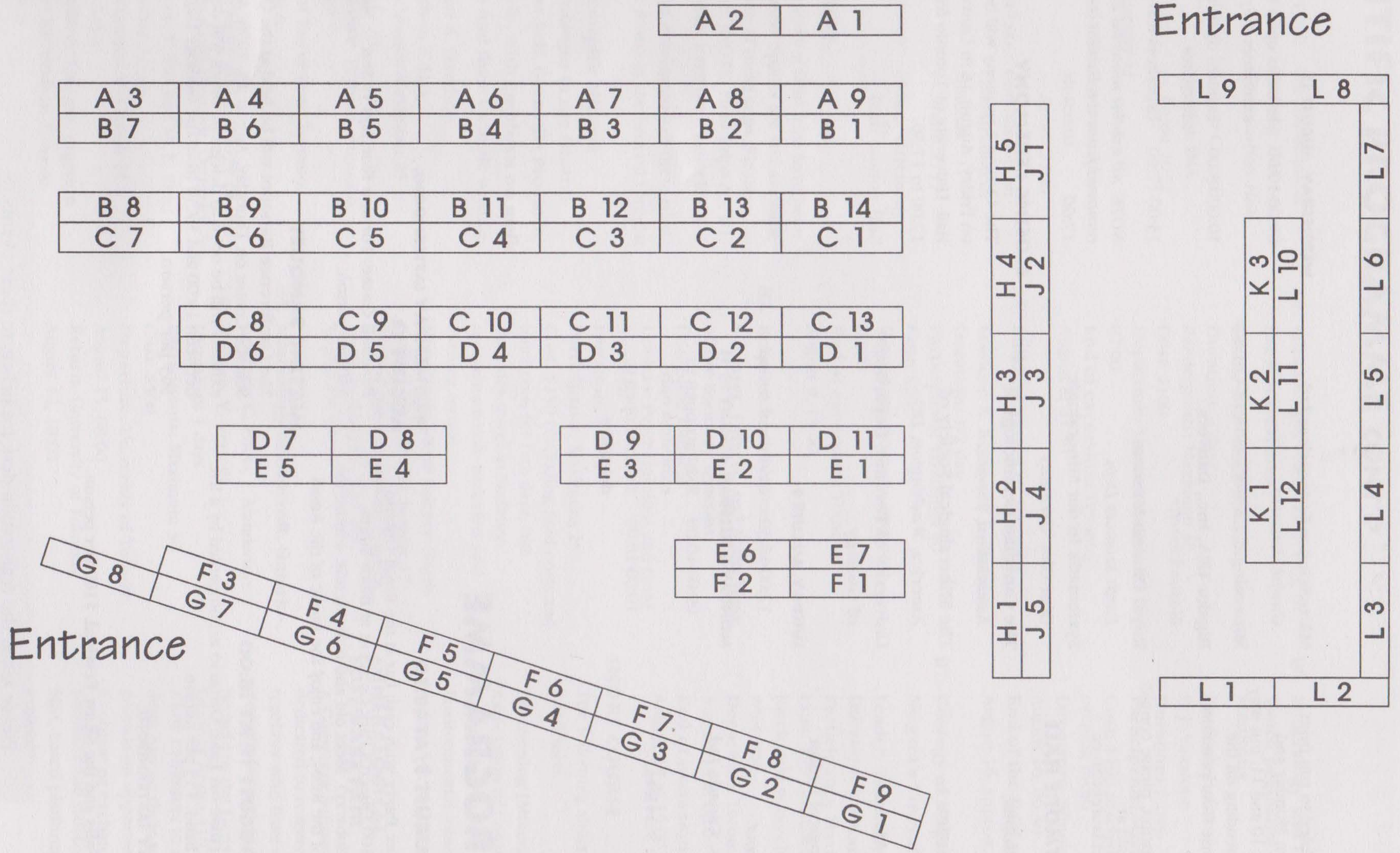

Plan of Posters in Wetmore Hall, New College.

The space is shared with exhibitors on Monday, Tuesday and Wednesday. A cash bar is in this area.

TECHNICAL SESSIONS PROGRAMME

	MONDAY	TUESDAY	WEDNESDAY	THURSDAY	FRIDAY
SYMPOSIA 08:30-12:00	**S1)** Mineral Deposits in Mafic and Ultramafic Rocks (in honour of A.J. Naldrett) [IMA/SEG/SGA/IGCP] MP 102 **S2)** Gems and Diamonds (in honour of the late Henry Meyer) MP 103			**S3)** Extraterrestrial Mineralogy: Traces of Nebula and Planetary Processes [WGCM/IGCP] M 134	
SESSIONS 08:30-12:00	**3)** Fluid Inclusions in Minerals [WGI] MP 134 **8)** Applied Mineralogy: Extractive and Metallurgical Processes [ICAM/CAM] MP 137 **15)** Recent Advances in the Crystal Chemistry of Rock Forming Minerals [PC] ES AUD **20)** Breakthroughs in Synchrotron Radiation in Mineralogy [CPM] MP 202 **23)** Mineralogical Museums Serving Science and Society [COMu] MP 203	**4)** Deep Earth Mineralogy: Lattice Dynamics to Mantle Dynamics [CPM] MP 137 **6)** Environmental Mineralogy [MSA/CMS] MP 202 **9)** Applied Mineralogy: Mineralogy of Ceramics and Cements [ICAM/CAM] MP 134 **16)** Mineralogy of Alkaline Rocks [CNMMN] ES 142 **17)** Mineral Synthesis [CGM/CCGM] MP 203	**7)** Crystal Structures and Topology [PC] MP 103 **10)** Gems Involving Organic and Amorphous Materials and Biomineralogy [CGM/WGOM] MP 134 **11)** Metamorphic Mineralogy: Fluid Flow associated with Metamorphism [PC] ES 142 **18)** Ore Mineralogy [COM] MP 203	**2)** Mineral Equilibria and Thermodynamics of Metamorphic Systems [WGME/IMA] MP 137 **5)** Comparative Mineralogy of Planetary Interiors [CPM] MP 102 **14)** Mineral Surface Studies [COM/CCGM] ES 149 **21)** Ore Mineralogy of Modern Sea Floor Hydrothermal Systems [COM] MP 203 **25)** Granite Pegmatites: Nature versus Experiment [MAC/MSA/PIG] ES 142 **26)** Descriptive Mineralogy at the Close of the 20th Century [PC] MP 202	**12)** Metal Adsorption on Clays [PC] MP 203 **13)** Crystal Morphology, Zoning and Growth [CCGM] MP 102 **22)** Ore Minerals in Hot Water [COM] MP 103 **24)** Mineralogy of Large and Superlarge Ore Deposits [IAGOD] MP 202
PLENARY LECTURES 12:15-13:15	**G. Rossman** What We Have Learned from Colour Minerals ES AUD **J. Craig** The Nature of Ore Assemblages, Textures and the Stories They Can Tell CONVOCATION HALL	**F. Hawthorne** Modern Perspectives in Mineralogy ES AUD **J. Parise** Real-Time Synchrotron X-ray Powder Diffraction CONVOCATION HALL	**D. Shaw** Fractionation Processes for Trace Elements — The IAGC Ingerson Lecture ES AUD	**D. Price** Bonding and Mineral Behaviour ES AUD **M. Zolensky** Mineralogy of the Solar System CONVOCATION HALL	**T. Yagi** Mineralogy from the Crust to the Core ES AUD **R. Ewing** Radwaste Mineralogy CONVOCATION HALL
POSTERS 14:00-17:00	S1, 3, 8, 15, 20, 23	S2, 4, 6, 9, 10, 16, 17	Free	S3, 5, 7, 11, 14, 18, 21, 26	2, 12, 13, 24, 25

IMA'98 SCIENTIFIC PROGRAMME
Abbreviations

CAM: Commission on Applied Mineralogy
CCGM: Commission on Crystal Growth of Minerals
CGM: Commission on Gem Materials
CMP: Commission on Mineral Physics
CMS: Clay Minerals Society
CNMMN: Commission on New Minerals and Mineral Names
COM: Commission on Ore Mineralogy
COMu: Commission on Museums
IAGC: International Association for Geochemistry and Cosmochemistry
IAGOD: International Association for the Genesis of Ore Deposits
ICAM: International Commission on Applied Mineralogy
IGCP: International Geological Correlation Program
IMA: International Mineralogical Association
MSA: Mineralogical Society of America
PC: Programme Committee
SEG: Society of Economic Geologists
SGA: Society for Geology Applied to Mineral Deposits
IUGS: UNESCO International Union of Geological Sciences
WGCM: Working Group on Cosmic Mineralogy
WGI: Working Group on Inclusions in Minerals
WGOM: Working Group on Organic Minerals
WGME: Working Group on Mineral Equilibria
§ Invited Paper

Plenary Lectures

Monday, 10 August 1998

§ 12:15 **George Rossman** *(Caltech, USA)*
What we have learned from colour in minerals rocks

§ 12:15 **James Craig** *(Virginia Tech, USA)*
Ore mineral textures and the tales they tell

Tuesday, 11 August 1998

§ 12:15 **Frank Hawthorne** *(University of Manitoba, Canada)*
Modern perspectives in mineralogy

§ 12:15 **John Parise** *(SUNY, USA)*
Real time synchrotron powder x-ray diffraction

Wednesday, 12 August 1998

§ 12:15 **Denis Shaw** *(McMaster University, Canada)*
IAGC Lecture: Trace element fractionation processes

Thursday, 13 August 1998

§ 12:15 **David Price** *(University of London , UK)*
Bonding and mineral behaviour

§ 12:15 **Michael Zolensky** *(NASA, USA)*
Mineralogy of the Solar System

Friday, 14 August 1998

§ 12:15 **Takehiko Yagi,** T.Kondo & T.Uchida *(U. of Tokyo, Japan)*
Mineralogy from the crust to the core

§ 12:15 **Rod Ewing** *(University of Michigan, USA)*
The design of nuclear waste forms: clues from mineralogy

Symposium 1. Mineral Deposits in Mafic and Ultramafic Rocks (in honour of A.J.Naldrett)

Sponsored by IMA/SEG/SGA and IUGS/IGCP Project 427 (Dynamics of Ore-Forming Magmatic Systems)

Convened by:
C.M. Lesher (Laurentian University)

*Monday, 10 August 1998, **MP 102***

Co-chairs:
Sarah-Jane Barnes (Université du Québec a Chicoutimi)
and
Mike Lesher (Laurentian University)

§ 08:30 **C.M.Lesher** *(Canada)*
Magmatic sulphide deposits in mafic and ultramafic rocks

§ 09:00 **R.R.Keays**, O.M.Burnham and C.M.Lesher *(Australia)*
Key factors in the generation of economic Ni-Cu-PGE sulphide deposits: the role of magma generation

§ 09:30 **S.J.Barnes**, R.E.T.Hill, J.Kauahikaua, S.E.Dowling and C.S.Perring *(Australia)*
Thermomechanical erosion by komatiites and the genesis of nickel sulphide deposits

COFFEE 10:00

§ 10:30 **P.C.Lightfoot** and staff of Voisey's Bay Nickel Company and Inco Technical Services Ltd. *(Canada)*
Geological and geochemical relationships in the breccias of the Reid Brook intrusive complex, Labrador: implications for the origin of the Voisey's Bay Ni-Cu-Co ores

§ 11:00 **G.E.Brügmann**, E.J.Hanski, A.J.Naldrett and V.F.Smolkin *(Germany)*
Sulfide segregation in ferropicritic flows and intrusions of the Pechenga Complex, Kola Peninsula

§ 11:30 **H.Papunen** *(Finland)*
Metamorphic sulphides in the komatiitic cumulates of the proterozoic Pulju Greenstone Belt, Western Lapland, Finland

*Tuesday, 11 August 1998, **MP 102***

Co-chairs:
Stephen J. Barnes (CSIRO, Perth)
and
Mike Lesher (Laurentian University)

§ 08:30 **S-J.Barnes** and R.D.Theriault *(Canada)*
The influence of assimilation and cooling rate on the composition of magmatic sulphides: examples from Muskox and Duluth

SGA

§ 09:00 **Z.Johan** *(France)*
Mineralogy of the Bushveld Upper Critical Zone Intercumulus: genetic considerations

§ 09:30 **A.H.Wilson**, S.Dawson and C.Z.Murahwi *(South Africa)*
Decoupling of nickel and major elements in olivine from the Bushveld Complex and the Great Dyke: a study of sulfide control

COFFEE 10:00

§ 10:30 **J.H.Crocket** *(Canada)*
PGE in Hawaiian basalt: implications for PGE mobility in volcanic fluids

§ 11:00 **L.J.Cabri**, T.Augé, G.McMahon and O.Legendre *(Canada)*
SIMS study of Pt in the New Caledonia Ophiolite

§ 11:20 **K.N.Malitch** *(Russia)*
Metallogeny of the unique Guli clinopyroxenite-dunite massif (Northern Siberia, Russia)

§ 11:40 **S.S.Gornostayev** *(Ukraine)*
Mineralogy of Pt-Fe natural alloys of the Aluchin Horst, Russian Far East: implications for genesis

POSTERS Monday, 10 August 1998

B14 **S.J.Barnes**, Z.Tang and V.Kunilov *(Australia)*
Chrome spinels associated with the Jinchuan and Noril'sk-Talnakh Ni-Cu sulphide deposits

C1 N.Caciagli and **J.M.Brenan** *(Canada)*
Fe-Ni exchange between olivine and sulphide melt: implications for magmatic Ni-sulphide deposits

C2 **O.M.Burnham**, A.M.McDonald and R.R.Keays *(Canada)*
Mineral chemistry of chromites from peridotite bodies along the Raglan Horizon, Cape Smith Belt, Northern Quebec

C3 **L.Cortesogno**, L.Gaggero and E.Jaho *(Italy)*
The multilayered gabbroic complex of the Mirdita Ophiolite Nappe (Northern Albania): mineral chemistry and geochemistry

C4 L.Cortesogno, **L.Gaggero** and A.Zanetti *(Italy)*
RE and trace elements behaviour during the subsolidus evolution of Mark Area Gabbros

C5 **G.Garuti**, F.Zaccarini, R.Cabella and G.Fershtater *(Italy)*
Origin of ruthenium, osmium, iridium and iron oxides by progressive desolforation and oxidation of laurite in Nurali Chromitites (Russia)

C6 **J.S.A.Krestow**, A.E.Litherland, J.C.Rucklidge, I.Tomski, G.C.Wilson and W.E.Kieser *(Canada)*
Development of *in situ* methods for the analysis of sub-ppb levels of PGE in silicates

C7 **M.Makovicky**, E.Makovicky, S.Karup-Møller and J.Rose-Hansen *(Denmark)*
Contribution to the mineralogy of the Os-Re pair: phase relations in the system Re-Fe-S at magmatic temperatures

C8 I.Yu.Badanina and **K.N.Malitch** *(Russia)*
Unusual PGE mineral associations from placer deposits of the Maimecha-Kotui Province (Nothern Siberia, Russia)

C9 **J.Mata** *(Portugal)*
$D^{ol/liq}_{Ni}$ on Madeira Island alkaline lavas: the influence of magmatic composition

C10 **M.J.Michaud** and S.A.Kissin *(Canada)*
The petrography and PGE-Ni-Cu-Au ore assemblage of the Roby Zone, Lac des Iles Mine, Northwestern Ontario

C11 **N.S.Rudashevsky** and V.N.Rudashevsky *(Russia)*
Porous crystals and grains of native osmium, ruthenium and iridium from alpine-type ultramafic rocks

C12 **S.V.Semenov**, B.V.Belyatsky, A.Zilberstein and V.S.Semenov *(Russia)*
Isotope-geochemical characteristics of the primary melts for the Lukkulaisvaara Mafic Complex (North Karelia, Russia)

C13 **N.A.Sharara**, G.C.Wilson and J.C.Rucklidge *(Egypt)*
Platinum-group elements and gold in Cu-Ni mineralized peridotite at Gabbro Akarem, Eastern Desert, Egypt

Symposium 2. Gems and Diamonds (in honour of the late Henry Meyer)

Sponsored by PC

Convened and chaired by:
Roger Mitchell (Lakehead University)
and
Fred Wicks (Royal Ontario Museum)

Monday, 10 August 1998, MP 103

§ 08:30 **I.Sunagawa** *(Japan)*
Growth, morphology and perfection of diamonds

§ 09:00 **J.E.Butler** *(USA)*
Chemical vapor deposition of diamond: synthesis in partial vacuums

§ 09:30 **E.Fritsch**, M.Moore and B.Lasnier *(France)*
The morphology of diamonds: a status report

§ 09:50 **E.Fritsch** and A.T.Collins *(France)*
Ultraviolet-visible-infrared absorption spectroscopy and cathodoluminescence of diamonds: a status report

COFFEE 10:10

§ 10:40 **S.E.Haggerty** *(USA)*
Diamonds in space and time (Meyer, 1989)

§ 11:00 **J.W.Harris**, B.Harte and M.T.Hutchison *(UK)*
Diamonds in the transition zone and lower mantle

11:20 **P.J.Wyllie** and I. D.Ryabchikov *(USA)*
Fluid inclusions in diamonds suggest critical end-point for solidus of peridotite-H_2O-CO_2 in upper mantle

11:40 **J.E.Shigley** *(USA)*
The identification of gem diamonds - natural, treated, synthetic or otherwise

Tuesday, 11 August 1998, MP 103

08:30 **W.D.Birch** *(Australia)*
The diamond-sapphire-zircon association in Victoria, Australia

08:50 **F.L.Sutherland** *(Australia)*
Gem corundum origins from eruptive sources

09:10 **P.T.Dung**, T.Häger, V.X.Quang and W.Hofmeister *(Germany)*
Rubies from Vietnam

09:30 **D.Tang** *(P.R. China)*
The colour and its origin of the Mingxi sapphires in Fujian, Southeastern China

09:50 **T.Häger** *(Germany)*
Interaction of trace elements in corundum

COFFEE 10:10

10:40 **M.I.Garland**, G.S.Henderson and F.J.Wicks *(Canada)*
Trace element and inclusion chemistry of the Montana alluvial sapphires

11:00 **J.L.Emmett** and T.R.Douthit *(USA)*
Color and clarity enhancement of colored gemstones

11:20 J.L.Emmett and **T.R.Douthit** *(USA)*
Development of heat treatment processing for the sapphire of Rock Creek, Montana

11:40 **B.M.Laurs** *(USA)*
Geology and exploration potential of gem-bearing pegmatites at Nuristan, Afghanistan

POSTERS Tuesday, 11 August 1998

L1 **A.V.Bovkun**, V.K.Garanin, G.P.Kudriavtseva and T.V.Possukhova *(Russia)*
Diamonds of the White Sea, Timan and North Yakutia: morphology, spectroscopy, origin

L2 **V.K.Garanin** and T.V.Possukhova *(Russia)*
Unusual diamonds from Arkhangelsk kimberlite province

L3 V.K.Garanin, **G.P.Kudriavtseva** and T.V.Possukhova *(Russia)*
Diamonds from the M.V.Lomonosov Deposit (Arkhangelsk Diamondiferous Province, Russia)

L4 **A.B.Makeyev**, N.I.Bryanchaninova, V.A.Dudar, V.G.Shametyko, V.N.Filippov, V.P.Lutoev and Yu.V.Glukhov *(Russia)*
Mineralogy of diamonds from Devonian placer Ichetju, Middle Timans, Russia

L5 **S.De**, P.J.Heaney, E.P.Vicenzi, R.B.Hargraves, Y.Fei and P.T.Taylor *(USA)*
Microstructural comparison between natural polycrystalline diamond (carbonado) and artificially sintered polycrystalline diamond

L6 **I.I.Moroz** and G.Panczer *(Israel)*
The Raman microspectroscopy and fluorescence of emeralds from various deposits

L7 I.I.Moroz and **I.Z.Eliezri** *(Israel)*
Phyllosilicates inclusions in emeralds from various deposits

L8 **W.Hofmeister** *(Germany)*
The influence of modular crystal structures on the quality of certain gemstones

L9 **J.Karfunkel**, M.L.S.C.Chaves, G.A.Banko and D.Hoover *(Brazil)*
Features of Espinhaço diamonds in Minas Gerais, Brazil, and their enigmatic source area

L10 **C.Kasipathy** and A.B.Rao *(India)*
Potentiality of Andhra Pradesh gem resources

L11 **A.B.Rao** *(Brazil)*
Geological and exploration characteristics of an aquamarine gem pegmatite sub-province in E.N.E. Brazil

L12 **T.J.Lu**, V.S.Balitsky, I.B.Makhina, J.E.Shigley, G.R.Rossman and B.A.Dorogovin *(USA)*
Synthetic iron-containing colored quartz (amethyst, citrine, and ametrine)

K1 H.J.Milledge, **F.L.Sutherland**, P.Kennewell and H.O.A.Meyer *(Australia)*
Copeton Diamonds, east Australia

Symposium 3. Extraterrestrial Mineralogy: Traces of Nebula and Planetary Processes

Sponsored by WGCM/IGCP Project 384 Impact and Extraterrestrial Spherules

Convened by:
Michael Zolensky (NASA Johnson Space Center)

Thursday, 13 August 1998, MP 134

Co-chairs:
Frans Rietmeijer (University of New Mexico)
and
Hiroshi Takeda (Chiba Institute of Technology)

08:30 **F.J.M.Rietmeijer**, J.A.Nuth and S.L.Hallenbeck *(USA)*
Aggregate IDPs: order in chaos before looking at nebular and planetary processes

09:00 **K.Ohsumi** and M.E.Zolensky *(Japan)*
Synchrotron XRD studies on interplanetary dust particles: L2005 AE6 and L2005 AG17

09:30 **M.E.Zolensky**, M.Weisberg, M.Prinz and K.Nakamura *(USA)*
Preserved nebular condensates in a primitive meteorite

COFFEE 10:00

10:30 **H.Takeda**, J.Chikami and M.Miyamoto *(Japan)*
Traces of planetary segregation of partial melts in the earliest solar system

11:00 **T.Mikouchi**, M.Miyamoto and I.Yamada *(Japan)*
Symplectic intergrowth of augite and magnetite in olivine from Martian meteorites

11:30 **M.A.Velbel** *(USA)*
Olivine hydration textures: comparison of extraterrestrial aqueous alteration in carbonaceous chondrites with terrestrial weathering and serpentinization

Friday, 14 August 1998, MP 134

Co-chairs:
Michael Zolensky (University of New Mexico)
and
Wolf Reimold (University of the Witwatersrand)

08:30 **W.U.Reimold** *(South Africa)*
Impact cratering in the solar system: the mineralogical angle

09:00 **Cs.H.Detre** and Gy.Don *(Hungary)*
The Proterozoic-Paleozoic, Paleozoic-Mesozoic and Mesozoic-Cenozoic boundaries associated with different cosmic events

09:30 **Sz.Bérczi**, Cs.Detre, Gy.Don, L.Dosztály, A.Gucsik, Á.Kiss and P.Solt *(Hungary)*
Interplanetary stratigraphy of the solar system

COFFEE 10:00

10:30 **M.Cloete**, R.Hart, H.Schmid, C.Demanet, V.Sankar, L.Maré and M.Drury *(South Africa)*
Crystallographic and magnetic orientations of magnetite particles in shocked quartz, Vredefort, South Africa

11:00 **O.Kákay Szabó** *(Hungary)*
Morphogenetic examination of extraterrestrial and terrestrial microspherules in Hungarian sediments by SEM and EDX methods

11:30 Y.Miura, S.Fukuyama, **M.Okamoto**, H.Kobayashi and A.Gucsik *(Japan)*
New impact evolution model of formation process at the end of Cretaceous Period

POSTERS Thursday, 13 August 1998

L1 **T.Di Valentin** and M.Zolensky *(Canada)*
Iron-nickel sulfides in carbonaceous chondrite matrix and chondrule rims

L2 **H.Hirai** and K.Kondo *(Japan)*
A possible genesis of cosmic diamond; transition of C_{60} fullerene to diamond

L3 **H.Nakazawa** *(Japan)*
Self-organized clusters in dilute allophane suspensions

L4 S.Maruyama, K.Kim, **S.Sueno** and H.Yurimoto *(Japan)*
Oxygen isotope measurements on compound chondrule-CAI objects in Allende Meteorite

Special Session 1. Mineral Equilibria and Thermodynamics of Igneous Systems

CANCELLED

Special Session 2. Mineral Equilibria and Thermodynamics of Metamorphic Systems

Sponsored by WGME/IMA

Convened and chaired by:
Leonid L. Perchuk (Moscow State University)
and
S.K. Saxena (Uppsala University)

Thursday, 13 August 1998, MP 137

08:30 **W.Heinrich** *(Germany)*
Experimental REE distributions between monazite and xenotime: a potential for temperature-calibrated geochronology

08:50 **T.Kawasaki** *(Japan)*
Partitioning of Fe^{2+} and Mg^{2+} between olivine and clinopyroxene: implications for mixing properties of $(Ca,Fe,Mg)_2SiO_4$ olivines

09:10 V.L.Vinograd and **A.Putnis** *(Germany)*
Cluster variation approach to the thermodynamics of Al, Si ordering in aluminosilicates

§ 09:30 **S.K.Saxena** *(Sweden)*
Thermodynamics of iron, silica, wustite, perovskite and iron hydride at lower mantle pressures

COFFEE 10:00

§ 10:30 **L.L.Perchuk**, T.V.Gerya, D.D.van Reenen and C.A.Smit *(Russia)*
Mineral equlibria and geodynamics of metamorphic complexes

11:00 **T.Boffa Ballaran**, M.A.Carpenter and C.A.Geiger *(UK)*
Hard mode IR spectroscopy of garnet solid solution

11:20 **G.L.Hovis**, J.Roux and P.Richet *(USA)*
Advances in hydrofluoric acid solution calorimetry: reduction of required sample size below ten milligrams

11:40 **A.Pilchin** *(Canada)*
Formation of plagioclase in the early Precambrian and the origin of anorthosites

Friday, 14 August 1998, MP 137

08:30 E.S.Grew, M.G.Yates, **P.Adams**, R.Kirkby and M.Wiedenbeck *(USA)*
Harkerite from Crestmore Quarry, California and from Cascade Slide, Adirondack Mountains, New York: a contrast in metamorphic pressure

08:50 W.-A.Kahl and **W.V.Maresch** *(Germany)*
Stability and thermodynamic properties of tremolite

09:10 **D.E.Harlov** *(Germany)*
High grade K-feldspar metasomatism in charnockites on both a local and regional scale

§ 09:30 **E.D.Ghent** *(Canada)*
Comments on geothermobarometry and P-T grids in medium-T, medium to high-P metamorphic rocks

COFFEE 10:00

§ 10:30 **K.-D.Grevel** *(USA)*
New P-V-T data for some high pressure phases in the system $CaO-MgO-Al_2O_3-SiO_2-H_2O$ and its consequences for internally consistent data bases

11:00 **Z.You**, Z.Zhang and Z.Zhong *(P.R. China)*
Corona textures in jadeite gneiss:evidence of post collision uplift of the ultrahigh pressure terrane in Dabieshan, China

11:20 **K.J.T.Livi**, J.M.Ferry and D.R.Veblen *(USA)*
Rare earth elements in low-grade metaclastic sediments: the what, where, and when of REE (re)distributions

11:40 S.W.Faryad and **G.Hoinkes** *(Slovakia)*
Two contrasting mineral assemblages in the Meliata blueschists, Western Carpathians, Slovakia

POSTERS Friday, 14 August 1998

A1 **D.Balen** *(Croatia)*
Compositional and optical zonation in amphibole from amphibole-bearing schists (Moslavacka Gora - Croatia)

A2 **M.Cho** and J.Kim *(Korea)*
Garnet-cummingtonite rocks in the Hyeondong Gneiss Complex, Northeastern Yeongnam Massif, South Korea

A3 **C.Grevel**, W.V.Maresch, K.P.Stanek, F.Grafe and G.Millan *(USA)*
High-pressure metamorphic rocks from the Escambray Massif, Cuba

A4 **M.Pilchin** and A.Pilchin *(Canada)*
Instability of some iron containing minerals under low temperature conditions

A5 **Yu.I.Pystina** *(Russia)*
Polymetamorphic complexes of the Urals: mineral-based reconstruction of evolutional environments

A6 **K.Yi**, M.Cho and S. R.Lee *(Korea)*
Reaction textures and P-T paths of the granulite to amphibolite transition in the Hwacheon Granulite Complex, South Korea

A7 **S.W.Faryad** *(Slovakia)*
Taramite as prograde-formed mineral in transition between greenschist and blueschist facies conditions

A8 **A.M.Pystin** *(Russia)*
Mineralogical record of polymetamorphism (on example of the Urals)

A9 **V.V.Fed'kin** *(Russia)*
Physicochemical conditions of formation of the eclogite-glaucophane rocks of the Atbashi Complex, South Tien Shan

Special Session 3. Fluid Inclusions in Minerals

Sponsored by WGI

Convened and chaired by:
Iain Samson (University of Windsor)
and
Maria-Luce Frezzotti (University of Siena, Italy)

Monday, 10 August 1998, MP 134

§ 08:30 **R.J.Bodnar** *(USA)*
Fluid inclusion systematics in porphyry copper deposits

§ 09:00 **J.S.Cline** and A.H.Hofstra *(USA)*
Ore fluid evolution at the Getchell Carlin-type gold deposit, Nevada, USA

§ 09:30 **T.Pettke,** J.D.Kramers and L.W.Diamond *(USA)*
Radiogenic isotopes in hydrothermal fluids: clues to understanding ore deposit genesis?

COFFEE 10:00

§ 10:30 **J.L.R.Touret** *(The Netherlands)*
Melt/fluid inclusions in granulites: carbonic metamorphism and "vapor-absent" melting

§ 11:00 **J.D.Webster**, F.Raia and B.DeVivo *(USA)*
Relationships involving magmatic volatiles and eruptive behavior at Mt. Vesuvius during interplinian volcanic activity (472 A.D. - 1944 A.D.)

§ 11:30 **E.Roedder** and J.F.Whelan *(USA)*
Ascending or descending water flow through Yucca Mountain tuffs? -- fluid inclusion evidence

§ 12:00 **P.F.Dennis** *(UK)*
The stable isotope composition of fluid inclusions in speleothems: palaoprecipitation, palaeothermometry and climate change

14:00 **Z.M.Cao** and Y. N.Huang *(P.R. China)*
Tellurium-bearing fluid: behavior and mechanics of the enrichment and dispersion

***POSTERS** Monday, 10 August 1998*

G1 **B.Bühn** and A.H.Rankin *(UK)*
Composition and significance of alkali- and halogen-rich natural carbonatite melts trapped in fluid inclusions

G2 **M.L.Frezzotti**, L.Dallai, G.Giorgetti and Z.D.Sharp *(Italy)*
Fluid inclusion and stable isotope evidence for fluid migration during metamorphism in the Priestley Metamorphic Complex (O'Kane Canyon, North Victoria Land, Antarctica)

G3 **E.Jonsson** and C.Broman *(Sweden)*
Fluid inclusion studies of hydrated Mn arsenates and associated minerals from the Långban Mine, Sweden

G4 **I.L.Komov** *(Ukraine)*
Diagnostics of captive minerals in inclusions

G5 **F.Molnár**, D.H.Watkinson, J.Everest and P.C.Jones *(Canada)*
Multi-stage fluid mobilization in the footwall units of the Sudbury Igneous Complex and the role of fluids in the formation of vein-type Cu-Ni-PGE deposits

G6 R.T.Walker and **I.M.Samson** *(Canada)*
Cryogenic Raman spectroscopic investigations of fluid inclusions in the $NaCl-CaCl_2-H_2O$ system

G7 **T.Sawaki**, M.Sasada and M.Sasaki *(Japan)*
Geochemical features of fluid inclusions of granitic rocks in Japan

G8 **S.N.Shanina** *(Russia)*
Pyrochromatography inclusions in salts

F9 **G.J.C.Viggiano**, P.E.González and M.G.Izquierdo *(Mexico)*
Fluid inclusion study in the Las Tres Virgenes, B.C.S. (Mexico): evidences of a magmatic uprising fluid

H1 **Z.Dehui** and L.Wei *(P.R. China)*
The fluid inclusions researches on the Yinshan polymetallic deposit, Jiangxi Province, China

H2 **L.Wei** and Z.Dehui *(P.R. China)*
Fluid inclusion study on the Shibangou gold ore deposit, Xixia, Henan, P.R.China

H3 **K.Yang** and S.D.Scott *(Canada)*
Volatitles in pre-erupted magmas and their possible contribution to a seafloor hydrothermal system in the Manus Back-Arc Basin, Western Pacific

H4 **H.Zhili** *(P.R. China)*
A brief of review of the decrepitation method development during the past 50 years

Special Session 4. Deep Earth Mineralogy: Lattice Dynamics to Mantle Dynamics

Sponsored by CPM

Convened and chaired by:
Francois Guyot (LMCP and IPG, Paris)

Tuesday, 11 August 1998, MP 137

§ 08:30 **R.J.Hemley** and H.K.Mao *(USA)*
X-rays on deep mantle and core dynamics

§ 08:50 **G.Fiquet**, A.Dewaele, D.Andrault, M.Kunz, T.LeBihan and D.Häusermann *(France)*
Thermoelastic properties and crystal structure of $MgSiO_3$ perovskite up to 86 GPa and 2700 K

§ 09:10 **G.D.Gwanmesia**, G.Chen, J.Lui and R.C.Liebermann *(USA)*
Elastic properties of polycrystalline pyrope-majorite garnets at high pressure and temperature, and the mineralogical constitution of the Earth's mantle

§ 09:30 **J.P.Brodholt** and D.Dobson *(UK)*
Electrical conductivity of mantle minerals and the temperature of the earth's lower mantle

§ 09:50 N.Tòmioka and **K.Fujino** *(Japan)*
Formation of $(Mg,Fe)SiO_3$ ilmenite (akimotoite) and perovskite in a shocked chondrite

COFFEE 10:10

§ 10:40 **R.E.Cohen** *(USA)*
Transition metal oxides at high pressures: magnetic and structural phase transitions

§ 11:00 **B.Reynard** *(France)*
Minor and trace elements in Earth's mantle minerals and melts: from microscopic substitution mechanisms to partitioning

11:40 **M.Matsui** *(Japan)*
MD study of the density and elastic constants of the olivine, modified-spinel, and spinel forms of Mg_2SiO_4 at mantle conditions

Wednesday, 12 August 1998, MP 137

08:30 **T.Arlt**, R.J.Angel, R.Miletich, T.Armbruster and T.Peters *(Switzerland)*
High pressure- $P2_1/c$-$C2/c$ phase transitions in pyroxene: influence of cation size and CFSE

08:50 **T.Yamanaka**, R.Kurashima and T.Tsuchiya *(Japan)*
Covalency/ionicity of SiO_2 rutile structure binds defined by k-refinement and by DV-Xα simulation

09:10 **F.Guyot**, L.Lemelle, H Leroux, J.C.Doukhan and G.Libourel *(France)*
Kinetic effects in metal silicate interactions consequences for core composition

09:30 **J.Xu** and X.Chu *(P.R. China)*
Sulfide- melt inclusions in mantle xenoliths of Hannuoba, China

09:50 X.L.Wu, Y.J.Han, **D.W.Meng**, W.R.Yang and D.X.Li *(P.R. China)*
A TEM and HRTEM study of microstructures in omphacite from UHP eclogites at Shima, Dabie Shan, China

COFFEE 10:10

10:40 **R.J.Harrison** and A.Putnis *(Germany)*
The kinetics of cation ordering in $MgFe_2O_4$: ordering mechanisms from the time-temperature dependence of magnetic susceptibility

11:00 **T.Kikuchi** *(Japan)*
New approach to the calculation of intracrystalline cation distribution equilibria in non-ideal solid solutions: application to the partitioning in olivine

11:20 **D.R.Neuville** and P.Richet *(France)*
Structure, viscosity and mixing between alkali and alkaline-earth silicate melts

POSTERS Tuesday, 11 August 1998

F4 **T.Akamatsu** and K.Kawamura *(Japan)*
Molecular dynamics of solid solution and coexisting liquid

F3 **S.Lévesque**, D.R.Neuville and P.Richet *(France)*
Influence of solid inclusions on the rheology of silicate melts

F5 **E.S.Persikov** *(Russia)*
Viscosity of model silicate and aluminosilicate melts at high water and super-high lithostatic pressures

F6 **T.Tsuchiya**, T.Yamanaka and K.Kawamura *(Japan)*
High pressure crystal chemistry of stishovite by potential renewing molecular dynamics simulation

F7 **H.Watanabe** *(Japan)*
Thermal properties of quartz, rutile, sapphire, silica glass, CoO, MgO, MnO, NiO and Ni at low temperatures

F8 **A.B.Woodland** and R.J.Angel *(Germany)*
High-pressure phase relations in the system magnetite-fayalite and the crystal chemistry of several spinelloid phases

Special Session 5. Comparative Mineralogy of Planetary Interiors

Sponsored by CPM

Convened and chaired by:
Yingwei Fei (The Geophysical Laboratory, CIW)

Thursday, 13 August 1998, MP 102

§ 08:30 **S.K.Saxena**, L.S.Dubrovinsky and P.Lazor *(Sweden)*
Mineralogy of the core and lower mantle

§ 09:00 **M.Akaogi**, A.Kubo, E.Ito, T.Suzuki, Y.Hamada and N.Kamii *(Japan)*
High-pressure transitions of aluminous phases in the deep mantle conditions

§ 09:30 **Y.Fei** and K.Hirose *(USA)*
The effect of alumina on physical properties and stability field of silicate perovskite

COFFEE 10:00

§ 10:30 M.Chen, A.El Goresy, **X.Xie**, B.Wopenka and T.G.Sharp *(P.R. China)*
Cooling rate in the shock veins of chondrites: constraints on the $(Mg,Fe)_2SiO_4$ polymorph transformations

11:00 Y.Miura, **S.Fukuyama**, M.Okamoto, H.Kobayashi and A.Gucsik *(Japan)*
Chemical separation of Fe-Ni particles after impact

11:20 **E.Ohtani** and H.Mizobata *(Japan)*
Stability of DHMS phases in the system Mg_2SiO_4-H_2O and $MgSiO_3$-H_2O up to 27 GPa

11:40 **Y.Kudoh** and T.Inoue *(Japan)*
Comparative crystal chemistry of hydrous wadsleyite and its relation to hydrous ringwoodite: structural modules and hydrogen contents

POSTERS Thursday, 13 August 1998

L5 **J.I.Chung**, S.Sueno and T.Kato *(Japan)*
The melting of basalt under hydrous conditions at 3.8 - 10 GPa

L6 **L.S.Dubrovinsky** and S.K.Saxena *(Sweden)*
Experimental mineralogy of earth's lower mantle - *in situ* high-P,T X-ray approach

L7 **T.Kuribayashi**, Y.Kudoh and M.Akizuki *(Japan)*
Single-crystal X-ray diffraction and FT-IR spectra of chondrodite, $Mg_5Si_2O_8(OH,F)_2$ under high pressure up to 6.0 GPa

L8 **A.Okada** and M.Shima *(Japan)*
Kijima meteorite: a new finding of free diopside-bearing EL6 chondrite

L9 A.Uchizono, **I.Shinno**, Y.Nakamuta, T.Nakamura and T.Sekine *(Japan)*
Residual effects in artificially shocked forsterite

Special Session 6. Environmental Mineralogy

Sponsored by MSA/CMS

Convened and chaired by:
G.D. Guthrie Jr. (Western Michigan University)
and
D. Bish (Los Alamos National Laboratory)

Tuesday, 11 August 1998, MP 202

§ 08:30 **A.E.Williams-Jones**, C.Normand, J.R.Clark, H.Vali, R.F.Martin and A.Dufresne *(Canada)*
Nature and distribution of asbestiform amphibole, Jeffrey Chrysotile Mine, Quebec

§ 08:50 **H.Vali**, N.Çiftçioglu and E.O.Kajander *(Canada)*
Biomineralisation by the smallest known nano-organisms in blood: implications for pathogenic diseases

§ 09:10 **T.J.Beveridge** *(Canada)*
Interaction, concentration and mineralization of environmental metal ions by bacterial surfaces

09:30 **B.L.Sherriff**, D.A.Brown and J.A.Sawicki *(Canada)*
Iron mineral reactions mediated by an environmental bacterial consortium

§ 09:50 **C.Zhang**, S.Brooks, S Fendorf, H.Vali and P.Jardine *(USA)*
Microbial uranium reduction and biomineralization: implication for immobilization of toxic metals and radionuclides

COFFEE 10:10

§ 10:40 **P.J.Heaney** and D.M.Yates *(USA)*
Adsorption of toxic metal cations to aqueous polymeric silica

§ 11:00 **D.K.McCarty**, J.N.Moore and W. Andrew Marcus *(USA)*
Mineralogy and trace element association in an acid mine drainage iron oxide precipitate; comparison of selective extractions

11:20 **E.F.Stumpfl**, D.Gregurek and C.Reimann *(Austria)*
Environmental impact by nickel-copper-PGE mining and smelting in the Kola Peninsula, NW Russia: the Kola Ecogeochemistry Project

11:40 **M.Boudeulle** and C.Mosser *(France)*
Structural characterization of quartz crystals from the Cigar Lake Uranium Deposit (Canada) : the effects of irradiation and/or hydrothermal alteration

POSTERS Tuesday, 11 August 1998

D1 I.Mascaro, F.Morelli, M.Benvenuti, **F.Corsini**, P.Parrini and G.Tanelli *(Italy)*
Mine wastes, drainage waters and stream sediments from the polymetallic sulfide deposit of Fenice Capanne (Southern Tuscany, Italy)

D2 **F.Q.Dong**, P.Wan, G.W.Li, T.J.Peng, J.Zhuang, Q.M.Feng and G.B.Song *(P.R. China)*
The biochemistry feature and environmental significance of industrial mineral fibers in Gamble solution and organic system

D3 **W.Dubbin**, G.Sposito and M.Zavarin *(UK)*
Mechanism of glyphosate inactivation by microcrystalline gibbsite

D4 **J.N.Dunlevey** *(South Africa)*
Rubification of the Berea Formation

D5 **R.García**, R.Vigil and J.A.González *(Spain)*
Periglacial loess fields in the Tajo River Valley, Spain

D6 C.J.Shull, D.S.Koenig and **M.E.Gunter** *(USA)*
Mineral content of glacial ice and snow from the Juneau Icefield, Alaska, U.S.A

D7 **J.Göske**, H.-G.Pankau and H.Pöllmann *(Germany)*
Cryo-SEM in environmental mineralogy research

D8 **X-Q.Hou**, R.J.Kirkpatrick and Y.Kim *(USA)*
^{77}Se NMR spectroscopic investigations of SeO_4^{-2} and SeO_3^{-2} hydrotalcite-like compounds (HTs)

D9 **S.Kobayashi** and T.Sakamoto *(Japan)*
Artificial chemical weathering of granite under earth surface conditions

D10 **U.Kolitsch** and A.Pring *(Australia)*
Antimony in the structure of dussertite, the Ba-Fe-arsenate end member of the Crandallite group

D11 **M.R.Lee** and I.Parsons *(UK)*
Si-rich layers at lichen-mineral interfaces as an indicator of biochemical weathering

E1 **O.Legendre**, F.Bodénan and V.Ettler *(France)*
Mineralogy and weathering of Pb-Zn slags from Pribram, Czech Republic

E2 **C.Lemaire**, F.Guyot, P.E.Petit and Ph.Gillet *(France)*
Vibrational spectroscopy of asbestos minerals in building materials

E3 **D.Li** *(USA)*
A novel USY zeolite-supported Ni-Mo sulfide catalyst for environmental clean-up

E4 **Y.Linard**, D.R.Neuville and P.Richet *(France)*
Thermochemistry of nuclear waste glasses

E5 M.F.Brigatti, P Frigieri, **C.Lugli** and M.Poppi *(Italy)*
Aminoacids sorption by Na-, Ca- and Cu-saturated smectites

E6 **A.Nayebzadeh**, A.Dufresne, B.Case and H.Vali *(Canada)*
Lung fiber burden of two groups of Québec asbestos miners and millers

H3 **S.S.Potapov** and E.V.Belogub *(Russia)*
The expansion of technogenesis as mineral formation process

E7 **R.A.Pushkareva** *(Ukraine)*
Tritium adsorbtion in the montmorillonite

F1 **S.K.Sears**, J.G.Raith, H.Vali and R.F.Martin *(Canada)*
TEM study of unique fibrous chlorite and muscovite

F2 **W.Sohn**, T.Shoji and H.Kaneda *(Japan)*
Hydrothermal crystallization of boro-silicate glasses containing Cs or Sr

H1 **N.P.Yushkin** *(Russia)*
Environmental mineralogy of natural and table salts

H2 **C.H.Jeong** and S.J.Kim *(Korea)*
Effect of solution chemistry on the sorption of radionuclides onto clay minerals

Special Session 7. Crystal Structures and Topology

Sponsored by PC

Convened by:
Stefano Merlino (University of Pisa)

*Wednesday, 12 August 1998, **MP 103***

Co-chairs:
Stefano Merlino (University of Pisa)
and
Emil Makovicky (University of the Copenhagen)

§ 08:30 **F.C.Hawthorne** *(Canada)*
Bond topology, bond valence and the structural chemistry of oxysalt minerals

§ 09:00 **S.Merlino** *(Italy)*
CSH (calcium silicate hydrates) minerals: unusual topologies, chain condensations and thermal behaviour

§ 09:30 **D.Yu.Pushcharovsky**, I.V.Pekov, J.Pluth and J.Smith *(Russia)*
Mn-silicates from alkaline rocks: crystal structures, topology and geochemistry

09:50 **T.Balić-Žunić** and E.Makovicky *(Denmark)*
Role of large cations in the feldspar structure

COFFEE 10:10

10:40 H.Yang, L.Finger, **C.Prewitt**, R.Hazen and P.Conrad *(USA)*
High-pressure single-crystal X-ray diffraction study of the protopyroxene structure: a first-order displacive phase transition observed at ~1.8 GPa

11:00 **H.Schlenz**, A.Kirfel and T.Vad *(Germany)*
New strategies for the precise and accurate determination of cation distributions in silicates

11:20 **G.Amthauer**, W.Lottermoser, G.Tippelt, G.Redhammer, W.Paulus and W.Treutmann *(Austria)*
Neutron powder diffraction, single crystal Mössbauer and magnetic susceptibility measurements on the synthetic clinopyroxene Li-acmite $LiFeSi_2O_6$

*Thursday, 13 August 1998, **MP 103***

§ 08:30 **E.Makovicky**, T.Balić-Žunić and P.N.Olse *(Denmark)*
OD phenomena and polytypy in sulfosalts

§ 09:00 **G.Vezzalini** *(Italy)*
Topological transformations induced by dehydration in zeolites

§ 09:30 **P.C.Burns** *(USA)*
Topological aspects of uranyl mineral structures

09:50 **V.Kahlenberg**, R.X.Fischer, C.Weidenthaler and T.Zeiske *(Germany)*
High temperature investigations on $Ca_2Fe_2O_5$ using X-ray and neutron diffraction

COFFEE 10:10

10:40 P.B.Moore, **A.R.Kampf** and P.K.Sen Gupta *(USA)*
Philolithite, a mineral with a close-packed trellis structure

11:00 **M.Schindler,** W.H.Baur and F.C.Hawthorne *(Canada)*
A new structural description for mineral and inorganic framework-structures containing isolated condensed polyhedra

11:20 **M.D.Welch** *(UK)*
Atomic ordering and superstructures in PbO related minerals

11:40 **Z.Yu** *(P.R. China)*
A study of the crystal structure of an unnamed mineral $(Ni,Fe)_9Cu_4(Ir,Pt)_8PbIr_2S_{27}$ with electron diffraction

POSTERS Thursday, 13 August 1998

C2 **J.Barbier** *(Canada)*
Sapphirine and surinamite analogs

C3 **L.C.Basciano**, R.C.Peterson, P.L.Roeder and I.Swainson *(Canada)*
Description of schoenfliesite, $MgSn(OH)_6$, and roxbyite, $Cu_{1.72}S$, from a 1375 BC shipwreck, and synthesis and Rietveld refinement of schoenfliesite, wickmanite, $MnSn(OH)_6$ and burtite, $CaSn(OH)_6$

C4 **D.Deneele**, M.D.Buatier, M.Dubois, M.Potdevin and M.Lopez *(France)*
Natural nacrite in the Lodeve Permian Basin: structure description and conditions of formation

C5 **I.Dódony** *(Hungary)*
Structural study of antigorite based on HRTEM image processing

C6 **H.Effenberger**, W.H.Paar, D.Topa, F.J.Culetto and G.Giester *(Austria)*
Towards the crystal structure of nagyagite

C7 **J.A.Foley**, J.Hughes and R.L.Schaefer *(USA)*
Determination of atomic occupancy in multiply-occupied cation and anion sites

C8 **A.Friedrich**, M.Wildner and E.Tillmanns *(Austria)*
Crystal chemistry of magnesium antimony hydroxide hydrate, $Mg(H_2O)_6[Sb(OH)_6]_2$

C9 J.Barbier, **E.S.Grew** and Paul B. Moore *(USA)*
Beryllian sapphirine from Casey Bay, East Antarctica: a superstructure with a 2× *a*-axis

C10 **F.C.Hill** and P.C.Burns *(USA)*
Investigations of the crystal chemistry of uranyl oxide hydrates

C11 **G.N.Lysiuk** *(Russia)*
Structure and properties of the fine dispersional manganese oxides

C12 **D.Lévy** and J.Barbier *(Canada)*
A new magnesium iron germanate

C13 **F.Mancini**, K.Marumo, N.Kohyama, R.Alviola and B.Marshall *(Japan)*
An HRTEM-AEM study of Mn-cummingtonite from Vittinki, Western Finland

D1 **F.Martignago** *(Italy)*
Accuracy of site occupancies in olivine: an interlaboratory study

D2 **A.Miyake**, M.Kitamura and K Kawamura *(Japan)*
Molecular dynamics simulation of PT - IT phase transition in pure anorthite

D3 **A.Mookherjee** and A.V.Phadke *(India)*
Thermo-dilatometric studies of cavansite from Wagholi, India

D4 **B.Niu** *(Japan)*
Differences of tetrahedral ^{27}Al in smectite illitization and discussion with NMR, FT-IR and HRTEM results in the Niigata Basin interbedded sandstone and mudstone

D5 **M.Pasero** and S.Merlino *(Italy)*
Enumeration of possible structures related to ZSM-5 and ZSM-11

D6 G.Giester and **F.Pertlik** *(Austria)*
Structure of hydrothermally synthesized $Ag_{10.5}Te_7$ and relationships to stuetzite

D7 **G.Salviulo**, S.Carbonin and A.Della Giusta *(Italy)*
A comparison of Rietveld and single-crystal X-ray structure refinement on a natural chromite

D8 **N.Shimobayashi**, E.Miura, A.Miyake and M.Kitamura *(Japan)*
Molecular dynamics simulation of high-pressure clinoenstatite

C1 **N.L.Smirnova** and O.E.Gorchakova *(Russia)*
Some space groups as combinations of modules

D9 **J.Stolz** and T.Armbruster *(Switzerland)*
X-ray single-crystal structure refinement of szenicsite, $Cu_3MoO_4(OH)_4$, and its relation to the structure of antlerite, $Cu_3SO_4(OH)_4$

D10 **I.C.Stretton**, P.F.Schofield, K.S.Knight, S.Hull, C.C.Wilson and S.F.Parker *(Switzerland)*
Neutron diffraction and spectroscopic studies of deuterated gypsum

D11 **P.Susse** *(Germany)*
Uniform ASCII symbols for space groups, point groups, and crystal systems

E1 C.L.Lengauer, **E.Tillmanns** and G.Hentschel *(Austria)*
A new magnetoplumbite-type mineral from the Eifel, Germany

E2 **E.V.Valyashko** and R.C.Peterson *(Canada)*
Synthesis and crystal chemistry of ferric hydrogen sulfate hydrate

E3 S.Quartieri, A.Sani, **G.Vezzalini**, E.Galli, E.Fois, G.Tabacchi and A.Gamba *(Italy)*
Bikitaite from North-Carolina: structure refinement and *ab initio* molecular dynamics simulations

Special Session 8. Applied Mineralogy: Extractive and Metallurgical Processes

Sponsored by ICAM/CAM

Convened and chaired by:
Richard Hagni (University of Missouri, Rolla),
Adrienne Wedepohl (MINTEK, Johannesburg)
and
William Petruk (Ottawa, Ontario)

*Monday, 10 August 1998, **MP 137***

§ 08:30 **R.D.Hagni** *(USA)*
Mineralogy of beneficiation problems involving fluorspar concentrates from carbonatite-related fluorspar deposits

§ 08:50 M.M.Tassinari, **H.Kahn**, L.Sant'Agostino and G.Ratti *(Brazil)*
Characterization of primary gold from Salamangone, AP, Brazil

§ 09:10 **K.Kojonen** and B.Johanson *(Finland)*
Determination of refractory gold distribution by microanalysis, diagnostic leaching and image analysis

§ 09:30 S.H.Poggi, **H.C.W.Skinner**, J.J.Ague and D.Carter *(USA)*
Using scanning electron microscopy to study biological mineral deposits

§ 09:50 **T.Chernet** and J.Jalava *(Finland)*
Effect of mineralogy and texture of sand and hard rock ilmenites in TiO_2 pigments production by sulfate process

COFFEE 10:10

§ 10:40 **W.Petruk** *(Canada)*
Current trends in applied mineralogy to extractive metallurgy

§ 11:00 **J.Graham** *(Australia)*
Some characteristics of weathered ilmenite which affect processing

§ 11:20 **A.Wedepohl** and P.Ellis *(South Africa)*
Ferrochromium: mineralogy applied to its production and use

11:40 **T.R.C.Fernandes** *(Zimbabwe)*
Chromite mineralogy and the ferrochrome industry

POSTERS *Monday, 10 August 1998*

J2 **T.A.Collyer**, B.Kotschoubey, H.Khan and B.Hieronymus *(Brazil)*
The hydrothermal tricolor quartz vein from Sao Geraldo do Araguaia, state of Para - Brazil, origin and application

J3 **I.S.Ismael**, M.K.Abd El-Rahman and M.S.Hassan *(Egypt)*
Influence of vibrating grinding and calcination on the physico-chemical properties of an Egyptian kaolinite

J4 **T.Ueno** and S.D.Scott *(Japan)*
Phase equilibria in the system Zn-Fe-Ga-S at 600°C to 860°C

J5 **J.P.Vaughan** *(Australia)*
Submicroscopic gold in sulphides from gold deposits in Western Australia

Special Session 9. Applied Mineralogy: Mineralogy of Ceramics and Cements

Sponsored by ICAM/CAM

Convened and chaired by:
Andrzej Szymanski (Warsaw University of Technology)
and
Benoit Fournier (CANMET, Ottawa)

Tuesday, 11 August 1998, MP 134

§ 08:30 **J.W.Carey** and G.D.Guthrie,Jr. *(USA)*
The alkali-silica reaction in concrete: silica minerals in high-pH environments

§ 09:00 **P.Rivard**, G.Ballivy and B.Fournier *(Canada)*
Automatic petrographic technique for the quantification of concrete damage due to alkali-silica reaction

09:30 **W.Kurdowski** and M.Soboñ *(Poland)*
Mineralogy of accretions in cement kiln preheater

COFFEE 10:00

10:20 **M.S.Hassan** and M.S.Elwan *(Egypt)*
Recycling of some Egyptian industrial solid wastes in clay bricks

10:40 N.Guscioni and **M.Maggetti** *(Switzerland)*
Stabilization of galvanic sludges in bricks

11:00 E.Kupiec and **A.Szymanski** *(Poland)*
Solid-state reactive transition of kaolinite and powdered aluminium mixture towards mullite ceramics matrix

11:20 G.J.C.Viggiano and **E.M.Alonso** *(Mexico)*
The petrology in the restoration: case example of the aqueduct of Morelia, Mich., México

11:40 **P.Yu** and R.J Kirkpatrick *(USA)*
Thermal stability of hydrous calcium silicates

POSTERS *Tuesday, 11 August 1998*

B8 **M.Franzini**, L.Leoni and M.Lezzerini *(Italy)*
The binder of medieval mortars

B9 **K.Ikeda**, T.Terai and H.Shima *(Japan)*
Crystal structure of synthetic ettringites in relevance to sulfur occupancies

B10 **O.A.Kamel**, A.Kh.El Gindy and A.M.Abbouda *(Egypt)*
Industrial applications of the clay beds of Wadi El Mehasham, East Bent Mazar, Egypt

B11 J.Serrano, **A.Sanz**, J.V.Clausell, J.Bastida and J.M Amigo *(Spain)*
SEM microstructure and XRD crystallite size of mullite in stoneware bodies obtained from ball clays of Teruel (Spain)

B12 **H.Xu**, P.J.Heaney, A.Navrotsky, L.Topor, J.Liu and R.C.Liebermann *(USA)*
Thermochemistry of stuffed quartz phases along the join $LiAlSiO_4$-SiO_2

Special Session 10. Gems Involving Organic and Amorphous Materials and Biomineralogy

Sponsored by CGM/WGOM

Convened and chaired by:
Margherita Superchi (CISGEM Italy)

Wednesday, 12 August 1998, MP 134

08:30 **R.Asada** and K.Tazaki *(Japan)*
Silica minerals in green biomats forming along Kamuiwakka Falls, Hokkaido, Japan

08:50 **H.Shikaura**, K.Tawara and K.Tazaki *(Japan)*
Formation of terrace-like sediment associated with iron-bacteria at Satsuma-Iwo Jima island

09:10 **K.Tazaki** *(Japan)*
A recent BIF showing bacterial rings

09:30 **J.Akai**, M.Ito, K.Akai, S.Nakano, Y.Maki, I.Sasagawa and S.Kuwa *(Japan)*
TEM observation of ancient and present biomineralization to form Biologically Induced Iron Ore: Gunma Iron Mine, Central Japan

COFFEE 10:00

10:30 **S.Yabuki**, A.Okada, Q.Chang and H.Kagi *(Japan)*
A new biomineral, potassium magnesium hydrogen carbonate hydrate [$KHCO_3.MgCO_3.4H_2O$], from secretion excluded by *Populus diversifolia* around the desert area, Xinjiang, NW China

10:50 E.Gambini and **M.Superchi** *(Italy)*
Analyzing gem materials from biomineralizations and amorphous compounds using mineralogical spectrometric techniques

11:10 C.Aurisicchio, **G.Graziani** and S.Nunziante *(Italy)*
A contribution to the identification of the Roman archaeological emerald origin

POSTERS *Tuesday, 11 August 1998*

F9 **K.Akai** and J.Akai *(Japan)*
Calcic, siliceous and manganese stromatolitic structures growing in some hot springs, Japan

G1 **A.Aoki** and K.Tazaki *(Japan)*
Bioremediation by *Gallionella* at mining area polluted by heavy metals

G2 **A.Banerjee** and D.Habermann *(Germany)*
Comparision of manganese contents of fresh water pearls by a 'hot cathode' cathodo-luminescence microscope

G3 **M.Ohno** and K.Tazaki *(Japan)*
Formative environment and micro-ecosystem of microbial mats in hot springs

G4 **H.Okuda** and K.Tazaki *(Japan)*
Air pollution influence on the concrete construction

G5 S.Yano, **N.Suzuki**, K.Matsumoto, M.Ohno, H.Wakabayashi and K.Tazaki *(Japan)*
Reservoir sediments and effective use in the Dashidaira Dam

G6 **M.Ueshima** and K.Tazaki *(Japan)*
Microscopic observations on bacterial biomineralization from K-feldspar

G7 **H.Watanabe** and K.Tazaki *(Japan)*
Biomats formed in the copper mine drainage

G8 **T.Yasuda** and K.Tazaki *(Japan)*
Crystal morphology of calcium carbonate associated with microbes

Special Session 11. Metamorphic Mineralogy: Fluid Flow associated with Metamorphism

Sponsored by PC

Convened and chaired by:
Barbara L. Dutrow (Louisiana State University)

*Wednesday, 12 August 1998, **ES 142***

09:00 A.Dombrowski, S.Hoernes and **M.Okrusch** *(Germany)*
Fluid flow along deep crustal shear zones within metaturbidites of an ancient accretionary prism, Damara Orogen, Central Namibia

§ 09:30 **J.A.D.Connolly** and Yu.Yu.Podladchikov *(Switzerland)*
The influence of rheology on regional metamorphic fluid flow

COFFEE 10:00

§ 10:30 **B.Dutrow**, C.T.Foster,Jr. and B.Travis *(USA)*
Deciphering signatures of fluid infiltration using 3D thermal and textural modeling

§ 11:00 **B.Jamtveit** *(Norway)*
Crystal growth and zonation patterns of hydrothermal garnets

***POSTERS** Thursday, 13 August 1998*

L10 **R.Compagnoni**, R.Conte, A.Facchinelli, P.Orione and P.Rossetti and C.Trossarelli *(Italy)*
The rodingite of Bellecombe (Val d'Aosta, Italy): a petrographic and fluid inclusion study

L11 **B.Dutrow**, D.J.Henry, C.Gable and B.Travis *(USA)*
Thermal evolution and fluid infiltration: development of metasomatic mineralogy adjacent to an alkalic dike

L12 **D.E.Moore**, S.Hickman, D. A.Lockner and R.Gunderson *(USA)*
Hydrothermal alteration in coreholes adjacent to the Great Sumatran Fault at Silangkitang, North Sumatra, Indonesia

K1 **T.Witzke** and J.Göske *(Germany)*
An unusual association containing oldhamite, bazhenovite, ye`elimite, hannebachite and other minerals from Ronneburg, Thuringia, Germany

K2 **Y.Ogasawara**, Y.Nakajima and K.Okamoto *(Japan)*
Interpretation of paragenetic relations and chemical compositions of carbonates from UHP terrane

K3 R.Cabella, **G.Lucchetti** and P.Marescotti *(Italy)*
Influence of the bulk rock chemistry and metamorphic conditions on the monazite growth in pelitic metacherts (Central Liguria, Italy)

Special Session 12. Metal Adsorption on Clays

Sponsored by PC

Convened and chaired by:
Jeanne B. Percival (Geological Survey of Canada)

*Friday, 14 August 1998, **MP 203***

08:30 **R.T.Cygan** and R.J.Kirkpatrick *(USA)*
Atomistic models of cesium and sodium sorption on illite clays

09:00 **R.J.Kirkpatrick**, Y.Kim, P.Yu and R.T.Cygan *(USA)*
NMR chemical shift and T_1 relaxation rate studies of surface sorbed species

§ 09:30 **M.F.Brigatti**, C.Lugli, M.Poppi and G.Venturelli *(Italy)*
Iron rich saponite: Cr uptake and dissolution reactions

COFFEE 10:00

10:30 **H.HE**, J.Guo and X.Xie *(P.R. China)*
Adsorption of heavy metals on clay minerals

11:00 **A.K.M.Attia**, M.E.Hilmy, S.N.Boulis and H.M.Bayoumi *(Egypt)*
Geochemistry of the argillaceous sediments intercalated with the phosphate deposits in the Nile Valley, Egypt

***POSTERS** Friday, 14 August 1998*

C7 **C.Poinssot**, B.Baeyens and M.Bradbury *(Switzerland)*
Sorption studies of Cs, Sr, Ni and Eu on illite

Special Session 13. Crystal Morphology, Zoning and Growth

Sponsored by CCGM

Convened and chaired by:
Richard Reeder (SUNY - Stony Brook)

*Friday, 14 August 1998, **MP 102***

§ 08:30 **M.Kitamura** and K.Nishioka *(Japan)*
Growth habit change between polyhedral shapes of the same crystalline substance: a theoretical study

08:50 **C.F.Woensdregt** and J.D.Meeldijk *(The Netherlands)*
Surface morphology of hydrothermally grown spessartine ($Mn_3Al_2Si_3O_{12}$)

§ 09:10 O.Grauby, **A.Baronnet** and B.Devouard *(France)*
Chrysotile-to-polygonal serpentines-to-lizardite reaction produced from a MgO-SiO_2- H_2O (MSH) gel

§ 09:30 **T.Abe** and K.Tsukamoto *(Japan)*
An attempt to visualize the concentration/ temperature field around silicate crystals growing at high temperature

§ 09:50 **K.L.Nagy** and R.T.Cygan *(USA)*
Growth of gibbsite on gibbsite, kaolinite, and muscovite

COFFEE 10:10

§ 10:40 **D.Bosbach**, C.M.Pina, U.Becker, P.Risthaus and A.Putnis *(Germany)*
Crystal growth of barite: an *in situ* AFM study

§ 11:00 H.H.Teng and **P.M.Dove** *(USA)*
The kinetics and mechanisms of calcite growth at near-equilibrium conditions

11:20 M.Temmam and **J.Paquette** *(Canada)*
Growth morphology and sectoral zoning of Cd, Mn, and Zn doped calcite crystals

11:40 **J.Rakovan** *(USA)*
Sectoral zoning (SZ) of REEs in fluorite: indication of the heterogenious nature and distribution of surface protosites

POSTERS *Friday, 14 August 1998*

B1 **A.Ahmadjan** and M.Kitamura *(Japan)*
Morphology of spinel-twinned crystals of natural diamond

B2 **A.M.Askhabov** *(Russia)*
"Hidden"-phase clusters and crystal growth

B3 E.Belluso, **A.Baronnet** and G.Ferraris *(France)*
Textures of alpine serpentinite veins containing asbestiform minerals as seen by TEM

B4 **I.K.Bonev** *(Bulgaria)*
Nature and origin of the twisted quartz crystals ("Gwindels") and of quartz with white strips ("Fadenquarz")

B5 **N.A.Bryxina** and O.I.Ripinen *(Russia)*
Oscillatory zoning in agate from Mongolia

B6 **B.Devouard** and P.R.Buseck *(France)*
Microstructure of fibrous micas from the Shunga Region, Russia

B7 **R.Gieré**, C.T.Williams, M.Braun and S.Graeser *(USA)*
Complex zonation patterns in monazite-(Nd) and monazite-(Ce)

§ B8 **J.A.Jaszczak** and G.W.Robinson *(USA)*
Spherical graphite from Gooderham, Ontario, Canada

B9 **N.I.Leonyuk** *(Russia)*
Teaching crystal growth of minerals

B10 **Sz.Leél-Őssy** *(Hungary)*
Evolution of a hydrothermal cave on the basis of the radiometric dating of speleothems

B11 **R.A.Mason** and L.J.Miller *(Canada)*
Recrystallization and the luminescence of synthetic calcite

B12 **T.Mizuta**, T.Miura and D.Ishiyama *(Japan)*
The crystal size distribution and geochemical characteristics of barite from the Motoyama Kuroko Deposits, Akita Prefecture, Japan

B13 **L.E.Mordberg**, M.D.Welch and I.G.Lyapitschev *(UK)*
The supergene occurrence of an unusual tetrasilicic mica related to taeniolite

B14 **A.Müller**, H.-J.Behr and R.Seltmann *(Germany)*
The multistage crystallization process of the Schellerhau Granites - a quartz CL study

C1 **T.Nagase** and M.Akizuki *(Japan)*
TEM observations of the disordered domain in marcasite from Ikezuki, Japan and Potosi, Bolivia

C2 **I.Parsons** and M.R.Lee *(UK)*
Chemical zoning in alkali feldspars and its relationship to exsolution microtextures

C3 D.G.Gazieva and **T.V.Possukhova** *(Russia)*
Gold morphology from Au-Ag ores of the Zarmitan and Marzhanbulak deposits (Uzbekistan)

C4 **V.I.Rakin**, S.K.Kuznetsov, I.V.Kodanev and V.P.Lutoev *(Russia)*
Zone crystals and deterministic chaos

C5 **R.J.Reeder** and N.G.Hemming *(USA)*
Growth-step-specific incorporation of borate anions on the calcite surface

C6 **J.Reinhardt** *(Germany)*
Chemical zoning in high-grade metamorphic garnets: results of a microprobe element mapping study

C8 **A.P.Santo** *(Italy)*
Textures and trace element in plagioclase as evidence of magmatic evolution processes

C9 **Z.Shanrong** *(P.R. China)*
Morphology, growth model and its fractal implication of the chrysanthemum stone in Qixia FM.,South China

C10 **V.D.Tikhomirova** *(Russia)*
Carbon and oxygen isotopic composition of carbonates from the deposits of the Copper Sandstone Formation

C11 **M.Gaft** and G.Panczer *(Israel)*
Laser-induced time-resolved luminescence spectroscopy of minerals

C12 **G.Panczer**, M.Gaft, P.Martin and B.Champagnon *(France)*
Diffusion of implanted europium in apatite probed by time-resolved photoluminescence

Special Session 14. Mineral Surface Studies

Sponsored by COM/CCGM

Convened and chaired by:
David J. Vaughan (University of Manchester)

*Thursday, 13 August 1998, **ES 149***

§ 08:30 **A.Manceau**, B.Lanson, V.A.Drits, J.Wu, W.P.Gates, J.W.Stucki and D.Chateigner *(France)*
Mechanism of Fe(III) to Fe(II) reduction in nontronite by X-ray diffraction, polarized EXAFS, and texture goniometry

08:50 **M.E.Hodson**, M.R.Lee and I.Parsons *(UK)*
Direct comparisons of naturally and experimentally weathered feldspar surfaces by scanning probe and electron microscopy

09:10 **C.M.Pina** and A.Putnis *(Germany)*
Crystallisation of solid solutions from aqueous solutions: growth mechanisms and composition relationships

§ 09:30 **S.L.S.Stipp** *(Denmark)*
Spontaneous movement of ions in calcite at room temperature: are there implications for fluid inclusion composition, isotope ratios and relative trace metal distributions?

§ 09:50 H.Teng, J.J.De Yoreo, **P.M.Dove** and C.Orme *(USA)*
Physical controls on calcite mineralization

COFFEE 10:10

10:40 **L.P.Lemelle**, Y.Fuchs, H.Leroux, G.Libourel and F.Guyot *(France)*
The role of surfaces in the reduction of olivine

§ 11:00 **J.A.Tossell** *(USA)*
Theoretical studies of the reactivity of ZnS and HgS surfaces using a molecular approach

§ 11:20 **H.W.Nesbitt**, G.M.Bancroft, A.R.Pratt and M.Scaini *(Canada)*
Sulphur and iron surface species on fractured pyrite surfaces

§ 11:40 **P.Möller** *(Germany)*
Gold deposition onto arsenopyrite surfaces

POSTERS *Thursday, 13 August 1998*

E6 **D.Banerjee** and H.W.Nesbitt *(Canada)*
Oxidation of chromium at birnessite surfaces and constraints on reaction mechanism

§ E5 **U.Becker**, D.Bosbach and C.Pina *(Germany)*
Dynamic simulation of crystal growth at the molecular scale

§ E4 **D.Bosbach** and A.Putnis *(Germany)*
Organic / inorganic interactions during crystallization and dissolution reactions: a microscopic perspective

E7 **R.A.Fellows**, A.R.Lennie, A.Munz, D.J.Vaughan and G.Thornton *(UK)*
Structures of $FeTiO_3$ (0001) surfaces obtained by scanning tunneling microscopy

F1 **Ye.A.Golubev** *(Russia)*
High-resolution STM and AFM investigation of shungites

F2 **R.B.Henriksen**, C.Nissen, E.Makovicky, S.L.S.Stipp and C.Eggleston *(Denmark)*
Nanometer scale morphology of franckeite obtained by scanning tunneling microscopy (STM)

F3 **J.Icenhower** and P.M.Dove *(USA)*
The dissolution kinetics of amorphous silica: structural controls on reactivity

F4 **J.Y.Jia**, Z.L.Pan, X.D.Xie, D.Q.Wu and B.M.Lan *(P.R. China)*
Electrochemical mechanism of pyrrhotite reducing Cr(VI) into Cr(III)

F5 Y.Miura, S Fukuyama, M.Okamoto and **H.Kobayashi** *(Japan)*
Reduced compositions of impact minerals

F6 **O.B.Kotova** *(Russia)*
Surface magnetism of fine dispersional minerals

F7 **D.L.Legrand**, H.W.Nesbitt and G.M.Bancroft *(Canada)*
Effect of dissolved oxygen on pentlandite and pyrrhotite oxidation under flotation related conditions

F8 **C.Nissen**, R.B.Henriksen, S.L.S.Stipp, E.Makovicky and C.M.Eggleston *(Denmark)*
Atomic-scale surface features of franckeite investigated by scanning tunneling microscopy (STM)

F9 **K.Okada**, Y.Kameshima and A.Yasumori *(Japan)*
Chemical shifts of silicon X-ray photo-electron spectra on various silicate minerals

H1 **M.J.Scaini**, G.M.Bancroft and H.W.Nesbitt *(Canada)*
Characterization of pentlandite and pyrrhotite alteration products by X-ray photoelectron spectroscopy

H2 **O.Tamada** and M.Tanimoto *(Japan)*
A molecular orbital research for the reaction or adsorption between silica (H_4SiO_4) and fluids (H_2O, HF and HCl)

H3 A.R.Lennie, **D.J.Vaughan**, A.W.Munz, T.Bertrams and G.Thornton *(UK)*
Studies of pyrite (111) and (001) surfaces by scanning tunneling microscopy

Special Session 15. Recent Advances in the Crystal Chemistry of Rock Forming Minerals

Sponsored by PC

Convened and chaired by:
Frank C. Hawthorne (University of Manitoba)

*Monday, 10 August 1998, **ES AUD***

§ 08:30 D.K.Teertstra, **P.Černý** and F.C.Hawthorne *(Canada)*
New developments in crystal chemistry and geochemistry of alkali felspars from rare-element granitic pegmatites

§ 09:00 **C.A.Geiger** *(Germany)*
Volumes and volumes of mixing in the garnet system (Ca, Mg, Fe^{2+}, Mn^{2+})$_3Al_2Si_3O_{12}$

§ 09:30 **R.H.Mitchell** and A.R.Chakhmouradian *(Canada)*
Crystal chemistry of perovskite group minerals and their synthetic analogues

COFFEE 10:00

§ 10:30 **F.C.Hawthorne** *(Canada)*
Short-range order in rock-forming minerals

§ 11:00 **D.J.Henry** and B.L.Dutrow *(USA)*
Tourmaline: new views of a garbage can mineral

§ 11:30 **J.-L.Robert**, G.Della-Ventura, F Delbove, M.Diaz, J.-P.Gourdant, A.Papin and J.Sergent *(France)*
Structural control of the OH → F exchange in rock-forming hydrous silicates: a review based on experimental and spectroscopic data

*Tuesday, 11 August 1998, **ES AUD***

08:30 **B.C.Chakoumakos**, Th.Leventouri and V.Perdikatsis *(USA)*
Atomic displacements in carbonate apatite

08:50 **D.M.Burt** *(USA)*
Vector derivation of a composition space for skarn garnets

09:10 **G.A.Lager**, E.Libowitzky and A.J.Schultz *(USA)*
Neutron diffraction study of the low-temperature phase transitions in lawsonite

09:30 **R.L.Millard**, R.W.Luth and B.L.Sherriff *(Canada)*
Si/Al distribution and site distortion in Di-CaTs clinopyroxenes, using ^{29}Si and ^{27}Al MAS NMR

09:50 **H.Annersten** and E.Hålenius *(Sweden)*
DAC Mössbauer spectroscopy of synthetic olivines at elevated temperatures and pressures

COFFEE 10:10

10:40 **C.Chopin**, F.Brunet, G.Ferraris, M.Prencipe and O.Medenbach *(France)*
Raadeite, $Mg_7(PO_4)_2(OH)_8$: toward a humite-type series in Mg-phosphates?

11:00 **G.B.Andreozzi**, S.Lucchesi and G.Graziani *(Sweden)*
Crystal chemistry of axinites

11:20 **G.Simon**, C.Chopin and M.Czank *(Germany)*
Magnesiostaurolite in UHP rocks: a HP phase with some uncommon features

11:40 **T.G.Weiszburg**, D.Pop, Z.Klencsár, S.Nagy and E.Kuzmann *(Hungary)*
Contribution to the crystal chemistry of glauconite

***POSTERS** Monday, 10 August 1998*

D1 **M.Andrut**, Th.Zeiske, R.Schulz and H.-G.Krane *(Austria)*
Low symmetry in garnets: caused by its "water" -component?

D2 **M.F.Brigatti**, C Lugli, L.Poppi, E.E.Foord and D.E.Kile *(Italy)*
Crystal chemistry of Li-bearing micas from the Pikes Peak Batholith, Central Colorado

D3 **T.F.C.Campos** and A.M.R.Neiva *(Brazil)*
Geochemistry of amphibole from hybrid granitoid rocks of Rio Espinharas Pb pluton, Northeastern Brazil

D4 **M.D.Dyar**, C.V.Guidotti, E.S.Grew, M.Yates, J.S.Delaney, J.J.McGee, A.V.McGuire, R.L.Paul, J.D.Robertson, L.Cross, V.M.Sisson, M.W.Wiedenbeck and G.Fowler *(USA)*
Interlaboratory comparison of tourmaline analyses: major elements including B, Li, and Fe

D5 **C.Ferraris** and C.Chopin *(France)*
HRTEM evidence for retrograde exsolution in phengite-*3T* from the Dora-Maira Massif (Italian Western Alps)

D6 A.Pavese, **G.Ferraris**, G.Ivaldi, V.Pischedda and M.Nespolo *(Italy)*
Cation ordering and thermal expansion in $2M_1$ and 3T micas by neutron diffraction - role of the *TOT* layer structural details

D7 C.Wagner and **M.Fialin** *(France)*
EPMA determination of trace elements: REE and metals in amphiboles and clinopyroxenes. a record of metasomatic effects in the mantle

D8 **H.-J.Förster**, D.Rhede and G.Tischendorf *(Germany)*
Crystal chemistry of lanthanide- and actinide-rich acessories from peraluminous granites

D9 **I.Galuskina,** E.Galuskin and A.Winiarski *(Poland)*
An unusual clinopyroxene - early mineral of the Achtarandite rocks from the Wiluy River (Yakutia)

D10 **M.Gottschalk,** S.Melzer, M.Andrut and J.Najorka *(Germany)*
Substitution of various cations on the A- and M4-site in amphiboles

D11 **D.C.Greenidge** *(USA)*
The significance of aluminum substitution for silicon intetrahedral sites, giving rise to defects and color centers in silicate minerals

E1 **D.Holtstam** and U.Hålenius *(Sweden)*
Mn^{3+}-bearing garnets and hydrogarnets

E2 **U.Hålenius** *(Sweden)*
Crystal field study of Mn^{3+} in diaspore

E3 **K.Kihara** and M.Matsui *(Japan)*
Crystal structure data of berlinite, $AlPO_4$, and molecular dynamics simulation

E4 **M.Kimata**, N.Nishida, M.Shimizu, S.Saito and T.Matsui *(Japan)*
Pyroanion linkage models for feldspar and silica minerals

E5 **M.Koch-Müller**, I.Abs-Wurmbach, W.Bubenik, M.Gottschalk and R.Wirth *(Germany)*
Crystal chemistry of synthetic high-pressure staurolite

E6 **Gy.A.Lovas**, Gy.Buda and S.Háden *(Hungary)*
Structural state of K-feldspars occurring in S-Hungarian and S-Bohemian (Austria) granitoids

E7 **V.P.Lutoev** *(Russia)*
Structural position and geological specificity of substitutional V^{4+} ions in wavellite

F1 M.Okui and **F.Marumo** *(Japan)*
A nonstoichiometric pyroxene synthesized under ambient pressure

F2 **P.Mata**, F.López-Aguayo and D.R.Peacor *(USA)*
Evidence for a low-P-T origin of cookeite polytypes in pelites of the Iberian Range (Spain): a TEM study

F3 **D.Pop**, T.G.Weiszburg and I.Bedelean *(Romania)*
Compositional and XRD Characteristics of Glauconites from Transylvania, Romania

F4 Ph.Blanc, E. A.Perseil, G.Roger and **C.Wagner** *(France)*
Cathodoluminescence of apatites: new data on potential activators and inhibitors and their bearing on geochemical interpretations

F5 **O.V.Yakubovich**, W.Massa, Y.V.Kucherinenko and I.V.Pekov *(Russia)*
Crystal chemistry of zeolites of the merlinoite family

F6 C.Paluszkiewicz and **W.Zabinski** *(Poland)*
The problem of ordering in the vesuvianite structure evidenced by vibrational spectroscopy

F7 **P.Zecchini**, H.Mérigoux, K.Yamni, C.Aurisicchio and O.Grubessi *(France)*
Multivariate analysis of natural garnets using IR reflectance spectra

F8 **W.X.Zhao** and X.W.Liu *(P.R. China)*
Study on the convergent-beam electron diffraction to dislocation of quartz

Special Session 16. Mineralogy of Alkaline Rocks

Sponsored by CNMMN

Convened by:
Giovanni Ferraris (University of Torino)

Co-chairs:
Giovanni Ferraris (University of Torino)
and
Joel Grice (Canadian Museum of Nature)

Tuesday, 11 August 1998, ES 142

§ 08:30 **A.P.Khomyakov** *(Russia)*
Mineralogy of hyperalkaline rocks: advances and prospects

§ 08:50 **J.D.Grice** *(Canada)*
Carbonate mineralogy, Mont Saint-Hilaire, Quebec, Canada

§ 09:10 **O.Johnsen** and J.D.Grice *(Denmark)*
Crystal chemical characteristics of the eudialyte group

§ 09:30 **P.C.Piilonen**, A.E.Lalonde and A.M.McDonald *(Canada)*
The crystal chemistry of astrophyllite-group minerals from Mont Saint-Hilaire, Quebec

09:50 **A.M.McDonald** *(Canada)*
The crystal structure of UK92, a potentially new silicoborate from Mont Saint-Hilaire, Quebec, with comments on layered alkali silicates of the reyerite mesotype series

COFFEE 10:10

§ 10:40 **E.V.Sokolova**, G.Ferraris and A.P.Khomyakov *(Russia)*
Alkaline - phosphate blocks in the crystal structures of minerals occurring in the hyperalkaline rocks of Kola Peninsula

§ 11:00 **G.Ferraris** *(Italy)*
Modularity in minerals of the hyperalkaline rocks: just classification categories or genetic mechanisms?

11:20 **J.N.Roelofsen** and D.R.Veblen *(USA)*
CL and TEM investigation of zirconosilicates in the subsolvus granite of the Strange Lake peralkaline complex, Quebec-Labrador, Canada

11:40 **F.Princivalle**, S.Greblo, E.M.Piccirillo and A.Cundari *(Italy)*
Crystal-chemistry of 10 natural *C2/c* pyroxene phenocrysts from Kamafugitic rocks of Katwe-Kikorongo (SW-Uganda, Africa)

POSTERS Tuesday, 11 August 1998

C6 **J.V.Belovitskaya**, I.V.Pekov and Yu.K.Kabalov *(Russia)*
RE-free and RE-poor burbankite from pectolite metasomatites: chemical composition and crystal structure refinement

B13 E.P.Reguir, **A.R.Chakhmouradian** and M.D.Evdokimov *(Canada)*
Unusual Zr- and Sn-rich titanite in association with baratovite and zircon from the Dara-i-pioz Complex, Tajikistan

§ B14 **A.R.Chakhmouradian** and R.H.Mitchell *(Canada)*
Evolution of the accessory Sr-LREE and Ti-Nb mineralization in nepheline syenite at Pegmatite Peak, Montana

C8 **N.V.Chukanov** and I.V.Pekov *(Russia)*
Microheterogeneity and structure ordering in apatite group minerals: IR spectroscopic investigation

C1 **J.M.V.Coutinho**, Oliveira M.C.B., D.Atencio and F.M.S.Carvalho *(Brazil)*
Genthelvite from Iapitangui, Sao Paulo, Brasil

C2 **I.A.Ekimenkova**, I.V.Pekov and N.N.Kononkova *(Russia)*
Rhabdophane group minerals in pseudomorphs after steenstrupine-(Ce) from Lovozero Alkaline Complex, Kola Peninsula

C3 **P.A.Matioli**, D.Atencio and J.K.Tsugawa *(Brazil)*
Recent contributinos to the mineralogy of Pocos de Caldas Alkaline Massif, Minas Gerais, Brazil

C4 **S.Nakano** *(Japan)*
Implication of calcium distribution patterns in syenite alkali feldspars

C7 D.Prelević, **Gy.Pantó**, G.Nagy and M.Jovanović *(Hungary)*
Phlogopites from lamprophyres, semilamprophyres and some alkaline basalts from Serbia, Yugoslavia

§ C5 **I.V.Pekov** *(Russia)*
Lanthanum-rich minerals in high-alkaline pegmatites and hydrothermalites of Khibiny Massif, Kola Peninsula

C10 ***D.Yu.Pushcharovsky***, *R.K.Rastsvetaeva and* S.A.Vinogradova *(Russia)*
Recent contribution to structural mineralogy of oxides and carbonates of alkaline rocks

C11 **E.A.Shamshina** and N.V.Zayakina *(Russia)*
Si-bearing ilmenite from tuff pipes of Olenyok Uplift, N.-E. of Siberian Platform (Russia)

C12 **C.S.J.Shaw** *(Germany)*
Origin of megacrysts in the alkaline volcanic rocks of West Eifel, Germany

C13 **Y.Togawa**, M.Kimata, T.Nakano, A.Kato and S.Matsubara *(Japan)*
Geochemistry of garnets in acid volcanics: influence by subduction-related magmas

H5 L.N.Kogarko, **C.T.Williams** and A.R.Woolley *(UK)*
Compositional variation in cumulus and inter-cumulus minerals from the Lovozero Alkaline Complex, Russia

H4 **A.G.Bazhenov** and E.V.Belogub *(Russia)*
Diversity of amphiboles of Ilmenogorsky Massif of nepheline syenites (the South Ural, Russia)

§ C9 **R.K.Rastsvetaeva**, N.V.Chukanov and I.V.Pekov *(Russia)*
New data on the minerals of the labuntsovite - nenadkevichite family and their systematization

Special Session 17. Mineral Synthesis

Sponsored by CGM/CCGM

Convened by:
Jean-Louis Robert (CRSCM-CNRS, Orléans)
Co-chaired by:
Charles Geiger (University of Kiel)
and
Henrik Skogby (Museum of Natural History, Stockholm)

Tuesday, 11 August 1998, MP 203

§ 08:30 **C.A.Geiger** and A.Stahl *(Germany)*
Synthesis and characterization of pyropic garnets

§ 09:00 **S.G.Eeckhout**, E.De Grave and C.McCammon *(Belgium)*
Mössbauer study of synthetic $Mg_{0.2}Fe_{0.8}SiO_3$ clinopyroxene

§ 09:30 **H.Skogby** *(Sweden)*
Hydrogen exchange kinetics in clinopyroxene

COFFEE 10:00

§ 10:30 **M.Akasaka**, Y.Suzuki and H.Watanabe *(Japan)*
Hydrothermal synthesis of pumpellyite-okhotskite series minerals

§ 11:00 **R.Vochten** and N.Blaton *(Belgium)*
A new method of synthesis of boltwoodite and related minerals

§ 11:30 **J.-P.Gourdant** and J.-L.Robert *(France)*
Structural control of solid solution limits and ionic distributions in synthetic tourmalines

POSTERS Tuesday, 11 August 1998

J2 K.Bente, T.Doering, G.Wagner, **G.P.Bernardini**, D.Borrini and C.Danti *(Italy)*
On the progress of ordering in the synthetic aikinite - bismuthinite series

J3 **F.Bernhard** and U.Barth-Wirsching *(Austria)*
Natural and experimental zeolitization of phonolitic glass: a comparison

J4 N.I.Leonyuk, Yu.V.Klimanova, **A.V.Lyutin**, S.N.Barilo, G.L.Bychkov and L.A.Kurnevich *(Russia)*
Synthetic ruby with unusual Cr^{3+} concentration

J5 **T.Nagase**, T.Iwasaki, T.Ebina, H.Hayasi, Y.Onodera, *M.Chatterjee and K.Torii (Japan)*
Synthesis of iron containing dioctahedral smectites

K2 **T.Rziha** *(Germany)*
Thermal behaviour of synthetic alkali-birnessites

K3 **J.Sergent**, J.-L.Robert and G.Della Ventura *(France)*
Ti in synthetic clinoamphiboles: influence of bulk composition, temperature and Fe content on Ti solubility and substitutional mechanisms

Special Session 18. Ore Mineralogy

Sponsored by COM

Convened and chaired by:
Alan Criddle (Natural History Museum, London)

Wednesday, 12 August 1998, MP 203

08:30 **M.G.Villaseñor-Cabral**, J.A.Gómez-Caballero and E.U.Petersen *(Mexico)*
Multistage lead sulfosalts from Zimapan, Hidalgo, Mexico

§ 08:50 **W.H.Paar**, M.K.de Brodtkorb, R.J.Sureda and D.Topa *(Austria)*
A microprobe study of complex Ag-Sn ores from Pirquitas, Jujuy Province, Argentine

§ 09:10 **O.C.Gaspar**, J.Bowles, J.Ferreira, A.Ferreira and P.Nelson *(Portugal)*
Unusual concentrations of tetrahedrite and tennantite in the VMS of Neves-Corvo Deposit

09:30 **S.N.Nenasheva** *(Russia)*
Peculiarities of composition of germanite subfamily minerals

§ 09:50 B.Grguric, R.Harrison and **A.Putnis** *(Germany)*
A new phase diagram for the bornite-digenite join: results from in situ neutron diffraction and DSC experiments

COFFEE 10:10

10:40 **A.M.El-Bouseily**, A.I.Arslan and K.I.Khalil *(Egypt)*
Geochemical prospecting and genetic study of gold mineralization at the Fawakhir gold mine area, Eastern Desert, Egypt

11:00 **G.N.Gamyanin** and Yu.Ya.Zhdanov *(Russia)*
Natural spheroids of minerals in the gold occurrence

11:20 **R.J.Herrington**, V.V.Maslennikov, C.J.Stanley and F.Buslaev *(UK)*
Tellurium bearing in black smoker chimney fragments from the Silurian Yaman Kasy nassive sulphide orebody, southern Urals, Russia

11:40 **E.H.Nickel** *(Australia)*
A remarkable occurrence of Pd-Pt-Au-Ag-Cu-Se mineralization in Western Australia

POSTERS Thursday, 13 August 1998

A1 **L.M.Alva-Valdivia**, J.C.Cruz Ocampo and W.Vivallo *(Mexico)*
Petromagnetic properties and opaque mineralogy of host rocks and magnetite-apatite ore from Cerro de Mercado, Mexico

§ A2 **A.Y.Barkov**, K.V.O.Laajoki, S.S.Gornostayev and O.Taikina-aho *(Finland)*
Substitution mechanisms in sorosite, Cu(Sn,Sb)

A3 **E.V.Belogub** *(Russia)*
Beaverite-osarisavaite series from oxidation zone of Alexandrinka massive sulphide deposite (South Ural, Russia)

A4 **C.Canet** and J.C.Melgarejo *(Spain)*
Contrasting mineralogy of Silurian and Carboniferous Sedex Deposits, SW Catalonia

A5 P.M.Nikolić, S.Đurić, D.M.Todorović, V.Blagojević, D.Urosević, P.Mihajlović, A.I.Bojičić, K.T.Radulović, D.G.Vasiljević-Radović and **M.Dimitrijević** *(Yugoslavia)*
Photoacoustic and some optical properties of mineral marmatite (ZnS+Fe)

A6 J.N.Dunlevey and **M.J.Duane** *(Kuwait)*
The Copper Queen Dome Northern Zimbabwe

A7 **M.E.P.Gomes** and A.M.R.Neiva *(Portugal)*
Mineralogical and geochemical characteristics of stanniferous quartz veins at Ervedosa, Northern Portugal

H4 **O.E.Gorchakova** and N.L.Smirnova *(Russia)*
Cationic composition of sulphide, selenide and telluride minerals

A8 **M.P.Kalinowski** and T.Ericsson *(Sweden)*
Mooihoekite and talnakhite studied by Mössbauer spectroscopy and other methods

A9 **T.Kerestedjian**, V.Mladenova, P.Petrov and E.Neykova *(Bulgaria)*
Solid state growth of argentopentlandite and mackinawite in chalcopyrite

B1 **J.Majzlan**, M.Orvošová and M.Chovan *(USA)*
Hydrothermal alteration of granitoid rocks in the Dubrava Sb-Au deposit, Western Carpathians

B2 Gy.Pantó and **Z.Maksimović** *(Yugoslavia)*
Two new rare earth minerals in an unusual mineralization of the Nisi Bauxite Deposit, Greece

B3 **P.Marescotti**, R.Cabella and G.Lucchetti *(Italy)*
The breakdown of braunite + quartz assemblages through syntectonic veining in manganese ores of Eastern Liguria (Italy)

B4 **M.F.Marquez-Zavalia** and J. R.Craig *(USA)*
Tetrahedrite-tennantite from Capillitas Mine, a high-sulfidation epithermal-type deposit from Northwestern Argentina

B5 **M.A.Mattash**, J.A.Diner and D.G.Strachan *(Yemen)*
Epithermal alteration of the Western Yemen rift-related volcanics and their gold potential

B6 A.Escusa and **J.C.Melgarejo** *(Spain)*
Mineralogy of the El Molar metamorphized deposit of Mn, Catalonia

§ B7 **Y.Moëlo** and N.N.Mozgova *(France)*
Revision of sulfosalt nomenclature and definition: 1998th situation

B8 **I.Mârza** *(Romania)*
Petrometallogeny and petrometallites

B9 Gy.Pantó, A.Demény, **B.Nagy**, R.Krouse and M.Vytik *(Hungary)*
$\delta\ ^{34}S$ systematics in polymetallic ore deposits in the Carpathian Continental Volcanic Arc

B10 A.G.Bushev, A.M.Portnov, **A.A.Rogozhin**, B.S.Gorobets and V.M.Tiulenev *(Russia)*
Photoluminescent mineral haloes around kimberlite pipes

B11 **V.P.Samusikov**, G.N.Gamyanin and L.A.Pavlova *(Russia)*
Ag-Cu isomorphism in minerals from silver deposits of Yakutia

B12 **M.N.Shawki** and M.A.Mattash *(Yemen)*
Structural patterns and their role in the formation of alteration and mineralization in the Western Yemen rift-related volcanics

B13 **X.Song**, Y.Guo, Q.Xu, S.Li and L.Qiao *(P.R. China)*
A preliminary study of O, Si, S, and Pb isotopic compositions for the Besshi-type Cu-Zn deposit at Faziba, SE Gansu, NW China

B14 **D.Topa** and W.H.Paar *(Austria)*
New data on the mineralogy of sulphosalts from the Felbertal scheelite deposit, Austria

H5 A.Garavelli, **F.Vurro**, Y.S.Borodaev and N.N.Mozgova *(Italy)*
Bonchevite and kirkiite: two rare sulfosalts from Vulcano (Aeolian Islands, Italy)

Special Session 20. Breakthroughs in Synchrotron Radiation in Mineralogy

Sponsored by CPM

Convened and chaired by:
Gordon E. Brown Jr. (Stanford University)
and
G. Calas (University of Paris)

*Monday, 10 August 1998, **MP 202***

§ 08:30 **G.M.Bancroft** *(Canada)*
Surface studies of minerals with XPS and XANES using synchrotron radiation

§ 08:50 **D.J.Vaughan**, J.M.Charnock, F.R.Livens, R. H.Parkman and R.A.D.Pattrick *(UK)*
Synchrotron studies of interactions at the surfaces of iron oxide and iron sulfide minerals--- probing the redox boundary

§ 09:10 **M.E.Fleet**, S.Muthupari, M.Kasrai and S.P.Farrell *(Canada)*
Applications of soft X-ray XANES spectroscopy to mineralogy and geochemistry

§ 09:30 **Ph.Sainctavit**, D.Cabaret, Ph.Ildefonse and C.Deudon *(France)*
X-ray absorption spectroscopy as a tool for the determination of crystallographic and electronic structures of minerals

09:50 **G.Cressey**, P.F.Schofield, B.A.Cressey and A.D.Smith *(UK)*
X-ray Photo-Emission Electron Microscopy (XPEEM): application to valence-state imaging and micro-area spectroscopy of mineral intergrowths

COFFEE 10:10

§ 10:40 **S.C.B.Myneni**, A.Warwick, Z.Hussain and W.Meyer-Ilse *(USA)*
Applications of soft X-ray spectromicroscopy to environmental geochemistry and mineralogy

11:00 F.Juillot, G.Morin, P.Ildefonse, **G.Calas**, M.Buatier, P.Chevallier, P.Populus, G.E.Brown Jr., T.Trainor and J.Ostergren *(France)*
Chemical forms of heavy metals in soils: contaminated fields *vs.* geochemical anomalies

§ 11:20 **S.R.Sutton** *(USA)*
Trace-element characterization of earth materials using the synchrotron X-ray fluorescence microprobe

§ 11:40 **R.J.Hemley**, A.F.Goncharov, R.Lu and H.K.Mao *(USA)*
Synchrotron infrared spectroscopy of earth and planetary materials

POSTERS Monday, 10 August 1998

L1 **U.Bismayer**, H.-W.Meyer, M.Zhang, L.A.Groat, L.Nistor and G. Van Tendeloo *(Germany)*
Titanite and malayaite: structural investigations and the 500 K anomaly

L2 **F.Farges**, S.Siewert, H.Büttner and G.E.Brown,Jr. *(France)*
Effect of pressure and water on the local environment of Ni in silicate glasses

L3 **L.Galoisy** and G.Calas *(France)*
High resolution Fe K- pre-edge spectroscopic study in minerals and glasses

L4 **S.Quartieri**, G.Antonioli, C.A.Geiger, J.Chaboy and G.Artioli *(Italy)*
Incorporation of Yb in synthetic pyrope and grossular garnets: XAFS/XRD study and multiple scattering calculations

L5 **A.H.Rankin**, B.Bühn, M.Haller and M.Radtke *(UK)*
Quantitative analysis of Sr-REE-Ba-daughter minerals in fluid inclusions by combined synchrotron micro-XRF and SEM-EDX techniques

L6 **M.Sachanbiñski** and J.Chojcan *(Poland)*
An attempt to estimate the age of obsidians using positron annihilation spectroscopy

L7 **A.G.Schaufuss**, H.W.Nesbitt and R.Szargan *(Germany)*
Fractured pyrite surfaces: evidence of site specific reactivity using synchrotron radiation

L8 **A.C.Scheinost**, H.Stanjek, D.G.Schulze, U.Gasser and D.L.Sparks *(USA)*
Structural environment and oxidation state of manganese in goethite-groutite solid-solutions: a Rietveld, EXAFS, XANES, and DRS study

L9 **P.F.Schofield**, E.H.Bailey and J.F.W.Mosselmans *(UK)*
Gold complexation by chloride bearing fluids

Special Session 21. Ore Mineralogy of Modern Sea Floor Hydrothermal Systems

Sponsored by COM

Convened and chaired by:
Mark Hannington (Geological Survey of Canada)

Thursday, 13 August 1998, MP 203

§ 08:30 **J.M.Peter**, W.D.Goodfellow and Leg 169 Shipboard Scientific Party *(Canada)*
Setting, mineralogy and geochemistry of the Middle Valley Sulfide Deposits: results of ODP Leg 169

08:50 **M.D.Buatier**, G.Früh-Green, C.Monnin and A.M.Karpoff *(France)*
Hydrothermal phyllosilicate formation at sedimented ridges: a comparison between axis and off-axis systems (Juan de Fuca Ridge)

§ 09:10 **S.Petersen**, P.M.Herzig and M.D.Hannington *(Germany)*
The third dimension of a presently forming Cyprus-type VMS deposit: TAG hydrothermal mound, Mid-Atlantic Ridge, 26°N

§ 09:30 **R.J.Herrington**, C.T.S.Little and B.Spiro *(UK)*
Fossil hydrothermal vent communities and associated features from exceptionally preserved massive sulphides in the geological record

§ 09:50 **D.Fortin** and F.G.Ferris *(Canada)*
Formation of Fe-oxides and Fe-silicates on bacterial surfaces in hydrothermal deposits collected near the Southern Explorer Ridge in the Northeast Pacific Ocean

COFFEE 10:10

§ 10:40 **K.Marumo** *(Japan)*
Mineralogy and geochemistry of hydrothermal plumes on the fast-spreading Southern EPR

§ 11:00 **U.Muench**, B.Pracejus and P.Halbach *(Germany)*
Mineral and metal composition of modern massive sulfides from different submarine geological environments

§ 11:20 **U.Schwarz-Schampera** and P.M.Herzig *(Germany)*
Mineralogy and geochemistry of indium in seafloor hydrothermal systems

11:40 **N.N.Mozgova** *(Russia)*
Specific features of ore mineralogy of modern sea floor hydrothermal systems

POSTERS Thursday, 13 August 1998

J1 **N.S.Bortnikov** *(Russia)*
Modern sea floor sulfide mineralization: mineralogical and isotopic contrasts

J2 **C.E.Loon**, S.D.Scott and J.C.Rucklidge *(Canada)*
Lead in sulfide and sulfate-rich chimneys from Guaymas Basin, Gulf of California, and the Pacmanus Deposit, Eastern Manus Basin

§ J3 **R.Moss** and S.D.Scott *(Canada)*
Geochemistry and mineralogy of silver in hydrothermal precipitates on the modern seafloor

Special Session 22. Ore Minerals in Hot Water

Sponsored by COM

Convened and chaired by:
Anthony Williams-Jones (McGill University)

Friday, 14 August 1998, MP 103

09:00 **I.-M.Chou** and W.A.Bassett *(USA)*
Minerals in hot water and hot fluids in minerals: visual observations and in-situ characterization of samples through diamond windows

09:30 **T.M.Seward** *(Switzerland)*
Spectroscopic studies of hydrothermal solutions

COFFEE 10:00

10:30 **S.A.Wood** *(USA)*
The solubility of siderophile elements (Pt, Pd, Os and Re) in hydrothermal solutions

11:00 **D.J.Wesolowski**, D.A.Palmer, P.Bénézeth and M.L.Machesky *(USA)*
Mineral/water interaction studies with *in situ* pH monitoring to 300°C

11:30 **W.E.Seyfried** Jr., K.Ding, D.E.Allen and M.E.Berndt *(USA)*
Mineral solubility constraints on metal mobility in subseafloor hydrothermal systems

Special Session 23. Mineralogical Museums Serving Science and Society

Sponsored by COMu

Convened and chaired by:
Carl Francis (Harvard Mineralogical Museum)

*Monday, 10 August 1998, **MP 203***

§ 08:30 **J.F.DeMouthe** *(USA)*
Interdisciplinary uses of mineral collections

§ 08:50 **V.W.Lueth** and R.W.Eveleth *(USA)*
Science and Service, the New Mexico Bureau of Mines and Mineral Resources Mineral Museum, Socorro, New Mexico, USA

09:10 J.Murphy and **J.F.Hurlbut** *(USA)*
Installation of a 6 x 8 foot rhodochrosite pocket in the Denver Museum of Natural History Coors Mineral Hall

§ 09:30 **S.C.Eriksson** *(USA)*
Is it real? The importance of minerals in education and research today

09:50 **C.J.Stanley** *(UK)*
The Earth Galleries: Natural History Museum, London, UK

COFFEE 10:10

§ 10:40 **G.E.Harlow** *(USA)*
The nature of diamonds: an exhibition integrating science, history, culture, and technology

11:00 **L.Touret** *(France)*
History of mineralogy through European mineralogy museums, the goal of Euromin

§ 11:20 **S.N.Monaghan** *(USA)*
Engaging museum visitors in mineralogy: the birthstone exhibit at the Harvard Mineralogial Museum

§ 11:40 **J.E.Post** *(USA)*
The new geology, gems and minerals exhibition at the Smithsonian Institution

POSTERS Monday, 10 August 1998

B8 **D.I.Belakovskiy** and D.M.Fiveyskiy *(Russia)*
MINSPEC- mineralogical database information system for museum collection management and mineral species fast diagnostic

B9 **C.A.Francis** *(USA)*
Catalogue of type specimens in the Harvard University mineral collection

§ B10 **A.R.Kampf** *(USA)*
Computer database design for effective mineral collection management

B11 **Y.Okuyama-Kusunose**, K.Kusunose, S.Togashi, N.Imai, M Haruna, A.Cho, T.Yanagitani and H.Kawakata *(Japan)*
Sample database and reference samples for science and society: an attempt of Geological Museum, GS Japan

B12 **K.U.Schuermann** *(Germany)*
Special exhibitions: a tool for connecting science and society?

B13 **H.A.Stalder** *(Switzerland)*
Catalogue of type mineral specimens - CTMS

Special Session 24. Mineralogy of Large and Superlarge Ore Deposits

Sponsored by IAGOD

Convened and chaired by:
D.V. Rundqvist (Moscow State University)

*Friday, 14 August 1998, **MP 202***

08:30 **D.V.Rundqvist** *(Russia)*
Are there mineralogical criteria of large and superlarge mineral deposits?

09:00 **A.J.Naldrett**, Jagmohan Singh and Sasa Krstic *(Canada)*
Mineralogy of the Voisey's Bay Ni-Cu Deposit, Labrador

09:30 **K.A.McCormick** and A.M.McDonald *(Canada)*
The crystal chemistry of amphiboles in the Footwall Breccia, at the Fraser Mine, Sudbury, Ont

COFFEE 10:00

10:30 **G.Y.Chen**, D.S.Sun, W.Shao and Y.Chen *(P.R. China)*
Mineralogy of the superlarge Linglong Gold Deposit in Shandong Province, N. China

11:00 **A.A.Chernikov** *(Russia)*
Mineralogical types of uranium ores of Russia and contiguous to countries, mineralogical types of large and superlarge deposits

11:30 **R.S.Krymsky** and B.V.Belyatsky *(Russia)*
Genesis of the large tungsten deposit Vostok-2 (Primorie, Russia): Sm-Nd and Rb-Sr isotope constraints

POSTERS Friday, 14 August 1998

E6 **Y.Chen**, W.Zang, W.S.Fyfe, G.Y.Chen and D.S.Sun *(Canada)*
The Jiaodong Gold Province of China: alteration and ore mineralogy

E7 **E.A.Kulish** and I.L.Komov *(Ukraine)*
Mineralogical peculiarities of large gold and platinum deposits

F1 **D.S.Sun**, G.Y.Chen, W.Shao and G.Y.Li *(P.R. China)*
Mineralogy of carbonates from large-superlarge gold deposits in Shandong Peninsula, N. China

Special Session 25. Granite Pegmatites: Nature versus Experiment

Sponsored by MAC/MSA PIG

Convened and chaired by:
Petr Černý (University of Manitoba)
and
David London (University of Oklahoma)

*Thursday, 13 August 1998, **ES 142***

§ 08:30 **P.Černý** *(Canada)*
Nature vs experiment in granitic pegmatites: what works and what does not

§ 08:50 **D.London** *(USA)*
Experimental simulation of pegmatite texture

§ 09:10 **P.Candela** and P.Piccoli *(USA)*
Pegmatitic and related textures in compositionally simple granitic rocks

§ 09:30 **D.R.Baker** and C.Freda *(Canada)*
Diffusion in pegmatite melts and the size of compositional gradients in front of growing crystals

§ 09:50 **T.Dewers** *(USA)*
Kinetics of oscillatory crystallization in granitic melts: internal versus external forcing

COFFEE 10:10

10:40 **R.F.Martin** *(Canada)*
Crystallization in granitic pegmatites: insights from my plate collection

§ 11:00 **D.B.Dingwell**, K.-U.Hess and C.Romano *(Germany)*
Water-rich silicic melt viscosities: influence of the alkali/aluminum ratio and implications for magmatic degassing

§ 11:20 **K.L.Webber**, Wm. B.Simmons and A.U.Falster *(USA)*
Cooling rates and crystallization dynamics of shallow level pegmatites, Calif., USA

§ 11:40 **R.Thomas** *(Germany)*
What can we learn from melt inclusions in granite pegmatites?

Friday, 14 August 1998, ES 142

08:30 **T.S.Ercit** *(Canada)*
Tantalum-niobium oxide minerals and pegmatite genesis

08:50 **C.Aurisicchio**, C.De Vito, V.Ferrini and P.Orlandi *(Italy)*
Geochemistry and crystal chemistry of Nb-Ta oxides from "Fonte del Prete" Dike (Elba Island, Italy)

09:10 **R.L.Linnen** *(Canada)*
Experimental constraints on the association of Li with Ta in granitic pegmatites

09:30 **F.Pezzotta**, A.Guastoni, V.Diella, C.M.Gramaccioli and F.Demartin *(Italy)*
Chemical and paragenetic data on gadolinite group minerals from Baveno and Cuasso al Monte, Southern Alps, Italy

09:50 **A.M.R.Neiva**, J.M.C.Neiva and J.Esson *(Portugal)*
Beryl from the granitic pegmatite at Namivo, Alto Ligonha, Mozambique

COFFEE 10:10

10:40 **Z.L.Li**, W.L.Zhang and R.Y.Yang *(P.R. China)*
The analysis of chemical composition of melt inclusion of beryl in pegmatite and discovery of zinc spinel by electronic probe

11:00 **R.B.Larsen** and M.Polvé *(Norway)*
Trace element distribution in pegmatitic quartz: petrogenetic applications to granite pegmatites in South-Norway

§ 11:20 **J.B.Selway**, P.Černý, F.C.Hawthorne and F.W.Breaks *(Canada)*
Compositional evolution of tourmaline in petalite-subtype pegmatites

11:40 **R.Seltmann**, B.Taylor, A.Aksyuk, A.Fedkin, F.Reyf, V.Shatov and G.Zaraisky *(Germany)*
Line rock formation in the Orlovka and Etyka tantalum deposits, Eastern Transbaikalia

POSTERS Friday, 14 August 1998

D1 ***P.Alfonso, J.C.Melgarejo and F.Fontan (Spain)***
Phosphates from the Cap de Creus granite pegmatite field, Eastern Pyrenees, Catalonia

D2 **Gy.Buda** *(Hungary)*
Characteristics of some variscan granitoids in Central Europe

D3 **J.M.Evensen**, D.London and R.F.Wendlandt *(USA)*
Solubility of beryl in haplogranite melts

D4 C.Aurisicchio, C.De Vito, **V.Ferrini** and P.Orlandi *(Italy)*
Complex Ti, Ta, Nb oxides from Baveno, Elba Island and Val Vigezzo (North of Italy)

D5 **P.Keller** *(Germany)*
Origin, emplacement and mineralization of rare-element pegmatites, Central Damara Province, Namibia

D6 H.Mäkitie, **S.I.Lahti**, N.Kärkkäinen and R.Alviola *(Finland)*
Mineralogy and chemical composition of granitic pegmatites in different metamorphic zones, Seinäjoki Region, Finland

D7 S.Nakano, T.Eriguchi and **K.Makino** *(Japan)*
FT-IR micro spectra of pegmatite alkali felspar from Hanazono, Japan

D8 **M.A.Morsy** and F.H.Mohamed *(Egypt)*
Geochemical study of the Muelha tin specialized granite, Eastern Desert, Egypt

D9 **P.N.Nysten** and E.Jonsson *(Sweden)*
Mineralogy of a late Svecofennian granitic pegmatite, Norrskogen, Uppland, Sweden

D10 J.C.Melgarejo, **R.M.Prol-Ledesma**, M.A.Sandoval-Miranda and M.Morales-Alvarado *(Mexico)*
The El Muerto Mine, Oaxaca, Mexico: an example of the allanite-subtype pegmatites

D11 R.Wegner, **H.Pöllmann**, Th.Witzke and W.Schuckmann *(Germany)*
Colquiriite, carlhintzeite, ralstonite and pachnolite from Serra Branca Pegmatite, Brazil

E1 **J.Quéméneur** *(Brazil)*
Trioctaedrical micas from the internal contact zone of two pegmatites from Minas Gerais, Brazil, as indicators of reflux fluids

E2 **M.M.V.G.Silva** and A.M.R.Neiva *(Portugal)*
Geochemistry of biotites from microgranular enclaves and host granites from Oporto-Gaia, Northern Portugal

E3 **T.K.Soldatos** *(Greece)*
The Elatia Granitic Pluton (North Greece): mineralogy, petrology, geochemistry

E4 M.C.Taylor and **M.A.Wise** *(USA)*
Primary petalite + spodumene assemblages in rare-element pegmatites of the Peninsular Ranges Batholith, Southern California

E5 **M.B.Wolf** and D.London *(USA)*
Experimental study of tourmaline stability in granitic magmas

Special Session 26. Descriptive Mineralogy at the Close of the 20th Century

Sponsored by PC

Convened and chaired by:
Joseph Mandarino (Royal Ontario Museum)

Wednesday, 12 August 1998, MP 202

08:30 **M.I.Novgorodova** *(Russia)*
Natural crystalline carbon polymorph from mantle xenolite

§ 08:50 **S.Graeser** *(Switzerland)*
The imhofite-jentschite group of Tl-As sulfosalts, Lengenbach, Switzerland

§ 09:10 **P.Orlandi** and S.Merlino *(Italy)*
Three new minerals from Tuscany, Italy

09:30 F.Pezzotta, **A.U.Falster**, Wm.B.Simmons and K.L.Webber *(USA)*
New data on rhodizite from Madagascar

09:50 **A.A.Almohandis** *(Saudi Arabia)*
Mineralogy and chemistry of desert roses, Ayn Dar Area, Abqaiq, Eastern Province, Saudi Arabia

COFFEE 10:10

§ 10:40 **D.S.Coombs** *(New Zealand)*
Nomenclature for zeolite minerals

§ 11:00 **S.Quartieri**, E.Galli, G.Vezzalini and A.Alberti *(Italy)*
An overview on zeolites from Antarctica

11:20 **J.L.Palmer** and M.E.Gunter *(USA)*
Optical properties of natural and cation-exchanged heulandite group zeolites

Thursday, 13 August 1998, MP 202

§ 08:30 **G.Raade** *(Norway)*
On the future of mineralogy and the CNMMN

08:50 **Y.Miura** *(Japan)*
Present and future of impact mineralogical sciences

§ 09:10 G.Ferraris and **S.Merlino** *(Italy)*
Role of the modular aspects of minerals for a crystal-chemically oriented descriptive mineralogy

09:30 **Ph.Sonnet** *(Belgium)*
An algebraic method for choosing exchange vectors that best describe a mineral

§ 09:50 **A.P.Khomyakov** *(Russia)*
Recent mineral discoveries and the number of mineral species: a reconsideration

COFFEE 10:10

§ 10:40 **D.Atencio** *(Brazil)*
The state of descriptive mineralogy in Brazil

§ 11:00 **G.Udubasa**, S.Szakall, R.Duda and V.M.Kvasnitsa *(Romania)*
Mineralogy of the Carpathians - a legend of the past-a challenge to the future

§ 11:20 **D.I.Belakovskiy** *(Russia)*
Natural modern mineralization process resulted from *in situ* coal self-ignition and burning

POSTERS Thursday, 13 August 1998

G1 **V.Bermanec**, T.Armbruster, R.Oberhänsli, V.Zebec and G.Kniewald *(Croatia)*
Solid solution in the epidote group of minerals: Pb and REE-rich piemontite from Nezilovo, Macedonia

G2 **G.Kniewald**, M.Rossbach, H.Amer and V.Bermanec *(Croatia)*
Distribution of rare earth elements in sediments from the Tuzla salt mine, Bosnia and Herzegovina

G3 **R.Cabella**, G.Lucchetti and P.Marescotti *(Italy)*
REE and Y minerals in an Fe-Mn deposit (Maritime Alps, Italy)

G4 C.Cipriani, V.Moggi-Cecchi, S.Rubechi, G.P.Bernardini and **C.Danti** *(Italy)*
A re-examination of the compositional fields of the members of the aikinite-bismuthinite series

G5 **A.Kovács**, Gy.A.Lovas, T.G.Weiszburg and E.Kuzmann *(Hungary)*
New data on coquimbite, paracoquimbite and copiapite-group minerals from Hungary

G6 P.Orlandi, A.Meerschaut, **Y.Moëlo** and P.Palvadeau *(France)*
Scainiite and pillaite, two new Pb-Sb sulfosalts from Tuscany: definition and crystal structures

G7 **E.P.Shcherbakova** *(Russia)*
Sulfate minerals. their possible technogene nature

G8 **J.Taucher**, F.Bernhard, F.Walter and K.Ettinger *(Austria)*
Pretulite, $ScPO_4$, a new scandium mineral from the Styrian and Lower Austrian lazulite occurrences, Austria

J4 **D.Tibljaš**, S.Šćavničar, V.Bermanec and R.Slavković *(Croatia)*
Celadonite-family mica in pyroclastic rocks from Hrvatsko Zagorje (NW Croatia)

J5 **G.C.Wilson** *(Canada)*
Evolution of MINLIB, a minerals-oriented bibliographic database

ABSTRACTS

for the Plenary Lectures, Symposia and Special Sessions
of the 17th General Meeting of the

International Mineralogical Association
Toronto, 1998

Abstracts are listed in the same order as the programme.
An index to the abstracts and the programme is at the back of this volume.

Plenary Lectures

WHAT WE HAVE LEARNED ABOUT COLOR IN MINERALS

Rossman G.R. *(Division of Geological and Planetary Sciences, California Institute of Technology, Pasadena, CA 91125, USA)*

Many portions of the electromagnetic spectrum are now used to study minerals. While instruments probe minerals with photons ranging from x-rays to microwaves, for most of us, the visible portion of the spectrum provides our first introduction to minerals. The beautiful colors of minerals are a major attraction to mineralogy. The technical understanding of the origin of color in minerals still provides significant scientific challenges. We have learned a lot about the origin of color in minerals and have had to revise many previously held ideas. The commonly held idea that "green indicates reduced iron and red indicated oxidized iron" is valid in particular circumstances, but certainly not in general. And, no, lithium does not cause pink color in mica and tourmaline.

Ions of common metallic elements are the dominant source of color in most silicate, phosphate and carbonate minerals. Color in these minerals is determined by the ion, its oxidation state, its coordination number and geometry, and by interactions with neighboring ions.

Examples from the garnets, tourmalines and the colored varieties of quartz will be used to illustrate the principles which govern color. The diversity of color in garnets is a direct result of the variety of sites which can accommodate a variety of elements in a variety of oxidation states. The complexity of color in tourmaline results from individual ions of Fe, Mn, Cr and V together with cations in arrangements which allow strong interactions with neighboring ions. The colored varieties of quartz are due, in part, to interstitial sites which accommodate Fe and other cations, and, in part, to microscopic inclusions of colored phases, some only recently recognized. The color of some varieties of both quartz and tourmaline result from changes in the oxidation states of cations brought about by natural background radiation.

MODERN PERSPECTIVES IN MINERALOGY

Hawthorne F.C. *(Dept. of Geological Sciences, Univ. of Manitoba, frank_hawthorne@umanitoba.ca)*

As this century draws to a close, we have a fairly detailed understanding of the structure, chemistry and properties of the rock-forming minerals. So "What's next?" In answering this question, we need to bear two points in mind: (1) Minerals provide us with a range of materials from the simple to the complex; (2) minerals form by natural processes, and hence are our window into geological processes. When we know the approximate atomic arrangement of a mineral, we can calculate the static and dynamic properties with increasing accuracy. Can we improve on these models to predict the onset of exotic properties (e.g., giant magnetoresistance, superconductivity). We need a better mechanistic theory of crystallization, one that adequately reproduces complex crystal morphology, oscillatory zoning, decoupled zoning, etc. Short-range order (SRO) can occur in solid solutions, yet we have very little data on SRO, even though it must impact significantly on thermodynamic modelling of geological processes. We know very little about long-range order (LRO) of trace elements and nothing about LRO of isotopes in minerals, and yet both features must affect the thermodynamics of trace-element and isotope exchange. Many processes occur at mineral surfaces, and yet there is still not much information on the real surface structure (static and dynamic) of most minerals. Another area that is crying out for more work involves the interaction between minerals (and mineral surfaces) and biological organisms; very little is yet understood at the atomic level, and yet this is an area that impacts greatly on our environment. Mineralogy abounds with challenging and fundamental problems that are waiting for us to solve them.

ORE MINERAL TEXTURES AND THE TALES THEY TELL

Craig J.R. *(Dept. of Geological Sciences, Virginia Tech, jrcraig@vt.edu)*

The ore minerals have served as the resource base for all of the metals used by humankind since the dawn of history. World production of refined metals in all time has been approximately 60 billion metric tons and today exceeds 1.3 billion metric tons annually. The continued availability of metals to serve in myriads of uses in modern society requires the discovery of economic deposits and the efficient extraction of the metals from the ores. The interpretation of ore mineral textures is generally second only in importance to the identification of the ore minerals in a deposit, and the textures often play the critical role in determining the actual extractability of the ore minerals as sources of the metals.

The ore textures, like the words on a page, are nature's record of the processes of formation and many of the subsequent events in the history of the deposit. "Texture", from the Latin "web" and French "to weave", relates to the basic fabrics from the most delicate to the most coarse. Conventional optical textural analysis, especially when interpreted in terms of known phase equilibria, simultaneously provides insights into the mechanisms of origin, sequences of deposition (including the existence of multiple generations), nature of post-depositional modification, grain size distribution, nature of intergranular relationships (inclusions, inter-penetration, intimate association), distribution of elements, secondary solid state reequilibration, secondary weathering and alteration, and likely fate of waste minerals after metal extraction. Furthermore, ore minerals are common accessory phases in non-economic deposits and can provide insights into the origins and histories of those rocks as well.

Chemical textural analysis, the examination of the distribution of minor and trace metals in ore minerals, can provide additional information on the origins of the minerals and the deposits and and can aid in predicting the fates of the metals during processing, disposal, and/or weathering. Ore textural analysis will be important in assuring efficient recovery of metals, especially from declining ore grades, and in the understanding of the fates of metals in the environment. Examination of the textures of ore mineral analogs formed on anthropogenic materials can provide archeological insights and is increasingly important in the understanding of metal corrosion, failure, and environmental dispersal.

REAL TIME SYNCHROTRON POWDER X-RAY DIFFRACTION

Parise J. B. *(Geosciences, State Univ. New York, Stony Brook, John.Parise@sunysb.edu)*

The availability of dedicated synchrotron radiation, coupled with the increased use of area detectors such as imaging plates and CCD's, has improved the quality of bulk powder diffraction data available with time resolutions of 1 - 5 seconds. A variety of detection systems are installed and have been tested at the X17B, X7A and X7B beamlines at the NSLS. These can be coupled to a variety of high temperature and high pressure devices or used to collect data from samples at ambient conditions. Examples from the following class of reactions have been studied using time resolved diffraction data and Rietveld structure refinement: 1) the mechanism of solid state phase transition from olivine to spinel, 2) the mechanism of order-disorder reactions in olivine 3) the kinetics of precipitation and transformation of pyrite and other sulfides and 4) the mechanism of ion-exchange in zeolites. In these studies high peak-to-background discrimination and high angular resolution are essential for Rietveld structure refinement. The ability to refine structure models provides insight into site-specific behavior. Useful information, however, on the phases present, their proportions and the kinetics of their transformation, can also be obtained from data of more marginal quality. Some of these experiments were carried out using a variety of cells which allow real time diffraction, while reagents are injected to vary reaction conditions. A new small environmental cell for real time studies (SECReTS) suitable for investigations of ion exchange, gas loading, dehydration and hydrothermal titration reactions will be described.

Several issues requiring further work will also be discussed and include: 1) solutions to the "data glut" expected when third generation synchrotrons make possible data collection at the sub-msec. time scale; 2) combined spectroscopy/diffraction to follow the pre-nucleation/nucleation behavior in solutions and gels; 3) the design and commissioning of cell designs which allow us to approach conditions of relevance to "real" reaction conditions and 4) possibilities for Rietveld refinement using energy dispersive data for the highest time resolution and minimal interference from cell assemblies.

Plenary Lectures

TRACE ELEMENT FRACTIONATION PROCESSES

Shaw D.M. *(Dept. of Geology, McMaster University, Hamilton, Canada; shawden@mcmaster.ca)*

The Goldschmidt school of geochemistry focussed on the behaviour of individual trace elements. Only in post-WW2 was it shown how they could be used to illuminate (some said to solve) geological problems. The first major effort in this direction was L.R.Wager and R.L.Mitchell's (1951) study of trace elements in the Skaergaard intrusion, although theoretical groundwork had already been laid by H.Neumann and by H.D.Holland & J.L.Kulp, based on Lord Raleigh's 1896 theory.

Improved analytical methods have since resulted in clearer understanding of element behaviour, augmented by resolution of contamination problems by ever-decreasing the sample size.

Basic fractionation theory, based on crystal chemistry, applies equally well to igneous, metamorphic, hydrothermal, oceanic and sedimentary heterogeneous (multiphase) systems; the details of such applications, and consequently of trace element behaviour, however, differ widely, because of variation of intensive parameters, and of kinetic, diffusional and mechanical transport factors.

The most useful concept in fractionation theory, is the equilibrium ***partition coefficient*** K_i of an element ***i*** between two phases. Early hopes that Henry's law, implying constant K_i, would govern trace element distributions have been dashed, and partition coefficient studies now support many careers. Paradoxically the concept of the constant partition coefficient has been very useful in elaboration of mantle melting schemes, particularly for so-called ***continuous or dynamic melting***. Few trace element data arrays have yet been sufficiently precise or well-controlled geologically, however, to test the assumptions invoked for such models.

MINERALOGY OF THE SOLAR SYSTEM

Zolensky M.E. *(SN2 NASA Johnson Space Center, Houston, TX 77058 USA, michael.e.zolensky1@jsc.nasa.gov)*

The coming decade + will see frequent fly-by and rendezvous missions to small bodies in our solar system performed by NASA, ESA and ISAS. We are also entering a new golden age of sample return missions from diverse extraterrestrial objects. The result of these efforts will be a dramatic expansion in our understanding of the origin and evolution of the Solar System. This presentation summarizes plans and goals for these planetary geology missions, so that mineralogists can begin to prepare. The schedule for these missions follows:

Near Earth Asteroid Rendezvous - Rendezvous with asteroid 433 Eros in 1998-2000

Deep Space 1 - Fly-bys of Mars, asteroid 3352 McAuliffe and comet P/West-Kohoutek-Ikemura in 1998-2000

STARDUST - Sample return from comet P/Wild 2 and interstellar dust in 2006

Muses-C - Sample return from asteroid 4660 Nereus in 2006

COUNTOUR - Fly-by of 3 comets including P/Encke and P/d'Arrest in 2004-2010

Deep Space 4: Champollion - Sample return from comet P/Tempel 1 in 2010

Rosetta - Rendezvous with comet P/Wirtanen in 2011-2013, with fly-bys of asteroid 3840 Mimistrobel and 2530 Rodari in 2006-2008

PLUS: Numerous missions to Mars including a sample return as early as 2008.

The Rendezvous and fly-by missions will be investigating mineralogy primarily by spectroscopy, although the Rosetta and Champollion landers will have limited microanalytical capabilities. The Stardust and Muses C sample returns will be in the microgram to gram level, necessitating clever and careful handing.

BONDING AND MINERAL BEHAVIOUR

Price G.D. *(Dept. Geological Sciences, University College London, d.price@ucl.ac.uk)*

All the properties and aspects of behaviour of a mineral depend upon the nature of bonding between the mineral's constituent atoms. Classically, such bonding has been discussed in qualitative terms such as ionic, covalent, *etc.* interactions. With the advent of powerful computing facilities in the past twenty years, however, it has been possible to quantitatively model the bonding within a mineral and to predict or rationalize its behaviour.

Computational mineral physics uses either empirical descriptions of interatomic interactions or, more increasingly, quantum mechanical solutions to calculate the variation of the energy and the resulting forces between atoms as a function of geometry. From the energy surfaces, it is possible to calculate a whole range of mineral properties including crystal morphology, elastic constants, equations of state, vibrational spectra, phase stability, defect properties, rheology and kinetic processes. In my talk, I will summarise the techniques used in simulations (including lattice dynamical and molecular dynamical methods), and show how they have been used to understand or predict the behaviour of minerals, with specific reference to:

(a) the equations of state of mantle phases

(b) the phase stability of Fe at high P and T

(c) the viscosity of liquid Fe in the Earth's core

(d) the ionic conductivity of $MgSiO_3$ -perovskite

(e) the morphology of calcite.

MINERALOGY FROM THE CRUST TO THE CORE

Yagi T., Kondo T. and Uchida T. *(Inst. Solid State Phys., Univ. of Tokyo, yagi@issp.u-tokyo.ac.jp)*

Pressure induced phase transformations in olivine, pyroxene, and garnet, and the physical properties of high pressure phases formed from these minerals are reviewed at the conditions from the crust to the core. Earth's mantle is believed to consist of three major minerals; olivine, pyroxene, and garnet. Intensive studies have been made to clarify the high pressure behavior of these minerals using various experimental techniques.

Development of synchrotron radiation combined with either multi-anvil apparatus or laser-heated diamond anvil cell made it possible to perform *in situ* X-ray observations of these minerals under the condition of the Earth's deep interior. It was believed that most of the high pressure phases of silicates are quenchable on release of pressure. Once the pressure range is extended to that of the lower mantle, however, it became clear that there exist many unquenchable high pressure polymorphs of silicates. This means, in order to discuss the mineralogy of the lower mantle, it is very important to make *in situ* observations under pressure. High pressure behaviors of olivine and pyroxene compositions are rather simple while that of garnet varies in a complicated manner depending on many factors such as pressure, temperature, and composition. Garnet breaks down into several phases when it is subjected to the condition of the lower mantle, but they eventually crystallize into a mixture of two perovskite phases under deep mantle condition. Transition pressure of garnet to perovskite assemblage phases is slightly higher than that of pure $MgSiO_3$ composition and the transition kinetics of this reaction is slower than that of olivine. These features may play important role for the dynamics of subducting slab.

The physical properties of the lower mantle are mainly controlled by the nature of composing phases, which is a complicated solid solution with perovskite structure. Further studies will be required to clarify the nature of these perovskite structured phases.

THE DESIGN OF NUCLEAR WASTE FORMS: CLUES FROM MINERALOGY

Ewing R.C. *(Dept. of Nuclear Engineering and Radiological Sciences, Univ. of Michigan, rodewing@umich.edu)*

Mineralogy has had only a limited impact on present nuclear waste disposal strategies. This is due to the emphasis in performance and safety assessments on "geologic isolation", rather than any significant reliance on "immobilization" or "containment" by durable materials, specifically designed for particular waste streams and defined geologic environments. However, highly durable ceramics can find unique applications in the immobilization and disposal of long-lived actinides, particularly the ^{239}Pu that results from the dismantling of nuclear materials. Radionuclides which are geochemically mobile, toxic, and fissile require special materials of high chemical and mechanical durability.

This presentation will review the areas in which mineralogy can contribute to the long-term isolation of actinide elements. The presentation will specifically discuss the considerations that are required for the design of materials for the immobilization of different waste streams. Critical to the design of the waste form are:

1) waste stream composition

2) processing technology

3) long-term chemical and mechanical durability

4) stability of alteration products

5) radiation-solid interactions.

Principal crystalline phases to be considered include: silicates (zircon and titanite), phosphates (monazite, apatite and sodium zirconium phosphate), oxides (zirconia, zirconolite, pyrochlore, and perovskite) and the UO_2 in spent nuclear fuel. Natural phases are used to evaluate long-term durability.

A specific example of how waste matrices can be designed for unique waste stream compositions (*e.g.* the immobilization of excess weapons plutonium in zircon and monazite) will be discussed. A powerful aspect of this approach is the use of natural phases to "confirm" projections of long-term behavior in a variety of geochemical environments.

Symposium 1. Mineral Deposits in Mafic and Ultramafic Rocks

MAGMATIC SULPHIDE DEPOSITS IN MAFIC AND ULTRAMAFIC ROCKS

Lesher C.M. *(Mineral Exploration Research Centre, Dept. of Earth Sciences, Laurentian Univ., lesher@nickel.laurentian.ca)*

Magmatic Fe-Ni-Cu-(PGE) sulphide deposits have been produced during all major phases of mafic-ultramafic magmatism on Earth. The mechanisms by which the magmas reached sulphide saturation and the mechanisms of ore emplacement are still poorly understood, but detailed geological, petrological, geochemical, and isotopic studies have shown that:

1) the magmas from which the ores segregated were derived by high degree partial melting of the mantle, but the composition of the source, the depth of melting, and the precise degree of partial melting were not critical;

2) all of the sulphides in the mantle were consumed during melting and the magmas remained undersaturated in sulphide during ascent and eruption;

3) the metals were derived (for the most part) from the host magmas, but the sulphur was derived from a mixture of crustal and mantle sources;

4) mineralized environments contain rocks exhibiting geochemical and isotopic evidence of local crustal contamination (*e.g.* LREE enrichment, Ta-Nb-Ti depletion, anomalous Sr-Nd-Pb-Os-S isotopic compositions) and local chalcophile element depletion (PGE>>Cu>Ni>Co), but the distribution of the contaminated and metal-depleted rocks varies from locality to locality depending on the environment of ore formation;

5) ore compositions vary with magma composition (degree of partial melting and/or fractional crystallization), sulphide/magma partition coefficients, the magma:sulphide mass ratio (R factor), and the degree of MSS fractionation.

Further work is required to improve our understanding of ore-forming fluid dynamic, thermodynamic, and chemical dynamic processes in these systems.

THERMOMECHANICAL EROSION BY KOMATIITES AND THE GENESIS OF NICKEL SULPHIDE DEPOSITS

Barnes S.J.[1], Hill R.E.T.[1], Kauahikaua J.[2], Dowling S.E.[1] and Perring C.S.[1] *([1]CSIRO Exploration and Mining, Australia. barnes.s@per.dem.csiro.au, [2]Hawaiian Volcano Observatory)*

The nickel sulphide deposits of the Archaean Yilgarn Block in Western Australia are associated with large komatiite flows. Type 1 deposits consist of basal accumulations of relatively high grade Fe-Ni sulphides at basal contacts of lava pathways. This contribution presents evidence for their origin by thermomechanical erosion and sulphide assimilation at the base of lava flows.

The Black Swan ultramafic complex near Kalgoorlie hosts Kambalda-style high grade linear nickel sulphide shoots. Massive sulphides contain abundant inclusions of felsic footwall lithologies, ranging from angular xenoliths through to totally molten and disaggregated plumes. Felsic ocelli, xenomelts and strongly contaminated geochemical signatures are widespread through the host flow complex. PGE signatures in ores record changing fluid dynamic conditions with time.

Partially digested xenoliths of distinctive footwall lithologies are seen in close association with ore in the Digger Rocks deposit in the Forrestania Greenstone Belt. Evidence for crustal contamination on regional scale is provided by a correlation between geochemical trends and substrate lithology. Komatiite sequences underlain by felsic volcanic rocks are characterised by Si and LREE enrichment, while those underlain by banded iron formation show Fe enrichment.

Thermal erosion at the base of basaltic lava flows has been observed in a lava tube draining the 1994 eruption of Kilauea. Lava was found to downcut a total of 5m into its basalt floor, an average rate of about 10cm per day, during steady laminar flow at low Reynolds numbers. There is therefore good reason to conclude that erosion beneath komatiite flows would have occurred vigorously during prolonged flow within lava tubes, and that this process generated Type 1 ores.

KEY FACTORS IN THE GENERATION OF ECONOMIC Ni-Cu-PGE SULPHIDE DEPOSITS: THE ROLE OF MAGMA GENERATION

Keays R.R., Burnham O.M. and Lesher C.M. *(Mineral Exploration Research Centre, Laurentian University)*

Economic Ni-Cu-PGE sulphide deposits are characterized by a number of features the recognition of which can provide powerful exploration guidelines. Because all economic Ni-Cu sulphide deposits are variably enriched in the PGE, which have extremely large sulphide/silicate melt partition coefficients, the primary requirement is that the ore-forming magmas must have been S-undersaturated (and hence PGE-bearing) when intruded to high crustal levels. The only magmas to satisfy this requirement are high MgO, high temperature partial melts such as komatiites and picrites produced by high degree partial melting. With the exception of boninites, such magmas are probably the products of mantle plumes and are hence associated with very voluminous quantities of tholeiitic magmas. Lower temperature, small degree partial melts such as MORB leave PGE-rich sulphides in the mantle and hence produce sulphides with low PGE contents. Another requirement is that the high-MgO magmas become S-saturated just prior to formation of immiscible magmatic sulphides and that these sulphides have high to very high R factor, the ratio of silicate magma to sulphides formed. S-saturation may be achieved by either mixing with a S-saturated magma, as in Merensky-style PGE-Ni-Cu sulphide deposits, or by assimilation of S-rich material, as in the case of Kambalda-style Ni-Cu-PGE deposits. The best mechanism to induce S-saturation and to achieve a high R factor is to thermally erode S-rich rocks, generate sulphide droplets and vigourously mix these with a large volume of silicate magma. To accomplish the latter, the magma must be high temperature and hence very energetic in order to thermally erode and assimilate S-rich material and to guarantee high R factors. Favourable magmas which have interacted with S-bearing crustal material can be recognized by features such as low chalcophile metal content, enrichment in the LREE, and high Th/Nb ratios.

Some of these principals will be illustrated with an example from the Cape Smith Fold Belt, Ungava, Quebec. Here, although both extrusive and intrusive ultramafic rocks were produced by co-magmatic S-undersaturated komatiitic basalt melts and both are associated with S-rich sediments, mineralization is only associated with the komatiitic basalt flows. The melts which formed the flows were apparently much more dynamic and voluminous than those which formed the sills

GEOLOGICAL AND GEOCHEMICAL RELATIONSHIPS IN THE BRECCIAS OF THE REID BROOK INTRUSIVE COMPLEX, LABRADOR: IMPLICATIONS FOR THE ORIGIN OF THE VOISEY'S BAY Ni-Cu-Co ORES

Lightfoot P.C. *(Inco Technical Services Ltd.)* and staff of Voisey's Bay Nickel Company and Inco Technical Services Ltd.

Geological and geochemical relationships in the 1.34 Ga Reid Brook Intrusive Complex, Labrador, provide information about the controls on the distribution of mineralization in the Voisey's Bay Deposit. The Complex consists of two troctolite-gabbro intrusions which are linked by a heavily mineralized sheet. The east-west trending sheet varies in attitude from 50° south-dipping in the west, through vertical on the Western Extension dyke, 60° north-dipping beneath the Ovoid Deposit, and 10-20° north dip along the northern margin at the base of the troctolite sheet which hosts the Eastern Deeps Deposit. The mineralization occurs as massive sulphide lenses and associated halos of disseminated mineralization which are spatially related to the troctolites and gabbros, but which locally cross-cut both dyke and country rocks. Breccias developed within the dyke and at the base of the Eastern Deeps intrusion contain fragments of country rock which appear to be derived dominantly from local Proterozoic-aged paragneisses. The breccias also contain xenoliths of gabbro, troctolite and melatroctolite. There is a close association between the breccias and zones of heavy mineralization, and these zones appear to plunge down the sheet from west to east. The geological relationships within the breccias indicate that they were formed after the solidification of the fine-grained marginal troctolitic rocks. The melatroctolite fragments have MgO=16-43wt.% and Cr=1000-6000 ppm; they are compositionally more mafic than most of the rocks of the Reid Brook Intrusion (typically 5-15 wt.% MgO), and tend to be displaced to higher Cr and MgO than the melatroctolites of the younger (1.314 Ga) Mushuau Igneous Complex (14-27 wt.% MgO; 200-700 ppm Cr). It is suggested that association of the sulphides and fragments within a distinct pulse of magma is consistent with emplacement of this fragment- and sulphide-laden magma from a deeper magma chamber, rather than in situ formation within the conduit system.

SULFIDE SEGREGATION IN FERROPICRITIC FLOWS AND INTRUSIONS OF THE PECHENGA COMPLEX, KOLA PENINSULA

Brügmann G.E. *(Max-Planck-Institut für Chemie, Mainz)*, Hanski E.J. *(Geol. Survey of Finland, Rovaniemi)*, Naldrett A.J. *(Dept. Geology, University Toronto)* and Smolkin V.F. *(Geol. Inst., Acad. of Science, Apatity)*

Ferropicritic rocks of the volcanic-sedimentary Pechenga Complex comprise massive flows, pillow lavas, tuffs and Ni-Cu-sulfide-bearing layered, differentiated flows and intrusions. Their ultramafic parental magmas have 15-17 wt.% MgO and are characterized by high FeO contents (>14 wt.%) and strong enrichment in incompatible elements.

Massive lavas and chilled margins from layered flows and intrusions contain <3-7 ppb Pd and Pt and >0.1-1.0 ppb Ir with very low Pd/Ir ratios of 5-11, which are typical for ultramafic magmas. The abundances of PGE correlate with each other and with chalcophile elements such as Cu and Ni, and indicate a compatible behavior during crystallization of the parental magma. Compared to the PGE-depleted central zones of differentiated flows (spinifex zone and clinopyroxene cumulate) the olivine cumulate zones at the base contain elevated PGE abundances up to 10 ppb Pd and Pt. A similar pattern is displayed in layered intrusions, such as the Kammikivi and Pilgujõrvi intrusions. The olivine cumulates at the base of these bodies contain massive and disseminated Ni-Cu-sulfides with up to 2 ppm Pd and Pt, but the PGE concentrations in the overlying clinopyroxene and gabbro cumulates are below detection limits.

These metal distribution patterns observed in samples representing liquid compositions and cumulates suggest that the parental magma was sulfide saturated and became depleted in these metals due to sulfide segregation during the emplacement. Modeling of the distribution of siderophile and chalcophile metals in sulfide-poor flows suggest that the sulfide-silicate partition coefficient increases in the order of Ni<Cu<Pt<Ir, which is consistent with experimental data. These calculations also estimate R-factors (silicate- sulfide mass ratio) of 10^3 to 10^6, which indicate the segregation of only a small amount of sulfide liquid. In contrast, the low PGE tenor in sulfide ores at the base of the intrusions is the result of a low R-factor. For example, it is calculated that the Ir content of the sulfide liquid ranged from 20-90 ppb, which implies an R-factor of about 100.

THE INFLUENCE OF ASSIMILATION AND COOLING RATE ON THE COMPOSITION OF MAGMATIC SULPHIDES: EXAMPLES FROM MUSKOX AND DULUTH.

Barnes S-J., and Theriault R.D. *(Sciences de la Terre, Universite du Quebec, Chicoutimi, Canada.)*

It has been known for some time that sulphides that form at the margins of intrusions have lower metal contents than those that are found further into the intrusions. This has been explained by suggesting that the sulphides closest to the margins collected metals from a smaller volume of silicate magma (low R-factor) than the sulphides further into the intrusion (high R-factor). The details of how this happens has been a little vague.

New trace element and S isotope data from the Muskox and Duluth sulphides indicate that there is an inverse relationship between the degree of country rock assimilation and the metal content of the ores *i.e.* the more country rock assimilation the lower the metal content of the sulphides. The closer the sulphides are to the contact the more evidence there is for country rock assimilation. The intimate relationship between degree of contamination and R-factor and distance from the contact suggests the following physical model to us. A primitive magma was emplaced into metasediments. The metasediments melted and mixed with the primitive magma provoking sulphide saturation.. This sedimentary derived melt contributed SiO_2, S, Sb and As to the mixed melt. The SiO_2 would have pushed the composition of the mixed melt towards norite. The more sedimentary melt that was present the more the mixed melt would resemble a norite. The sedimentary derived melt would also have had a lower temperature than the mantle derived melt. Thus, the more sedimentary melt that was present in the mixed melt the lower the temperature of the mixed melt. The lower the temperature of the mixed melt the less time available for the sulphides to collect metals from the mixed melt before solidification, *i.e.*, the more magma is contaminated the lower the R-factor.

METAMORPHIC SULPHIDES IN THE KOMATIITIC CUMULATES OF THE PROTEROZOIC PULJU GREENSTONE BELT, WESTERN LAPLAND, FINLAND

Papunen H. *(Turku University, Finland)*

The Pulju Greenstone Belt (PGB) is a part of a rift-related Paleoproterozoic volcanic-sedimentary sequence trending in NW-SE direction across Lapland in northern Finland and Norway. The belt evolved during a long period of time, c. 500 Ma, with initial phases of continental and shallow-marine volcanism, cratonic margin sedimentation and volcanism and recurrent submarine volcanism and sedimentation in opened rift basin. The regional metamorphism and rejuvenation of granitoids occurred at c. 1.9 Ga ago. Thin beds of intensely contaminated ultramafic komatiitic volcanics exist at the initial, intracratonic phase of the supracrustal evolution, and again higher up in the sequence during opening of the oceanic basin, where they overlie a sedimentary sequence composed of graphitic and sulphidic pelitic sediments (the Matarakoski Formation MF). This "Sattasvaara type" of ultramafic volcanism is about 2.05 Ga of age and had two major centres in the central Lapland.

Polyphase deformed sequence of PGB is a flat-lying relatively thin sheet above the rejuvenated Hetta granitoid complex.The main effect of the felsic intrusion has been a voluminous fluid activity during the main phase of regional metamorphism. The fluids have altered the ultramafic olivine cumulates to tremolite-chlorite rocks, chlorite schists and locally also to pyroxenites, depending on the regional metamorphic grade. The metamorphic tremolite-chlorite rocks are very similar to metamorphic equivalents of the A-zones of fractionated komatiitic flows and only trace element geochemistry is the indicator of their origin. The metamorphic fluids deliberated sulphur from underlying MF type sediments and precipitated sulphides in the ultramafics, where redox-conditions were suitable for the mineralization process. This secondary sulphide dissemination is abundant in the ultramafics, but as nickel was not remobilized in metamorphism, the sulphides are mainly iron sulphides and contain only up to 0.25 % Ni which was the tenor of Ni in primary magmatic olivine. Chemical compositions of metamorphic silicates and oxides reflect the deposition of metamorphic sulphides, the Ni tenor of olivine is only 200-300 ppm, metamorphic pyroxenes contain less than 100 ppm Ni and due to low oxidation state all the phases have low ferric to ferrous iron ratio, for example a metamorphic low-ferric chromite has evolved from chromiferous chlorite. The metamorphic sulphides have caused problems in sulphide exploration and primary magmatic sulphides can be recognized only by their high and constant Ni/S ratios in samples where sulphides are abundant.

MINERALOGY OF THE BUSHVELD UPPER CRITICAL ZONE INTERCUMULUS: GENETIC CONSIDERATIONS

Johan Z. *(BRGM, Orléans, France, z.johan@brgm.fr)*

The Upper Critical zone (UCZ) intercumulus was studied in the Union Section from UG-1 to Bastard reef. The Cl content of phlogopite varies cyclically, being the highest about half way between the chromitites or reefs and the lowest within these horizons; this indicates the presence of a fluid phase during the chromitite and reef deposition. Plagioclase contains inclusions of K-feldspar rimmed by celsian, Cl-rich apatite associated with loveringite, ilmenite and Nb-bearing rutile. Chromite included in plagioclase is Ti and V rich. Loveringite is commonly associated with baddeleyite. Chromitite horizons contain a phlogopite + rutile + loveringite + baddeleyite association filling chromite negative crystals, as well as sodium phlogopite and pargasitic amphibole. Zircons occur at quartz-clinopyroxene contacts. Base-metal sulphides (pyrrhotite, chalcopyrite, pentlandite) included in plagioclase show exsolution of Pt-Fe alloys, Pd-tellurides, and sperrylite. Cu-Zn and Pd-Ge alloys, galena and clausthalite are also observed associated with BMS.

Raman study reveals the presence of fluid with a variable CH_4/CO_2 ratio. The Pothole reef section is characterized by CH_4-rich fluid, whereas gas chromatography shows the highest CH_4 concentration (0.21-0.25 μm/g) at Merensky reef - the pyroxenites and chromitites of the UCZ only contain 0.04-0.10 μm/g. CO_2 concentration varies from 1.08 to 3.25 μm/g. Within Merensky reef, Cl- and REE-rich apatite has been altered by the late fluid into REE-poor, OH-rich apatite.

REE distribution in the UCZ rocks reveals the highest REE concentration at the top of Merensky reef. Furthermore, a remarkable cyclic variation is observed in Eu concentration, leading respectively to positive and negative Eu-anomalies. This behaviour which cannot be interpreted in terms of magmatic evolution reflects fO_2 variation in the fluid phase.

DECOUPLING OF NICKEL AND MAJOR ELEMENTS IN OLIVINE FROM THE BUSHVELD COMPLEX AND THE GREAT DYKE: A STUDY OF SULFIDE CONTROL

Wilson A.H., Dawson S. *(Geology Department, University of Natal, Durban, South Africa)* and Murahwi C.Z. *(Prospecting Ventures, Harare, Zimbabwe)*

Variations of nickel content in olivine as a result of competition with sulfide are important indicators of primary magmatic processes and are also used as an exploration tool. Details of the variation between nickel contents and major element compositions in olivine in large layered intrusions are for the most part lacking but sections of drill core through dunite sections from the Great Dyke and Bushveld Complex have allowed evaluation of such trends.

A section through the dunite/harzburgite units in the C3 Subunit of the Lower Critical Zone of the Bushveld Complex shows strong systematic variation for olivine compositions. A symmetrical distribution for compositions though the section indicates a magma mixing event which resulted in Mg# increasing upwards and ending in the formation of a chromitic layer. This is followed by fractionation with decreasing Mg#. Nickel in olivine shows a completely opposite trend with high Ni content corresponding to low Mg# and being controlled by the development of minor sulfide through the succession.

Olivine compositions through part of the dunite succession of the Great Dyke (Darwendale Subchamber) show highly systematic variations for Mg# (0.91 - 0.89) and also for Mn and Ni. Near the top of one cyclic unit the olivine NiO content decreases from 0.26% to 0.05% over less than 10 m corresponding to a zone where sulfide rises from 0.05 wt.% to 3.5 wt.%. However, Ni content in the whole rock follows that of olivine-Ni thereby indicating that sulfide was initially in competition with olivine and was enriched in Ni but was subsequently removed from the system. There is also evidence that olivine in this section of the Great Dyke has been depleted in Ni compared with general trends.

Olivine compositional trends from the Bushveld Complex and the Great Dyke are compared, together with small-scale variations which resulted from boundary layer effects in the magma chambers.

SIMS STUDY OF Pt IN THE NEW CALEDONIA OPHIOLITE

Cabri L.J. *(CANMET, Ottawa)*, Augé T. *(BRGM, Orléans)*, McMahon G. *(CANMET, Ottawa)* and Legendre O. *(BRGM, Orléans)*

In New Caledonia, an Upper Eocene ophiolite nappe covering some 40% of the territory consists of depleted mantle peridotites, locally covered by mafic and ultramafic cumulates. The mantle harzburgites in places show sulphide enrichment: total rock analyses of five such samples also show anomalous PGE concentrations, as do the sulphide concentrates. The sulphides formed relatively early in the host rocks since they occur included in pyroxenes and are also layered within the host rock. The paragenesis of the ore minerals varies between the different localities, although graphite is everywhere present. In the Yaté 1 locality, the ore minerals are heazlewoodite, pentlandite, awaruite, millerite and native copper. The host rocks contain dominant olivine, orthopyroxene, rare clinopyroxene and minor chromite, with serpentinization ranging from 20 to 60%.

Earlier studies to determine the PGE-carrier minerals by SEM-EDS were unsuccessful. However, SIMS depth profiles show that Pt is strongly enriched in awaruite, varying widely between grains, and ranging from 4 to 1210 ppm for 21 grains in one sample. In contrast, 11 pentlandite grains in the same sample do not exceed 10 ppm Pt. Ten of 12 heazlewoodite grains show no detectable Pt, and the Pt content of the other two grains is estimated to be very low (<1 ppm). SIMS ion images confirm that awaruite is a preferential host for Pt and also that the Pt concentration depends on the awaruite's composition in Fe, Cu, Ni and Co. SIMS ion images also show that awaruites, whether or not Pt-bearing, contain some Au, whereas heazlwoodites are Au-free.

In conclusion, we have determined that, where base-metal sulphides and alloys co-exist, Pt concentrates preferentially in the alloys. Variations in the Pt content of awaruite suggests a two-step crystallisation in a process yet to be elucidated. We can also conclude that the Pt enrichments found in some ore minerals account for the elevated PGE contents of the concentrates.

PGE IN HAWAIIAN BASALT: IMPLICATIONS FOR PGE MOBILITY IN VOLCANIC FLUIDS

Crocket J.H. *(School of Geography and Geology, McMaster University, crocketj@mcmail.cis.mcmaster.ca)*

Gold, Pd, Ir, Os and Pt were determined by radiochemical neutron activation in fresh and altered basalt, and fumarolic condensates from Kilauea volcano, Hawaii. The objective was to evaluate the mobility of these metals in basaltic rock in response to surficial hot water - rock reactions, and to evaluate transport properties as reflected in fumarolic condensates. Most of the samples were collected from outcrops of post-1970 flows of Kilauea. The hydrothermal alteration suites were taken from the Halemaumau and Mauna Ulu crater areas while the condensate material includes samples of native sulfur and sulfate-dominated minerals from Sulfur Bank and occurrences on the East Rift system.

The fresh, unaltered suite of 24 basalts average 0.38, 2.4 and 1.8 ppb Ir, Pd and Au respectively with coefficients of variation of 36, 43 and 32%. In the hydrothermally altered suite higher average metal contents of 0.75, 3.9 and 5.5 ppb were found for Ir, Pd and Au in a suite of 20 samples. The variation in metal content from sample to sample was much larger in the alteration suite with coefficients of variation ranging from 70 to 80%. Gold is higher in the alteration suite by a factor of 3 and may have been added in the alteration process. Palladium and Ir, although higher in the alteration suite, are present in similar proportions in both altered and fresh rocks. The differences may reflect volume changes in the rock resulting from hydrothermal alteration rather than addition of metals from fluids.

Condensate suites included two different types : native sulphur and suites with sulphate minerals as major constituents. Relative to fresh basalt, native sulphur has lower metal contents with average Ir, Pd and Au of 0.056, 1.0 and .74 ppb. The Pd/Ir ratio is 18 compared with 6 for fresh basalts. In contrast the sulphate rich suite (thenardite, alunogenite and ralstonite) is enriched in all metals, but especially Ir, compared to the fresh rocks. Individual samples, which occur as vesicle fillings in basalt, carry up to 26, 10 and 31 ppb of Ir, Pd and Au respectively. For Ir this represents 68 times the average Ir content of the fresh basalt suite. The presence of ralstonite, a fluorine-bearing mineral, suggests the possibility that halogen complexes may transport noble metals in Kilauea magmas.

METALLOGENY OF THE UNIQUE GULI CLINOPYROXENITE-DUNITE MASSIF (NORTHERN SIBERIA, RUSSIA)

Malitch K.N. *(Dept. of Petrology and Metallogeny, VNII Okeangeologiya, malitch@g-ocean.spb.su)*

Original data on the geology, mineralogy and geochemistry for the world's largest Guli clinopyroxenite-dunite Massif and associated gold-PGE placers were obtained in 1985-1995 as a result of a geological survey on a scale of 1:200 000, exploration and research. These data have made it possible to re-assess a metallogenic potential of the Maimecha-Kotui Province located in the northern part of the Siberian Craton.

The Guli ultramafic Massif possesses transitional features between platiniferous placer-forming clinopyroxenite-dunite massifs of the Urals, Aldan, Russian Far East, Alaska, British Columbia, East Australia, and Alpine-type dunite-harzburgite massifs of the Urals, Koryakia, Tasmania, New Caledonia and some other regions. The Guli Massif is similar to the former in the paragenetic association of rocks (dunites, chromitites, wehrlites and clinopyroxenites), and the significant PGE placer-forming potential (the first tens of tons of the useful component), and to the latter, by a considerable areal size of outcrops (hundreds of square kilometres) and metallogenic specialization for the infusible platinoids. Uniqueness of PGE placers derived from the Guli clinopyroxenite-dunite Massif sterms from the revealed platinum-group minerals (PGM) as well as by the considerable predicted resources of noble metals, and, in particular, osmium. These resources can be compared only with the commercial placer deposits of Witwatersrand in South Africa, with an enigmatic primary source.

The high ratio of uplift and considerable volume of mantle diapir which appeared to be a protholith for the Guli Massif provide the preservation of the primary PGM associations.

Symposium 1. Mineral Deposits in Mafic and Ultramafic Rocks

MINERALOGY OF Pt-Fe NATURAL ALLOYS OF THE ALUCHIN HORST, RUSSIAN FAR EAST: IMPLICATIONS FOR GENESIS

Gornostaev S.S. *(National Mining University, Dnepropetrovsk, Ukraine, ssg@apex.dp.ua)*

The nuggets of Pt-Fe natural alloys in the Aluchin horst, Russian Far East have been observed in placer deposits, spatially associated with areas of Late Jurassic sediments, containing the conglomerates of rocks which represent the Alaskan-type ultramafic complexes. The are also large Alpine-type ophiolitic (dunite-harzburgite) pluton of Permian or Triassic (?) age exposed in the area of platinum-bearing placers.

Pt-Fe natural alloys (native platinum and isoferroplatinum) contain numbers of inclusions of other platinum-group minerals (PGM), most of them are rhodium minerals or Rh-rich phases (Rh-content in wt.%): bowieite (two varieties; 35.6 - 39.7), kashinite (19.8 - 23.2), cuprorhodsite (three varieties; 24.15 - 37.0), hollingworthite (23.6 - 30.2), Rh-laurite (up to 3.86), prassoite (67.9 - 69.7), unnamed $(Pt,Rh,Pd,Ir)_{3.44}(Cu,Fe)_{0.69}As_{0.91}$ (16.8), unnamed $(Rh,Pd,Pt)_2As$ (32.14 - 34.0). The host minerals (Pt-Fe alloys) are also enriched by Rh-content (0.43 - 4.56).

The data on PGM and other minerals inclusions (magnetite, plagioclase) in Pt-Fe nuggets as well as compositions of chromian spinels from conglomerate boulders in Late Jurassic sediments support the hypothesis which suggest that the primary source rocks of Pt-Fe natural alloys in this area is an Alaskan-type ultramafic complexes and not the ophiolitic rocks. It shown, that Pt-Fe natural alloys migrate to alluvials indirectly within two stages: (1) disintegration of Alaskan-type plutons and formation of conglomerates of PGM-bearing rocks in Late Jurassic period; (2) disintegration of conglomerates of PGM-bearing Late Jurassic rocks in Quaternary period.

Fe-Ni EXCHANGE BETWEEN OLIVINE AND SULPHIDE MELT: IMPLICATIONS FOR MAGMATIC Ni-SULPHIDE DEPOSITS

Caciagli N. and Brenan J.M. *(Dept. of Geology, University of Toronto, brenan@zircon.geology.utoronto.ca)*

Ni-sulphide deposits hosted in mafic and ultramafic igneous rocks are generally considered to be the product of sulphide liquid immiscibility and segregation at magmatic conditions. A robust test of this hypothesis is the preserved Fe-Ni equilibrium between olivine and coexisting sulphide, expressed as: $FeS(liq) + Ni_2SiO_4(ol) = NiS(liq) + Fe_2SiO_4(ol)$, with an apparent equilibrium constant (Kd) equal to: (Fe/Ni)ol/(Fe/Ni)liq. Many experimentally derived Kd-values are in the range of 30-35, whereas values measured from natural samples are significantly lower, ranging from 2-20. However, no single data set exists that systematically documents the effect of T or composition on Kd at controlled fO_2 or fS_2. In order to assess these effects, and possibly account for the apparent discrepancy between the experimental and natural database, we have measured Kd at T ranging from 1200-1400°C, log fO_2 = -8.2 and log fS_2 = -2.1.

Samples consisted of a mixture of Fe-Ni-S powder + powdered San Carlos olivine ±a polished and oriented San Carlos olivine wafer. This material was contained in a crucible fabricated from a San Carlos olivine megacryst and equilibrated in a gas-mixing furnace at high T for 1 - 4.5 days. Control of fO_2 and fS_2 was achieved using $CO\text{-}CO_2\text{-}SO_2$ mixtures. Run products were analyzed by electron microprobe. Consistent with the approach to equilibrium are analyses that show resulting olivine grains which are both homogeneous and shifted in composition with respect to the starting material. Moreover, Kd values measured in experiments run for 1 and 3 days duration at 1300°C are essentially identical.

Kd-values measured thus far are found to be only weakly dependent on temperature. However, combining our data measured at 15 and 30 wt% Ni in the melt with that of Gaetani and Grove (*GCA* **61**, 1829-1846), reveals that, at constant fO_2, Kd values decrease linearly with the Ni content of the sulphide liquid. In contrast to the high Ni contents employed in many previous experimental studies (> 40wt%), the Ni contents of natural sulphide liquids are in the range of 3-15wt%. Thus, low Kd values in natural systems simply reflect the low nickel content of natural sulphide liquids. We conclude that Kd's from natural samples are indeed consistent with sulphide formation at magmatic conditions.

CHROME SPINELS ASSOCIATED WITH THE JINCHUAN AND NORIL'SK-TALNAKH Ni-Cu SULPHIDE DEPOSITS

Barnes S.J. *(CSIRO Exploration and Mining, Australia. barnes.s@per.dem.csiro.au)*, Tang Z. *(Gansu Bureau, China)* and Kunilov V. *(Noril'sk Kombinat, Russia)*

The Jinchuan intrusion in north-west China and the Noril'sk-Talnakh intrusions in Siberia host major concentrations of Ni-Cu sulphides. Cr-spinels in both intrusions show Fe^{3+} and TiO_2 enrichment trends, coupled with decreasing Mg#, attributable to extensive reaction between spinels and solidifying interstitial melt.

These trends are particularly clear in the Talnakh intrusion, which shows a continuous spectrum from chromite to Ti-rich magnetite, in some cases within a single sample, reflecting prolonged equilibration due to continuous magma flow-through within the intrusion. Noril'sk-Talnakh spinels are enriched in Fe^{3+} at a given Mg# compared with Jinchuan spinels and typical layered intrusions, possibly due to melt oxidation during evaporite assimilation. Mg-ilmenites in the Siberian intrusions reflect advanced trapped liquid equilibration coupled with buffering of Mg/Fe by cumulus olivine.

Jinchuan spinels show less advanced TiO_2 enrichment, as a consequence of entrapment of spinel within olivine. Spinels associated with sulphide ores show distinctive Al-rich Cr-magnetite compositions, attributable to oxidation of normal chromite during oxygen exsolution from the sulphide melt fraction.

Both Jinchuan and Noril'sk-Talnakh spinels are systematically depleted in Ni for a given Fe^{3+} content, and in Co at a given Mg/Fe^{2+}, relative to neighbouring unmineralised intrusions. Spinel-olivine pairs in the mineralised intrusions record somewhat lower blocking temperatures than in comparable barren intrusions, implying lower cooling rates due to prolonged magma flow-through.

The distinctive composition of ore-associated spinels suggests a possible application of chromites as resistate indicator minerals for Ni-Cu sulphide deposits.

MINERAL CHEMISTRY OF CHROMITES FROM PERIDOTITE BODIES ALONG THE RAGLAN HORIZON, CAPE SMITH BELT, NORTHERN QUEBEC.

Burnham O.M., McDonald A.M., Keays R.R. *(Mineral Exploration Research Centre, Dept. of Earth Science, Laurentian University)*

The Raglan horizon of the Cape Smith Fold Belt contains a number of Fe-Ni-Cu-(PGE) sulphide deposits associated with komatiitic peridotite lava channels and channelised gabbro/peridotite sheet flows at the base of the Chukotat Group komatiitic basalts. The ultramafic bodies are primarily composed of serpentinised orthocumulate peridotite and are characterised by 50-75% serpentine pseudomorphs after fine to medium-grained olivine surrounded by fresh to partially altered oikocrystic augite ± acicular tremolite and fine grained chlorite. In addition to variable amounts of disseminated Fe-Ni-Cu sulphides, almost all of the peridotites contain accessory (≤ 5%) fine to medium-grained, subhedral to euhedral chromite, either as inclusions within the serpentinised olivine or as disseminated intercumulus grains.

Most of the chromite grains are zoned and comprise a relatively homogenous Mg-chromite core towards a chromite or ferrichromite margin. Whereas the Cr/(Cr+Al) ratio exhibits little variation within the grains and is close to the range in komatiites *sensu stricto*, $Mg^{\#}$ decreases between the cores and rims, consistent with diffusion-controlled exchange between chromite and olivine during cooling. The cores of the majority of the chromites from the mineralised lava channels and channelised sheet flows exhibit low Fe^{3+} (<10 at%) and TiO_2 contents (<1 wt%) and are depleted in Ni relative to those from associated non-mineralised levee-facies sheet flows and the ultramafic portions of co-magmatic non-mineralised differentiated sills in the underlying Povungnituk Group sediments. Whereas the higher Fe^{3+} and Ti contents of the chromites from non-mineralised peridotites may be accounted for by the accumulation of chromite from more evolved magmas, the lower Ni contents of the chromites from the mineralised peridotites cannot result from differences in magma evolution and indicate that either a) the Ni contents of the chromites are controlled by crystal chemical effects (the high OSSE of Ni should lead to higher Ni contents in Fe^{3+}-rich spinels with inverse structures than Fe^{3+}-poor chromites with normal structures), b) the olivine+chromite cumulates of the mineralised ultramafic bodies crystallised from Ni-depleted magmas, or c) the chromite and intercumulus sulphide phase underwent post-magmatic re-equilibration, leading to the loss of Ni from the chromite.

THE MULTILAYERED GABBROIC COMPLEX OF THE MIRDITA OPHIOLITE NAPPE (NORTHERN ALBANIA): MINERAL CHEMISTRY AND GEOCHEMISTRY.

Cortesogno L., Gaggero L. and Jaho E. *(Department of Earth Sciences, University of Genoa, Italy, cortez@dister.unige.it, gaggero@dister.unige.it).*

The paired belts of Albanian ophiolitic sutures are characterized by two distinct stratigraphic and compositional signatures, MOR-type to the W and IAT to the E.

The western ophiolite shows some similarities with Western Tethyan ophiolites; however, detailed investigations on mineral and rock chemistry revealed that such layer 3 is the product of multiple intersection of i) early subcontinental (?) magmatic activity, ii) high grade granulitic metamorphism associated with lateral deplacement, iii) cumulus and fractionation of the major magma batch of melatroctolites, troctolites, norites, Ox-gabbros and Ox-diorites, iv) rare intrusions of IAT basalts at the bottom of gabbro sequence, v) emplacement of plagiogranites vi) basaltic MOR volcanism yielding a sheeted dike complex at the top of the gabbro, and pillow lavas, vii) amphibolite to subgreenschist facies seafloor alteration with zoneography in space and time.

The chemistry of igneous minerals in gabbros allows to infer pressures for the beginning of the crystallization slightly higher that in present-days slow spreading ridges (*e.g.* MAR). The modelization for the crystallization of gabbros suggest fractional crystallization within the cumulus sequence, and is consistent with field evidence.

Estimated P and T for the evolution in the subsolidus again indicates higher pressures than gabbros of the MARK area.

On the whole, igneous and metamorphic features, as well as the thickness and composition of the basaltic cover on gabbros, support that the western belt of Albanian ophiolites was a ridge of intermediate spreading rate.

ORIGIN OF RUTHENIUM, OSMIUM, IRIDIUM AND IRON OXIDES BY PROGRESSIVE DESOLFORATION AND OXIDATION OF LAURITE IN NURALI CHROMITITES (RUSSIA)

Garuti G., Zaccarini F. *(Dept. of Earth Sciences, Univ. of Modena, garutig@unimo.it)*, Cabella R. *(Dept. of Earth Sciences, University. of Genoa)* and Fershtater G. *(Inst. of Geology and Geochemistry, Ekaterinburg)*

The Nurali ultramafic complex, located in the southern Urals (Russia), is composed of mantle tectonite overlaid by dunite-wehrlite-gabbro sequence containing small chromitites. Serpentine, chlorite, zoisite, prehnite develop in the layered sequence as a consequence of post-magmatic hydrothermal or metamorphic event.

During the investigation by optical microscopy and EPMA of the Nurali chromitites both sulfides pertaining to laurite-erlichamanite serie and Ru-Os-Ir-Fe oxides were found.

In the ternary diagram Ru-Os-Ir both sulfides and oxides fall in the same compositional field indicating a possible origin of the oxides by a progressive desolforation and oxidation of laurite.

Conclusive support of this assumption is brought by the new discovery of several zoned grains consisting of a laurite core rimmed by an oxide. EPMA analyses reveals the presence of an intermediate zone composed of an Fe rich Ru-Os-Ir sulfides varying from XS to XS_{1-x} stoichiometry.

The observed alteration process of laurite involves progressive loss of S and gain of Fe and O, apparently without change in volume, since the external shape of the original laurite crystal is generally preserved. The replacement of laurite by Ru-Os-Ir-Fe oxides possibly take place under hydrothermal conditions at low pressure and temperature.

RE AND TRACE ELEMENTS BEHAVIOUR DURING THE SUBSOLIDUS EVOLUTION OF MARK AREA GABBROS.

Cortesogno L., Gaggero L. *(Department of Earth Sciences, University of Genoa, Italy, gaggero @dister.unige.it)* and Zanetti A. *(Department of Earth Sciences, University of Pavia, Italy, zanetti@crystal.unipv.it)*

The gabbroic rocks intruded in peridotites at the western wall of the Mid-Atlantic Ridge between 23° and 24°N, at the ridge-Kane transform intersection, display significant compositional and textural heterogeneity. Investigations following ODP Leg 153 showed that the intrusives emplaced as successive magma batches during the ascent of peridotites to the ocean floor and were affected by subsolidus re-equilibration through granulite, amphibolite, actinolite - oligoclase, and prehnite - actinolite facies. The concentrations of 21 trace elements (REE, HFSE, LILE) were determined by SIMS analyses on clinopyroxene, amphiboles and plagioclase in selected gabbros and Ox-gabbros. Cumulate clinopyroxene have LREE-depleted patterns ($La_N/Yb_N \sim 0.1$), with no or slight negative Eu anomaly. In all magmatic phases, REE abundances increase in more evolved rocks. In granulite and high-grade amphibolite assemblages, characterized by the early appearance of Ti-pargasite, trace-element concentrations and REE patterns largely reflect the magmatic signature; however, REE and Zr contents increase in neoblastic clinopyroxene. Green hornblende (amphibolite facies) has LREE-depleted patterns ($La_N/Yb_N \leq 0.2$), with large negative Eu and Sr anomaly; REE contents are variable, but can reach very high values (*e.g.* La_N=115). Ti and Zr decrease in hornblendes at decreasing metamorphic conditions; they are preferentially concentrated into neoblastic phases (*e.g.* titanites). Tremolite replacing olivine in greenschist facies, shows very low trace-element concentrations; REE contents increase from core to rim of olivine site (La_N/Yb_N =0.1 - 1.4), with positive Eu anomaly (Eu*/Eu up to 5.2). On the whole, the increasing fluid activity and the acceptance of REE in amphiboles, which correlate to the metamorphic grade, are important factors controlling the partitioning and mobility of trace elements.

DEVELOPMENT OF *IN-SITU* METHODS FOR THE ANALYSIS OF SUB-PPB LEVELS OF PGE IN SILICATES

Krestow J.S.A., Litherland A.E., Rucklidge J.C., Tomski I., Wilson G.C. and Kieser W.E. *(IsoTrace Laboratory, University of Toronto, Toronto, Ontario, Canada M5S 1A7, krestow @quartz.geology.utoronto.ca)*

Successful *in-situ* analysis of platinum group elements (PGE) in silicate minerals promises a new tool for petrogenetic modelling of the chemical evolution of mafic magmas, relevant to segregation of siderophile and chalcophile metals. However, applications to natural systems require minimum detection limits (MDLs) in the 10^{-12} to 10^{-9} (ppt-ppb) range. Routine methods for determining PGE in bulk samples have MDLs for the most often-analysed precious metals (Pt, Pd, Au) ~1-10 ppb. Two new methods, with prospects of MDLs at least as low as the ppt range for the best-suited elements, have been proposed; preliminary results are promising. The methods employ Accelerator Mass Spectrometry (AMS), previously used successfully for PGE determinations in sulphide, oxide and metal samples, to analyse non-conducting silicate matrices. The typical mode of AMS trace-element analysis, using Cs^+ sputtering, has yielded routine MDLs in ore minerals of 10 ppt to 5 ppb for most precious metals (up to 20-50 ppb for Os and Re, which form negative ions with great reluctance). In the new AMS techniques the usual positive (Cs^+) primary beam, which leads to charge build-up on the sample surface, is replaced by a negative primary beam which sputters the samples and generates positive secondary ions. The positive ions can often be (1) transformed into negative ions by charge changing in metal vapours for further analysis by conventional AMS, or (2) neutralized with high efficiency after focussing onto a tandem accelerator stripping canal where they can be readily re-ionized to positive ions and accelerated further for AMS analysis. The first method needs less development than the second but the latter holds promise for higher sensitivity in the future. Early tests with 25 keV C^- sputtering produced beams of 350 pA Al^+ from pyrophyllite. Feasibility tests were conducted on low-energy charge-changing of PGE secondary ions to negatives or neutrals. Initial tests on negative-ion sputtering and charge- changing with organic and alkali-metal vapour cells have been completed. Current experimental and theoretical data suggest that sub-ppb levels of PGE such as Pd will be detectable in mm-sized silicate mineral grains, opening an avenue of research previously limited mostly to specific cases of bulk analysis, *e.g.*, RNAA of Ir.

CONTRIBUTION TO THE MINERALOGY OF THE Os-Re PAIR: PHASE RELATIONS IN THE SYSTEM Re-Fe-S AT MAGMATIC TEMPERATURES

Makovicky M., Makovicky E., Karup-Møller S. and Rose-Hansen J. *(The Geological Institute, University of Copenhagen and The Institute for Geology and Geol. Engineering, The Technical University, Lyngby, Denmark, emilm@geo.geol.ku.dk)*

The increasing geochemical importance of the Os-Re pair led us to investigate their behaviour in the phase systems with Fe and S, relevant for their mantle and lower crust mineralogy and geochemistry.

The Fe-Re-S system contains at 1200°, 1100° and 1000° a series of Fe-Re alloys, the Fe-S based sulfide melts, below 1200°C the $Fe_{1-x}S$ solid solution, and the only rhenium sulfide found, ReS_2. There is a skewed gap between gamma(Fe,Re) and "Fe_3Re_2" and between "FeRe" and (Re,Fe) which recedes with decreasing temperature from 72 to 85 at.%Re. At 1200° and 1100°C these alloys coexist with a sulfide melt, at 1000°C only the first alloy pair does so. The melts contain no Re or only traces of it (below 0.15 at.%).

The association $Fe_{1-x}S$ (or melt)-ReS_2-alloy shows less than 1.5 at.% Fe in the alloy, maximum 0.6 at.% Fe in ReS_2 and 0.2 or less at.% Re in $Fe_{1-x}S$. The latter are the maximum Re contents in mss; at 1200°C the melts with about 51 at.%S have 0.3-0.4 at.% Re. The associations richest in S show lower solubilites.

The most characteristic feature of the Fe-Re-S system is the association of practically the entire spectrum of alloys with low-S Fe-S melts and/or $Fe_{1-x}S$ which contain only traces of Re even at 1200°C. The composition ranges of the central alloys are rather insensitive to temperature. ReS_2 associates with nearly Fe-free alloys and intermediate melt/mss. Solubility of Fe in ReS_2 is low, that of Re in $Fe_{1-x}S$ or in the sulfide melt is very low. For the majority of S fugacity values rhenium will accumulate in its alloys with Fe and will be depleted from sulfides (sulfide melts).

$D^{ol/liq}_{Ni}$ ON MADEIRA ISLAND ALKALINE LAVAS: THE INFLUENCE OF MAGMATIC COMPOSITION

Mata J. *(Centro de Geologia, University of Lisbon, Portugal, jmata@fc.ul.pt)*

Lavas from Madeira Island (North Atlantic; 32°N, 17°W) are alkaline and range in composition from basanites (and picrobasalts) to mugearites. In all lithotypes but mugearites, olivine is present as a *liquidus* phase having crystallized at temperatures ranging from 1360°C to 1135°C.

For 21 olivine/magma pairs considered as in equilibrium, based on $K_{DFe/Mg}$ values, the calculated D_{Ni} values range from 4.7 to 16.8, being inversely correlated with the MgO content of lavas and with the calculated olivine saturation temperatures.

However, the obtained correlation, D_{Ni}= (86.27/MgO) + 0.685, is clearly distinct from those proposed by Hart & Davis (1978) and Kinzler *et al.* (1990), which, for a given magma MgO content, overestimate the D_{Ni} values when applied to Madeira samples. Since these authors established their equations from experiments performed at temperatures not significantly different from those obtained for olivine crystallization on Madeira lavas, those differences can be explained essentially as a consequence of magma composition on Ni partition coeficients.

Indeed, starting materials used on those experiments were silica-saturated while Madeira lavas are usually ne-normative being, thus, representative of magmas with lower degrees of polimerization, a characteristic that we consider as having favoured the relatively lower Ni partion coefficient reported for olivines in Madeira lavas.

References

Hart S.R. & Davis K.E. (1978) - *Earth Planet. Sci. Lett.*, **40**: 203-219.

Kinzler R.J., Grove T.L. & Recca S.I. (1990) - *Geochim. Cosmochim. Acta*, **45**: 1255-1265.

UNUSUAL PGE MINERAL ASSOCIATIONS FROM PLACER DEPOSITS OF THE MAIMECHA-KOTUI PROVINCE (NOTHERN SIBERIA, RUSSIA)

Badanina I.Yu. and Malitch K.N. *(Dept. of Petrology and Metallogeny, VNII Oceangeologiya, malitch@g-ocean.spb.su)*

Our communication deals with first data on natural polycomponent solid solutions of the Ru-Os-Ir-Pt-Fe system which were discovered in the recent and Upper Quaternary alluvial sediments of the Ingaringda River. The latter is localized within the Guli clinopyroxenute-dunite massif of the Maimecha-Kotui Province, in the northern part of the Siberian Platform.

The new unusual polycomponent solid solutions of platinoids, (Ru,Pt,Os,Ir), (Pt,Ru,Os,Fe,Ir), (Pt,Ru,Os,Fe) and (Pt,Ru,Fe), form polymineral associations with other PGM, these associations having some characteristic morphological features. In particular, the ideally preserved hexagonal-tabular crystals of osmium minerals (according to the classification by Harris and Cabri, 1991) are localized between or within the half-rounded crystalline individuals represented by isoferropatinum, laurite (RuS_2), and the polycomponent solid solutions of the Ru-Os-Ir-Pt-Fe system. The latter are found as relicts of the unchanged primary proto-solution and as exsolution lamellae in isoferroplatinum. Saturated chemical formulae of these minerals may be represented correspondingly as $Pt_{.53}Ru_{.18}Fe_{.16}Os_{.09}Rh_{.04}Ir_{.03}Ni_{.01}$ and $Ru_{.32}Pt_{.25}Os_{.19}Ir_{.12}Fe_{.08}Rh_{.03}Ni_{0.01}$.

It is characteristic that polycomponent PGE solid solutions similar in composition were discovered (Feather, 1976) in the unique Witwatersrand placers, with enigmatic primary source.

Taking into account that platinum forms limited isomorphic mixtures with infusible PGE, the discovery of natural polycomponent solid solutins containing these elements indicates to stable conditions of generation of their ultramafic host substrata at significant mantle depths, characterized by increased P-T parameters. Thus, the polycomponent solid solutions of the Ru-Os-Ir-Pt-Fe system allow for determining their host ultramafic substrata as ore-producing systems of mantle genesis.

THE PETROGRAPHY AND PGE-Ni-Cu-Au ORE ASSEMBLAGE OF THE ROBY ZONE, LAC DES ILES MINE, NORTHWESTERN ONTARIO

Michaud M.J. *(SRK (Canada) Inc., mmichaud@srk.com)* and Kissin S.A. *(Dept. of Geology, Lakehead Univ.)*

The Archean Lac des Iles Complex is a mafic-ultramafic intrusive complex within granite gneiss terrain, northwestern Ontario. The Roby Zone deposit, located within the gabbroic portion of the complex, contains an estimated resource of 8.9 million tonnes grading 5.0 g/t Pd, 0.34 g/t Pt, 0.30 g/t Au, 0.1% Cu and 0.1% Ni. The northern portion of the Roby Zone is composed of a layered sequence of pristene, intrusive phases of leucogabbro, gabbro, clinopyroxenite and gabbronorite. The southern portion is composed of a very lithologically and texturally complex unit, termed heterolithic gabbro, that consists of numerous irregularly shaped and sized sections ranging in composition from anorthosite to pyroxenite. The various sections, which occur within a gabbroic matrix, are compositionally congruent with the northern layered sequence. The ore zone within the heterolithic gabbro is largely enclosed by sericitic, chloritic and talc alteration. PGMs in the layered sequence consist of fine grained disseminations and net-textured sulphides, including primarily chalcopyrite, pyrrhotite, pyrite and braggite. Sulphide minerals within the heterolithic gabbro consist of irregularly shaped blebs up to 1.0 cm. dia. and typically account for up to 5 vol.% of the rock. Braggite, kotulskite and vyskoskite are the dominant PGMs and occur within sulphide blebs and at the sulphide-silicate boundary. It is proposed that the heterolithic gabbro is the result of brecciation of the northern layered sequence possibly related to an explosive magmatic injection. Partial melting of the fragments during brecciation triggered liquid immisicibility between felsic and mafic magmas, resulting in the precipitation of PGE-Au-Cu-Ni sulphides. Deuteric fluids remobilized PGE-Au-Cu-Ni within the heterolithic gabbro and produced the observed alteration.

POROUS CRYSTALS AND GRAINS OF NATIVE OSMIUM, RUTHENIUM AND IRIDIUM FROM ALPINE-TYPE ULTRAMAFIC ROCKS

Rudashevsky N.S. and Rudashevsky V.N. *(St.Petersburg St. C. Mekhanobr-Analyt; Mineralogical Museum of Russian Academy of Science, Moscow; geolog@mail.nevalink.ru)*

Characteristic microporous structure was revealed in individual of crystals and grains of native osmium, ruthenium and iridium (over 100 samples, 0.3-3 mm in size) of placer deposits from some alpine-type rock complexes of Russia, located in the Koryak Highland (Ust-Belsky and Khatyrsky massifs), in Kamchatka (Ust-Kamchatsky massif), and in the Urals (in the Miass River Basin).

In crystals of osmium and ruthenium, the porous areas are mainly associated with apexes and edges. Pores are localized in the most permeable zones of PGM grains: on cleavage or joint planes. Micropores are circular or ovate-oblong in cross-section (in place they are typical microtubes: canals!). They are usually less than a micrometer in diameter, but separate pores can be as large as 10-20μm. The most porous are round grain of native osmium which are typical dissolution bodies, mineral "microsponges".

Revealed were contrasted variation in chemical composition of primary native mineral in the zones (1-10 μm) adjacent to pores: drastic depletion in Ru and, to a lesser degree, in Pt, Rh, in places, Os: (Ru,Os,Ir) → (Os,Ir) → (Ir,Os). Pores and canals inside grains of native platinoids can be hollow, partly or completely filled in various PGM (16 minerals in Ust-Belsky samples).

The porosity of grains of native osmium, ruthenium and iridium is the result of reactions of the "solid-gas" type (at temperatures not below 900° C neocrystallization in PGM pores, corresponding to conode $Pt_{0.6}Ir_{0.4}$ - $Pt_{0.4}Ir_{0.6}$). This is explained within the model of carbonil differentiation of primary native platinoid mineralization of alpine-type ultramafic rocks under the action of mantle fluid CO.

PLATINUM-GROUP ELEMENTS AND GOLD IN Cu-Ni MINERALIZED PERIDOTITE AT GABBRO AKAREM, EASTERN DESERT, EGYPT.

Sharara N.A.[1], Wilson G.C.[2] and Rucklidge J.C.[2], *([1]Department of Geology, University of Assiut, Assiut, Egypt; [2]IsoTrace Laboratory, University of Toronto, Toronto, Ontario, Canada M5S 1A7)*

The Akarem mafic-ultramafic complex is located at 24°01'N, 34°08'E, 130 km east of Aswan in the southern part of the Eastern Desert of Egypt. The late-Proterozoic complex includes an earlier, mostly layered, gabbroic phase and a later peridotite phase. The latter was emplaced in two successive stages with barren followed by mineralized (Cu-Ni sulphide -bearing) peridotites. The gabbroic rocks are largely gabbronorite, olivine gabbronorite, troctolite and hornblende gabbro. Unmineralized peridotite is lherzolite, while the mineralized peridotite is dunite and harzburgite. The rocks are highly serpentinized. The estimated mode of the mineralized peridotite includes ≤35% olivine, 15% serpentine, ≤3% plagioclase, 16% clinopyroxene, 4% orthopyroxene, 6% amphibole, ≤15% pyrrhotite, ≤3% pentlandite and 3% chalcopyrite. Sulphidic peridotite averages 0.716 wt.% Cu, 0.654 wt.% Ni, 0.045 wt.% Co and 6.033 wt.% S. An old resource estimate is ~700,000 tonnes. The primary sulphides are pyrrhotite, pentlandite, chalcopyrite and cubanite. These minerals exhibit disseminated, massive and net textures in the olivine-rich ultramafic cumulate host. Secondary minerals include violarite, pyrite, monoclinic pyrrhotite, magnetite, mackinawite and millerite.

Analyses of bulk rocks and selected coarse sulphide grains were made by a combination of NAA, ICP, EPM and AMS (Accelerator Mass Spectrometry) methods. *In-situ* Au levels measured by AMS are low: pyrrhotite contains 1.8-25 ppb, pentlandite 2.8-8.4 ppb and chalcopyrite 0.7-8.2 ppb. These values are much below bulk-rock levels (67-1080 ppb). Trace Pt (0.5-1.4 ppb) is detected in the sulphides, also far below bulk levels (31-326 ppb). Coarse pyrrhotite carries more Rh (20-120 ppb, mean 60 ppb) than bulk rock (mean 21 ppb) and other major sulphides. Ir is similar - other sulphides and bulk samples carry much less (a few ppb) than coarse pyrrhotite (30-100 ppb, mean 60 ppb). Granular magmatic pentlandite has the highest Pd contents, up to 1030 ppb. Mass balance calculations suggest that most Au and Pt probably form discrete grains of native Au and PGM. In contast, most Pd, Rh and Ir are present within Fe-Ni-Cu sulphides, probably incorporated in the lattice of their host(s). PGE distributions can be explained by fractional crystallization of mss from parental sulphide liquid.

ISOTOPE-GEOCHEMICAL CHARACTERISTICS OF THE PRIMARY MELTS FOR THE LUKKULAISVAARA MAFIC COMPLEX (NORTH KARELIA, RUSSIA).

Semenov S.V., Belyatsky B.V., Zilberstein A. and Semenov V.S. *(IPGG RAS, St.Petersburg, Russia, boris@BB1401.spb.edu)*

The Lukkulaisvaara intrusion was dated by U-Pb at 2442±1 Ma. It cuts rocks of the Archean granite-migmatite-gneissic basement and is disconformably overlain by Proterozoic metaeffusive rocks. The thickness of the layered intrusion does not exceed 4600 m. Its weight-average composition is comparable with magma of the marianite-boninite series. However, the solution of the problem whether this composition corresponds to parental magma has met some difficulties because of a multi-phase structure of the intrusion. It is quite possible that fine-grained gabbro-norite which forms large and small lenticular bodies whose fabric suggests rapid crystallization is associated with injections of fresh magma. Structures in which fine-micrograined rocks (FMGR) occur do not differ from "potholes" in morphology and the set of structure-forming rocks. Two geochemical types of fine-micrograined norite and gabbronorite are present: boninites and tholeiites. We consider both of them are mantle primary melts. They have high MgO contents and Mg# 0.73-0.83. REE patterns have subhorisontal shape with very slight LREE enrichment and do not exceed 8 chondrite norms for boninite and 3 - for tholeiite. Initial isotope characteristics: ε_{Nd}=+3.5±0.5 and I_{Sr} = 0.7015-0.7018 evidence depleted mantle source for these rocks without any significance of contamination or assimilation processes. The rocks of main layered series, at the same times, are characterized by negative ε_{Nd} values (-2.2±1.0) and more evolved values of I_{Sr} (0.7030±2).

Position of bodies of FMGR in the cross-section suggests that additional intrusions have taken place at the time when not less then 50% of melt in magma chamber had crystallized. Temperature of liquidus and densities of resident evolved residual melt and FMGR for dry conditions are: 1200°C and 2.70-2.74 g/cm³ for resident melt; 1460°C and 2.69-2.71 g/cm³ for boninites; 1280°C and 2.66-2.69 g/cm³ for tholeiites.

Symposium 2. Gems and Diamonds

GROWTH, MORPHOLOGY AND PERFECTION OF DIAMONDS

Sunagawa I. *(Yamanashi Inst. Gemmology and Jewellery Arts)*

External morphology, surface microtopography of crystal faces, spatial distribution of dislocations, chemical inhomogeneities in single crystals, and polycrystalline textures are the records of growth and/or post-growth histories of crystals. How and under what conditions a particular crystal grew may be deduced if these features can be visualized. In the talk, the following will be demonstrated, based on the available information on these features observed in macro- and micro- natural diamond crystals.

1) Natural diamond crystals grew in a silicate solution phase (magma). Eclogitic and ultramafic suites are assumed to be two different chemical environments.

2) The morphologies can be classified into single crystalline, poly-crystalline and combined types, and correlated to the differences and changes of driving force.

3) The {111} behaves as the only smooth interface on which spiral growth takes place, whereas the {100} always behaves as a rough interface in natural diamond crystallization. The {110} is an S face, and may appear both by growth and dissolution processes.

4) Some diamonds experienced drastic change in the driving force during their growth histories. Some early-formed micro- diamonds acted as seeds of macro-diamonds.

5) The growth rates fluctuated considerably even in single crystalline growth, which are responsible for chemical zoning.

6) Diamonds have experienced partial dissolution and plastic deformation during their post-growth histories.

THE MORPHOLOGY OF DIAMONDS: A STATUS REPORT

Fritsch E.[1], Moore M.[2] and Lasnier B.[1] *([1]Université de Nantes, France, and [2]Royal Holloway College, U.K.)*

Diamond morphology is extremely diverse. It provides information on the growth history of diamond crystals, and is of interest to a wide audience.

Simple observations of the outside shape of crystals have been complemented by X-ray topographs, which show the successive growth episodes and their morphology. Such studies have revealed three different basic growth morphologies for natural diamond: octahedral, cuboid and fibrous.

- Octahedral growth is the stable shape for most natural gem diamonds while they grow. However, perfect octahedra are rare. They grow in a solution by a spiral growth mechanism around a screw dislocation under very low supersaturation.

- Cuboid growth is not growth along cube faces, but along an undulating surface of mean orientation corresponding to a cube face (hence the name). A small portion of such crystals are gems. The cause of cuboid growth is not well understood, but cuboid diamonds have specific properties, such as a high hydrogen content and micron-size lenticular fractures. At the Jwaneng mine in Botswana, it leads to skeletal crystals.

- Fibrous growth forms opaque fibrous aggregates. The growth orientation of the fibers is the (111) direction, so it could be considered as a special variety of octahedral growth. It is due to a large supersaturation of carbon and/or the presence of numerous inclusions. It is never gem quality. However, it can overgrow gem diamonds to form "coated crystals" or "speculative rough".

All these basic growth morphologies of natural diamond can be combined and are often modified by dissolution, fracture, cleavage, deformation, preferred growth directions, the presence of twinning or inclusions. This results in a variety of shapes such as rounded dodecahedra or the rare tetrahedra.

In SYNTHETIC DIAMOND, other growth morphologies are present. In particular the true cube can play a major part in the morphology, with minor influence from the true dodecahedron and the trapezohedron. The method of production (high-pressure, high temperature or chemical vapor deposition) does not have a major influence.

CHEMICAL VAPOR DEPOSITION OF DIAMOND: SYNTHESIS IN PARTIAL VACUUMS

Butler J.E. *(Gas/Surface Dynamics Section, Code 6174 Chemistry Division, Naval Research Laboratory, Washington DC 20375)*

During the last 15 years the chemical vapor deposition (CVD) of diamond has grown from scientific skepticism through enthusiastic investigation to technological impact. CVD materials are currently in production for applications in cutting tools, thermal management of electronics, optical windows, photodetectors and radiation detectors. These materials can vary from black (Ballas like) to white (better than type IIa) with grain structures from nanometers to mm in size. Plates of CVD as large as 300 mm diameter and 1 mm thick have been fabricated. This talk will present an overview of the science behind the synthesis, and the range of materials which can be produced.

ULTRAVIOLET- VISIBLE-INFRARED ABSORPTION SPECTROSCOPY AND CATHODOLUMINESCENCE OF DIAMONDS: A STATUS REPORT

Fritsch E. *(Université de Nantes, France)* and Collins A.T. *(Kings College, London, United Kingdom)*

Spectroscopies and optical methods of all kinds have been very important tools in the study of the extraordinary properties of diamond as a material, a mineral and a gem. The last ten years have seen significant advances in ultraviolet (UV) - visible (Vis) - infrared (IR) absorption and cathodoluminescence (CL) spectroscopies. Several of these discoveries came from the renewed interest in diamond synthesis by high pressure-high temperature or chemical vapor deposition techniques.

Most of the UV-Vis-NIR absorption of diamond is due to color centers, some intrinsic, many related to nitrogen, most of unknown nature. Several absorptions have been discovered related to the presence of impurities less common than nitrogen in diamond, such as nickel, cobalt, silicon or unusually high amounts of hydrogen. Many of those are found in synthetic diamonds only. New absorptions responsible for color in diamond have been described (H- and Ni-related centers, "Caïman jaw" spectrum, "725 nm triplet"). Further research on relatively well-known color centers (GR1, H1b, H1c, H2, H3, H4, 595 nm line) have proved useful in separating untreated from treated colored diamonds.

Isotopic effects are possible to observe because of newly developed synthesis techniques enabling pure ^{12}C or pure ^{13}C diamond , as well as ^{15}N-doped diamonds to be produced. The spectra of such crystals show shifts in peak positions that help understand the nature of some absorptions of electronic or vibrational nature. Remarkably pure near-colorless synthetic diamonds recently produced make it possible to study the edge emission, rather than defects in the band gap.

Cathodoluminescence can be useful in two ways. First, the simple observation of the cathodoluminescence pattern can help separate natural from synthetic gem diamonds. Secondly, CL spectroscopy reveals a large number of emissions. Many found in the middle of the visible range in diamond thin films are not found in natural diamonds.

Symposium 2. Gems and Diamonds

DIAMONDS IN SPACE AND TIME (MEYER, 1989)

Haggerty S.E. *(Geosciences, Univ. of Massachusetts, Amherst, haggerty@eclogite.geo.umass.edu)*

Carbon is the fourth most abundant element in the solar system and four distinct settings are recognized for the primary formation of diamond. Meyer set the tone and these are some of the advances:

Presolar: Primitive chondritic meteorites have presolar (>4.5 Ga), nm-size diamonds in concentrations up to 1400 ppm. In association with SiC, and exotic WC, ZrC, and TiC, and based on unusual, non-solar elemental distributions and rare gas isotopic signatures, these diamonds are attributed to formation by carbon vapor deposition in the high-energy plasmas of supernovae explosions. Significantly, the carbon isotopic composition (CIC) of diamond = -32 to -38 ‰, which, given the setting, is clearly non- biological.

Impact: Ureilitic meteorites contain solar (4.5 Ga) diamond (CIC= -5 ‰) of planetismal impact origin. The characteristic polymorph is hexagonal lonsdaleite, which is also found in terrestrial impact craters, in sheets of impact melts (CIC= -16 to -22 ‰), and in diamonds (CIC= -25 ‰) in high Ir sediments at the K-T boundary.

Crustal: Micro-diamonds (1-100 μm), associated with coesite, are present in felsic gneisses in continental collision zones in Norway (375-420 Ma), Kazakhstan (520-530 Ma) and China (210-250 Ma). Peak metamorphism was ~2-4.5 GPa; mineral assemblages are regressed, and diamond and coesite preserved in garnet and zircon. Intraplate subduction to depths of ~120 km is possibly related to supercontinent assembly, and mega-terrain exhumation is thought to be buoyancy-driven. Carbon (CIC= -10 to -20‰) in diamond is of mantle origin, but some C may be biologically mediated.

Mantle: Macro-diamonds (1-4 ppm) in kimberlite and lamproite intrusions are globally distributed in stable cratons, typically >2 Ga in age. Diamond is xenolithic to these melt breccias, and the host rocks, based on assemblages and mineral inclusion chemistries, are dominated by harzburgite and eclogite; sulfide is the single most abundant inclusion in diamond, whereas calc-silicate and Lz inclusions are rare. Majorite in diamond is from the transition zone (410-660 km), and diamonds enclosing magnesiowustite + opx, or ferropericlase + wo + tetragonal garnet are from the lower mantle (>660 km). Model ages for Hz diamonds are >3 Ga; Lz diamonds are ~2 Ga; and Ecl diamonds are ~1 Ga. Carbon is primordial and CIC peaks at -5‰. Diamond precipitation is redox controlled by oxidation of CH_4 or reduction of CO_2 at >180 km. A partisan view is that diamonds are erupted in superplume events.

DIAMONDS IN THE TRANSITION ZONE AND LOWER MANTLE

Harris J.W. *(Dept. of Geology and Appl. Geology Univ. of Glasgow, UK)*, Harte B and Hutchison M.T. *(Dept. of Geology and Geophysics Univ. of Edinburgh, UK.)*

The information reported concerns a study of inclusions in diamonds recovered from an alluvial deposit at Sao Luiz (Brazil), where the diamonds are believed to be derived from kimberlites of Cretaceous age. Diamonds from the deeper zones within the Earth are recognised principally by the mineralogy and chemical compositions of syngenetic inclusions. In the transition zone, the compositions of majorites associated with clinopyroxenes indicate continuous diamond formation down to beyond 450km. The presence in diamonds of ferropericlases (fPer) coexisting with ($Mg,Fe,CaSiO_3$) type compositions, (presumed to be perovskite structured) are the expected minerals of lower mantle assemblages (>660km), as determined from experimental - theoretical work. The natural assemblages show the occurrence of Al-rich phases: a new tetragonal structured garnet type mineral, (pyr-alm ss); Al-rich pervoskite; and corundum.

Majorite inclusions are commonly composite, the garnet coexisting with smaller grains of clinopyroxene. Garnets are of normal-Si or high-Si types, with similar ranges in Ca-Mg-Fe. Associated clinopyroxenes (Di-Hd-Jd ss) are also not chemically distinct. Ion microprobe analyses show that high-Si garnets have positive correlations between the abundances of MREE, HREE,Y and Zr with Fe.

$Mg/(Mg+Fe^{2+})$ ratios of fPers range from 0.38 to 0.85. Blebs within fPer are magnesioferrites. MgSiPvks have up to 10 wt% Al_2O_3, CaSiPvks are virtually stoichiometric and the tetragonal garnet type mineral has an extremely low Ca content. REE compositions show low abundances for all phases except CaSiPvk, which is an REE sump.

Transition zone diamonds from Sao Luiz have bimodal $\delta^{13}C$ values ranging from -8 to -12 ‰. Nitrogen impurities are low (<100ppm), but are aggregated into the higher states. The lower mantle diamonds have carbon isotope values near -5‰ and generally contain no nitrogen.

The wide range in the Mg# number for fPer inclusions at Sao Luiz is unusual. The Fe-rich members, which invariably occur separately in diamond, may not be part of the general mineralogy associated with the upper/lower mantle boundary, but be derived from depths perhaps as great as the D" layer, the diamonds and fPers being brought to the 660km discontinuity entrained in convection cells.

FLUID INCLUSIONS IN DIAMONDS SUGGEST CRITICAL END-POINT FOR SOLIDUS OF PERIDOTITE-H_2O-CO_2 IN UPPER MANTLE

Wyllie P. J. *(Div. Geol. Planet. Sci., Cal. Inst. Technology)* and Ryabchikov I. D. *(Inst. Geol. Ore Deposits, USSR Acad. Sci.)*

Schrauder and Navon (1994) interpreted the trapped fluid compositions in a suite of Botswana diamonds in terms of fluids from which the diamonds grew. Inclusions in a single diamond define a single fluid composition. The range of inclusion compositions among diamonds show linear correlation between a carbonatitic end member (calcic dolomite), and a hydrous end member. These two compositions correspond to those expected in upper mantle peridotite, given CO_2 and H_2O and suitable redox conditions. Experiments confirm that the near-solidus liquid in peridotite-CO_2-H_2O deeper than about 65 km (at least to 200 km), is dolomitic (calcic) carbonatite. A vapor phase if present, either subsolidus or coexisting with a liquid, must be hydrous.

The high total solubilities of silicate components in vapors in several systems at high pressures suggest that a critical end-point could exist on the solidus for peridotite-CO_2-H_2O. At greater depths, there would be no phase boundary between vapors and liquids, and no solidus where melting begins. Homogeneous fluids coexist with peridotite, changing from aqueous at lower temperatures to carbonatitic at higher temperatures, with the main (nearly linear) composition change occurring within a narrow temperature interval. Within a small range of depths (with associated temperature variations), the complete range of fluid compositions could be present. Individual diamonds transported from a small mantle volume therefore could sample very different fluid compositions. The reported fluid compositions appear to fit diamond growth somewhat deeper than a critical end-point on the mantle solidus (depth not known).

THE IDENTIFICATION OF GEM DIAMONDS - NATURAL, TREATED, SYNTHETIC OR OTHERWISE

Shigley J.E. *(Gemological Institute of America (GIA), Carlsbad, California, jshigley@gia.edu)*

Jewelers are legally required to disclose the identity of gemstones at the time of sale, a task complicated by the availability of treated, synthetic, and imitation gem materials. One important goal of gemological research is to provide jewelers with practical gem identification criteria that use only basic, often portable, gem-testing equipment and practical identification techniques.

Some natural gem diamonds are treated to alter their color or clarity. Irradiation and/or annealing processes create a wide variety of colors that visually overlap the range of naturally occurring colors. Clarity is enhanced by filling open fractures with a high-refractive index glass to reduce their visibility, or by the laser drilling and bleaching of dark inclusions. To date, gem-quality synthetic diamonds have been seen in the jewelry trade only in very small numbers. Imitations like cubic zirconia (CZ), and now synthetic moissanite (SiC), are encountered more frequently.

These gem materials can be gemologically distinguished on the basis of visible features (inclusions, color zoning, and other growth characteristics), ultraviolet luminescence, and their visible and infrared absorption spectra. Imitations, because they are different materials from diamond, are distinctive in terms of physical properties such as specific gravity and refractive index, and in their chemical composition. Jewelers should utilize several features to identify a gemstone, and not rely on just one criterion.

Symposium 2. Gems and Diamonds

THE DIAMOND-SAPPHIRE-ZIRCON ASSOCIATION IN VICTORIA, AUSTRALIA

Birch W.D. *(Geology Department, Museum of Victoria, bbirch@mov.vic.gov.au)*

Alluvial diamonds have been found in localities across Victoria but in considerably lower concentrations than in other eastern Australian (especially New South Wales) fields. The sources of the diamonds are unknown, despite extensive exploration focussed on kimberlitic indicator minerals. Recently a subduction model has been developed for the formation of eastern Australian diamonds. This would allow for diamonds to crystallise during episodes of Palaeozoic subduction, at half the pressures associated with kimberlitic sources, and preserve them for transport to the surface during Tertiary volcanism. Corundum (including gem sapphires) which formed in different crustal environments, and zircons which crystallised in felsic intrusives, could be brought to the surface in the same volcanic episodes. This model ultimately provides an explanation for the close coincidence of the NSW diamond fields with commercial deposits of gem sapphires found in volcaniclastic deposits associated with Tertiary alkali basalt volcanism.

In Victoria, alluvial sapphires are more widespread than diamonds. They show the full range of habits and colours typical of the more extensive deposits in eastern Australia. They also show regional distinctions, and many exhibit magmatic resorption suggesting they are derived from nearby volcaniclastic deposits. Zircons in each alluvial field often show a range of ages, indicating mixed sources, but with the oldest age often coinciding with the known age of Tertiary basaltic lavas in the region. The relationship between diamond, sapphire and zircon in Victoria therefore tends to support a regional subduction-diamond model. While the kimberlitic model should not be abandoned in Victoria, sapphires and dated zircons should be considered as additional diamond 'indicators'.

RUBIES FROM VIETNAM

Dung P.T.[1,2], Häger T.[1], Quang V.X.[2] and Hofmeister W.[1] *([1]Dept. of Gemstone research, Univ.of Mainz, Germany, haeger@goofy.zdv.uni-mainz.de, [2]Inst. of Material Research, Hanoi, Vietnam)*

There are several deposits of rubies in Vietnam. The most important occurrences are located in the provinces Yen Bai and Nghe An. Both deposits are of great commercial interest, because of their excellent coloured and high quality rubies comparable to those from Mogok (Myanmar).

The deposits of the Yen Bai province are located 200 km north-west of Hanoi, 50 km west of the city of Yen Bai near the town Luc Yen. The genesis of rubies from the Luc Yen mining area may be related to the Ailao Shan-Red River shear zone (ASSR) as the major geological discontinuity in East Asia. The high grade metamorphic rocks (amphibolite facies) are combined with the emplacement of leucocratic melts with typical pegmatitic crystallisation products like topaz and tourmaline. Metasomatic processes with marbles obviously yield the formation of rubies.

Rubies from Doi Ty, Mo Coi, Khe Nga, Doi Nga and Doi Ca belonging to Quy Chau mining area (a city and a district of the province Nghe An), are related to granitic pegmatite introduced into mica-sillimanite-garnet schist.

The trace element contents of rubies from these two occurrences are determined with electron microprobe (wavelength dispersiv system). Rubies from the Quy Chau region show significant higher Ti-contents in solid solution, while those from Luc Yen have more rutile inclusions. Further common inclusions in rubies from Luc Yen are calcite-dolomite, zircon, apatite and tourmaline (all determined with the electron microprobe).

Additionally the trace element contents of the Vietnamese rubies are compared to those of different synthetic rubies (Chatham, Duros, flame fusion, flux-grown from Novosibirsk, Inamori, Kashan, Knischka, Lechleitner, Ramaura and Tairus).

GEM CORUNDUM ORIGINS FROM ERUPTIVE SOURCES

Sutherland F.L. *(Australian Museum, lins@amsg.austmus.gov.au)*

Sapphires and rubies of many colours come from alkali basaltic eruptives in various localities (Australia, S.E. Asia, China, Africa, Madagascar, Europe). Two distinctive suites appear, a dominant blue-green-yellow zoned suite and a fancy coloured sapphire-ruby suite. Some basalt fields produce both suites, showing magmatic corrosion.

Blue-green-yellow suite crystals range to 12cm. Primary mineral inclusions form feldspars, zircon, Fe-Ti oxides, Nb-Ta oxides, U-Th oxides and rare earth phosphates. Scarce corundum-bearing xenoliths contain similar, coarser minerals in syenitic associations. Fluid-inclusions of CO_2 and CO_2 with saline aqueous fluid and daughter minerals indicate corundum crystallization above 680°C. Secondary exsolutions of Fe and Ti oxides in corundum-bearing xenoliths indicate original crystallization around 900°C. Trace element contents are highest in Fe and Ti, with noticeable Ga (to 0.04 wt%) and Ga/Ti >1. Colour absorption spectra show Fe^{2+}/Fe^{3+} intervalence change transfer.

Various origins for this suite have been proposed, ranging from metamorphic crystallization in subducted Al-rich rocks to various magmatic scenarios. Models of direct crystallization from syenitic melts, include some favouring mantle origins. Using the MELTS program, corundum can be generated by residual crystallization at mantle TP from melts derived from amphibolized mantle xenoliths from sapphire-producing fields. Another model involves a hybrid magmatic origin between carbonatites and silica-rich rocks at mid-crustal levels. Detailed studies of corundum-basalt genesis in eastern Australia suggests repeated gem eruptions and an origin linked to migration of amphibolized lithosphere over mantle plume systems.

The fancy coloured sapphire-ruby suite show more limited primary mineral inclusions (Mg-rich spinel, sapphirine and rare fassaite pyroxene) which suggest a metamorphic origin. This is supported by trace element contents that typify metamorphic corundums. Cr and Fe dominate the deeper pink, purple and ruby range and Ga is distinctly low (<0.01 wt% Ga_2O_3, with Ga/Ti <1). Colour absorption spectra of blue sapphires show only minor $Fe^{2+}Fe^{3+}$ intervalence charge transfer. Spinel-sapphirine thermometry gives crystallization temperatures between 780° - 940°C. Mixed suites of magmatic and metamorphic corundums may be more prevalent than generally realized.

THE COLOUR AND ITS ORIGIN OF THE MINGXI SAPPHIRES IN FUJIAN, SOUTHEASTERN CHINA

Tang D. *(Dept.of Environ. & Resource, Univ of Fuzhou, Fujian, China, dptang@fzu.edu.cn)*

The Mingxi sapphires occur in the Tertiary basalts in the Mingxi area of Fujian Province, southeastern China. The color of the sapphires is dominantly greenish blue, but yellow, green and brown species are also found. The chromatic measurement indicates that the Mingxi sapphires have a stronger yellow tone and dichroism than the sapphires from Shandong, China. Microprobe analyses show the sapphire have high FeO and low TiO_2 with an average of 1.34 wt% and 0.07 wt%, respectively. No correlation between composition and colors has been found. UV-Vis spectroscopic studies reveal that all Mingxi sapphires have 377, 388 and 451nm absorption bands, in which 451nm band causes the yellow color. A 810nm band has been observed in the different color sapphires and its absorption varies with the species of sapphires. The stronger 810nm band is accompanied by a weak 510 nm band and produces the blue or green color, which is attributed to Fe^{2+}- Fe^{3+} intervalence change transfer. A 570nm band produces the blue color of the Mingxi sapphires. IR spectroscopic 3310, 3234 and 3188cm^{-1} band are found in the sapphires. The blue sapphires have a stronger 3310 cm^{-1} band and, therefore, a higher H content in the lattice, which are estimated based on Beer's law, than yellow ones. These provide evidence for the hypothesis that the blue color of Mingxi sapphires are produced by a H, Fe, Ti-containing defect cluster proposed by Moon *et al* (1994).

Symposium 2. Gems and Diamonds

INTERACTION OF TRACE ELEMENTS IN CORUNDUM

Häger T. *(Dept. of Gemstone Research, Univ.of Mainz, Germany, haeger@goofy.zdv.uni-mainz.de)*

Blue and yellow sapphires of different localities were heat-treated at 1850°C in a gas furnace with slightly oxidising atmosphere to destroy structurally bonded OH-groups (proved with IR-spectroscopy) and to develop the strongest possible colour. Afterwards the trace element contents (electron microprobe) and the absorption coefficients of the spin forbidden Fe^{3+} transition bands, the Fe^{2+}/Ti^{4+}- and Fe^{2+}/Fe^{3+}-charge transfer band (UV-VIS-NIR-microscope) were determined.

The transition at 25750 cm^{-1} shows a linear correlation between the Fe^{3+}-content and the respective absorption coefficient. The absorption bands at 30250, 29180, 26470 cm^{-1} due to Fe^{3+} show an exponential growth of the absorption coefficient with increasing Fe^{3+}-content. The Band at 22080 cm^{-1} does not show a unequivocal linear or exponential growth with increasing Fe^{3+} content.

No correlation between the Fe- and/or Ti-content and the absorption coefficient of the absorption bands due to Fe^{2+}/Ti^{4+}- or Fe^{2+}/Fe^{3+}-charge transfer were found. Also the statistical calculation of the Fe^{2+}/Ti^{4+}-cluster content and a complex cluster model have shown no relation to the absorption coefficients. If we calculate at first colourless $MgTiO_3$-clusters and afterwards with the remaining Ti- and Fe-content $FeTiO_3$-clusters, these (so called effective $FeTiO_3$-clusters) show a linear correlation to the absorption coefficient of the Fe^{2+}/Ti^{4+}-charge transfer band.

It should be noted, that all those yellow sapphires coloured by defect centres have shown an excess of Mg after calculating the colourless $MgTiO_3$-clusters. It was proved with flame-fusion grown sapphires, that in addition to the excess of Mg small amounts of Fe (about 50 atom mol ppm) are necessary to develop similar defect centres like the natural ones.

For the system Al^{3+}-$Fe^{2+/3+}$-Ti^{4+}-Mg^{2+} a complete graphical model of the interaction of trace elements with respect to causes of colour in corundum will be presented.

TRACE ELEMENT AND INCLUSION CHEMISTRY OF THE MONTANA ALLUVIAL SAPPHIRES

Garland M.I., Henderson GS and Wicks F.J. *(Dept. of Geology, Univ. of Toronto, garland@afm1,geology.utoronto.ca)*

Alluvial sapphires occur within several drainages over a large area in southwest Montana. Discovered by placer miners over 100 years ago, the origin and source of these sapphires is not known. Several deposits have been in almost continuous production since discovery, producing sapphires first as jewel bearings, then with the application of colour-enhancing heat-treatment, as coloured gemstones. This project was designed to extrapolate a possible source for the sapphires using their trace element and inclusion chemistry.

Gem corundum is formed by either crustal metamorphic processes or by a process in the vicinity of the crust-mantle boundary and brought to the surface via alkali basalt magmatism. Work on known sapphire (and ruby) deposits has indicated that corundum formed by crustal metamorphism has Ga contents up to 100 ppm while corundum associated with alkali basalts is characterized by Ga contents from 100 to around 300 ppm. The direct substitution of Ga for Al in the corundum structure reflects the Ga content of the source environment and therefore can be used as a discriminating trace element signature. The major difference in inclusion chemistry is the exclusive presence of Nb-Ta and U pyrochlore in the alkali basalt corundum.

The Montana alluvial sapphires are remarkable in their consistent Ga contents, between 40 and 60 ppm. This would indicate a crustal metamorphic source, based on the Ga contents of corundum from other deposits. Raman spectroscopy is being used to look at the chemistry of the inclusions in the sapphires. To date, no Nb-Ta minerals have been found, nor has Nb-Ta been indicated by the trace element chemistry, indicating a probable metamorphic origin.

COLOR AND CLARITY ENHANCEMENT OF COLORED GEMSTONES

Emmett J.L. and Douthit T.R. *(Crystal Chemistry)*

Altering the color and/or clarity of colored gemstones to enhance value dates back to antiquity. In modern times, post-mining gemstone enhancement is required for most mining projects to achieve economic viability. The sophistication and effectiveness of modern gemstone enhancement techniques has raised many ethical questions. Among gemstones routinely enhanced today are corundum (ruby and sapphire), quartz (citrine), beryl (aquamarine and emerald), tourmaline, and zoisite (tanzanite). The processing of these materials will be outlined. High temperature solid state defect chemistry provides the modern basis for enhancement process development. As an example, the specific application of these techniques to the development of heat treatment processes for corundum will be reviewed in detail. The techniques developed result in a very substantial increase in value of the processed gemstones.

DEVELOPMENT OF HEAT TREATMENT PROCESSING FOR THE SAPPHIRE OF ROCK CREEK, MONTANA

Emmett J.L. and Douthit T.R. *(Crystal Chemistry)*

Several major sapphire deposits in Montana have been known since their discovery prior to the turn of the century. One of these, the Rock Creek deposit near Philipsburg, Montana, was mined from the early 1900s through World War II to provide corundum for watch and instrument bearings. Hundreds of tons were recovered. The development of synthetic sapphire terminated mining. The success of heat treatment for enhancing the value of other sapphire deposits motivated an extensive study of heat treatment of Rock Creek sapphire. The methodology and results achieved are described in detail. The impact of heat treatment on the viability of mining the Rock Creek deposit for gem sapphire is discussed, and the heat treatment facility developed to support the mining operation is described.

Symposium 2. Gems and Diamonds

GEOLOGY AND EXPLORATION POTENTIAL OF GEM-BEARING PEGMATITES AT NURISTAN, AFGHANISTAN

Laurs B.M. *(Gemological Institute of America, Carlsbad, CA, blaurs@aol.com)*

Granitic pegmatites containing rare-metal (Li, Be, Ta, and Sn) mineralization are known from four plutonic belts in northeastern and central Afghanistan: Western Nuristan, Safed Khers, Helmand, and Western Badakhshan. Miarolitic pegmatites with gemstones (elbaite, kunzite, and beryl) are known only from the Western Nuristan belt in the Hindu Kush Mountains, at elevations ranging from 800 to 6,000 m. These pegmatites are spatially and genetically related to peraluminous Oligocene S-type biotite- and two-mica granites that are elongate NE-SW, parallel to the regional structure, but generally undeformed. The pegmatites are most commonly hosted by Mid-Cretaceous gabbro-diorite and Permian-Upper Triassic amphibolite-grade mica schists, and least commonly by Proterozoic high-grade gneisses. Individual pegmatite bodies range from tens of meters up to 2,000-5,000 m long, and 1-60 m thick. Structural types include steeply dipping dikes, subhorizontal to gently dipping dikes, and small lens shaped veins with moderate to steep dip.

Economically important gemstone deposits (*e.g.*, Nilaw-Kolum and Darre Pech) are mined from gently dipping, internally zoned, albitized microcline-schorl-muscovite-beryl pegmatites. Well-formed crystals occur in cavities (10 cm to 3 m in size) that are irregularly distributed within the pegmatite core, nearer to the hanging wall. The cavities contain microcline and quartz, commonly with albite (cleavelandite), kunzite, multicolored tourmaline, morganite, lepidolite, and numerous accessory minerals.

Exploration for gem-bearing pegmatites in Afghanistan should concentrate on areas known to contain Oligocene granitoids and/or rare-metal mineralization. Regional geologic mapping and reconnaissance sampling will be most effective when combined with remote sensing of this sparsely vegetated area.

UNUSUAL DIAMONDS FROM ARKHANGELSK KIMBERLITE PROVINCE

Garanin V.K. and Posukhova T.V. *(Dept. of Geology, Moscow State University, Russia, mineral@geol.msu.ru)*

The diamonds from the Pioneerskaya kimberlite pipe were studied. At the upper horizons were established usual diamond crystals: round rhombododehedral (>2mm), octahedral and combination O-D forms (0.5 - 1mm), which are typical for kimberlites.

At the depth were found unusual microcrystals (<0.1mm): hollow box skeletal round octahedron which irregular and incompletely filled by thin diamond plates, growing at the angle to the surface; tabular and cross-looked fragments of zone-sector crystals and the smooth licked grain in plating cover.

Such types of crystals are similar to diamonds from metamorphic rocks of the Kokchetav massif in Kazakhstan and therefore we propose the similarity between conditions of their genesis.

The experimental data show that such crystals are characterized by fibrous mechanism of growth, which takes place at unequilibrium conditions when temperature decreases. The result of such deviation from equilibrium may be spherical isometric forms of diamonds.

Skeletal growth of crystals is due to fast deposition of carbon, sharp increasing of saturation degree and high content of impurities. The impurities increase the speed of growth and make the diamond crystals defective and they acquire sector and zone-sector structure.

Fast saturation (cooling) of mineral solution is the cause of forming a great number of nuclei, that explains the very small size of diamond crystals and the wide-spreading occurrence of twins.

DIAMONDS OF THE WHITE SEA, TIMAN AND NORTH YAKUTIA: MORHPOLOGY, SPECTROSCOPY, ORIGIN

Bovkun A.V., Garanin V.K., Kudriavtseva G.P. and Possoukhova T.V. *(Geological Dep., Moscow State University, Russia, mineral@geol.msu.ru)*

Systematic morphological and spectroscopic research of representative collections has revealed features of diamond crystals from the north East-European (the White sea, Timan) and Siberian platforms. The main features of similarity of the diamond of those regions are a significant prevalence of rhombododecahedra and low content of octahedra at their appreciably small sizes. Distortions of the forms of crystals, traces of plastic deformation, wide distribution and variety of the sculptures of resorbtion on crystal surfaces should be also related to the common features. Spectroscopic of diamonds from these regions are also close. They, in overwhelming majority, belong to Ia- type. The similarity is marked in distribution of crystals as spectra, distinguished on features of presence of the own and impurity defects.

General geological attribute for these regions is the position on a board of platforms. The prevalence of the round rhombododecahedra can be explained by active influence of resorbtión during the transportation of diamonds in kimberlite melts. Octahedra sharply predominate in kimberlites of the central areas of platforms. The contradiction between availability of diamond placers and low contents of diamonds in Timan and Northern Yakutia kimberlites can be eliminated at the account of established vertical zoning of pipes. The diamondiferous "Pionerskaya" pipe (White Sea) is an example. In the tops predominate dodecahedra with mosaic-block relief and the size more than 0,5 mm, and at the depth of more than 500 m - microcrystals (<1 mm) of a corrosian diamond prevail. Picrochromite is distributed in a kimberlite groundmass on top sections, and on bottom ones - perovskite, titanomagnetite and zone grains of chromium spinels.

These features are explained by unequal solution of crystals in kimberlite melts, with varying chemical composition, thermodynamic conditions and time of crystallization. The bottom parts of kimberlite bodies, revealing at a modern erosion level sharply differed from the tops of pipes.

DIAMONDS FROM THE M.V.LOMONOSOV DEPOSIT (ARKHANGELSK DIAMONDIFEROUSE PROVINCE, RUSSIA)

Garanin V.K., Kudriavtseva G.P. and Possoukhova T.V. *(Geological Dep., Moscow State University, Russia, mineral@geol.msu.ru)*

M.V.Lomonosov deposit is the first hard rock diamond deposit in the Europe. The diamonds have unique morphological and physical properties. More than 50% of them have gem quality. The round rombododecahedra prevail. Then round tetrahexahedra follow. Octahedra are rare, but their shave in small classes (<1mm) is rather high. Cubic crystals are rare also. The diamonds have numerous sculptures and channels of corrosion. They have undergone an oxidizing solution at the final phases of crystallization under the mantle conditions. Several diamond generations (embryos, zoning, inclusions of "a diamond in a diamond" type) and traces of plastic deformation were established by a color cathodoluminescence method. It shows on complicated history of diamond formation in the mantle.

Most of the crystals, according to their absorption spectra, contains many nitrogen impurity's defects. The concentration of A-defects makes up (30-40) × 10^{19} cm^{-3}. The low concentration of A-defects was determined in microdiamonds. The content of IIa-type diamonds is low. N_2, CO_2 and H_2O (up 70%) are the main fluid inclusions. It is another proof that the crystallization of the diamonds was under the oxidizing conditions. The isotopic composition varies and the content of ^{13}C changes from -2.9 up to -22.2 ‰. It shows on different carbon sources. Chemical composition of the mineral inclusions indicates on peridotitic and eclogitic paragenesis of a diamond. There are no inclusions of sulfides, wustite and native iron.

Thus, the diamond crystallization of this deposit was long, with several stages and occurred under oxidizing conditions in the environment enriched by N_2, CO_2 and H_2O. The reductive low part of the mantle didnÆt take part in convergation of the mantle flow and didn't give the microdiamonds in association with native iron, troilite and wustite as embryos to the region of birth of diamond-bearing magmas at upper parts of the mantle.

MINERALOGY OF DIAMONDS FROM DEVONIAN PLACER ICHETJU, MIDDLE TIMANS, RUSSIA

Makeyev A.B., Bryanchaninova N.I., Dudar V.A., Shametyko V.G., Filippov V.N., Lutoev V.P. and Glukhov Yu.V. *(Institute of Geology Russ. Acad. of Sci., Syktyvkar, Terra-2 Ltd., Ukhta, Russia, rmin@geo.komi.ru)*

A complex Devonian placer Ichetju, where Terra-2 Ltd. conducts prospecting and exploration of useful components, is a diamond - gold - raremetal placer. More than 160 diamonds and several kilograms of gold have been extracted to date. Most of the diamonds average about 0.25-0.5 carats in weight. One 2-carat and ten 1-carat diamond crystals have been also found. A large portion of the diamonds is of jewelry quality. There are colour diamonds, yellowish, greenish, brown and black ones among them. The diamonds mainly display pseudotetrahexahedral, bow-facet habit, twins are abundant. Pseudo-octahedral, pseudotrigonalthreeoctahedral crystals and fragments are rarely found. A relatively fresh shape of the bow-facet crystals does not give the basis to assume a distant source of washaway. The diamonds are reminiscent of krasnovishersky ones (Uralian type). Timanian diamonds have been investigated for their morphologies, inclusions composition and physical properties (photoluminescence, X-ray luminescence, EPR spectra). The diamond edges' sculpture is variable: vicinals, etch pits, traces of plastic deformation, steps, marks of minerals-companions, diamond chips, edge deterioration, outputs of inclusions and cracks. The mineral inclusions diagnosed in the diamonds are: graphite, chrome spinellide, olivine, enstatite, anthophyllite, Nd-perovskite, ilmenite, TR alumo-sulfite-phosphate, a mineral of the djerfisherite type. The EPR and luminescence spectra indicated A, P1, P2 centres in the diamonds and permitted to calculate their concentrations. All these features testify two source areas for the diamonds - proximal and distal. The geological data suggest that terrigenous material was carried from the east. The diamond content in the Ichetju placer exceeds the one in Krasnovishersky (Uralian type) placers.

THE RAMAN MICROSPECTROSCOPY AND FLUORESCENCE OF EMERALDS FROM VARIOUS DEPOSITS

Moroz I.I. *(Institute of Earth Sciences, The Hebrew University of Jerusalem)* and Panczer G. *(Laboratoire de Physico-Chimie des Materiaux Luminescents, Université Claude Bernard-Lyon 1, France)*

Emeralds from nine gem-mining regions in Afghanistan, Brazil, Colombia, Nigeria, Russia, Tanzania, Zambia and a synthetic emerald were studied by non-destructive Raman microspectroscopy using Laser Raman microspectrometer DILOR XV at the Laboratoire de Physico-Chimie des Materiaux Luminescents, Université Claude Bernard-Lyon, which allowed simultaneous Raman and luminescence studies. Conventional luminescent techniques used to obtain luminescence of minerals are far from being perfect and are applicable only to a limited number of "luminescent" gems. Emerald is usually considered a "not luminescent" gem (Samsonov *et al.*, 1984; Smith, 1984). The technique intensity is significantly larger than the luminescence excited by conventional light sources and it can be induced practically in every mineral showing dielectric behaviour and containing dopant ions.

Descriptive comparative presentation of the vibrational single crystal Raman and luminescence spectra of emeralds of various deposits is given. The spectra were obtained for two different orientations of the incident and scatterred light polarizations with respect to the crystal.

The present investigation shows that Raman microspectrometry is quite sensitive to the crystal chemistry of emerald. The use of this method provides the possibility to define reference bands for more quantitative spectral analysis as a means of contributing to the fast identification of the gem, of synthetic analogues of natural emeralds.

It is evident that the efficiency of the method may be fully realized when a data bank of information on the Raman and luminescence spectra for gems is established.

MICROSTRUCTURAL COMPARISON BETWEEN NATURAL POLYCRYSTALLINE DIAMOND (CARBONADO) AND ARTIFICIALLY SINTERED POLYCRYSTALLINE DIAMOND

De S., Heaney P.J., Vicenzi E.P., Hargraves R.B. *(Department of Geosciences & PMI, Princeton University)*, Fei Y. *(Geophysical Laboratory, Carnegie Institution of Washington)* and Taylor P.T. *(NASA/ Goddard)*

Carbonado, found in alluvial deposits in Brazil and Central African Republic (CAR), occurs as black, irregularly shaped, polycrystalline diamond aggregates with exceptionally high porosities. Carbonado exhibits the extreme hardness and high thermal conductivity of single-crystal diamond but is less vulnerable to catastrophic cleavage. In the last two decades, scientists have offered many hypotheses to account for the origin of carbonado, including deep mantle subduction, irradiation of organic matter, and meteoritic impact. Using transmission electron microscopy (TEM), we have observed two kinds of defect structures in carbonado: 1) polygonalization networks that outline subgrains ranging from 1.0 to 10.0 mm in size; and 2) pervasive defect lamellae oriented roughly parallel to {111} with periodicities of 40 nm.

In an effort to reproduce the textures observed in natural carbonado, we have performed several sintering experiments using a multianvil press. Diamond powders of different grain sizes were sintered at high pressures ranging from 6-8 GPa and temperatures ranging from 1200°-1800°C. Examination of the first set of sintered materials by TEM revealed a range in the grain size from 1-7 mm. Dislocations were heterogeneously distributed in the form of tangles. Additionally, we observed a second set of microstructures that were very regular and periodic with a wavelength ranging from 15-40 nm. These defect lamellae appear to be very different from those in natural carbonado in that they were flat planar and often occurred in multiple sets parallel to {111}. Diffraction patterns of these areas confirm the diamond structure but show streaking along <111>* due to the planar disorder. HRTEM of the region across the defect lamella shows kinking of the lattice fringes, and in some areas amorphization has occurred at the defect boundaries. The comparison of the microstructures present in these artificially sintered diamonds with those of carbonado will help us constrain the temperature-pressure regime in which carbonado formed.

PHYLLOSILICATES INCLUSIONS IN EMERALDS FROM VARIOUS DEPOSITS

Moroz I.I. *(Institute of Earth Sciences, The Hebrew University of Jerusalem)* and Eliezri I.Z. *(Colgem EL 97 Ltd, Israel)*

Emerald is the most important gemstone of the beryl group. The commercial value of emeralds is affected by many factors, that include not only their colour and clarity, but also by their geological source - region. For the gemmologist the identification of inclusions in gems is of the utmost importance both for their authentification and for the determination of their geological origin (Dele-Dubois *et al.*, 1987).

Phyllosilicates (micas, scolite, talc, pyrophyllite and chlorite) are the most common mineral inclusions in studied emeralds; a rich diversity of these inclusions in emeralds from ten gem mining regions were chemically characterized by use of the electron microprobe JEOL JXA-8600 Superprobe at the Institute of Earth Sciences of the Hebrew University of Jerusalem.

The stone occurrences in Australia, Brazil, Mozambique, Russia, Tanzania (Lake Manyara) and Zambia belong to 'schist-type' deposits. We found micas, margarite, aluminiferous glauconite (scolite), talc, pyrophyllite, chlorite as inclusions in emeralds from these deposits. The results of the study allow us to distinguish even among the same mineral inclusions in emeralds from different deposits. For example, micas and talc inclusions differ in composition.

The specific geological settings for Colombian, Nigerian and some Tanzanian (specifically Sumbawanga) emerald deposits result in a unique suite of mineral inclusions in these emeralds (*e.g.* chlorine-rich scolite in Nigerian emerald, titanium-rich mica in emerald from Sumbawanga, aluminiferous talc in Colombian emerald being found).

The results of the study can be of great use in determining gem sources, distinguishing from synthetics and, more generally, in understanding conditions under which gems are formed.

Symposium 2. Gems and Diamonds

THE INFLUENCE OF MODULAR CRYSTAL STRUCTURES ON THE QUALITY OF CERTAIN GEMSTONES

Hofmeister W. *(Department of Gemstone Research, University of Mainz, Germany, hofmeis©goofy.zdv.uni-mainz.de)*

Certain unit cells of special mineral structures may be described as to be built of smaller symmetry related sub- or supergroup unit cells of chemically nearly identical subcells. These usually pseudosymmetric subcells (relativ to the larger unit cells) may therefore be defined as modules of modularily constructed structural families.

For the family of pyroxene-minerals some of these approaches are used to describe a relationship between clino- and orthopyroxene structures. The real power of the concept of modular structures is to be seen when interpreting certain properties of special minerals like topaz, prehnite, pumpellyite, zoisite-tanzanite or vesuvianite as examples that are not conform with their conventionally presumed crystal structures and crystal chemistry.

The modular crystal structure of prehnite, $Ca_2Al(Si_3AlO_{10})(OH)_2$, gives the background for a concept of group - subgroup related substructures, that is able to explain all those structurally nonconforming properties like piezo- /pyroelectricity, cation-ordering and optical anomalies. Basing on this structural proof, all those hitherto unexplicable properties of topaz, $Al_2SiO_4(F,OH)_2$, (strictly limited OH/F-replacement, optical anomalies, piezo-/pyroelectricity) are due to the pronounced modular crystal structure of the gem-mineral. As a further aspect, some of the different colours of topazes can be related to the actual crystal chemistry.

Another structural familiy is built by all the mono-disilicates like epidote-zoisite-pumpellyite, $Ca(Al,Fe)Al_2(SiO_4)(Si_2O_6/O/OH)$-$(O/OH)_2/(OH)$. All the chemical variations within this large mineral-group are due to the great structural variance basing on different symmetrical stacking of a single principle module. This ability prepares the mode in which the zoisite gem-mineral tanzanite gets its famous blue colour . The ability of the structural modul for chemical twinning with the result of topologically different coordination polyhedra enables the crystals of tanzanite to incorporate special colouring cations

POTENTIALITY OF ANDHRA PRADESH GEM RESOURCES

Kasipathi C. *(Dept. of Geology, Andhra University, India)* and Rao A.B. *(Dept. of Mineral Resources, University of Brasilia)*

Gemstones are coveted due their rarity and value, and qualities like colour, beauty, brilliance, and durability are their attracting factors. India has the historical record both in gem production and industry. With the exception of diamond, ruby corundum, chrysoberyl, alexandrite and cats eye, besides topaz, tourmaline, amethyst, moonstone, garnet and zircon occur in parts of Khammam, East Godavari and Visakhapatnam Districts in the Andhra Pradesh State.

Geological Conditioning Eastern Ghats are known to extend from Orissa to Tamilnadu through Andhra Pradesh in the East and to Kerala in the West. These hills are constituted of granitic gneisses rich in alkalis, flanked by khondalites and charnockitic suites rich in aluminium, westward.

Alexandrite and chrysoberyl in the East Godavari and Visakhapatnam Districts are found in granitic (to charnockitic) pegmatites at the contact of mafic and khondalitic suite of Eastern Ghats. Ruby corundum in Khammam District is hosted by pegmatites at the contact of mafic/ultramafic suites, high-grade pelitic systems and nepheline syenites.

Mineralogy Mineralogically a variety of gems occurs in parts of Andhra Pradesh. Besides the mentioned species, varieties of quartz, agate, sapphire and kornerupine also are known.

Genesis Gems are mostly in pegmatites of granitic (quartz-K feldspar-mica-tourmaline), and also gabroic or alkaline nature. Nevertheless, their interception by /with mafics/ultramafics, vocano-sedimentaries and alkaline complexes, also could condition the generation of the principal gem minerals. The origin of the pegmatitic fluids and their stages of evolution from a high temperature magmatic intrusive to a late stage hydrothermal enrichment and related mineralisation, is evidenced. However, the gem evolution, in each case, needs to be systematised and not generalised. It is also important that a pegmatite growth in a consequence of slow crystallisation and the paragenetic association of the then prevailing chemical environment. Thus Be with high Al and Si produces aquamarines and emeralds, while Be with Al and scarce Si produces chrysoberyl and alexandrite. Production The Government of Andhra Pradesh has accorded leases for exploration and mining in the localities mentioned for semi-precious stones. Prospective areas for further development with improved mining methods can be assured with a systematic conceptual modelling both of exploration and exploitation of known gem deposits of the State.

FEATURES OF ESPINHAÇO DIAMONDS IN MINAS GERAIS, BRAZIL, AND THEIR ENIGMATIC SOURCE AREA

Karfunkel J., Chaves M.L.S.C. *(Dept. of Geology, Fed. Univ. of Belo Horizonte, Brazil, jokarfun@igc.ufmg.br)*, Banko G.A. *(Dept. of Mineralogy, Univ. of Vienna, Austria)* and Hoover D. *(Hoover Associates, Springfield MO.65803, USA)*

Prior to the findings of diamonds in S. Africa, Brazil (mainly the Minas Gerais State - MG) was the major supplier of the world's diamonds for 150 years. Although barren pipes are known from MG, primary sources for Espinhaço diamonds remain unknown and subject to controversy. Some advocate that diamond in metaconglomerates came from nearby sources, situated within the Espinhaço-Range, while others postulate the cratonic area in the west to be the primary source area. The time of pipe emplacement took place around or >1.75 Ga.

Statistics regarding physical properties of diamonds were conducted on diamond populations from the Espinhaço-Range. The results are: percentage of gem are extremely high; deposits have an average size of ±0.25 ct per stone; gemological characteristics are good; predominant crystal habit is the dodecahedron; percentage of broken stones is very low; bort is absent, and percentage of coated stones is high. These features are in concordance with a long geologic history. Espinhaço diamonds have been processed through a number of sedimentary cycles, starting in Middle Precambrian up to recent time. These led to spotty occurrence of the stones in MG over a region of 300,000 km², which are believed to be remnants of what earlier in time was a more dense distribution of diamond-bearing sediments.

The ability of diamond to withstand most surface processes is evident in the large size of Espinhaço fields and features of its stones, reflecting processes, from their release from pipes to dispersal to actual site, increasing the quality of diamond populations. An exception is the high percentage of coated stones, which originated in secondary deposits.

Present studies show effects of transport and reworking on diamonds during a long history from a distant area. The exact geographic site of the primary pipes, however, remains an enigma.

GEOLOGICAL AND EXPLORATION CHARACTERISTICS OF AN AQUAMARINE GEM PEGMATITE SUB-PROVINCE IN E.N.E. BRAZIL

Rao A.B. *(Dept. of Mineral Resources)* and Adusumilli M.S. *(Univ. of Brasilia, 70910-900 Brasilia. Brazil.bra@tba.com.br)*

Brazilian aquamarines are famous in the world. In ENE Brazil, in Borborema Pegmatite Province, pegmatites are : 1) Borborema Province Type (BPT). 2) Aquamarine Gem Pegmatite (AGP), and 3) Tourmaline Gem Pegmatite (TGP). AGPÆs are much different and simple (authors, 1993-1997) and during our investigations five detailed are aquamarine type, within an extension around 80 X 20 km forming an Aquamarine Sub-Province. Geologically they are enclosed in a degraded Neo-Proterozoic host system with a trend ENE-SSW, constituted mainly of biotite schists. The sequence is squeezed forming a set of fan-shaped syn- and anticlines, plunging towards S, and flanked by antiforms constituted of granitic orthogneisses.

Immediate host system is a compact biotite schist, occasionally feldspathised, locally deformed, fractured and faulted. Morphologically pegmatites don't show relief due to intense biotite schist degradation and denudation.

Pegmatites are granitic, K-Si rich, showing interdigestion with pods of vein/rose quartz, and bands of K-feldspar. Not zoned, and show medium granularity, sharp contacts with host system, frequent bulging and tapering, with dimensions like 100 X 10 X 50m. Substitutions by Na-feldspars and presence of Li- minerals both characteristic of BPT and TGP are absent. Alterations are very sporadic to absent and occasional kaolin and Mn hydroxides are noted as secondary products. Lateritic converings are not known. Mineralogy: Milky vein quartz dominates (60%) the pegmatite with sporadic but consistent rose quartz variety. Quartz veins and pods intercept coarse K- feldspar masses in veins or blocks (nearly 40%). Biotite flakes, occasionally as books, are studded in vein quartz. Schrol as acicular to radial aggregates develop on fracture surfaces of vein quartz. Sporadic yet not uncommon, red almandine granules develop along the contacts of the pegmatite and the host system. Economic minerals are aquamarine, rose quartz, beryl and K-feldspars.

Exploration guides are: 1) Pegmatites in low topographic terrain, degraded and enclosed in biotite schist host system; 2) Pegmatites partially zoned and poorly mineralised, mainly with quartz and feldspar veins; 3) Constant presence of rose quartz, biotite flakes and schrol needles; 4) Absence or very sporadic alterations; and 5) Growth of beryl in quartz zone, and gem variety mostly along the nucleus of the opaque beryl of the first generation.

Symposium 2. Gems and Diamonds

SYNTHETIC IRON-CONTAINING COLORED QUARTZ (AMETHYST, CITRINE, AND AMETRINE)

Lu T.J. *(Gemological Inst. of America(GIA), tlu@gia.edu)*, Balitsky V.S. *(Inst. of Experimental Mineralogy(IEM), RAS, balvlad@iem.ac.ru)*, Makhina I.B. *(IEM, RAS)*, Shigley J.E. *(GIA, jshigley@gia.edu)*, Rossman G.R. *(California Inst. of Technology, grr@juliet.caltech.edu)* and Dorogovin B.A. *(Russian Research Inst. for the Synthesis of Materials, ofi@vniisims.vladimir.su)*

Both natural and synthetic amethysts have been mass produced worldwide. Natural citrine and ametrine (amethyst-citrine) are relative rare, and most of the citrine available today is produced by heat treatment in the laboratory.

There are characteristic differences of morphology, twinning, inclusions, growth sectors and zoning, color bands, IR spectra, and trace element chemistry between natural and synthetic amethyst, citrine and ametrine. For example, synthetic amethyst grown from fluoride solutions exhibits stream-like structure, color bands parallel to the seed plates, IR spectra in a range of 3,000 - 3,700 cm^{-1}, and F and Li trace elements. Amethyst grown from alkaline solutions is characterized by specific growth sectors, color zonation, IR spectra, and pleochroism. It also has a higher color stability than either natural amethyst or synthetic material grown from fluoride solutions. A characteristic IR absorption peak at 3540 cm^{-1} existing in most synthetic amethysts. Its response to the effects of γ -ray irradiation, heat treatment, and crystallographic orientation will be presented and its gemological significance discussed. Also presented are the orientations of color bands, IR characteristics, and other features which distinguish synthetic ametrine from its natural counterparts.

Detailed comparison tables of gemological characteristics of natural and synthetic amethyst and ametrine will be presented and discussed.

STUDIES ON COPETON DIAMONDS, EAST AUSTRALIA

Milledge H.J., *(Dept of Geological Sciences, University College, London)*, Sutherland F.L. *(Dept. Mineralogy, Australian Museum)*, Kennewell P. *(Cluff Resources Pacific, Sydney)* and Meyer H.O.A. *(deceased)*

Nearly 200 diamonds from the New England gem fields, New South Wales, Australia have been studied to examine the origin of these unusual diamonds. Some 70% of the stones come from various Copeton mines, 25% from Bingara mines and 5% from other workings. New mining at Copeton is yielding further stones.

The diamonds are characterised by an unusual mineral inclusion suite (coesite, calcic garnet, calcic clinopyroxene), and relatively heavy carbon isotope ratios, but rare diamonds (Bingara) contain inclusions typical of eclogitic diamonds. The main suite contains two roughly equal proportioned varieties *viz* yellow, high nitrogen and white, low nitrogen diamonds, with nitrogen concentrations ranging from under 20 to over 2500ppm.

Many diamonds show roughly hemispherical depressions or substantial broad rough cracks, which contain minerals that reveal information about the origin and history of these diamonds. One coesite-bearing Copeton diamond contained scapolite, as a high pressure, CO_2,H_20 and sulphur-bearing phase, as well as ilmenite, rutile and SiO_2 in a deep gouge as fillings unexposed on the diamond surface. The diamonds exhibit fractures and cleavages, some of which are old (etched) and many have matt surfaces. Sharp octahedra are not abundant and many stones have relatively sharp edges approximating to dodecahedra. Others are smooth, well rounded crystals, confirming substantial resorption has taken place.

Infrared transmission spectra measurements and analyses on the diamonds were baselined using the automatic correction in the Optus software. Many spectra are of good quality, but off scale and these results are being further analysed.

The New England diamonds are presently the focus of several separate studies, which will help elucidate their enigmatic origin.

AGGREGATE IDPs: ORDER IN CHAOS BEFORE LOOKING AT NEBULAR AND PLANETARY PROCESSES

Rietmeijer F.J.M. *(Inst. of Meteoritics, Univ. of New Mexico)*, Nuth J.A. and Hallenbeck S.L. *(NASA Goddard Space Flight Center)*

Interplanetary dust particles (IDPs) include aggregates of sub-micron matrix units, Mg,Fe-silicates and Fe,Ni-sulfides that accreted in the solar nebula 4.5 Gyrs ago. The properties of matrix units that define a transition from presolar to solar nebula dust shed light on the nature of dust-forming processes. The sub-spherical units (0.1-0.5μm in diameter) include (i) ferromagnesiosilica material ± sulfur with a trace of Ni, (ii) magnesiosilica material with Fe,Ni-metal and -sulfide, and (iii) ferromagnesio-aluminosilica material ±Ca. The compositions of the units match serpentine dehydroxylate, $(Mg,Fe)_3Si_2O_7$, Fe/(Fe+Mg) (fe) = 0.3 - 0.8, and saponite dehydroxylate, $(Mg,Fe)_6Si_8O_{22}$ (fe = 0 - 0.3). The first two units contain Mg,Fe- pyroxene and -olivine, kamacite and pyrrhotite grains <50 nm in an amorphous matrix. The third unit has coarse-grained (10-410 nm) Mg,Fe-pyroxene, -olivine and amorphous Ca,Al-silica grains. Thermal alteration of IDPs occurs during flash heating (<15 s; 200-1100°C) on entry in the Earth's atmosphere. The silicates and iron oxides may be secondary phases due to *in situ* crystallization of amorphous units during flash heating or in a parent body 4.5 Gyrs to ~ 10^5 years ago. The dust in the Galaxy and solar system initially formed by vapor to solid condensation. We conducted condensation and thermal annealing experiments showing that the compositions of amorphous matrix units are predictable metastable equilibria defined by the metastable eutectics in the system MgO-'FeO'-SiO_2 ('FeO' denotes FeO and Fe_2O_3). The experiments and matrix units show a critical role of the oxygen fugacity on the FeO-Fe_2O_3/Fe_3O_4 buffers during condensation and subsequent thermal annealing. We have not (yet) found metallic iron in our samples. The experiments defined metastable "serpentine and smectite dehydroxylate mixing lines" that match compositions of the matrix unit in a Mg-Fe-Si (el. wt %) diagram. The results reveal much more order among the apparently chaotic mineral compositions in ultra-fine-grained aggregate IDPs and that does not necessarily require a planetary environment.

PRESERVED NEBULAR CONDENSATES IN A PRIMITIVE METEORITE

Zolensky M.E. *(SN2 NASA Johnson Space Center, Houston, TX 77058 USA, michael.e.zolensky1@jsc.nasa.gov)*, Weisberg M., Prinz M. *(American Museum of Natural History, New York, NY 10024 USA)* and Nakamura K. *(Lockheed-Martin ESS, Houston, TX 77058 USA)*

Ningqiang is a unique carbonaceous chondrite with similarities to the oxidized CV3s, but with somewhat lower refractory lithophile- element content and a higher carbon and H_2O abundance. We have been examining a large (5 mm) Ningqiang dark inclusion (DI) for which our previous work indicated a very primitive nature.

This Ningqiang DI appears to record the following early Solar System processes: (1) Formation (condensation and Fe-enrichment) of generally submicron-sized olivine and pyroxene crystals in the nebula. (2) Either irradiation, resulting in partial amorphization of the olivine and pyroxene to varying degrees, or partial melting at the edge of a turbulent nebula. We prefer the former explanation based upon the noble-gas composition. (3) Partial annealing resulting in fairly large, euhedral, olivine and pyroxene grains with remnant amorphous sharply-bounded rims. (4) In some cases prolonged annealing resulting in the microcrystalline rims; the latter annealing would have been a natural consequence of irradiation near the critical temperature for olivine. (5) Mixture of the above materials (lithology A) with nebular clinopyroxene and olivine, which escaped nebular processing to become lithology B. Admixture of apparently unrelated (?) aggregates of olivine, hedenbergite and kirschteinite, magnetite and pyrrhotite, as well as aggregates of calcium-aluminum rich minerals (called CAI).

SYNCHROTRON XRD STUDIES ON INTERPLANETARY DUST PARTICLES: L2005 AE6 AND L2005 AG17

Ohsumi K. *(Inst. of Materials Structure Science, KEK)* and Zolensky M.E. *(NASA/Johnson Space Center)*

Iron-nickel sulfides are the only phases present in all types of extraterrestrial materials. We have therefore initiated a comprehensive electron beam determination of the compositions and structures of carefully-selected of sulfides in chondritic materials.

1) Chondritic interplanetary dust particle L2005 AE6

The chemical formula of the sample is determined as $Fe_{0.89}Ni_{0.02}S$ analyzed with EPMA. The Laue pattern was obtained by 30 min. exposure at the BL-4B1 of the PF, KEK.

More than 40 Laue spots were recorded on the imaging plate. An important feature of the Laue pattern is that some satellite reflections accompanied with missing main spots are observed. This type of pyrrhotite is regarded as the NA type, and its c-axis is three times of that of the niccolite type subcell. The periodicity of the a-axis is estimated to be 41.84 times (N = 41.84) longer than that of the niccolite type FeS subcell. Observed Laue intensities excluding those of satellites agree well with the calculated ones based on the twinned 3C-pyrrhotite.

2) Chondritic interplanetary dust particle L2005 AG17

The chemical formula is determined as $Fe_{0.83}S$ by EPMA. Laue pattern was obtained by 15 min. exposure. Diffuse streaks are observed along the zone. In order to clarify the diffuse streaks, six oscillation patterns were also taken by monochromatic SR to cover 180°. Most of the diffuse diffractions peaks can be indexed based on the 3C-pyrrhotite. Four weak but distinct powder lines are also observed in all oscillation patterns; these lines correspond to those of magnetite (Fe_3O_4). This sample is thus revealed to be composed of 3C-pyrrhotite and magnetite.

TRACES OF PLANETARY SEGREGATION OF PARTIAL MELTS IN THE EARLIEST SOLAR SYSTEM

Takeda H. *(Research Institute, Chiba Institute of Technology, takeda@cc.it-chiba.ac.jp)*, Chikami J. and Miyamoto M. *(Mineral. Inst., Univ. of Tokyo)*

Mg-rich mafic silicates of lodranites/acapulcoites and winonaites/ IAB irons groups have been known as residues of partial melting, and iron meteorites as product of differentiation. However, basalts representing the solidified partial melt have not been too well characterized in the meteorite collections. We present here discovery of basaltic materials with Na-rich plagioclase and Cr-rich augite in iron meteorites, which are the products of partial melting.

We found Ca-Al-rich regions in a large slab of Caddo County (IAB). Two thin sections represent an area adjacent to metal, and consist of augite crystals ($Ca_{43.7}Mg_{54.1}Fe_{2.1}$, 30 vol. %) up to 1 mm in diameter surrounded by a much larger sodic plagioclase crystal ($Or_3Ab_{75}An_{21}$, 43 vol. %). Minor orthopyroxene ($Ca_{2.5}Mg_{90.1}Fe_{7.4}$) and olivine is often found to co-exist with augite. Such materials were also found in the Colomera IIE irons by Caltech group [1]. The most common were dominated by sodic plagioclase ($Or_{3.2}Ab_{91.4}An_{5.4}$ to $Or_{3.5}Ab_{96.1}An_{0.4}$), devitrified glass with similar composition, and Cr-diopside ($Ca_{44}Mg_{48}Fe_8$ to $Ca_{35}Mg_{42}Fe_{23}$). Minor minerals are orthopyroxene (Opx), chromite, troilite, Ca-phosphates, silica etc. One inclusion contained an Na-, Cr-,Ti-pyroxene (kosmochlor-diopside) and sodic plagioclase. Irregular K-feldspar and SiO_2 in Opx and Cr-Di occur around olivine nodules in a large surface inclusion[1].

Close association of the plagioclase-augite area with metal supports the formation model as partial melt. One thin section represents a recrystallized chondritic material and shows textural transition towards the plagioclase-augite assemblage. This assemblage can be interpreted as a region where all partial melts were segregated from the source regions by large difference in their surface energy and are collected and brought together with another Fe-Ni-S eutectic melt. The K-Si-rich melt is the lowest temperature eutectic melt in the quartz-$KAlSiO_4$ system. These products of partial melting are distinct from the eucrites.

Reference

1. Takeda H., Hsu W., Huss G. and Wasserburg G. J. (1998) *Lunar & Planet. Sci.* **29**

Symposium 3. Extraterrestrial Mineralogy

SYMPLECTIC INTERGROWTH OF AUGITE AND MAGNETITE IN OLIVINE FROM MARTIAN METEORITES

Mikouchi T., Miyamoto M., Yamada I. *(Mineral. Inst., Univ. of Tokyo, mikouchi@min.s.u-tokyo.ac.jp)*

Among the many interesting mineralogical properties of the Martian meteorites is that they contain minerals suggesting formation under oxidizing environments. The nakhlite Martian meteorites (Nakhla, Governador Valadares, and Lafayette) consist of cumulus augite and olivine in plagioclase-rich mesostasis. The nakhlites are considered to be a series of simple cumulate rocks having undergone various degrees of late-magmatic and subsolidus annealing. Nakhla is the least affected and Lafayette is nearly completely re-equilibrated. Governador Valadares is intermediate between the two, but more similar to Nakhla. Some Canadian Archean extrusive flow shows a remarkable match to nakhlites in petrography. Recently, we have found symplectic intergrowth of augite and magnetite in Nakhla and Governador Valadares olivines. Lafayette olivine does not contain such intergrowth, possibly because more extensive annealing erased the symplectites. The intergrowth in Nakhla and Governador Valadares olivines is usually lamellar form and perpendicular to (100) of the host olivine. Although the intergrowth texture of augite and magnetite is very complex, the (111) plane of magnetite is parallel to (100) of the host olivine. Such symplectic intergrowth of augite and magnetite in olivine is reported only from some terrestrial rocks and considered to be an exsolution product due to the presence of Fe^{3+} in olivine. Fe^{3+} in olivine causes exsolution from the host olivine to form such inclusions on cooling because ionic radius of Fe^{3+} is too small for the olivine structure at low temperature. The typical lamellar shape of symplectite might suggest a reaction involving an intermediate phase of Fe^{3+}-rich kirschsteinite lamellae and subsequently decomposed into augite and magnetite. Although similar intergrowth is reported from lunar rocks, the symplectites are composed of pyroxene and chromite, reflecting reducing conditions on Moon. The presence of the augite-magnetite symplectite in nakhlite Martian meteorites is consistent with the oxidizing formation environment of nakhlites based on the composition of magnetite-ulvöspinel compositions, and supports that Martian redox conditions more resemble terrestrial ones rather than lunar ones.

IMPACT CRATERING IN THE SOLAR SYSTEM: THE MINERALOGICAL ANGLE

Reimold W.U. *(Dept. of Geology, Univ. of the Witwatersrand, Johannesburg, S.Afr., 065wur@cosmos.wits.ac.za)*

The significant role that meteorite and comet impact cratering has played on all solid bodies throughout the evolution of the Solar System has been sufficiently demonstrated as the result of remote sensing investigations of the planetary bodies, as well as of hands-on mineralogical analysis of lunar and terrestrial rocks, and meteorites. The most vital of clues for the recognition of impact-generated and impact-deformed rocks, and, thus, of the presence of an impact structure or of impact ejecta is provided in the form of *shock metamorphic deformation* effects providing unequivocal evidence for ultra-high (>10 GPa) shock pressure deformation in upper crustal rocks. Comparison of shock experimental data for a broad range of rock-forming minerals with naturally deformed rocks not only established a series of shock metamorphic indicator effects (changes of physical properties with pressure; occurrence of shock fracturing, PFs, PDFs, diaplectic glasses, mosaicism, selective mineral or bulk rock melting), but also calibrated the respective shock pressure ranges for these effects. In recent years, detailed TEM studies have resolved the submicroscopic nature of some of these effects. In addition, petrographic analysis is a prerequisite for the understanding of impact breccia formation, recognition, and classification (in the latter case, the identification of impact or tectonic melt breccias represents a particular problem). Finally, chemical or chronological study of impactites is doomed to failure, unless they are preceeded by thorough petrographic studies. Verification of the existence of distal impact ejecta layers in the Archean rock record and detection of carrier phases of meteoritic trace element signatures rely on micro-petrographic and -chemical techniques. Detailed mineralogical studies are required for analysis of the thermal and hydrothermal effects of impact events, which especially in the case of large impact structures could have economic geological implications.

OLIVINE HYDRATION TEXTURES: COMPARISON OF EXTRATERRESTRIAL AQUEOUS ALTERATION IN CARBONACEOUS CHONDRITES WITH TERRESTRIAL WEATHERING AND SERPENTINIZATION

Velbel M.A. *(Dept. of Geological Sciences, Michigan State Univ., velbel@pilot.msu.edu)*

Phyllosilicates in CM2 carbonaceous chondrites are widely regarded as having formed by aqueous alteration of anhydrous precursor phases. Both partial and complete replacement of primary silicates by phyllosilicates in CM2 chondrites can be observed petrographically. Some masses of chondritic phyllosilicate are pseudomorphic (or alteromorphic) after primary coarse anhydrous constituents (chondrules, monocrystalline olivine). Some have outlines characteristic of the precursor (*e.g.*, pseudomorphic after euhedral olivine), and some exhibit uniform simultaneous optical extinction across the entire alteromorph. This suggests that hydration in these cases was controlled by anisotopy of the parent-mineral structure. Partially-replaced coarse primary olivine in CM2 chondrites occurs as olivine remnants surrounded by centripetally oriented phyllosilicate. This suggests a process in which the alteration product is developing at right angles to, and simultaneously on, each exposed face of the parent mineral, replacing it at a uniform rate. For the rate to be uniform on all exposed faces, such replacement must be isotropic.

CM2 chondrite alteration textures resemble terrestrial weathering textures of some silicate minerals. The uniform optical orientation shown by some meteoritic alteromorphs resembles terrestrial weathering of olivine; the centripetal crystallite orientation in partial alteromorphs resembles terrestrial weathering of garnet. Differences include the mineralogy of the phyllosilicate products (smectite in terrestrial weathering, serpentine in CM2 chondrites), and the widespread occurrence of dissolution etch pits on terrestrially weathered olivine.

Alteration textures of CM2 chondrites are strikingly similar to "meshwork" textures in partially serpentinized terrestrial mafic/ultramafic rocks. Serpentine-group minerals are the products, and etch pits are absent, from both chondritic and terrestrially serpentinized olivine. However, the temperature conditions inferred for hydrous alteration on the carbonaceous chondrite parent body overlap terrestrial weathering conditions, whereas most terrestrial serpentinites are believed to have formed at much higher temperatures.

THE PROTEROZOIC-PALEOZOIC, PALEOZOIC- MESOZOIC AND MESOZOIC-CENOZOIC BOUNDARIES ASSOCIATED WITH DIFFERENT COSMIC EVENTS

Detre Cs. H. and Don Gy. *(Cosmic Matter Res. Gr., Geol. Inst. Hungary, detre@mafi.hu)*

In the last ten years it became obvious that all great events of the history of the Earth are connected with different extraterrestrial influences. Major accepted types include **impacts**, increase in **cosmic radiation**, and massive infall of **cosmic dust** to the Earth surface.

These extraterrestrial effects produced spectacular extinctions in the living world, however, important prosperities also are observed.

This paper deals only with the Phanerozoic time, when the extraterrestrial influences have been reflected by the evolutionary dynamics of the living world.

The main geological changes (boundaries) connected with documented extraterrestrial influences are as follows:

Proterozoic-Paleozoic (Pc/Ca) boundary:

Suggested vast meteorite falls: very rich occurrences of Ni-Fe meteoroid spherules in the Himalaya and Siberia. In this case the connection with the prosperity of the biosphere is not clear. The latter may be caused by a rapid phase of decrease in H_2O on the Earth, produced by plate tectonic subductions: a "**sump effect**" whereby O_2-rich shelf regions were formed along the shorelines .

Paleozoic-Mesozoic (P/Tr) boundary:

The most dramatic extinction produced by a nearby supernova event. Accompanying world-wide phenomenon : anoxia.

Mesozoic-Cenozoic (K/T) boundary:

Impact "**drum-fire**" of previously-captured meteorite or comet cloud. Arguments: exponentially increasing occurrence of glassy impact spherules during the uppermost Cretaceous.

Symposium 3. Extraterrestrial Mineralogy

INTERPLANETARY STRATIGRAPHY OF THE SOLAR SYSTEM

Bérczi Sz.[1], Detre Cs.[2], Don Gy.[2], Dosztály L.[2], Gucsik A.[3], Kiss A.[4], Solt P.[2] *([1]Eötvös Univ, Dept. Petrology and Geochemistry, Cosmic Materials Res. Gr. H-1088 Budapest, Múzeum krt 4/a. Hungary. [2]Geological Inst. of Hungary, H-1143 Budapest, Stefánia út 14. Hungary. [3]Yamaguchi Univ., Dept. Chemistry and Earth Sci. Yoshida, Yamaguchi 753, Japan. [4]ATOMKI, Nuclear Res. Institute, H-4001 Debrecen, P.O.Box. 51. Hungary. berczi szani@ludens.elte.hu)*

The stratigraphy of the Moon was the first topics where both refreshment of principles and extension of classical tolls for correlation were important to develop[1,2]. Interplanetary correlation needs new ‚inclusions": spherules fulfills many requirements, they occur in lunar and terrestrial strata, and in meteorites as chondrules.

SPHERULE HORIZONS ON EARTH

Deep sea spherules were discovered in the last century, but spherules came to focus by their occurrence in lunar strata[3]. On the Moon they were of two different origin: impact and volcanic. The role of spherules in terrestrial stratigraphy formed during the last 3 decades (deep sea, tektite related types, Antarctic types, *etc.*). The IGCP 384 formulated the goal to use them as new tool for correlation. It is important goal of spherule horizons on Earth that they can be used even in Archaicum[4].

THE 5 MAIN SPHERULE TYPES

Common shape of spherules come the fact that they were once molten. But their composition and environment also contributed to their final form and composition. In our spherule stratigraphy overview the following basic types will be used:

- Refractory spherules from carbonaceous chondritic meteorites (Murchison, Allende, Kaba),
- Chondrules from stony meteorites,
- Spherules from Moon: a) impact (lunar samples and lunar meteorites), b) volcanic, (lun. soil),
- Terrestrial spherules with impact, cosmic, and other processes,
- Terrestrial industrial spherules.

References

1.Shoemaker E.M., Hackman R.J., Eggleton R.E. (1962) *Advances Astronaut. Sci.* **8**. 70-89.
2.Wilhelms D.E. (1987) *U.S.G.S. Prof. Paper* **1348**.
3.Lindsay J.F. (1976) Lunar Stratigraphy and Sedimentology
4.Simonson B.M., Beukes N.J., Hassler S. (1996) *LPSC* **28**, 1323.

MORPHOGENETIC EXAMINATION OF EXTRATERRESTRIAL AND TERRESTRIAL MICROSPHERULES IN HUNGARIAN SEDIMENTS BY SEM AND EDX METHODS

Kákay Szabó O. *(Hungarian Geological Institute, kakay@mafi.hu)*

Extraterrestrialá and terrestrial microspherules are to be found in sediments of differents ages and in placers. Based on their chemical composition, textural structure and morphogenetics different types of spherules can be identified by means of SEM and EDX study. The spherules reveal the process which created them.

I. EXTRATERRESTRIAL TYPES (size: 50-200 μm)

A. Blenddrops sprayed in the upper part of the atmosphere. These microspherules are those which result as blenddrops from the cold meteorites which were abruptly heated up in the atmosphere and then burst and disintegrated into their elements. They formed plastic blenddrops of iron and silicate, rich in gases, namely:

1. Glassy tektites (Si).
2. Magnetospherules (Fe).
3. Tektiteformation siderospherules (Si-Fe).

B. Blenddrops separated from heated meteorites in the lower layer of the atmosphere. The upheated blenddrop, as a result of the decrease of its caloric energy (CE), separates into droplets, the iron and silicate content of which depends on the quantity of their CE. CE is a function of the distance between the place of the separation from the meteorite and the Earth's surface. They are:

1. Perfectly disintegrated siderospherule (Fe-SiFe).
2. Non perfectly disintegrated siderospherule (Si-Fe).
3. Non disintegrated siderospherule (SiFe).

II.TERRESTRIAL TYPES (size: 300-400 μm)

Terrestric magnetopearls (Fe): These are formed in sediments of reductive environment by low temperature, slow and quiet crystallization of iron reach solutions in the sediment pores. They differ in their shape from extraterrestrial spherules.

Glassy tektites with high Ca contents from sediments of different ages have a similar morphogenesis and chemical composition, thus they were formed from the same material by the same genetic process. Strata enriched in microtektites signify major cosmic events. The appearance of magneto- and siderospherules is likewise of significant value concerning the type and measure of meteorite falls.

CRYSTALLOGRAPHIC AND MAGNETIC ORIENTATIONS OF MAGNETITE PARTICLES IN SHOCKED QUARTZ, VREDEFORT, SOUTH AFRICA

Cloete M., Hart R., Schmid H., Demanet C., Sankar V., Maré L. and Drury M. *(Council for Geoscience, S. Africa, mcloete@geoscience.org.za)*

Quartz grains in a gneiss from the centre of the Vredefort structure contains abundant planar deformation features (PDFs), phenomena generally considered diagnostic of meteorite impact. The PDFs locally contain ultra fine-grained microscopic magnetite, too fine to be positively identified by standard petrographic and secondary electron microscopic techniques. The well established techniques of transmission and scanning transmission microscopy were used to identify the micron-sized magnetite particles in terms of their microstructure and composition.

The magnetite particles in some rocks were found to be highly orientated in space, despite the orientations of the host quartz grains being different. Three quartz grains were investigated containing a sum of 22 magnetite particles. Two quartz grains each have special lattice orientation relationships with the magnetite particles whereas the other grain has no special orientation relationship, *i.e.* a low degree of lattice coincidence. One magnetite grain within amorphous silica also showed the same crystallographic orientation as the other magnetite particles.

Magnetic force imagery of the PDF-hosted magnetite particles show well defined arrays of magnetic signals set in a neutral background. Intensities of the signals vary with size of the magnetite particles. Magnetite particles >2μm have weak (low amplitude), complicated, maze-patterned signals whereas particles <2μm have high amplitude, concentric signals consisting of well defined attractive centres associated with slightly offset repulsive outer halo's. The magnetic and physical attributes of the magnetite particles satisfy theoretically predicted criteria of multi- and single domain (SD) magnetite. The consistent offset of the cores relative to outer halo's suggests a consistent plunge for the direction of magnetization of the SD particles. A uniform magnetization direction and crystallographic orientation of the magnetite, implies that magnetization occurred along a single crystallographic (easy) direction.

NEW IMPACT EVOLUTION MODEL OF FORMATION PROCESS AT THE END OF CRETACEOUS PERIOD

Miura Y., Fukuyama S., Okamoto M., Kobayashi H. and Gucsik A. *(Department of Earth Sciences, Yamaguchi University, Japan)*

Since the first report[1], there has been wide acceptance of the idea that the special features of the Cretaceous- Tertiary (K/T) boundary are explicable by the impact upon Earth of an iron meteorite ≈10 km in diameter. Evidence includes anomalous enrichments in Ir, shocked minerals including quartz, tektites and microtektites, stishovite, Ni-rich spinels and a range of platinum-group elements (PGE) found at K/T boundary sites worldwide. A large, buried impact crater at Chicxulub, Yucatan, Mexico is a plausible K/T impact site[2]. But anomalous distributions of shocked materials and spherules below and above the boundary are difficult to explain by a single impact[3-7]. Taken together, the Ir anomalies, shocked quartz, impact craters, spherules and calcite below and above the boundary are inconsistent with a single 10-km asteroid impact[1-9]. The varieties of spherules offer significant data in determining the exact nature of the impact at the boundary[7,9].

Spherules found in the northern hemisphere increased gradually ≈5 million years before the K/T boundary. Gradual increase of spherules after the boundary in the southern hemisphere was found in lowermost Paleocene (Danian) strata considered to be formed by tsunamis radiating out from the Yucatan[8]. Now, spherules are found also at the Permian-Triassic (P/T) boundary in many regions including Hungary[9]. A multi-step impact model from a terrestrial ring at the K/T event[7] cannot be applied to the P/T boundary, but a single sharp impact in the deep ocean can be postulated to explain anomalous spherules and terrestrial activity. Evidence suggests that progressive impacts began before the K/T boundary proper, and that small impacts, by ring fragments from a single asteroid orbiting the Earth, started ≈5 million years before the ≈65 Ma K/T boundary, and progressive impacts by small fragments persisted after the main boundary event.

References.

1. Alvarez, W.L. *et al.* (1980): *Sci.Am.* **263**, 78-84
2. Hildebrand, A.R. *et al.* (1991): *Geology* **19**, 867-871
3. Miura, Y. *et al.*, (1985): *ESR Dating and Dosimetry* **1**, 469-476
4. Miura, Y. (1989): *Meteoritics* **24**, 305; also **25**, 387
5. Miura, Y. (1991): *Shock Waves* **1**, 35-41
6. Miura, Y. *et al.* (1992): *Meteoritics* **27**, 261
7. Miura, Y. *et al.* (1997): *Proc. ISAS* **30** (in press)
8. Albertao, G.A. *et al.* (1994): Terra Nova **6**, 366-375
9. Detre, C. *et al.* (1997): *LPSC* **XXVIII**, 297-298

Symposium 3. Extraterrestrial Mineralogy

IRON-NICKEL SULFIDES IN CARBONACEOUS CHONDRITE MATRIX AND CHONDRULE RIMS

Di Valentin T. *(University of Ottawa)* and Zolensky M. *(Johnson Space Center, NASA)*

Iron-nickel sulfides are found in most solar system environments, including the most primitive extraterrestrial material, which is comprised of cometary and asteroidal particles. The most common Fe-Ni sulfides in chondrites are troilite (FeS), pyrrhotite ($Fe_{1-x}S$) and pentlandite $(Fe,Ni)_9S_8$. Troilite is believed to have resulted from sulfidation of metal (Fe-Ni) grains in an H_2S-containing environment. Pyrrhotite is produced when friable troilite grains, which are exfoliated from the metal nucleus, are submitted to continued sulfidation. Pentlandite is commonly formed during aqueous alteration. Each sulfide has its own particular determined stability conditions. What remains unclear is how these laboratory-determined conditions apply to actual environments in the early solar system.

The long-term objective of this research is to characterize sulfides in chondritic meteorites in order to better establish the conditions under which they formed, and the subsequent processes they experienced. Ultimately, by examining the precise chemical composition of the sulfides, it will be possible to infer whether the sulfides in the chondrites were formed in the solar nebula or on asteroids, and if formed on the asteroids, deduce how much alteration has occurred there.

Sulfides from four chondrites were analyzed during the course of this study. The sulfides were taken from chondrule rims and the matrix of the meteorite samples. The Fe, S and Ni atom percentages from the various analyses were plotted in triangular diagrams. The data for the two CM2 chondrites revealed that sulfides from the chondrule rims and the matrix have resembling compostions, suggesting that they were formed in similar conditions, probably on the asteroid. As for the CV3 chondrites, the matrix and chondrule rim sulfides have distinct compostions, suggesting that they are not directly related.

SELF-ORGANIZED CLUSTERS IN DILUTE ALLOPHANE SUSPENSIONS

Nakazawa H. *(National Institute for Research in Inorganic Materials, Japan, nakazawa@nirim.go.jp)*

Earth and planetary sciences are recently succeeding to draw the picture of the early abiotic Earth, an entirely inorganic world. The organic world was constructed after existence of the life. In between, there must be a transition period from inorganic to organic world where inorganic materials played a vital role in the formation of the life or they might even themselves play parts of life's functions as precursors. The origin of life problem is, therefore, a realistic subject opened especially for mineralogists.

Following the hypothesis of the upper-crust origin of life (Nakazawa *et al.*, 1993), the present investigation attempts to find possible mineral precursor of the individual in clay suspensions under possible conditions of the abiotic Earth.

Some "X-ray amorphous" clay minerals such as allophane and imogolite are known to have macromolecule nature and are reactive with greater affinity to organic molecules. Colloidal suspensions of such materials behave very similar to proteins when pH, temperature, concentration, dielectric constant are tend properly with the right choice of solvents and additives.

Dilute suspensions of allophane were used varying their concentration in the range from 0.3 to 0.01 % or less in weight. Allophanes were collected from Kitakami and Kanuma, Japan, and purified by previously reported processes. When once the pH of the suspensions was controlled by H_3PO_4 with/without a sluggish increase of ethanol concentration, spherical or even cell-like clusters in the order of 10 micrometer diameter range were often appeared. The cluster changed into crystals of hexagonal morphology similar to that of tarnakite-like mineral (Wada, 1958) after keep long for more than 1 year at room temperature. Formation and crystallization mechanisms of these clusters have not yet been made clear, but such self-organized clusters of allophane or its derivatives are very suggestive for the possible precursor of the individual being made entirely of inorganic macromolecules.

The concept that functions of inorganic precursors might have been taken over by organic ones in more elegant style is fairly well known (Bernal, 1953; Cains-Smith, 1982). The present results show that it may also be applicable for the origins of the individual.

A POSSIBLE GENESIS OF COSMIC DIAMOND; TRANSITION OF C_{60} FULLERENE TO DIAMOND

Hirai H. *(Inst. Geoscience, Univ. of Tsukuba, hirai@arsia.geo.tsukuba.ac.jp)* and Kondo K. *(Materials Structures Lab., Tokyo Inst. of Technology)*

C_{60} fullerene has recently become of major interest as the third form of carbon because of its wide variety of physical properties and practical applications. This substance was originally found during research in cosmic particles and interstellar media. A more plausible source of fullerenes is giant red stars which are continuously puffing out vast quantities of dusts, which are possibly rushing in space.

Shock compression can generate environments close to those caused by impact and collisions among cosmic media. In this work, shock compression experiments of C_{60} fullerene were carried out, applying rapid quenching technique under 8 to 55 GPa at 1000 to 3000 K by a single-stage powder gun. C_{60} fullerene transformed to diamond under rather lower pressure and temperature than graphite-based materials did, suggesting a unique transition mechanism. The diamond crystallites were a few nanometers to dozens of nanometers in size, depending on shock temperature and shock duration. The characteristic transition process from C_{60} fullerene to diamond was examined, exploring changes in structure and electron state by using electron diffractometry and electron energy-loss spectroscopy for the recovered samples. The experimental results suggested a possible genetic model for cosmic diamond formation; *i.e.* collision or impact among cosmic fullerenes rushing around in space.

OXYGEN ISOTOPE MEASUREMENTS ON COMPOUND CHONDRULE-CAI OBJECTS IN ALLENDE METEORITE

Maruyama S., Kim K., Sueno S. *(Inst. of Geoscience, Univ. of Tsukuba, sueno@arsia.geo.tsukuba.ac.jp)* and Yurimoto H. *(Earth & Planetary Science, Tokyo Inst. of Technology)*

Recently chondrule-CAI and CAI-CAI compound objects have been found in Allende meteorite. Study of these objects may clarify the genesis of chondrules and the relationship between CAI and chondrule. *In-situ* O isotopic measurements were carried out for (1) a chondrule which include spinel grains and (2) a compound CAI, using a Cameca 1270 SIMS with Cs^+ beam. The mass resolution power was set to ~6000 to resolve ^{17}O from the interference of ^{16}OH. Measurements were made by magnetic scanning through the following mass sequences; the tail of $^{16}O^-$, $^{16}O^-$, $^{17}O^-$, $^{16}OH^-$, and $^{18}O^-$. Data were corrected for the deadtime and the instrumental mass fractionation by utilizing a spinel standard.

(1) A chondrule, in which olivine and spinel grains are enclosed in the plagioclase assemblage, was selected from Allende. The oxygen isotopic compositions of the spinel grains are $\delta^{17}O_{SMOW}$ = -34.3±1.3 ‰, $\delta^{18}O_{SMOW}$ = -30.5±1.8 ‰ and are similar ^{16}O-excess to those of CAI spinels. The oxygen isotopic compositions of olivine are ($\delta^{17}O_{SMOW}$ = -12.5±1.3 ‰; $\delta^{18}O_{SMOW}$ = -11.8±1.4 ‰) and those for pyroxenes are essentially equal. This is the evidence that these spinel grains are the relict phase and the origin of the spinel may be directly related to CAI precursors or CAI itself according to the similarity of ^{16}O-enrichment.

(2) Oxygen isotopic measurements among mineral phases in a compound CAI from Allende were carried out. The CAI consists of three major parts, such as host part, inclusion 1 and inclusion 2. In previous reports on CAI, oxygen isotopes in spinel and fassaite exhibit excesses of ^{16}O, and those in melilite and anorthite are near the terrestrial fractionation line. However, melilite and anorthite in the host part in this CAI show ^{16}O excesses and those from melilite in the inclusion 1 show the compositions near the terrestrial fractionation line as previous observation. Those for the inclusion 2 are at the intermediate between the host and inclusion 1. Since all refractory phases in the host show oxygen isotopic anomaly, it can be suggested that CAI precursors of the host may havehad oxygen isotopic anomaly, at least during their melt stage. It is also considerable that oxygen isotopic compositions of melilite in the inclusion 1 and inclusion 2 may be resulted by the remelting of proto-CAIs such as the host.

2. Mineral Equilibria and Thermodynamics of Metamorphic Systems

EXPERIMENTAL REE DISTRIBUTIONS BETWEEN MONAZITE AND XENOTIME: A POTENTIAL FOR TEMPERATURE-CALIBRATED GEOCHRONOLOGY

Heinrich W. *(GeoForschungsZentrum Potsdam, whsati@gfz-potsdam.de)*

Solid solutions of the REE+Y orthophosphates monazite and xenotime were synthesized hydrothermally between 300°C and 800°C at 2 and 5 kbars using REE+Y-oxides and H_3PO_4 as starting materials. The REE bulk composition was similiar to those found in metapelitic rocks. All experiments produced two solid phases, monoclinic monazite and tetragonal xenotime, in volumetric ratios similiar to relative abundances in metapelites. REE concentrations of coexisting monazite-xenotime pairs were determined by EMP analysis, and REE distribution coefficients

$$D_{REE} = X_{REE}^{monazite}/X_{REE}^{xenotime}$$

were derived for the entire REE+Y suite. The values of D_{REE} depend strongly on ionic radii of the REEs and on temperature. The log D_{REE} versus ionic radius curve shows a nearly linear decrease from La to Lu and comprises almost five orders of magnitude from $D_{La} \approx 10^3$ to $D_{Lu} \approx 10^{-2}$. Between 450° and 800°C, most D_{REE} values vary continuously by a factor of about 2 to 3. D_{Nd} decreases from 48 to 16 and D_{Sm} from 9 to 5; D_{Tb} increases from about 0.2 to about 0.4, D_{Dy} from 0.1 to 0.2 and D_Y from 0.06 to 0.12 along this temperature range. Experimentally determined values of D_{REE} are in close agreement with those derived from natural monazite-xenotime pairs equilibrated between 400° and 700°C.

REE partitioning between monazite and xenotime is appropriate for geothermometry. The most useful application is that equilibrium and disequilibium partitioning of REE in metamorphic rocks are easily recognized. In the case of equilibrium distributions, U-Pb chronometry of single monazites or xenotimes provides a direct link to their growth conditions and information on temperature-time paths. Equilibrium distributions of Sm and Nd, expressed in molar fractions, result in

$$K_D=(X_{Sm}^{monazite}X_{Nd}^{xenotime}/(X_{Sm}^{xenotime}X_{Nd}^{monazite}) = 0.2 \text{ to } 0.3$$

from 600° to 800°C, and Sm-Nd chronometry should provide reasonable two-mineral isochrons for such monazite-xenotime pairs.

CLUSTER VARIATION APPROACH TO THE THERMODYNAMICS OF Al, Si ORDERING IN ALUMINOSILICATES

Vinograd V.L. and Putnis A. *(Institut für Mineralogie, Univ. Münster, Germany, vinogra@uni-muenster.de)*

The recent development of spectroscopic methods such as the ^{29}Si NMR has shown that most aluminosilicates have a strong degree of short-range Al,Si ordering (SRO). This suggests that the thermodynamics of Al,Si ordering in aluminosilicates should be described by models which can incorporate the spectroscopic information on SRO. The Bragg-Williams models, multisite-ideal (reciprocal-solution) models and Landau models which are traditionally used in mineralogy are not able to describe variable degrees of SRO simply because the SRO parameter does not appear in their free energy expressions.

The cluster variation method (CVM) has been designed for the problem of description of systems with SRO (Ising models). It would seem to be an ideal tool for the description of aluminosilicates, but so far it has had very few applications in mineralogy. The main problem which stops further development of the CVM is its mathematical complexity. To apply CVM successfully to aluminosilicate structures one has to be able to calculate probability distributions (PD) and functions of PD (entropies) for rather large clusters. The description of PD of large clusters requires many cluster-configuration variables and this is where the complexity appears. One has to perform minimization of the total CVM free energy with respect to a generally large number of parameters.

We have recently developed a mathematical technique which allows one to reduce significantly the number of cluster-configuration variables, and to simplify the derivation and evaluation of CVM models for complex aluminosilicate lattices. In our paper we will demonstrate that CVM models can be successfully applied to the description of SRO and LRO in layer silicates, feldspars and cordierite.

PARTITIONING OF Fe^{2+} AND Mg^{2+} BETWEEN OLIVINE AND CLINOPYROXENE: IMPLICATIONS FOR MIXING PROPERTIES OF $(Ca,Fe,Mg)_2SiO_4$ OLIVINES

Kawasaki T. *(Div. of Earth Sciences, Dept. of Bio-Geosphere Sci., Fac. of Sci., Ehime Univ., kawasaki@sci.ehime-u.ac.jp)*

The exchange reaction of Fe^{2+} and Mg^{2+} between olivine and clinopyroxene was experimentally determined at 1150°C and atmospheric pressure by varying the value of Ca/(Ca+Fe+Mg) in the system where the bulk ratio Fe/(Fe+Mg) was fixed at about 0.5 under controlling oxygen fugacity (WI buffer). The CaO contents of olivine seriously affect the Fe-Mg partition coefficient K_D $[=(X^{Cpx}_{Mg}\ X^{Ol}_{Fe})/(X^{Cpx}_{Fe}\ X^{Ol}_{Mg})]$, which increases with increasing X^{Ol}_{Ca}. I found the K_D as 1.89 for the assemblage of clinopyroxene and olivine with X^{Ol}_{Ca}=0.0152, in contrast to 2.93 for the Ca-enriched system coexisting with clinopyroxene, olivine with X^{Ol}_{Ca}=0.1362 and ferroan monticellite.

In order to explain the Ca-effect on the K_D, it is sufficient that mixing properties of $(Ca,Fe,Mg)_2SiO_4$ olivines can be approximated by the disordered multi-site regular solution model which is very similar to a symmetric regular solution model. Using the Fe-Mg mixing data of olivine and clinopyroxene, and the free energy change of the Fe-Mg exchange reaction by Kawasaki and Ito 1994, thermodynamic analyses of the present Fe-Mg partition data yielded as

$$W^{Ol,M2}_{MgCa} = 30.69 \pm 0.32 \text{ kJ/mol}$$

and

$$W^{Ol,M2}_{CaFe} = 23.23 \pm 0.45 \text{ kJ/mol.}$$

The present results are consistent with Davidson and Mukhopadhyay's 1984 analysis of miscibility gap in Ca-Fe-Mg olivines and the experimental data on the fayalite-kirschsteinite solvus (Mukhopadhyay and Lindsley 1983). The Ca-Mg mixing is slightly less non-ideal than the Adams and Bishop's 1985 results estimated from the forsterite-monticellite solvus.

THERMODYNAMICS OF IRON, SILICA, WUSTITE, PEROVSKITE AND IRON HYDRIDE AT LOWER MANTLE PRESSURES

Saxena K. *(Dept. of Earth Sciences, Uppsala University)*

The high pressure polymorphs of iron, silica and wustite and the phase perovskite are important phases in the lower mantle. Although experimental data are sparse, it is possible to obtain a fairly quantitative thermodynamic description of these phases which include the double hexagonal closest packed (DHCP) beta iron, the cubic, hexagonal and B8 phases of wustite and the high pressure silica phase (*Pnc*2). The latter phase data together with that of MgO must support the dissociation of $MgSiO_3$-perovskite between 70 and 80 GPa at moderate to high temperatures as indicated by the experimental data.

Until experiments become feasible on iron above 200 GPa, extrapolation of thermodynamic data on iron is necessary for the study of the core. The assessed data on iron is based on experimental data on a) melting to 200 GPa, b) the location of the triple point hcp-dhcp-fcc at 36 GPa and 1450 K and c) the location of the triple point dhcp-fcc-melt close to 60 GPa and 2800 K. If no other phase transition intervenes, the melting of beta-iron at 360 GPa takes place at temperatures less than 5000 K.

The thermodynamic data on iron hydride is assessed based on new experiments to 40 GPa and 2000 K.

The data base is only preliminary requiring further detailed study of the stability of $MgSiO_3$ and of iron phase diagram. The data may be used to design new experiments and verification.

2. Mineral Equilibria and Thermodynamics of Metamorphic Systems

MINERAL EQULIBRIA AND GEODYNAMICS OF METAMORPHIC COMPLEXES

Perchuk L.L., Gerya T.V. *(Department of Petrology, Moscow State University, llp@geol.msu.ru)*, van Reenen D.D. and Smit C.A. *(Department of Geology, Rand Afrikaans University, Republic of South Africa, ddvr@rau3.rau.ac.za)*

Local mineral equilibria allow correct calculation of PT-paths that are powerful tools in understanding the geodynamic processes. This statement can be exemplified by data from two very similar in terms of their geology Precambrian complexes, *i.e.* the Limpopo Granulite Complex from South Africa and the Lapland granulite complex from Kola Peninsula and Fennoscandia. Both of them are situated among green-stone belts. The major mineral equilibria in the Limpopo metapelites are Grt+Qtz = Opx+Crd and Grt+Qtz+Sil = Crd, which form typical coronitic and symplectitic textures. Similar textures well developed in many other complexes (*e.g.* the S.W.Baikal, S.India *etc.*). Two types of retrograde PT-paths, isobaric cooling and common decompression cooling are recorded by these textures from the same granulite complex. The only difference is in location of the samples. Samples of isobaric cooling calculated from the Grt+Qtz = Opx+Crd reaction texture normally are collected near the contact of granulite with the cratonic wall rocks, while the decompression cooling path is common for samples collected far from the contact. Mineral equilibria from the schists adjacent to the granulite complexes have recorded PT-loop that suggest circulation (crustal convection) of the wall rocks caused by ascent of a granulite complex. Such gravitational redistribution of the rocks has been tested by numerical modeling (Newton's flow) that allows to follow movement of each given sample in the crust. While granulites move up to the surface, relatively cool metabasalts and komatiites move down cooling the granulites along the contact zone. This causes change in direction of movement of some uprising granulite blocks toward the contact with the cratonic rocks and isobaric cooling at a given level of the Earth's crust while others ascent to the Earth's surface. This model is numerically compared with a collision-erosion model widely used for explanation of granulite facies terrenes formation.

ADVANCES IN HYDROFLUORIC ACID SOLUTION CALORIMETRY: REDUCTION OF REQUIRED SAMPLE SIZE BELOW TEN MILLIGRAMS

Hovis G.L. *(Department of Geology & Environmental Geosciences, Lafayette College, Easton, PA 18042, USA, hovisguy@lafvax.lafayette.edu)*, Roux J. *(CNRS-CRSCM, 1A, rue de la Ferollerie, 45071 Orleans Cedex 2, FR, jroux@cnrs-orleans.fr)* and Richet P. *(Institut de Physique du Globe, 4, place Jussieu, 75005 Paris, FR, richet@ipgp.jussieu.fr)*

For many years hydrofluoric acid solution calorimetric experiments have been known for the large sample sizes that they require. Although samples of one gram per dissolution were not unusual for such experiments twenty years ago, the availability of new instrumentation has improved the precision with which temperature and energy can be measured in these experiments, as well as the accuracy and precision with which samples can be weighed. To test sample requirements based on improvements to the solution calorimetric system at Lafayette College, we have made a systematic study of the enthalpy of solution of coarse unground hexagonal GeO_2 crystals in 20.1 weight % HF at 50°C as a function of sample weight for samples ranging from 185 to 10 milligrams.

The resulting calorimetric data demonstrate that precision of the highest degree (±0.1%) is maintained down to sample sizes of 50mg. There is some loss of precision with smaller samples, but even 25 mg and 10 mg samples produce calorimetric data having quite respectable standard errors equal to just 1% of the enthalpies of solution, precision that is adequate for many purposes.

Since GeO_2 yields relatively low heats of solution on the basis of energy per weight, even smaller samples than the ones above can be utilized for substances producing greater energy per gram. Many silicates, for example, produce weight-based heats of solution that are about twice those of GeO_2. Minimum sample sizes for these will be half those required for germanium oxide, that is, 5 to 25 mg depending on phase and application.

These improvements make possible many new kinds of projects for HF solution calorimetric investigation, including those on high-pressure phases, where sample quantity is at a minimum. Moreover, we continue to seek ways of further reducing sample size, including the development of a smaller more energy-sensitive dissolution vessel.

HARD MODE IR SPECTROSCOPY OF GARNET SOLID SOLUTIONS

Boffa Ballaran T., Carpenter M.A. *(Dept. of Earth Sciences, Univ. of Cambridge, UK, tiziana@esc.cam.ac.uk)* and Geiger C.A. *(Mineralogisch-Petrographisches Inst., Univ. of Kiel, D)*

Hard Mode Infrared Spectroscopy (HMIS) was used to investigate the mixing properties of three synthetic garnet solid solutions: pyrope ($Mg_3Al_2Si_3O_{12}$)-almandine ($Fe_3Al_2Si_3O_{12}$), almandine-grossular ($Ca_3Al_2Si_3O_{12}$) and pyrope-grossular in the frequency range 50-1400 cm^{-1}. Changes in frequency and line broadening of the different phonons are associated with the cation substitutions of Mg, Fe and Ca in the dodecahedral sites. A new method based on the use of the autocorrelation function has been developed to obtain the average line width of the absorption bands over a given frequency interval. This statistical tool does not require peak fitting and therefore may be applied also in those regions with overlapping peaks; moreover it gives results which show less scatter than line widths obtained by traditional fitting.

Line broadening is assumed to be associated with local heterogeneities arising from the cation substitution in the structure of samples at intermediate compositions. Three different frequency regions were analysed for each spectrum and the results compared with the enthalpy of mixing of the investigated solid solutions. Non linearities of the line broadening have a shape similar to the excess enthalpies of mixing. This is tentatively explained as indicating that the enthalpy of mixing arises from elastic energies accompanying local strain within the garnet structure.

FORMATION OF PLAGIOCLASE IN THE EARLY PRECAMBRIAN AND THE ORIGIN OF ANORTHOSITES

Pilchin A. *(Universal Geoscience and Environmental consulting company, pilchin@sprint.ca)*

The research shows that the principal petrologic and mineralogical peculiarities of composition of Early Precambrian rocks of cratonic regions are: presence of anorthosites; predominance of felsic rocks; absence or extremely rare presence of olivine and relatively rare presence of orthopyroxenes; content of huge amounts of plagioclase and quartz; content of chlorite, hornblende, biotite and augite as the main mafic minerals; absence or lack of water during the Early Precambrian rocks formation. Formation of the Early Precambrian rocks was controlled by medium to low temperature, high to medium pressure and specific environmental conditions. Huge amounts of plagioclase in the Precambrian was formed by breakdown of garnet and clinopyroxene. This supposition is confirmed by such field and experimental data as: presence of plagioclase as secondary mineral in eclogites; occurrence of garnet, clinopyroxene and amphibole in anorthositic rocks; formation of garnet-plagioclase pairs; formation of orthopyroxene - spinel - plagioclase symplectites around garnet in contact with clinopiroxene; plagioclase inclusions in garnet core; growth of plagioclase collars between clinopyroxene and garnet; plagioclase inclusions in clinopyroxene; garnet - pyroxene coronas in anorthositic gabbros; formation of clinopyroxene - plagioclase symplectites around garnet by breakdown of omphacite; formation of plagioclase eclogite; replacement of garnet by amphibole - plagioclase coronas; replacement of clinopyroxene by amphibole - sodic plagioclase symplectite; formation of plagioclase - amphibole -magnetite assemblages as coronas around garnet; pyroxene megacrysts from anorthosites, *etc.*

Areas of anorthosite formation are characterized by increasing content of iron (Franceschelli *et al.* 1982, Bogdanova 1984, Sukhanov *et al.* 1984). It allows the supposition that one of the causes of garnet and clinopyroxene breakdown is the instability of two - valence iron.

2. Mineral Equilibria and Thermodynamics of Metamorphic Systems

HARKERITE FROM CRESTMORE QUARRY, CALIFORNIA AND FROM CASCADE SLIDE, ADIRONDACK MOUNTAINS, NEW YORK: A CONTRAST IN METAMORPHIC PRESSURE.

Grew E.S., Yates M.G. *(Dept. Geol. Sci., Univ. Maine)*, Adams P. *(The Aerospace Corp., El Segundo, Calif.)*, Kirkby R. *(Scottsdale, Ariz.)*, and Wiedenbeck M. *(Inst. Meteoritics, Univ. New Mexico)*

Of two new U.S. localities for harkerite (Hrk), ~ $Ca_{48}Mg_{16}[AlSi_4(O,OH)_{16}]_4(BO_3)_{16}(CO_3)_{16}(H_2O,Cl)_2$, the contact aureole in the Crestmore Quarry ($T \geq 800°C$ and, $P \approx 1$ kbar, Wiechmann, 1995 Ph.D. thesis) is typical for this mineral, whereas the deep-seated Cascade Slide xenolith ($T \approx 720$-$850°C$, $P \approx 6.4$-8.4 kbar, *e.g.*, Valley, Spear and others) in anorthosite is unique. Critical assemblages are (1, in blue calcite marble) Hrk + forsterite (Fo) + clintonite (Cln) ±spinel (Spl) (Crestmore); Hrk + monticellite (Mtc) ± Fo + Spl and Hrk + clinopyroxene (Cpx) + Mtc (Cascade Slide); and (2, in skarn) Hrk + vesuvianite + Mtc + Cln (Crestmore). The sequence of crystallization is (1) Cpx (Cascade Slide only), (2) Mtc, (3) Fo, (4) Hrk. The analyzed Hrk differ from one sample to another significantly in SiO_2 and B_2O_3, and, to a lesser extent, in CO_2. Variations among Si, Al and B approximate $Al_{0.75}Si_{4.25}O_{15.25}(OH)_{0.75} \leftrightarrow (BO_3)_4$. Hrk SiO_2 content reflects both mineral assemblage and B_2O_3 activity. Hrk from Crestmore contains 0.08-0.23 wt% SO_3. Large cages in the Hrk structure might incorporate minor SO_3 and CO_2, as well as H_2O and Cl. Distribution of Fe and Mg is regular (Fe increases Fo < Hrk < Cpx < Mtc << Spl < magnetite), consistent with $Fe = Fe^{2+}$ in Hrk and with approach to chemical equilibrium among the minerals. Crestmore Hrk formed at close to peak T when solutions dominated by Al penetrated the aureole; boron was presumably introduced by these solutions. On the other hand, boron could have been present in the protolith at Cascade Slide. The Cascade Slide Hrk probably formed at high T and low P in a marble xenolith entrapped in anorthosite at a high crustal level and re-equilibrated during granulite-facies metamorphism after burial to $P = 6.4$-8.5 kbar. Hrk was stable at this P, but the decarbonation required for its original formation is probably possible only at very low P as at Crestmore.

HIGH GRADE K-FELDSPAR METASOMATISM IN CHARNOCKITES ON BOTH A LOCAL AND REGIONAL SCALE

Harlov D.E. *(GeoForschungsZentrum Potsdam, dharlov@gfz-potsdam.de)*

The Ivrea-Verbano Zone, N. Italy, represents a traverse of steeply dipping lower crustal rocks consisting of basal metagabbros in the NW followed by 3 km of Amph-free, metasedimentary, metavolcanic charnockites and stronalites (Ti-Bt, Rt, Hm poor Ilm, Po, Graphite) towards the SE with a steady decrease in P-T from granulite to amphibolite facies ($P = 8$-4 kbars and $T = 800$-$600°C$). Cl-rich basalt underplating, represented today by the basal metagabbros, is the most likely source of the heat and fluids for these granulites. In distinct contrast, charnockites from the Seward Peninsula, W. Alaska (Ti-Bt, Hm-poor Ilm, Po, Graphite) represent a localized event in which fluids from an Fo-Di-Phl-(minor Scp) containing marble layer effectively charnockitized 85 cm of amphibolite facies gneiss, in contact with the marble, to an Opx-Cpx-bearing gneiss at 800°C and 8 kbars.

BSE images from either set of charnockites show an extensive and continuous system of Kfs veins along Qtz/Plg grain boundaries, some of which can be traced across the entire length of the sample. These are always associated with Qtz. Qtz grain rims in contact with these veins show evidence of extensive corrosion. Isolated Qtz blebs are commonly found within the Kfs veins and may represent secondary deposition of Qtz from a silica supersaturated fluid. Contact between the Kfs veins and Opx or Grt grains show no signs of secondary alteration. Kfs veins in contact with Ti-Bt show no evidence of a melt texture. Kfs also takes the form of patches of variable size (5 - 70% of the grain) in the form of "replacement anti-perthite" in approximately half of the Plg grains. The Kfs veins and patches diminish in abundance with decreasing metamorphic grade and/or distance from the fluid source and disappear once full amphibolite facies is reached. The only real difference is that the highly localized effect seen in the Seward charnockites (85 cm) is identical to that seen in the Ivrea charnockites (3 km). We postulate that these Kfs veins are evidence of a pervasive, high temperature, low H_2O activity, Cl-rich fluid, most likely a brine, coupled with a separate CO_2-rich phase. And that these H_2O-poor brines could be the principle dehydration mechanism for charnockite formation - not just on a localized scale but on a regional scale as well. Brines might account for the highly reduced nature of both charnockites with K resulting from the breakdown of Bt and Hbl.

STABILITY AND THERMODYNAMIC PROPERTIES OF TREMOLITE

Kahl W.-A. and Maresch W.V. *(Inst. Mineralogie, Ruhr-Univ. Bochum, walter.v.maresch@ruhr-univ-bochum.de)*

End-member tremolite (Tr) $Ca_2Mg_5[Si_8O_{22}(OH)_2]$ is an "anchor" phase in internally-consistent thermodynamic data sets and for formulations of amphibole solid-solution models, due to its presumed crystal-chemical simplicity and its importance as a major component of many complex natural amphibole solid solutions.

However, there is debate on how closely ideal end-member tremolite can be approached for thermodynamic description, because natural material is rarely pure and synthetic products are often difficult to characterize accurately. Material from Nuristan, Afghanistan, appears to satisfy requirements for natural, sufficiently pure tremolite for experimental work and for calorimetric measurements. Gem quality fragments can be isolated. Details on the occurrence are scarce. Talc, dolomite and magnesite are associated with the tremolite. Analysis yields a typical composition $K_{0.002}Na_{0.016}Ca_{1.954}Mg_{4.931}Fe^{2+}_{0.056}Mn_{0.004}Al_{0.025}Si_{8.003}O_{21.980}(OH)_{2.019}$ $F_{0.001}$ (H_2O content analysed; Fe^{2+} confirmed by ESR; HRTEM indicates no planar defects).

The Nuristan tremolite and samples of the classical "Edinburgh" tremolite quoted in the literature have been hydrothermally recrystallized with excess diopside + quartz and with excess enstatite/talc + quartz to bracket miscibility on the tremolite- $Mg_7Si_8O_{22}(OH)_2$ join at 700-800°C and 1-2 kbar. Depending on chosen calculation procedures, the scatter of microprobe analyses corresponds to maximum Tr contents between 96% and 100%. This agrees with bromide-fluxed syntheses reported in the literature and underscores the problem with standard amphibole synthesis techniques, which usually lead to larger compositional scatter and higher magnesiocummingtonite contents at similar P-T conditions.

Lead borate drop-solution calorimetry as well as transposed-temperature-drop and DSC heat capacity measurements on the Nuristan tremolite are in progress; refined results will be reported.

COMMENTS ON GEOTHERMOBAROMETRY AND P-T GRIDS IN MEDIUM-T, MEDIUM TO HIGH-P METAMORPHIC ROCKS

Ghent E. D. *(Dept. of Geology and Geophysics, University of Calgary, ghent@geo.ucalgary.ca)*

Common end members for medium-T, medium to high-P metamorphosed (MTMHP) pelitic rocks, with few exceptions, *e.g.* staurolite, have reasonably well-defined P-T stability fields. Experimental activity-composition (a-X) data for crystalline solutions are limited. Many a-X relationships are derived from field-based data. Independent estimates of P-T are necessary and it is assumed that all of the phases close reaction and exchange at the same P-T. P-T estimates in pelitic rocks straddling the kyanite-sillimanite isograd in Mica Creek, B.C. provide some quantitative data on the consistency of P-T estimates with experimental data on the kyanite-sillimanite equilibrium. Pressure-temperature grids for MTMHP can be compared with field data from SE B.C. The difference in pressure between the staurolite-out and the muscovite-plagioclase-quartz solidus intersections with the kyanite-sillimanite P-T curve is at least 1.5 kbar.

For MTMHP metabasites the P-T stability relations for the end member Ca-Na amphiboles are known for very few phases and a-X relations for the amphiboles are derived from field-based data. P-T estimates based upon amphibole-clinopyroxene-garnet-plagioclase-quartz equilibria do not agree well with the kyanite-sillimanite equilibrium curve (Mica Creek area).

Most estimates of T for eclogites are derived from garnet-clinopyroxene Fe-Mg exchange, but there is disagreement over the calibrations. Minimum P limits are estimated from albite = jadeite + quartz. An upper P limit can be set for low-T epidote-bearing eclogites which lack lawsonite. For kyanite-eclogite, diopside + kyanite = grossular + pyrope+quartz is a possible geobarometer. Diopside + clinozoisite = grossular + pyrope + quartz + H_2O, is another possible geobarometer, if one makes an assumption about H_2O activity.

2. Mineral Equilibria and Thermodynamics of Metamorphic Systems

NEW P-V-T DATA FOR SOME HIGH PRESSURE PHASES IN THE SYSTEM CaO-MgO-Al_2O_3-SiO_2-H_2O AND ITS CONSEQUENCES FOR INTERNALLY CONSISTENT DATA BASES

Grevel K.-D. *(Ruhr-Universität Bochum, Institut für Mineralogie, Klaus-Dieter.Grevel@ruhr-uni-bochum.de)*

Due to the lack of experimental data, Berman (1988) as well as Holland & Powell (1990) estimated several values for compressibility and thermal expansion when they derived their internally consistent data bases. Therefore we investigated the P-V-T behaviour of some high pressure minerals in the system CaO-MgO-Al_2O_3-SiO_2-H_2O recently. All powder X-ray diffraction experiments were carried out using synchrotron radiation (HASYLAB at DESY, Germany) and a multi-anvil-X-ray-apparatus (MAX-80, Peun *et al.*, 1995). The isothermal bulk moduli were calculated using the Murnaghan equation of state (Murnaghan, 1951); k′ was assumed to be equal 4:

zoisite	(1249 ± 22 kbar)	lawsonite	(1080 ± 14 kbar)
diaspore	(1300 ± 12 kbar)	kyanite	(1684 ± 31 kbar)
pyrophyllite	(413 ± 6.7 kbar)	clinochlore	(758 ± 12 kbar)
Mg-chloritoid	(1284 ± 23 kbar)	Mg-staurolite	(1685 ± 33 kbar)
tremolite	(775 ± 7.0 kbar)		

These compressibility data as well as P-V-T data for the phases listed above were used to calculate several mineral equilibria at high pressures. As an example some equilibria involving zoisite and lawsonite are discussed. The calculated positions of the equilibria

zoisite =grossular+kyanite+coesite+H_2O (Schmidt & Poli, 1994); zoisite+kyanite+coesite+H_2O=lawsonite (Skrok *et al.*, 1994), and zoisite =grossular +kyanite +coesite +lawsonite (Poli & Schmidt, 1998)

using the Berman (1988) data base and including our new P-V-T measurements are in good agreement with the experimental results in contrast to the investigations by Holland *et al.* (1996).

Additionally, some calculations on the stability of Mg-staurolite (Fockenberg, 1998) will be presented.

RARE EARTH ELEMENTS IN LOW-GRADE METACLASTIC SEDIMENTS: THE WHAT, WHERE, AND WHEN OF REE (RE)DISTRIBUTIONS.

Livi K.J.T., Ferry J.M. and Veblen D.R. *(Dept. of Earth and Planetary Sciences, Johns Hopkins University, klivi@jhu.edu)*

The rare-earth and actinide element distributions in rocks and minerals have important implications for a wide range of studies, ranging from tectonics to radioactive waste disposal. Investigation of diagenetic and low-grade metamorphic clastic sediments is relevant because they occur in collisional mountain belts worldwide and because they experienced elevated temperatures similar to those in radwaste environments. Our study investigates clastic sediments from the Liassic black shale in Central Switzerland. The concentrations of 39 elements, including selected REEs, Pb, Th, and U, were determined using high-precision electron microprobe analyses. Results show that diagenetic-grade samples (~100°C) contain a diverse array of REE-rich phosphate and silicate phases, including monazite (La ≤ 13.8 wt%, Nd ≥ 9.2%), La-depleted monazite (La ≥ 5.5%, Nd ≤ 14.2%), brabantitic monazite (Th = 8.6%), Ce-silicate (Ce = 61.3%), xenotime, apatite, and zircon. Sr-rich barite is common in these samples. In higher- temperature samples (400-450°C), allanite formed from coexisting monazite and apatite, and low-La, brabantitic monazite, and barite are missing. Analysis of the modal abundance of REE phases and LREE/whole-rock ratios for sheet silicates indicate that LREEs reside predominantly in monazite (which hosts up to 50% of the LREEs) and white micas. Chlorite and pyrophyllite contain less than the whole-rock concentration. HREEs appear to reside almost exclusively in xenotime. The LREE concentrations in Central Switzerland sediments vary from 100 times chondritic values in samples with little monazite present to 200 times in samples with the highest abundance of REE-phosphates. Preliminary investigations indicate that REEs were lost from clay minerals when they reacted to form higher-grade sheet silicates. Dating of monazite and xenotime crystals by the Pb-Th-U chemical method yields a concordant age of 380 ma and other older ages that reflect their detrital source. This indicates that monazites are resistant to diagenetic processes but are affected by reactions at higher temperatures.

CORONA TEXTURES IN JADEITE GNEISS:EVIDENCE OF POST COLLISION UPLIFT OF THE ULTRAHIGH-PRESSURE TERRANE IN DABIESHAN, CENTRAL CHINA

You Z., Zhang Z. and Zhong Z. *(Faculty of Earth Sciences, China University of Geosciences, Wuhan, zdyou@sky.cugb.edu.cn)*

Various types of jadeite-bearing rocks are discovered along the south eastern part of Dabieshan. The typical mineral assemblage is: jadeite (Jd_{85-90}) + garnet (Alm_{69-70}) +quartz + glaucophane. The rock types differ widely in the amount of jadeite ranging from jadeite quartzite through quartz jadeite gneiss to jadeitite in which jadeite dominates over quartz. Polycrystalline quartz pseudomorphs after coesite have been found as microinclusions within jadeite which is a decisive evidence for an ultrahigh-pressure (UHP) metamorphic event of a felsic protolith. The petrochemistry and trace elements in jadeite gneiss indicate a protolith of greywacke type or other felsic rock types of crustal origin.

The jadeite gneiss occurs as lenses or layers intercalated within granitic gneisses and are associated with marble layers and eclogite pods. Most of the jadeite gneisses are medium grained granular rocks but always highly foliated showing a ductile deformation fabric formed during their uplift.

The UHP jadeite gneiss has commonly undergone amphibiolite facies of retrograde metamorphism. The most prominent feature is the compound corona textures along the boundaries between jadeite and quartz. The outermost rim of the corona is a moat of aegirine and the inner part of the corona is composed of plagioclase with needle-like taramite inclusions radially grown against the margin of the jadeite.

The plagioclase in the corona displays a strong compositional zonation: the outer part is nearly pure albite (An_{0-3}) while towards the jadeite host it turns out to be oligoclase (An_{15-2}). Therefore, the corona-forming reaction is apparently diffusion-controlled. The process can be related to a mosaic re-equilibrium under PT conditions prevailing in the middle crust. This kind of retrometamorphism provides an evidence of the post orogenic uplift in Dabieshan UHP terranes.

TWO CONTRASTING MINERAL ASSEMBLAGES IN THE MELIATA BLUESCHISTS, WESTERN CARPATHIANS, SLOVAKIA

Faryad S.W.[1,2] and Hoinkes G.[1] *([1]Institute of Mineralogy, Univ. Graz, Austria, [2]Dept. Geol. & Mineralogy, Univ. Kosice, faryad@tuke.sk)*

Textural relations and mineral compositions of blueschist facies metabasites from the Meliata unit indicate the presence of two mineral assemblages in thin section scale formed at different P-T conditions. The first assemblage is represented by zoisite with inclusions of muscovite, paragonite and Al-rich titanite. The Zoisite, having Al_2Fe content of 3-5%, is rimmed by clinozoisite with maximum Al_2Fe of 75% and enclosed by glaucophane. Besides clinozoisite and glaucophane, the second assemblage involves Na-pyroxene, phengite, chlorite and relatively Al-poor titanite. The metabasite contains tabular idiomorphic shaped pseudomorphs of phengite (probably after lawsonite) which are in sharp contact with Na-pyroxene. Glaucophane cross cuts both Na-pyroxene and phengite pseudomorphs.

According to textural relations, the zoisite-bearing assemblage corresponds to the early stage of metamorphism and was formed at pressure of <0.5 Gpa at 350°C. Na-pyroxene shows strong compositional variations (Jd_{4-70}, Aeg_{10-49},Q_{17-49}) and contains jadeite-rich domains which are visible in back-scattered electron images. Some of these domains have idiomorphic forms and probably were formed by local equilibrium and replacement of an Al-rich phase. Glaucophane reveals progressive zoning with increase of Al and Na and decrease of Ca towards rims. Accessory Ca-rich glaucophane, enclosed in Na-pyroxene, is also present. Phengite is characterized by high Si content of 3.5 a/f.u.. Pressures of >1.2 GPa at 450°C are estimated using the maximum jadeite content in pyroxene and thermodynamic calculations. Different P-T conditions, obtained for the two assemblages indicate a very steep geothermal gradient for the blueschist facies metamorphism of the Meliata unit. The presence of clinozoisite, rimming zoisite, suggests that transformation from orthorhombic to monoclinic epidote group minerals is dependent not only on temperature but also on pressure.

2. Mineral Equilibria and Thermodynamics of Metamorphic Systems

COMPOSITIONAL AND OPTICAL ZONATION IN AMPHIBOLE FROM AMPHIBOLE-BEARING SCHISTS (MOSLAVAÈKA GORA - CROATIA)

Balen D. *(Inst. for Mineralogy and Petrology, Dept. of Geology, Univ. of Zagreb, drbalen@public.srce.hr)*

Polymetamorphic amphibolite facies complex of Moslavaèka gora (Croatia) consists of amphibolite, mafic schists (diopside-amphibole schist, garnet-diopside-amphibole schist), gneiss, cordierite schist and hornfels, marble and migmatite. Older metamorphic rocks are disturbed by the Hercynian (?) granite intrusion.

Amphibole bearing schists with zoned amphibole have layered structure ("sandwich") with three different mineral associations: garnet association in "centre" of rock (grossular-clinozoisite- clinopyroxene-plagioclase), surrounded by the clinopyroxene association (clinopyroxene-plagioclase-titanite) and embedded in the amphibole association (hornblende-plagioclase-clinopyroxene-ilmenite-quartz).

The increase of metamorphic conditions are plotted with respect to growth zonation of amphibole grains with Si- and Mg- concentrations decreasing from core to rim along with increasing Al-, Na- and Ti-content. Changes in the chemical composition are also visible in plane polarised light as an obvious colour change for Y and Z vibration directions of indicatrix (Y_1= green, Y_2=brown, Z_1=dark green, Z_2=dark brown). This chemical and colour changes are interpreted through coupled substitutions in amphibole and reactions with minerals during the increase of metamorphic (P, T) conditions.

Paragenesis with zoned amphibole are: amphibole (6.70 Si p.f.u., $Mg/(Mg+Fe^{2+})$ = 0.493 - rim), plagioclase (0.62 Ca p.f.u. - rim), clinopyroxene (diopside) and ilmenite.

Geothermobarometric evaluation of temperature and pressure conditions during metamorphism with aid of various calibrations and mineral sensors gives 585°C and 200 MPa for core and 650°C and 200 MPa for rim of zoned amphibole grains.

GARNET-CUMMINGTONITE ROCKS IN THE HYEONDONG GNEISS COMPLEX, NORTHEASTERN YEONGNAM MASSIF, SOUTH KOREA

Cho M. *(Dept. of Geological Sciences., Seoul National University, moonsup@plaza.snu.ac.kr)* and Kim J. *(Korea Basic Sci. Inst.)*

Garnet-cummingtonite (Grt-Cum) rocks containing up to 24 wt% Fe_2O_3* (total iron) rarely occur in the Hyeondong Gneiss Complex, NE Yeongnam Massif. This Massif, often correlated with North China Craton, primarily comprises granitic gneisses, porphyroblastic gneisses and cordierite schists together with minor amphibolites and calc-silicates. The Grt-Cum rock occurs as concordant layers together with amphibolites and metasedimentary rocks. Garnet and cummingtonite reach up to 90 modal %, and minor phases include quartz, biotite, plagioclase, magnetite, and ilmenite. Garnets, 4 - 5 mm in size, are the product of peak metamorphism belonging to the upper amphibolite facies, and occur as euhedral or subhedral poikiloblasts enclosing cummingtonite, quartz, plagioclase, and ilmenite. Secondary minerals such as hornblende and chlorite commonly occur along the grain boundaries between garnet and cummingtonite. P-T conditions of the Grt-Cum rock as well as garnet-bearing metapelite and amphibolite were estimated with various geothermobarometers. The results indicate the peak metamorphic condition of 630~690°C and 4 - 5 kbar, and the retrograde temperature of 510~600°C. The whole rock compositions of Grt-Cum rocks and amphibolites range from tholeiitic basalt to basaltic andesite, and the similarity in trace and rare earth element chemistries advocates their origin from an identical parental magma formed at the arc environment. In addition, the enrichment of iron in the Grt-Cum rock is interpreted to result from hydrothermal exhalative volcanic activity.

HIGH-PRESSURE METAMORPHIC ROCKS FROM THE ESCAMBRAY MASSIF, CUBA

Grevel C.[1], Maresch W.V.[1], Stanek K.P[2], Grafe F.[1] and Millan G.[3] *([1]Inst. Mineralogie, Ruhr-Univ. Bochum, klaus-dieter.grevel@ruhr-uni-bochum.de, [2]Inst. Geologie, TU Bergakademie Freiberg, [3]Instituto de Geología y Paleontología, La Habana, Cuba)*

The Escambray massif, an isolated mountainous area of metamorphic rocks in the south-central part of Cuba, consists of two morphological domes, the western Trinidad dome and the eastern Sancti Spiritus dome (Somin & Millan, 1974). Impure metacarbonates and quartz-mica schists, in part garnetiferous, as well as metaquartzites are the most predominant rocks of the area (Somin & Millan, 1981). Basic and ultrabasic bodies of various dimensions are found locally in the form of slightly altered gabbro, greenschist, blueschist, eclogite, amphibolite and serpentinized ultramafic rock.

We have studied the geology and petrology of the eastern Sancti Spiritus dome, which is composed of three main lithotectonic units. The Gavilanes and Pitajones units have been strongly deformed and thrust over the Yayabo unit exposed only along the northeastern margin of the dome.

P-T-estimates for pods of garnetiferous blueschist belonging to the Gavilanes unit yield maximum metamorphic conditions of 16 kbar at 500°C. Eclogites from this same unit yield even higher metamorphic conditions of 16-20 kbar at 570-600°C. An independent indicator for high-pressure metamorphism in the Escambray is the occurrence of deerite in ferruginous metaquartzite (Grevel *et al.*, 1996). At 460°C (quartz-magnetite oxygen-isotope geothermo-metry; S.Hoernes, pers. comm., 1997) the low-pressure stability limit for deerite is about 14 kbar, according to the experimental study of Lattard & Le Breton (1994). Deerite-quartzites are an integral part of the Gavilanes stratigraphy and prove that the entire unit was subjected to high-pressure metamorphism.

INSTABILITY OF SOME IRON CONTAINING MINERALS UNDER LOW TEMPERATURE CONDITIONS

Pilchin M. and Pilchin A. *(Universal Geoscience and Environmental consulting company, pilchin@sprint.ca)*

Physical, geochemical and metallurgical data show that iron suboxide (FeO) is unstable under low temperature conditions (570°C or less) and that the iron oxide is unstable under high temperature conditions (Nagata 1961, Tretyakov 1967, Pilchin 1983). Below the temperature of its stability FeO transforms to magnetite and native iron. The occurrence of native iron and secondary magnetite and hematite in different types of rocks is well known. Instability of olivine under low temperature conditions is proven experimentally (Johannes 1968, Normand & Williams-Jones 1996, O'Hanley 1996). Results of magnetic (Pechersky *et al.* 1975) and paleomagnetic (Mikhailova *et al.* 1985) researches also point at the low temperature formation of magnetic minerals. The transformance of two-valence iron to three-valence iron also strongly depends on pressure and with increase of pressure FeO becomes more stable under low temperature conditions. Such a transformation is well known from experimental data (Nagata 1961, Green & Ringwood 1967) and field data (serpentinization of olivine containing rocks, breakdown of solid solutions of pyroxenes, formation of iron formations, transformation of chlorite to serpentine). Since three-valence iron is unstable under medium and high temperature conditions, it is evident that that rocks and minerals containing three-valence iron could be only of secondary origin. It also means that all rocks and minerals containing two-valence iron are unstable under upper crust thermodynamic conditions and could be altered to other rocks and minerals containing three-valence iron. Such minerals as andradite, hastingsite, riebeckite, arfvedsonite, glauconite, biotite, acmite, iron containing jadeite, some types of omphacite, magnetite could be only of secondary origin. On the other hand, such minerals as almandine, most of amphiboles, augite, pigeonite, hedenbergite, fayalite, antigorite, siderite, clinochlore are unstable under the upper crust conditions.

2. Mineral Equilibria and Thermodynamics of Metamorphic Systems

POLYMETAMORPHIC COMPLEXES OF THE URALS: MINERAL-BASED RECONSTRUCTION OF EVOLUTIONAL ENVIRONMENTS

Pystina Yu.I. *(Inst. of Geology, Komi SC, Uralian Div. of RAS)*

The Urals is one of the best studied Phanerozoic folded systems, comprising numerous complexes of strongly metamorphosed rocks. Age and origin of the complexes are open to various interpretations since their links with the adjacent geosynclinal deposits are indeterminate.

The accumulated data on the accessory minerals from the polymetamorphic complexes of the South, Middle (Alexandrovsk, Taratashsk, Ilmenogorsk complexes), Circumpolar (Nerkayusk, Nyartinsk) and Polar Urals (Khordyusk) suggest that morphologic features, internal structure, composition as well as spectroscopic properties of particular accessory minerals, first and foremost zircon, are good indicators of the polymetamorphites' genesis and environments in which the polymetamorphic complexes have evolved. Our study showed that the habit, zonality and composition of zircon crystals vary depending on the metamorphic conditions, which allows to distinguish typomorphic features for particular P-T parameters.

TARAMITE AS PROGRADE-FORMED MINERAL IN TRANSITION BETWEEN GREENSCHIST AND BLUESCHIST FACIES CONDITIONS

Faryad S.W. *(Institute of Mineralogy, Univ. Graz, Austria, Dept. Geol. & Mineralogy, Univ. Kosice, faryad@tuke.sk)*

Taramite is usually known as retrograde phase in amphibolized eclogites and its thermodynamic properties and stability field are not well known. The Ca-Na amphibole of taramite composition occurs in metabasalts which are a part of about 100 km long belt of metabasites and quartz phyllites in the northern and eastern part of the early Paleozoic of the Gemericum (Western Carpathians). Metbasites, containing albite, epidote and actinolite and quartz phyllite with chlorite and white mica, indicate greenschist facies metamorphism. The presence of taramite is restricted to ca 2 km zones of metabasites with preserved structures of pillow lavas and porphyric basalts. Taramite-bearing metabasites have relatively higher FeO_t (X_{Mg} = Mg/Mg+FeO_t = 0.5) contents compared to actinolite-bearing rocks with X_{Mg} of 0.17-0.36. Taramite associates with albite, epidote, grossular-and andradite-rich garnet, titanite, chlorite and rarely also with biotite. With exception of retrograde chlorite, all these minerals are in textural equilibrium. Besides fine-grained taramite in the matrix, it occurs in albite pseudomorphs after plagioclase or replaces igneous pyroxene. The X_{Mg} and Si contents in taramite are in the range of 0.36-0.45 and 6.0-6.4 a./f.u., respectively. A site in the amphibole formula is occupied by 0.51-0.96 atoms and Na^{M4} contents are 0.51-0.8 a/f.u. Large amphibole crystals are zoned with Si increasing and Na decreasing towards rims of grains. Garnet has average composition of Grs_{73}, And_{18}, Sps_2, Alm_2, $Py_{0.2}$ and the grossular content decreases and andradite increases from core ($Grs_{72}And_{20}$) to rim ($Grs_{44}And_{54}$).

Comparing metabasites from different sector of the greenschist belt, the metabasites near taramite-bearing rocks contain actinolite with relatively higher Na and lower Ca contents. Some amphibole analyses indicate transition to Ca-Na amphibole of winchite composition. Metamorphic conditions of 0.6-0.9 GPa and 440-480°C for taramite formation were estimated using thermodynamic calculation for the assemblage albite-taramite-garnet-quartz. Quartz phyllites, intercalated in metabasites contains phengite with maximum Si content of 3.3 a./f.u.

REACTION TEXTURES AND P-T PATHS OF THE GRANULITE TO AMPHIBOLITE TRANSITION IN THE HWACHEON GRANULITE COMPLEX, SOUTH KOREA

Yi K., Cho M. *(Dept. of Geol. Sci., Seoul Nat'l. Univ., keewook@plaza1.snu.ac.kr)* and Lee S. R. *(Korea Inst. of Geol., Mining & Materials)*

The Hwacheon Granulite Complex (HGC) occurring in central Korean Peninsula represents a coherent volume of migmatitic granulites first reported in S. Korea. This complex is commonly assumed to be a part of the Imjingang Belt, whose tectonic history is one of the current issues in east Asian geology. The HGC consists of migmatitic, felsic and pelitic gneisses together with subsidiary mafic granulites and amphibolites. Mafic rocks occur as either isolated blocks or concordant layers in migmatitic granulites. One mafic outcrop showing the transition between mafic granulite and garnet amphibolite was studied in detail. In the transition zone, 5 cm in width, a wide variety of reaction and exsolution textures is present. In particular, concentric reaction coronas consisting of outer monomineralic garnet and inner symplectic hornblende develop between pyroxene and plagioclase, and were used to constrain retrograde P-T paths. The garnet coronas formed during an isobaric cooling from 830°C to 680°C at 6 - 7 kbar, probably in association with fluid flux resulting from the crystallization of partial melt. Subsequently, the honblende symplectite formed in response to a decompression from 7 kbar to 3 kbar at *ca.* 600~700°C. In conjunction with our preliminary geochronologic and thermobarometric results from the HGC, we conclude that these contrasting P-T trajectories result from two distinct metamorphic events at Early Proterozoic and Permian-Triassic times, respectively.

MINERALOGICAL RECORD OF POLYMETAMORPHISM (ON EXAMPLE OF THE URALS)

Pystin A.M. *(Inst. of Geology, Komi SC, Uralian Div. of RAS)*

Polymetamorphism is a widespread phenomenon; its manifestations can be inferred in nearly any metamorphic complex. However, readily observed in real natural objects are parageneses of only the latest metamorphic episode, hence reconstruction of polymetamorphism presents a complicated problem.

In the Urals, polymetamorphic complexes proper showing no signs of the original rocks, mostly belong to pre-Riphean structural stages. Of major importance for the reconstruction of the metamorphic history of these complexes are: (a) relict minerals and mineral parageneses; (b) optical and chemical zonality in rock-forming and accessory minerals; (c) geochronologic reference dates in the history of mineral metamorphism.

The following sequence of metamorphic events has been outlined:

1. Aureole (?) metamorphism of granulitic facies (ball-like zirkon crystals of the "granulitic" type, over 2.2 bln years of age).

2. Diaphthoresis of amphibolitic facies (mineral parageneses of the amphibolitic facies, garnets with regressive zonality, prismatic zonal zircon crystals of the "amphibolitic" type, over 1.7 bln years of age).

3. Zonal metamorphism, reaching the conditions of the epidote-amphibolitic facies (mineral parageneses of epidote-amphibolitic and greenschist facies, garnets with progressive zonality, metamict zirkon crystals, about 0.9-0.6 bln years of age).

4. Greenschist facies metamorphism (mineral parageneses of greenschist facies, low-temperature pseudomorphs after garnet and hornblende, about 0.4 bln years of age).

PHYSICOCHEMICAL CONDITIONS OF FORMATION OF THE ECLOGITE-GLAUCOPHANE ROCKS OF THE ATBASHI COMPLEX, SOUTH TIEN SHAN

Fed'kin V.V. *(Inst. of Experimental Mineralogy, RAS. Russia, fedkin@iem.ac.ru)*

The Atbashi metamorphic complex is involved in the Hercynian folded terrane of the South Tien Shan and forms its Precambrian basement. Detailed petrography studies of the eclogite-glaucophane and other attendant rocks included in the Cheloktore suite, indicate that these rocks were formed at high pressure and intermediate temperature conditions as the result of the joint action of metamorphic and metasomatic processes. The available petrochemical data and the observed sequence of the mineral reactions that took place during the transformations of the high grade metamorphic rocks of the complex (eclogites and eclogite-like rocks with garnet -clinopyroxene mineral assemblages) to glaucophane-bearing and muscovite-quartzitic schists, testify that the chemical composition of the rocks was changed in the course of the Atbashi complex forming. These changes appeared as the decrease of Ca, Mg, and Fe in the rocks, smooth increase of Si, Al, and K, and increase of sodium activity at the different stages of metamorphism. These processes occured against the background of the total prograde metamorphic evolution of the complex.

Intensive microprobe studies of the main rock-forming mineral composition, mineral zoning, inclusions, and contact zones (more than 450 analyses) allow us to distinguish the metamorphic evolution features and the rock composition changes. Compositions of minerals from both primary (garnet-clinopyroxene) and secondary (garnet-glaucophane) mineral assemblages indicate the temperature increase of the equilibrium core-rim growth from 500-550°C to 600-740°C and from 400-450°C to 515-600°C, respectively. The prograde zoning of garnet and the retrograde transformation of rocks (glaucophane growth, muscovitization, carbonatization *etc.*) are interpreted in terms of volume acid leaching metasomatism and metamorphic processes. The geotectonic position of the Atbashi metamorphic complex is discussed based on the petrological data.

3. Fluid Inclusions in Minerals

FLUID INCLUSION SYSTEMATICS IN PORPHYRY COPPER DEPOSITS

Bodnar R.J. *(Department of Geological Sciences, Virginia Tech, bubbles@vt.edu)*

It is well known that porphyry copper deposits are associated with both an early magmatic fluid that exsolves from the crystallizing magma, and a later fluid of dominantly meteoric origin that convects through the pluton late in its history. Fluid inclusions in porphyry copper deposits provide a record of this magmatic/hydrothermal fluid system and its evolution during mineralization and alteration. Previous models for porphyry copper genesis called upon the early magmatic fluids to introduce the metals into the system and cause early-high temperature (potassic) alteration. Later alteration (phyllic) (and perhaps copper deposition) was thought to be associated with lower temperature meteoric waters. More recently, however, results of fluid inclusion studies have shown that the low to moderate salinity, moderate temperature fluids associated with phyllic alteration in many deposits are of magmatic origin.

In order to better understand the types of fluid inclusions that should be produced during cooling of a porphyry copper pluton, the room temperature phase ratios of fluid inclusions as a function of time and position within the overall porphyry system have been calculated. The results of these calculations show consistent variations and also predict previously unrecognized inclusion types. For example, the model calculations predict a zone of halite-saturated vapor above the cooling pluton early in its crystallization history. This zone evolves to a liquid plus vapor zone as the pluton cools and the crystallization front moves to greater depths. Additionally, the PTX conditions along the sides of the pluton are such that it is possible for magmatic fluids to migrate from the pluton into the overlying rocks without intersecting the two-phase field to produce fluid inclusions at shallow depth that have low salinities, moderate Th, and show no evidence of immiscibility. In the past such fluid inclusions were interpreted as being of meteoric origin, but results of recent studies of porphyry systems and these model calculations indicate that they could be of magmatic origin. A discussion of how the distribution of these inclusion types in time and space can be used in exploration for porphyry deposits will be presented.

ORE FLUID EVOLUTION AT THE GETCHELL CARLIN-TYPE GOLD DEPOSIT, NEVADA, USA

Cline J.S. *(Geoscience Dept., Univ. of Nevada, Las Vegas, jcline@nevada.edu)* and Hofstra A.H. *(U.S.G.S., Denver, CO)*

Getchell is a large, low-grade, sediment-hosted Carlin-type deposit. Gold occurs as submicron particles in As-rich pyrite. The main ore stage includes gold + As-rich pyrite + quartz + orpiment + fluorite; orpiment and fluorite precipitated late in this event. The late ore stage contains realgar + calcite + pyrite + Au.

Primary and secondary aqueous fluid inclusions from main ore stage quartz yield pressure corrected temperatures of 180 - 220°C. Fluorite trapped primary aqueous inclusions at 155 - 200°C and secondary aqueous inclusions at 115 - 155°C. Fluorite also trapped secondary, three-phase inclusions that record the influx of a 240°C CO_2-rich fluid. CO_2-H_2O phase equilibria constrain trapping to a minimum of ~330 bars and provide a pressure correction for ore stage inclusions. Realgar trapped secondary, single-phase inclusions. Aqueous inclusions in calcite are typically necked; sparse secondary inclusions with consistent phase ratios were trapped at 115 - 155°C.

Quadrupole mass spectrometer gas analyses show that ore-stage fluids in quartz, fluorite, and orpiment are generally H_2O-dominant, but contain significant concentrations of CO_2 and H_2S. Trace amounts of hydrocarbons (HC) and N_2 may be present. Late ore calcite inclusions are H_2O-dominant and contain minor to moderate CO_2, minor HC, and occasionally, traces of N_2 and H_2S.

Inclusion fluids in main ore stage quartz, fluorite, and orpiment have the highest δD_{H2O} (-50 to -97‰) and $\delta^{18}O_{H2O}$ (+12 to 0‰) values. Inclusion fluids in late ore realgar have low δD_{H2O} (-133 to -151‰) and $\delta^{18}O_{H2O}$ (-13.6 to -17.0‰) values characteristic of meteoric water. Inclusion fluids in late ore stage calcite exhibit a wide range of δD_{H2O} (-74 to -125‰) and $\delta^{18}O_{H2O}$ (14 to 2‰) values.

The high δD_{H2O} and $\delta^{18}O_{H2O}$ values of main-ore stage fluids provide clear evidence for a deep-sourced ore fluid at Getchell that is either metamorphic or magmatic in origin. Mixing of the deep-sourced fluid with cooler, variably exchanged meteoric water may have reduced ore fluid temperature, diluted ore fluid CO_2 and H_2S concentrations, and produced the lower isotope values of late ore stage fluids. The low δD_{H2O} and $\delta^{18}O_{H2O}$ values of secondary realgar inclusions may record the collapse of cool, dilute meteoric water into the system.

RADIOGENIC ISOTOPES IN HYDROTHERMAL FLUIDS: CLUES TO UNDERSTANDING ORE DEPOSIT GENESIS?

Pettke T.*, Kramers J.D. and Diamond L.W. *(Isot. Geol. Group., Min.-Petr. Inst., Univ. of Bern, Switzerland; tpettke@umich.edu; *present address: Dept. Geol. Sci., The Univ. of Michigan, USA)*

Contradictory genetic models for late-metamorphic gold lodes of various formation ages world-wide emerge from literature, testifying to the need of discriminating analytical tools to reliably constrain the source of the fluid and the gold, and the timing of gold vein formation relative to orogenic events. We elucidate the power and possible pitfalls of radiogenic isotope systematics as applied to hydrothermal gold veins on the basis of the Alpine Monte Rosa Gold District (MRGD; NW Italy).

Vein emplacement was diachronous over the MRGD between 32 and 11 Ma ($^{40}Ar/^{39}Ar$ in mica), always ~10 m.y. post peak metamorphism of the adjacent country rock. Primary fluid inclusions in the gold were revealed by step-wise degassing. Their trapped disequilibrium He-Ar abundance patterns are (a) indicative of retrograde boiling coeval with free gold deposition and (b) devoid of any atmospheric contribution. The fluid inclusion He-Ar isotope compositions reveal a mixture between a crustal and a very subordinate mantle-type component. The initial Sr isotopic compositions of fluid inclusions and vein minerals (a) are in disequilibrium with those of the adjacent host rocks and (b) monotonically evolve away from the host rock signatures with progressive vein growth. Combined with the CO_2-H_2O-NaCl-KCl-H_2S fluid chemistry, Sr isotopes demonstrate that (1) fluid flow in the veins was upward, and (2) the fluid most likely was derived from devolatilization of calcschists. Thus, the hydrothermal fluid ascended at least 10 km vertically. Gold and the hydrothermal fluid, however, have different source rocks. Gold is derived from metaophiolites intercalated with and overlying the calcschists as is indicated by the primitive initial Pb isotope compositions of the gold and cogenetic quartz.

Our detailed study underscores similarities between Tertiary and Archean lode gold deposits, suggesting a common genetic driving force, regional metamorphism. However, the principal sources of the fluid may have changed through time; Mesozoic veins often appear to be genetically linked to graphitic calcschists whereas such rocks are notably scarce in the late Archean. Radiogenic isotopes carefully applied to fluid inclusions and hydrothermal vein minerals have the potential, as no other technique available to date, to confine the selection of possible genetic scenarios for a given hydrothermal deposit.

MELT/FLUID INCLUSIONS IN GRANULITES: CARBONIC METAMORPHISM AND "VAPOR-ABSENT" MELTING.

Touret J.L.R. *(Dept of Petrology and Isotope Geology, Free University Amsterdam, The Netherlands, touj@geo.vu.nl)*

Two major processes are involved during the formation of the lower continental crust, assumed to have an overall granulite composition: fluid-assisted (carbonic) metamorphism and vapor-absent melting. In the first case rocks equilibrate at depth in the presence of an abundant free fluid phase, mostly externally derived (CO_2 and highly saline brines). In the second no free fluids exist: all are bound in mineral structures or dissolved in melts. In fact, both types involve a complex interaction between magmatic (melting) and metasomatic processes, which partly overlap, but can be deciphered by a detailed study of the many inclusions occurring in granulite rock-forming minerals. Much work has been done on inclusions related to fluid-assisted metamorphism, recently emphasizing the importance of highly saline solutions, much less on inclusions obviously related to melting. Melt inclusions have been discovered in various granulites, either regional (Sulawesi, Indonesia) or occurring as xenoliths in recent volcanoes (Eastern Pamir, part of the large Pamir-Himalayas collision belt). The exceptional preservation of inclusions in this case, as well as the information that they can provide on the nature of the lower crust below the Himalayas, make them especially interesting. Primary melt inclusions have been observed in major (kyanite, garnet) as well as in accessory minerals (apatite, zircon), all showing comparable phase relations at room temperature : glass (K-rich rhyodacite composition), heterogeneous glass bubble and eventually one or several microcrystals (mostly silicates). Measured T homogenization are above 1000°C, probably well above the real formation temperature. Some inclusions contain high-density CO_2, corresponding to 1.5 to 1.8 wt% CO_2 in the melt. H_2O-content is lower (0.83 wt %). Th and LREE- contents are low, Y and HREE relatively high (ion microprobe data). Chlorine is very variable, high (up to 0.3 wt %) in massive granulites, not detectable in gneissic granulites.

These results show that "vapor-absent" melting in the lower crust can in fact happen in the presence of free, low H_2O-activity fluids, either locally derived or introduced from an external source. Fluid-assisted and "vapor-absent" metamorphism are two complementary facets of the various processes occurring in the lower crust, involving complicated interaction between rocks, fluids and melts.

3. Fluid Inclusions in Minerals

RELATIONSHIPS INVOLVING MAGMATIC VOLATILES AND ERUPTIVE BEHAVIOR AT MT. VESUVIUS DURING INTERPLINIAN VOLCANIC ACTIVITY (472 A.D. - 1944 A.D.)

Webster J.D. *(Dept. Earth and Planetary Sci., AMNH, jdw@amnh.org)*, Raia F. *(Dept. Earth and Planetary Sci., AMNH, raia@amnh.org)* and DeVivo B. *(Dept. Geophys. and Volcanol., Univ. of Naples, devivo@biol.dgbm.unina.it)*

As part of a systematic study of pre-eruptive magma geochemistry, we have analyzed silicate melt inclusions in clinopyroxene phenocrysts from 9 rock samples (lava and scoria) from Mt. Vesuvius. Most melt inclusions require reheating and quenching to a glass prior to analysis because they contain daughter minerals. Inclusions were analyzed for major, minor, and trace elements by electron and ion microprobes and FTIR. The rock samples are products of two intervals of interplinian volcanic activity: the 472 A.D. - 1139 A.D. medieval period and the 1631 A.D. to 1944 A.D. modern period. These two eruptive periods were interrupted by the 1631 plinian eruption of Vesuvius, and each interval exhibits dramatically different eruptive behavior.

The melt inclusion data provide important constraints on magma geochemistry. The major element compositions of the magmas ranged from phono-tephrite to tephri-phonolite. Although the magmas of the medieval and modern periods were roughly similar in major-element composition, the trace and volatile elements show distinctly different behavior. The compositions of melt inclusions from samples of the modern period are consistent with simple silicate melt evolution (via fractional crystallization) characterized by increasing Cl, S, Rb, Cs, Si, Al, and K and decreasing Ca and Sr. Conversely, melt inclusions from samples of the medieval period show evidence of melt evolution via fractional crystallization, multiple inputs of more-primitive magma, and strong evidence of a volatile phase or phases. Exsolution of at least one volatile phase, before entrapment of the inclusions and before eruption, is indicated by fixed Cl contents, a small range in S contents, and relationships involving other elements soluble in aqueous volatile phases (*e.g.* H_2O, B, Li).

The presence of a volatile phase in medieval magmas, which displayed comparatively greater violence during eruptions, contrasts with the apparent lack of a volatile phase prior to eruption of the modern magmas which erupted much more frequently and in a relatively passive manner.

THE STABLE ISOTOPE COMPOSITION OF FLUID INCLUSIONS IN SPELEOTHEMS: PALAOPRECIPITATION, PALAEOTHERMOMETRY AND CLIMATE CHANGE

Dennis P.F. *(Stable Isotope Laboratory, School of Environmental Sciences, University of East Anglia, Norwich, NR4 7TJ, UK)*

The speleothem archive is unique containing a high-resolution palaeotemperature, palaeoprecipitation and palaeogroundwater isotopic composition record. Most speleothems contain up to 0.1 wt. % of water in the form of fluid inclusions that were trapped in the host calcite at the time of growth. This relict seepage water is closely related to the mean annual meteoric precipitation composition of the cave site during the time of speleothem growth. Provided the speleothem grew in thermal isotopic equilibrium, then measurement of both the inclusion and host calcite compositions can be used to define the palaeoprecipitation isotope composition and cave palaeotemperature. There are, however, considerable technical problems associated with the extraction and measurement of small, sub micro-litre volumes of inclusion water and measuring both the hydrogen and oxygen isotopic compositions to the better than ± 2 (δ^2H) and ±0.2 ($\delta^{18}O$) ‰ precisions that are required for palaeoclimate work.

In this paper I present results from a series of experiments on synthetic inclusions that demonstrate that reliable and robust recovery of inclusion water is possible without modification of its isotopic composition. Using these techniques fluid inclusion data obtained from Holocene speleothems covering a known climate range from northern Norway to southern Europe are used to show that the inclusions accurately record the range of modern meteoric precipitation compositions reported for this region. Finally high-resolution (approximately 100 years) fluid inclusion isotopic records from several speleothems from western England are presented.

The techniques used in this work have wider applications in other areas of fluid inclusion study including low temperature hydrothermal veins, diagenetic studies *etc.*

ASCENDING OR DESCENDING WATER FLOW THROUGH YUCCA MOUNTAIN TUFFS? – FLUID INCLUSION EVIDENCE.

Roedder E. *(Dept. Earth and Planetary Science, Harvard Univ. roedder@shore.net)* and Whelan J.F. *(U.S.Geological Survey, jfwhelan@usgs.gov)*

The potential site for a high-level nuclear waste repository at Yucca Mountain, Nevada, lies within a thick series of volcanic tuffs, more than 300 meters above the present water table. Recent reports (*e.g.* Hill *et al.*, 1995, Dublyansky *et al.*, 1996) claim that (1) *ascending* ground water, possibly at elevated temperature, has in the past risen through the thick unsaturated zone and discharged at the surface, and (2) should this recur in the future, it could flood the repository, with serious consequences.

We have studied the fluid inclusions in vein and vug calcite from the tuffs and find that all unsaturated zone calcite contains abundant inclusions that are full of liquid, and lesser numbers of inclusions that are full of gas mixtures of atmosphere-like composition at about one atm. pressure. These latter probably formed by the trapping of exsolved gas bubbles sticking to the crystals as they grew from a film of cool water (probably ≤ 40°C), infiltrating from the surface and *descending* through the unsaturated zone. Calcite also occurs well below the water-table, deep in the saturated zone; textural, stable isotope, and fluid inclusion evidence indicates that this calcite formed predominantly during a moderate-temperature hydrothermal event at about 10.4 Ma.

Our fluid inclusion studies of numerous samples from the underground workings of the Exploratory Studies Facility and from Yucca Mountain boreholes have revealed no evidence of either hydrothermal activity or ascending fluids during formation of unsaturated-zone secondary minerals, but have confirmed our earlier conclusions that these minerals formed from descending cool waters, above the level of the water table.

TELLURIUM-BEARING FLUID: BEHAVIOR AND MECHANICS OF THE ENRICHMENT & DISPERSION

Cao Z.M. *(Dept. of Min. Res. & Eco. Chengdu Univ. Of Tech., P. R. China, czm@cdit.edu.cn)* and Huang Y. N. *(Bureau of Geo. & Min. Pros., Chengdu, P. R. China)*

Samples were collected from the Dashuigou telluride lode deposit in the mineralizing belt of Te-Au-Ag. By various test methods, such as isotopes, fluid inclusion (Laser microprobe with Raman spectrum), experimental simulation (285°C, 300°C), it suggests that the Te-bearing fluid originated from the upper mantle. Some conclusions follow such as: 1. Telluride occurs in the Kangdian axis and Dadu River gold ore belts. This suggests that the regional geochemical field be characterized by enrichment in tellurium. 2. A transcrustal fracture near the ore district could be a pathway for Degasification (H_2Te) of the mantle. Existence of a high content of CO_2, H_2, BO_3^-, F^-, Na^+ etc. indicates that the ore fluid was rich in mineralizer. 3. Preliminary enrichment in tellurium was got in the residual magmatic melts. $\delta^{13}C_{CO2}$ (5.7‰, mean value of 6 samples) and $^3He/^4He$ (1.21×10^{-5}, mean value of 3 samples) values for the dolomite associated with Te mineralization are similar to those for degasification of the upper mantle. Migration of tellurium could be related to HCO_3^-. The oxyphile character of tellurium enable it to migrate in the form of fluoride or bicarbonate complex and to precipitate with Bi, Au and Ag to form tetradymite-dolomite veins. 4. Tellurium underwent transition from a mineralizer to an ore-forming element. Tellurium acting as mineralizer played an important role in the formation of the precious metals (Au, Ag, Pt, and Pd) deposits. Au and PGE occur in the form of metallic telluride other than metallic sulfides. The fTe_2, fS_2, fCO_2 and the temperature controlled the precious metal mineral facies in the hydrothermal ore deposits. Perhaps a limited recharge of tellurium in the source region was responsible for the predominance of native gold over Au and Ag telluride. Changing from a mineralizer to an ore-forming element, Te was bound together with Bi in residual magma forming tetradymite. 5. Accumulation of tellurium depends upon both pre-enrichment of vaporous H_2Te in an unmixing system and shielding effect of the structural trap. Vice versa, tellurium may be dispersing.

The project was supported by National Nature Sciences Foundation of China.

3. Fluid Inclusions in Minerals

COMPOSITION AND SIGNIFICANCE OF ALKALI- AND HALOGEN-RICH NATURAL CARBONATITE MELTS TRAPPED IN FLUID INCLUSIONS

Bühn B. *(Univ Giessen, Germany, and Kingston Univ, UK, Bernhard.Buehn@geo.uni-giessen.de)* and Rankin A.H. *(Kingston Univ, UK, a.rankin@kingston.ac.uk)*

Carbonatites generally have low alkali contents due to exsolution and expulsion of a fluid phase at late stages of crystallization. The existence of fenitized aureoles around most carbonatites shows that these melts do not represent initial melt compositions and therefore cannot directly prove the generally supposed alkali-rich nature of mantle-derived carbonatite melts.

The alkali-poor Kalkfeld carbonatite complex (Namibia) has expelled a fluid into quartzitic country rocks which is interpreted to represent an alkali- and halogen-rich carbonatite melt. Most fluid inclusions have high densities and consist of abundant daughter minerals like nahcolite, halite, sylvite, burbankite, cryolite, rouvilleite, Ca-Mn-Fe-carbonate, fluorite and Fe-Cu-Zn sulfides (+ alkali feldspars/feldspathoids). In addition, both a CO_2 phase and a Na-K-Ca aqueous phase is present in very variable proportions of a melt-CO_2-H_2O system. This peculiar fluid and mineral assemblage is the result of magma entrapment in quartz crystals, which has preserved the composition of an unexsolved carbonatite melt including alkalis and halogens. This assemblage therefore comprises all fugative and solid components otherwise separated by carbonatitic melt-mineral-fluid fractionation and/or immiscibility. We have investigated this melt system through a geochemical characterization of individual mineral phases, individual inclusions and the bulk carbonatite melt system by microthermometric, SEM-EDX, Synchrotron-XRF, ICP-AES and ICP-MS techniques. The melts represent a very rare case where an unexsolved carbonatite melt can be investigated, and therefore add to the understanding and direct characterization of carbonatitic melt-fluid systems.

FLUID INCLUSION STUDIES OF HYDRATED Mn ARSENATES AND ASSOCIATED MINERALS FROM THE LÅNGBAN MINE, SWEDEN

Jonsson E. *(Dept. of Mineralogy, Swedish Museum of Natural History, Stockholm, Sweden)* and Broman C. *(Dept. of Geology and Geochemistry, Stockholm Univ., Sweden)*

Mineralogical and fluid inclusion (FI) data from the complex Pb-Mn-As-Sb-bearing fissure mineralizations in the Långban mine (59.86°N, 14.27°E), in Värmland, Sweden, suggest formation at low T and P at or close to atmospheric pressure, from low to moderately high saline fluids. FI have been studied in allaktite, sarkinite, barite and calcite. The T_h (g->l) of 2-phase FI in calcite and barite range between 70-165°C with the majority around 125°C. $T_{m(ice)}$ range between -19 to -3°C, *i.e.*, 21.7-5 eq. wt% NaCl), with the majority between c. 10-14 eq. wt% NaCl. Eutectic melting (T_{fm}) temperatures of ice in the range -25 to -40°C suggest a complex composition with NaCl, $MgCl_2$ and possibly $CaCl_2$ as the main dissolved components. Primary 2-phase (g+l) FI in allaktite ($Mn_7(AsO_4)_2(OH)_8$) exhibit T_h (g->l) between 78-103°C; $T_{m(ice)}$ range between -3 to -0.5°C, *i.e.*, 5-0.9 eq. wt% NaCl. T_s range between -40 to -55°C and T_{fm} -40 to -52°C. Primary 2-phase (g+l) FI in sarkinite ($Mn_2(AsO_4)(OH)$) exhibit T_h (g->l) between 89-99°C with the majority around 90-94°C. $T_{m(ice)}$ range between -0.1 to -1.7°C, *i.e.*, salinities of 0.2-2.9 eq. wt% NaCl. Eutectic melting (T_{fm}) temperatures of ice lie in the interval -33 to -44°C (with Ts -44 to -57°C). Eutectic melting data from FI in the Mn arsenates suggest a fluid composition different than FI in calcite and barite, possibly dominated by $CaCl_2$ as a dissolved component

FLUID INCLUSION AND STABLE ISOTOPE EVIDENCE FOR FLUID MIGRATION DURING METAMORPHISM IN THE PRIESTLEY METAMORPHIC COMPLEX (O'KANE CANYON, NORTH VICTORIA LAND, ANTARCTICA)

Frezzotti M.L., Dallai L., Giorgetti G. *(Dip. di Scienze della Terra, Univ. of Siena, frezzotti@dst.unisi.it)* and Sharp Z.D. *(Dept. of Earth and Planetary Sciences, Univ. of New Mexico)*

The present study was performed in syn-metamorphic quartz ± calcite in upper-greenschist facies and lower-amphibolitic facies rocks of the Priestley metamorphic complex (western Wilson Terrane), that crop out in the O'Kane Canyon area (northern Victoria Land), inland of Terra Nova Bay Italian station. Fluid inclusions, fluid-mineral equilibria and stable isotope studies have been used to derive pressure, temperature, composition and origin of fluids during low-P high-T metamorphic events (Cambrian-Ordovician Ross Orogeny).

Fluid inclusions are preserved in veins in two localities. Two veins (MR17 and 18) were sampled in a C-bearing metapelite belonging to the upper-greenschist facies; two veins (MR19 and 25) were sampled in lower-amphibolitic facies C-bearing marbles and metapelites. A single grouping of structurally controlled early fluid inclusions have been recognised in each vein set. In lower-amphibolitic facies rocks, trapped fluids are H_2O-CO_2-CH_4 mixtures (Fluid A: 50 mole % CO_2 and 4 mole % CH_4) in marbles, and H_2O-CO_2-N_2 mixtures (Fluid B: 50 mole % CO_2 and 10 mole % N_2) in schists. Entrapment of fluids with different compositions occurred during vein formation, at about 500 - 550°C and 3 - 3.5 kbars fluid pressure. These inclusions underwent re-equilibration during cooling that resulted in density increase, without change in composition. In lower-grade schists, veins were formed from a single H_2O-CO_2-CH_4 fluid phase (Fluid C: 30 - 60 mole % CO_2 and 4 mole % CH_4) at 350 - 400°C and 2 kbars fluid pressure.

Vein formation occurred in the Priestley metamorphic complex during the waning stages of metamorphism, followed by near isobaric cooling at metamorphic depths. Stable isotopes indicate an external origin for aqueo-carbonic mixtures (Fluid A and C), ranging from metamorphic to meteoric with considerable fluid chemistry control by the local granitic wall-rocks. H_2O-CO_2-N_2 fluids (Fluid B) likely represent independent internally-derived fluids.

DIAGNOSTICS OF CAPTIVE MINERALS IN INCLUSIONS

Komov I. L. *(State Sci. Centre of Envir. Radiogeochemistry, Kiev, Ukraine. CENTER@radgeo.freenet.kiev.ua)*

It is known that the diagnostics of captive mineral in multiphase inclusions is a labour-consuming operation (optical and thermal methods are used).The inclusions can be easily diagnosed under ionising irradiation. In this case NaCl inclusions are coloured yellow, KCl are lilac-coloured or dark-blue, NaF inclusions are of brown colour, which indicates that captive minerals can be diagnosed without opening the inclusions. Visually it is possible to discern the forms of existing hard inclusions at a high reliability and minimum energy, to determine with sufficient precision the availability of even a minor quantity of NaCl in solutions, and in rather simple in form inclusions to state the concentration thereof. Used for investigation are transparently polished sections, slices or chips of minerals without polishing. Investigated in plates by use of an optical microscope are gas and liquid inclusions and the character of distribution thereof. Then the samples are irradiated and the captive minerals are diagnosed by use of reference phases. Large inclusions (>10 μm) are extracted from vacuoles, after pressed into a special pot, irradiated and subjected to inclusions diagnosis. In the complex with irradiation it is possible to conduct the neutron-activation analysis of cylindrical specimens (height 10 μm, diameter 9 μm) drilled out of the samples. The specimens are held for a week and then again irradiated with neutrons within 3 hours where upon the contents of K, Na, Br and As are fixed on the spectrometer. By use of IR-spectroscopy the main components (H_2O, OH -group, CO_2) in mineral inclusions are determined.

Aside from minerals diagnostics, gamma-irradiation permits to obtain reliable information about crystal growth conditions.

3. Fluid Inclusions in Minerals

MULTI-STAGE FLUID MOBILIZATION IN THE FOOTWALL UNITS OF THE SUDBURY IGNEOUS COMPLEX AND THE ROLE OF FLUIDS IN THE FORMATION OF VEIN-TYPE Cu-Ni-PGE DEPOSITS

Molnár F., Watkinson D.H., Everest J. and Jones P.C. *(Dept. Earth Sci., Carleton Univ., fmolnar@ccs.carleton.ca)*

Vein-type and disseminated sulfides occur in Sudbury Breccia hosted by the footwall units as far as several hundred metres from the magmatic segregational sulfide bodies near the base of the Sudbury Igneous Complex at the Lindsley 4b and Little Stobie deposits along the South Range, and McCreeady-East and West deposits along the North Range. Major minerals in these ores are chalcopyrite, pyrrhotite, pentlandite, millerite, and bornite. Pd-Pt-Bi-Te-As minerals, hessite, electrum, native silver, bismuthinite, cubanite, Ni-Bi-sulfides, magnetite, galena, and sphalerite are the most common accessories. Hydrous silicates have elevated Cl-content. Type 1, NaCl-CO_2-H_2O fluids in inclusions of rock-forming quartz are related to the late stages of the contact metasomatic recrystallization of the Levack Gneiss Complex. These fluids underwent immiscibility during pressure decrease from 3 to 0.5 kbars at 300-350°C (McCreedy-East and West deposits). Type 2, NaCl-$CaCl_2$-H_2O fluids in primary inclusions of K-feldspar are related to the K-metasomatic alteration of the Murray Granite between 360-410°C (Lindsley 4b deposit). Type 3, NaCl-$CaCl_2$ ±(KCl-$FeCl_2$-$MnCl_2$-$BaCl_2$-PbCl)-H_2O fluids occur in primary and secondary inclusions of quartz associated with sulfides in all deposits. Minimum temperatures for these fluids are 200-400°C. Type 4, NaCl-$CaCl_2$-H_2O fluids in secondary inclusions of quartz also occur in all studied deposits. Their trapping temperatures are below 200-240°C. Type 3 and Type 4 fluids were ocasionally immiscible with carbonic fluids in the South Range. Fluids of all stages are characterized by 20-50 wt% salinity; lower salinities also occur in the carbonic-aqueous inclusions of the South Range. Type 3 fluids post-dating Type 1 and Type 2 fluids can be related to the formation of the Cu-Ni-PGE enriched vein-type ores. Type 4 fluids are post-ore basinal fluids.

GEOCHEMICAL FEATURES OF FLUID INCLUSIONS OF GRANITIC ROCKS IN JAPAN

Sawaki T., Sasada M. and Sasaki M. *(Geothermal Research Department, Geological Survey of Japan, sawaki@gsj.go.jp)*

We have studied fluid inclusions in quartz mainly from granitic rocks (pegmatites) in Japan, additionally from metamorphic rocks, in order to elucidate geochemical features of volatiles released from granitic magma during crystallization. Gases of the inclusions were analyzed by a quadrupole mass spectrometer and a capacitance manometer. In granitic rocks in Japan, (1) aqueous two-phase liquid-rich, (2) aqueous two-phase vapor-rich, (3) monophase liquid, (4) liquid CO_2-bearing aqueous, and (5) daughter mineral (*e.g.* halite)-bearing multiphase inclusions occur. Aqueous two-phase liquid-rich inclusions are common in all granitic rocks, and liquid CO_2-bearing inclusions occur in Cretaceous ones. Coexistence of daughter mineral-bearing and vapor-rich inclusions are frequent in Tertiary granitic rocks, and indicates that these inclusions trapped two-phase fluids. Granitic rocks whose fluid inclusions trapped two-phase fluids were probably emplaced at shallower than 5 km in depth in the crust, based on a phase diagram of NaCl solution and solidus of granitic rocks.

Gas analyses show that H_2O is the main component of all fluid inclusions (88 mol% <), and that CO_2 is the main gas for almost the samples (12 mol% >) with subordinate amounts of N_2 (1.9 mol% >), CH_4 (2.8 mol% >) and Ar (0.0004 mol% >), except for inclusions in pegmatitic quartz from the Hidaka belt where granitic magma was probably produced by anatexis of metamorphic rocks. Fluid inclusions from the Hidaka belt are characterized by relatively high CH_4 (0.16-9.6 mol%) and N_2 (0.03-1.8 mol%) contents, compared to CO_2 (0.09-0.94 mol%). Fluid inclusions from S-type granitic rocks in the Outer Zone of southwestern Japan also have slightly high contents of CH_4. The high CH_4 and N_2 contents possibly related to the partial melt of sediments. The variation of CO_2/CH_4 ratios may reflect the difference of fO_2 around the granitic rocks where the fluids flew. CO_2/CH_4 ratios of inclusions from magnetite-series granitic rocks are slightly higher than those from ilmenite-series ones. Magnetite-series granites are thought to be formed under higher fO_2 condition than ilmenite-series. The gas ratios are consistent with it, and the analytical results suggest that gas compositions of fluid inclusions are probably controlled by source of granitic magma.

CRYOGENIC RAMAN SPECTROSCOPIC INVESTIGATIONS OF FLUID INCLUSIONS IN THE NaCl-$CaCl_2$-H_2O SYSTEM

Walker R.T. and Samson I.M. *(Dept. of Earth Sciences, University of Windsor, ims@uwindsor.ca)*

We have characterized the solid assemblages present in frozen, natural fluid inclusions and synthetic fluids using Raman spectroscopy in order to test whether this method can yield useful information about the composition and phase behaviour of aqueous fluid inclusions. Specifically, we were interested in characterizing the presence and abundance of a $CaCl_2$ component, which is commonly hypothesized as being responsible for low eutectic temperatures, and as a justification for modelling phase equilibria in the system NaCl-$CaCl_2$-H_2O. In order to obtain spectra which represent the bulk fluid composition, analyses were carried out on fine-grained aggregates of ice and hydrate, rather than large hydrate crystals. After initial, rapid freezing, most inclusions and synthetic solutions yield spectra that indicate the presence of hexagonal ice, but not salt-hydrates. On warming, the fluids commonly exhibit a phase transition between about -70 and -50°C, that is manifested as a wave of crystallization or coarsening and darkening of the inclusion. Raman spectra acquired after immediate cooling, indicate that this transition represents hydrate crystallization. As this phase transition could be mistaken for eutectic melting in natural inclusions, some low eutectic temperatures reported in the literature may be erroneous, and in such cases, additional components may not be required to explain the observed phase behaviour. Frozen inclusions from a rare-element granite pegmatite and the Mt. Pleasant W-Mo deposit contain detectable ice + hydrohalite ± antarcticite. Mathematical modelling and comparison with the synthetic fluids indicate that other hydrates were absent or below detection and that NaCl > $CaCl_2$. These results are supported by EDS-decrepitate analysis which also indicate small amounts of K in some inclusions. Modelling of phase equilibria in these inclusions using the NaCl-$CaCl_2$-H_2O system therefore seems justified.

PYROCHROMATOGRAPHY INCLUSIONS IN SALTS

Shanina S.N. *(Institute of Geology, RAS Ural Division, Russia, common@geo.komi.ru)*

Pyrochromatography is one of the most perspective methods of research of inclusions in minerals. The method includes sample destruction and extraction of inclusion content by heating. Our equipment is gas chromatograph "Chrom-5" and self-made attachment for breaking down inclusions and transfer of the released gases into gas chromatograph. The method is suitable to determine volatile oxygen and oxygen-free compounds of basic elements of organic chemistry (carbon, hydrogen, nitrogen, rarely sulphur) and to compare the composition of the gases by step heating.

It is known that organic inclusions up to oil are widespread in natural salts. Their origins vary from syngenetic to epigenetic. Our task is to study the types of organic inclusions present in salts, their origins and evolution in minerals from different salt deposits. Moreover, it is necessary to establish whether there are any differences in composition of volatile gases in the salts overlying oil and gas accumulations. Of special interest is study of organic inclusions in minerals from the Komi Republic salt deposits (Seregovo, Kechmes) where such kind of investigations have never been carried out.

Chromatographic analyses of organic inclusions were carried out on halite crystals from several salt deposits: Kechmes (Komi), Klodava (Poland), Karvakh (Yemen). The analyses were used to determine the presence and specify the nature, quantities and location of organic substance.

3. Fluid Inclusions in Minerals

FLUID INCLUSION STUDY IN THE LAS TRES VIRGENES, B.C.S. (MEXICO): EVIDENCES OF A MAGMATIC UPRISING FLUID.

Viggiano G.J.C. *(C.F.E., Exploración, UMSNH, Facultad de Ingenieria Civil; UNLA, Ingeniería de la Construcción, Morelia, Mich. México)*, González P. E. and Izquierdo M. G. *(IIE, Cuernavaca, Mor.,México, geoexplo@mich1.telmex.net.mx)*

The study of fluid inclusions in minerals has long been a useful tool in investigating geothermal field to:

a) Fluid types and their relation to the processes of boiling and mixing.
b) Compositional variations of chloride fluids.
c) Interpretation of the Th data: thermal history.
d) Boiling points constraints on temperature profiles.

A good example is the Las Tres Vírgenes geothermal field which lies at the center of Baja California, México and is geologically installed in granodioritic rocks (≈84 m.y. old) which are the aquifer rocks overlaied by other complex sequence constituted by sandstones, andesites, *etc.* The whole pile of rocks displays variables ranks and predominantly low intensities of alteration minerals represented by quartz, calcite, chlorite, montmorillonite, illite, epidote, *etc.* as result of water-rock interaction. The percolating fluid according to this mineralogy is near neutral Ph alkali-chloride. The main mineral deposit style is the replacing meaning therefore low permeability at the time of mineral formation. The scientific interdisciplinary intervention has estimated about 25 MW as proven reserve. In order to contribute on fluid evolution knowledge a fluid inclusion study in well cuttings was undertaken. Based upon this study is roughly stated:

The parental (*i.e.* unboiled or better non boiled) fluid is typical of orthomagmatic deposits in its pneumatolithic-hydrothermal state with ranging temperatures between 250-300ºC and with even 30000 ppm TDS. This fluid has given place to a forced up-flow, due to its low permeability, which is greisenizing (presence of tourmaline and mica among other minerals) the nearest rock to the skarn, that is, the granodiorite. The meteoric water, also identified in the fluid inclusions according to the salinities, could have infiltrated during the forced convective flow and its presence can be verified in the diluted fluid inclusions of relatively high temperature which frecuency is subordinated respect to those of high salinity. This fact, however, does not implies a low availability of fluid as for mineralization: let's recall the huges ore deposits disseminated worlwide, but it does as regards geothermal exploitation because the obvious restrictions of meteoric recharge toward the reservoir.

FLUID INCLUSION STUDY ON THE SHIBANGOU GOLD ORE DEPOSIT, XIXIA, HENAN, P.R.CHINA

Wei L. and Dehui Z. *(Faculty of Earth Resources, China Univ. of Geosciences, Wuhan, P.R.CHINA,430074, ZYb@ cug. edu. cn)*

The Shibangon lode-type gold ore deposit Xixia, Henan Province, P.R.China, is hosted in ductile-brittle shear zones. Fluid inclusions characteristics, and natures of ore-forming fluids were deduced by 53 samples in this area.

Microthermometry of fluid inclusions in quartz indicates five types of inclusions:

(1) two phase gas-rich inclusions (Type I)
(2) two phase liquid-rich inclusions (Type II)
(3) polyphase inclusions that contain daughter crystals (Type III)
(4) secondary two phase liquid-rich inclusions (Type IV)
(5) secondary one phase liquid inclusions (Type V)

Type I inclusions have homogenization temperatures of 330°C to 350°C. Type II inclusions have homogenization temperatures of 170°C to 310°C. Type III inclusions have homogenization temperatures of 278°C to 371°C. Type IV inclusions have homogenization temperatures of 130°C to 230°C. Type II inclusions have a salinity range of 4.4 to 13.6 NaCl equiv. Wt%. Type III inclusions have a salinity range of 36.2 to 43.0 NaCl equiv. Wt%. Type IV inclusions have a salinity range of 4.6 to 11.3 NaCl equiv. Wt%. Type V inclusions have a salinity range of 2.3 to 6.5 NaCl equvi. Wt%. Ore-forming fluids are basically of the NaCl-KCl-H_2O system.

The most striking character of the fluid composition is that in cations, K^+ and Na^+ are most numerous and in anions, F^- is slightly more than Cl^-. In gas phase, H_2O is dominant, followed by CO_2. δD_{H2O} values of inclusion in the range of -24.0 to -37.3 ‰, and δO_{H2O} in the range of -2.49 to 1.99 ‰, and $\delta^{13}C_{CO2}$- values of CO_2 gas in inclusions are -11.12 to -14.59 ‰. This suggests that ore-forming fluid was a mixed fluid.

THE FLUID INCLUSIONS RESEARCHES ON THE YINSHAN POLYMETALLIC DEPOSIT, JIANGXI PROVINCE, CHINA

Dehui Z. *(China Univ. of Geosciences, Beijing, 100083, P.R.China, Zyb@cug.edu.cn)* and Wei L. *(China Univ. of Geosciences, Wuhan, 430074, P.R.China,)*

The Yinshan deposit, which is one of the large-scale Cu-Pb-Zn-Au-Ag polymetallic deposit, is located 2km north of Dexing, Jiangxi Province, China. In this paper, new advances of fluid inclusions research of Yinshan deposit have been presented. The study shows:

1. In polymetallic ore veins, some fluid inclusions of halite daughter minerals-bearing have been discoveried.

2. The fluid inclusions data may be divided into two groups, which is respectively high salinity and low salinity group. The salinity of high saline fluid inclusions vary from 30 to 45 wt% NaCl equivalent and the salinity of low saline fluid inclusions vary from 2.86 to 14.4 wt% NaCl equivalent.

3. There are the fluid inclusions of liquid-CO_2 -bearing in polymetallic ore veins.

4. The homogenization temperatures of fluid inclusions range from 95°C to 520°C displaying a very wide range.

5. In the plot of homogenization temperature and salinity, there are two group of data and the curvilinear correlation between homogenization temperature and salinity.

6. A southwesterly and a upwards trend of decreasing salinity and homogenization temperatures are indicated.

From the points mentioned-above, the conclusions can be drawn as follows: The high estimated salinities of fluid inclusions indicate that the hotter hydrothermal fluid was most consist with a magmatic origin. The two group of data of temperature and salinity has been attributed to mixing of a hot, saline fluid with a cool, dilute fluid. It is inferred that it is possible there is a concealed igneous body and a concealed porphyry copper deposit at depth of the deposit.

VOLATITLES IN PRE-ERUPTED MAGMAS AND THEIR POSSIBLE CONTRIBUTION TO A SEAFLOOR HYDROTHERMAL SYSTEM IN THE MANUS BACK-ARC BASIN, WESTERN PACIFIC

Yang K. and Scott S.D. *(Dept. of Geology, Univ. of Toronto, e-mail: kaihui@quartz.geology.utoronto.ca)*

The degassing of magma may have contributed significant amounts of volatiles to the formation of the PACMANUS massive sulfide deposits in the eastern Manus back-arc basin, western Pacific. Microanalysis has been carried out on melt inclusions in phenocrysts and the matrix glass of the volcanic rocks ranging in composition from basalt, basaltic andesite, dacite to rhyolite. The glass of the melt inclusions has relatively high and homogenous concentrations of H_2O (7.41 ± 0.68 wt %) and Cl (0.23 ± 0.04 wt%). In contrast, the matrix glass is extremely inhomogenous in the concentrations of H_2O (4.47 ± 2.33 wt%) and Cl (0.15 ± 0.15 wt%). Relatively high concentrations of Cl are noted in the dacite and rhyolitic glass. Unlike H2O and Cl, F is highly variable with no significant concentration difference between the glass of melt inclusions (0.05 ± 0.06 wt %) and that of the matrix (0.06 ± 0.07 wt %). The major element composition of the glass in the melt inclusions and of the glass in the matrix are similar.

The high concentrations of H_2O and Cl in the melt inclusions are compatible with those of subduction-related volcanic rocks elsewhere and are typical of pre-erupted magmas at convergent plate margins. The remarkable differences in the volatile contents between the glass of the melt inclusions and the matrix glass of the PACMANUS volcanic rocks suggest that significant amounts of magmatic volatiles were released during the degassing process. This is further supported by the presence of an ore metal-rich volatile phase in bubbles in the melt inclusions and in vesicles in the matrix glass. Such a magmatic fluid may have been contributed to the hydrothermal systems that are presently forming massive sulfide deposits in the Manus back-arc basin.

3. Fluid Inclusions in Minerals

A BRIEF REVIEW OF DECREPITATION METHOD DEVELOPMENT DURING THE PAST 50 YEARS

Zhili H. *(#FKDept. of Geol., Univ. of Science and Technology Beijing, licylxj@public.bta.net.cn)*

The University of Toronto is the birthplace of the decrepitation method (DM). The phenomenon and the origins of decrepitation in heated minerals were studied in the first half of the last century. Before 1908, the problems were studied intermittently.

However, the DM of temperature measurement of mineral inclusions was invented by Scott in Toronto in 1948. A series of papers about DM was published by Smith, Peach and other young researchers from the University, during the development of DM. The method spread rapidly to Europe, Asia and elsewhere at the beginning of the 1950s. Scientists from the USSR were especially interested in the method. Automatic thermo-pressure decrepitators under vacuum was made in the USSR (1966) and China (1981) for elimination of sound interference. The results of studies from USSR and China indicated that this method has many uses, although it has some demerits in geothermometry.

It is very useful in prospecting for new ore deposits / blind ore bodies, and can also be applied to study the genesis, history and metamorphic processes of minerals. The steaming- through halo method for prospecting ore deposits and blind orebodies suggested by Ermakov and the 12-channel automatic decrepitators were made in USSR (1966). The new prospecting method spread to China in the same year, and the primary steaming-through halo was discovered in a skarn iron deposit. 4-channel automatic thermosonic decrepitators were also made in China (1981) as proposed by the author. Many studies about practical decrepitators, elimination of interfering factors and the application of the DM for mineral prospecting have been conducted by geologists from the former USSR and China. In recent years, data have been collected in the CIS at a rate of ~50,000 decrepitation measurements per year. Based on the characteristics of decrepitation graphs and related data, a decrepitation parameter model for gold exploration has been established by two Chinese geologists and some blind gold orebodies have been found by application of the method. For exploration applications, DM will continue to develop as follows; (1) comprehensive analysis of accumulated data to establish new models, and (2) design and deployment of portable, rapid, high-quality automatic decrepitators. The author believes that the people will never forget the pioneers' names and their distributions.

4. Deep Earth Mineralogy

X-RAYS ON DEEP MANTLE AND CORE DYNAMICS

Hemley R.J. and Mao H.K. *(Geophysical Laboratory and Center for High-Pressure Research Carnegie Institution of Washington, Washington, D.C. 20015).*

Recent developments and applications of diamond-anvil cell synchrotron x-ray diffraction techniques are providing new views of the mineralogy, structure, dynamics of the deep mantle and core. Laser-heating experiments indicate that the partitioning of Fe and Mg between coexisting $(Mg,Fe)SiO_3$-perovskite and (Mg,Fe)O-magnesiowüstite strongly depends on pressure, temperature, bulk Fe/Mg ratio, and ferric content. Ferrous iron in the perovskite phase is highly depleted at conditions pertinent to the top of the lower mantle and gradually increases at greater depth. The multivariable dependence of the partitioning leads to a continuous variation of Fe content in perovskite along the geotherm, which has important implications for geochemical and geophysical dynamics of the mantle. The perovskite stability field expands relative to magnesiowüstite + SiO_2 on increasing pressure and temperature, with α-PbO_2-type silica likely to be stable at the highest pressures. The rhombohedral phase found previously in FeO has been tracked as a function of pressure in magnesiowüstites, and high P-T transitions in Fe_2O_3 have been characterized. New insights on the dynamics of the core, including its anisotropy and super-rotation, have been obtained from laser heating and radial x-ray diffraction techniques. Double-sided laser heating studies to above 100 GPa show that (hcp) ε-Fe exhibits a large P-T field of stability field. Radial x-ray diffraction measurements carried out at room temperature to above 200 GPa have been used to constrain the elasticity, rheology, and sound velocities of ε-Fe at core pressures. The elastic anisotropy is larger than expected from theoretical calculations, but the observed orientation dependence of differential strain may indicate a variation of stress among individual grains due to basal-plane slip.

Aggregate velocities, especially the shear, are significantly higher than those of the inner core. The results suggest large temperature effects on the shear velocities, additional low velocity phases, and/or complicated textures in the inner core.

ELASTIC PROPERTIES OF POLYCRYSTALLINE PYROPE-MAJORITE GARNETS AT HIGH P & T, AND THE MINERALOGICAL COMPOSITION OF THE EARTH'S MANTLE

Gwanmesia G.D., Chen G., Liu J. and Liebermann R.C. *(Mineral Physics Institute and Center for High Pressure Research, SUNY at Stony Brook, gwanmesia@sbmp04.ess.sunysb.edu)*

Elastic properties of the high pressure phases of mantle minerals at high pressure and high temperature are essential for investigating the mineralogical compostion of the Earth by comparing laboratory velocity and density models for the Earth with the seismic velocity and density profiles of the transition zone of the Earth (400-700 km) obtained from earthquake studies. In particular, majorite, a garnet-structured high pressure phase of pyroxene is an important constituent of the upper mantle and forms extensive solid solution with aluminous garnet. Dense isotropic polycrystalline garnet specimens (Py_{100}, $Py_{40}Mj_{60}$, $Py_{20}Mj_{80}$, Mj_{100}, where Py = $Mg_3Al_2Si_3O_{12}$; Mj = $Mg_4Si_4O_{12}$) within the pyrope-enstatite join have been hot pressed in a 2000 ton uniaxial split sphere anvil apparatus (USSA-2000). These specimens have bulk densities within 0.3 % of x-ray densities and exhibit ambient compressional and shear wave velocities within 0.2% of the Hashin-Shtrikman bounds calculated from their single crystal elastic moduli. Sound wave velocities have been measured to 8 Gpa, at room temperature on these polycrystalline garnet specimens in a 1000-ton uniaxial split-cylinder-anvil high pressure apparatus (USCA 1000), using phase comparison ultrasonic interferometry. Acoustic compressional (Vp) wave and shear (Vs) wave travel times have also been measured for the polycrystalline specimens at simultaneous high pressures (to 8 Gpa) and high temperatures (to 1000 K) using phase comparison ultrasonic interferometry adapted for use with a DIA-type cubic anvil high pressure apparatus (SAM-85) installed at the National Synchrotron Light source (X17B1 beam line) of the Brookhaven National Laboratory, which allows simultaneous measurement of the travel times of acoustic waves and synchrotron x-ray diffraction spectra from both the sample and NaCl, from which the unit cell volumes for the sample and cell pressures at P and T are retrieved. We report results of the elastic wave velocities for the garnet polycrystalline specimens in the pyrope garnet majorite solid solution as a function of pressure and temperature, and compare the new elasticity data to acoustic data for other compositions in the pyrope-majorite solid solution series. We also discuss the implication of the new results on the seismic velocity gradients in the Earth's transition zone.

THERMOELASTIC PROPERTIES AND CRYSTAL STRUCTURE OF $MgSiO_3$ PEROVSKITE UP TO 86 GPA AND 2700 K.

Fiquet G., Dewaele A. *(Ecole Normale Supérieure de Lyon, Lyon 69364 Cedex, gfiquet@ens-lyon.fr)*, Andrault D. *(Institut de Physique du Globe de Paris, Paris 75252 Cedex)*, Kunz M., LeBihan T. and Häusermann D. *(ESRF, Grenoble 38043 Cedex)*

The chemical composition of the lower mantle is estimated on the basis of a reliable equation of state for $MgSiO_3$ perovskite, obtained by an *in situ* X-ray diffraction study up to 86 GPa and 2700 K. Angle-dispersive X-ray diffraction experiments were carried out at high pressure and temperature in a laser-heated diamond-anvil cell at the ID30 beamline of the ESRF (Grenoble, France). A doubly focused monochromatic X-ray beam at a wavelength of 0.4255 Å was used in association with image plates to collect data over a 2θ interval from 4 to 25°.

Silicate perovskite $MgSiO_3$ samples were synthesized (1) from synthetic $MgSiO_3$ enstatite, (2) from synthetic $MgSiO_3$ glass, mixed with platinum powder and transformed at high-pressure and high-temperature into silicate perovskite $MgSiO_3$. These starting materials were loaded cryogenically in argon, used as pressure transmitting medium. Temperatures were measured from the analysis of the sample thermal emission and pressures inferred from the PVT equation of platinum, used as an internal pressure calibrant.

Le Bail profile refinements were applied to the diffraction patterns, in order to obtain reliable high-pressure high-temperature cell parameters for $MgSiO_3$ perovskite as well as for the pressure calibrant. Rietveld structural refinements were achieved on selected pattern at these extreme pressure and temperature conditions, yielding detailed structural information on these compounds. Data analysis allowed us to identify a set of thermoelastic parameters, that are used to constrain the compositional model of the Earth's lower mantle. The comparison with the density and KT profiles calculated for PREM model is satisfactory for a lower mantle composition close to 83vol% $(Mg_{0.93}Fe_{0.07})SiO_3$ and 17vol% $(Mg_{0.79}Fe_{0.21})O$, thus making a pure perovskite lower mantle very unlikely.

ELECTRICAL CONDUCTIVITY OF MANTLE MINERALS AND THE TEMPERATURE OF THE EARTH'S LOWER MANTLE

Brodholt J.P. and Dobson D. *(Dept. of Geological Sciences, University College London)*

Thermal profiles of the Earth's upper mantle are well constrained from geothermometry, heat flow measurements, and the temperature of the olivine-spinel-post spinel phase transitions. In contrast lower mantle temperatures are poorly constrained with estimates of temperatures at 700 km differing by as much as 1000 K and at the base of the mantle by more than 2000 K. Such widely varying models have very different implications for Earth processes and properties.

Electrical conductivity measurements could, in principle, be used to distinguish between different lower mantle thermal models provided a) the geophysically measured response functions have sufficiently high resolution and b) that high quality laboratory measurements for the appropriate minerals exist.

We present new laboratory measurements on the electrical conductivity of upper and lower mantle minerals. We also present the results of forward modelling the Earth's geomagnetic response functions using these data together with different geotherms. Although the results are not sensitive enough to constrain the deeper lower mantle geotherm, they are sensitive to temperatures in the upper part of the lower mantle (700 to 1500 km). We find that the predicted response is only consistent with the Earth's observed geomagnetic response if a cool geotherm is used.

4. Deep Earth Mineralogy

FORMATION OF (Mg,Fe)SiO3 ILMENITE (AKIMOTOITE) AND PEROVSKITE IN A SHOCKED CHONDRITE

Tomioka N. and Fujino K. *(Division of Earth and Planetary Science, Hokkaido University, fujino@cosmos.sci.hokudai.ac.jp)*

Natural $(Mg,Fe)SiO_3$ ilmenite and perovskite were identified in the shock induced veins in the Tenham meteorite. They were adjacent to clinoenstatite in pyroxene fragments and have the same composition (Fe/(Mg+Fe)≈0.21) with clinoenstatite. This indicates that both phases have converted from enstatite in a solid state transition by the shock event.

Ilmenite grains have two morphologies, columnar (<1.4 μm in length) and granular (<0.4 μm), and columnar grains have a topotaxial relationship with clinoenstatite, $(0001)_{ilm}//(100)_{cen}$, indicating shear transformation. No decomposed phases of β- or γ-spinel and stishovite were observed between clinoenstatite and ilmenite. Perovskite grains are granular (~0.2 μm) and easily become amorphous by the electron beam irradiation.

Higher iron contents in both ilmenite and perovskite than those experimentally obtained may indicate that both phases have metastably transformed from enstatite by the shock event. Existance of perovskite and majorite, which is thought to have crystallized from the melt, indicates a generated pressure and temperature in excess of ~23 GPa and ~2000°C.

The proposed name akimotoite for silicate ilmenite, in honor of Prof. S. Akimoto, has been approved by the Commission on New Minerals and Mineral Names, International Mineralogical Association.

MINOR AND TRACE ELEMENTS IN EARTH'S MANTLE MINERALS AND MELTS: FROM MICROSCOPIC SUBSTITUTION MECHANISMS TO PARTITIONING

Reynard B. *(Laboratoire de Sciences de la Terre CNRS UMR 5570, ENS Lyon, France, breynard@ens-lyon.fr)*

The knowledge of the microscopic mechanisms of minor and trace element incorporation in both crystalline and liquid oxides is a clue to the understanding of their geochemical behaviour in the Earth's mantle. This behaviour can be rationalised in terms of their various bonding properties and various other electronic contributions such as the ligand field stabilisation energy for transition elements. These properties can be used to quantify the free energies of trace element incorporation in crystals and melts through simple models, and to quantify partition coefficients between various phases. This microscopic approach requires that all terms be estimated, either through modelling or through spectroscopic measurements. They can then be used to account for, to test and to extrapolate the macroscopic petrologic data on partition coefficients in natural or experimental systems. In order to resolve some of these issues, various spectroscopies can be applied to provide information about the local environment of the trace element and its stabilisation by the ligand field. The possibility for obtaining information on the crystal-chemistry of trace elements in mantle minerals and glasses from luminescence spectroscopy is tested, on the example of Cr^{3+}, which yields an intense luminescence in the near infrared to red. It may thus be studied even at the very low concentration levels relevant to mantle materials. For high ligand field, it presents narrow luminescence lines, which allow the resolution of different local environments. At low ligand fields, it presents broad bands which position is directly related to the ligand field. Transition between these two regimes may be obtained, in favourable cases, by varying the pressure and temperature, which allows to study both the detailed structural environment of Cr^{3+}, and its ligand field stabilisation energy as a function of pressure. The results obtained on Cr^{3+}-doped mantle minerals (spinel, pyroxenes, olivine) and glasses used as analogues of melts are described. They are used to discuss the substitution mechanisms in crystals and to model the high pressure evolution of mineral/melt partition coefficients which is compared to available experimental data. Some of the results obtained for Cr^{3+} can also be generalised to other trace elements, especially those concerning the effective charge compensation mechanisms in crystals.

TRANSITION METAL OXIDES AT HIGH PRESSURES: MAGNETIC AND STRUCTURAL PHASE TRANSITIONS

Cohen R.E. *(Geophysical Laboratory and Center for High Pressure Research, Carnegie Institution of Washington, cohen@gl.ciw.edu)*

A full and quantitative understanding of the transition metal oxides (*e.g.* FeO, MnO, CoO, and NiO) has remained elusive, and still forms one of the most difficult and important problems of condensed matter physics and mineral physics. An understanding of these materials is crucial not only in developing a fundamental understanding of materials, but also for geochemistry and geophysics since electronic and magnetic transitions will change their physical properties and the partitioning behavior of minor and trace transition metal ions. Study of these materials under pressure also will separate useful predictive theories from those which work fortuitously at zero pressure, or cannot predict high pressure behavior. A rich phase diagram is expected at high pressures, including Mott or charge transfer transitions (delocalization transitions), high-spin low-spin transitions, structural phase transitions, and metal-insulator transitions.

We have performed extensive electronic structure computations on these materials and find high-spin low-spin transitions at high pressures (Cohen *et al.*, *Science*, **654**, 1997). Observations of structural transitions to the NiAs-type structure in FeO (Fei and Mao, *Science*, **266**, 1678, 1994) have been reinterpreted in terms of a polytype between normal and anti-NiAs with Fe in the As site and O in the Ni site (Mazin et al., Am. Mineral., in press, 1998). Current theoretical and experimental work, especially the recent M÷ssbauer experiments on FeO that show a magnetic transition (Pasternak *et al.*, *PRL*, **79**, 5046, 1997) on these complex materials will be reviewed.

This work is supported by NSF and is performed in collaboration with I. Mazin, Y. Fei, R. Downs, and D. Isaak.

MD STUDY OF THE DENSITY AND ELASTIC CONSTANTS OF THE OLIVINE, MODIFIED-SPINEL, AND SPINEL FORMS OF Mg_2SiO_4 AT MANTLE CONDITIONS

Matsui M. *(Dept. of Earth and Planetary Sciences, Kyushu Univ., matsui@geo.kyushu-u.ac.jp)*

Molecular dynamics (MD) simulation is used to predict the density and elastic constants of the olivine, modified-spinel, and spinel forms of Mg_2SiO_4 at high temperatures and high pressures prevailing in the mantle. The interionic potential is taken to be the sum of pairwise additive Coulomb, van der Waals attraction, and repulsive interactions. In order to take account of non-central forces in crystals, the breathing shell model (BSM) is introduced in MD simulation, in which the repulsive radii of O ions are allowed to deform isotropically under the effects of other ions in the crystal, with each core and breathing shell being linked by a harmonic spring with force constant k. The same potential model is used for the three Mg_2SiO_4 polymorphs. Required energy parameters, including k, were obtained empirically by fitting the parameters to the observed structural and elastic properties of the three Mg_2SiO_4 polymorphs.

In spite of the simplicity of the present potential model, the MD simulation is found to be very successful in reproducing accurately the observed values for the structural parameters, the linear and volume thermal expansivities, the bulk and shear moduli, and the individual elastic constants of the three Mg_2SiO_4 polymorphs over wide temperature and pressure ranges, where experimental data are available. The MD simulation is further applied to predict the densities and P- and S-wave velocities of the three Mg_2SiO_4 polymorphs at high temperatures and high pressures corresponding to the upper mantle and the transition zone. Then the simulation results are compared with the seismological model PREM, with paying special attention to the density and velocity jumps at the 400-km and 520-km (if any) discontinuities which are considered to be due to the olivine to modified-spinel and the modified-spinel to spinel transformations, respectively.

4. Deep Earth Mineralogy

HIGH PRESSURE- $P2_1/c$-$C2/c$ PHASE TRANSITIONS IN PYROXENE: INFLUENCE OF CATION SIZE AND CFSE

Arlt T.[1,2], Angel R.J.[2], Miletich R.[2], Armbruster T.[3] & Peters T.[1] *([1]Mineral.-petrograph. Inst., Univ. Bern, Switzerland, thilo.arlt@uni-bayreuth.de; [2]Bayerisches Geoinstitut, Universität Bayreuth, Germany; [3](Laboratorium. f. chem. u. mineral. Kristallographie, Univ. Bern, Switzerland)*

The high-pressure behaviour of the $P2_1/c$-clinopyroxenes kanoite $Mn_{0.9}Mg_{1.1}Si_2O_6$, $CrMgSi_2O_6$ and $MnSiO_3$ was studied by single-crystal X-ray diffraction in a diamond-anvil cell at room temperature. Phase transitions from space group $P2_1/c$ to HP-$C2/c$ were found and reversed at 5.1 GPa in kanoite, at 3.6 GPa in $CrMgSi_2O_6$ and at 2.9 GPa in $MnSiO_3$-cpx. The phase transitions are rapid, reversible, first-order in character and are accompanied by a volume decrease of approx. 2%. The structure of HP-$C2/c$ kanoite was determined by structure refinement from single-crystal X-ray intensity data collected at 5.2 GPa, and is very similar to that of HP-$C2/c$-ferrosilite[1] and HP-$C2/c$-enstatite[2]. Although the space group $C2/c$ is the same as for HT-kanoite[3], the two phases have significantly different structures. The silicate chains are extremely kinked in HP-kanoite while they are almost straight in HT-kanoite. In $MnSiO_3$, the $P2_1/c$ - HP-$C2/c$ phase transition at 2.9 GPa shows that the *C-centred* pyroxene is actually the stable phase in the MnO-SiO_2 system, whereas the $P2_1/c$ -pyroxene described previously[4] is metastable with respect to the pyroxenoid structures.

A comparision of the transition pressures of clinoenstatite (6.5 GPa, large hysteresis), kanoite and $MnSiO_3$ shows that increasing M cation size decreases the transition pressure. However in the (Mg,Fe)-cpx series the decrease with cation radius is much stronger; the transition pressure is 1.7 GPa in clinoferrosilite. Furthermore, the transition pressure of $CrMgSi_2O_6$ at 3.7 GPa fits the trend of (Mg,Fe)-clinopyroxenes. These observations suggest that the effective ionic radii of M1 and M2 cations are not the exclusive control on the transition pressure, but there appears to be a contribution from crystal field effects (CFSE). These are expected to stabilize HP-$C2/c$ clinopyroxenes with Cr^{2+} and Fe^{2+} because the M2 sites are more regular than in the low pressure $P2_1/c$ structure.

References

1. Hugh-Jones D., Woodland A., Angel R., 1994, *Am. Mineral.*, **79**, 1032-1041
2. Angel R.J., 1992, *Nature*, **358**, 322-324
3. Arlt T., Armbruster T., 1997, *Europ. J. Mineral.*, **9**, 953-964
4. Akimoto S., Syono Y., 1972, *Am. Mineral.*, **57**, 76-84

KINETIC EFFECTS IN METAL SILICATE INTERACTIONS CONSEQUENCES FOR CORE COMPOSITION

Guyot F. *(Laboratoire Minéralogie-Cristallographie and IPGP, Paris, France; guyot@lmcp.jussieu.fr)*, Lemelle L. *(LMCP, Paris, France)*, Leroux H, Doukhan J.C. *(LSPEA, Lille, France)* and Libourel G. *(CRPG, Nancy, France)*

The formation of metallic cores is a major differentiation event which determines the chemical compositions and layering of planetary interiors. In recent years, experimental studies of the pressure and temperature effects on metal/silicate equilibration have been strongly developed. The role of kinetics, however, has not been much studied, although metal/silicate differentiation is probably associated to relatively short characteristic times, in differentiated meteorite parent bodies as well as in the Earth.

In this study, we present the results of mineralogical experiments designed for evaluating kinetic effects on metal/silicate differentiation:

(1) Measurements of rate constants of transfer reactions of Ni, Fe and Si between silicate and metal phases at P = 1 bar and T = 1600°C, under reducing conditions. A correlation is observed between rate constants and thermodynamical affinities.

(2) Measurements of Fe-Mg profiles induced by metal extraction in olivines equilibrated at P = 1 bar and T varying between 1100°C and 1600°C, under reducing conditions. It is shown that Fe-Mg interdiffusion in olivine is not, as usually assumed, systematically the rate-controlling factor of liquid metal/solid silicate equilibration

(3) Measurement of quenched liquid metal and quenched liquid silicate compositions resulting from dynamic high pressures.

The potential relevance of these kinetic effects to the formation and composition of the core of the Earth will be discussed.

COVALENCY/IONICITY OF SIO_2 RUTILE STRUCTURE BONDS DEFINED BY k-REFINEMENT AND BY DV-Xα SIMULATION

Yamanaka T., Kurashima R. and Tsuchiya T. *(Dept. of Earth and Space Science, Osaka Univ., b61400@center.osaka-u.ac.jp)*

In order to elucidate the bonding character of earth interiors, the covalency/ionicity and the other bonding character of rutile structure SiO_2, GeO_2, SnO_2 and α-PbO_2, high pressure form of quartz, were investigated by X-ray diffraction study using monopole refinement (k-refinement) and molecular orbital simulation (DV-X_α). Those single crystals were synthesized using multianvil high pressure apparatus. The refinement of the charge density was undertaken by κ-parameter (Coppens *et al.*, 1979; van der Wal, 1984) on the basis of the structure factor F(hkl). Electron density in consideration of the perturbed valence density was

$$\rho'_{valence}(r)=P_{valence}\cdot\kappa^3\cdot\rho_{valence}(\kappa\cdot r),$$

where $\rho_{valence}(r)$ is the electron density of free atom ground states, $P_{valence}$ is the valence-shell population which is assigned to the occupancy parameter of scattering factor for core and valence electron, and the factor κ^3 is required for normalization.

The M—O bonding characters were estimated by κ-refinement applied to the valence electrons of oxygen. Each oxygen κ-parameter was 0.91 (SiO_2), 1.06 (GeO_2), 1.14 (SnO_2). This indicates that the electron distributions are more localized with increasing the atomic number.

DV-X_α simulation was carried out to elucidate the bonding character of these dioxides. In the present study, DV-X_α results were obtained in the condition of the second neighbor cluster (M.P. ±4, ±4, ±6). The calculating total DOS (density of states) about the energy levels of main peaks for SiO_2, GeO_2, SnO_2, is in good qualitative agreement with the XPS experiment (Barr, 1991). The bond overlap populations based on Mulliken population analysis were degreased with increasing the atomic number. DOS wave function maps and deformation maps of electronic charge density interpretated that the bond character of SiO_2 is much different from GeO_2 and SnO_2. There are wide spread distributions of Si excited-3d more than Ge excited-4d and Sn excited-5d. This characteristic of Si excited-3d has a connection with the stronger covalency of d-p π-bond nature of SiO_2 compared with GeO_2 or SnO_2. However, SiO_2 rutile structure indicate more ionic than quartz lower pressure polymorph.

SULFIDE- MELT INCLUSIONS IN MANTLE XENOLITHS OF HANNUOBA, CHINA

Xu J. *(1.University of Science and Technology Beijing, Beijing 100083)* and Chu X. *(Institute of Geology, Chinese Academy of Sciences, Beijing 100029)*

The samples of this study were collected from Damaping, Qingyanggou, and Jieshaba of Hannuoba in Zhangjiakou area, China, where alkali-basalt and tholeiite occur horizontally as alternating beds. Mantle xenoliths were captured whthin some alkali-basalt strata, dominantly comprised by spinel lherzolite and accompanied with pyroxenite, dunite and pyroxene megacryst. Fluid (and melt) inclusions can be divided into five types based on main components and phases: 1) pure CO_2 inclusion; 2) CO_2 melt inclusion; 3) CO_2 melt inclusion; 4) sulfide-melt inclusion; and 5) CO_2 sulfide-melt inclusion. LRM analysis of gas composition shows that CO_2 content is a range of 50 - 60mol% in different types of inclusions. The contents of H_2S, SO_2 and CH_4 are detected too, but N_2,H_2 and H_2O were detected only in some samples. Sulfur (H_2S+SO_2) occupies larger proportion in gas composition, generally more than 20 mol%. Sulfide-melt inclusions (type 4 and type 5) of Hannuoba are usually seen in spinel-lherzolite and olivine pyroxenite, and usually contain two phases, sulfide and glass phases, or only one sulfide phase. Under polarizing microscope, sulfide phase shows a dark bubble, but it appears a bright yellow spot when exposed on the surface of polished thin section. The EPMA analyses have been made for sulfides in the melt inclusions. The components of sulfide inclusions in lherzolite (Q117, DA5) are mainly pentlandite, with small amount of chalcopyrite, while those in olivine pyroxenite (J131, D15) are pentlandite, and pyrrhotine too. However, the components of sulfide bubbles in pyroxene megacrysts are mainly pyrrhotine, according Huang et al. (1987). One important feature is that sulfide phases are rich in As, which are as 10 - 40 times as in host minerals, but the contents of As do not reach that of gersdorffite ([Ni,Co,Fe]AsS). Meanwhile, both sulfide inclusions and sulfide minerals in mantle xenoliths of Hannuoba are rich in Cu, Zn, Au and Ag in some degree.

The research is aided by financial support from National Natural Science Foundation(49673175). The authors thank Profs. Fan Qichen, Li Shuyan and Li Qianmao for their great help.

4. Deep Earth Mineralogy

A TEM AND HRTEM STUDY OF MICROSTRUCTURES IN OMPHACITE FROM UHP ECLOGITES AT SHIMA, DABIE SHAN, CHINA

Wu X.L., Han Y.J., Meng D.W., Yang W.R. *(Faculty of Earth Science, China University of Geosciences, Wuhan, China, dwmeng@dns.cug.edu.cn)* and Li D.X. *(Laboratory of Atomic Imaging of Solids, Institute of Metal Research, Academia Sinica, Shenyang, China)*

Transmission electron microscopy (TEM) and high-resolution transmission electron microscopy (HRTEM) analyses have been performed on omphacite from ultra-high-pressure (UHP) eclogites at Shima, Dabie Shan, China. TEM reveals that a prominent feature of the microstructure is dislocation substructures in the studied omphacite samples. A dense distribution of free dislocations are observed. Some free dislocations interact to form dislocation networks. These dislocation networks are composed of dislocation nodes and some complex but are regular organization of the dislocations form a quasihexagonal net indicating recovery. Some are curved or form dislocation loops that are present in (100) plane and have Burgers vector [001], defining the slip system [001](100). The [001] loops are generally associated with straight dislocations that have a crystallographic control on their directions, parallel to [001] loops indicating strong Peiers (structural) forces which control the generation and motion of dislocation. They are produced by high-temperature ductile deformation and the recovery-accommodated dislocation slip became the main mechanism of deformation.

In addition, antiphase domain boundaries (APBs) are detected by TEM in the studied samples. The antiphase domains (APDs) have an average domain size in the range of 0.10 - 0.45μm with 0.20 - 0.25μm being in the majority reflecting a long period of annealing at high temperatures followed by relatively rapid cooling.

HRTEM reveals C2/*c*, P2/*n* and P2 space groups in different parts of one single-omphacite crystal. It is attributed to metastable transformations. Therefore it provides new valuable information on exhumation mechanism of UHP eclogites and dynamic analysis of the UHP metamorphic belt in the Dabie Shan.

NEW APPROACH TO THE CALCULATION OF INTRACRYSTALLINE CATION DISTRIBUTION EQUILIBRIA IN NON-IDEAL SOLID SOLUTIONS: APPLICATION TO THE PARTITIONING IN OLIVINE

Kikuchi T. *(Dept. Earth and Planetary Sci., Hokkaido Univ, Japan, takes@cosmos. sci. hokudai. ac. jp)*

In this study we establish a new approach in which the equilibrium distribution is calculated by a combination of molecular dynamics (MD) and a chemical thermodynamical approach. In olivine $(A,B)_2SiO_4$, the cations in M_1 site are classified into the following ten types according to the number of surrounding divalent cations of the other kind, $A_1(n)$ and $B_1(n)$ where n=0 to 4. Similarly, cations in M_2 site are distinguished by two surrounding M_1-cations, $A_2(n)$ and $B_2(n)$ where n=0 to 2. It becomes obvious from the result of MD that the site potentials of divalent cations in M_1 and in M_2 sites increase (or decrease) in the order of the number n. This reflects the following eleven elementary equilibrium reactions:

$(4-n)A_1(0) + nA_1(4) = 4A_1(n)$ where n=1 to 3

$(4-n)B_1(0) + nB_1(4) = 4B_1(n)$ where n=1 to 3

$A_2(0) + A_2(2) = 2A_2(1)$, $B_2(0) + B_2(2) = 2B_2(1)$

$A_1(0) + B_1(0) = A_1(4) + B_1(4)$, $A_2(0) + B_2(0) = A_2(2) + B_2(2)$

$A_1(0) + B_2(0) = B_1(4) + A_2(2)$

The equilibrium constant of the above eleven reactions can be obtained in the form $K=\exp(-\Delta G/nRT)$ using the data from MD and the configurational entropy of the product.

The above sixteen unknown concentrations are calculated by adding five more equations which restrict the condition. Attempts to calculate distribution coefficient Kd for Mg-Ni, Co-Mg, Co-Ni, Mn-Fe and Fe-Mg olivines at 873K under 1 atm were successful.

THE KINETICS OF CATION ORDERING IN $MgFe_2O_4$: ORDERING MECHANISMS FROM THE TIME-TEMPERATURE DEPENDENCE OF MAGNETIC SUSCEPTIBILITY

Harrison R.J. and Putnis A. *(Institut für Mineralogie, Münster)*

We present the results of a kinetic study of cation ordering in the inverse spinel $MgFe_2O_4$ using measurements of alternating-field magnetic susceptibility (χ). The starting material for the kinetic experiments was a synthetic sample of stoichiometric $MgFe_2O_4$ quenched from 900°C, which displays the relatively disordered equilibrium cation distribution characteristic of this temperature. This material was then ordered by annealing isothermally at temperatures ranging from 450 to 700°C, and the changes in cation distribution as a function of annealing time were monitored by periodically removing the sample from the furnace and measuring its Curie temperature (T_c) from the temperature dependence of the magnetic susceptibility.

The Curie temperature of $MgFe_2O_4$ is extremely sensitive to the intracrystalline distribution of Fe^{3+} and Mg cations between tetrahedral and octahedral sites of the spinel crystal structure, with T_c varying from 260 to 422°C as the cation distribution varies from fully random to fully inverse. Consequently, the χ-T curves provide a very sensitive probe of the ordering process, and, although such measurements yield the susceptibility averaged over the whole crystal, the source of the magnetic signal can be ascribed to very localised areas of magnetic order. Using this technique, therefore, it is possible to detect the presence of fine-scale heterogeneities in the cation distribution, which would otherwise be missed using macroscopic measurements such as X-ray diffraction.

The results clearly demonstrate that ordering in $MgFe_2O_4$ proceeds via a heterogeneous mechanism, involving nucleation and growth of ordered domains within a disordered matrix. During the early stages of ordering, the χ-T curves develop a pronounced superparamagnetic tail, extending from the Curie temperature of the disordered phase (303°C) to the Curie temperature of the equilibrium ordered phase (varying between 345 and 370°C depending on the annealing temperature). In the intermediate stages of ordering, the size of the ordered domains have grown such that they are larger than the critical size for single-domain magnetic behaviour, at which point sharp magnetic transitions can be observed for both the ordered and disordered phases. The χ-T curves reveal that a small fraction of disordered material remains even after extensive annealing, implying that recrystallisation is required to achieve a fully homogeneous cation distribution.

STRUCTURE, VISCOSITY AND MIXING BETWEEN ALKALI AND ALKALINE-EARTH SILICATE MELTS.

Neuville D.R. and Richet P. *(Laboratoire de Physique des Géomatériaux, ESA7046-CNRS, Institut de Physique du Globe, France, neuville@ipgp.jussieu.fr*

The configurational properties of melts and glasses provide fundamental information needed to characterize magmatic processes. A principal difficulty, however is to link the "macroscopic" configurational entropy with the structure of melts. This has been done by combining viscometry with Raman spectroscopic structural studies. From the viscosity measurements at low and high temperatures, we have obtained the configurational entropy, S^{conf} ($log\ \eta = A_e + B_e/TS^{conf}$, where η is the viscosity, T the temperature and A_e, B_e two constants).

We are using Raman spectroscopy at room temperature between the alkali and alkaline-earth silicate melts. For these compositions, we establish some link between the variation of the viscosity, the configurational entropy as the function of chemical composition and the Q species obtained from the Raman spectroscopy. These structural variations are related to the changes in configurational entropy. It is possible, to understand this variation of viscosity.

4. Deep Earth Mineralogy

MOLECULAR DYNAMICS OF SOLID SOLUTION AND COEXISTING LIQUID

Akamatsu T. *(Fac. of Education, Kochi Univ., akamatsu@cc.kochi-u.ac.jp)* and Kawamura K. *(Dept. of Earth and Planet. Sci., Tokyo Inst. of Technology, kats@geo.titech.ac.jp)*

The differentiation of elements between solid and coexisting liquid is an important phenomenon in the fields of material and earth sciences. The purpose of this study is to observe and consider the mechanism of the differentiation of elements in atomic scale through molecular dynamics (MD) simulation.

Two-phase MD simulations of coexisting solid and liquid were performed for binary systems MgO-CaO and NaCl-KCl. Solid solution crystal and its melt having the same composition were placed in a basic cell, and the compositional change of solid and liquid during MD calculation was observed. The starting compositions were Mg-rich ($Mg_{0.875}$, $Ca_{0.125}$)O, Ca-rich ($Mg_{0.125}$, $Ca_{0.875}$)O, Na-rich ($Na_{0.875}$, $K_{0.125}$)Cl, and K-rich ($Na_{0.125}$, $K_{0.875}$)Cl. The total number of particles in the basic cell was 3456 [(Mg, Ca)O and (Na, K)Cl] or 8192 [(Mg, Ca)O]. The MD program MXDORTO was used and the step time was 2 fs. Periodic boundary conditions were applied to x-, y-, and z- directions.

Crystallization or melting of the system was observed according to the temperature. Concentration of "minor element" into liquid was detected for some calculations where solid-liquid interface was maintained for a long period of time, more than 400 ps (= 200 × 10^3 steps). These minor elements were swept out into liquid during the growth of the crystal lattice, because of the mismatch of cationic size, which was reflected by the shape of the potential curve for cation-anion bond. There occurred positional fluctuation of solid-liquid interface during the calculation. This fluctuation caused the effective differentiation of cations between solid and liquid.

It was easier to cause the differentiation in MgO-CaO system than in NaCl-KCl system. This is consistent with the shape of phase diagrams: The distance between solidus and liquidus curves of MgO-CaO system is larger than that of NaCl-KCl system. In microscopic view, the magnitude of cation-anion interaction of Mg-O and Ca-O bonds is higher than that of Na-Cl and K-Cl bonds. This may cause the higher differentiation in MgO-CaO system.

VISCOSITY OF MODEL SILICATE AND ALUMINOSILICATE MELTS AT HIGH WATER AND SUPER-HIGH LITHOSTATIC PRESSURES

Persikov E.S. *(Institute of Experimental Mineralogy, RAS, Russia)*

The composition and pressure dependenceis of the viscosity both water bearing and water-free full polimerized aluminosilicate (albite, jadeite) and high depolimerized both $Ab_{25}Di_{75}$ and metasilicate (diopside) melts have been studied by falling-floating sphere method at water pressure up to 0.8 GPa and lithostatic pressure up to 12 GPa and temperature range: T =1200-1900°C. The accuracy of temperature measurements was ±5°C, the relative uncertainty in pressure measurements was ±1 rel.%. The relative error of the viscosity measurements was 15-25%.

The results show: 1. The viscosity as well as activation energy of viscous flow of water bearing and water free albite and jadeite melts dramatically decrease with increasing both water and lithostatic pressure. For example, the viscosity of jadeite melt decreases by about three orders of magnitude under 0.4 GPa water pressure (T = 1000°C) and by about five orders of magnitude under 9 GPa lithostatic pressure (T =1900°C). 2. In contrary, the viscosity and activation energy of water bearing and water free diopside melts increase with increasing both water and lithostatic pressure. 3. The pressure dependence of viscosity and activation energy for all aluminosilicate melts has minima and pressure value for minimum points decreases regularly with increasing basicity of the melts. 4. The activation energies are approximately equal for minimum conditions, *i.e.* it is independent on melt compositions and approximately equal to the activation energy for any metasilicate melts.

Using these as well as early results (Persikov E.S., 1991) some generalized patterns has been received on composition and pressure dependences of magmatic melts viscosity at crust and upper mantle T, P - conditions.

We acknowledge the support of RFBR grant N 9705-64448 to Persikov.

INFLUENCE OF SOLID INCLUSIONS ON THE RHEOLOGY OF SILICATE MELTS.

Lévesque S., Neuville D.R. and Richet P. *(Lab. de Physique des Géomatériaux, CNRS-ESA7046, IPGP, neuville@ipgp.jussieu.fr)*

The viscosity of a magma is an important parameter for understanding magmatic processes and volcanic eruptions. A lot of work has been done to understand how the viscosity of silicate melts depends on temperature, on chemical composition, and even on pressure. But natural magmas are not made of only a melt phase; they carry a lot of solid and gas inclusions whose influence on viscosity is now starting to become known.

For solid phase inclusions, reliable and accurate data have previously been gathered for melts with spherical crystalline inclusions of constant size. The viscosity of these melts increases abruptly and becomes non-newtonian when the crystal fraction is about the threshold value of 40% vol. The rheology of real magmas is more complicated because of the diversity of form and size of the crystalline species and the possibility of orientation effects.

This study aims at filling some important gaps which still exist in understanding the rheology of magmas. This work is done with high viscosities where the kinetic of growth of crystals is slow, so the crystal fraction is well known during the experiments. The influence of non-spherical crystals with different sizes will be determined for melts having the same composition as the crystals (for example anorthite, cordierite). Thus we avoid strong variations of viscosity due to a change of the chemical composition of the melt by crystallization, and we just consider the physical effect of the crystal fraction.

The rheological laws obtained with simple systems will be compared with measurements on lavas. The results will be directly pertinent to a better understanding of the dynamics of volcanic eruptions.

HIGH PRESSURE CRYSTAL CHEMISTRY OF STISHOVITE BY POTENTIAL RENEWING MOLECULAR DYNAMICS SIMULATION

Tsuchiya T., Yamanaka T. *(Dept. of Earth and Space Science, Osaka University, taku@ess.sci.osaka-u.ac.jp)* and Kawamura K. *(Dept. of Earth and Planetary Sciences, Tokyo Institute of Technology)*

Stishovite is the high pressure polymorph of SiO_2 and the rutile-type structure ($P4_2/mnm$, z=2) in which structure Si ions are in sixfold-coordinated states and SiO_6 octahedra make chains with sharing edges of octahedra along c axis. X-ray diffraction measurement showed the shared O—O edge of the octhedron is shorter than the unshared O—O distance at ambient conditions (Bolzan *et al.* 1997). In spite of this fact, it was reported by high pressure experiments using diamond anvil cell that the shorter shared edge has greater compressibility than the longer unshared edge (Sugiyama *et al.* 1987, Ross *et al.* 1990). The reason for this strange behavior was elucidated by the newly derived MD simulation.

The conventional MD method based on fixed interatomic pair potential (Tsuneyuki et al. 1988, Belonoshko and Dubrovinsky 1994) cannot reproduce this phenomenon. The charge equilibration method was used to estimate charge transfer between atoms in molecules and periodic systems under static conditions (Mortier *et al.* 1985, Rappe and Goddard III, 1991). Our new MD method in which potential is variable with changes of interatomic distances by the charge equilibration method was developed in order to comprehend the compression mechanism of stishovite. Simulation using this new method with Mortier's parameters about atomic electronegativities and self energies and semi-empirical pair potential (van Beest *et al.* 1992) was successful in reproducing the strange behavior of stishovite. It was clearly found that a little change in the nature of chemical bond under high pressure is essential to account for the strange behavior of stishovite.

4. Deep Earth Mineralogy

THERMAL PROPERTIES OF QUARTZ, RUTILE, SAPPHIRE, SILICA GLASS, CoO, MgO, MnO, NiO AND Ni AT LOW TEMPERATURES

Watanabe H. *(Dept. of General Education, Osaka Sangyo University, hwatasan@mbox.las.osaka-sadai.ac.jp)*

New data for heat capacities, thermal diffusivities, thermal conductivities and linear thermal expansions of seven single crystals, quartz, rutile, sapphire, CoO, MgO, MnO and NiO, silica glas and nickel were obtained at low temperatures, 100K to 570K, using a laser flash calorimeter and a push-rod dilatometer.

The effects of magnetic transition, Neel transition, on heat capacities, thermal diffusivities, thermal conductivities and linear thermal expansions of CoO, MnO and NiO were shown.

The anisotropic properties for thermal diffusivities, thermal conductivities and linear thermal expansions of quartz, rutile and sapphire were shown.

HIGH-PRESSURE PHASE RELATIONS IN THE SYSTEM MAGNETITE-FAYALITE AND THE CRYSTAL CHEMISTRY OF SEVERAL SPINELLOID PHASES

Woodland A.B. *(Mineralogisches Institut, Universität Heidelberg, D-69120 Germany, alan@classic.min.uni-heidelberg.de)* and Angel R.J. *(Bayerisches Geoinstitut, Universität Bayreuth, D-95440 Germany)*

The crystal chemical behavior of Fe^{3+} in silicate spinel and wadsleyite has important implications for the oxidation state of the Earth's transition zone. However, the thermodynamics of such solid solutions containing both Fe^{3+} and Si^{4+} is poorly known. Therefore, the Fe_2SiO_4 - Fe_3O_4 binary system has been investigated experimentally by equilibrating various molar proportions of magnetite (mt) and fayalite (fay) in Ag or Au capsules at 2.0-9.0 GPa and 900°C-1200°C in a belt apparatus and a multi-anvil press.

The max. Fe_2SiO_4 content in mt increases with increasing pressure; $X_{fay} \approx 0.1$ at 2.5 GPa and $X_{fay} \approx 0.2$ at 5.0 GPa. Temperature has only a minor effect on this limit. At low P (<3.5 GPa at 900°C and <2.6 GPa at 1100°C), mt-rich spinel coexists with fay. At higher P, three intermediate phases appear with their respective stability fields being dependent on P, T and bulk composition. All three phases are spinelloid (spd) polytypes and are structural analogues of spinelloids II, III and V in the Ni-aluminosilicate system. At 900°C, only spd V is stable. At >1000°C and 3-4 GPa, spd II coexists with either fay or mt-rich spinel. Spd II gives way to spd V at higher P and spd III appears in bulk compositions ≥50 mol% fay. The max. Fe_2SiO_4 content in spd III ($X_{fay} \approx 0.68$) appears to be limited by the reaction spd III + fay = iscorite + opx. Between 6.0 and 8.0 GPa at 1100°C the stability fields of spd V and III terminate and a complete spinel solid solution exists.

The cell parameters of the three spd phases exhibit smooth but distinct trends with composition. Spds II and III are previously unidentified phases in this system. Single-crystal structure refinements show that Spd II has two distinct tetrahedral sites, T1 and T2, arranged to form T_3O_{10} groups, with partial ordering of Si onto the smaller T2 site. Spd III has only one symmetrically distinct tetrahedral site, joined in pairs to form T_2O_7 groups with no evidence of significant ordering of Fe^{3+} and Si^{4+} on this site. Spd III is isostructural with Mg_2SiO_4-wadsleyite, indicating that this structure type can be stabilised by the presence of Fe^{3+}.

5. Comparative Mineralogy of Planetary Interiors

MINERALOGY OF THE CORE AND LOWER MANTLE

Saxena S.K., Dubrovinsky L.S. and Lazor P. *(Dept. of Earth Sciences, Uppsala University)*

The existence of the high temperature condensates in the solar nebula has been established both by their occureence in meteorites (*e.g.* Allende) and by condensation calculations. A protocore which formed from a mixture of planetesimals rich in iron and in refractory oxides would eventually differentiate to form a D″ layer at the core-mantle boundary. A large solid iron (Fe-Ni-S) protocore would react with wustite and possibly iron hydride (Fe-FeO-H_2O) which separated from the dissociating silicates and oxides in the surrounding accreted mantle. An outer liquid core would grow at the expense of the solid protocore.

The support for this model is derived from the experimental information out lined below:

a. The stability of the high pressure silica polymorph (possibly space group *Pnc*2);
b. The structural transformation in Fe_xO and the probable unmixing of magnesiowustite and
c. The dissociation of perovskite.

All these reactions appear to take place between 70 and 80 GPa at moderate to high temperatures. Additionally we have extended the study of the Fe-H_2O system to high pressure and temperature and find iron hydride (FeH_x) stable at 40 GPa and 1500 K.

THE EFFECT OF ALUMINA ON PHYSICAL PROPERTIES AND STABILITY FIELD OF SILICATE PEROVSKITE

Fei Y. and Hirose K. *(Geophysical Lab and Center for High Pressure Research, Carnegie Institution of Washington, fei@gl.ciw.edu)*

Silicate perovskites are important minerals in the Earth's lower mantle. Magnesium-iron silicate has been extensively studied, in terms of its physical properties, crystal chemistry, and stability field. In this study, we report the effect of alumina on bulk modulus, unit cell parameters, and stability field of silicate perovskite.

Perovskites with different alumina content were synthesized at pressures above 23 GPa and temperatures between 1500 and 2000°C in a multi-anvil apparatus. The solubility of alumina in perovskite increases with pressure, from 1.5 mole% at 23 GPa to 13 mole% at 27 GPa at 1750°C. It decreases with increasing temperature for a given pressure. The unit cell parameters of Al-bearing perovskites were determined as a function of alumina content by synchrotron x-ray diffraction. The nature of Al substitution in perovskite structure was also studied by Raman spectroscopy.

Static compression data for perovskite with 4 mole% alumina were obtained by using a monochromatic synchrotron x-ray beam and the image plate technique. The experiment was conducted in a diamond-anvil cell, using neon as a pressure medium and gold as a pressure calibrant. The unit cell parameters at different pressures were refined by GSAS. The data were fitted to the Birch-Murnaghan equation of state to obtain the bulk modulus. The effect of alumina on the bulk modulus of perovskite will be discussed.

HIGH-PRESSURE TRANSITIONS OF ALUMINOUS PHASES IN THE DEEP MANTLE CONDITIONS

Akaogi M., Kubo A., Ito E.*, Suzuki T., Hamada Y. and Kamii N. *(Department of Chemistry, Gakushuin University, Japan masaki.akaogi@gakushuin.ac.jp; *Institute for Study of Earth's Interior, Okayama University)*

Phase transitions in the system MgO-FeO-SiO_2 at high pressures have been studied in detail in recent decade. Although Al_2O_3 is the other abundant component of the mantle, phase transition studies on aluminous phases are insufficient and in controversy. We have studied phase transitions of several aluminous phases in the deep mantle conditions by direct high pressure experiments together with some calorimetric measurements and thermodynamic calculation. Pyrope dissociates into aluminous perovskite and corundum at about 27 GPa with a positive slope boundary, and further recombine into an almost single perovskite solid solution at about 37 GPa.

Calorimetric study shows that garnet-perovskite transition in the system $Mg_4Si_4O_{12}$-$Mg_3Al_2Si_3O_{12}$ occurs at about 23-27 GPa, almost consistently with high pressure experimental results. $MgAl_2O_4$ spinel decomposes into periclase and corundum at 16 GPa, which recombine into calcium ferrite phase at about 25 GPa. $CaAl_2O_4$ with nepheline structure transforms to calcium ferrite at 9 GPa. In the system $MgAl_2O_4$-$CaAl_2O_4$, a hexagonal phase with calcium ferrite-like structure is also stable. $KAlSi_3O_8$ sanidine dissociates into $K_2Si_4O_9$ wadeite, kyanite and coesite at 6 GPa, and recombine into $KAlSi_3O_8$ hollandite at 9 GPa. Calorimetric study confirms positive slope boundaries of the two transitions in $KAlSi_3O_8$. The results described above suggest that magnesian silicate perovskite is a major aluminous phase in the lower mantle, and that calcium ferrite phase and K-hollandite are important constituents of the subducted oceanic crust and sediment, respectively.

COOLING RATE IN THE SHOCK VEINS OF CHONDRITES: CONSTRAINTS ON THE $(Mg,Fe)_2SiO_4$ POLYMORPH TRANSFORMATIONS

Chen M., Xie X. *(GZ Inst. of Geochem., Academia Sinica)* El Goresy A. *(MPI fur Kernphysik)* Wopenka B. *(Dept. of Earth & Planet. Sci., Washington University)* and Sharp T.G. *(Dept. of Geol.,Arizona State University)*

P-T regimes in the shock veins of meteorites were estimated to be 20-24 GPa ~2000°C in the Sixiangkou chondrite, 14-23 GPa 1800-2000°C in the Peace River and Mbale chondrites. The occurrence of wadsleyite(β-phase) and ringwoodite (γ-phase) phases were constrained by cooling rate after impact events.

The shock veins of Sixiangkou chondrite consist of polycrystalline γ-phase and majorite grains, plagioclase glass, FeNi-FeS eutectic nodules, fine-grained majorite-pyrope garnet and magnesiowustite. The veins of Peace River chondrite contain polycrystalline grains both γ-phase and β-phase, pyroxene grains, plagioclase glass, metal and troilite eutectic nodules, fine-grained majorite-pyrope garnet, β-phase. The shock veins of Mbale chondrite consist of polycrystalline olivine and pyroxene grains, plagioclase glass, FeNi-FeS nodules, fine-grained majorite-pyrope garnet, olivine and small amounts of β-phase.

The greater cooling rate (>10000°C s^{-1}) in the shock veins of Sixiangkou made all high-pressure phases to be immediately frozen after pressure release. No back-transformation of high-pressure phases took place. Polycrystalline grain of β-phase plus γ-phase in the Peace River were formed as a result of transformation-exsolution from olivine with a homogeneous composition (Fa_{24}). Most γ-phase subsequently reverted to β-phase due to a cooling rate 1000-2000°C s^{-1} in the veins. The vein of Mbale experienced a cooling rate (<500°C s^{-1}). The lower cooling rate in the meteorite results in that nearly all high-pressure polymorphs reverted to their low-pressure phases after pressure release. In the fine-grained matrix, the coexistence of olivine and small amounts of β-phase is evidence that most of β-phase reverted to α-phase. The occurrence of small amounts of γ-phase in polycrystalline olivine shows the back-transformation from γ-phase to α-phase.

The heat dissipation in shock veins took place after the parent body asteroid was broken into fragmental pieces. Cooling rate in the shock veins constrained the back-transformations of $(Mg,Fe)_2SiO_4$ high-pressure polymorphs.

CHEMICAL SEPARATION OF Fe-Ni PARTICLES AFTER IMPACT

Miura Y., Fukuyama S. and Gucsik A. *(Yamaguchi University, Japan)*

Compositional changes of the Fe-Ni system formed in planetesimals are analyzed from artificial and natural impact craters. Fe-Ni phases are significant in the context of (a) characterization of natural alloys, (b) Ni-rich separation after impact melt events, and (c) the main source of Ni anomalies of extraterrestrial origin[1-3]. From artificial impact experiments with the railgun facility at ISAS, Japan, (≈7 km/sec with PCR projectile) on the Barringer (Canyon Diablo) iron, it is found that (a) Fe readily becomes enriched in Si (the Fe-Si system) whereas Ni is associated with such elements as Cl and S, and (b) Ni content increases from ≈7% in kamacite to as much as 49%. Fe-rich mixed impact fragments from the Barringer and Wolf Creek craters reveal that particles of Fe-Ni phases formed by slow crystallization in the planetesimals can be recognized, with an Fe-Si mixing signature, as melted brecciated grains. However, alloys of the Fe-Ni system cannot be found as crystalline particles under vapour-melt conditions of impact where Fe-Si alloys form as impact veins or spherules. The Widmanstatten texture of Fe-Ni iron meteorites formed at slow cooling rates (several °C/My) cannot form after short-lived impact-induced reactions under high-P/T conditions which form Ni-rich, Fe-rich, or Fe-Si compositions. Among these grains, Ni (but not Fe) content is considered a significant indicator of extraterrestrial origins. Thus some Ni ore deposits on the Earth may indicate probable locations of (a) impact sites of small iron meteorites, (b) impact sites of large iron meteorites with mixing evolution in the Earth's interior, and (c) hot or cold plume sites of mantle convection which transports some of the Ni contribution of large iron-rich bodies penetrating to the upper mantle. Present results indicate (a) grains of Fe-Ni system in major composition can survive solid- (or melt)-solid impact reactions, (b) grains in the Fe-Si system can be formed under vapour condition of impact, and (c) those with Ni-Cl,S -rich chemistry formed under vapour conditions at impact. Spherules found at the K/T and P/T boundaries are considered to be products of impact melting and mixing. Ni separation from Fe-Ni alloys can best be obtained by impact on thin suboceanic crust, with penetration to mantle layers allowing mixing and separation, forming some of the Ni-rich ore deposits found today. A key example may be Sudbury where evidence includes shatter-cones, breccias with Ir anomaly, and shocked quartz.

References
1. Miura, Y. *et al.* (1994): *Shock Waves* **3**, 293-298
2. Miura, Y. *et al.* (1995): *Shock Waves Proc.* **19**, 399-410
3. Miura, Y. *et al.* (1997): *Proc.Int.Conf.H-P Sci.& Tech* (in press)

COMPARATIVE CRYSTAL CHEMISTRY OF HYDROUS WADSLEYITE AND ITS RELATION TO HYDROUS RINGWOODITE: STRUCTURAL MODULES AND HYDROGEN CONTENTS

Kudoh Y. *(Institute of Mineralogy, Petrology, and Economic Geology, Tohoku University, ykudoh@mail.cc.tohoku.ac.jp)* and Inoue T. *(Department of Earth Sciences, Ehime University, inoue@sci.ehime-u.ac.jp)*

The crystal structures of two hydrous wadsleyite crystals with formula $Mg_{2-x}SiH_{2x}O_4$ have been analysed in this study. The crystals with 2x=0.50 and 2x=0.28 (denoted by 0.5H-β and 0.3H-β, respectively in this study) were synthesized under conditions of 1300°C and 15.5 GPa in an MA8-type apparatus. The single-crystal X-ray diffraction intensity distributions and lattice parameters showed that the 0.5H-β is orthorhombic and the 0.3H-β monoclinic, confirming our previous result for the 0.5H-β (Kudoh *et al.*, 1996). In order to determine the cause of the change of symmetry from orthorhombic to monoclinic in the 0.3H-β, atomic parameters of the 0.5H-β and the 0.3H-β were refined with monoclinic space group *I2/m* and the deviations of atomic parameters from orthorhombic symmetry were compared. The Fourier and the difference Fourier syntheses were calculated and small but significant Fourier peaks were found in both orthorhombic and monoclinic structures at the same site, Si2, in a normally vacant tetrahedral void adjacent to the Mg3 site as reported for the monoclinic hydrous wadsleyite by Smyth *et al.* (1997). Atoms at Si2 are considered to have migrated from the Si1 site in association with the vacancy at the Mg3 site. The dilution of symmetry from orthorhombic to monoclinic in the 0.3H-β is interpreted qualitatively by the Si2-Mg3 repulsion due to asymmetrical distribution of Mg atoms at Mg3 site around Si2 site along the direction of the **a**-axis. From the comparison of the 0.5H-β and the 0.3H-β structures, the Mg-vacant structural modules were found to be the building units for the structures of hydrous wadsleyite. The mode of arrangement of the Mg-vacant structural modules interprets the symmetry and hydrogen content of the hydrous wadsleyite and gives the structural relationship between hydrous wadsleyite and hydrous ringwoodite.

STABILITY OF DHMS PHASES IN THE SYSTEM Mg_2SiO_4-H_2O AND $MgSiO_3$-H_2O UP TO 27 GPa

Ohtani E. and Mizobata H. *(Inst. of Mineral. Petrol. and Econ. Geol., Tohoku University, ohtani@mail.cc.tohoku.ac.jp)*

Phase relations in the bulk compositions of $MgSiO_3$-15wt.%H_2O, Mg_2SiO_4-5wt.%H_2O and Mg_2SiO_4-11wt.%H_2O were studied in the pressure range from 20 to 27 GPa. Phase E, phase G (which is identical to phase D by Yang *et al.*,1997) and superhydrous phase B (phase C, Kanzaki, 1993) appear in this pressure range. The stability field of phase G expands in the bulk compositions with higher H_2O contents and lower Mg/Si ratios.

The water content in γ-Mg_2SiO_4 was measured by a secondary ion mass spectrometry. γ-Mg_2SiO_4 synthesized at 23 GPa and 1450-1800°C in the Mg_2SiO_4-5wt.%H_2O system contains about 0.3 wt.% H_2O. Whereas γ-Mg_2SiO_4 synthesized at 20-23 GPa and 1300-1450°C in the system Mg_2SiO_4-11wt.%H_2O contains 1.5-2.6 wt.% H_2O. Further careful studies are needed to clarify the relationship between the water content in γ-Mg_2SiO_4 and the bulk composition. The amount of water stored in γ-Mg_2SiO_4 in the mantle may be smaller than that in β-Mg_2SiO_4.

On the basis of the present results and those for the systems Mg_2SiO_4-20.5wt.%H_2O (Ohtani *et al.*, 1995; Frost and Fei, 1998), $MgSiO_3$-13.9wt.%H_2O and $MgSiO_3$-4wt.%H_2O (Ohtani *et al.*, 1997), and the serpentine bulk composition (Kuroda and Irifune, 1998), we estimated the phase relations in the system MgO-SiO_2-H_2O containing a few weight % H_2O in the pressure range from 10 to 30 GPa and temperatures corresponding to the cold slabs. Hydrous phases in the sediment and basalt layers of the cold subducting slabs might carry water into the depth about 300 km. Serpentine, which exists in the basaltic and peridotite layers in the slabs, might transport water into the 200 km depth. After decomposition of serpentine, phase A might carry water to the depth of 450 km, phase E to 500 km, superhydrous phase B and phase G into the transition zone and the lower mantle.

THE MELTING OF BASALT UNDER HYDROUS CONDITIONS AT 3.8 - 10 GPa

Chung J.I., Sueno S. and Kato T. *(Inst. Geosci., Univ. of Tsukuba, chon@arsia.geo.tsukuba.ac.jp)*

Melting behavior of oceanic tholeiite has been investigated under hydrous condition at pressures of 3.8 to 10 GPa. All experiments were carried out by a MA-8 type apparatus, a uniaxial 2000-ton press at the Earthquake Research Institute, University of Tokyo. The starting material used in the experiments is natural MORB with addition of water. The water content of the starting material is 1.2 ±0.4 wt.%.

The solidus temperature at 3.8 GPa is lower than 600 °C and it rises to the vicinity of 1000°C at 7.2 GPa. The melting interval is over 700°C at 3.8 GPa and decreases to 550°C at 7.2 GPa. This wide melting interval is an important characteristic of the hydrous system, in contrast to the small melting interval of the dry basalt. The melts adjacent to the solidus temperature are highly silicic and coexist with garnet, clinopyroxene, coesite (stishovite at 10 GPa) and TiO_2 phase. Still higher degrees of melting (≥ 40%) results in mafic liquid corresponding to basaltic composition. High percentage melts coexist with eclogitic residues composed of garnet and clinopyroxene.

The results of this study support the idea that eclogite xenoliths in kimberlites originate from high-pressure melting of subducted oceanic crust. Although several hypotheses have been proposed for the origin of eclogite xenoliths, some geochemical studies have revealed that the significant chemical features of eclogite inclusions in diamond from xenolith and host eclogite xenolith prove eclogite formation in equilibrium with melts. Furthermore, recent experimental studies of hydrous basalt at pressure lower than 3 GPa show that silicic melt and the resultant mafic residue with 20-30% melting represent TTG melts and eclogite [Winther, 1996; Rapp and Watson, 1995]. Therefore, the partial melting of subducted hydrous basaltic crust at pressure higher than 3 GPa may also have been an essential element in the growth of continental crust and the formation of diamondiferous eclogites that are stable at the depth deeper than 150 km.

5. Comparative Mineralogy of Planetary Interiors

EXPERIMENTAL MINERALOGY OF EARTH'S LOWER MANTLE - *IN SITU* HIGH-P,T X-RAY APPROACH

Dubrovinsky L.S. and Saxena S.K. *(Dept. of Earth Sciences, Uppsala University)*

The experimental study of geophysically important materials at high pressure and temperature require *in situ* x-ray diffraction. It is practically the only method which provides direct information on phase relations and structures. Our in-house x-ray facility allows us to collect diffraction patterns in megabar pressure range at temperature to 1500°C. X-ray facility includes rotating anode generator (18 kW), capillary collimating system and CCD area detector. The radiation from a rotating anode with molybdenum target is filtered with zirconium foil such that the Kβ is 1% of that Kα. The beam of initial size 1 × 0.5 mm is collimated to 0.08 mm diameter using capillary system. Special collimator is used to reduce the size of the X-ray spot to 30 μm. The CCD area detector placed on goniometer platform at various distances from 150 to 250 mm is used as a detector. Typical exposure time is 120 s for 5 μm thin iron foil on air at 1 bar.

To generate pressure and temperature simultaneously we used diamond anvil cell with electrical heating. We developed a technique of placing a thin foil (5 μm) or wire between two gaskets in a high-pressure cell using periclase or corundum as a pressure medium. The advantage of the two gasket design is that the metal does not bend and it decreases risk for the wire to be damaged by the diamond, at the same time, the diamonds are better preserved from touching the hot wire. With specially designed graphite heaters (foils and carbon-carbon composite) we were able to reach temperature of 1500°C at pressure 85 GPa and we applied this method of heating to study geophysically important materials - magnesiowustite with different compositions and silica.

KIJIMA METEORITE: A NEW FINDING OF FREE DIOPSIDE-BEARING EL6 CHONDRITE

Okada A. *(Inst. Phys. Chem. Res., aokada@postman.riken.go.jp)* and Shima M. *(Natl. Sci. Mus., Tokyo, masako-sh@aix.or.jp)*

Kijima meteorite is a stony meteorite that fell at Kijima-mura (the present name: Kijimadaira-mura), Shimotakai-gun, Nagano Prefecture, Japan (36°51'N, 138°23'E), on June 15, 1906. The stone has long remained uninvestigated, but the recent reinvestigation has revealed that Kijima belongs to the enstatite chondrite group, and that its chemical-petrologic type is EL6. The most unique aspect is that the silicate phase of Kijima contains a significant amount of free diopside, while most enstatite chondrites which have been investigated to date are diopside-free, excepting a few cases such as the Yamato 691 and Qingzhen EH3 chondrites, in which diopside is present as fine exsolution lamellae in the host enstatite. The matrix is highly recrystallized, chondrules quite absent. However chondrule relict-like silicate aggregates composed of large enstatite and forsterite grains, 100-250 μm in size, are observed in places in the recrystallized matrix consisting of much smaller silicate grains, less than 20-30 μm in size, in the thin section. Undulatory extinction prevails in most silicate grains. Several enstatite grains show shock-induced kink bands. The silicate phase is dominantly composed of enstatite (Wo_1Fs_1), and colorless and transparent plagioclase (An_{11-13}) is prevalent in the matrix. The accessory silicate minerals are nearly iron-free forsterite (Fa_1) and diopside ($Wo_{46}En_{53}Fs_1$) up to 80 μm in size. The opaque minerals are kamacite (5-6 wt.% Ni), schreibersite [$(Ni,Fe)_3P$], troilite (FeS), Mn-bearing daubreelite ($FeCr_2S_4$), ferroan alabandite [(Mn,Fe)S], mackinawite [$(Fe,Ni)_9S_8$], graphite (C), and taenite (32-47 wt.% Ni). Oldhamite (CaS) was not found in the sections of Kijima investigated in this work. Although the occurrence of taenite is very sparse, the cooling rate, 10-100°K/myr, was tentatively estimated by the metallographic method using Ni distribution in the taenite grains. This result implies the cooling at the burial depth of about 10 km within the parent body, 50-100 km in radius.

SINGLE-CRYSTAL X-RAY DIFFRACTION AND FT-IR SPECTRA OF CHONDRODITE, $Mg_5Si_2O_8(OH,F)_2$ UNDER HIGH PRESSURE UP TO 6.0 GPa

Kuribayashi T., Kudoh Y. and Akizuki M. *(Institute of Mineralogy, Petrology and Economic Geology, Tohoku University, ykudoh@mail.cc.tohoku.ac.jp)*

The crystal structure of chondrodite, $Mg_5Si_2O_8(OH,F)_2$ is built up by the olivine-like layer of the chemical composition, $Mg_2SiO_3(OH,F)$ and the brucite-like layer of MgO(OH,F). The bulk modulus of chondrodite, K_T=136.2 GPa (Faust and Knittle, 1994) is significantly larger than the simple average of the bulk modulus values of forsterite, Mg_2SiO_4 (K_T=122.6 GPa (Kudoh and Takeuchi, 1985)) and brucite, $Mg(OH)_2$ (K_T=42 GPa (Duffy *et al.*, 1995)). In the view of these situations, high-pressure measurements of single-crystal X-ray diffraction and FT-IR spectra of chondrodite were undertaken up to 6.0 GPa using a diamond anvil high pressure cell at room temperature. With the single-crystal X-ray diffraction data obtained at 1.3, 2.4, 3.0, 3.2, 3.9, 4.1, 4.4, 4.9, 5.7, 5.9 and 6.0 GPa, the isothermal bulk modulus was determined using the Birch-Murnaghan equation of state. The bulk modulus and linear compressibilities of each axis of chondrodite thus obtained were:

K_T=136.0 ± 2.1 GPa (K_T' = 4);

βa = 1.71(3), βb = 2.80(5) and βc = 2.66(4) ($\times 10^{-3}$/GPa)

The bulk modulus value obtained in this single-crystal X-ray study is vely close to the 136.2 GPa value obtained with the high pressure powder X-ray DAC method by Faust and Knittle (1994). In the variation plots of cell parameters versus pressure, there was not any significant discontinuity up to 6.0 GPa. The compressibility of the b-axis in chondrodite is much smaller compared to the compressibilities of olivine (βa=1.65, βb=3.34 and βc = 2.55 ($\times 10^{-3}$/GPa) in forsterite (Kudoh and Takeuchi, 1985)), giving the relatively large bulk modulus value compared to that of forsterite. In the FT-IR spectra, five peaks of OH-vibrations were observed at ambient conditions. With increasing pressure, three peaks around 3550 cm^{-1} were shifted to higher wave numbers, while the other two peaks around 3400 cm^{-1} were shifted to lower wave numbers, suggesting the formation of hydrogen bonding due to shortening of O-O distances.

RESIDUAL EFFECTS IN ARTIFICIALLY SHOCKED FORSTERITE

Uchizono A., Shinno I. *(Grad. Sch. Soc. & Cult. Stud., Kyushu Univ.)*, Nakamuta Y., Nakamura T. *(Dept. Earth & Planet. Sci. Fac. Sci., Kyushu Univ.)* and Sekine T. *(National Inst. Res. Inorg. Materials, shinno@rc.kyushu-u.ac.jp)*

Many studies on shocked olivines have been done so far. We have examined synthetic single crystal of forsterite (10 ϕ × 2mm thickness) shocked up to 82GPa using a single stage propellant gun. Shocked forsterites displayed unique extinction features as observed in various shock stages of chondritic olivines and considerable fracturing under polarizing and fluorescence microscopes, respectively. Even in forsterites shocked to 82 GPa, any decomposition phases such as olivine or silica glasses and fine grained MgO could not be detected.

Profile analyses of X-ray diffraction and Raman scattering peaks of the forsterites, where Gandolfi camera and micro Raman spectroscopy methods were applied respectively, have been done to detect residual strain and stress. Photo-luminescence and ESR spectra were also measured to identify defect type in strain parts.

The strain derived from Williamson-Hall plot of 20 diffraction angles and their peak broadening had a linear relation to the shock pressures. Raman peak 824 cm^{-1} assigned to an internal stretching decreased linearly contrary to the prediction in chondritic olivines, while the translational vibration of M2 site at 340 cm^{-1} shifted to higher wavenumber with increasing shock pressures. Although unit cell dimensions did not show any changes against the shock pressures, there exists residual stress in the shocked forsterites. The relation was applied to estimate the experienced shock pressures of Dhrumsala chondrites; it ranged from 24.0 to 37.8GPa.

The luminescence was intensified by the shock pressures, and its spectrum was composed of 5 bands. Their intensity and band width increased with the pressures, however, those parameters did not change simply.

Any meaningful ESR signals could not be detected even at liquid N_2 and variable microwave intensities, which may show nothing any types of defect with electron-hole or radicals in the forsterites.

6. Environmental Mineralogy

NATURE AND DISTRIBUTION OF ASBESTIFORM AMPHIBOLE, JEFFREY CHRYSOTILE MINE, QUEBEC

Williams-Jones A.E., Normand C., Clark J.R, Vali H., Martin R.F. *(Dept. Earth Planet. Sci., McGill Univ., willy_j@geosci.lan.mcgill.ca)* and Dufresne A. *(Dept. Occup. Health, McGill Univ.)*

Occupational health studies have demonstrated that exposure to asbestiform amphibole constitutes a major factor in lung deceases afflicting workers in asbestos mines and mills. A detailed study of the Jeffrey mine was conducted in order to characterize amphibole phases, to determine the concentration, distribution and controls of asbestiform amphiboles, and to develop criteria that can be used to avoid areas contaminated by these minerals.

Samples from serpentinized harzburgite ore zones and adjacent slate, serpentinized dunite and pyroxenite, and felsic dyke rocks, were studied by optical and electron microscopy, X-ray diffraction, and whole-rock geochemistry. Lower detection limits for amphibole in serpentinite were reduced to 0.1 wt% by the development of an acid-base dissolution method. Amphibole was not detected in ore zone serpentinite. However, fibrous amphibole was found commonly at altered serpentinite-dyke contacts and in altered serpentinite xenoliths in dykes, and less significantly in fracture zones in dykes, and in slate and serpentinized pyroxenite. Amphibole developed in felsic dyke rocks and slate tends to have actinolitic compositions ($Mg/[Mg+Fe^{2+}]$=0.56 to 0.67), whereas that from serpentinite-dyke contacts and xenoliths is more tremolitic (0.77 to 0.95). The distribution of asbestiform amphibole is thus controlled primarily by felsic dyke emplacement, and by syn- to post-magmatic hydrothermal fluids that interacted with compositionally contrasting dykes and serpentinite.

Extraction of amphibole-free chrysotile from serpentinized harzburgite-hosted orebodies is possible if precautions are taken to avoid felsic dyke rocks, serpentinized pyroxenite and serpentinite-slate contact zones.

INTERACTION, CONCENTRATION AND MINERALIZATION OF ENVIRONMENTAL METAL IONS BY BACTERIAL SURFACES.

Beveridge T.J. *(Dept. of Microbiology, College of Biological Science, Univ. of Guelph, tjb@micro.uoguelph.ca)*

The surfaces of bacteria are highly interactive with their environment. Whether the bacterium is gram-negative or gram-positive, most surfaces are charged at neutral pH because of the ionization of the reactive chemical groups which stud them. Since prokaryotes have a high surface area-to-volume ratio, this can have surprising ramifications. For example, many bacteria can concentrate dilute environmental metals or contaminating toxic heavy metals on their surfaces and initiate the development of fine-grained minerals. The mechanisms of this process will be presented. In natural environments, it is not unusual to find such bacteria closely associated with the minerals which they have helped develop. It is possible that this ability of bacteria to interact and concentrate dilute metals into *bona fide* minerals can be used as a bioremediation process to detoxify heavy metal contaminated environments.

BIOMINERALISATION BY THE SMALLEST KNOWN NANO-ORGANISMS IN BLOOD: IMPLICATIONS FOR PATHOGENIC DISEASES

Vali H. *(Electron Microscopy Centre, McGill Univ., vali_h@geosci.lan.mcgill.ca)*, Çiftçioglu N. and Kajander E.O. *(Dept. of Biochem. & Biotech., Univ. of Koupio)*

Unique culturable nano-organisms, capable of producing biominerals and likely responsible for pathogenic mineralisation (*e.g.* kidney stone, tooth plaque and various tissue mineralisation), have been isolated from mammalian blood and blood products. These nano-organisms have also been detected in human blood and their antigens found in kidney stones. The chemical composition and morphological features of mineralised nano-organisms resemble mineral particles found in calcified tissue cells and kidney stones. The surface morphology and internal structure of the nano-organisms were investigated in Pt/C replica, ultrathin section and cryo-ultrathin section in TEM. The nano-organisms are hundreds of micrometres in size and are not initially visible under the optical light microscope. After several days of incubation, however, and depending on culture conditions, the nano-organisms can be observed easily.

The mode of formation of minerals within the nano-organisms seems to be distinct from known biologically induced or biologically controlled mineralisation. The surfaces of the nano-organisms show a granular aggregation of particles of ~30 nm in size embedded in an organic matrix. In HRTEM, the internal structure of the nano-organisms show the ubiquitous presence of fine-grained hydroxyapatite. The chemical composition and structure of the crystals formed by the nano-organisms are similar to crystallites in enamel. The overall morphology and texture (*e.g.* size, shape, orientation and growth pattern) of the crystals within these organisms, however, resemble features observed in pre-dentin and pre-bone matrices. Mechanisms of mineralisation in bone and dentin are not well understood. There is general agreement, however, that glycosylated phosphoproteins are responsible for mineralisation in dentin and bone. Although the morphological characteristics of the mineralised nano-organisms are distinctive, and the presence of glycosylated protein in nano-organisms uncertain, a similar protein-based process of mineral formation in nano-organisms is conceivable. If so, these nano-organisms will have significance for understanding the mechanisms of pathogenic mineralisation and may provide insight into biomineralization processes in bone and dentin.

IRON MINERAL REACTIONS MEDIATED BY AN ENVIRONMENTAL BACTERIAL CONSORTIUM

Sherriff B.L., Brown D.A. *(Dept. Geol. Sci., Univ. of Manitoba, BL_SHERRIFF@ Umanitoba.Ca)* and Sawicki, J.A. *(AECL, Chalk River Laboratories)*

Iron rich sediments contain both Fe(II) and Fe(III) as a variety of oxides and hydroxides. A bacterial consortium, which produces a biofilm, controls Eh and pH in the aqueous environment. This consortium has been shown to be actively involved in various dissolution, precipitation and alteration reactions of iron minerals. In this paper the interactions between the consortium and various iron oxides and hydroxides are discussed.

Dissolution: the consortium removed grains of magnetite from thin sections of Lac du Bonnet grey granite.

Alteration: when magnetite was incubated in a flask with the consortium, 11% was converted to hematite within 3 weeks.

Precipitation: TEM and DIC images show that iron minerals precipitate directly onto the cell wall or S-layer of bacteria as well as being disseminated throughout the biofilm. Iron chelated by citrate in aqueous solution was precipitated as a mixed ferric/ferrous gel with the ratio of Fe(II):Fe(III) dependant on the ratio of C:Fe. The ferric ion was then partially reduced to ferrous by the metabolic reactions of the bacteria. These biologically precipitated iron gels (both ferrous and ferric) were aged under varying oxygenic conditions at 80 and 4°C to simulate low temperature diagenesis. The products were monitored using Mössbauer spectroscopy. The ferrous gel remained completely reduced except when aged at 80°C under air. The more oxic gel formed ferrous hydroxide at 4°C and hematite at 80°C. Goethite was only formed under sterile conditions with chemically precipitated iron when aged at 80°C. Only fine grained hematite was formed when the consortium was present.

6. Environmental Mineralogy

MICROBIAL URANIUM REDUCTION AND BIOMINERAL - IZATION: IMPLICATION FOR IMMOBILIZATION OF TOXIC METALS AND RADIONUCLIDES

Zhang C. *(Environmental Sciences Division, ORNL; zg9@ornl.gov)*, Brooks S. *(Environmental Sciences Division, ORNL)*, Fendorf S. *(University of Idaho)*, Vali H. *(McGill University)* and Jardine P. *(Environmental Sciences Division, ORNL)*

Reduction of uranium by microorganisms has potential applications in bioremediation of uranium- contaminated environments. The objective of this study was to examine the rate, extent, and the mechanisms of bacterial uranium reduction so that *in-situ* bioremediation of U-contaminated aquifers can be effective.

Batch experiments were conducted to evaluate the effects of environmental conditions on bacterial U(VI) reduction by using *Shewanella alga* strain BrY. Rates of U(VI) reduction were examined at temperature of 10 to 45°C, pH of 4 to 8, and dissolved-oxygen of 0.0 to 8.6 mg/L (air-saturated). Reduction rates were fastest at 45°C (rate constant = 0.2/hr) and lowest at 10°C (rate constant = 0.02/hr). Holding temperature constant (20°C), U(VI) reduction increased with increasing pH; the rate coefficient increased from < 0.01/hr at pH 4 to about 0.08/hr at pH 8. In abiotic controls, however, increases in pH had little effect on U(VI) reduction, and the decrease in U(VI) was less than 15% of initial concentration, compared with > 80% in cell suspensions at the same pH. Oxygen content had little effect on U(VI) reduction when dissolved oxygen was <1.0 mg/L; at 8.6 mg/L concentration, however, reduction of U(VI) decreased by eight- to 10-fold. Microbial reduction of U(VI) was confirmed by X-ray absorption spectroscopy, which provides information about the chemical and structural environments of U(VI) and U(IV) species. Interaction of uranium with BrY was examined by transmission electron microscopy in ultrathin sections. After two days of incubation, about 50% of BrY population showed uranium mineral precipitation on the cell membrane. This suggests that BrY is effective in immobilizing soluble uranium. Results of this study demonstrated that under the experimental conditions examined, maximum reduction of U(VI) occurred at temperature, pH, and redox conditions optimal for anaerobic growth of the bacterium. These results should help implement bioremediation strategies by providing information on optimizing microbial immobilization of toxic metals and radionuclides in heterogenous environments.

MINERALOGY AND TRACE ELEMENT ASSOCIATION IN AN ACID MINE DRAINAGE IRON OXIDE PRECIPITATE; COMPARISON OF SELECTIVE EXTRACTIONS

McCarty D.K. *(Texaco EPTD)*, Moore *J.N. (University of Montana)*, and Marcus W. Andrew *(Montana State University)*

Mineral and trace element characterization of an Fe-rich precipitate from an acid mine system was accomplished by X-ray diffraction (XRD), differential X-ray diffraction, and ICP chemical analysis. A primary objective was to evaluate the effectiveness of common selective dissolution treatments in determining the association of minerals with potentially toxic trace elements. The precipitate consisted primarily of goethite, a poorly crystalline phase resembling synthetic ferrihydrite, dolomite, and gypsum in clay-size fractions. The ammonium oxalate and EDTA treatments, which are thought by some workers to dissolve only poorly crystalline phases, were found to dissolve a significant amount of crystalline goethite. However, the oxalate extraction did dissolve more ferrihydrite than the other treatments tested. A solution of 0.1 M hydroxylamine hydrochloride in 0.1 M HNO_3, which is thought by some to dissolve mostly the highly soluble Mn-oxides was found to also dissolve goethite, as did 0.25 M hydroxylamine hydrochloride in 25% (v/v) acetic acid, 0.25 M hydroxylamine hydrochloride in 0.25 M HCl, 0.5 M HCl, and Na-dithionite buffered with Na-citrate and 1.0 M $NaHCO_3$. Both trace and major elements that were extracted with the various treatments were found to vary significantly and non-systematically when compared to the proportion of total extractable Fe. These selective extractions can not be used to make reliable conclusions about trace metal and mineral associations. Gypsum was identified by XRD in clay-size separations from the sample, but this phase was not detected in diffraction scans of the bulk sample. This finding indicates that individual phases can be segregated by particle size.

ADSORPTION OF TOXIC METAL CATIONS TO AQUEOUS POLYMERIC SILICA

Heaney P.J. and Yates D.M. *(Dept. of Geosciences, Princeton University)*

Charged colloidal particles in aqueous solutions can control the migration of dissolved metal cations in contaminated groundwaters. If colloids are immobilized within an aquifer system, adsorbed species may be concentrated well beyond the levels predicted by solubility data (Gschwend and Reynolds, 1987; Backhus *et al.*, 1993). Alternatively, mobile colloidal particles can serve as vectors for solute migration hundreds of meters from the contaminant source (Penrose *et al.*, 1990).

Although environmental scientists typically treat clay particles as the reactive fraction of suspended colloids, we argue that aqueous polymeric silica also plays a significant role as an adsorbent of metal cations in many groundwater systems. The comparative neglect of the sorptive behavior of polymeric silica may be traced to small colloid sizes and inadvertent removal during groundwater analysis. Our size exclusion chromatography has revealed that silica colloid dimensions fall in the nanoscale range (molecular weights of ~10^4 Daltons) in solutions that are only slightly supersaturated with respect to amorphous silica. In addition, we have shown that filtration of groundwaters with cellulosic filters effectively removes the polymeric silica fraction due to strong polymeric silica-cellulose attraction.

That polymeric silica can outcompete other colloidal adsorbents in nature is demonstrated by the common occurrence of such metalliferous chert varieties as jasper (Fe^{3+}-silica), chrysocolla (Cu^{2+}-silica), chrysoprase (Ni^{2+}-silica), and coffinite (U^{4+}-silica). Unlike clays, which will release bound metals during the transition from smectite to illite, metalliferous cherts can remain stable for billions of years, as metals are retained even during polymorphic diagenesis from opal-A to microcrystalline quartz. The petrogenesis of these cherts by metal-induced polymer coagulation is suggested by experiments involving polymeric silica and dissolved transition metals, such as Pb^{2+} (Patra and Ganguly, 1992), Th^{4+} (Östhols, 1995), and Cu^{2+} (Yates *et al.*, 1998). Our studies reveal that: 1) Transition metal adsorption to polymeric silica occurs as inner-sphere bonding; 2) Much lower concentrations of transition metals will coagulate silica than is the case with alkali cations; and 3) The pH dependence of adsorption isotherms for polymeric silica differs markedly from that involving colloidal crystals, such as clays. The strong adsorption of dissolved metal cations to nanoscale silica polymers presents a role for silica in polluted aquifer remediation.

ENVIRONMENTAL IMPACT BY NICKEL-COPPER-PGE MINING AND SMELTING IN THE KOLA-PENINSULA, NW RUSSIA: THE KOLA ECOGEOCHEMISTRY PROJECT

Stumpfl E.F., Gregurek D. and Reimann C. *(Inst. of Geol. Sciences, Univ. of Leoben, stumpfl@unileoben.ac.at)*

The International Kola Ecogeochemistry Project (Finland, Russia, Norway, Austria) has been devoted to the analysis of environmental damage near the nickel mining and processing centers of Zapoljarnij, Nikel and Monchegorsk, Kola-Peninsula, NW Russia. Technogenic deserts of up to 10 km diameter have developed around the main emitters; these can be recognized on satellite images. Total emissions are in the order of 300,000 t SO_2, and several hundred tons of copper and nickel per annum. This has resulted in maximum Ni- and Cu contents in topsoils exceeding 2% in some areas, with accompanying PGE contents reaching several ppm. We report here results of mineralogical and geochemical investigations of snow (1995/96 winter) and soil samples (summer 1997), taken at varying distances from the main emitters. Snow filter-residues and soil samples have been analysed for up to 40 trace elements and precious metals; there are distinct differences in the Pd/Te, Pt/Pd and Au/Pd ratios in snow filter-residues. These may be attributed to different ores being processed - Noril`sk ore is mixed with Pechenga ore at Nikel and Monchegorsk - and/or different process technologies. PGE distribution patterns in snow filtrates and soil samples reveal pronounced similarities suggesting more or less complete transfer of metals from snow to soil. Filtrates of snow samples have been embedded in araldite resin and polished; grain sizes range from 3 - 50µm. In the Zapoljarnij area (mines, roasting plant) a vast spectrum of primary pyrrhotite, pentlandite and chalcopyrite ore particles are dominant constituents. Typical intergrowths between Ni-Cu sulphides and phyllosilicates as seen in primary ores from Pechenga can frequently be observed in these filtrates. At the Nikel and Monchegorsk smelters, technogenic particles (Cu-Fe-Ni-(Co)-S and Fe-Ni-(Cu)-oxide globules, slag particles, coke) are widespread. They allow conclusions to be drawn as to the technological processes used; their compositions differ, however, slightly from those of standard blast furnace and converter products. This may be attributed to the fact that many industrial installations have not been modernized since the 1930s.

6. Environmental Mineralogy

STRUCTURAL CHARACTERIZATION OF QUARTZ CRYSTALS FROM THE CIGAR LAKE URANIUM DEPOSIT (CANADA) : THE EFFECTS OF IRRADIATION AND/OR HYDROTHERMAL ALTERATION.

Boudeulle M. and Mosser C. *(LPCML, Université Claude Bernard Lyon I, France, boudeull@pcml.univ-lyon1.fr)*

The Cigar Lake uranium deposit (Saskatchewan, Canada) developed at the unconformity separating the micro-conglomeratic sandstones of the Athabasca group from the metasediments and plutonic rocks of the Wollaston Group. Alteration haloes, reflecting several alteration phases, surround the deposit.

In the sandstones, around the uranium mineralization of the main pod episode (1341 Ma) and in some perched orebodies, an alteration zone containing hydromuscovites and vanadium bearing ferri-kaolinites surrounds secondary pitchblende (323 Ma). According to the petrological and geochemical data, the sandstones detrital quartz underwent dissolution in probably very aggressive fluids (T,P, sulphide,..) carrying radionucleides.

In the clay fraction, SEM imaging shows, together with well-shaped, well crystallized kaolinite flakes, rounded sponge-like grains of quartz, dotted with circular craters. At high magnification, it puts into evidence a high degre of surface alteration, without any even faces nor sharp edges. Circular holes, with regular diameters, are observed on every grain, like etch pitches or revealed fission tracks. Such features have been described previously for neutron irradiated graphite.

Raman spectra were collected using a microspectrometer which optics, according to the grain sizes, just allow to detect them in the clayey matrix. The weak spactra are characterized by a noticeable broadening and shifting of the vibration bands, specially the soft mode, and very anisotropic signals are recorded in some cases : they are characteristic of highly defective lattices and very similar to those resulting from neutron irradiation of quartz at a high dose. A careful heating, *in situ*, under the focused laser beam of the spectrometer, induces a noticeable increase of the local crystalline order, like fission track annealing.

Our observations are perfectly coherent with the proposed hypothesis of an hydrothermal alteration associated with particle irradiation : in this respect, quartz grains from Cigar Lake sandstones represent good models for the simulation of the evolution of nuclear waste disposals.

THE BIOCHEMISTRY FEATURE AND ENVIRONMENTAL SIGNIFICANCE OF INDUSTRIAL MINERAL FIBERS IN GAMBLE SOLUTION AND ORGANIC SYSTEM*

Dong F.Q., Wan P., Li G.W., Peng T.J., Zhuang J., Feng Q.M. and Song G.B. *(Inst. of Min. & Appl., Southwest Inst. of Tech., P.R. China)*

The Industrial mineral fiber dusts included fibrous and block brucite (Br), wollastonite (Wo), chysotile asbestos (CA), Lizardite (Liz), fibrous and clay sepiodite (Sep) and palygorskite (Pal), and clinoptilolite (Cp) collected from more than 7 provinces of China.

1. The solubility of industrial mineral fibers in organic system. Acetic acid, oxalic acid, lemon acid, tartaric acid were chosen to compound a concentration series. Br, Wo can completely dissolved in all organic acid and produce Mg and Ca salts, and forms Si complex compound in Wo. Sep, Pal and Cp only some Mg^{2+}, Al^{3+} exchange out, mineral structures aren't no change and total dissolving loss upto 8 - 10%. Liz and CA not only cation come out but also some SiO_2 dissolved (at 37°C, 24h and l/s = 50:1).

2. The feature of mineral dust in Gamble solution. The 12 different mineral dusts were chosen under pH=3,5,7 Gamble solution at 37° C, speed 5ml/h. The chemical analysis from each 15 days collected acting liquid solution show that Mg^{2+}, Ca^{2+} had dissolved easily from all dusts. Ca^{2+} character in Wo is same as Mg^{2+} in Br but in Cp as cation exchanging out. Si can be a little dissolved in silicates as a less 5%. The pH3 and pH5 Gamble solution dissolving speed far exceed the pH7 because pH3 is a HCl - ((Na K, Ca) Cl,) - $C_6H_6O_6$ - $NaHCO_3$ - $KHC_8H_4O_4$ system, pH5 is a salt and sugar system and pH7 is salt, sugar and contain NaOH system. $C_6H_6O_6$ doesn't influence the dusts dissolving but salts solution will increase dissolving capacity of pH7 and decrease of pH3.

3. The dissolving feature of the dusts containing SiO_2 in organic system and all elements in Gamble solution submit a way to explain the forming mechanics of silicosis and treat similar decease, as well as good for discussing the mineral dusts moving in human body.

**Project was supported by National Natural Sciences Foundation.*

MINE WASTES, DRAINAGE WATERS AND STREAM SEDIMENTS FROM THE POLYMETALLIC SULFIDE DEPOSIT OF FENICE CAPANNE (SOUTHERN TUSCANY, ITALY)

Mascaro I., Morelli F., Benvenuti M., Corsini F., Parrini P. and Tanelli G. *(Department of Earth Sciences, University of Florence)*

In the Fenice Capanne area exploitation and processing of a polymetallic Cu-Pb-Zn-(Ag-Au) deposit have left many mine wastes; the ore bodies occurred with a vein attitude linked to two tectonic dislocations in the east flank of Serrabottini horst.

Mine waste materials (roasting and flotation tailings) show high, even if variable, contents of toxic elements. The maximum contents, in ppm are: Pb (10000), Zn (13500), As (750), Cu (7500), Cd (30). Tailings commonly show pH values in the range 3.3-7.8.

Water and stream sediment samples have been collected as far as 6 km both up and downstream from the mine wastes. Waters present two different chemical compositions. All river waters collected downstream from mine wastes are Ca-sulfate, mostly acidic and with high contents of Cu, Pb, Zn, Fe, Cd and Mn, exceeding the drinking water level as established by the Italian law. Waters sampled upstream from wastes are Ca-bicarbonate with neutral pH and low contents of metals.

Both stream bed sediments and suspended particulate have high metal loads as well; maximum values in ppm: are Cu (13300), Pb (2100), Zn (7100), As (420). Close to the mine wastes they are composed of relics of py, ccp, sp, gn, amorphous Fe (Al) oxyhydroxides with trace contents of Cu, Pb and Zn, malachite and chrysocolla.

The alteration processes of mine waste materials (oxidation of sulfides, dissolution of carbonates and silicates) have produced pollution in surficial waters and sediments. The occurrence on the river-bed and in suspension of particulate sediments, mainly composed of Fe(Al) oxyhydroxides, is of interest for metal dispersion. In fact these colloid materials can be easily transported by stream waters. Moreover entrapment of metals in these amorphous particulates may be only temporary in relation to the changing chemicophysical conditions.

MECHANISM OF GLYPHOSATE INACTIVATION BY MICROCRYSTALLINE GIBBSITE

Dubbin W. *(Dept. of Mineralogy, Natural History Museum, London)*, Sposito G. and Zavarin M. *(Ecosys. Sci. Div., UC Berkeley)*

Glyphosate [N-(phosphonomethyl)glycine] is a nonselective broad-spectrum herbicide that is widely used in agriculture, forestry, and urban settings. It is one of the most heavily applied pesticides in the U.S., with an annual usage of 11 to 13 million kg. Upon addition to soil, glyphosate is readily sorbed, losing both its efficacy as an herbicide and its potential for translocation. Oxides of Al such as gibbsite are abundant in earth surface environments and possess surfaces capable of chemisorbing and inactivating various xenobiotic organic compounds. Attempts to elucidate the mechanism of glyphosate sorption to gibbsite, and thereby provide an explanation for this rapid inactivation, have thus far been unsuccessful. The goal of this research, therefore, was to derive the architecture of gibbsite-Cu-glyphosate surface complexes, in which Cu serves as a probe of the local bonding environment.

Copper K-edge EXAFS spectra of 10 mM aqueous Cu-glyphosate complexes at pH 5.5 revealed Cu complexation at the phosphonate moiety. Formation of a ternary surface complex by introduction of microcrystalline gibbsite resulted in loss of P from the coordination sphere of Cu, suggesting a direct coordination of the phosphonate group to the oxide surface. EXAFS spectra of Cu in the gibbsite-Cu-glyphosate ternary complex give a close fit with spectra for the Cu-glycine and Cu-methylglycine aqueous systems, thereby providing evidence for Cu complexation at only the carboxyl O and amine N of glyphosate. The EXAFS-derived structure of the surface complex reveals that rapid inactivation of glyphosate occurs due to chemisorption via the phosphonate group. Furthermore, despite tenacious binding of glyphosate to gibbsite by this mode of attachment, the amine N is vulnerable to microbial attack and glyphosate may, therefore, be degraded rapidly.

6. Environmental Mineralogy

RUBIFICATION OF THE BEREA FORMATION

Dunlevey J.N. *(Dept. Geology, Univ. Durban-Westville, South Africa)*

The Berea Formation (BF) is composed of rubefied, Pleistocene Age dune sands and forms a band over 500km long on the eastern coast of southern Africa. Although only modern dune sands (MDS) are mined in South Africa, units equivalent to the BF are, in the East African Coastal Plain a potentially important source of titanium-rich heavy minerals.

The BF lack the calcite, feldspar and silicate heavy minerals (except zircon) found in MDS, and the characteristic red colouration is concentrated in the sticky, fine-grained phase coating sand grains. This fine-grained material formed by rubification is normally ascribed to haematite and 'clay-minerals'. However; XRD indicates that although the coating contains a little kaolinite, no crystalline iron-bearing minerals are present; but, a significant quantity of an amorphous phase is present.

The bulk BF has, relative to MDS, an enhanced SiO_2 content, and the <63μm and <25μm fractions lower SiO_2 contents. The enhanced TiO_2 content of the BF bulk sample suggests material loss during rubification, and high TiO_2 values in the fine fractions indicate heavy mineral comminution. The Al_2O_3 values of all BF samples are elevated, but highest in the fine-grained material. The enhanced Fe_2O_3 and depleted FeO values of all BF samples, compared to MDS, indicate oxidation; and the drastically reduced MgO, CaO, Na_2O, CO_2 and strontium content signify leaching. BF bulk sample zirconium content is enhanced relative to MDS, but the fine-fractions depleted; indicating rubification does not reduce zircon grain sizes. The most dramatic differences are in the moisture content, MDS contain very little water, but the BF whole sample has significant water, and fine fractions high moisture contents.

The fine-grained material produced by rubification that coats the sand-size grains of the BF is a hydrated aluminium and iron hydroxide, best represented by the formula $(Al, Fe)(OH)_3\ nH_2O$. The ionic radii of ferric iron and aluminium are not considered compatible, but both are well known for their amorphous and gelatinous hydroxides. Thus the formation of a non-crystalline double hydroxide is not contradictory to the principles of crystal structure, as a lattice structure is not present.

MINERAL CONTENT OF GLACIAL ICE AND SNOW FROM THE JUNEAU ICEFIELD, ALASKA, U.S.A.

Shull C.J., Koenig D.S. and Gunter M.E. *(Dept. of Geology, University of Idaho, mgunter@uidaho.edu)*

Mineralogists have a unique opportunity to assist in many current environmental issues, for example the mineralogical content of atmospheric dust. Many countries have regulations on acceptable levels of dust, but rarely is the mineralogical composition of the dust considered. Historical levels of dust and mineralogical composition are preserved in glacial ice. The Juneau Icefield in Alaska is an excellent location in which to conduct research on atmospheric dust in ice and snow due to its remote location and lack of local human interference.

During the summer of 1997 we collected seven ice and nine snow samples of approximately 1 liter of water obtained from melting the snow or ice. The ice samples were collected below an icefall in a series of ogives. An ogive is a iceflow feature that repeats annually. Samples were collected from ogive number 1, 5, 10, 15, 20, 30, and 50; thus, spanning 50 years of time. The nine snow samples were collected over an aerial distribution of approximately 20 by 50 kilometers and represent snow from the 1996-1997 winter.

In the lab, each liter of water was filtered through silver membrane filters to prepare the dust for powder X-ray diffraction analysis; the before and after weight of the filter gave the dust content of the ice or snow. Ice sample dust content ranged from 0.41 mg/l to 15.27 mg/l and snow sample dust content ranged from 0.18 mg/l to 1.72 mg/l. The highest dust concentrations came from the oldest ice samples.

The samples contained only mg quantities of dust; thus, long scan times were required to obtain diffraction patterns sufficient to identify the minerals. A Siemens D-5000 theta-theta powder diffractometer equipped with a solid state detector was used to scan over 2-62 degrees 2-theta with a step size of 0.02 degrees and 15 second count times. The mineral assemblages in both the snow and ice samples are complex and are a mixture of clays, feldspars, and quartz. In general, the snow samples vary less in mineralogy than the ice samples. The younger ice samples consist more of clay minerals than quartz and feldspar.

PERIGLACIAL LOESS FIELDS IN THE TAJO RIVER VALLEY, SPAIN.

García R., Vigil R. *(Dep. Geoquímica, Fac. Ciencias, U.A.M. Madrid, Spain)* and González J.A. *(Dep. Geografía, Fac. Filosofía y Letras, U.A.M., Madrid, Spain).*

Aeolian structures have been investigated in Aranjuez-Colmenar de Oreja zone (Madrid, Spain), to know if these structures are loess, depending on particle size.

The periglacial conditions are created by long-lasting temperatures below 0°C and frequent variations of air temperatures around this point.

We have constructed the corresponding grain size sequence curve with small fractions. Every fraction has been studied by X-Ray Difraction, EDAX and heavy mineral analyses.

The aeolic origin of all samples has been demostrated by Electron Microscope. This study has been accomplished by shocking quartz particles during materials transport. Most of these sediments were transported by wind at short distances as proved by direct mineralogic connections of these sediments with bedrock outcrops in adjacent areas.

If we take into consideration the fact that there are iron silicates on quartz particles, it is therefore is possible to consider aeolic structures joined underlying soil.

CRYO-SEM IN ENVIRONMENTAL MINERALOGY RESEARCH

Göske J., Pankau H.-G. and Pöllmann H. *(Dept. of Mineralogy, Univ. of Halle /S., Germany, goeske@geologie.uni-halle.de)*

Low temperature stages for scanning electron microscopy (SEM) were developed initially to avoid the water loss from hydrated specimens which occurs at room temperature in the high vacuum of the microscope. Cryo-preparation can be completed within a few minutes. The effect of shock freezing is completed within some msec. An *in situ* examination of hydrated systems like cement or cementitious compounds (lamellar metal-metal-hydroxisalts) in the vacuum environment of a SEM at ambient temperature is often not possible. Such samples can be cryo stabilized by freezing, transferred to a cryo preparation chamber under vacuum where they can be fractured, sputter coated with a conductive layer and finally examined on a cold stage in the SEM. Fracturing such samples gives information on the distribution, size of the various phases and components, beginning of the crystal growth and *in situ* orientation of the crystals and crystal aggregates in solution (without sedimentation due to the texture or size of the crystals).

Crystals of the lamellar calciumaluminatehydrates are hexagonal and platy. In solution the crystals grow from stoichiometric composition of the starting mixture. For standard SEM-examination the substances must be dried before the preparation. This process is responsible for a preferential orientation of the crystals || 001. Therefore it is generally possible to examine only these crystal faces with standard SEM. After the drying process no statement is possible about the size of the educts and products in solution or about the development of the reaction.

With the help of the cryotransfer SEM the crystals or aggregates of crystals in solution can be frozen and growing of crystals can be studied *in situ*.

With this technique it is possible to obtain time-resolved information on crystal growth mechanisms in hydrous systems.

6. Environmental Mineralogy

^{77}Se NMR SPECTROSCOPIC INVESTIGATIONS OF SeO_4^{-2} AND SeO_3^{-2} HYDROTALCITE-LIKE COMPOUNDS (HTs)

Hou X-Q. *(xhou@uiuc.edu)*, Kirkpatrick R. J. *(kirkpat@uiuc.edu)* and Kim Y. *(Dept. of Geology, University of Illinois at Urbana-Champaign)*

Selenium plays a critical role in both inorganic and biogeochemical systems, but its molecular-level behavior remains incompletely understood. Hydrotalcite-like compounds (HTs) are mixed oxides with layer structures and contain anions in the interlayer. Thus, they are expected to interact strongly with Se-O anions. HTs with interlayer SeO_4^{2-} and SeO_3^{2-} have been synthesized by exchange reaction, ^{77}Se NMR spectra were collected under conditions of variable humidity, temperature and pH and in aqueous suspensions to understand the structural environments and dynamical behavior of the selenium-containing species on a molecular scale, and their exchange in hydrotalcite-like compounds. Selenate and selenite are remarkably different in this regard. Selenate in HT has a relatively narrow peak and a chemical shift close to that of sodium selenate solution. It is relatively loosely held in the interlayer. Selenite in HT has a much broader peak than in solution. XRD data suggest that it occurs in the interlayer, but it may also react by a ligand exchange reaction based on ^{77}Se NMR data. Dependence of the structural environments and dynamical behavior on pH and humidity is also discussed.

ANTIMONY IN THE STRUCTURE OF DUSSERTITE, THE Ba-Fe-ARSENATE END MEMBER OF THE CRANDALLITE GROUP

Kolitsch U. and Pring A.*(Dept. of Mineralogy, South Australian Museum, Adelaide, Australia, ukolitsc@geology.adelaide.edu.au)*

The crystal structure of an antimony-bearing dussertite has been refined from single crystal intensity data. Dussertite is the Ba-Fe-arsenate end member of the crandallite group of arsenates and phosphates within the alunite family of compounds $AB_3(XO_4)_2(OH,H_2O)_6$, where A = monovalent (H_3O, Na, K, Ag, Tl, ...), divalent (Ca, Sr, Ba, Pb, Hg, ...), trivalent (Bi, REE) or quadrivalent cation (Th, Zr), B = trivalent cation (Al, Fe, Cr, and minor Cu^{2+}, Zn^{2+}) and X = P^{5+}, As^{5+}, S^{6+}, Se^{6+} and minor Si. The present contribution is part of a project on the immobilization of toxic heavy metals in specific mineral structure types.

The crystal investigated has the composition $Ba(Fe^{3+}_{0.84},Sb^{5+}_{0.16})_3(AsO_4)_2(OH,H_2O)_6$ and shows rhombohedral symmetry, $R\bar{3}m$ with a = 7.410(3), c = 17.484(4) Å, Z = 3; the structure has been refined to R = 3.2 % and R_w = 3.7 % using 377 observed reflections [I >3 σ(I)]. The hydrogen bonding network was modeled using bond valence calculations.

Dussertite has the alunite-type structure and consists of sheets of corner sharing $(Fe^{3+},Sb^{5+})O_6$ octahedra parallel to (001), BaO_{12} polyhedra in between the sheets, and AsO_4 tetrahedra. The substitution of Fe by Sb is unambiguously demonstrated by refinement, electron microprobe analysis and crystal-chemical considerations. The investigated dussertite sample represents the first example of a member of the crandallite group which contains substantial antimony. The structural parameters are compared with those of other members of the alunite family. The role of antimony in secondary arsenates is discussed.

ARTIFICIAL CHEMICAL WEATHERING OF GRANITE UNDER EARTH SURFACE CONDITIONS

Kobayashi S. *(Division of Earth Sciences, Kurashiki Univ. of Sci. and Arts, shoichi@las.kusa.ac.jp)* and Sakamoto T. *(Faculty of Sci., Okayuma Univ. of Sci., sakamoto@das.ous.ac.jp)*

In order to predict the effect of acid precipitation, artificial chemical weathering of polished plates of the so-called Kitagi Granite, Okayama, southwestern Japan, was conducted using a Soxhlet extraction apparatus with distilled water and HNO_3, H_2SO_4 and HCl of pH 3 at 55°C for a different period of time up to 824 days. The granite was composed mainly of quartz, plagioclase ($Ab_{86}An_{12}Or_2$), alkali feldspar ($Or_{92}Ab_8$) and biotite. Samples of the leached solution were collected, and analyzed for major and minor elements using ICP, ICP-MS and Ion-Chromatography. Morphological and chemical changes of the each mineral surface were studied by SEM, EPMA and microscopy techniques. Alteration products, collected from the surface of each mineral on the polished plates by hand picking, were also examined by XRD.

The results showed the release of elements and the degree of weathering of minerals as a function of leaching time. Molar ratios of the each element in the leached solutions to the granite are differed by the element. The ratios of the elements such as Mn, Mg, Fe, Sc, Zn and Yb, which reflect the dissolution of biotite, are shown relative high. Similarly, the ratios of Na, Ca, Gd and Sr, which reflect dissolution from plagioclase, are also shown relative high. The plots of the ratio versus ionic radius are similar to the partition coefficient-ionic radius diagram for plagioclase and biotite systems (Matsui *et al.*, 1977). It is seem, therefore, that plagioclase and biotite are weathered extremely. The ratio also described that the sequence of reactivity of the acid solutions for plagioclase is H_2SO_4, HCl and HNO_3, and for biotite is H_2SO_4, HNO_3, and HCl.

It is evident that biotite changed into mica-clay minerals and/or interstratified minerals of mica and vermiculite by all kinds of acid solution used in the experiment. Smectite appeared to be formed from plagioclase during the artificial chemical weathering. No altered product from quartz and alkali-feldspar, however, was detected.

SI-RICH LAYERS AT LICHEN-MINERAL INTERFACES AS AN INDICATOR OF BIOCHEMICAL WEATHERING

Lee M.R. and Parsons I. *(Department of Geology and Geophysics, University of Edinburgh, martin.lee@ed.ac.uk)*

Si-rich "leached layers" have been widely reported on the surfaces of silicate minerals used in laboratory dissolution experiments. These layers are typically thin (sub-micrometer) and thus difficult to characterise. There are also very few reports of such layers on the surfaces of silicate minerals from soils and so their relevance to our understanding of silicate weathering in nature is questionable.

We have found Si-rich layers on silicates from the Lower Devonian Shap Granite, NW England. The layers occur on grains of alkali and plagioclase feldspar and biotite that are encrusted by the lichen *Rhizocarpon geographicum*. Their thickness is typically less than 10 micrometres and the layers are composed of Si and O, with minor concentrations of Al and S. Significantly, the layers bridge fractures and cleavages within mineral grains and also infill small pores. The presence of these layers at the lichen-mineral interface confirms their biochemical origin, but they could either be true residual layers formed by the leaching of silicates, or biochemical precipitates.

Other evidence for biochemical weathering of the Shap Granite is scarce. Oxalate minerals, which are diagnostic of biochemical weathering by lichens, are absent. Cleavage surfaces within alkali feldspars have been etched, but this weathering may have predated colonisation of the granite by *R. geographicum*. Importantly, the best evidence for biochemical weathering comes from biotite grains that have been biomechanically fragmented by penetration of fungal hyphae along cleavage planes. Elements including Mg, Al, K, Ti and Fe have been leached from these grains, leaving a Si-enriched relic. The origin of these Si-rich layers remains unclear, but dissolution of silicates followed by reprecipitation of an impure silica gel, is the most likely mechanism. In addition to being a diagnostic indicator of biochemical weathering, such layers may play an important role in protecting mineral surfaces from subsequent biochemical action.

6. Environmental Mineralogy

MINERALOGY AND WEATHERING OF Pb-Zn SLAGS FROM PRIBRAM, CZECH REPUBLIC

Legendre O., Bodénan F. *(BRGM, Orléans, o.legendre@brgm.fr)* and Ettler V. *(Charles University, Prague)*

This study is part of a program aimed at understanding heavy metal behavior in vitrified waste material exposed to weathering. At Příbram, 100-year-old Pb/Ag pyrometallurgical slag was sampled and studied for its similarity with such material. The slag occurs as massive (30 × 30 cm) casts of glassy material mainly composed of silicates; a metallic fraction is present as spherical inclusions, a centimeter to a few microns in size, derived from the separation of a sulfide matte at the liquid stage. A large amount of the metallic fraction is often observed at the bottom of the casts.

The mineralogical study shows that the three main components of the silicate fraction are olivine-type minerals [with the general formula $(Fe,Ca,(Mg))SiO_4$], Ca-rich clinopyroxene [$(Ca,Fe)_2Si_2O_6$], and melilite-family minerals [$(Ca)_2(Fe,Mg,Al^{VI})(Si,Al^{IV})_3O_7$]. Fe-Al- Zn spinels are also observed. Dendritic Fe-poor sphalerites are very common in the silicate phase. A glass phase forms chilled borders to the slag and fills interstices of the silicate crystals. Electron-probe analyses show Pb enrichment in the glass. The metallic fraction is an intergrowth of sulfides with minor alloys, arsenides and oxides, the most common species being pyrrhotite, galena, sphalerite, bornite, and lead, present as rounded inclusions. As is associated with Fe, mostly as löllingite. Sb and Sn are found as alloys with minor Cu.

Evidence of weathering has been observed, such as a wash out (to 100 μm depth) of the chilled glass borders of the slag, which leaves a framework of untouched silicates with no *in-situ* redeposition of the mobilized material. Another weathering feature comprises 10-20 μm banded layers of secondary minerals deposited at the surface of the slag. These minerals, very finely crystallized and difficult to identify. are composed of Pb, Zn and Fe sulfates and oxides-hydroxides. The solution precipitating the minerals probably results from leaching nearby metallic inclusions at the surface.

A NOVEL USY ZEOLITE-SUPPORTED NI-MO SULFIDE CATALYST FOR ENVIRONMENTAL CLEAN-UP

Li D. *(EES-1, Los Alamos Natl. Lab., dienli@lanl.gov)*

New environmental regulations require that sulfur, nitrogen and toxic metals in fuels used be reduced very significantly. The γ-Al_2O_3 based catalysts which have been widespread used in industry are not suitable for deep hydrodesulfurization (HDS). Zeolite supported transition metal sulfides may be new generation catalysts for the deep HDS, because of their high activity in both hydrogentation and hydrocracking (HC). A novel ultrastable Y-type (USY) zeolite supported Ni-Mo sulfide catalyst has been developed in this work.

The USY zeolite was made by dealumination of NaY zeolite (faujasite). The USY and NaY zeolite supported Ni-Mo catalysts were prepared by co-impregnation of Ni and Mo aqueous ammonia solution. The catalysts were dried at 200°C for 2h, calcined at 550°C for 3h in air, and sulfided under a stream of H_2-H_2S mixture at 400°C for 2h before reactions. The catalytic HDS of dibenzothiophene (340°C) and HC of decalin (340°C), tetralin (375°C) and diphenylmethan (375°C) were tested. The catalytic activities were calculated based on gas chromatography measurements. The catalysts were characterized using powder x-ray diffraction (XRD), NH3 temperature programmed desorption (TPD), diffuse reflectance spectroscopy (DRS), x-ray photoelectron spectroscopy (XPS) and transmission electron microscopy (TEM).

USY zeolite and its supported Ni-Mo sulfide catalyst are much active for the tested reactions than NaY and its supported catalyst, respectively. The USY zeolite supported Ni-Mo catalyst also has much higher HDS and HC activity than γ-Al_2O_3 supported catalyst. The NH_3 TPD indicated the presence of a very strong Bronsted acid site in the USY zeolite. XPS, DRS and TEM showed that Ni and Mo may enter the sodalite cage or great cavity of the USY zeolite. Both strong Bronsted acid structure and the Ni-Mo sulfide phase in the cage or supercage of USY zeolite may contribute to the high HDS and HC activities of USY zeolite supported Ni-Mo sulfide catalyst.

VIBRATIONAL SPECTROSCOPY OF ASBESTOS MINERALS IN BUILDING MATERIALS

Lemaire C., Guyot F. *(Lab. de Minéralogie et Cristallographie and IPGP, Paris, France, lemaire@lmcp.jussieu.fr)*, Petit P.E. *(BRGM Orleans France)* and Gillet Ph. *(ENS Lyon France)*

Vibrational spectroscopies are potentially interesting sensors of asbestos minerals, since portable systems can be taken on site for characterization without specific sample preparation. In order to test the capabilities of such spectroscopies in realistic situations, we have recorded mid-infra-red (MIR), near infra-red (NIR, 1.3 to 2.5 μm) and Raman spectra of standard asbestos minerals, as well as of several asbestos-containing materials typically found in building constructions. The samples were also studied by analytical transmission electron microscopy in order to characterize unambiguously the asbestos minerals in the materials.

The vibrational spectra of pure reference asbestiform minerals obtained by the 3 techniques have been analysed, with special attention to orientation effects related to the fibrous nature of these minerals. Possible overlaps with characteristic signals of other common minerals and organic materials are discussed.

The main conclusions for asbestos-containing materials, such as asbestos-cement, vinyl pavement, spray-on fireproofing, cord and cardboard are :

1. NIR spectra recorded with a portable apparatus provide good quality signals of the first overtones of O-H stretching modes and combination bands of fundamentals of O-H stretching and M-O-H bending modes in most materials investigated and can lead to unambiguous characterization of chrysotile in asbestos-bearing materials. The difficulties of application of this method to the detection of asbestos amphibole minerals are discussed.

2. Raman microspectrometry allows discrimination of fibrous chrysotile and amphiboles in most materials, based on vibrational modes related to Si-O and Si-O-Si oscillators. Additionally, this technique allows characterizations of fiber orientation parameters. However, in numerous cases, sample fluorescence prevents the use of this method.

A combination of both approaches therefore generally leads to unambiguous qualitative determinations of asbestos minerals in the materials investigated. More advances toward quantitative estimates will be discussed.

THERMOCHEMISTRY OF NUCLEAR WASTE GLASSES

Linard Y. *(Service de confinement des déchets, CEA-Valrho, Marcoule; Laboratoire de Physique des Géomatériaux, Institut de Physique du Globe, ESA-CNRS 7046)*, Neuville D.R. and Richet P. *(Laboratoire de Physique des Géomatériaux, Institut de Physique du Globe, ESA-CNRS 7046)*

Knowledge of basic thermochemical properties of borosilicate glasses used for long-term storage of nuclear waste is a prerequisite for a quantitative understanding of water-glass reactions. For a large part, the current lack of Gibbs free energies of dissolution of these glasses stems from the fact that, as disordered substances, glasses do not obey the third principle and have indeed large configurational entropies (S^{conf}). As the complex compositions of borosilicate glasses used for nuclear waste storage prevent determining configurational entropies by calorimetric methods, we used the Adam and Gibbs theory of relaxation processes to determine them from viscosity and calorimetry measurements through the equation : $\log \eta = A_e + B_e / T S^{conf}(T)$ where A_e and B_e are constants.

For this purpose, we have thus measured the heat capacities and high- and low- temperature viscosities of a series of glasses that include the SON68 glass developed by the Commissariat à l'Energie Atomique (CEA) to immobilize Light-Water type fission product solutions. The configurational entropies determined from these measurements will be discussed along with the implications of these results for modelling water-glass interactions.

6. Environmental Mineralogy

AMINOACIDS SORPTION BY Na-, Ca- AND Cu-SATURATED SMECTITES

Brigatti M.F., Frigieri P, Lugli C., Poppi M. *(Dept. of Earth Sciences, Univ. of Modena, Italy, brigatti@unimo.it)*

A thorough understanding of the capacity of clay minerals to adsorb organic pollutants is essential in order to predict the fate of contaminants in the environment. Because of the large surface area and common occurrence of smectites in clay fractions they are important in sorption/desorption reactions of organic pollutants entering soils and sediments.

The aim of this work is to evaluate the stability of the smectite- amino acid- metal systems in order to predict the capacity of these minerals to adsorb and to retain pollutants as heavy metals and organics. As aminoacids glycine and cysteine, which are abundant in soils around landfill and common in freshwaters, were chosen.

Sorption and desorption of glycine and cysteine by Na-, Ca- and Cu-saturated smectites (a montmorillonite from Cheto Apache County, Arizona, USA and a beidellite from Rasta, Recoaro Terme, Italy) were investigated; two grams of each natural and exchanged sample were suspended and stirred overnight, at room temperature, in 100 mL of 0.2M cysteine or glycine in aqueous solutions. Results showed that: i) glycine and cysteine can be sorbed by natural and Cu^{2+}-exchanged smectites; ii) the amino acid content depends on clay mineral chemistry and the amino acid type; iii) glycine is readily and nearly completely released by natural and Cu^{2+}-smectites treated with acidified distilled water (pH = 5), while cysteine is strongly retained by the mineral; iv) in the temperature range between 200-400°C, Cu^{2+}-smectite-glycine complexes show an exothermic reaction at about 300°C, whereas Cu^{2+}-smectite -cysteine complexes show an endothermic reaction at about 250°C, followed by an exothermic peak at about 300°C. v) in Cu^{2+}-smectite-amino acid complexes $d_{(001)}$ reflections shift from 15.5Å to about 17Å (Cu^{2+}-smectite-glycine) and to 22Å (Cu^{2+}-smectite-cysteine).

THE EXPANSION OF TECHNOGENESIS AS MINERAL FORMATION PROCESS

Potapov S.S. and Belogub E.V. *(Institute of Mineralogy of UB RAS, Miass, Russia, spot@imin.urc.ac.ru)*

Technogenesis as the process of change of natural complexes under effects of industrial activity of person causes the geochemical and mineralogical consequences, results in diverse mineralformation. Technogenesis mineralogy as the specific scientific direction was issued in connection with creation on the initiative of B.V.Chesnokov in beginning of 80's of Laboratory.

The modern mineral formation in burning coal heaps, in petroleum wells and oil equipment, at corrosion of metals in extreme conditions, in potassium salt heaps, in heat-and-power engineering equipment, at petroleum fires is studied in Laboratory of Technogenesis Mineralogy. We were investigated of new formation minerals in wall covers, in drainage water of pig farm, in sculptures too. All new and new technogenesis objects are involved in sphere of our researches with development of technical progress. B.V.Chesnokov studied 209 minerals in burning coal heaps, from them 46 new mineral kinds is established. 70 mineral phases have become known in oil and gas equipment. We make the list of mineral formations in heat-and-power engineering equipment from 50 minerals. We established 7 minerals in products of petroleum fire, 11 minerals in wall covers and 4 minerals in drainage water of pig farm. Only employees of our Laboratory is found out more 350 technogenesis minerals (approximately 10% of known =mineral kinds).

Mineralogy of series of technogenesis objects is not investigated practically: in nuclear desalinization of water installations; in zones of underground nuclear explosions; on burial place of liquid and firm nuclear wastes; on sites underground petroleum, coal, pyrites and gas fires and explosions; in zones of nuclear failures *etc.* I think, that to 20% of mineral kinds known on present moment is formed in technogenesis conditions. That is, technogenesis is all amplifying by geological force. The time has come to say about expansion of technogenesis as a real mineral formation process.

LUNG FIBER BURDEN OF TWO GROUPS OF QUEBEC ASBESTOS MINERS AND MILLERS

Nayeb zadeh A., Dufresne A. *(Dep. Occupational Health, McGill University)*, Case B. *(Dep. Pathology, McGill University)* and Vali H. *(Electron Microscopy Center, McGill University)*

One of the health effect of long-term exposure to asbestos fibers is an interstitial lung fibrosis called asbestosis. To investigate the lung fiber burden of asbestosis cases of Québec asbestos miners and millers, lung tissues of 88 former employees of two mining regions were analyzed. Thirty six cases from Jeffry mines and 46 cases from Thetford mines were included in this study. Two methods, digestion and ultra-thin sectioning were used to prepare the lung tissues. Transmission electron microscope (TEM) equipped with Energy Dispersive Spectrum (EDS) were used to characterize the morphology of the fibers and to analyze them. The average number of fibers analyzed was 85 per each case. The results showed a higher concentration of tremolite fibers in the lung of Thetford miners. Amosite and crocidolite asbestos fibers were observed in the lungs of Jeffrey mine miners and millers. Primarily statistical analysis on the first part of our data also showed that mean length, diameter, and aspect ratio of two groups were not different. In addition, a higher mean average concentration of fibers among Thetford miners was observed. Since Asbestos fibers were analyzed and sized in three ranges of length, $L < 5\mu m$, $10\mu m > L > 5\mu m$, and $L > 10\mu m$, we expect that the statistical analysis reveals further differences between the two groups.

Primarily results of TEM analysis of ultra thin sections of both group of miners suggest the accumulation of variety of mineral particles, including amphiboles, micaceous and opaque minerals, associated with presence of alveolar machrophase and pulmonary lesions. There was and extensive variation in the concentration and distribution of particles in the individual cells. We have also conducted a comparative analysis on standard samples of chrysotile and tremolite to compare their morphology with the detected fibers in the lungs of exposed miners.

TRITIUM ADSORBTION IN THE MONTMORILLONITE

Pushkareva R.A. *(State Science Center of Environmental Radiogeochemistry, gnc-r@olinet.isf.kiev.ua)*

Tritium accumulation in the underlying loess-like loam of the radioactive waste repositories site was established.

The main rock-forming minerals are quartz, feldspar and montmorillonite. To find out the structural position of tritium thermal and nuclear-physics analysis of the main rock-forming minerals was performed. Quartz and feldspar hold moisture in the temperature range to 1000°C. As a consequence, tritium accumulation is unlikely in these minerals. Moisture losses resulting from heating of loess-like loam are caused by dehydration and dehydroxylation of montmorillonite.

Eduction of water extracts occurs in the range 16-140°C, 140 - 230°C, 230 - 450°C, 450-700°C in accordance to endoeffect of montmorillonite. First endoeffect (98°C) conform to exuding free water, second (190°C) - to eduction of adsorption and interlayer molecular water, third - to exuding of admixture getite water. The major volume of the structural water constitutional hydroxyls educed in the course of the forth endoeffect. The eduction of constitutional hydroxyls in temperature range 450-700°C and free water - in 16-140°C was corroborated by data of the nuclear-physics analysis.

The specific Tritium activity in water extracts distilled off loess-like loam increased in respectively 100, 100, 40 and 30 times upon interaction of the loess-like loam with heavy tritium water having activity 4000 Bq/l for 180 days. This supports the theory that tritium can enter and exchange in the structural OH-groups and positions of clay minerals at normal conditions of the earth surface.

Consequently, *in situ* and laboratory tests evidence that loess-like layers can be effective geological-geochemical barrier to tritium contamination.

6. Environmental Mineralogy

TEM STUDY OF UNIQUE FIBROUS CHLORITE AND MUSCOVITE

Sears S.K. *(E&PS, McGill Univ., sksears@geosci.lan.mcgill.ca)*, Raith J.G. *(Inst. Geol. Sci., Univ. of Leoben, raith@unileoben.ac.at)*, Vali H. *(EM Centre, McGill Univ.)* and Martin R.F. *(E&PS, McGill Univ.)*

Phyllosilicates of unusual elongate platy to fibrous morphology have been identified in the matrix and in syn- to late-metamorphic quartz veins of graphitic schist of the Kaisersberg graphite mine, Styria, Austria. Mineral aggregates with acicular to asbestiform habit in hand sample and identified previously as "asbestos" or "hornblende asbestos", consist of Mg-Fe-bearing chlorite and alkali-deficient muscovite. In SEM, aggregates of fibrous chlorite, with diameters of 1 to 10s of μm, appear to have developed by "rolling-in" of platy chlorite. Elongate, lath-shaped muscovite also show "rolling-in" parallel to their long axis. TEM imaging of Pt-C replicas of chlorite and muscovite fibres show, in addition to the typical cleavage surface perpendicular to the c^* direction, a cleavage plane perpendicular to the *a* or *b* axis. The cleavage surfaces of these minerals show fine-scale growth steps along the long axis of the fibres, with some chlorite appearing to have more curved edges than the flat muscovite and overgrowths of distinct crystal phases. HRTEM imaging of octadecylammonium (C18) cation-exchanged ultrathin sections containing muscovite fibres show packets of coherent sequences of 2:1 layer silicates with 1 nm spacing. No structural defects, bending or "rolling-in" features could be observed. The lack of interlayer expansion after C18 cation exchange was surprising, considering the deficit of interlayer K in EMP analyses. This muscovite thus has not been altered and is distinct from illite, which shows an interstratification of expanded and non-expanded interlayers after C18 cation exchange. For a mineral to be considered as asbestos, single fibers must have a length >5 μm, a width <5 μm, and a length/width ratio of >3. The chlorite and muscovite identified in this study partially fulfill these criteria. Although individual fibres are typically elongate platy crystals, the bending and "rolling-in" of these aggregates parallel to the long axis result in the formation of a true fibrous morphology. The internal structure and, to some extent, the surface topography of these minerals, are more similar to asbestiform amphiboles than chrysotile. As the physical properties of the fibrous chlorite and muscovite resemble asbestos, their pathogenicity in humans and their environmental impact must be determined.

ENVIRONMENTAL MINERALOGY OF NATURAL AND TABLE SALTS

Yushkin N.P. *(Institute of Geology, Syktyvkar, Russia, yushkin@geo.komi.ru)*

Crystalline products of salt basins (halite, sylvite, carallite, etc.) contain inclusions of not only authigenic minerals of evaporite paragenesis but also atmospheric dust particles which can provide important information about the state of natural environment during salt deposition.

The insoluble salt residue from many deposits throughout the world showed a dramatic predominance of atmospheric dust particles derived from minerals occurring in the neighbouring territories. Tiny metal balls of cosmic origin are rather abundant, their nature suggested by their structural peculiarities, presence of nickel and other indicative elements. Salts from modern salines contain a large number of technogenic particles, including metal and metal-silicate balls. Revealed in a number of European salt lakes are levels with radioactive particles which are a consequence of Chernobyl holocaust.

After technological treatment, a large portion of insoluble inclusions in natural salts passes into the table salt. During a life span, the man takes up with salt about a dozen kilograms of insoluble minerals (anhydrite, gypsum, calcite, dolomite, quartz, hematite, radioactive minerals, *etc.*). They frequently occur as sharp needles and blades. The mineral inclusions in salt can cause local physical and chemical damage in the alimentary tract, exert a negative influence on human health.

Our study showed that natural salts can be one of the most important sources of environmental mineralogical information.

HYDROTHERMAL CRYSTALLIZATION OF BOROSILICATE GLASSES CONTAINING Cs OR Sr

Sohn W., Shoji T. and Kaneda H. *(Dept. of Geosystem Engineering, Univ. of Tokyo).*

Borosilicate glasses of various compositions were hydrothermally annealed in order to evaluate high-level radioactive waste disposal. The compositions were R_2O (R = alkalis of Li, Na, K)-B_2O_3-SiO_2 plus 5 wt.% of either Cs_2O or SrO. The experiments were carried out at 200 °C under vapor pressure (15.3 MPa) for 1, 3, 7, 14, 28, 56, 182 day(s) using an autoclave.

XRD characterization revealed that quartz, tridymite, Li-silicate, Li-borate, Na-borosilicate (searlesite) and Sr-borate (veatchite) were formed. SEM observation suggested two types of crystallization: 1) replacement type (R type) and 2) dissolution-precipitation type (DP type). A grain of the R type kept the original shape with crystallization progressing inward. On the hand, each grain of the DP type was changed into a balloon shape, where the inner part of the grain dissolved out, and new phases grew up from the original surface. Crystallization of the DP type was observed in most of the products, while that of the R type was seen only in some cases where alkali was rich.

Microprobe analysis and XRD patterns suggest that Sr is included in its own minerals, such as veatchite, one of whose major constituents is Sr. In contrast, Cs seems to substitute for alkali ions of solid solution minerals.

EFFECT OF SOLUTION CHEMISTRY ON THE SORPTION OF RADIONUCLIDES ONTO CLAY MINERALS

Jeong C.H. and Kim S.J. *(Dept. of Engineering Geology, Uni. of Taejon, chjeong@dragon.taejon.ac.kr)*

The transport rates of radionuclides leached from radioactive wastes disposed in crystalline rocks would largely be controlled by sorption process in water-mineral reaction systems along their transport pathways. In this study, sorption characteristics of hazardous nuclides such as ^{137}Cs and ^{90}Sr onto fracture-filling clay minerals, *i.e.*, kaolinite, illite and smectite clay, were investigated considering various chemical conditions of aqueous solutions such as ionic strength, pH and complex-forming ions.

Three-dimensional Kd modelling designed using a statistical method was performed to compare the relative effect among hydrated radii, charge and concentration of competing cations on the adsorption of Cs and Sr. The results of modelling indicate that the hydrated radii of competing cations are the most important factor for the adsorption of Cs and Sr followed by their charges and concentrations.

The pH exerts significant effect on ^{90}Sr sorption, whereas it has a little effect on ^{137}Cs sorption. The effect of pH on ^{137}Cs and ^{90}Sr sorption is relevant to the deprotonation of amphoteric clay surface. The effect of pH on the amphoteric surface charge of clay particles is recognized by zeta potential measurement.

The complexing agents such as SO_4^{2-} and HCO_3^- exert an effect on ^{90}Sr sorption by the pH change, the precipitation of a secondary phase such as a strontianite ($SrCO_3$), and aqueous complexation. The speciation of Sr and the saturation state of a secondary phase were thermodynamically calculated using the program, WATEQ4F.

The affinity of clay minerals for the removal of ^{137}Cs and ^{90}Sr from the solution were discussed considering the surface complexation model including the inner- (or outer-) sphere complex at the interlayer siloxane cavity of clay minerals. The ionic strength-dependence of ^{137}Cs and ^{90}Sr sorption by clay minerals indicates that ^{137}Cs and ^{90}Sr are weakly sorbed as outer-sphere complex at surface sites. It was also concluded that the difference of ^{137}Cs sorption between illite and smectitic clay is related to the reactivity of siloxane cavity.

7. Crystal Structures and Topology

BOND TOPOLOGY, BOND VALENCE AND THE STRUCTURAL CHEMISTRY OF OXYSALT MINERALS

Hawthorne F.C. *(Dept. of Geological Sciences, Univ. of Manitoba, frank_hawthorne@umanitoba.ca)*

It can be shown that the energy difference between two structures is primarily dependent on the first few disparate moments of their respective electron-energy density-of-states. Putting this in structural terms, the important energetic differences between structures involve differences in coordination number and local polyhedral connectivity. This supports the contention that structures may be usefully hierarchically ordered according to the polymerization of coordination polyhedra with higher bond-valences.

Bond-valence theory may be considered as a simple form of molecular-orbital theory, parameterized via interatomic distance rather than electronegativity or ionization potential, and arbitrarily scaled via the valence-sum rule. Combination of bond-valence theory with bond topology/energetic considerations leads to a very simple way of expressing complex structures. The structural unit is a strongly-bonded, usually anionic, polyhedral array whose charge is balanced by large low-valence interstitial cations. This gives a simple binary representation of even the most complicated structure; moreover, we can calculate the Lewis basicity and acidity of the two components, and examine their interaction via the valence-matching rule. This allows us to (1) account for why there are systematic differences in interstitial-cation chemistry in structural-groups with different structural units (*e.g.* collinsite: $Ca[Mg(PO_4)_2(H_2O)_2]$ *vs* brackebuschite: $Pb_2[Mn(VO_4)(H_2O)]$), (2) explain the presence and predict the amount of 'water of hydration' in minerals (*e.g.* botryogen: $Mg_2[Fe^{3+}_2(SO_4)_4(OH)_2(H_2O)_2](H_2O)_{10}$), and (3) rationalize the crystallization sequence of minerals in (some) complex environments (*e.g.* saline lakes).

Mn-SILICATES FROM ALKALINE ROCKS: CRYSTAL STRUCTURES, TOPOLOGY AND GEOCHEMISTRY

Pushcharovsky D.Yu., Pekov I.V. *(Dept. of Geology, Moscow State University, dmitp@dgeo.phys.msu.su)*, Pluth J. and Smith J. *(Dept. of Geophysical Sciences, CARS, Univ. of Chicago)*

This work summarizes the most recent results of XRD studies of Mn-silicates discovered in Lovozero and Dara Pioz alkaline massifs. Their structural topology, comparative crystal chemistry and petrogenetic significance are considered.

The structure of raite, $Na_3Mn_3Ti0_{0.25}[Si_8O_{20}](OH)_210H_2O$ was studied using SR (effective crystal size ~ 6μ m ; R 0.059 for 916 reflections). The structure comprises the silicate layers with tetrahedron inversion. In raite the regions of equal directedness of the SiO_4 tetrahedra are 2 *zweier* single chains, in sepiolite - 3 *zweier* single chains, in kalifersite both types of tetrahedral ribbons are characterized by tetrahedron inversion. The crystallization of aqueous layered silicate raite followed the formation of unhydrous nordites.

In 1997 nordite family with general formula $Na_3Sr\mathit{REE}M^{2+}Si_6O_{17}$ (M^{2+}=Zn,Mn,Fe,Mg; *REE*=Ce,La) was completed by two new minerals - manganonordite-Ce and ferronordite-Ce, discovered in Lovozero alkaline massif . They were characterized by the excess of Ce among REE and of Mn and Fe among M^{2+}cations, respectively. The size of M^{2+} tetrahedron correlates with its composition. The silicate bands $[Si_6O_{17}]$ of nordites are comparable with topologically related new silicate bands of haiweeite, $Ca(UO_2)[Si_5O_{12}(OH)_2]5H_2O$ - typical secondary mineral of U-deposits, connected with alkaline pegmatites of Dara-Pioz (Tajikistan) and Teofilo Otoni, Brazil.

Calcybeborosilite-Y,$(Y_{.42}\mathit{REE}_{.13}Ca_{.45})(Fe_{.125}Mn_{.05})[SiO_4](B_{.5}Be_{.5})[O_{.35}(OH)_{.65}]$ was discovered in Dara-Pioz. In contrast to all minerals of the datolite-gadolinite family it contains both B and Be. Co-occupation of a common position by Be and B is well confirmed by bond lengths of a corresponding tetrahedron. The distortion of Si tetrahedra decreases with the increase of ionic component in (B,Be)-O bonds.

The new discoveries of Mn silicates allows discussion of specific features of mineral geochemistry of Mn in alkaline pegmatites.

CSH (CALCIUM SILICATE HYDRATES) MINERALS: UNUSUAL TOPOLOGIES, CHAIN CONDENSATIONS AND THERMAL BEHAVIOUR

Merlino S. *(Dip. Scienze della Terra, Università di Pisa, merlino@dst.unipi.it)*

CSH (Calcium silicate hydrate) minerals include two wide group of phases: those which were collected under the name of 'calcium sheet silicates', because of their chemical composition and distinct basal cleavage and those characterized by the presence of single or double wollastonite chains.

The first group presents some of the most unusual and appealing topologies: simultaneous presence of silicate chains and silicate sheets in okenite; presence of two distinct silicate sheets in truscottite and gyrolite: the two distinct kinds of silicate layers, alternating with calcium octahedral layers, give rise trough different module combinations to the structures of reyerite, gyrolite, tungusite, fedorite, K- and Z-phases, and the somewhat modified structures of minehillite and baratovite. Moreover the various sets of module combination present polytypic and OD modifications.

The second group is characterized by the presence of single or double wollastonite chains which are grasped to 'octahedral' ribbons or layers: typical feature of all these minerals is the 7.3 Å periodicity of the tetrahedral part as compared with the halved 3.65 Å periodicity of the 'octahedral' module, which is at the origin of the widespread manifestation of polytypism and OD character by all the phases in the group: hillebrandite, xonotlite, foshagite,..... and all the members of the tobermorite subgroup (clinotobermorite, tobermorite-9Å, tobermorite-11Å, tobermorite-14Å).

Both group of minerals display interesting phenomena of topotactical transformations: the heating behaviour in the first group and the condensation and decondensation of wollastonite chains in dehydration processes taking plae in the second group will be described and discussed at the light of X-ray and electron diffraction studies and MASNMR investigations.

ROLE OF LARGE CATIONS IN THE FELDSPAR STRUCTURE

Balić-Žunić T. and Makovicky E. *(The Geological Institute, University of Copenhagen, Denmark, tonci@geo.geol.ku.dk)*

The large cation in the feldspar structure resides in a cavity defined theoretically by up to 11 oxygen atoms. The geometrical characteristics of the cavity and the bonding of large cations in known feldspar-type structures have been analysed using the parameters related to a centroid of coordination (Balić-Žunić and Makovicky, 1996; Makovicky and Balić-Žunić, 1998). Bonding characteristics were defined from the weighted coordination number for these cations as introduced by O'Keeffe (1979) and from the coordination number of the cavity that is derived from the Voronoi polyhedron of the centroid. Further geometric characteristics of the coordination polyhedron/cavity are the cation eccentricity, polyhedron sphericity and quantitative global distortion, all of these being centroid parameters.

The results show two distinct structural trends, one connected with the group of relatively small cations (Ca,Na) and another one valid for the group of relatively large cations (K,Rb). These trends converge in the middle region (Eu,Sr,Pb,Ba) where the coordination polyhedra show the smallest deformations. They meet in the structure of the H^+-feldspar (Paulus and Müller, 1988) which can therefore be regarded as presenting an undisturbed cavity in the feldspar structural framework. Incorporation of cations having the bond distance to oxygen greater than 2.86 Å (sum of Shannon's crystal radii for CN 9) produces straining of the framework with a tendency to inflate the cavity symmetrically. Cations with shorter bond distances also produce strain, but this time deforming the cavity and lowering its CN by bonding predominantly to one side of the cavity. For the former cations the cavity CN is therefore increased to 10 and O'Keeffe's weighted CN to 7.0 - 8.9. For the latter cations these values decrease to 8-7 and to 5.4 - 5.7, respectively. The ideal, "undisturbed" values are 9 and about 6.0. Trends for the other geometric characteristics based on the centroid concept will be discussed in the presentation.

HIGH-PRESSURE SINGLE-CRYSTAL X-RAY DIFFRACTION STUDY OF THE PROTOPYROXENE STRUCTURE: A FIRST-ORDER DISPLACIVE PHASE TRANSITION OBSERVED AT ~ 1.5 GPA

Yang H., Finger L., Prewitt C., Hazen R. and Conrad P. *(Geophysical Laboratory, Carnegie Institution of Washington, prewitt@gl.ciw.edu)*

A single-crystal X-ray diffraction study on a $(Mg_{1.54}Li_{0.23}Sc_{0.23})Si_2O_6$ protopyroxene crystal has been undertaken at various pressures up to 6.1 GPa to understand the pressure effects on the crystal structure of protopyroxene. A first-order displacive phase transformation from the *Pbcn* to $P2_1cn$ symmetry was observed between 1.11 and 2.50 GPa. The transition is characterized by a discontinuous change in all unit-cell dimensions and appearance of intensities of some *0kl* reflections with $k \neq 2n$. From 1.11 to 2.50 GPa, the a and c dimensions and the unit-cell volumes decrease by 1.28, 2.59, and 3.24%, respectively, whereas the *b* dimension increases by 0.63%. Differing from the low- protopyroxene structure, which contains only one type of the O-rotated silicate chain, the high-protopyroxene structure consists of two types of single silicate chains, the O-rotated A and the S-rotated B chains. Most strikingly, these two differently-rotated silicate chains in the high-protopyroxene structure occur alternately along the *b* axis in a tetrahedral layer parallel to (100). Such a mixed arrangement of two different types of silicate chains in a tetrahedral layer has not been observed in any other pyroxene structures. The O3-O3-O3 kinking angle in low protopyroxene at 1.11 GPa is 166.6°, whereas it is 153.9 and 147.9° for the A and B chains, respectively, in high protopyroxene at 2.50 GPa. The marked change in the kinking angles of the silicate chains at the transition is responsible for the decrease in the *c* dimension and the increase in the *b* dimension in high protopyroxene. Associated with the phase transition is the change in the compression anisotropy of the protopyroxene structure. The relative linear compressibilities (β_a:β_b:β_c) are 1.00:1.77:1.00 for low protopyroxene, whereas they are 1.00:1.24:1.77 for high protopyroxene. The bulk moduli of low and high protopyroxene are 134(1) and 137(2) GPa, suggesting that the phase transition has insignificant influence on the compressibility of the protopyroxene structures. The *Pbcn*-to-$P2_1cn$ phase transition is regarded to result from the collapse of the M2 polyhedral site.

NEUTRON POWDER DIFFRACTION, SINGLE CRYSTAL MÖSSBAUER AND MAGNETIC SUSCEPTIBILITY MEASUREMENTS ON THE SYNTHETIC CLINOPYROXENE Li-ACMITE $LiFeSi_2O_6$

Amthauer G., Lottermoser W., Tippelt G., Redhammer G. *(Institute of Mineralogy, Univ. of Salzburg, georg.amthauer@sbg.ac.at)*, Paulus W. *(Laboratoire Léon Brillouin, CEA Saclay)* and Treutmann W. *(Institute of Mineralogy, Univ. of Marburg)*

Mössbauer experiments on a Li-acmite single crystal section with the crystallographic **b**-axis (*P*21/*c*) parallel to the **k**-vector of the incident γ-rays were performed at room temperature and at several temperatures around the previously reported Néel point T_N (19.5(5)K). The observed iron is found to be exclusively in the trivalent state on one crystallographic site. In the antiferromagnetic region below T_N, we observe strong relaxation effects which diminish with decreasing temperature. In spite of this, the Mössbauer spectra could be satisfactorily refined yielding a slightly temperature-dependent angle of ~ 42° between the main component of the electric field gradient efg, V_{ZZ}, and **b**. In contradiction to early Mössbauer powder experiments, the quadrupole splitting QS does not disappear below T_N - a recalculation of the latter spectra with our single crystal parameters ($QS \neq 0$, $\Theta \neq 0$) yields a least equal goodness-of-fit as the early results. The internal magnetic field H(0) is mainly aligned parallel to the **c**-axis in agreement with magnetic susceptibility measurements of single crystals. A slight canting towards a corresponds with the results of neutron powder diffraction measurements at low temperatures. The different methods applied yield slightly different temperatures of the onset of magnetic ordering. This will be discussed in terms of long range order and short range order.

The results are compared to those of other pyroxenes, in particular to acmite $NaFeSi_2O_6$ and hedenbergite $CaFeSi_2O_6$. In many respects, Li-acmite can be considered as a model compound of one dimensional magnetic systems.

NEW STRATEGIES FOR THE PRECISE AND ACCURATE DETERMINATION OF CATION DISTRIBUTIONS IN SILICATES

Schlenz H., Kirfel A. and Vad T. *(Mineralogisch-Petrologisches Institut, Universität Bonn, Germany, schlenz@uni-bonn.de)*

The intracrystalline cation distribution of *e.g.* Fe^{2+} and Mg in silicate crystal structures is a complex function of chemical composition, temperature, pressure, oxygen fugacity, cooling rate of the host rock and possibly other variables. Orthopyroxene can *e.g.* serve as a geospeedometer (Kroll *et al.*, 1997), provided the accurate distribution of Fe^{2+} and Mg over the non-equivalent octahedral sites M1 and M2 as a function of composition, temperature and time. In order to obtain such precise and accurate information by X-ray diffraction experiments, including synchrotron radiation, improved and more sophisticated measurement and refinement strategies are required to yield reliable data for further thermodynamic and kinetic calculations, as recently demonstrated by Kroll et al. (1997).

We will present new X-ray and synchrotron data for orthopyroxene and olivine, demonstrate other measurement strategies and consider new techniques for site refinement, alternatively to the recently published LOT analysis (Schlenz *et al.*, 1997; Kroll *et al.*, 1997). We will introduce a new so called Q-Method (Vad, 1997), that is particularly based on the use of sensitive HO-reflections, and the method of charge integration which uses integrated electron densities for the distribution analysis.

References

Kroll, H., Lueder, T., Schlenz, H., Kirfel, A., Vad, T. (1997): *Eur. J. Mineral.*, **9**, 705-733.

Schlenz, H., Kroll, H., Fischer, A., Kirfel, A., Vad, T. (1997): *Terra Nova*, **9**, 426.

Vad, T. (1997): PhD. dissertation, Universität Würzburg, Germany.

OD PHENOMENA AND POLYTYPY IN SULFOSALTS

Makovicky E., Balić-Žunić T. and Olsen P.N. *(The Geological Institute, Univ. of Copenhagen, Denmark, emilm@geo.geol.ku.dk)*

OD phenomena and polytypy of various kinds were recognized in the crystal structures of owyheeite $Pb_{10}Sb_{11}Ag_3S_{28}$ (Olsen *et al.*, in prep.), imhofite $Tl_3As_{7.66}S_{13}$, gillulyite $Tl_2(As,Sb)_8S_{13}$ and in the pair rebulite $Tl_5As_8Sb_5S_{22}$ - jankovicite $Tl_5As_3Sb_{10}S_{22}$ (original structure determinations were made by Divjaković & Nowacki 1976, Foit *et al.* 1995, Balić-Žunić *et al.* 1982 and Libowitzky *et al.* 1995).

They range from classical OD phenomena obeying the groupoid theory to non-OD polytypes/polytypoids. Two or more such phenomena of different kind can be alternatively present in the same structure. OD layers with idealized symmetry *P* (2/*n*) $2_1/m$ $2_1/m$ alternate with layers *P(1) 1* $2_1/m$ in owyheeite; two such alternative sets of layers (012) and ($0\bar{1}2$) are present. Two distinct sets of (001) OD layers *P(1) 1* $2_1/m$ and either *P(1)* $2_1/m$ *1* (with a doubled b dimension) or *A (1) 2/m 1* alternate in gillulyite.

Part of the OD phenomena in gillulyite as well as those in imhofite stem from the introduction of regular As_2S_5: TlS_5 sequences (and of AsS_5: TlS_5 sequences in jankovicite) into atomic arrays in which adjacent sequences are shifted by either a half-width or a full width of one of the above polyhedra (polyhedral group). In imhofite these phenomena (OD rods in one set of layers) lead to distinct crystal structures when the other layers, the "inert matrix" of the structure, are taken into consideration. In jankovicite the *A (1) 2/m 1* unit OD layers result in two ordered stackings, *P-1* and *A 2/m*. The rebulite - jankovicite pair is formed by unit-cell twinning which is distinct from the above OD phenomena on Tl-As rows.

All these phenomena were observed in real, not idealized covalent structures of complex minerals.

7. Crystal Structures and Topology

TOPOLOGICAL TRANSFORMATIONS INDUCED BY DEHYDRATION IN ZEOLITES

Vezzalini G. *(Dip. Scienze della Terra, Univ. of Modena, Italy, vezzalini@imomn1.unimo.it)*

A large number of aluminosilicate zeolites may be reversibly dehydrated with only minor distortions of the framework. Others, characterized by a very flexible framework, exhibit a considerable framework distortion and a large decrease of the cell volume during the dehydration process. In these cases, rehydration is fast and complete reversion of the structure at room conditions occurs. A third type of zeolite is characterized by a framework that is less flexible, and so dependent on channel stuffing that it becames structurally unstable upon dehydration and subsequent migration of exchangeable cations. As a consequence, the framework collapses and the resultant stretching produces the breaking of some T-O-T bridges and the migration of tetrahedral cations to new "face sharing tetrahedra". As an effect of this migration, new topologies, characterized by new T-O-T bridges or by interrupted frameworks, are formed and the dehydration is partially irreversible.

These topological transformations affect only zeolites whose framework can be described by 6R or 4-4-1 SBU's. One example is, for the 6R zeolites, the synthetic zeolite (Na,TMA)-EAB which is characterized by the ABBACC stacking sequence and at around 360°C transforms into a sodalite-type product with a ABCABC sequence. On the contrary, all zeolites with 4-4-1 SBUs (heulandite, stilbite, barrerite, stellerite and brewsterite) are characterized by topological changes during dehydration, due to the breaking of T-O-T bridges in the 4-rings. The presence of OH in the frameworks, due to interrupted oxygen bridges, has been observed in NIR spectra for both the collapsed and partially rehydrated phases, thus suggesting a possible rearrangement of the framework, albeit a substantial stability of the new topologies is retained.

Water is expected to play a major role in these topological transformations, acting as a necessary catalyst. Different types of extraframework cations may give rise to variations in the thermal stability and the products obtained.

HIGH TEMPERATURE INVESTIGATIONS ON $Ca_2Fe_2O_5$ USING X-RAY AND NEUTRON DIFFRACTION

Kahlenberg V., Fischer R.X. *(FB Geowissenschaften, Univ. Bremen)* Weidenthaler C. *(Inst. f. Anorg. Chem., Univ. Frankfurt)* and Zeiske T. *(Hahn-Meitner-Institut, Berlin)*

The ferrite solid solution $Ca_2(Fe_{1-x}Al_x)O_5$ with $(0 < x < 0.7)$ is one of the four major phases in Portland cements. Differential thermal analysis of the iron-rich ferrites in this system revealed two very weak (order of magnitude 0.1 cal/g) signals at about T_1= 443°C and T_2 = 688°C, respectively. The present structural investigation was focussed on the end member $Ca_2Fe_2O_5$ and was aimed to characterize these transitions in more detail. The results of our high temperature X-ray experiments can be summarized as follows :

The structure stable at room temperature can be described in space group *P n m a*. The first signal at about T_1 is not accompanied by systematic integral or special extinctions of diffraction lines in addition to the extinction rules of *P n m a*. However, a sudden contraction of the unit cell parameters is observed. In the powder pattern recorded above the second transition several weak diffraction lines disappeared. The Laue indices of the remaining lines belong to the reflection class $h+k+l=2n$, indicating that the high temperature phase crystallizes in a body centered structure.

The Rietveld analysis of the neutron diffraction data recorded at 23°C revealed an anti-ferromagnetic ordering of the magnetic moments of the Fe^{3+} cations parallel to the *a*-axis. The ordering is compatible with the Shubnikov group *P n'm'a*. Above T_1 the magnetic reflections disappeared, indicating that this value corresponds to the Néel temperature of the compound. No additional structural changes relative to the room temperature structure could be detected.

TOPOLOGICAL ASPECTS OF URANYL MINERAL STRUCTURES

Burns P.C. *(University of Notre Dame, Peter.Burns.50@nd.edu)*

The crystal structures have been determined and refined for only 59 of the more than 200 uranyl minerals that have been described. Despite this, uranyl minerals show incredible structural diversity, owing largely to the details of the coordination polyhedra about U^{6+}. In minerals, the U^{6+} cation is invariably strongly bonded to two O atoms at distances of ~1.8 Å, forming an approximately linear $(U^{6+}O_2)^{2+}$ uranyl ion. The uranyl ion occurs in structures coordinated by four, five or six additional anions arranged at the equatorial corners of square, pentagonal, and hexagonal bipyramids, with the O atoms of the uranyl ions forming the apices of the polyhedra. The bond-valence requirements of the O atoms of the uranyl ion are largely met by the U^{6+}-O bond, but the bonds between the equatorial anions and the U^{6+} cation are weaker. As a result, the equatorial anions require substantial additional bonding, permitting extensive polymerization involving the equatorial corners and edges of the uranyl polyhedra. Considering uranyl polyhedra and other polyhedra of higher bond-valence only, polymerization of polyhedra in uranyl mineral structures usually results in infinite sheets (46 examples), but can also result in infinite chains (5 examples), finite clusters (5 examples), and frameworks (3 examples).

The 46 uranyl mineral structures that are based upon sheets contain 24 topologically distinct sheets. However, when only the anions contained within the sheets are considered, only 15 distinct topological arrangements result. The sheet anion-topology may be obtained for any sheet, and contains only anions that are at least two-connected within the sheet. It is constructed by drawing a line between anions that are separated by less than ~3.2 Å. The sheet anion-topology may be regarded as a two-dimensional tiling that possesses translational symmetry. It is straightforward to construct all observed anion topologies by using a set of chains of polygons that contain squares, triangles, pentagons and hexagons. This approach not only provides a means to compare structures, but also a means to predict new structures, and of relating the structural hierarchy to mineral paragenesis.

PHILOLITHITE, A MINERAL WITH A CLOSE-PACKED TRELLIS STRUCTURE

Moore P.B. *(Warwick, New York)*, Kampf A.R. *(Los Angeles County Museum of Natural History)* and Sen Gupta P.K. *(Deceased, Memphis State University)*

The atomic arrangement of the new Långban mineral, philolithite, $Pb_{12}Mn(Mg,Mn)_2(Mn,Mg)_4(SO_4)(CO_3)_4Cl_4O_6(OH)_{12}$, $P4_2/nnm$, a = 12.627(9), c =12.595(9) Å, Z=2, is remarkable for accommodating an assortment of ion sizes in an elegant framework based upon cubic-closest packing (c.c.p.). This and hundreds of other oxysalt structure types can be viewed as close-packed (c.p.) frameworks that lack some anions required for c.p. filling. These structures, which we refer to as trellis structures, are based upon open frameworks of octahedra and tetrahedra. The open c.p. trelliswork we call the structure's basis and the remaining ions, which fill the openings within the trellis, we call the structure's compliment.

In the philolithite trellis, linear edge-sharing Mn,Mg-O octahedral chains run parallel to [110] and [1$\bar{1}$0]. When the structure is viewed normal to c.p. layers, *e.g.* down [111], one set of chains lies in the plane of the projection, while the other appears as descending octahedral edge-sharing staircases, a common motif for c.c.p. structures. The two sets of chains are welded together by MnO_4 and SO_4 tetrahedra, forming an open, but rigid ediface.

The crystal-chemical formula can be written $^{[7]}Pb^{2+}_{12}O_6Cl_4(OCO_2)_4$ $[^{[4]}Mn^{2+}\ ^{[6]}Mn^{2+}_6\ (SO_4)\ (OH)_{12}]$, 3-ccc-, where the trellis portion, contained in brackets, is preceded by the framework's compliment. Two carbonate O atoms are associated with the c.c.p. trellis, while the remaining carbonate O, another O and the Cl are associated with Pb. The MnO_4 tetrahedron, infrequently encountered, is nearly regular and may contribute to the green color of philolithite. The trellis occupies 44% of available anion space. Betpakdalite possesses another type of connected trellis, $[^{[6]}Mo^{6+}_{16}\ ^{[5]}Fe^{3+}_6\ O_{58}\ (As^{5+}O_4)_4]^{14-}$, 2-chhhc-, which occupies 48% of available anion space.

We consider it noteworthy that structures of such apparent complexity can be resolved to relative simplicity.

A NEW STRUCTURAL DESCRIPTION FOR MINERAL AND INORGANIC FRAMEWORK-STRUCTURES CONTAINING ISOLATED CONDENSED POLYHEDRA

Schindler M.[1], Baur W.H.[2] and Hawthorne F.C.[1] *([1]Dept. of Geol. Sciences, University of Manitoba, schindl0@cc.umanitoba.ca. [2]Department of Geophysical Sciences, University of Chicago)*

Frameworks of condensed finite polyhedral groups can be described as three-dimensional nets with inserted functional groups. The functional groups are the condensed finite polyhedral groups, which are connected to each other by single polyhedra. The single polyhedron is "topologically active", and the condensed polyhedra group is "topologically passive". Connecting the centre of the topologically active polyhedra results in an arrangement of simple polyhedra (or units), which are isostructural to AB_x structure-types. The functional groups are inserted in these polyhedra (or units) and they are exchangable. Inserted in the same topology, they can be of radically different sizes, geometries and compositons. Examples of AB_2 type are: (1). The recently synthesized microporous vanadium and molybdenum phosphates, where $[V_5O_9]$ or $[Mo_4O_8]$-groups are inserted in square planar four-rings formed by phosphate tetrahedra. The square-planar units form twisted-square (ts) chains, similar to the rho and sodalite nets. (2). The jagowerite structure $Ba[Al(PO_4)(OH)_2]$ contains condensed octahedral pairs, surrounded by eight tetrahedra, forming distorted cubes (CaF_2 structure-type). The AB_3 structure-type is represented by the minerals of the pharmacosiderite- $(K[(FeOH)_4(AsO_4)_{6/2}\cdot 6H_2O$ and boracite- $(Mg_3[(B_4O)(BO_4)_{6/2}]Cl$ groups. In the pharmacosiderite structure there are four condensed iron octahedra surrounded by six arsenate tetrahedra; in the boracite structure, there are four condensed borate tetrahedra in an octahedral unit, built up by six other borate tetrahedra. The octahedra are arranged as in the ReO_3 structure-type and can contain other functional groups like $[Zn_4O]$ and $[MO,OH]_4$ with M = Al, Mo, Ge. An example of an AB_6 structure-type is the synthetic $Zn_4O(BO_2)_6$, where the Zn_4O groups are surrounded by twelve borate tetrahedra, forming rhombic dodecahedra (CaB_6 structure-type).

A STUDY OF THE CRYSTAL STRUCTURE OF AN UNNAMED MINERAL $(Ni,Fe)_9Cu_4(Ir,Pt)_8PbIr_2S_{27}$ WITH ELECTRON DIFFRACTION

Yu Z. *(Institute of Geology, CAGS, Beijing, China)*

The mineral $(Ni,Fe)_9Cu_4(Ir,Pt)_8PbIr_2S_{27}$ occurs in chromium-bearing dunite. It is a superstructure phase, composed of the $4CuIr_2S_4\cdot(Fe,Ni)_9S_8\cdot PbIr_2S_3$ or $(Ni,Fe)_9Cu_3(Ir,Pt)_6S_{20}\cdot CuPb(Ir,Pt)_4S_7$. Observed from its X-ray powder diffraction data, the primary isometric system of the mineral $Cu(Ir,Rh)_2S_4$ ($Fd3m$, a=9.91Å) has been transformed to trigonal unit cell a=7.0Å, c=11.3Å. The multiple single-crystal studies of this mineral were performed with transmission electron microscopy. A schematic diagram of all the observed diffraction patterns from individual domains in [111], [1$\bar{1}$0], [321], and [211] foils were obtained. The superlattice spots in pattern [111] foil exhibit six-fold symmetry, which indicates the presence of either a three- or a six-fold axis in the unit cell. This symmetry belongs to either the hexagonal (including trigonal) or the cubic crystal class, because only these classes have this type of symmetry. The demonstration for the cubic system cannot be obtained from its X-ray powder diffraction data. The dimensions of the unit cell can be obtained from the d spacings, which are associated with various discovered superlattic reflections. In the [111] foil, the orientation of the superlattice unit cell with respect to the primary unit cell is as following: $<01\bar{1}>_{SL}\|<111>_{PL}$, $<1\bar{0}0>_{SL}\|<4\bar{2}\bar{2}>_{PL}$. In the (111) primary foil, the $(10\bar{1}0)_{SL}$ spot is located in $1/\bar{3}_{PL}(422)_{PL}$ distance, $g(1010)=(\sqrt{24}/9.95)/3 = 2/\sqrt{3}a$, a=7.03Å. The length of c-axis corresponds to six complete {111} layers of atoms in the cubic lattice, which can be seen in the [321] foil, such as $(01\bar{1}1)$, $(01\bar{1}4)$, $(02\bar{2}2)$, $(4\bar{4}5)$, $(02\bar{2}5)$, $(03\bar{3}3)$, and $(03\bar{3}6)$. In the [1$\bar{1}$0] foil, the superlattice spot (0003) is located in the $\frac{1}{4}(111)_{PL}$ distance, c = ($\sqrt{3}$/9.91)/4=3/c, *i.e.* c=68.6Å, v=2936Å^3, z=6. Since c is three fold, [*i.e. 0001* = 3n and $-h+k+l \neq 3n$, such as $(10\bar{1}0)$], the S.G. must be $P3_112$, $P3_121$, $P3_212$, $P3_221$, $P3_1$ or $P3_2$.

ATOMIC ORDERING AND SUPERSTRUCTURES IN PbO-RELATED MINERALS

Welch M.D. *(Division of Mineral Sciences, The Natural History Museum, London, mdw@nhm.ac.uk)*

Minerals with structures based upon that of litharge PbO have a wide variety of elements partially substituting for Pb, including Mo, V, As, Sb, W, S, P, Si and possibly H. These minerals occur in Pb-Mn-Cu ore bodies that have reacted with low-temperature (<200°C) metalliferous brines. Atoms of the substituting species are highly ordered within the PbO sheets, with the development of a range of novel superstructures and incommensurate behaviour.

This presentation will focus upon the Pb-oxychlorides, which consist of alternating PbO and Cl sheets. The crystal chemistry and superstructures of mereheadite ($Pb_2O(OH)Cl$), parkinsonites ($Pb_7MoO_9Cl_2$, $Pb_9MoO_{11}Cl_2$), sundiusite ($Pb_{10}SO_{12}Cl_2$) and $Pb_{10}SO_{11}Cl_4$ will be discussed in the light of recent TEM studies. Electron diffraction (TEM) indicates that valuable information about superstructures and, hence, atomic ordering, is often missed by X-ray diffraction because of the weakness of superstructure reflections and the very high X-ray absorption coefficients of these minerals (800-1100cm^{-1}). As a result, the tetragonal or pseudotetragonal subcell has usually been erroneously identified as the true cell, and the atomic ordering has passed undetected. Crystallites observed by TEM are thin enough to allow weak superstructure reflections to be recorded (using exposure times of 90-120s). Superstructures are deduced from the relations between substructure and superstructure reflections observed in electron diffraction patterns.

SAPPHIRINE AND SURINAMITE ANALOGS

Barbier J. *(Dept. of Chemistry, McMaster University, Canada - barbier@mcmaster.ca)*

The crystal structures of sapphirine and surinamite analogs forming in the MgO-Ga_2O_3-GeO_2 system have been determined by X-ray diffraction using single crystals grown from potassium molybdate fluxes. Sapphirine, $Mg_{8.9}Ga_{14.2}Ge_{4.9}O_{40}$, is isostructural with the triclinic silicate mineral sapphirine-1Tc. It crystallizes in the $P\bar{1}$ space group with a = 8.822(2), b = 9.794(2), c = 10.256(2) Å, α = 63.82(3), β = 84.77(3), γ = 65.32(3)°, Z = 1 (wR(F^2) = 0.080 for 6770 unique reflections). Surinamite, $Mg_{7.6}Ga_{8.8}Ge_{5.6}O_{32}$, crystallizes in the $C2/c$ space group with a = 10.329(1), b = 23.722(1), c = 10.072(1)Å, β = 110.44(1)°, Z = 4 (wR(F^2) = 0.154 for 2820 unique reflections). The $C2/c$ structure of the surinamite analog corresponds to a polytypic modification of the $P2/n$ natural surinamite, $Mg_3Al_4Si_3BeO_{16}$.

The refinements of the octahedral populations indicate strong Mg/Ga orderings in both structures which correlate very well with the mean octahedral bond distances. The tetrahedral Ga/Ge distributions were not refined, but the average tetrahedral bond distances suggest a higher degree of Ga/Ge ordering in surinamite than in sapphirine. This difference is also observed in the corresponding silicate minerals and can be correlated with the different tetrahedral chain topologies in the two structures.

TEM examination of microcrystals of the sapphirine and surinamite analogs has revealed the common formation of intergrowths as expected from their close structural relationship and their similar chemical compositions. Lattice images are consistent with the description of the sapphirine and surinamite structures in terms of a polysomatic series based on the stacking of spinel and pyroxenes modules.

DESCRIPTION OF SCHOENFLIESITE, $MgSn(OH)_6$, AND ROXBYITE, $Cu_{1.72}S$, FROM A 1375 BC SHIPWRECK, AND SYNTHESIS AND RIETVELD REFINEMENT OF SCHONEFLIESITE, WICKMANITE, $MnSn(OH)_6$, AND BURTITE, $CaSn(OH)_6$

Basciano L.C. *(Dept. of Earth and Ocean Sciences, Univ. of British Columbia)*, Peterson R.C. and Roeder P.L. *(Dept. of Geological Sciences, Queen's Univ.)* and Swainson I. *(Neutron Program for Materials Research, Steacie Institute for Molecular Sciences, National Research Laboratory)*

Schoenfliesite, $MgSn(OH)_6$, and roxbyite, $Cu_{1.72}S$, have been identified as corrosion products of a 1375 BC bronze harpoon head from a shipwreck in the eastern Mediterranean Sea. The sample is very fine grained and appears to be layered. The atomic structures of isostructural, synthetic schoenfliesite, burtite $CaSn(OH)_6$ and wickmanite $MnSn(OH)_6$ have been studied by neutron powder diffraction at 4K. The results show that the $Sn(OH)_6$ octahedral bond lengths and polyhedral volumes for the three compounds are similar and the octahedra exhibit a systematic change in angle variance. The $M(OH)_6$ octahedral bond lengths and polyhedral volumes change systematically with the increase in radii of the enclosed metal. The hydrogen atoms are disordered over two positions in these cubic minerals. However, within an isolated hydrogen-oxygen system, the hydrogen is not disordered. These isolated systems are not correlated with each other, resulting in long range disorder. The O-H bond lengths are often increased due to the hydrogen bonding, with the presence of a second more distant oxygen. For $MgSn(OH)_6$ and $MnSn(OH)_6$, the $O\text{-}H_2$ distances are longer than expected. This may be due to incorporation of water into the crystal structure. The water molecules interacting with the bonded hydrogen atoms causes additional lengthening of the O-H bonds. Free water in the crystal structure was confirmed with an infrared spectrum of a synthetic partially-deuterated $MgSn(OH)_6$ sample.

STRUCTURAL STUDY OF ANTIGORITE BASED ON HRTEM IMAGE PROCESSING

Dódony I. *(Dept. of Mineralogy, Eötvös L. University, Budapest, dodony@ulixes.geobio.elte.hu)*

The existing structural models of antigorite are partly hypothetic due to the lack of proper single crystal data. TEM studies revealed some important real structural features of antigorite and its microtextural characteristics in serpentinites.

The structure of antigorite can be regarded as a modulated lizardite supercell. There are two inversions in tetrahedral sheet within these supercell. At every second one there are four- and eight-membered rings instead of six-membered lizardite-type ones. The octahedral sheet is also modulated, the (020) planes of lizardite octahedra are in antiphase positions at the places of every tetrahedral inversions. At the accuracy level of refinements made so far, the basal plane of tetrahedral sheet as well as the apical oxigens and the hydroxiles of the octahedral sheet are co-planar. The crucial characteristics of antigorite are the non six-membered rings, inversions in tetrahedral layers and the antiphase-like boundary in the octahedral layers. Except for the inversion, these characteristics are invisible in the most studied [010] projection.

Validity of the Kunze-Spinnler model is evaluated in the present work. Simulated SAED patterns and HRTEM micrographs are compared to experimental ones. Contrasts of crucial importance are overlayed in [001] projected HRTEM images and blurred by the dominant lizardite component. Structural layers in HRTEM images were enhanche and decompose by special image filtering. The validity of this filtering technique was controlled on simulated micrographs. No experimental evidence of four- and eight-membered rings in tetrahedral layer were found. The density of antiphase-like boundary in octahedral layer were found to be less than half of what the Kunze-Spinnler model requires. A new structural model is proposed that fits well all the experimental results.

This work was supported by the MKM grant # FKFP 0202/97.

NATURAL NACRITE IN THE LODEVE PERMIAN BASIN: STRUCTURE DESCRIPTION AND CONDITIONS OF FORMATION

Deneele D., Buatier M.D., Dubois M., Potdevin M. and Lopez M. *(Laboratoire. de Sédimentologie, Université Lille 1, France, Martine.Buatier@univ_lille1.fr)*

Petrogenetic and significance of kaolin polymorph is not clearly understood and still debated. Nacrite crystallizes in the space group Cc with a two layer staking sequence. It is the rarest kaolin polymorph generally considered to be formed at high temperature and most occurences support a hydrothermal origin.

Authigenic euhedral nacrite of nano to millimeter size were found in dolomite cavities in the Cambrian basement of the Lodève Permian basin, France. Nacrite can be associated to barite mineralizations which are atttributed to underbasinal fluid discharge and trapping during the Late Permian extensional regime. Petrological investigations suggest that both minerals growed contemporaneously. XRD, DTA and IR demonstrated that nacrite is the only kaolin mineral present in these cavities.

The combination of transmission electon microscopy (TEM) images with electron diffraction pattern (SAED) confirm the two layers perodicity of nacrite. In low magnification images, nacrite also display a lamellar structure with a high density of planar defects parallel to (001). Each lamellae is from 1.4 to 600 nm thick. According to SAED and high resolution images, these planar defects correspond to twin boundaries.

Stable isotope analyses of nacrite and fluid inclusions present in the barite crystals have been investigated in order to characterize the nature and temperature of fluids from which nacrite and barite precipitated. Fluid inclusions are mostly one-phase, coexisting with rare two-phases. Ice melting temperatures indicate a high salinity brine (up to 25 wt% NaCl). Heating runs indicate a formation at low temperature, of about 80 to 100°C, consistent with oxygen isotope data on nacrite. These data imply that nacrite has formed at relatively low temperatures in the Lodeve Permian basin.

Key Words : Nacrite, fluid rock interaction, TEM, SAED, fluid inclusions, stable isotopes...

TOWARDS THE CRYSTAL STRUCTURE OF NAGYAGITE

Effenberger H. *(Inst. für Mineralogie und Kristallographie, Univ. Wien)*, Paar W.H. *(Inst. für Mineralogie, Univ. Salzburg)*, Topa D. *(Inst. für Mineralogie, Univ. Salzburg)*, Culetto F.J. *(Kärntner Elektrizitäts AG, Klagenfurt)* and Giester G. *(Inst. für Mineralogie und Kristallographie, Univ. Wien)*

For high-temperature superconductive materials search purposes synthetic nagyagite was grown from melts. Electron-microprobe investigations of nagyagite from the type locality Nagyág, Transylvania (now Săcărîmb, Romania) are compared with data from literature using the crystal chemical formula $[Pb(Pb,Sb,As)S_2][(Au,Te)]$ derived from investigations of the crystal structure.

Nagyagite is pseudotetragonal, but crystallizes monoclinic, the space group is $P2_1/m$, a = 4.220(1)Å, b = 4.176(1)Å, c = 15.119(3)Å, β = 95.42(3)°, Z = 2. The average crystal structure was determined from both synthetic and natural samples and was refined from the synthetic material to R = 0.045 for 657 single-crystal X-ray data.

Nagyagite features a pronounced layer structure formed by slices of a distorted PbS type with formula $Pb(Pb,Sb,As)S_2$ parallel to (001) with a thickness of 9.15 Å. Te and Au are arranged in a *pseudo*-square planar net which is sandwiched between the PbS-type layers; $Au^{[4\ Te]}$ and at least in part zig-zag chains formed by Te—Te links have to be assumed. Ordering within the PbS-type and gold-tellurium layers seems to be responsible for intense twinning and stacking variants which cause superstructure reflections.

Morphology, cell metric and chemical composition suggests that buckhornite, $[(Pb_2Bi)_{\Sigma 3}S_3][(AuTe_2)_{\Sigma 3}]$, and nagyagite, $[(Pb_3(Pb,Sb)_3)_{\Sigma 6}S_6][(Au,Te)_3]$, can be considered as part of a homologous series. It is assumed that in buckhornite two horizontal (Pb,Bi)S sheets form a slice of the PbS archetype which is intercalated between the Au-Te layers whereas in nagyagite four (Pb,Sb)S layers form the corresponding slice.

DETERMINATION OF ATOMIC OCCUPANCY IN MULTIPLY-OCCUPIED CATION AND ANION SITES.

Foley J.A., Hughes J. *(Dept. of Geology, Miami Univerity, foleyja1@muohio.edu)* and Schaefer R.L. *(Mathematics and Statistics, Miami Univ.)*

Among the most fundamental areas of mineralogical research is elucidation of chemical substitutions. In binary solid solutions occupancy is determined by interpolation between <bond lengths> or electron count of the 2 occupying species, but with ≥ 3 substituents the <bond length> or electron occupancy can be described by numerous solutions of the occupants. We previously reported a method for least-squares minimization of the difference between observed and calculated electron occupancy and observed and calculated bond-valence sums for multiply-occupied sites. Here we extend the method and demonstrate that the solutions can be solved analytically.

The nonlinear relation between bond length and site occupancy is well-modeled by Brown's bond valence $v_{ij} = \exp\{(R_{ij}-d_{ij})/b\}$ and atomic valence $V_i = \sum^{bonds}_{j=1} v_{ij}$. Site occupancies are nonlinear in bond lengths but linear in electron count. Using these empirical observations we find that with x-ray data, coupled with knowledge of the *possible* substituents at a site, we are able to match the chemical analysis with remarkable accuracy. By including the chemical analysis we have devised a set of linear equations for calculating site occupancies of all sites. To obtain a set of linear equations to solve for occupancy of each site m and substituent i, we take partial derivatives with respect to x_{ml} of

$$f(\mathbf{x}) = \sum_{m=1}^{M} L_m^2 \left[\sum_{i=1}^{N} x_{im}^2 (Z_i - V_{im})^2 + \left(\sum_{i=1}^{N} x_{im} Q_i - Q_{obs,m} \right)^2 \right]$$

$$+ \sum_{i=1}^{N} \left(\sum_{m=1}^{M} L_m x_{im} - C_{obs,i} \right)^2 Q_i^2$$

The terms enclosed by [ ] involve only the x-ray data. If chemical analyses are available, the rest of the function may be computed.

BERYLLIAN SAPPHIRINE FROM CASEY BAY, EAST ANTARCTICA: A SUPERSTRUCTURE WITH A 2 × a -AXIS

Barbier J. *(Dept. Chem., McMaster Univ.)*, Grew E.S. *(Dept. Geol. Sci., Univ. Maine)* and Moore Paul B. *(101 Big Island Road, Warwick, NY)*

Sapphirine (Spr) incorporates significant BeO, which reaches 2.51 wt% (ion probe analyses) in Spr from Casey Bay with a composition of $Mg_{5.46}Fe_{2.00}Al_{14.28}Be_{1.44}B_{0.02}Si_{4.80}O_{40}$. The minerals surinamite, musgravite and sillimanite associated with Spr at Casey Bay saturate it in BeO, and thus its BeO content could be close to the maximum possible. The weak superstructure first reported by A. Christy using electron diffraction has been confirmed by single-crystal X-ray diffraction using a diffractometer equipped with a Mo rotating anode and a CCD area detector. $(F_o^2)_{max}$ of the super-cell reflections is only 0,4% of $(F_o^2)_{max}$ of the sub-cell reflections. The superstructure corresponds to a doubling of the a-axis in monoclinic sapphirine-2M ($P2_1/c$ setting) with the following unit-cell parameters: a =19.800(1), b =14.371(1), c =11.254(1)Å, β =125.53(1)°, Z = 4. The fully anisotropic structure refinement leads to final reliability indices $wR(F^2)$ = 0.108 for 14,349 reflections and R(F) = 0.036 for 10,220 reflections with $F_o > 4\sigma(F_o)$. Refinement of all sixteen octahedral (M) and twelve tetrahedral (T) site occupancies yields cation distributions of $(Al_{8.61}Mg_{5.46}Fe_{1.93})^{[6]}$ and $(Al_{5.67}Si_{4.80}Be_{1.44}Fe_{0.07}\ B_{0.02})^{[4]}$. The 2 × a superstructure is found to result primarily from ordering in the doubled (T1→T6, T7→T12) tetrahedral chain, which is parallel to the a-axis. The strongest contribution comes from Al-Si-Be ordering on the T2 (33-16-51%) *vs.* T8 (0-95-5%) and T3 (4-78-18%) *vs.* T9 (30-0-70%) sites. The Be distribution in Spr demonstrates a strong preference for Be/Al mixing over Be/Si mixing, which is in agreement with the structures of other silicates incorporating variable amounts of Be substituting for trivalent cations: Be ↔ Al in cordierite and Be ↔ B in hyalotekite.

CRYSTAL CHEMISTRY OF MAGNESIUM ANTIMONY HYDROXIDE HYDRATE, $Mg(H_2O)_6[Sb(OH)_6]_2$

Friedrich A., Wildner M. and Tillmanns E. *(Institut für Mineralogie, Universität Wien, Austria, manfred.wildner@univie.ac.at)*

A first structural model for synthetic $Mg(H_2O)_6[Sb(OH)_6]_2$ has been proposed by Beintema (1936) who reported space group $P\bar{3}1m$ with a=16.079, c=9.841Å. A few years ago the same compound was found in nature in the Brandholz-Goldkronach-area, Fichtelgebirge, NE-Bavaria, Germany. Identity of the mineral with the synthetic compound was proven by thermo-gravimetric, infrared, X-ray single crystal and powder diffraction measurements and by electron microprobe analyses. After the recent investigation of the crystal structure it has been proposed as a new mineral to the IMA-commission for New Minerals and Mineral Names. Crystals of natural $Mg(H_2O)_6[Sb(OH)_6]_2$ were found up to 1.5mm in diameter with predominant forms {10$\bar{1}$0} and {0001}. They are transparent, colourless with a vitreous luster and a white streak, nonfluorescent, brittle and show a conchoidal fracture. VHN=60 kg/mm², which corresponds to Mohs-hardness 2-3. The calculated density is 2.605 g/cm³. The optical behaviour is uniaxial (-) with n_ω=1.570(2) and n_ε=1.569(2). Thermogravimetric analyses show a loss of water of 39 weight%, corresponding well with the theoretical value. The crystal structures of natural and synthetic $Mg(H_2O)_6[Sb(OH)_6]_2$ were investigated using single-crystal X-ray CCD data and proved to be isotypic with bottinoite (Bonazzi & Mazzi, 1996). Both crystals are twinned with {10$\bar{1}$0} as twinplane and consequently show a strong pseudo-symmetry towards space group $P\bar{3}1m$, the true space group, however, is $P\bar{3}$; the cell parameters of the natural crystal are a=16.114(1), c=9.863(1)Å, Z=6, V=2217.9(1)Å³, the refinement converged to R=2.96%. The structure is built up by nearly regularly shaped isolated $Mg(H_2O)_6$- and $Sb(OH)_6$-octahedra forming two types of layers which are stacked along the c-axis. One layer consists of $Sb(OH)_6$-octahedra only, the other of $Mg(H_2O)_6$- and $Sb(OH)_6$-octahedra with a Mg/Sb-ratio of 2:1. The octahedra within these layers as well as the layers themselves are interconnected by hydrogen bonds.

INVESTIGATIONS OF THE CRYSTAL CHEMISTRY OF URANYL OXIDE HYDRATES

Hill F.C. and Burns P.C. *(Univ. of Notre Dame, fhill@nd.edu)*

Uranyl oxide hydrates encompass an important group of mineral and inorganic phases that occur in diverse chemical environments. As minerals, they commonly occur as major components of the oxidized portion of U deposits, and have been documented in soils contaminated with U. These phases also have been observed as alteration products growing on the surface of spent nuclear fuel. Knowledge of the crystal chemistry of uranyl phases, however, is only beginning to approach that of other mineral groups, owing primarily to the experimental difficulties associated with these phases, such as poor crystal-quality and high absorption of X-rays by the crystals.

We have undertaken a crystal-chemical study of the uranyl oxide hydrate system, with emphasis on crystal growth and the determination of structures of uranyl phases containing mono and divalent cations of mineralogical interest. To date, two phases that have not been previously reported have been obtained, and their structures determined. The first, $Sr_{2.84}[(UO_2)_4O_4(OH)_3]_2(H_2O)_2$, is the synthetic Sr analogue of curite and contains sheets of uranyl polyhedra composed of UrO_4 square bipyramids ($Ur = (UO)_2^{2+}$) and UrO_5 pentagonal bipyramids linked by sharing equatorial edges and corners. To date, this arrangement of uranyl polyhedra has only been observed in curite. It is orthorhombic, *Pnam*, a=12.3143(7), b=12.9609(8), c=8.4053(5) Å, with an R of 5.30%. The second phase, $Cs_6[(UO_2)_{24}O_{14}(OH)_{26}](H_2O)_6$, is structurally related to compreignacite and clarkeite, and contains the (α-U_3O_8-type sheet of uranyl polyhedra that is found in those minerals as well as in becquerelite, billietite, and richetite. It is rhombohedral with a=14.1241(6), c=22.407(1) Å, and an R of 4.06%. The discovery of these two structures suggests that greater chemical and structural diversity may exist in the uranyl oxide hydrate system than the small sampling of known phases previously available suggests.

7. Crystal Structures and Topology

STRUCTURE AND PROPERTIES OF THE FINE DISPERSIONAL MANGANESE OXIDES

Lysiuk G.N. *(Institute of Geology, RAS Ural Division, Russia, Syktyvkar, common@geo.komi.ru)*

The object of our investigations is fine-grained minerals from pelagic ferromanganess nodules. There are three different crystalline manganese phases in the nodules: 10Å manganite, 7Å manganite and vernadite. Among the 10Å mineral series there are minerals with tunnels and layered crystal structures. Todorokite is a mineral with tunnel structure, and asbolan has layered structure. 7Å manganite is called birressite and has layered structure too.

The predominant crystalline phase of the ore samples studied is the 10Å phase. Comparing diffraction and TGA data on the samples from different zones reveated that central parts of the nodules are most enriched in the phase. Investigation of variations in physical properties of the 10Å phase in direction from the centre to periphery showed that reflectance coefficient and hardness values increase from periphery to center. That is a consequence of the degree of mineral crystallinity increasing in the same direction, and growth from center to periphery going through several stages for a long period of time.

Great contents of native metals and intermetal compounds are found in ore zones of the nodules studied (native copper copper-zinc compounds, iron, aluminium, zinc).

Occurrence of native metals in the nolules is interpreted by different authors in terms of cosmic, terrestrial, magmatogenic, volcanogenic-hydrothermal, and biogenic origins. On the contrary, our data particularly imprints observed on the surface of the inclusion grains, indicate that nucleation and growth of these metals occurred in pores of the nodules. Although the majority of the nodules consist of intensively oxidized matter, there exist inclusions of metals in reduced forms, which are signs of microlocalities of markedly reduced state (we call this "microlocal geochemical zonality of nodules"). These localities may be formed by segregation of organic matter.

AN HRTEM-AEM STUDY OF Mn-CUMMINGTONITE FROM VITTINKI, WESTERN FINLAND

Mancini F. and Marumo K. *(Geol. Surv. of Japan)*, Kohyama N. (NIIH, Tokyo), Alviola R. *(Geol. Surv. of Finland)* and Marshall B. *(Univ. of Technology, Sydney)*

We have investigated, by electron microscopy, the fine structures of a Finnish mangano-cummingtonite-"tirodite", and correlated them with the metamorphic conditions.

The tirodites ($P2_1/m$) are from a regionally metamorphosed (T=700-750°C, P=4-8 kbars) quartz-tirodite schist intercalated with various Svecokarelian Mn-rich gneisses and host various fine textures: i) exsolution lamellae of ($C2/m$) mangano-actinolite; ii) micrometer scale polysynthetic twinning; iii) polysomatic replacement reactions, including chain multiplicity faults that form a triple-chain Mn-analogue of clinojimthompsonite and topotactic replacement to talc.

The exsolution lamellae show a large scatter in the orientation ("$\bar{1}01$" oriented 1.5-6.5° from ($\bar{1}01$) and "100" oriented 3.7-4.5° from (100)) consistent with a wide range of exsolution temperatures as confirmed by the optimal phase boundary (OPB) calculations. The lattice adjustment occur by rotation of 2.1° and 2.6° respectively of the (110) and (001) fringes. The lamellae vary from nanometers to micrometers in width, do not correlate with orientation, and presumably reflect local increase in the diffusivity of the chemical elements.

The contrast differences on either side of some of the (100) boundaries of the polysynthetic twinning suggests that the off-set is not strictly the classical $\pm c/2$, and the mismatch also occurs along the **b**-direction.

The sporadic triple chain defects of "unit-cell scale" width (50-100 Å at most in **b**-direction), formed as "faults" in a predominantly ordered double-chain host. The defects and the polysomatic replacement to talc, are evidenced by chemical compositions intermediate between amphibole and talc. The scarcity of triple chain pyriboles at Vittinki correlates with the conditions of metamorphism. Based on the mineral assemblages, textures, and natural occurrences of triple chain silicates in the literature, we conclude that the equilibrium paragenesis in the quartz-tirodite schist are in excess of those required for the metastable formation of triple chain silicates.

A NEW MAGNESIUM IRON GERMANATE

Lévy D. and Barbier J. *(Dept. of Chemistry, McMaster University, Canada)*

The investigation of the MgO-Fe_2O_3-GeO_2 system at 1 atm pressure has led to the characterization of a new germanate phase with a narrow solid solution range including the $Mg_{2.14}Fe_{3.16}Ge_{2.56}O_{12}$ composition. This composition and the crystal structure have been determined by electron microprobe analysis and X-ray diffraction using single crystals grown from a potassium molybdate flux. The new germanate phase crystallizes in the tetragonal $I\bar{4}2d$ space group with a = 6.815(1), c = 18.669(1)Å, Z = 4 ($wR(F^2)$ = 0.063 for 1158 unique reflections). The refinement of site occupancies yields a structural formula of $(Mg,Fe)^{[8]}_{0.85}(Mg,Fe)^{[6]}_4(Fe,Ge)^{[4]}_3O_{12}$. This synthetic germanate is the room-pressure analog of a high-pressure silicate mineral recently identified as inclusions in diamonds (tetragonal almandine pyrope phase, with a garnet-like composition $(Mg,Fe)_{0.94}(Mg,Al,Fe,Cr,Mn)_{3.93}(Al,Si)_3O_{12}$).

A particular feature of this tetragonal structure is the presence of a partially occupied eight-coordinated dodecahedral site. This site contains mixed Mg^{2+}/Fe^{3+} populations in both the silicate and the germanate structures (occupancies of 94% and 85% respectively) and its coordination environment (with $\bar{4}$ symmetry) is similar to that of the eight-coordinated sites in the garnet structure, *e.g.* $Ca_3Fe_2Ge_3O_{12}$. The structure refinement of a partially Ca-substituted germanate phase, $(Mg,Ca,Fe)_{0.92}(Mg,Fe)_4(Fe,Ge)_3O_{12}$, shows a complete partitioning of Ca^{2+} ions on the dodecahedral site but the Ca/Mg substitution remains limited to about 15%. Indeed, the similarity between the tetragonal and garnet phases is only compositional, and the two phases are clearly structurally distinct. On the other hand, the tetragonal structure is also found for the arsenates $M_3As_2O_8$ (or $M_{4.5}As_3O_{12}$) with M = Mg, Ni, Co.

ACCURACY OF SITE OCCUPANCIES IN OLIVINE: AN INTER-LABORATORY STUDY.

Martignago F. *(Dept. of Mineralogy and Petrology, Univ. of Padova)*

Determination of cation distributions in minerals is crucial for any thermodynamic application. In order to define the reliability of X-ray results and their limitations in terms of precision and accuracy of site occupancies, a methodological and interlaboratory study was undertaken. Two crystals of olivine (Fo_{90} and Fo_{45}) were used to collect diffraction data up to 2θ = 110° ($MoK\alpha$) in three Italian laboratories (Padova, Pavia, Trieste) with different single crystal diffractometers. Each laboratory carried out several data collections, changing crystal orientation for every experiment. All data were refined using STRUCSY, ORFLS and SHELXL'93 programs with differing refinement models, refinement strategies, weighting schemes without chemical constraints. The main results are as follows:

- The atomic coordinates obtained by refining data sets at various resolutions (1.1-0.7) with differing refinement programs and orientations do not change significantly. Structural geometry is therefore not affected either by resolution or refinement strategy.

- All the data sets collected in the three laboratories and refined with the same program (SHELXL'93) only suffer from different crystal-mounting and experimental apparatus. These refinements using Mg^{2+} *vs.* Fe^{2+} show that site occupancies for sample Fo_{90} change from 0.906 (2) to 0.913 (1) for M1 site and from 0.919 (1) to 0.923 (1) for M2 site, with differences of 0.007 and 0.004 respectively; while for sample Fo_{45} site occupancies change from 0.425 (5) to 0.455 (3) for M1 site and from 0.473 (5) to 0.494 (2) for M2 site with differences of 0.03 and 0.02 respectively.

- Refining a single set of data with differing programs the difference obtained in site occupancies .approaches the previously quoted values for a resolution of 1.1 for both Fo_{90} and Fo_{45} crystals due to changing refinement models (valence states, extinction correction), refinement strategies (refinement on F^2 or F, blocking, damping, *etc.*) and weighting schemes.

MOLECULAR DYNAMICS SIMULATION OF PĪ-IĪ PHASE TRANSITION IN PURE ANORTHITE

Miyake A., Kitamura M. *(Dept. of Geology and Mineralogy, Kyoto University, miya@mine.kueps.kyoto-u.ac.jp)* and Kawamura K. *(Dept. of Earth and Planetary Sciences, Tokyo Institute of Technology)*

Phase transition of pure anorthite between PĪ and IĪ phases at around 515K has been extensively studied. Details of the transition mechanism has not been fully understood while various models have been proposed. Al and Si atoms occupy tetrahedral sites in the crystal structure of pure anorthite. The arrangement of Al and Si must be in a fully ordered state as far as it obeys the Al-avoidance rule. A NMR study has suggested that natural specimens are not in the fully ordered state but have partial Al/Si disorder violating the Al-avoidance rule. Since the degree of the Al/Si ordering can not be controlled in experiments using actual specimens because of the extremely sluggish exchange of Al and Si below 1000K, the effect of the partial Al/Si disorder to the transition has not been elucidated.

Molecular-dynamics (MD) simulation using appropriate inter-atomic potentials between atoms has been widely used for investigating the physical properties of materials. Any degree of the Al/Si ordering can be chosen in an initial structure for MD simulation. Two kinds of structures were chosen in the present study in order to investigate the influence of the partial Al/Si disorder on the transition; fully ordered anorthite and partly disordered anorthite. MD simulations on the structures were carried out by changing temperature at the atmospheric pressure.

Discontinuous changes in unit cell volumes and structure factors at the transition temperature are observed in the fully ordered anorthite but not in the partly disordered anorthite. These results show that the orders of the transitions of the fully ordered anorthite and the partly disordered anorthite are first (not nearly second) and non-first, respectively. The motions of Ca and the framework are strongly correlated during the transition in both the MD-simulated anorthites. A high-temperature X-ray study has shown that the transition of real anorthite is non-first. The result can be interpreted as that the real anorthite has a partially disordered arrangement of Al and Si.

DIFFERENCES OF TETRAHEDRAL ^{27}Al IN SMECTITE ILLITIZATION AND DISCUSSION WITH NMR, FT-IR AND HRTEM RESULTS IN THE NIIGATA BASIN INTERBEDDED SANDSTONE AND MUDSTONE

Niu B. *(Geology and Geochemistry Lab., Technology Research Center, Japan National Oil Corporation, niu-ben@jnoc.go.jp)*

There are two representative changes are discussed in the chemical compositions during the transformation from smectite to illite, which is also called smectite illitization. The first compositional change is the substitution of the potassium for the interlayer cations, as K^+exchange Na^+, Ca^{2+} and is preserved and fixed in the interlayer position. The second compositional change is the initial octahedral Al^{3+} (or environmental fluid Al^{3+}) substituted Si^{4+} in the tetrahedral sheet, which the change are considered as an important reason to increase negative charges in the interlayer for fixing interlayer potassium. Hence, the problem is what mechanism of the illitization takes place during the diagenetic process. Depended on X-ray diffraction crystal structure studies, the theory of mixed-layer illite/smectite (I/S) conversion have been established. However the mechanism of compositional substitution have been not explained satisfactorily with the enough evidences.

The NMR ^{27}Al analytical results show that the lower diagenetic smectite have higher tetrahedral Al^{4+} than the higher diagenetic mixed-layer I/S in the deep formations from the Niigata basin. And the octahedral Al^{3+} of I/S increase are detemined with the degree of diagenesis increase. The FT-IR results show the low intensity of Al-OH absorption bend of smectite in the young sediment. The difference of the smectite in the sandstone and mudstone affect the rate of illitization, which is called heterogeneous conversion during diagenetic process.

THERMO-DILATOMETRIC STUDIES OF CAVANSITE FROM WAGHOLI, INDIA

Mookherjee A. and Phadke A.V. *(Department of Geology, University of Pune,Pune 411 007, apte@ unipune.ernet.in)*

A very rare mineral cavansite, $[Ca(VO)Si_4O_{10}\cdot 4H_2O]$ occurring at Wagholi, about 14 km from Pune, the only other known locality in the western region of the Deccan Volcanic Province (DVP), of India, apart from the two other known occurrences from Oregon, USA, is hosted in cavities in tholeiitic basaltic lava flows of the DVP, in association with zeolites and other associated minerals like calcite, okenite, apophyllite *etc.* The mineral was subjected to thermo-dilatometric studies for the first time using the Hungarian "Derivatograph". During these investigations fine powder of the pure sample of cavansite was pressed into a hollow cylindrical pellet and was continuously heated in the temperature range of Room temperature - 1000°C, keeping the rate of heating at 10°C/minute. and TD and DTD curves were photographically recorded. The results provide precise temperatures of maximum of each reaction at which volume changes reflecting cell modifications take place four times before complete dehydration and twice thereafter with further heating.

These results highly correspond with the four steps of dehydration, earlier shown by Phadke and Apte (1994), modifying the cell dimensions manufactured on expulsion of the four H_2O molecules in succession. Amongst the four stages of the cell contractions, the second one at a peak temperature 350°C is quite appreciable and the transformed phase is designated here as Metacavansite-I. A complete structural collapse of cavansite on complete dehydration occurs at 560°C. This transformation is designated as Metacavansite-II. It is also well established here that on further heating of the dehydrated x-ray amorphous phase, there is structural re-organisation with dissociation into two separate phases *viz.*,(i) cristobalite and (ii) CaV_3O_7, precisely at 905°C and 975°C respectively.

ENUMERATION OF POSSIBLE STRUCTURES RELATED TO ZSM-5 AND ZSM-11

Pasero M. and Merlino S. *(Dept. of Earth Sciences, Univ. of Pisa, pasero@dst.unipi.it)*

The zeolite molecular sieves ZSM-5 and ZSM-11 are members of an important family of structures (the so-called pentasil family) with selective ion-exchange capabilities, by means of a two-dimensional system of channels. These two structures are based on the same fundamental building blocks, namely the cage formed by eight pentagonal rings of $[(Si,Al)O_4]$ tetrahedra.

The possible existence of variants of these structures could be of some relevance. Therefore the set of structures related to those of ZSM-5 and ZSM-11 was modeled.

Cages can be stacked one above the other to give rise to columns. Depending on how subsequent cages are connected between each other, three different columns with miminum structural complexity can be obtained.

These columns (1*d* modules) can be arranged into layers (2*d* modules: a total of nine different layers was set up), and layers can be arranged into frameworks (3*d* modules).

Eventually a total of 19 different framework structures was established. A general outline will be presented; moreover, basic structural parameters (space group symmetries, unit cell parameters, atomic fractional coordinates idealized by means of DLS geometrical refimenent) will also be given for a number of them.

Two out of the 19 structures obviously correspond to those of ZSM-5 and ZSM-11. The other ones represent possible structural models for both natural and synthetic zeolite-like compounds. The newly discovered mineral species mutinaite, a zeolite from Antarctica, represents the first example of a natural compound topologically related to the pentasil family of structures.

7. Crystal Structures and Topology

STRUCTURE OF HYDROTHERMALLY SYNTHESIZED $Ag_{10.5}Te_7$ AND RELATIONSHIPS TO STUETZITE

Giester G. and Pertlik F. *(Institut für Mineralogie und Kristallographie, Universität Wien, Austria)*

Synthetic stuetzite was obtained from hydrothermal synthesis experiments which were carried out in Teflon-lined steel autoklaves, with a volume of approximately 5 cm^3, an isothermal reaction time of 60 hours and 420 K under autogenous pressure. Synthesis experiments were started from homogenous mixtures of the elements in an aqueous 10n NaOH solution. Predominant crystallographic forms of the synthesized crystals (0.20 x 0.20 x 0.35 mm^3) are {10.0} and {00.1}.

Structural data determined by single crystal X-ray experiments are: a = 13.480(2), c = 8.482(1) Å; Z: 3; space group $P\bar{6}2m$ (No.189); R value: 0.059 for 2046 observed X-ray data [$Fo > 4\sigma(Fo)$] and 93 parameters. The atomic arrangement is characterized by a more or less ordered framework of 21 tellurium atoms on six crystallographic different positions and ~ 31 highly mobile silver atoms distributed in this framework on seven positions, statistically occupied.

By Te atoms of two equivalent positions Te-Te dumbbells with interatomic distances of 2.748(4) Å and 2.846(2) Å are formed. In the first case both of these Te atoms are each equidistant connected to three Ag atoms [Te-Ag = 2.740(2) Å]. The corresponding Ag-Te-Ag and Ag-Te-Te angles are 112.63(5)° , 3x, and 106.09(5)°, 1x. In the second case the Te atoms are each connected to five Ag atoms and Te-Ag within the range 2.874(2) Å to 2.980(2) Å. The Ag-Te-Ag and Ag-Te-Ag angles vary from 90.73(6)° to 121.67(4)°. The generating symmetry elements for these two dumbbells are a $\bar{6}m2$ point, and a mirror plane, respectively. The remaining four Te atom positions are irregularly coordinated to Ag atoms and Te-Ag distances from ~ 2.7Å to ~ 3.1 Å and a clear gap up to 3.5 Å.

The Ag atoms are distributed disordered over seven crystallographic different positions showing Ag-Te ≥ 2.7 Å and shortest Ag-Ag distances ≥ 2.9 Å (for comparison Ag-Ag in Ag^0 = 2.889 Å) and irregular coordination polyhedra. Within a range up to 3.5 Å two Ag atoms are coordinated to two Te atoms, the rest uniform to four Te atoms. The number of nearest Ag neighbours is three to six.

MOLECULAR DYNAMICS SIMULATION OF HIGH-PRESSURE CLINOENSTATITE

Shimobayashi N., Miura E., Miyake A. and Kitamura M. *(Dept. of Geology and Mineralogy, Kyoto Univ., shimo@kueps.kyoto-u.ac.jp)*

Polymorphism of enstatite ($MgSiO_3$) has been extensively studied at high temperatures and high pressures. In addition to the previously-known four polymorphs: orthoenstatite, protoenstatite, and low- and high-clinoenstatite, the fifth pyroxene-type polymorph was reported by the recent high-pressure experiments in this decade. This new polymorph has been identified as a high-density monoclinic phase with the *C2/c* structure (denoted as high-pressure clinoenstatite [CEN(HP)]). The high-temperature clinoenstatite [CEN(HT)] has the same *C2/c* symmetry as CEN(HP), but the phase relation and the structural comparison between both *C2/c* clinoenstatites have not been fully elucidated. In this study, the CEN(HP) structure was studied using a molecular dynamics (MD) simulation technique.

The MD simulation was carried out on the basis of an interatomic potential model whose potential parameters were determined empirically. The periodic boundary condition was imposed with the MD basic cell composed of 16 unit cells (2**a** × 2**b** × 4**c**, containing 640 atoms). Starting from the experimentally determined structural parameters of low-clinoenstatite as the initial state, the CEN(HT) structure was firstly simulated by increasing temperature up to 2000K at the atmospheric pressure. Taken from the MD simulated structural parameters of CEN(HT), subsequent calculations were carried out by increasing pressures up to 18GPa at intervals of 3GPa at the same temperature (2000K). As the result, the changes in cell parameters indicate apparent discontinuity between at 12GPa and 15GPa. The MD simulated structures above 15GPa were CEN(HP) whose structures are characterized with the significantly small β angles (99-100°). The calculated CEN(HP) structure has symmetrically equivalent "O-rotated" chains with the substantially smaller O3-O3-O3 chain extension angle (135-137°) than 180° for the ideal CEN(HT) structure, and therefore the coordination of the M2 sites is limited to 6-fold in the CEN(HP) structure. The pressure-induced phase change from CEN(HT) to CEN(HP) looks like a first-order phase transition, but the more detailed inspection reveals that CEN(HT) does not directly transform into CEN(HP) but through an intermediate phase with $P2_1/c$ structure.

A COMPARISON OF RIETVELD AND SINGLE-CRYSTAL X-RAY STRUCTURE REFINEMENT ON A NATURAL CHROMITE

Salviulo G., Carbonin S. and Della-Giusta A. *(Dept. Of Mineralogy, Univ. of Padova, Italy, gabri@dmp.unipd.it)*

A natural chromite sample was used to evaluate site occupancy variations obtained by Rietveld structure refinement and single-crystal X-ray diffraction. X-ray powder data were collected in conventional Bragg Brentano geometry, using CuKα radiation in step scan mode in the 16°-140° 2θ angular range, with step size of 0.02° and counting times of 15 sec for four samples 1500, 300, 150 and 50μm thick. For the sample 50μm, two additional patterns were collected in the same angular range with a step size of 0.03° and counting times of 5 and 9 sec, respectively. Single-crystal X-ray diffraction data on four crystals were collected with monochromatized MoKα radiation up to 2θ =110° and refinements were carried out with the SHELXL93 program. Three Rietveld refinements for each data collection were performed using the same initial model but differing in parameter turn-on sequence. Numerical and graphical criteria show that, for each set of data, profile shapes and background descriptions are acceptable, but statistical parameter values decrease with decreasing sample thickness. The atomic coordinates do not change, while, T and M site occupancies are very sensitive to sample thickness, and for the same sample to the counting statistic. Values obtained for the 1500 μm and 50 μm samples 5 and 9 sec time/step show really inconsistent results. The powder results well approach those from single crystal decreasing sample thickness. Best-fit factors in single-crystal refinement were obtained when total electrons from T and M site occupancies were closer to those calculated from chemical composition. Experiments on the 50 μm sample showed that the best results were obtained using fully ionized scattering curves for cations and partially ionized for oxygen, as observed in the single-crystal experiment. In conclusion, the powder thickness is crucial when the material shows a high absorption coefficient, and the best results are obtained only with a high rate of statistical counting.

SOME SPACE GROUPS AS COMBINATIONS OF MODULES

Smirnova N.L. and Gorchakova O.E. *(Dept. of Geology, University of Moscow, Russia, hydr@geol.msu.ru)*

Ordered and disordered isomorphism and parsimony are universal phenomena. These phenomena are a basis of alloranized systems. In accordance with isomorphism all systems (objects) are composed of 0 - 3 dimensional modules. According to parsimony the number of essentially different types of at least one of constituent modules in a system tends to be small (1 - 4). Why? It is well known that all crystalline structures are built of 11 Kepler-Schubnikov nets. Tetragonal and cubic structures are composed of nets: e - 4^4, n - 3^2434, v - 48^2 perpendicular to axis 4. The nets are in planar sections of space groups. The symmetry of these planar sections is described by three plane symmetry groups: *p*4 (**1**), *p*4*m* (**2**), *p*4*g* (**3**). These sections are at arbitrary height *z*. Most of tetragonal groups also have five sections at a fixed height: **1**, **2**, **3**, *c*4 (**4**), *c*4*m* (**5**). Combinations of arbitrary and fixed sections are: **1**, **11**, **2**, **22**, **3**, **33**, **12**, **112**, **13**, **113**, **123**, **14**, **114**, **124**, **134**, **25**, **225**, **35**, **335**. Among 15 theoretical combinations of 1 - 4 sections six are absent. In the same planar section there is one and the same combination of nets: **1** - *p*4 e_1; $e_4n_1v_1$; **2** - *p*4*m* e_1; e_2; e_3; v_1; v_2; **3** - *p*4*bm* e_2; n_2e_5; e_6v_3, **4** - *c*4, **5** - *c*4*m*. Relative values of lattice parameters 1 - 1, 4 and larger ones have nets e_1, e_2; 1,9 - 2,4 e_3, e_4, e_5, n_1, n_2, v_1, v_4; 2,8 e_6, v_2, v_3. All the nets can be obtained by deformation of nev net. The space group module is the space between two sections. In accordance with parsimony there are only few symmetry group modules containing a small number of nets. That is why different structures consist of few related modules and combinations of the same or different modules. The modules are translated along axis 4 by symmetry operations *t*, *c.*, *.c*, 2_1, 4_1 and by sections symmetry elements. Some minerals are considered as a combination of modules.

7. Crystal Structures and Topology

X-RAY SINGLE-CRYSTAL STRUCTURE REFINEMENT OF SZENICSITE, $Cu_3MoO_4(OH)_4$, AND ITS RELATION TO THE STRUCTURE OF ANTLERITE, $Cu_3SO_4(OH)_4$

Stolz J. and Armbruster T. *(Laboratorium für chem. und mineral. Kristallographie, Universität Bern, Switzerland, jano@mpi.unibe.ch)*

The crystal structure of szenicsite, $Cu_3MoO_4(OH)_4$, from Inca de Oro, Atacama, Chile (type locality) was investigated at room temperature using a single-crystal X-ray diffractometer (MoKα radiation) equipped with a CCD area detector. The structure was solved and refined in the orthorhombic space group *Pnnm* (a = 12.559(2), b = 8.518(3), c = 6.072(1) Å, V = 649.5(3) Å^3) with 772 unique reflections up to $(\sin\theta)/\lambda = 0.65$ leading to R1 = 2.64% and wR^2 = 6.37%. The structures of szenicsite, $Cu_3MoO_4(OH)_4$, *Pnnm*, and antlerite, $Cu_3SO_4(OH)_4$, *Pnma* (a = 8.244(2), b = 6.043(1), c = 11.987(3) Å, V = 597.1(2) Å^3), are characterized by triple chains of copper octahedra running parallel to 6Å axes. These triple chains are linked by MoO_4^{2-}- and SO_4^{2-}-tetrahedra, respectively. The different size of these tetrahedra governs their different linkage to the triple chains and the orientation of the Jahn-Teller distortion of the Cu^{2+} octahedra.

Keywords: szenicsite, antlerite, crystal structure, Jahn-Teller distortion, molybdate, sulfate

UNIFORM ASCII SYMBOLS FOR SPACE GROUPS, POINT GROUPS, AND CRYSTAL SYSTEMS

Susse P. *(Inst. of Mineralogy and Crystallography, University of Göttingen, psusse@gwdg.de)*

The use of subscript and superscript characters in space group and point group symbols is quite disadvantageous for printing as well as for electronic data processing. While preparing the *6th* edition of the mineral database *MINABS*, new symbols were designed, consisting of a string of *5 ASCII* characters for *Schoenflies* style, and of up to 7 characters for *Hermann-Mauguin* style description. It proved to be very useful to extend the new symbols to space groups, point groups, as well as to crystal systems.

The symbol for the **crystal system** is made taking the *Schoenflies* symbol of the *holoedric* point group, bringing the subscript characters in line, and filling the remainder of the 5 spaces with *asterisks* (*ASCII* 42), while in the **point group** symbol the remaining spaces are filled with *periods* (*ASCII* 46). The **space group** symbol is made adding the superscript number of *Schoenflies*.

The *ASCII* format for the *Hermann-Mauguin* style symbols is achieved by denoting inversion axes with the " ~ " character (*ASCII* 126), and screw axes of all kind with the " ' " character (*ASCII* 39). Following are some examples of the new symbols:

Crystal system		*Point group*		*Space group*	
ci***	triclinic	ci...	1~	ci..1	P 1 ~
c2h**	monoclinic	c2h..	2/m	c2h.5	P 2 ' / c
d2h**	orthorhombic	c2v..	mm2	c2v12	C m c 2 '
d4h**	tetragonal	d2d..	4~2m	d2d.3	P 4 ~ 2 ' m
d3d**	trigonal	c3v..	3m	c3v.4	P 3 1 c
d6h**	hexagonal	d6h..	6/mmm	d6h.4	P 6 ' / m m c
oh***	cubic	td...	4~3m	td..5	F4~3c

For retrieving purposes in databases, the *Schoenflies* symbols are useful because of their hierarchical nature and of being independent of crystal settings. The advantage of *Hermann-Mauguin* symbols is the orientational information they contain. The combination of both, using the new *ASCII* symbols, is being successfully applied in the database *MINABS*.

NEUTRON DIFFRACTION AND SPECTROSCOPIC STUDIES OF DEUTERATED GYPSUM

Stretton I.C. *(ETHZ, Switzerland. Iona@erdw.ethz.ch)*, Schofield P.F. *(Mineralogy, Natural History Museum, UK)*, Knight K.S, Hull S., Wilson C.C. and Parker S.F. *(ISIS, Rutherford Appleton Lab, UK)*

Structural parameters of deuterated gypsum have been extracted from Rietveld analysis of powder neutron diffraction data within the temperature range 4.2 to 370 K and up to 5.4 GPa pressure, at room temperature. From such data we have measured the thermal expansivity, the static compressibility and monitored the structural and hydrogen bond controls on this behaviour and the dehydration of gypsum.

The thermal expansion of gypsum is highly anisotropic along the **b**-axis due principally to the effect of the H2···O1 hydrogen bond. Single-crystal neutron studies at 50, 115 and 200 K have allowed us to adopt an anisotropic thermal parameter model confirming the structural behaviour of, and associated with, the hydrous component. Inelastic neutron scattering at 5, 200 and 250 K shows the temperature dependence of the H-bonding and the H_2O molecular dynamics.

The high temperature limits for the expansion coefficients of the cell edges a, b and c are 3.98×10^{-6}, 4.36×10^{-5} and 2.53×10^{-5} K^{-1}, respectively, and for the cell volume it is 6.96×10^{-5} K^{-1}. The β angle displays oscillatory variation reflecting a change in the influence of at least two coupled processes. Empirical data analysis, of the data set prior to dehydration, results in

$$a_b = 1.251 \times 10^{-6} \sin(0.0116T + 0.311)\ K^{-1}$$

The static compressibility measurements of powdered gypsum, made using the Paris-Edinburgh cell, when fitted to a Birch-Murnaghan equation revealed values of 42 GPa for K and 0.48 for K′, the pressure derivative of the bulk modulus.

A NEW MAGNETOPLUMBITE-TYPE MINERAL FROM THE EIFEL, GERMANY

Lengauer C.L., Tillmanns E. *(Institut für Mineralogie, Universität Wien, Austria, ekkehart.tillmanns@univie.ac.at)* and Hentschel G. *(Sinzig, Germany)*

Within the group of hexagonal compounds in SG $P6_3/mmc$ with the general formula $(A^{XII})(M^{IV,V,VI})_{12}O_{19}$ the iron rich 'ferrites or hexa-ferrites' with $A(Fe_6Fe_{6-x}M_x)O_{19}$ play an important role because of their ferrimagnetic properties. Crystallographic studies mainly done on synthetic end-members proved these compounds to be isotypic with the mineral magnetoplumbite (A= Pb, M= Mn). Three further isotypic but non-ferrimagnetic minerals nezilovite (A= Pb, M= Mn, Zn, Ti), yimengite (A= K, M= Cr, Ti, Mg), and hawthorneite (A= Ba, M= Cr, Ti, Mg) have been reported in the literature.

The EMP-analyses of the title compound revealed also a barium dominated chemistry of the A-site, the overall chemistry of the M-site, however, is two times higher in iron than in hawthorneite and shows no chromium content. Mg and Mn were only observed as minor substituents. Due to the high iron content, which is in the range of magnetoplumbite, this material also exhibits ferrimagnetic properties. The idealized chemical formula can be given as $Ba[Ti_2Fe_{10}]O_{19}$.

The structure is an alternating sequence of two building units R and S, which can be derived from a A-cation substituted closed anion packing of magnetite. The R unit consists of AM_6O_{11} layers, the S unit (M_6O_8) is identical to the *ccp*-packing of spinel along [111]. This anionic arrangement gives rise to one tetrahedrally (M3), one five-fold bipyramidally (M2), and three octahedrally coordinated voids (M1, M4, M5), which can be occupied by various small cations. The single crystal data refinement using constraints as derived from chemical analysis ($R_{4\sigma}$ = 0.033) revealed the following crystallographic site occupancies: the M1-3 sites are fully occupied by iron and the Fe content of the M5-site can be partially replaced by magnesium as a substituent of all 'light' cations. The M4 position, however, is domi-nated by almost all of the titanium content. The M2 position (s.o.f. = 0.5) is shifted from the mirror plane with a M2-M2 distance of 0.45(1)Å. The cell parameters are a=5.909(1)Å, c=23.369(4)Å, (d_x= 5.01).

7. Crystal Structures and Topology

SYNTHESIS AND CRYSTAL CHEMISTRY OF FERRIC HYDROGEN SULFATE HYDRATE

Valyashko E.V. and Peterson R.C. *(Dept. of Geological Sciences, Queen's University, Kingston, aliona@geol.queensu.ca)*

A new crystal phase of hydrated ferric sulfate was synthesized from a mixture of ferricopiapite and sulfuric acid. Run durations of 20-30 days and a temperature of 140°C produced well-defined tabular crystals with rhombohedral morphology up to 1mm. The phase is stable at 140°C for long periods in the solution from which it precipitated and at room temperature after being removed from the solution.

Twinning is evident in all crystals in polarized light. X-ray powder and single crystal diffraction techniques were used to characterize this ferric sulfate. The X-ray diffraction pattern closely matches that of an aluminum sulfate with the chemical formula $AlH(SO_4)_2 \cdot H_2O$. The electron microprobe results show that metal to sulfur ratio is two. This combined with the similarity to $AlH(SO_4)_2 \cdot H_2O$ indicates a formula $FeH(SO_4)_2 \cdot H_2O$.

The crystal structure of the hydrated ferric sulfate was solved to R = 13% with *P*1 space group and cell dimensions: a = 8.303(9)Å, α = 89.99°(1), b = 7.88(3)Å, β = 100.4°(1), c = 15.81(2)Å, γ = 90.02°(8)

The pseudo-rhomboherdal structure consists layers of corner sharing Fe-octahedra and S-tetrahedra with H_2O in between layers, which is consistent with platy morphology of the crystals.

This phase is related to other sulfates such as rhomboclase, kornelite and lausenite.

BIKITAITE FROM NORTH CAROLINA: STRUCTURE REFINEMENT AND *AB-INITIO* MOLECULAR DYNAMICS SIMULATIONS.

Quartieri S., Sani A., Vezzalini G. *(vezzalini@imomn1.unimo.it)*, Galli E. *(Dip. di Scienze della Terra, Modena, Italy.)*, Fois E., Tabacchi G. *(Ist. di Scienze Mat., Fis. Chim., Como, Italy)* and Gamba A. *(Dip. di Chim. Fis. ed Elettrochim., Milano, sede di Como, Italy)*

Bikitaite, $Li[AlSi_2O_6] \cdot H_2O$, is a quite rare zeolite, found for the first time at Bikita, Zimbabwe (B) and later at King's Mountain, North Carolina, USA (NC). Two X-ray and one neutron diffraction studies are reported for bikitaite from the type locality. Different space groups (P21 or P1) were determined, depending on the Si,Al ordering degree present in the crystals. No structural refinements have been reported before for bikitaite from North Carolina, and it is particularly interesting to examine its actual space group and Si,Al distribution.

In this work we report the results of an accurate single-crystal X-ray diffraction study on a sample of bikitaite NC and we compare these data with those of the other refined bikitaite samples. X-ray diffraction data collection was carried out over the range $5 < 2\theta < 84$. 8270 reflections were collected in the triclinic s.g. *P*1, out of which 8225 with $I > 3\sigma(I)$ were used in the structure refinement, performed in the s.g *P*1. At the end of the last anisotropic refinement cycle, the Rw index was 3.02%. The single crystal used for the X-ray diffraction study was also employed to collect the IR spectrum, by means of a FTIR microscope.

The results of the structure refinement indicate that bikitaite from NC is triclinic, with a strongly ordered Si,Al distribution. Hydrogen positions are consistent with those determined by neutron diffraction.

We have also performed *ab-initio* molecular dynamics simulations on two different configurations of bikitaite, the former of which is completely ordered, while the latter is characterized by a disordered Si/Al distribution.The simulated X-ray and neutron diffraction patterns from the two trajectories were compared to the experimental patterns.The simulated vibrational spectra, in agreement with the experimental IR spectrum, are consistent with the presence of a one dimensional chain of hydrogen-bonded water molecules. No evidence for proton transport along the hydrogen chains of water molecules has been observed during a simulation 2 ps long.

8. Applied Mineralogy: Extractive and Metallurgical Processes

MINERALOGY OF BENEFICIATION PROBLEMS INVOLVING FLUORSPAR CONCENTRATES FROM CARBONATITE-RELATED FLUORSPAR DEPOSITS

Hagni R.D. *(Dept. of Geology and Geophysics, Univ. of Missouri-Rolla, rhagni@umr.edu)*

The World's three largest producers of fluorite from carbonatite-related fluorspar ore deposits are located at Okorusu, Namibia, Amba Dongar, India, and Mato Preto, Brazil. Beneficiation problems involving fluorite concentrates from those three deposits share some similar aspects that are related to their mineralogy. The most important of these problems involves their phosphorus, silica, and lime contents.

Because the fluorite-depositing hydrothermal fluids were partly or largely derived from carbonatite sources, and carbonatites typically are rich in phosphorus, carbonatite-related fluorite deposits are expectably characterized by significant amounts of phosphorus minerals,especially apatite. Apatite may occur as free particles and especially as particles locked with fluorite. The presence of apatite in fluorite concentrates may contribute significant amounts of phosphorus, a deleterious constituent in fluorspar concentrates used in the steel-making industry.

Fluorite concentrates from some carbonatite-related fluorspar deposits are characterized by significant amounts of silica. The silica occurs in the form of quartz, potash feldspar, and sericite. Quartz occurs as free particles and particles locked with fluorite. Quartz was deposited late in the paragenetic sequence and typically fills small vugs between the fluorite crystals. Potash feldspar formed during early potassic fenitization associated with the magmatic carbonatite emplacement. Potassic feldspar forms intricate intergrowths with fluorite that result in locked feldspar-fluorite particles in the fluorspar concentrates. The potash feldspar is intensely altered to sericite.

Fluorite deposits that occur within a carbonatite host, such as some deposits at Mato Preto, may have the grades of their fluorite concentrate diluted by the presence of calcite. The calcite commonly is present as binary locked calcite-fluorite particles.

Although the beneficiation problems concerning fluorite concentrates from carbonatite-related fluorspar deposits may be effectively studied by petrographic and ore microscopic techniques, cathodoluminescence microscopy is uniquely suited to the rapid recognition and study of the minerals involved in these problems.

DETERMINATION OF REFRACTORY GOLD DISTRIBUTION BY MICROANALYSIS, DIAGNOSTIC LEACHING AND IMAGE ANALYSIS

Kojonen K. and Johanson B. *(Geological Survey of Finland, Kari.Kojonen@gsf.fi, Bo.Johanson@gsf.fi)*

A refractory gold deposit recently discovered in Northern Finland has disseminated gold-bearing pyrite and arsenopyrite in graphite-bearing albitite host rock. The minor ore minerals include chalcopyrite, sphalerite, tetrahedrite, gersdorffite, galena, bournonite and rutile.

Ore and concentrate samples were studied under polarising microscope using reflected light. To reveal the texture of pyrite and arsenopyrite the samples were etched with $KMnO_4$ dissolved in concentrated sulfuric acid with etch times of 1-2 minutes.

The diagnostic leach tests show that only a minor part of the gold is in cyanide leachable form, *i.e.*, free gold. Most of the gold is liberated in nitric acid leach, which means that it is bound to pyrite and arsenopyrite as inclusions or as "invisible" gold.

The relationship between arsenopyrite and pyrite in the concentrate was determined using image analysis of backscattered electron images. Optical image analysis was used for determination of the grain size distribution of the concentrates.

As result of the rare-phase search runs with EPMA a total of 111 gold grains were located in the polished sections of ore samples and concentrates. The grains have a large compositional variation from silver bearing gold to electrum and Au-Ag amalgam.

In the EPMA trace Au analyses, the average gold content in pyrite (n=192) is 46 ppm, the average Au content in arsenopyrite (n=135) is 279 ppm. The SIMS analyses average 69 ppm Au in pyrite (n=16) and 217 ppm Au in arsenopyrite (n=22).

Based on cyanide leach results, trace analyses and image analysis the calculated average percentages of gold in the concentrate are: free gold 4.1%, gold in pyrite 22.7% and gold in arsenopyrite 73.2%.

CHARACTERIZATION OF PRIMARY GOLD FROM SALAMANGONE, AP, BRAZIL

Tassinari M.M. *(M.Sc., Polytechic School, Univ. São Paulo)*, Kahn H. *(Prof., Polyt.. Sch., Univ. São Paulo, henrkah@usp.br)* Sant'Agostino L. *(Prof. , Geoscience. Inst., Univ.. São Paulo)* and Ratti,G. *(Ph.D., Polytechic School, Univ. São Paulo)*

Three samples from Salamangone primary ore were studied as a part of an economic feasibility study. Applied mineralogical studies were carried out trough mineral separations coupled to cyanidation and amalgamation tests, with support of chemical and mineralogical analysis - optical microscopy, SEM and XRD. The objectives were to define the gold association and distribution, identify the presence of fortuitous "cyanicides" minerals, as well as to suggest a preliminary process flowsheet and the gold recovery potential.

The ore presented an average grade of 12.6 ppm. After grinding it bellow 0.6 mm the gold recovery for the amalgamated heavy fraction was 61% with the following distribution - 40% as free gold, 11% in locked particles with silicates, 7% locked with sulphides and 3% with quartz plus sulphides. Cyanidation tests performed from float fractions and amalgamation residues showed that an additional of 27% of the gold content cold be recovered - 15% associated with silicates and the others 12% to sulphides. The unrecoverable gold portion represents 8% - 5% associated with silicates and 3% with sulphides. Cyanicides minerals were not found.

A process flowsheet could be established without any other mineral or metallurgical processes tests. Later on, the operation of industrial plant showed a total, as well as individual gold recoveries for the gravity and cyanidation circuits, very close to the predicted values from the applied mineralogy studies.

USING SCANNING ELECTRON MICROSCOPY TO STUDY BIOLOGICAL MINERAL DEPOSITS

Poggi S.H. *(UCLA Medical School)*, Skinner H.C.W. *(Yale Univ. Catherine.Skinner@Yale.edu)*, Ague J.J. *(Yale Univ.)* and Carter D. *(Yale Medical School)*

Examination of thin sections of breast tissue are the second stage of identifying tumors after mammography. The sections often exhibit mineral deposits among the cells and cellular products. The significance of these deposits and their potential to aid the diagnosis and treatment of patients are not yet fully explored nor understood.

We have investigated the use of SEM/BSE with EDS/WDS to study the morpohology and composition of the deposits in situ, that is in association with other tissue components. We utilized standard laboratory thin sections but removed the parafin and did not polish the samples. Five samples, selected from 152 breast tissue specimens collected at Yale in 1994, showed deposits in a variety of tissue sites. The microcalcifications were imaged and range in size from less than 1 μm to over 40 μm. The larger size mineral material was recognizable as calcium oxalate but the predominant mineral form in the calcifications was calcium phosphate as tiny spherules and spheulitic aggregates.

Because of the small size and rough surface the energy spectra results varied widely but we elected to calculate Ca/P ratios for multiple analyses on each type. The results showed that the Ca/P of the microcalcifications are comparable to normal calcium phosphate deposits in bone, and other pathologic deposits. However two distinct types of deposits were identified: those in the ducts of the tissue and those in the matrix. The ducts had higher Ca/P ratio material although the reproducability of the measurments suggests that the mineral may not be a homogeneous phase, even when a single aggregate is examined.

We suggest that the mineral reflects the composition of the biolgical environment in which it is precipitating. It appears that SEM may be a useful and effective technique to document the reactions of cells under different conditions and may help in clinical diagnosis and treatment.

8. Applied Mineralogy: Extractive and Metallurgical Processes

EFFECT OF MINERALOGY AND TEXTURE OF SAND AND HARD ROCK ILMENITES IN TiO_2 PIGMENTS PRODUCTION BY SULFATE PROCESS

Chernet T. and Jalava J. *(Geological Survey of Finland tegist.chernet@gsf.fi and Kemira Pigments Oy, FIN-28840 Pori)*

In producing TiO_2 pigments by sulfate process the reactivity of the raw material with sulfuric acid is crucial. Two ilmenite concentrates from sand and hard rock deposits were studied. For the former, the recovery of TiO_2 into the pigment was only moderate, whereas the latter showed a high recovery. This study shows that mineralogical and textural characteristics correlate with the observed recoveries. In the sand ilmenite, alteration advances along grain boundaries and fractures resulting in the formation of poorly soluble phases that prevents the acid reaching the soluble ilmenite. Furthermore, the trace elements that tend to be concentrated during the alteration and the trace element signature of ilmenites from multiple source rocks affect the quality of the pigment.

Rare alteration in the hard rock ilmenite favours good solubility. Magmatic features *i.e.* exsolution and twinning have a positive effect on solubility. The dissolution of ilmenite and extent of hematite exsolution was found to correlate. Hematite lamellae are partially dissolved and shown by oriented pits that promote percolation of the acid and result in a positive effect on the leaching of ilmenite. Structural discontinuities *i.e.* twinning and fracturing are favourable for the penetration of the leachates into the grains. The effect of a trace element on the quality of pigment is highly dependent on whether it is incorporated in the lattice of ilmenite or some insoluble phases.

A knowledge of Ti bearing phases including their quantification and alteration can throw light on the raw material treatment enabling the metallurgist to deal with the problems in TiO_2 recovery. The distribution and the content of trace elements and deleterious minerals provide a useful guide to controlling both the quality of final product and tailing. To conclude, careful mineralogical examination of any ilmenite concentrate is useful in evaluating its suitability for the process.

SOME CHARACTERISTICS OF WEATHERED ILMENITE WHICH AFFECT PROCESSING

Graham J. *(SRCAMMP, University of Western Australia, jgraham@chem.uwa.edu.au)*

Australian ilmenites generally occur as heavy mineral sands which result from weathering of granitic host rocks, and have been transported over long distances to form strand lines subsequently buried. The mineral has been altered to varying extent in the process, resulting in a mixture of more or less oxidised phases with a range of physical and chemical properties which must be taken into account in processing. Each deposit is a unique mixture of the same minerals, and in general East Coast deposits are less altered than those in the West.

Magnetic properties can be altered significantly by quite minor heat treatment in air or in a reducing medium. These changes can be utilised in separation of an improved ilmenite fraction which is less altered and has reduced chromite impurity.

Chemical reactivity of altered ilmenite is a complex function of mineralogy and FeO content. Suitability for the sulphate process for TiO_2 pigment production can be assesed from a thermogram of a small sample in an oil bath.

CURRENT TRENDS IN APPLIED MINERALOGY TO EXTRACTIVE METALLURGY

Petruk W. *(Petruk Mineral Characterization, Ottawa, huguette@magmacom.com)*

Unprecedented improvements have been made in applied mineralogy to extractive metallurgy by adapting new analytical equipment to solve problems encountered by metallurgical engineers. The main requirements of applied mineralogy to extractive metallurgy are to determine mineral identities, mineral textures (including grain sizes), mineral quantities, mineral liberations, mineral compositions, trace element contents in minerals, and surface coatings on mineral grains. The optical microscope continues to be used as the preliminary instrument for all studies, and in many instances is the only instrument. The scanning electron microscope is a major second instrument and is used for identifying minerals and determining mineral textures. It is also used in conjunction with an image analyzer to automatically determine mineral identities, quantities, textures, and liberations, and to search for rare minerals. X-ray diffraction (XRD) has been used for many years to identify minerals and to determine approximate mineral quantities. Recent developments in computerizing XRD data has led to more accurate results for mineral quantities. Similarly, other techniques such as cathodoluminescence, are used in mineral identification and determining textures. The microprobe has been widely used since it was developed to identify the minerals and to determine mineral compositions and trace element contents in minerals. The very low quantities of trace elements, which may be either valuable by-products or deleterious impurities, can now be determined with such equipment as a PIXE, LIMS, or SIMS. Surface coatings, such as metallurgical reagents or elements on mineral grains and particle surfaces, and which may cause metallurgical problems, can be determined with TOF-LIMS and TOF-SIMS.

FERROCHROMIUM: MINERALOGY APPLIED TO ITS PRODUCTION AND USE

Wedepohl A. *(Mintek-now retired)* and Ellis P. *(Mintek)*

Due to the vast reserves of chrome ore existing in the Bushveld Complex of South Africa, this country has become the largest producer of ferrochromium in the world. As a result, much effort has gone into optimizing its production and usage in South Africa. Mineralogical investigations have contributed to the optimization process and this paper will review some work of this nature, which the authors have undertaken at Mintek, a research organization specializing in mineral technology.

Case histories which will be discussed are the following :

1. The reduction of chrome ore in a traditional submerged-arc furnace. A study was made of the reduction mechanism, using samples taken during the dig-out of a 48MVA submerged-arc ferrochromium furnace, by a team from the Pyrometallurgical Division at Mintek, led by Dr N.A.Barcza.

2. The reduction of chrome ore in a transferred-arc plasma furnace. Samples from a pilot furnace at Mintek were analyzed and the reduction mechanism compared with that taking place in a submerged-arc furnace.

3. Binding strength of chromite briquettes. In order to avoid the danger of blowouts caused by feeding fines directly to a submerged-arc furnace, it is necessary to agglomerate chromite fines. Studies were done of the high- and low-temperature strength of briquettes made with a variety of binding materials, and the temperatures at which reactions took place.

4. Characterization of ferrochromium. This was required when a particular type of ferrochromium e.g. charge chrome or low-carbon ferrochromium was under consideration as a starting material for some other process.

5. Leaching of ferrochromium.

In order to produce chromium chemicals from ferrochromium fines, generated during handling of the material, a leaching study was undertaken with a mineralogical component.

8. Applied Mineralogy: Extractive and Metallurgical Processes

CHROMITE MINERALOGY AND THE FERROCHROME INDUSTRY

Fernandes T.R.C. *(Inst. of Mining Research, Univ. of Zimbabwe, reifern@imr.uz.zw)*

Future demands for ferrochromium alloys for the stainless steel industry are likely to be met from Southern Africa where 89% of the worlds chromium reserves occur. Zimbabwe has good quality metallurgical grade chromite ores that have been used for premium grade alloys with carbon levels of 4-6% which command a better price. Traditionally the preferred qualities for the production of these alloys are lumpy ore with a minimum of 48% Cr_2O_3, a high Cr:Fe ratio (>2.8:1) and a high proportion of refractory to non-refractory components. Recent studies reveal that mineralogical factors, resulting mainly from transformation-induced microstructures, have an influence on the quality of the ores.

Spinels in undisturbed chromites are commonly euhedral and essentially defect-free. Narrow line profiles in the XRD spectra confirm that the crystals are strain-free.

Tectonic stress in the Great Dyke has resulted in brittle fracture and stress-induced cation migration resulting in measurable strain and a change from perfect cubic symmetry. These crystal imperfections act as nucleation sites during metallurgical reduction and lead to a poorer quality ferroalloy with a greater carbon content.

Different cation distributions over tetrahedral and octahedral sites in spinels of similar composition detected by channelling enhanced microscopy and by subtle differences in convergent beam electron diffraction patterns, allow for enhanced exchange interactions between magnetically active cations, resulting in ferrimagnetism in the sheared spinels. The effect appears to be greater in the more iron-rich ores thus affording a possible means of using the magnetic properties of chromite for *in situ* ore evaluation, beneficiation and process control.

INFLUENCE OF VIBRATING GRINDING AND CALCINATION ON THE PHYSICO-CHEMICAL PROPERTIES OF AN EGYPTIAN KAOLINITE.

Ismael I.S., Abd El-Rahman M.K. and Hassan M.S. *(Central Metallurgical R & D Institute, P.O.Box 87, Helwan, Cairo, Egypt, rucmrdi@rusys.eg.net)*

The effects of vibrating grinding and calcination on the structure and reactivity of Kalabsha kaolinite have been studied by means of XRD, IR, DTA and BET surface area. Leaching experiments on ground and calcinated samples were carried out using 20% HCl for aluminum extraction.

In the earliest stages of grinding the partial destructive of stacking kaolinite layers is occurred. These changes are associated with increase in surface area due to formation of fine grains with great number of boundaries. Further grinding or calcination leads to a deterioration of kaolinite structure. A significant increase of surface area is observed, starting from 18m²/g for original sample to reach maximum value 42 m²/g at 120 min. grinding time and 30 m²/g at 300°C for calcination.

The extraction of aluminum after 30 min. leaching time is about 97.52% for the ground kaolinite at 240 min. grinding time and about 93.47% for calcinated kaolinite at about 550°C.

THE HYDROTHERMAL TRICOLOR QUARTZ VEIN FROM SÃO GERALDO DO ARAGUAIA, STATE OF PARÁ - BRAZIL, ORIGIN AND APPLICATION

Collyer T.A. *(Institute of Economic-Social Development the State of Pará)*, Kotschoubey B. *(Center of Earthsciences of the Federal Univ. of Pará)*, Khan H. *(Polytechnic School of the Univ. of São Paulo)* and Hieronymus B. *(University Pierre and Marie Curie, Paris VI)*

Occurrences of tricolor zoned quartz showing the violet, yellow and red associated colors were discovered close to São Geraldo do Araguaia Town, in the southeastern part of the State of Pará, Brazil. The tricolor quartz vein is a subvertically dipping, N 10° W oriented and approximately 2.5 m thick body which crops out for about 50 m along the strike. The host rocks are meta-arkoses and meta-sandstones and the vein exhibits a rough zonation. The outer zone it's mainly composed by smoky quartz, and the intermediate zone is constitited by irregularly banded and undulated tricolor cluster quartz. The inner part consists of clay with enclosing angular quartz fragments.

The inclusions of the border quartz zone showed the H_2O-$CaCl_2$-NaCl system, salinity range 20.6 to over than 23.2 wt% NaCl and temperature range 488 to 492°C. In the crystals bicolored zone have been identified the presence of the H_2O-$CaCl_2$-NaCl and H_2O-$FeCl_2$-NaCl systems and salinity ranging from 13.8 to 17.3% and 19.9 to higher than 23.2 wt% NaCl, respectively. The red zone the H_2O-$FeCl_2$-NaCl system shows a salinity range from 8.68 to 10.1 wt% NaCl and temperature ranging from 267 to 199°C.

Chemical analyses of the quartz applied in the silicon metallurgy, showed a weight composition of 99.72 % SiO_2, 0.2% Fe_2O_3, 0.08% Al_2O_3, 0.01% CaO, 0.01% MgO and 0.02% TiO_2. The presence of the two different hydrothermal fluid systems and a relatively high salinity suggest a hydrothermal origin for the tricolor quartz relationship as a magmatism as the regional metamorphic activities.

The decrease of the salinity of the basal to the upper crystalline zone and the change of the chemical fluid composition also suggest a different crystalline phase growth or a several hydrothermal pulses in specifics pressure and temperature conditions. The meteoric or supergenic water contribution cannot be ruled out in the crystal generation mainly in the final hydrothermal process. Rough tricolor quartz is used actually for the mineral craftmanship made in São Geraldo do Araguaia region and the quartz border zone is applied to silicon metallurgy.

PHASE EQUILIBRIA IN THE SYSTEM Zn-Fe-Ga-S AT 600°C TO 800°C

Ueno T. *(Dept. of Earth Sciences, Fukuoka Univ. of Education, Japan, uenot@fueipc.fukuoka-edu.ac.jp)* and Scott S.D. *(Dept. of Geology, Univ. of Toronto, scottsd@zircon.geology.utoronto.ca)*

In the system Zn-Ga-S, three solid solutions were found: $(Zn,Ga)_{1-X}S$ solid solution, phase V solid solution and phase U solid solution. In the system Ga-Fe-S, three new ternary phases (phase Z, phase X and phase W) and two binary phases (alloy Y and α-iron) were found. In the central portion of the Zn-Fe-Ga-S system, there is a wide range of $(Zn,Fe,Ga)_{1-X}S$ solid solution at 900°C and 800°C. This solid solution has the sphalerite structure along the ZnS-FeS join. Adding only a small amount of GaS component to the solid solution results in the appearance of a mixture of sphalerite and wurtzite, and extensive incorporation of GaS component and FeS component stabilizes the wurtzite structure. Scott & Barnes (1972) have examined the sphalerite-wurtzite equilibrium and showed that both phases can coexist over a range of temperatures well below 1020°C as a function of sulfur fugacity. In the case of $(Zn,Fe,Ga)_{1-X}S$ solid solution, the inversion temperature for sphalerite → wurtzite structure varies with chemical composition. Phase V has a solid solution area that extends into the Zn-Ga-Fe-S tetrahedron; the maximum iron content is 12.5 atomic % at 900°C and 11.9 atomic % at 800°C. Phase X and Ga_2S_3 have very small solid solution areas into the Zn-Fe-Ga-S tetrahedron.

SUBMICROSCOPIC GOLD IN SULPHIDES FROM GOLD DEPOSITS IN WESTERN AUSTRALIA

Vaughan J.P. *(Dept. of Mining Geology, Western Australian School of Mines, tvaughan@cc.curtin.edu.au)*

The submicroscopic gold contents of sulphide minerals from sixteen refractory and free-milling gold ores from Western Australia have been determined using SIMS (secondary ion mass spectrometry). Pyrite, arsenopyrite and pyrrhotite are overwhelmingly the dominant sulphide minerals in these ores. Of these, arsenopyrite and pyrite are the main carriers of submicroscopic gold, which is consistent with findings from other refractory gold ores. Pyrrhotite does not appear to carry submicroscopic gold in any of the deposits investigated. Arsenopyrite almost always carries the higher levels of submicroscopic gold in refractory ores where both pyrite and arsenopyrite are present. However, in some pyrite + arsenopyrite ores, neither sulphide carries significant submicroscopic gold, and these ores are not refractory. In purely pyritic ores (i.e. without arsenopyrite), it is only arsenian pyrites which carry submicroscopic gold, but generally at lower levels than those which are typically found in arsenopyrite. Arsenic-free varieties of pyrite carry virtually no submicroscopic gold.

Other sulphides of interest which are potential carriers of submicroscopic gold include loellingite, gersdorffite and cobaltite, which are present in a few ores. Limited numbers of analyses on these minerals indicate that loellingite carries significant amounts of submicroscopic gold, but not gersdorffite or cobaltite.

In conclusion, submicroscopic gold was shown to be the main cause of refractory behaviour in almost all of the deposits investigated. Other reasons which contributed to refractory behaviour in a few deposits included gold-bearing tellurides and fine-grained inclusions of native gold in pyrite.

9. Applied Mineralogy: Mineralogy of Ceramics and Cements

THE ALKALI-SILICA REACTION IN CONCRETE: SILICA MINERALS IN HIGH-pH ENVIRONMENTS

Carey J.W. *(Los Alamos Natioanl Lab, bcarey@lanl.gov)* and Guthrie G.D., Jr. *(Western Michigan Univ., guthrie@wmich.edu)*

Pore fluids in concrete are alkali rich with a pH that exceeds 12.5. High-silica materials in the aggregate (*e.g.*, silica polymorphs, volcanic glass) can react with the pore fluids to produce a swelling silica gel. This is known as the alkali-silica reaction (ASR) and can lead to deterioration of concrete structures via a characteristic map-pattern cracking.

Petrographic studies document a complex reaction mechanism. Alkali-rich silica gels develop at the aggregate-paste interface and within the aggregate. In the early stages of ASR, these gels are localized near the aggregate but may also fill air voids. As ASR develops, distinct chemical reaction zones form that consist of bands of alkali-rich gel, calcium-rich gel, and possibly gel-free aggregate. During this stage, ASR-generated gel migrates away from the aggregates along fracture surfaces and is modified to a Ca-rich form, apparently by cation exchange with the cement paste. Extensive gel migration has been correlated with advanced stages of deterioration in concrete.

The geochemistry of gel formation is unclear. For example, the alkali content of cement is important because it raises the pH, but the chemical variability and "equilibrium" behavior of the ASR gel is not well understood. The apparent relative reactivity of silica polymorphs including the difference between quartz and strained quartz suggests that kinetics plays an important role in ASR. Surprisingly, the same reactive minerals occurring in aggregate can prevent ASR when they are present in a finely ground (pozzolonic) form. Mineralogical and geochemical tools will be useful in finding answers to these and other riddles presented by alkali-silica reactivity in concrete.

AUTOMATIC PETROGRAPHIC TECHNIQUE FOR THE QUANTIFICATION OF CONCRETE DAMAGE DUE TO ALKALI-SILICA REACTION

Rivard P., Ballivy G. *(Department of Civil Engineering, Sherbrooke University)* and Fournier B. *(CANMET, Natural Resources Canada)*

A new automatic petrographic technique for the quantification of concrete damage due to alkali-silica reaction (ASR) was developed as part of this study. The amount of microcracking and alkali-silica gel due to ASR is determined from polished concrete specimens impregnated with fluorescent exoxy resin covered with uranyl acetate solution. The above parameters are quantified using magnified images treated by a computer image analysis program designed specifically for this research project.

The new image analysis method showed good correlation between the concrete damage and measured expansions of the laboratory concrete prisms. The total length of cracks was the parameter that gave the best correlation with the level of expansion of the test specimens. Coefficients of correlation (R^2) of 0.9 and 0.6 were obtained for the samples incorporating the reactive Spratt limestone and Potsdam sandstone aggregates, respectively. The variation in coefficient of correlation is explained by the different petrographic and mineralogical characteristics of these rocks. Microcrystalline silica sparsely distributed within the matrix of the limestone and intergranular siliceous cement in the sandstone cause the above aggregates to be ASR susceptible. The results of this technique showed good correlation with those obtained from the Damage Rating Index method (DRI) performed on the same concrete samples.

The quantitative petrographic technique was also applied to a ten meter long core taken from the Beauharnois Dam, located in the Montreal area. The analysis of the selected samples along the core confirmed previous reports that some parts of the dam are seriously affected by ASR. Higher damage was observed close to the surface of the dam, while the damage was observed to decrease going towards the centre of the dam. Most of the cracking in the core was horizontal, confirming the confinement of the concrete in the horizontal direction.

MINERALOGY OF ACCRETIONS IN CEMENT KILN PREHEATER

Kurdowski W. and Soboñ M. *(University of Mining and Metallurgy, Cracow, Poland)*

In a short rotary kiln with the cyclone preheater an internal recirculation of volatile constituents is generated, essentially containing compounds of potassium, chlorine and sulphur.

These compounds are subject to partial condensation on the raw material grains which consist mainly of calcite.

The increasing concentration of volatile costituents creates convenient conditions for crystallization of new phases, panicularly sylvite. Beautiful crystals of this phase are formed, probably by the VLS mechanism.

As the thermal analysis has shown, a liquid phase is formed in the system at relatively low temperature about 630° C, which enhances the reaction of silica with calcium carbonate and spurrite is formed. The preheater can be divided into two parts: in higher temperature prevails spurrite and sylvite; in lower anhydrite and calcium langbeinite.

Thus the build-ups are mainly of calcite, sylvite and spurrite, and in some cases also of calcium oxide and anhydrite. "Sulphospurrite", gehlenite, calcium langbeinite, dicalcium silicate and calcium aluminate - $12CaO.7Al_2O_3$, can be found as minor components.

Key words: thermal analysis, accreation, sylvite, spurrite, anhydrite, calcite, rotary kiln, preheater.

RECYCLING OF SOME EGYPTIAN INDUSTRIAL SOLID WASTES IN CLAY BRICKS

Hassan M.S. and Elwan M.S. *(Central Metallurgical R & D Institute, P.O.Box 87, Helwan, Cairo, Egypt, Email: rucmrdi@rusys.eg.net)*

In the present work an attempt is made to study the possibility of using clay with industrial waste products such as blast furnace slag and converter slag cooled by air-water for brick manufacture.

The materials used are investigated by chemical analysis, DTA, X-ray as well as grain size distribution. Solid bricks are made using hand moulding. Firing is carried out at 800 - 900°C with rate 2.5°C/min up to the desired temperature for 2 hours duration. The ceramic properties are measured.

The results show that the substitution of 10% clay by blast furnace slag fired at 900°C, 1000°C, improves the compressive strength, bulk density, but the substitution by converter slag decreasing the above properties at the same temperature. It can be concluded that granulated slag is suitable for brick making than the converter slag.

9. Applied Mineralogy: Mineralogy of Ceramics and Cements

STABILIZATION OF GALVANIC SLUDGES IN BRICKS

Guscioni N. and Maggetti M. *(Min. Petr. Institute, University of Fribourg, marino maggetti@unifr.ch)*

CrIII-rich galvanic sludge was mixed in various amounts to a German clay ceramic body and fired at different temperatures in order to establish a) the possibility of the stabilization of this industrial waste and b) to characterize the properties of the ceramic bodies obtained. The sludge, the clay and the fired products were analyzed by XRF, XRD, mercury pressure prosimetry, optical microscopy, SEM, microprobe, leaching tests and various laboratory tests for the physical parameters relevant for industrial application (*e.g.* compressive strength). We present only the results obtained with 2 and 10 wt% admixture and firing temperature of 1000°C.

The sludge is very fine, mainly amorphous with Ca, P, Al, Cr, H, S, Cl and traces of Sr, Rb, Ba, Zn and Pb. Its leachate satisfies the Swiss limits for "stabilized residues" but the high solubility of the sludge in HCl 2n cannot be tolerated. The German clay has a granulometry adequate for the production of bricks only and contains quartz, muscovite-illite, kaolinite, siderite and dolomite.

Clay samples without any sludge addition show after firing at 1000°C new phases such as hematite, anorthite, K-feldspar and mullite. 2 and 10 wt% sludge addition produces supplementary apatite and eskolaite, *i.e.* a Cr-phase. Leaching tests of the samples show as positive result that all the Cr is incorporated in the insoluble eskolaite. Measurements of the physical parameters of the fired products (*e.g.* compressive strength) show sligthly better results for the mixed samples. Cr-addition in ceramics can therefore be considered as a valorization with the possibility of an official acceptance for a stabilizing procedure.

THE PETROLOGY IN THE RESTORATION: CASE EXAMPLE OF THE AQUEDUCT OF MORELIA, MICH., MÉXICO

Viggiano G.J.C. and Alonso E.M. *(Facultad de Ingeniería Civil, UMSNH, Mich., México, geoexplo@mich1.telmex.net.mx)*

The Aqueduct of Morelia Mich., México, is a baroque monument built in the XVIII century, totally with ignimbrite stone known locally as pink stone (of Tertiary) which proveneance quarry is virtually uncertain. It has about 1700 m length and is formed by 253 stilted archs. Since the end of the past century left working adequatelly due to many causes -but of, course, the main one, its deterioration- and therefore was constituted a real architectural monument and a city symbol. The stones of the monument have indurated a strong alteration due mainly to atmospheric agents, without underestimate the human-caused deterioration, through the time and the work has periodically been restored but seemingly neglecting the petrological characterization of the stones. This paper focuses firstly on the petrological featuring of stones in order to describe either the primary and the secondary mineralogy; the latter one ascribed to atmospheric causes and, secondly, on the study of 3 nearby quarries with the same philosophy to provide the best choice of supply materials in any stage of restoration. The stones of the monument were clasified as devitrified and oxidized ignimbrites with low to medium degree of welding, constituted by quartz >plagioclase >glass> ± biotite displaying strong ferrugination (bearing-Fe oxides appearence), considerable montmorillonite- clay generation and very incipient calcitization (calcite formation), as products of atmospheric alteration. This alteration confers the stones the typical beautiful patina colors especially when the phenomenon is not so advanced, but unfortunatelly when the stone decay becomes highly advanced, the stone must be replaced. Thus, the most adequate quarry to replace petreous pieces is the so called the El Tejocote quarry not only because its mineralogical similarity respect to the original stones but because its geomechanical (compressive strenght, apparent density and adsorption) properties.

SOLID-STATE REACTIVE TRANSITION OF KAOLINITE AND POWDERED ALUMINIUM MIXTURE TOWARDS MULLITE CERAMICS MATRIX

Kupiec E. *(Power Engineering Institute, Boguchwala, Poland)* and Szymański A. *(Warsaw University of Technology, Faculty of Chemistry, Poland)*

Single-phase, pure mullite ceramics show a number of attractive chemical, thermal and mechanical properties. Previous application of the mullite ceramics as refractory material accepted small admixtures of the different phases. Mass-production based on the high temperature sintering of kaolinite maintain many heterogeneties in the body. To-day technology of hi-tech mullite ceramics formation towards to the lower temperature synthesis which to make possibilities for raw materials composition programming.

Solid-state reactive transition of kaolinite, mixed with precisely calculated admixture of the metallic aluminium powder, there was process of mullitization which we studied. Addition of powdered aluminium give us possibility to elimination of free silica, both: connected with raw kaolinite clay, as well as, come into being in kaolinite thermal decomposition process. That metallic admixture compensated stoichiometric ratio between alumina and silica in the final mullite ceramics body.

In our experiments we observed complexity of the physicochemical processes, which take place in that mixture sintering. At the temperature range from 100 to 1730°C appeared and disappeared eleven crystalline phases. Into kaolinite-aluminium powder mixture, contained make-up water, reactive interaction to start with a 100°C, and created many essential technological problems.

Independently of process complexity, that way of kaolinite mullitization give us possibilities to obtain roentgenographically single-phase mullite bodies.

Key words: kaolinite mullitization, reactive sintering, mullite ceramics.

THERMAL STABILITY OF HYDROUS CALCIUM SILICATES

Yu P. *(Dept. of Materials Science and Engineering, Univ. of Illinois, p-yu@uiuc.edu)* and Kirkpatrick R.J *(Dept. of Geology, University of Illinois, kirkpat@uiuc.edu)*

Tobermorite and jennite are important model compounds for the calcium silicate hydrate (C-S-H) phase of Portland cement and are also natural minerals. Understanding their dehydration behavior is important to understanding both the structures and properties of the individual phases and the mechanical and thermal properties of cement paste at elevated temperatures.

We present here NMR, DSC and TGA, IR, and powder XRD data for heated tobermorite and jennite. Tobermorite undergoes a series of phase transformations from room temperature to 600°C by lose of interlayer water and SiOH groups. Wollastonite forms as the main phase in the temperature range of 800°C to 1000°C. The silicate chains become crosslinked and the fraction of bridging oxygen increases during heating. Jennite transforms to metajennite at 110°C by loss of interlayer water. When further heated to 350°C the metajennite loses its layer structure and transforms to an amorphous phase by loss of interlayer water and CaOH groups. When the CaOH groups leave the structure, the residual non-silicate oxygens coordinate to silicon to form non-bridging oxygens. Thus the silicate chains depolymerize, and the fraction of bridging oxygen decreases during heating.

The layer structure of jennite has lower thermal stability than that of tobermorite due to its lower layer-charge density and the existence of non-silicate oxygens. Cement pastes containing more tobermorite-like structural elements may be preferable for high temperature applications.

THE BINDER OF MEDIEVAL MORTARS

Franzini M., Leoni L., Lezzerini M. *(Dip. Scienze della Terra, Univ. Pisa, Italy, Franzini@dst.unipi.it)*

More than 100 samples of mortar from various European medieval buildings have been analysed. Chemical (XRF), mineralogical (XRD), petrographical (optical microscopy and modal analysis) and physical data have been collected on bulk samples. An X-ray energy-dispersive system (EDAX) applied to a SEM was used to determine the chemical composition of binder and of grains of pozzolanic materials. The components or properties of binder which couldn't be directly assessed (CO_2, H_2O^+, density *etc.*) have been indirectly derived through a computation method. The binder of all the analysed mortars may be regarded as composed of a carbonate crystalline fraction and a non-carbonate amorphous fraction. The non-carbonate fraction, whose amount varies from 0% up to 60% by weight of the binder, is made up by hydrated calcium alumino-silicates similar to the CSH components of cement. Binders are characterised by a ratio of silica to other hydraulic components very close to that of added pozzolanic materials.

On the whole, collected data suggest that medieval mortars were prepared with slaked lime; the more or less marked hydraulic properties are due to the addition of pozzolanic materials.

The mortars from some Pisa monuments, which include the famous Leaning Tower, have binders characterised by high contents of non-carbonate fraction, though they don't exhibit any residue of pozzolanic materials. It is inferred that these mortars were prepared adding diatomaceous earth to sand and slaking lime; this would explain the absence of any detectable residue of unreacted pozzolanic material, since we have observed that diatoms fully dissolve in slaked lime in a very short time (about 30 minutes). Laboratory tests proved that a mixture of slaked lime and diatomite (20% by weight) sets to a very light, hard material in about a day; therefore, we believe that Pisa mortars were prepared by first mixing diatomite with sand and then adding the mixture to the slaked lime.

INDUSTRIAL APPLICATIONS OF THE CLAY BEDS OF WADI EL MEHASHAM, EAST BENT MAZAR, EGYPT

Kamel O.A. *(Geology Department, El Minta University, Egypt)* and Abbouda A.M. *(El Minta Governate, Egypt)*

The Wadi El Mehasham clay deposit is mainly represented by two clay beds of variable thickness, and belonging to the Midawara Formation of Lower Lutetian (Middle Eocene) age. The upper bed consists of a thick yellowish grey calcareous claystone (31.4 - 34 m), while the lower bed consists of a yellowish brown calcareous claystone with gypsum and iron oxides of moderate thickness (11.9 - 13.6m). The maximum thickness of the claystone unit is generally about 42m, and it is intercalated with two thin red ferruginous claystone beds.

Based on the results of X-ray diffraction, textural and chemical analyses and technical properties of the technological clay samples (compactness and slaking in water, plasticity, drying and firing behaviours), it is suggested that Wadi El Mehasham clays can be recommended for the manufacture of building bricks. However it seems more useful to mix them with some sands to get convenient values of the drying sensitivity coefficients, and to increase the safety area of Bigot's curves. Also the results of chemical analysis indicate that these clays are suitable for the production of a normal Portland cement.

CRYSTAL STRUCTURE OF SYNTHETIC ETTRINGITES IN RELEVANCE TO SULFUR OCCUPANCIES

Ikeda K., Terai T. and Shima H. *(Department of Advanced Materials, Science and Engineering, Yamaguchi University, Japan, k-ikeda@po.cc.yamaguchi-u.ac.jp)*

Ettringite characterized by extremely large content of water is a naturally occurring mineral designated as $Ca_6[Al(OH)_6]_2(SO_4)_3.26H_2O$ and has wide applications to cement and concrete industries. It has been suggested that $[SO_4]^{2-}$ substitution with $2OH^-$ will take place in ettringite, *i.e.*, $Ca_6[Al(OH)_6]_2\ [(SO_4)_{3-x/2}(OH)_x].26H_2O$ where x=0 corresponding to pure ettringite. According to Moore and Taylor (1970) there are 8 possible sites for $[SO_4]$ in a unit-cell for ettringite structure (Z=2). For pure ettringite 6 sites are filled with $[SO_4]$ and 2 remain unfilled, that is 6/8 occupancy. If the substitution above-mentioned occurs, $[SO_4]$ occupancies will decrease with increasing x. The authors will clarify this point by the conventional X-ray structure refinement technique for 4 synthetic poly-crystalline ettringites each labelled [0], [1], [2] and [3],expecting 6/8, 6/8, 5/8 and 4/8 occupancies.

All samples were prepared at room temperature with extra water. R values 0.12 to 0.15 were reached. Results are summarized as follows. $[SO_4]$ occupancies obtained were smaller than the expected values and samples [1] and [2] were reversed from the expected order.

Sample [0] prepared by the precipitation method in solutions showed 5/8 occupancy, corresponding to x=1.

Sample [1] prepared by mixing Ca-hauyne $Ca_4Al_6O_{12}(SO_4)$ gypsum $CaSO_4.2H_2O$ and portlandite $Ca(OH)_2$ in 1:8:6 molar proportion showed 3/8 occupancy, corresponding to x=3.

Sample [2] prepared by mixing Ca-hauyne, gypsum and portlandite in 4:23:33 molar proportion showed 4/8 occupancy, corresponding to x=2.

Sample [3] prepared from only Ca-hauyne showed 2/8 occupancy, corresponding to x=4.

SEM MICROSTRUCTURE AND XRD CRYSTALLITE SIZE OF MULLITE IN STONEWARE BODIES OBTAINED FROM BALL CLAYS OF TERUEL (SPAIN).

Serrano J., Sanz A., Clausell J.V., Bastida J. and Amigo J.M. *(Dto. Geología, Universidad de Valencia, Spain)*

The coal mining district of Teruel (NE, Spain) produces china clays and ball clays, wich are used mainly in the ceramic factories of East Spain (Bastida *et al.*,1993). The crystallinity of kaolinites from different deposits was studied by Amigo et al. (1993), and the crystallinity of kaolinite in ball clays used for stoneware was studied in Serrano *et al.* (1993a). Some results concerning crystallite size of mullite in the produced stoneware were discussed in Serrano, Bastida & Amigó (1993b).

The Dv crystallite size (De Keijser *et al.*182) for [001], [110], [120], [210],[111] and [121] directions, in mullite of stonewares produced with different temperatures and different annealing times are analysed in the present paper. Microstructure is also observed by SEM, and the SEM aspect ratios of grains on prismatic faces are compared with those obtained from apparent crystallite sizes used as normal distances of crystallite faces in different combination of possible prismatic faces.

The performed comparation allows to consider that the number of apparent crystallites in the direction of elongation is significantly greater than in other directions perpendicular to grain elongation, so the crystallites may be arranged in such a way to produce grain elongation parallel to [001] and this elongation increases with the firing duration as well as with temperature, in the studied range (up to 1150°C).

A simultaneous growth of length in needle-like grains and of crystallite sizes has been observed during the annealing; the observed agreement of aspect ratio between apparent prismatic crystallite sizes and aspect ratio in prisamtic grains is interpreted as indicative of parallel growth.

THERMOCHEMISTRY OF STUFFED QUARTZ PHASES ALONG THE JOIN $LiAlSiO_4$-SiO_2

Xu H., Heaney P.J. *(Dept. Geosciences, Princeton Univ., Email: hongwuxu@princeton.edu)*, Navrotsky A., Topor L. *(Dept. Chem. Eng. & Mater. Sci., UC-Davis)*, Liu J., and Liebermann R.C. *(Dept. Geosciences, SUNY)*

$Li_{1-x}Al_{1-x}Si_{1+x}O_4$ aluminosilicates ($0 \le x \le 1$), which crystallize in either the β- or α-quartz structure, are of considerable industrial interest because of their near-zero thermal expansion and one-dimensional superionic conductivity. In addition, as quartz is a common structure type, the $LiAlSiO_4$-SiO_2 join offers an ideal system for systematically investigating the effects that charge-coupled substitutions exert on structure, thermodynamics, and physical properties. Despite the importance of this group of materials, few thermodynamic data are available, and thus the energetics of this solid solution series remain largely undetermined.

We have measured the enthalpies of drop-solution (DHdrop-soln) of a suite of stuffed quartz phases $Li_{1-x}Al_{1-x}Si_{1+x}O_4$ ($0 \le x \le 1$) by high-temperature calorimetry in molten $2PbO{\cdot}B_2O_3$ at 974 K. As Si^{4+} substitutes for $Li^{+}+Al^{3+}$, the enthalpies become more exothermic. A slope change in $\Delta H_{drop\text{-}soln}$ *vs.* composition (x) at x=~0.3 is interpreted as a result of an Al/Si order-disorder transition, as revealed by synchrotron X-ray diffraction. Thus, this solid solution series can be divided into two energetically distinct regimes: $0 \le x < \sim 0.3$ and $\sim 0.3 \le x \le 1$, which feature ordered and disordered Al/Si configurations, respectively. By extrapolating a straight line through the $\Delta H_{drop\text{-}soln}$ data of the disordered regime, the enthalpy change associated with the Al/Si disordering for the end-member β-eucryptite is determined to be ~16.6 kJ/mol. This value is consistent with our direct measurements of $\Delta H_{drop\text{-}soln}$ on a series of b-eucryptite samples with varying degrees of Al/Si order.

Standard molar enthalpies of formation of the stuffed quartz phases from constituent oxides ($\Delta H^0_{f,oxi}$) and elements ($\Delta H^0_{f,ele}$) at 298 K were derived. A $\Delta H^0_{f,oxi}$ of 67.21 ± 2.76 kJ/mol and a $\Delta H^0_{f,ele}$ of -2111.7 ± 2.2 kJ/mol for β-eucryptite are in good agreement with the results previously determined by HF solution calorimetry at 346.7 K (Barany and Adami, 1966). We also have determined the enthalpies of formation of intermediate compositions for the first time.

SILICA MINERALS IN GREEN BIOMATS FORMING ALONG KAMUIWAKKA FALLS, HOKKAIDO, JAPAN

Asada R. and Tazaki K. *(Graduate School of Natural Science and Technology, Kanazawa Univ.)*

The behavior of silica in association with green biomats forming along the riverbed of Kamuiwakka River in Hokkaido, Japan was examined in this study. Biomats are forming in specific environments, such as hot springs and geothermal areas, and are appropriate objects to study the transportation and crystallization of silica materials correlated with the activities of microorganisms. Microorganisms live in almost places of the Earth's surface and largely influence on the transportation and crystallization of almost all elements in the Earth's environment. Although many studies on the behavior of silica in hot springs and geothermal areas have been carried out, only a few cases of the behavior of silica associated with microorganisms have been reported.

Acid hot spring water (pH 1.6) flows in Kamuiwakka Falls. Green biomats form on the riverbed and consist mainly of spherical microorganisms about 3 μm in diameter. It has been found through analyses and observations of these microorganisms and the habitat that the microorganisms belong to unicellular red algae. White sediments comprising mainly dead algae were found just under the green biomats. The two colored parts were cultivated and observed by SEM-EDX, XRD and TEM. The results have indicated that green biomats accumulate the fine particles of amorphous silica from acid hot spring water, that the spherical algae influence the shape and structure of amorphous silica and that amorphous silica can be changed to cristobalite by alteration.

A RECENT BIF SHOWING BACTERIAL RINGS

Tazaki K. *(Dept. of Earth Sciences, Kanazawa University, Japan, kazuet@kenroku.ipc.kanazawa-u.ac.jp)*

A recent BIF (banded iron formation) fumarolic microbial system growing in the sea around an active volcanic island in southern Kyushu, Japan has been investigated by electron microscopy. Occurrences throughout the continents of voluminous Archean-Proterozoic iron beds in the form of BIF demonstrate the important role of bacterial biomineralization in the early stages of the Earth's history.

Recent iron oxide deposits and iron-hydroxide suspensions from and in fumarolic sea water in an inlet at Satsuma-Iou Jima Island (sulphur island), Kagoshima, Japan, give an engrossing insight into the active formation of BIF. The surface seawater of the inlet is colored reddish brown by jets of smoky fumarolic emanations from the inlet floor.

Thin-sections of this BIF show coexisting periodic precipitation of Fe and Mn layers with bacteria in brown and black biomats. Fe and Mn bacterial biomineralization is forming periodic patterns with alternating Fe and Mn concentrations. The bacteria have territories within elemental layers resembling the periodic precipitation patterns of Liesegang rings.

FORMATION OF TERRACE-LIKE SEDIMENT ASSOCIATED WITH IRON-BACTERIA AT SATSUMA-IWO JIMA ISLAND

Shikaura H., Tawara K. and Tazaki K. *(Graduate School of Natural Science and Technology, Kanazawa University, Japan)*

Various colored microbial mats have been found at Satsuma-Iwo Jima Island (SIJ). The color of seawater in and around SIJ is full of variety; white, reddish brown and transparent blue. SIJ is a small volcanic island located in the northernmost of Tokara Islands, southwest Japan. SIJ still continues to gush high-temperature volcanic gas. Mixture of this acidic gas and groundwater creates the acidic and mineral-rich hot springs along the coast of the island. Furthermore, mixture of seawater and acidic and mineral-rich hot springs causes tonal changes of seawater ranging from white to red, depending on the mineral composition of the various hot springs. This is the base of various colored microbialmats. Nagahama-Port is one of these typical cases. The port is colored allover in reddish brown. A characteristic of Nagahama Hot Springs is intense concentration of Fe^{2+} (151 ppm) and free CO_2 gas, which upon reaction with the seawater, produces ferric colloid. At Nagahama Port there are sandy beaches and breakwaters. Inside the breakwater, typical reddish brown terrace-like sediment is formed. The build-up of sediment is very fast and reaches over 2 meters in just 3 years. The XRD analysis of the reddish brown terrace-like sediments identified amorphous materials with broad 2.5Å reflection suggesting the presence of ferrihydrite. TEM observations of oil slicks floating around the terrace-like sediments revealed numerous colonizing microorganisms, the cells of which are covered with granular or needle-shaped Fe-minerals. This oil slick is a colony of bacteria which derives energy by the oxidation of Fe^{2+} to Fe^{3+}. It seems to be abundant Fe^{2+} and iron bacteria in addition to grains of sand and the existence of breakwaters shutting out the horizontal flow of water, that have promoted the formation of this rapid sedimentation.

TEM OBSERVATION OF ANCIENT AND PRESENT BIOMINERALIZATION TO FORM BIOLOGICALLY INDUCED IRON ORE : GUNMA IRON MINE, CENTRAL JAPAN

Akai J., Ito M. *(Dept. of Geology. Niigata University, Japan, akai@sc.niigata-u.ac.jp)*, Akai K. *(Kamo-gyosei High School)*, Nakano S. *(Shiga Univ.)*, Maki Y. *(Iwate Univ.)*, Sasagawa I. and Kuwa S. *(Nippon Dent. Univ)*

Sedimentary iron ore of recent to very young geologic age at Gunma Iron mine, Japan was examined from the viewpoint that the present processes may be a key to past ore formation. Some characteristic ore specimen types were distinguished: thin and thick banded iron ore type, aggregate of moss fossil types , *etc*. The ore-composing minerals are goethite of fine particle size, well crystallized jarosite and small crystalline strengite. These minerals and ore textures were examined by SEM, EPMA, TEM and HRTEM. Thick banded ore type was clarified to algal fossil aggregate. Thin banded iron ore was composed of spherical ball-like aggregates. Fe distribution strongly correlated to textures of organism and is positively related to As and V distribution. S and K are reversely correlated to this. Concentric ring textures of algal vertical sections were observed by TEM. In HRTEM, goethite crystals were often of nanometer dimension.

In the present mineral spring water stream, varieties of biomineralization were found: amorphous Fe-phosphate precipitates by bacteria and diatoms, and Fe hydroxides by coccoid and bacillus-shaped bacteria. Mosses and green algae are also collecting Fe hydroxide in and around the living cells. TEM observation of ultra-thin sectioned specimen of living moss confirmed that cell wall itself is directly mineralized by iron. Chemical compositions, and T, pH, DO, ORP and EC data were obtained: Fe rich (- 20ppm) and SO_4 rich , and pH 2-3, *etc*. In the experiments of bacterial biomineralization using the natural water, coccus type bacteria with Fe hydroxides were the most predominant. Bacteria, moss and algae might have played an important role in formation of this iron ore. Based on these observations, Gunma Iron Ore can be characterized as an example of Biologically Induced Iron Ore.

10. Gems Involving Organic and Amorphous Materials and Biomineralogy

A NEW BIOMINERAL, POTASSIUM MAGNESIUM HYDROGEN CARBONATE HYDRATE [$KHCO_3 \cdot MgCO_3 \cdot 4H_2O$], FROM SECRETION EXCLUDED BY *Populus diversifolia* AROUND THE DESERT AREA, XINJIANG, NW CHINA

Yabuki S., Okada A. *(The Inst. of Phys. and Chem. Res. (RIKEN), syabuki@postman.riken.go.jp)*, Chang Q. *(Dept. of Environmental Science, Kumamoto Univ.)* and Kagi H. *(Fac. of Science, the Univ. of Tokyo)*

Potassium magnesium hydrogen carbonate hydrate [$KHCO_3 \cdot MgCO_3 \cdot 4H_2O$] was found as one of the major components of the poplar salt, an evaporitic salt material produced at the mechanically damaged part of the trunk of halo-tolerant plant, *Populus diversifolia* at Kuitun area, Xinjiang, northwestern China. It occurs as small colorless and transparent crystals, platy and columnar in shape and ranging from a few microns up to 100μm in size, coexisting with sylvite [KCl], lansfordite [$MgCO_3 \cdot 5H_2O$], dypingite [$4MgCO_3 \cdot Mg(OH)_2 \cdot 5H_2O$], calcite [$CaCO_3$], monohydro-calcite [$CaCO_3 \cdot H_2O$], natrite [$Na_2CO_3$], thermonatrite [$Na_2CO_3 \cdot H_2O$], nahcolite [$NaHCO_3$] and gaylussite [$Na_2CO_3 \cdot CaCO_3 \cdot 5H_2O$].

This is the first occurrence of $KHCO_3 \cdot MgCO_3 \cdot 4H_2O$ in natural environment, and we named this biomineral as kuitunite after Kuitun City, where the poplar salt was collected.

Crystallographic parameters, chemical composition, physical and optical properties were determined and the results were consistent with those of synthetic ones. Infrared absorption spectra of kuitunite are very similar to that of trona [$NaHCO_3 \cdot Na_2CO_3 \cdot 2H_2O$]. Thermal analysis showed a strong endothermic peak at 95°C corresponding to the amorphization.

There are three possibilities about the origin of carbonate and hydrogen carbonate ions of kuitunite: 1. Populus diversifolia takes carbonate and hydrogen carbonate ions from groundwater and secretes them from its salt glands. 2. Some organic compounds such as oxalates decompose to carbonate or hydrogen carbonates. 3. When secreted sap is exposed to the air, organic acid is decomposed and the excess alkaline and alkaline earth elements absorb carbon dioxide from the atmosphere. Our experimental results support the third possibility as the most likely origin, but the second one cannot be totally excluded.

A CONTRIBUTION TO THE IDENTIFICATION OF THE ROMAN ARCHAEOLOGICAL EMERALD ORIGIN.

Aurisicchio C. *(C.S. Equilibri Sperimentali Minerali e Rocce CNR.)*, Graziani G. *(Dept. of Earth Sciences, University of Rome "La Sapienza")* and Nunziante S. *(C.S. Per la Termodinamica Chimica alle alte Temperature CNR)*

Emeralds, fascinating stones, pay the attention of scientists, gemologists and why not of the our ladies since the olden time. The recent findings in the Roman area of funeral stores (1st century AD), rich of gold goods decorated with precious stones (emeralds, saffires, and a diamond), suggested an investigation on the possibility to link each gem to its deposit. This work reports the results of an infrared spectroscopy study on emeralds collected from archaeological sites as well as from other deposits, not quoted in the literature, but perhaps utilized in the Roman age. The study of the physical characteristics, and of the inclusions have been omitted because usually they do not allow meaningful identification of gems origin. The IR spectra were collected at room and liquid Helium temperature in the range NIR FIR (10000 - 30 cm^{-1}), on powdered samples, where possible, and on the cut stones under IR microscope, using different set up of the interferometer. The obtained patterns show meaningful peculiarites which allow to classify the emeralds in a number of groups collecting samples having different place of origin. In order to share gems belonging to the same group EMPA and X-ray analyses were used and the results compared with infrared data. The reported results seem to be promising for our purpose even if other analytical tecniques like the new microanalysis LAM-ICP-MS could help to reach a better characterization of each deposit.

ANALYZING GEM MATERIALS FROM BIOMINERALIZATIONS AND AMORPHOUS COMPOUNDS USING MINERALOGICAL SPECTROMETRIC TECHNIQUES

Gambini E. and Superchi M. *(CISGEM of the Milan Chamber of Commerce, Superchi@mi.camcom.it)*

Gemmology deals with a composite group of materials ranging from diamonds, corundums, beryls (and several other mineral species and rocks) to materials from animal and vegetable kingdom, artificial products and "synthetic minerals".

Mineralogical methods and, among them, infrared spectrophotometry, energy dispersive spectrometry and, more recently, Raman spectrometry are useful not only to identify different gem materials but, as well, to prove the presence of a treatment. The use of non destructive methods is considered unconditional.

To open a discussion on the subject, some cases have been chosen:

A. a natural coloured red Corallium compared with a red stained Corallium

B. a white Madrepora (mainly calcitic Hexacorallia) compared with a white Corallium (aragonitic Octocorallia)

C. white cultured pearls coated with an artificial resin to improve their lustre

D. a comparison between Strombus pink pearls and cultured light pink freshwater pearls, both natural coloured

E. the qualitative and semiquantitative chemical composition of archaeological carved glasses from different localities as a proof of authenticity and as an orientation about the area of production

F. the control of hydroxiles amount present in an ancient glass window to detect the level of its corrosion and of its chemical composition to predict its durability.

These are just some fields of gemmological investigation that should be "cultivated" together with mineralogists.

CALCIC, SILICEOUS AND MANGANESE STROMATOLITIC STRUCTURES GROWING IN SOME HOT SPRINGS, JAPAN

Akai K. *(Kamo-gyosei High School, Japan)* and Akai J. *(Dept. Geology, Niigata University, Japan, akai@sc.niigata-u.ac.jp)*

Some small stromatolitic structures which are now growing in hot springs are also known although Precambrian stromatolites are famous. Using these recent samples, we can directly examine their fromation processes and intimate relations between microbes and mineral components at present conditions. We have investigated various types of stromatolite structures found in hot spring environments, Japan. Growing calcic stromatolitic structures (Akakura hot spring, Niigata Prefecture), silicic stromatolitic structures (Onikoube hot spring, Miyagi Prefecture) and manganese stromatolitic structures (Yunokoya hot spring Gunma Prefecture) were examined. Geochemical characteristics of hot spring water, biological features of the microbial mats on the surfaces of stromatolitic structures and mineralogical characters of component minerals were examined by Light Microscope, XRD, SEM and TEM. Formation processes of these calcic and silicic stromatolite structure were intimately related to cyanobacteria: adhereing and cementation of precipitated mineral grains, and finally dissoluving filamentous structures of cyanobacteria. On the other hand, the black and brittle manganese stromatolitic structures are hemispherical, and are composed of amorphous manganese minerals. Cyanobacteria were not found in these conditions. Many bacteria of bacillus type that were coated with amorphous Mn minerals were found. It was suggested that the formation processes of these structures are closely related to the activities of these bacteria. This may become an example that the stromatolitic structure or similar structure is formed by bacterial actions. We have reported Precambrian Mn stromatolite (Akai *et al.*, 1997) and the structures found in this study is very similar to this Precambrian one although the size is small.

BIOREMEDIATION BY *Gallionella* AT MINING AREA POLLUTED BY HEAVY METALS

Aoki A. and Tazaki K. *(Graduate school of Natural Science and Technology, Kanazawa University, Japan)*

Jinzu River noted for Itai-Itai disease has been polluted by Cd from Kamioka Mine in Japan. Jabara Valley in the mine is polluted by heavy metals, due to spreading wastes and slag contained sphalerite, galena and chalcopyrite. Although inspections have been regularly carried out, continuing removal of heavy metals is required. Accordingly environmental studies on biomats are available for a bioremediation.

The stream bed of Jabara Valley is covered with red-brownish biomats occurring in colloidal states. The stream water was analyzed by ICP-AES, which showed the concentration of Pb, Cd, Fe, Zn and Cu was 23ppb, 3.1ppb, 10ppm, 0.12ppm and 25ppb respectively.

XRD analysis revealed that the biomats consisted mainly of amorphous materials. Significant peaks corresponding to lepidocrocite and goethite were also detected. XRF analysis showed the biomats contain Zn (6454ppm) and Cu (324ppm). Excretions of *Gallionella*, an iron bacterium, in twisted stalks were mostly recognized in the mats by optical microscope and SEM. EDX analysis of the excretions detected abundant Fe with traces of Si and Ca. An electron diffraction analysis of the excretions indicated the distinct rings of lepidocrocite.

This clarifies that *Gallionella* fixate Fe^{2+} as lepidocrocite (γ -FeOOH), excretions of which develop biomats. FeOOH is known to make polymer involving heavy metal ions such as Pb^{2+}, Cd^{2+}, Zn^{2+} and Cu^{2+}. Consequently, the result indicates that *Gallionella* can be applied to bioremediation.

FORMATIVE ENVIRONMENT AND MICRO-ECOSYSTEM OF MICROBIAL MATS IN HOT SPRINGS

Ohno M. and Tazaki K. *(Graduate School of Natural Science and Technology, Kanazawa University, Japan)*

Formative environmental conditions with micro-ecosystem of microbial mats (biomats) at Hirayu Hot Springs, Gifu Prefecture in Japan have been evaluated. White, brown and green biomats are formed in this hot springs area. White biomats can be seen on the walls of hot springs source pool, whereas brown and green belt-like biomats are distributed along the drainage ditch. The pH-Eh, pH-DO and pH-WT phase diagrams of the hot spring water have shown the tendency of environmental conditions of biomats respectively. White biomats occur in low pH, reducing, microaerobic and high temperature circumstances. Brown biomats form over a wide range environment. In contrast, the occurrence conditions of green biomats are restricted to high pH, oxidizing, aerobic and middle temperature circumstances. Sulfide ions were detected from white biomats, while not detected from both brown and green biomats. Microscopic observations (optical and fluorescence microscope, SEM and TEM) have revealed micromorphological characterizations of bacteria associated with biominerals in biomats. XRD analyses were also carried out for the identification of the biominerals. White biomat comprising sausage shaped bacteria contains abundant sulfur. Brown biomat with many bacilli and filamentous bacteria contains granular materials. Green biomat consists of filamentous bacteria with abundant calcite.

The results have revealed that the color of biomats reflects the environmental conditions and micro-ecosystem. Bacteria share the formative places according to biomineralization in hot springs.

COMPARISION OF MANGANESE CONTENTS OF FRESH WATER PEARLS BY A 'HOT CATHODE' CATHODOLUMINESCENCE MICROSCOPE

Banerjee A. *(Inst. of Geosciences, Mainz University,Germany)* and Habermann D. *(Inst. of Geology, Bochum University, Germany)*

Pearls are composed of concentric layers, which are built up of minute crystals of calcite and aragonite, cemented together with conchiolin. The calcite and aragonite crystals in freshwater pearls contain variable amounts of Mn^{2+}.

The distribution and amount of Mn^{2+} in thin sections of freshwater natural pearls from N. America and 'tissue graft' fresh water cultured pearls from China were investigated for the first time by using a 'hot cathode' cathodoluminescence (CL) microscope. The luminescence spectra were obtained by using an EG & G digital triple grating spectrograph with LN_2-cooled CCD camera attached to the CL. The digital spectra were processed using a non commercial software for **Q**uantitative **H**igh **R**esolution **S**pectral analysis of CL- Emission, QHRS-CL. CL provides a unique tool to identify the domains of Mn^{2+} activated calcite and aragonite in thin sections of pearls. Calcite activated by Mn^{2+} show a typical orange CL. As proved by QHRS-CL in combination with **P**roton **I**nduced **X**-ray **E**mission (PIXE) analysis, aragonite activated by low Mn^{2+} concentration (<10 ppm) shows blue and aragonite activated by high Mn^{2+} concentration (about 1109 ppm) shows green CL.

From the present investigation two main conclusions can be drawn: (1) Cultured pearls from China contain domains of calcite in the middle which are absent in natural pearls from N. America. (2) The concentration of Mn^{2+} in natural pearls from N. America is marked by regular fluctuations from the middle to the periphery, whereas in case of the cultured pearls from China the Mn^{2+} concentration decreases from the place of implantation of the tissue graft in the middle towards the periphery of the pearl.

AIR POLLUTION INFLUENCE ON THE CONCRETE CONSTRUCTION

Okuda H. and Tazaki K. *(Graduate School of Natural Science and Technology, Kanazawa University, Japan)*

Air pollution has been investigated in Ishikawa Prefecture, Japan, since 1971. Ishikawa Prefecture has NO_2 concentration of middle level air pollution compared with other prefectures. But, some time the measurement of NO_2 shows high values. In order to show elaborate situation of air pollution, NO_2 concentration in Kanazawa city, Ishikawa Prefecture, was measured during a two year period. The average of NO_2 concentration was 0.019 ppm in 1996 and 0.021 ppm in 1997. These values were under environmental standard (0.040-0.060 ppm). But, NO_2 concentration in the central area of the city tend to be high, because of heavy traffic.

NO_2 concentration is low after rain, because the precipitation contains the acidic components such as NO_x, SO_x, and CO_2. In fact, melting snow shows low pH (pH 4.8), and influences on the concrete construction. The concrete material was corroded by the acidic snow, and secondary calcite is formed with organics on the surface of concrete. The pH values changed to high pH (pH 6.7) after corrosion of concrete materials. The results suggest that acidic snow influences corrosion of concrete construction more than acid rain and air during winter at snowy areas.

10. Gems Involving Organic and Amorphous Materials and Biomineralogy

RESERVOIR SEDIMENTS AND EFFECTIVE USE IN THE DASHIDAIRA DAM

Yano S., Suzuki N., Matsumoto K., Ohno M., Wakabayashi H. and Tazaki K. *(Graduate School of Natural Science and Technology, Kanazawa University, Japan)*

Storage dams are generally useful for riparian work and irrigation. Reservoir sediments in storage dams cause many problems such as the decline of the capacity of dam functions and beach erosion. Rivers in Japan are generally rapid currents, especially, the Kurobe River, running through Toyama prefecture, which is very rapid and has fast reservoir sedimentation. Therefore, a hydroelectric power generation dam, the Dashidaira Dam, which has sand-flash gates in order to remove sediment, was constructed on the upper reaches of the Kurobe River. In 1991, it was 6 years since the completion of the dam, the first discharge of reservoir sediments resulted in the influence of dirty water with a bad smell. The following five times discharges had been improved.

Although, in the case of other dams, sediments can be used for reclamation after removal, the Dashidaira Dam with the function capable of discharging reservoir sediments affords a wide margin of more effective use of the sediments for the lower reaches of the river. It seems possible to utilize the sediments as manure or nutriment for fluvial organisms, provided that the sediments contain nitrogen, phosphorus, potassium, and so on. The purpose of this study is to identify clay minerals and organics involved in the sediments, and to detect chemical composition of the sediments. Additionally the characterizations of microbes living in and around the sediments, for consideration of effective use of the sediments.

BIOMATS FORMED IN THE COPPER MINE DRAINAGE

Watanabe H. and Tazaki K. *(Graduate School of Natural Science and Technology, Kanazawa University, Japan)*

Microbes form colonies called biomat, which concentrate various metal elements. Biomats attract attention from the point of view of formation processes of ore deposit and biominerals. The occurrences of brown or black biomats have been reported in the mining drainage, concentrated Fe and/or Mn. Generally, in copper mines, iron accumulated in brown biomats is widely recognized, whereas copper is hardly identified. On the contrary, blue-green biomats contain copper as a major element, found at Dohgamaru mine, Shimane Prefecture, Japan where copper mine was once developed. Occurrences, micromorphologies and chemical composition of the blue-green biomats are introduced in this paper.

Dohgamaru Mine, characterized as fissure-filling vein type deposit, had been once operated as a prominent copper mine in San-indistrict and closed in 1909. At present, though the entrance of mining galleries are filled with concrete wall, but drainage is still continually flowing out. Cobalt blue biomats are found along the rock surface of "waterfall". At the waste dump area, blue colored biomats occur on the rock surface flowing drainage. Green and blue-green colored biomats mainly consist of ribbon-shaped algae. Gravels, on the basin of the waterfall, are covered with green crust about 1mm in thick. Colloform texture and banded structure like stromatolites are recognized with optical and scanning electron microscope. Microbes are also observed in almost everywhere in this crust. Blue biomats are found the place where drainage seeps. The biomat assumes a vivid blue color, but the color tends to be dull in a few days after sampling, and turns green by drying. Optical and scanning electron microscopic observations show that tubular microbes covered with granules are predominant. EDX analysis showed that these biomats are composed of a high concentration of Al, Si, S and Cu with trace of Ca, K and Zn. XRD pattern shows that biomats contain illite, pyrophyllite, brochantite and cyanotrichite.

MICROSCOPIC OBSERVATIONS ON BACTERIAL BIOMINERALIZATION FROM K-FELDSPAR

Ueshima M. and Tazaki K. *(Department of Earth Sciences, Kanazawa Univ., Japan, ueshi@kenroku.ipc.kanazawa-u.ac.jp)*

Microorganisms are influential in environmental earth materials. Elemental circulation, environmental changes and the Earth evolution associated with microorganisms have been reported. Biomineralization of clay minerals and biodegradation of granite were identified by XRD, optical microscope and SEM-EDX. Illite-vermiculite inter-stratified layer was recognized around root of lichen grown on weathered granite.

Bioweathering experiments were also carried out using thin section of granite in river water under pH 6.6, Eh -26 mV, EC 0.426 mS/cm, DO 1.3 mg/l, WT 11.9°C conditions, with iron bacteria (*Toxothrix* and *Leptothrix*). Microbial mats were formed on the surface of the thin section after 10 days. Cavities and chaps with bacilli and filamentous bacteria were observed on the surface of feldspars and biotite. Si content was reduced at flake materials (Si:Al=3:2) with bacilli on the surface of K-feldspar. It was considered that bacteria dissolved silicate ions from K-feldspar. The results suggest that the weathering of granite were accelerated by microorganisms and lichen dissolving potassium and silicate ions from K-feldspar.

CRYSTAL MORPHOLOGY OF CALCIUM CARBONATE ASSOCIATED WITH MICROBES

Yasuda T. and Tazaki K. *(Graduate School of Natural Science and Tecnology, Kanazawa University, Japan)*

Microbial influences to the crystal morphology of calcium carbonate in two different conditions have been clarified in this study. Brown biomat is formed just under green biomat at Cyugu hot springs in Ishikawa Prefecture, Japan. The hot spring water indicates the pH 8.1, Eh 25mV, EC 4.5mS/cm, DO 9.4mg/l, and WT 42°C. XRD analyses of both biomats identified presence of calcite. SEM observation shows that green biomat has calcite with sharp edges. Brown biomat comprise spherical calcite. The existence of cyanobacteria was observed in the both biomats by optical microscope. TEM observations revealed the cell walls of cyanobacteria provide the sites of nucleation into crystallization of calcite.

In contrast, water chemistry with biomats at Hakusan Yanagidani-Valley is gradually different comparing the upper to the lower reaches, such as pH 6.2→8.2, Eh 80→210mV, EC 1.6→1.4mS/cm, DO 2→10mg/l, WT 21→18°C. SEM observation shows that cyanobacteria, green algae and *Gallionella* live on the surface of the sediment. XRD analyses identified the sediment is composed of calcite and aragonite. Crystal morphology of these minerals are various. The crystallinity of calcium carbonate tend to develop gradually as downward. Consequently, crystal morphology of calcium carbonate in these places is influenced by a diversity of microbes.

FLUID FLOW ALONG DEEP CRUSTAL SHEAR ZONES WITHIN METATURBIDITES OF AN ANCIENT ACCRETIONARY PRISM, DAMARA OROGEN, CENTRAL NAMIBIA

Dombrowski A. *(Mineral. Institute, Univ. of Würzburg)*, Hoernes S. *(Mineral.-Petrogr. Institute, Univ. of Bonn)* and Okrusch M. *(Mineral. Institute, Univ. of Würzburg)*

The Khomas Trough in central Namibia comprises metamorphosed deep-sea turbidites within an ancient accretionary prism setting at an active continental margin. Contemporaneous shearing and thrusting played an important role throughout the structural evolution providing excellent pathways for migrating fluids. Thus, within the northern Khomas Trough extensive scapolitization of metapelites and metapsammites occurred leading to the formation of two conspicuous marker horizons. The scapolite-bearing lithologies are characterised by the mineral assemblage scapolite + biotite + quartz + epidote ± plagioclase ± calcite ± Ca-amphibole ± titanite. Modal abundances of scapolite attain up to 50% of the total rock volume. Scapolites are of mizzonitic compositions with an EqAn content of 54-67%. Fluid salinities calculated from scapolite compositions revealed values of 0.16-0.43 X_{NaCl} in the coexisting fluid with an average of 0.22. Fluid inclusion studies revealed corresponding fluid salinities of 10-20 wt.% NaCl equivalent. While in the southern scapolite-bearing sequence the X_{NaCl} values are quite uniform, in the northern horizon differences of 0.18 X_{NaCl} are preserved within a single sample. Thus, fluid compositions must have changed at least within the northern scapolite-bearing sequence of the Khomas Trough and fluid/rock ratios must have been considerably low otherwise chlorine gradients would have been smoothed out. Stable isotope studies confirm fluid-rock interaction with saline pore fluids of the sediment pile from where they were expelled during progressive deformation. Fluid migration along prominent shear zones caused extensive scapolitization of predominantly pelitic sequences in the northern Khomas Trough.

DECIPHERING SIGNATURES OF FLUID INFILTRATION USING 3D THERMAL AND TEXTURAL MODELING

Dutrow B. *(Dept. Geology, LSU, dutrow@geol.lsu.edu)*, Foster, C.T., Jr. *(Dept. Geology, Univ. Iowa)* and Travis B. *(Geoanalysis, LANL)*

Mineralogical and textural features of metamorphic (mm) rocks often contain subtle signatures related to fluid infiltration. Spatial variations in mineral chemistry, mineral zoning patterns, intricate texture relationships and/or specific mineral assemblages may reflect the presence and composition of infiltrating fluids. However, these features are often difficult to interpret unambiguously.

We developed an approach linking sophisticated thermal models of intruding plutons with texture models in mm rocks in order to relate mm textures to pluton geometry and host rock permeability, features which control heat and fluid flow around the intrusion. Thermal and flow fields are calculated for a specific pluton geometry and permeability distribution using a 3D heat and mass transfer code. This calculation provides P, T, X, t data for specific locations in the aureole. In turn, these data are used as input for textural modeling calculations to simulate development of rock textures at these host rock locations. Texture models utilize a differential approach to calculate whole rock reactions and a kinetic model of mm reaction mechanisms. This approach produces a sequence of rock textures for any position in the metamorphosed region as the mm event progresses. Textures and minerals produced by a specific thermal model can then be compared to features observed in the field to evaluate the thermal/flow field responsible for their formation. For example, calculations with and without pore fluid convection, completed for conditions approximating metamorphism in Maine, USA, show that two distinct distributions of mineral textures develop depending on infiltration of fluids. These calculations suggest that rocks from NW Maine more closely resemble the convective case.

This approach allows refinement of thermal histories of mm events, interpretation of subtle lateral variations in mineral textures and P-T paths, and illustrates how reaction mechanisms that develop in regional contact metamorphism are influenced by the influx of fluids.

THE INFLUENCE OF RHEOLOGY ON REGIONAL METAMORPHIC FLUID FLOW

Connolly J.A.D. and Podladchikov Yu.Yu. *(Department of Earth Sciences, ETH-Zentrum, connolly@erdw.ethz.ch).*

Episodic fluid flow is an inescapable consequence of the deformable nature of crustal rocks; thus, even given the existence of a constant metamorphic fluid source, lower-to-mid crustal fluid flow must be accomplished by pulses of fluid-filled porosity (*i.e.* porosity waves) that are propagated by fluid pressure anomalies. The spatial and temporal distribution of porosity waves is critically dependent on rheology. To address this problem we have studied the character of wave propagated fluid flow for the entire range of rheologies realized in the lithosphere by numerical and analytical techniques. In the viscous limit, the stable mode of fluid flow consists of isolated waves that detach from the fluid source, but cannot propagate through regions without pre-existing hydraulic connectivity. Negative effective pressures are required for viscous wave propagation. For normal geothermal gradients, thermally activated creep stabilizes sill-like horizontal waves, a geometry that was thought to be unstable on the basis of constant viscosity models. Implications of this stabilization are that: the vertical length scale for wave-propagated flow is generally constrained by the activation energy for viscous deformation rather then the viscous compaction length; and lateral fluid flow may occur on greater length scales than anticipated from earlier estimates of compaction length scales in viscous regimes. In viscous rock, inverted geothermal gradients stabilize vertically elongated waves or vertical channels. Unlike viscous waves, elastic waves cannot detach from the fluid source and propagate as shocks accompanied by a fluid pressure surge. A critical fluid overpressure is necessary for nucleation of an elastic shock, but the shock may be propagated by positive effective pressures. Elastic waves can propagate through a matrix with no prior connectivity, thus in viscous regimes without hydraulic connectivity fluid flow must be accomplished by an elastic shock front. The propagation of the shock is limited by the rate of fluid supply by viscous compaction at depth. The time scale for viscous wave propagation increases exponentially toward the earth's surface so that a transition from viscous to elastic dominated wave propagation becomes inevitable. Below the transition fluid flow is accomplished by short wavelength, large amplitude waves; above the transition flow is by high velocity, low amplitude surges. The resulting transient flow patterns vary strongly in space and time. Plastic yielding is an effective mechanism for vertical channelization of crustal fluids.

CRYSTAL GROWTH AND ZONATION PATTERNS OF HYDROTHERMAL GARNETS

Jamtveit B. *(Department of Geology, University of Oslo, Norway)*

Hydrothermal garnets often show complex growth morphologies and extensive intracrystalline chemical zonation. Both features generally reflect growth in a system where the pore- or fracture-filling fluid is out of thermodynamic equilibrium with the surrounding rock matrix. This is commonly associated with fracture-controlled flow where the rate of fluid-rock mass transfer is limited by transversal diffusion and low mineral surface areas.

Hydrothermal garnets occasionally show morphological transitions from planar via cellular to hopper-like structures. Faceted cells develop when initially wavy perturbations on dodecahedral {110} surfaces become parallel to other low-index surfaces such as {211}. Facet instability may arise when the crystals reach a critical size through the coupling between transport and anisotropic growth kinetics. However, it may also occur without the presence of concentration gradients in the solution if a change in the environment causes a change in which surface orientation is the most stable. A changeover in surface morphology may occur like a first-order phase-transition. The transition from one morphology to another may arise by faceting of vicinal surfaces by 'surface reconstruction' and this may be a continuous transition. If this phase transition occurs after a crystal has reached a minimum size, the macroscopic response may be formation of new crystallites or a sawtooth pattern on the initially flat surface. Thus morphological instability may in some cases not be driven by concentration (or heat) gradients in the solute (constitutional supersaturation), but represent a facet instability that in many respects resembles spinodal decomposition of one homogeneous phase (surface structure) to a mixture of two or more phases (low index surfaces).

Complex intracrystalline zonation of hydrothermal minerals in fractures is driven by the external forcing imposed by the composition of the local pore fluid. The zonation patterns are in general non-periodic and in some cases show 'fractal-like' scaling over two decades. A simple crystal growth model has been constructed that examines the coupling between external forcings imposed by infiltrating fluids, modelled as fractional Browninan noise, and local crystal growth processes. Unless, the mineral solution composition is a non-unique function of the pore-fluid composition at the interface, the observed mineral zonation pattern closely resembles the external forcing.

11. Metamorphic Mineralogy: Fluid Flow Associated with Metamorphism

THE RODINGITE OF BELLECOMBE (VAL D'AOSTA, ITALY): A PETROGRAPHIC AND FLUID INCLUSION STUDY

Compagnoni R., Conte R., Facchinelli A., Orione P., Rossetti P. and Trossarelli C. *(Dip. di Scienze Mineralogiche e Petrologiche - Università di Torino-Via Valperga Caluso, 35-10125 Torino, Italy)*

The studied rodingite occurs as an alignment of boudins, ca. 1m long and 20 to 50 cm thick in an antigorite serpentinite of the Piemonte Zone, W Alps. Each boudin consists of a fine- and a coarse-grained portion. The fine-grained portion is foliated and crenulated, and consists of grossular (Gr), diopside (Di), chlorite (Chl) and minor vesuvianite (Ves). The coarse-grained portion consists of a network of polyphase mono- and/or poly-mineralic veins, including Gt, Di, Chl and Ves. Most veins formed after the development of the main regional foliation, but during or later than crenulation. In the veins, Gt is changing composition from Gros- to Andr-rich, and non-coeval Ves shows different composition. A fluid inclusion (**FI**) study was performed on coarse grained Ves crystals of different colour and composition. A great variety of two phases (L+V) **FI**, often with an unusual coloured-like, from brown to blackish, vapor phase, occurs. Microthermometric results for primary **FI** are in rather good agreement: T_{hom}=285.4°C ± 17 (n=51), T_{im}= -26.4°C ± 5, T_{fm}= -9.8°C ± 3, consistent with an aqueous fluid with 12.8 wt% NaCl equiv. and a density of 0.88 g cm^{-3}. A Ft-IR study gave absorption bands referable to H_2O, to CH-bonds of possible aromatic hydrocarbons, but no evidence of CO_2. A Mass Spectroscopy analysis on gases released upon decrepitation suggests the presence of H_2, CH_4, C_2H_6, C_3H_8, H_2O and molecules with A.M.U.>90. In conclusion, the **FI** study indicates that the Bellecombe rodingite formed during the Alpine greenschist facies metamorphic event and suffered at T ≥ 285°C, during the post-climactic retrograde history, an important influx of hydrocarbon-bearing aqueous fluids of still unknown origin. Fluids of similar compositions not yet described in other metamorphic minerals of the western Alpine belt, have been reported from rodingites of the Bowman Asbestos Mine, Canada (Schandl *et al.*, 1990).

HYDROTHERMAL ALTERATION IN COREHOLES ADJACENT TO THE GREAT SUMATRAN FAULT AT SILANGKITANG, NORTH SUMATRA, INDONESIA

Moore D. E., Hickman S., Lockner D. A. *(U. S. Geological Survey)* and Gunderson R. *(Unocal)*

The character of hydrothermal mineralization at Silangkitang varies systematically with measured temperatures and proximity to the Great Sumatran fault (GSF). The GSF is an active, NW-striking, right-lateral fault largely coincident with the Sumatran magmatic arc; it accommodates the arc-parallel component of oblique subduction at the Java trench. Numerous surface thermal features with hydrothermal mineralization occur locally along the fault. Unocal made available 13 core samples from three exploratory geothermal wells located along the GSF near Silangkitang in North Sumatra. Wells A and C were drilled nearly vertically ≈1 km west of the principal trace of the GSF, with well C located ≈1.2 km northwest of well A. The 4 examined core samples from well A come from 1645-1910 m depth at T = 270-290°C, and the single well C core sample is from 2115 m depth and T = 180-200°C. Well B was drilled at a dip of 60° eastwards from the site of well A to within ≈100 m of the main fault; the 8 core samples are from the deepest part of this well, at 1760-2030 m and T = 300-320°C. Boiling springs at Silangkitang yield nearly neutral, Cl brines whose source is the active geothermal system. The studied core samples are rhyolite ash-flow tuffs with phenocrysts of andesine, quartz, sanidine, biotite, and hornblende. The well B samples are extensively altered along open fractures and brecciated zones. Adularia is the principal hydrothermal mineral in well B, associated with chlorite, quartz, calcite, titanite, pyrite, albite, anhydrite, and rare epidote. In well C, the plagioclase phenocrysts are thoroughly albitized, and the minerals lining open veins include quartz, calcite, K-mica, and pyrite. Samples from well A have been least affected by hydrothermal fluids and consequently have the best preserved igneous feldspar compositions. The main alteration minerals in well A are calcite, hematite, K-mica, quartz, chlorite, and albite; vein adularia and pyrite are rare. The vein assemblages are consistent with well temperatures, and they have many similarities to hydrothermal assemblages at Ohaki-Broadlands, N.Z. and the Salton Sea, CA. The differences in feldspar mineralogy and degree of fracturing suggest that well A is the least permeable and well B the most permeable. The well B core samples are closest to the principal strand of the GSF, and their inferred high permeability may be maintained by repeated fracturing and brecciation within the fault zone.

THERMAL EVOLUTION AND FLUID INFILTRATION: DEVELOPMENT OF METASOMATIC MINERALOGY ADJACENT TO AN ALKALIC DIKE

Dutrow B., Henry D.J., *(Dept. Geology, LSU, dutrow@geol.lsu.edu)*, Gable C. and Travis B. *(EES-5, Geoanalysis, LANL)*

Fluid infiltration and concomitant mass transfer associated with contact metamorphism provides a mechanism to substantially alter host rock mineralogy. For example, in subsurface Louisiana, USA, a drill core records the presence of an apparent 11 m section of intrusive alkalic igneous rock that penetrates a sequence of thinly-bedded carbonate mudstones and organic-rich siliciclastic siltstones at 1.9 km depth. The original sedimentary mineral assemblage is: calcite + quartz + pyrite + organics ± dolomite ± anhydrite. The dike metamorphosed and metasomatized these sediments to form an asymmetric contact aureole that extends 4 m above and 3 m below the dike. New mineral assemblages are rich in alkali and alkaline earth elements as well as fluorine. Approaching the dike, isograds include: diopside, pectolite + apophyllite, fluorite, and F-bearing grossular garnet, with sodalite and analcime developing at the dike margin. The assemblage diopside-albite-K-feldspar, first developed within the diopside zone, persists up to the contact. F-apophyllite is also found up to the contact after initial formation. Anisotropic garnets display minor zoning with rims enriched in F. Fluorite is a late stage mineral, developing on pectolite clusters or in veins. Modal abundance, mineralogical textures and C and O isotopic signatures also vary as a function of protolith composition and thermal environment.

Numerical heat transport calculations suggest maximum temperatures in the aureole were ≈400°C adjacent to the dike ≈0.3 yrs after intrusion. At the outer limit of the aureole, temperature rises slowly to a maximum of 80°C at ≈15 yrs. after intrusion. Significant fluid flow accompanied dike emplacement, with a maximum time integrated fluid flux in the aureole of 169 m^3 H_2O/m^2 rock within siltstone laminae. These mineralogical features necessitate that metasomatic alteration was an important process accompanying metamorphism.

AN UNUSUAL ASSOCIATION CONTAINING OLDHAMITE, BAZHENOVITE, YE`ELIMITE, HANNEBACHITE AND OTHER MINERALS FROM RONNEBURG, THURINGIA, GERMANY

Witzke T. and Göske J. *(Dept. of Mineralogy, Univ. of Halle /S., Germany, goeske@geologie.uni-halle.de)*

The Ronneburg mining area is known as Europe´s most important uranium mining field. From 1951 to 1990 several mines and an open cast were active. The mining was permanently complicated by spontaneous self-ignition of silurian graptolithic shale rich in pyrite and organic matter. Due to the pyrometamorphic processes minerals like mullite, indialite, osumilite-(Mg), cristobalite and others were formed. Elevated gases like H_2S and SO_2 from an *in situ* burning shale migrated through overlying Silurian and Devonian limestone. As a result of the metasomatosis parts of the limestone were completely replaced by oldhamite (CaS) and anhydrite ($CaSO_4$). In Si- and Al-rich parts hydroxylellestadite ($Ca_{10}(SiO_4)_3(SO_4)_3(OH)_2$) and ye`elimite ($Ca_4Al_6O_{12}SO_4$) were formed. Alteration of oldhamite leads to the formation of several secondary minerals inclucing the calcium polysulfide thiosulfate hydroxide hydrate mineral bazhenovite ($Ca_8S_5(S_2O_3)(OH)_{12}.20H_2O$), hannebachite ($Ca(SO_3).½H_2O$), portlandite ($Ca(OH)_2$), ettringite ($Ca_6Al_2(SO_4)_3(OH)_{12}.26H_2O$), gypsum and others.

The association represents a disequilibrium as shown by the several sulfur valencies: S^{2-} (oldhamite), S_5^{2-} (polysulfide in bazhenovite), S^0 (native sulfur), S^{2-} and S^{6+} with the formally valence S^{2+} (thiosulfate in bazhenovite), S^{4+} (sulfite in hannebachite), and S^{6+} (sulfate in gypsum, anhydrite and ettringite).

INTERPRETATION OF PARAGENETIC RELATIONS AND CHEMICAL COMPOSITIONS OF CARBONATES FROM UHP TERRANE

Ogasawara Y., Nakajima Y. *(Institute of Earth Science, Waseda University, yoshi777@mn.waseda.ac.jp)* and Okamoto K. *(Department of Earth and Planetary Sciences, Tokyo Institute of Technology)*

Discovery of coesite inclusion in dolomite from Dabie Shan, has directly shown that host carbonate and calcsilicate rocks were subjected to UHP metamorphism together with eclogite blocks. Many attentions should be paid to carbonates from UHP terranes because carbonates may be a "container" of information which cannot be obtained from silicates. Carbonates, particularly from the Kokchetav Massif give interesting information to constrain P-T path and carbonate stability during UHP metamorphism because peak-P is expected as higher than other UHP terranes. The following things have been reported on the Kokchetav carbonates; (1) microdiamond in carbonate rocks, (2) very high-$MgCO_3$ calcite (25 mol% in $MgCO_3$), (3) calcite exsolution from dolomite; however, their stability relations are still unclear. On the basis of phase relations in the system $CaCO_3$-$MgCO_3$, this paper is to provide the interpretations of carbonates stability and their chemical compositions that have been reported so far and will be expected in the Kokchetav Massif in the future.

Important factors related with paragenetic relations of carbonates are: (1) aragonite+dolomite paragenesis, and (2) eutectoid point between them, in the system $CaCO_3$-$MgCO_3$, and $FeCO_3$ effect on aragonite+magnesite coexistence under UHP should be considered. Coexistence of aragonite with dolomite significantly shifts aragonite-calcite equilibrium curve to high-P side at high T. With increasing P, the eutectoid point moves to high-T and high-$MgCO_3$ side. At extremely high-P, the eutectoid point may reach the crest of calcite-dolomite solvus.

The following subjects should be examined for UHP carbonates, particularly those from the Kokchetav Massif: (1) compositional variation of calcite and heterogeneity of Mg-calcite in a single grain: to search almost pure $CaCO_3$ portion as well as higher $MgCO_3$ portion, (2) composition and paragenetic relations of carbonate inclusions in garnet, (3) calcite (aragonite)-magnesite paragenesis and $FeCO_3$ effect on this paragenesis at UHP conditions, (4) paragenetic relations of diamond with carbonates and silicates.

INFLUENCE OF THE BULK ROCK CHEMISTRY AND METAMORPHIC CONDITIONS ON THE MONAZITE GROWTH IN PELITIC METACHERTS (CENTRAL LIGURIA, ITALY)

Cabella R., Lucchetti G. and Marescotti P. *(Dept. of Earth Sciences, Univ. of Genova, lucchett@dister.unige.it)*

The mineralogy and chemistry of the first occurrence of monazite developed under pumpellyite-actinolite facies conditions are compared with other known monazite from different genetic environments.

Monazite was recently found in the siliceous metasediments overlying the ophiolitic basalts of the Jurassic Piedmont-Ligurian basin (Mt. Figogna Unit, Sestri-Voltaggio Zone), equilibrated under pumpellyite-actinolite facies conditions ($P \cong 3$-4 kbar and $300°C \leq T \leq 350°C$) during alpine tectono-metamorphic events.

These sediments consist of rhythmic repetitions of millimetric to centimetric beds of reddish siliceous cherts (hematite-bearing) and greenish siliceous mudstones (phengite- and chlorite-rich).

Monazite occurs, commonly associated with quartz, rutile, xenotime and albite, as euhedral prismatic elongated crystals (generally up to 150 μm in length) in phengite+chlorite-rich beds, in millimetric quartz veins and in open fissures.

Quantitative chemical analyses were carried out with an ARL-SEMQ electron microprobe in a wavelength dispersive mode using an accelerating voltage of 20 kV (sample current of 20 nA) with a beam spot size of about 4μm; natural and synthetic compounds were used to standardize, verify and eliminate the interferences taking into account the peak overlaps.

All the analyzed samples are monazite-(Ce) with other LREE in variable amounts and HREE generally below the detection limits.

The LREE patterns, normalized to the NASC (North American Shales Composite), show flat distribution with strong analogies with those occurring in metapelites from greenschist to anfibolite facies conditions.

Mineralogical and chemical features suggest that monazite formed as a result of the sedimentary phyllosilicate breakdown during the metamorphic re-equilibration and as a consequence of mobilization processes that concentrated the LREE originally dispersed in the siliceous mudstones.

12. Metal Adsorption on Clays

ATOMISTIC MODELS OF CESIUM AND SODIUM SORPTION ON ILLITE CLAYS

Cygan R.T. *(Geochemistry Dept., Sandia National Laboratories, rtcygan@sandia.gov)* and Kirkpatrick R.J. *(Dept. of Geology, Univ. of Illinois, kirkpat@uiuc.edu)*

An atomistic understanding of mineral-water interactions is important for the evaluation and prediction of sorption properties for clays and other minerals that may be used in the remediation of hazardous wastes. Molecular simulations are proving useful in this effort. Such simulations for metal sorption onto clays typically incorporate empirical forcefields, based on molecular orbital calculations and spectroscopic data, that account for Coulombic, van der Waals attractive, and short-range repulsive energies. We have used several different forcefields to examine molecular cluster and periodic assembly representations of the illite structure (based on a paragonite surrogate) and the energetics of cesium and sodium sorption. In addition to energy minimization and molecular dynamics (MD) simulations, energy sorption maps of the illite surface are used to identify and evaluate the crystallographic control of the low energy sites for metal sorption.

Energy minimization calculations indicate the sorption sites for the free cesium and sodium ions are determined primarily by electrostatic interactions with the clay substrate. Surface protonation state and local tetrahedral aluminum substitution influence the binding energy and optimum sites for the metal sorbate. MD calculations, accounting for molecular water and solvent effects, suggest the existence of inner sphere cesium complexes for all illite surfaces while the sodium ion occurs as both inner and outer sphere complexes depending on the surface. The modeling results are consistent with recent spectroscopic observations using dynamical MAS NMR spectroscopy.

Research was supported by the U.S. Nuclear Regulatory Commission and the U.S. Department of Energy, Office of Basic Energy Sciences, Geosciences Research, under contract DE-AC04-94AL85000 to Sandia National Laboratories.

IRON RICH SAPONITE: Cr UPTAKE AND DISSOLUTION REACTIONS

Brigatti M.F., Lugli C., Poppi M. *(Dept. of Earth Sciences, Univ. of Modena, Italy, brigatti@unimo.it)* and Venturelli G. *(Dept. of Earth Sciences, Univ. of Parma, Italy)*

To gain a deeper understanding of the geochemical processes involved in the interactions between ionic solutions and clay minerals in natural system, the ability of an iron-rich saponite ($^{[12]}(Ca_{0.34}Na_{0.12}K_{0.01})^{[6]}(Fe^{3+}_{1.58}Mg_{4.15}Mn_{0.04}Ti_{0.03})^{[4]}(Si_{5.95}Al^{3+}_{1.34}Fe^{3+}_{0.71})O_{20}(OH)_4$) to adsorb Cr was studied at constant temperature (25°C) with varying metal concentration (3.22, 5.50, 8.50 meq/L) and accompanying anion (NO_3^-, Cl^-, CH_3COO^-). Results show that the amount of Cr adsorbed increases in line with its concentration in the solution. Adsorption produces preferential release of Ca .

For each concentration used, the amount of Cr sorbed is significantly affected by the accompanying anion in the order : $NO_3^- \cong Cl^- >> CH_3COO^-$. A kinetic study of the adsorption during the first thirty minutes, when the most Cr is sorbed, display that at some concentration of the component added, K increases in the following order: $K_{CH3COO-} < K_{Cl-} < K_{NO3-}$.

The dissolution rates of natural and Cr-treated saponite were studied as a function of pH and time at 25°C. The saponite dissolution rates were determined on the basis of the release of Si. In both natural and exchanged-saponite a linear dependence of K from pH in both acidic and basic solutions was observed: in acidic solution the K correlate negatively with pH, whereas the opposite occurs in basic solution. The iron-rich saponite dissolves via destruction of the tetrahedral and octahedral layers, as indicated by the loss of Si and Mg.

NMR CHEMICAL SHIFT AND T_1 RELAXATION RATE STUDIES OF SURFACE SORBED SPECIES

Kirkpatrick R.J., Kim Y.[1], Yu P. *(Depts. of Geology and Materials Science and Engineering, Univ. of Illinois, kirkpat@uiuc.edu; [1]Present address: Korea Environment Institute, Seoul, Korea)* and Cygan R.T. *(Geochemistry Dept., Sandia National Laboratories.rtcygan@sandia.gov)*

Nuclear magnetic resonance (NMR) methods provide otherwise unobtainable information about the structural environments and dynamical behavior of surface sorbed species via the chemical shift, line shape analysis and relaxation rate measurements. The value of the chemical shift provides direct structural information, and the number of peaks represents the number of observable, magnetically distinct structural environments that are not in rapid exchange. For Cs adsorbed on illite, for instance, multiple peaks, representing inner sphere and outer sphere complexes on both the tops and bottoms and sides of crystallites can be observed at relative humidities (R.H.) near 30%. At R.H.s approaching 100%, however, Cs on these sites are in rapid exchange at room temperature, and multiple sites and the exchange among them can only be understood via line-shape analysis of low-temperature data.

Because many surface species exchange with the bulk solution at frequencies greater than kHz at room temperature, often only one peak is observed for paste and slurry samples, and low temperature experiments cause the solution to freeze. In such cases, T_1 relaxation rate measurements can provide significant insight. For illite in pastes of CsCl solution, the Cs T_1 data can be modelled with simple 2-site exchange to give surface site density as a function of solid/solution ratio. The maximum values observed are essentially identical to those determined from the spectra at 30% R.H., and this observation is consistent with the dominance of inner sphere complexes. For situations where outer sphere complexes apparently dominate, the T_1 values change much less and cannot be modeled with 2-site exchange. This is the situation for Na on illite and silica gel and Cs on tobermorite and jennite. For situations where little or no sorption occurs, such as Cl on jennite and tobermorite, the T_1 values do not change significantly with solid/solution ratio.

ADSORPTION OF HEAVY METALS ON CLAY MINERALS

HE H., Guo J. and Xie X. *(Guangzhou Institute of Geochemistry, Chinese Academy of Sciences, Wushan, Guangzhou 510640, P.R. China.)*

Heavy metal contamination has been a serious problem and the interaction between heavy metals and minerals has been widely studied in the world. In this paper, interaction of heavy metals (Cu^{2+}, Pb^{2+}, Zn^{2+}, Cd^{2+} and Cr^{3+}) with clay minerals (Ca-monmorillonite, illite and kaolinite) are studied. Montmorillonite is treated for extracting FeOOH in the original sample.

Kaolinite is a very pure commercial product. Illite is untreated. The amount of clay mineral is no less than 100mg in each sample. A modified nitric acid extraction scheme is used in this study. The experiment is conducted in plasticware. Heavy metal concentrations of solutions before and after reaction are determined using Atomic Absorption Spectrophotometer.

Subtracting the amount of the heavy metal in the solution after absorption from the amount of the heavy metal added to the solution before absorption is that sorbed by the clay mineral.

The experimental results show that the absorption ability of the three minerals is: montmorillonite >> illite >> kaolinite. Also, it is revealed that, for montmorillonite, the affinity of the five heavy metals is: Cr^{3+} (3054.8 μg/g) >Pb^{2+} (2240.6μg/g) >Cu^{2+} (2197.6 μg/g) ≈ Cd^{2+} (2182.3 μg/g) >Zn^{2+}(1877.0 μg/g); for illite, Pb^{2+}(534.3 μg/g) >Cd^{2+}(373.9 μg/g) >Cr^{3+}(340.3 μg/g) ≈ Zn^{2+} (239.7 μg/g) >Cu^{2+}(196.4 μg/g); for kaolinite, Cr^{3+}(148.4 μg/g) > Pb^{2+} (88.2 μg/g) > Cd^{2+} (29.3 μg/g) ≈ Zn^{2+} (27.8 μg/g) ≈ Cu^{2+} (24.8 μg/g). The value in the parentheses is the absorption capacity for the mineral to the heavy metal ion. Cr^{3+} is most effectively sorbed by montmorilonite and kaolinite.

Pb^{2+} shows a strong affinity for illite. To demonstrate the absorption mechanism, samples sorbing heavy metals are being studied using MAS NMR and EPR.

12. Metal Adsorption on Clays

GEOCHEMISTRY OF THE ARGILLACEOUS SEDIMENTS INTERCALATED WITH THE PHOSPHATE DEPOSITS IN THE NILE VALLEY, EGYPT.

Attia A.K.M. *(Central Metallurgical R & D Institute, Cairo, Egypt, rucmrdi@rusys.eg.net)*, Hilmy M.E. *(Dept. of Geology, Ain Shams University)*, Boulis S.N. and Bayoumi H.M. *(CMRDI)*

The geochemistry of the shales and marls intercalated with the phosphate deposits in the Nile Valley area is used to throw some light on the source rock, environment regime of deposition, diagenesis and weathering modifications.

About 60 samples were analysed for the major elements SiO_2, Al_2O_3, Fe_2O_3, MnO, P_2O_5, TiO_2, CaO, MgO, Na_2O, K_2O, SO_3 and Cl, as well as the trace elements Sr, Ba, V, Ni, Co, Cr, Zn, Cu, Y, Zr, Mo and Cd.

The results obtained reveal that the shales have a provenance materials varying from basaltic and granitic to basaltic rocks while marls have a provenance materials varying from mixed granitic and basaltic to basaltic and granitic to basaltic rocks.

The trace elements in general may be of organic origin where the elements occur as metalo-organic compounds or of inorganic origin where the elements occur as accessory minerals or adsorbed cations.

The data obtained reveal the shales and marls are of detrital origin and that the environmental conditions of deposition were mainly alkaline. The data also reveal that the phosphorites and intercalated shales were mainly deposited under two different environmental conditions.

SORPTION STUDIES OF Cs, Sr, Ni AND Eu ON ILLITE

Poinssot C. *(Commissariat à l'Energie Atomique, DCC/ DESD/ SESD, poinssot@cea.fr)*, Baeyens B. and Bradbury M. *(Paul Scherrer Institut, Labor für Entsorgung, baeyens@psi.ch, bradbury@psi.ch)*

Radionuclides released from the near-field of a radioactive waste repository will undergo sorption reactions with the minerals in the host rock. For many of the rock types being considered, the sorption on clay minerals such as smectites, illites and kaolinites may be of particular importance. The aim of the work presented here was to investigate the sorption of Cs(I), Sr(II), Ni(II) and Eu(III) on an illite from a mechanistic view point.

A natural illite (illite du Puy) was initially purified and conditioned to the homo-ionic Na-form. The conditioned Na-illite was then characterised in terms of mineralogy, chemical inventories and surface properties. The mineralogical composition was analysed by means of XRD and IFTR and the structural formula determined from EDS analyses (SEM/TEM). The Na-CEC at neutral pH was evaluated to be 12.8 meq/100g. Titration measurements on illite suspensions were carried out at two ionic strengths using the batch back titration technique. The evolution of solution composition in equilibrium with Na-illite was investigated as function of pH, time, solid/liquid ratio and ionic strength.

The sorption data were measured in suspensions of Na-illite in $NaClO_4$ as background electrolyte under inert atmosphere controlled conditions (CO_2 and O_2 ~5 ppm) using the batch technique. For each radionuclide kinetic, sorption edge and isotherm data were determined and are given. In principle such measurements combined with titration and physico-chemical characterisation data can be interpreted in terms of "near-mechanistic" sorption models. This study will focus on just one of the radionuclides measured, namely Cs, and the interpretation of its sorption behaviour in terms of a 3 site cation exchange model. The site capacities and corresponding Cs-Na selectivity coefficients are given.

13. Crystal Morphology, Zoning and Growth

GROWTH HABIT CHANGE BETWEEN POLYHEDRAL SHAPES OF THE SAME CRYSTALLINE SUBSTANCE: A THEORETICAL STUDY

Kitamura M. *(Dept. of Geology and Mineralogy, Kyoto University, kitamura@mine.kueps.kyoto-u.ac.jp)* and Nishioka K. *(Dept. of Optical Science and Technology, University of Tokushima, nishioka@opt.tokushima-u.ac.jp)*

It is a common observation that many crystals of the same substance undergo a change in habit during their growth from one polyhedral shape to another, such as the change between a cube and an octahedron. Such habit change requires the relative growth rates of two distinct faces to become inverted. The effect of impurities has been stressed, based on both experimental studies and the fact that a crossover of growth rates between different faces due to supersaturation (σ) is not generally expected in the published theories of growth in pure systems.

Two processes can be distinguished for the incorporation of a growth unit from the surrounding media onto a kink site: a series process via terrace and/or step sites and a direct process. A concept of crystal growth where the incorporation of growth units by series processes can be faster than the direct incorporation under certain conditions reveals two new growth mechanisms; (1) under certain conditions where activation energies and the energy differences between growth sites are large, a series process via an intermediate site in an appropriate free energy state becomes the fastest among series processes and acts as a high speed path, and (2) surfaces without chemical bonds along them can be stabilized by "layer growth" controlled by a new mechanism like the nucleation-growth. Habit change between polyhedral shapes can be explained by the two growth mechanisms.

A formulation of σ where spiral growth of cubic faces and "layer growth" of octahedral faces of a simple cubic crystal from solution have the same rate shows that a change from cubic to octahedral shapes can occur when σ and/or activation energies increase or when temperature decreases. Impurity effects on habit change can be treated as an increase of activation energies. The formulation is equally applicable to other kinds of growth systems such as from vapor and melt.

CHRYSOTILE - TO - POLYGONAL SERPENTINES - TO - LIZARDITE REACTION PRODUCED FROM A MgO-SiO_2- H_2O (MSH) GEL

Grauby O. *(CRMC2, Marseille)*, Baronnet A. *(CRMC2, Marseille, baronnet@crmc2.univ-mrs.fr)* and Devouard B. *(Dept. Geology, Clermont-Ferrand)*

There is a need to better understand the meaning of serpentine microstructures such as conical scrolls, chrysotile rolls, polygonal serpentines, and lizardite. For that purpose hydrothermal syntheses of serpentine are conducted from an aluminum-free $3MgO$, $2SiO_2$-excess H_2O gel at T = 300°C, $P_{(H2O)}$ = 700 bar, solid/liquid mass ratio of 0.25. Quenched products for durations ranging from one hour to one year are characterized by XRD, IR, HRTEM and FEG-SEM.

Serpentine is the unique product of all runs. The systematic suite of serpentine microstructures is observed with increasing run duration: conical + cylindrical chrysotile → polygonal serpentines (with 15 and 30 sectors) → lizardite. Early transformation of the gel into "corn-flakes" of proto-serpentine precedes nucleation and growth of cones and tubes at the transformed gel-free solution interface. Some of these "corn flakes" close up either as cylindrical tubes, 6-7 unit-layers thick, or as cone-in-cone structures. Grain-size and shape factor analysis of the fibres show that both cones and tubes grow first along the fibre axis. Then they thicken rapidly once their radius exceeds some 100 nm. This sudden change of the radius growth rate of tubes is caused by the chrysotile-to-polygonal serpentine transformation. The latter takes place *via* a solid-state polygonization mechanism followed by overgrowth. Eventually lizardite platelets nucleate in longest runs while supersaturation is sufficiently decreased.

This isochemical, isobaric, isothermal chrysotile → polygonal serpentine → lizardite sequence illustrates ripening controlled by the decrease of the elastic energy stored in the microstructures rather than by decrease of surface energy. According to the Ostwald step rule, chrysotile and polygonal serpentine are metastable phases while lizardite is the only possible stable phase. The Al-free system used here indicates that Al (or Fe^{3+}), expected to reduce the misfit between the tetrahedral and the octahedral sheets, is not necessary to maintain serpentine flatness at equilibrium. The suite of microstructures reported here may be useful as markers of the maturation of serpentinites.

SURFACE MORPHOLOGY OF HYDROTHERMALLY GROWN SPESSARTINE ($Mn_3Al_2Si_3O_{12}$)

Woensdregt C.F. and Meeldijk J.D. *(Faculty of Earth Sciences, Utrecht University, Geodynamical Research Institute, P.O. Box 80.021, 3508 TA Utrecht, The Netherlands, woens@earth.ruu.nl)*

Spessartine ($Mn_3Al_2Si_3O_{12}$) shows {112} as the most important crystal form instead of {110}. According to the computed theoretical growth forms of garnets [1] the growth forms depend on the effective charge on oxygen, q_O. At lower effective charges of q_O, thus taking into account the covalent nature of the Si-O bond, {110} and sometimes minor {100} determine the garnet habit. Crystals grown from stoichiometric melts at temperatures just below the melting temperature (1170°C) show dominant {112} and subordinate {110}. Since these garnets have grown under oxidising conditions the typical spessartine {112} habit could be due to the presence of Mn^{3+} as an impurity in the melt. Spessartine has also been grown from hydrothermal solutions at temperatures ranging from 550°C (1.0 kbar) to 650°C (3.0 kbar) during runs of one hour, one day and 14 days. The starting material consist of a stoichiometric coprecipitated gel of $Al(NO_3)_3{\cdot}9H_2O$, $Mn(NO_3){\cdot}2H_2O$ and TEOS ($C_8H_{20}O_4Si$). Gold capsules have been filled with a fluid/solute ratio of 4. At the highest pressure and temperature (> 2.5 kbar and 650°C) spessartine crystals display {110} as the only form or otherwise in combination either with {100} or with both {100} and {112}. At intermediate temperatures and pressures (~2.5 kbar and 600°C) corroded {100} determines the habit, while {110}, {112} and {111} are present as minor flat faces. At pressures below 2 kbar {100} is the most important crystal form. Under these conditions the cube faces are not corroded, but slightly curved. Other forms present on these crystals, such as {110}, are completely flat. The surface topology at subnanometric scale has been investigated by AFM.

Reference

[1] M.M.R. Boutz and C.F. Woensdregt, *J. Crystal Growth*, **134** (1993), 325

AN ATTEMPT TO VISUALIZE THE CONCENTRATION/ TEMPERATURE FIELD AROUND SILICATE CRYSTALS GROWING AT HIGH TEMPERATURE

Abe T. *(Dept. of Earth Sciences, Faculty of Science, Yamaguchi Univ.)* and Tsukamoto K. *(Inst. Mineralogy, Petrology & Economic Geology, Faculty of Science, Tohoku Univ.)*

In order to understand the interaction between crystals and the high temperature solutions during crystal growth, an attempt has been made to visualize and measure the solute concentration and temperature fields around the growing or dissolving crystals.

The concentration and temperature fields are affected by (1) the growth kinetics of the crystal, and *vice versa*, and by (2) the fluid dynamics and statics (i.e., flow and density difference), which also cause the movement of the crystals. The growth rate of crystals would vary due to the fluctuating surface supersaturation caused not only by diffusion but also by surface kinetics. These subjects, however, had not been directly investigated by conventional *ex-situ* methods.

Such visualization has been realized successfully by high resolution laser interferometry for the crystal growth at room temperature, but not as yet for high-temperature crystal growth. However, we had the prospect of visualizing this crystal growth process by means of our sample holding method used in our previous *in-situ* observations. In this study we employed a Mach-Zehnder interferometer for the test on the crystal growth of forsterite in the system Fo-An-Silica at temperatures up to 1400°C.

This attempt at such high temperature has been successful and thus the concentration gradient can quantitatively be analyzed by processing the interference fringes. It was demonstrated first that the gradient of concentration becomes large with the increase of ΔTs and inverse in growth and dissolution. This method is now being applied to the subjects mentioned above. However, the fringes were distorted with the curved meniscus of the thin film of the solution, which impedes a more-detailed analysis of the concentration gradient. This problem is now being addressed.

13. Crystal Morphology, Zoning and Growth

GROWTH OF GIBBSITE ON GIBBSITE, KAOLINITE, AND MUSCOVITE

Nagy K.L. *(Dept. of Geological Sciences, Univ. of Colorado, nagyk@spot.colorado.edu)* and Cygan R.T. *(Geochemistry Dept., Sandia National Laboratories, rtcygan@sandia.gov)*

New data for gibbsite growth on powdered kaolinite and single crystal muscovite at 80°C in pH 3 solutions were combined with published data for gibbsite growth on gibbsite powders. All rates obey the same rate law provided reactive surface area is specifically considered. The rate law is $Rate_{ppt} = (1.57 \pm 0.18) \times 10^{-10}\ g^{(1.06 \pm 0.01)}$ where $g \equiv |\Delta G_r|/RT$, $\Delta G_r = RT[\ln(Q/K)]$ for the reaction $Al^{3+} + 3H_2O = Al(OH)_3 + 3H^+$, and rates are in units of mol/m²/sec. Rates on kaolinite were determined using steady-state measured changes between inlet and outlet solutions in single-pass stirred-flow experiments. Rates on muscovite were determined by measuring the volume of precipitated crystals in images obtained by Tapping Mode™ atomic force microscopy (TMAFM). Rates were normalized to total BET surface areas for powdered gibbsite, to 30% of the BET surface area for powdered kaolinite (percentage of edge surface), and to the basal surface area imaged by TMAFM for single crystal muscovite. Two-dimensional mechanisms for nucleation and growth are suggested by the following observed morphologies of gibbsite grown on muscovite: (1) epitaxial films with hexagonal edge outlines and thicknesses of 30-40 Å, (2) elongate crystals 30-40 Å thick aligned with the structure of the distorted Si-tetrahedral sheet of the $2M_1$ muscovite as determined by energy-minimization calculations, and (3) micron-scale three-dimensional clumps of intergrown platy crystals. Rates and crystal morphologies can be explained in terms of both geometric and chemical (permanent and pH-dependent surface charge) characteristics of the substrates.

Research was supported by the U.S. Department of Energy, Office of Basic Energy Sciences, Geosciences Research, under contract DE-AC04-94AL85000 to Sandia National Laboratories.

THE KINETICS AND MECHANISMS OF CALCITE GROWTH AT NEAR-EQUILIBRIUM CONDITIONS

Teng H.H. and Dove P.M. *(School of Earth and Atmospheric Sciences, Georgia Tech., Atlanta, GA 30332, dove@eas.gatech.edu)*

The abundance of calcium carbonate minerals in natural and engineered earth systems have motivated extensive investigations of calcite crystallization. Most studies infer average rates and mechanisms of calcite growth using indirect methods that monitor changes in bulk solution chemistry or conduct mesoscale *ex situ* examinations of growth hillocks, the products of step assembly. At microscopic scales, direct observations of calcite growth to date have yielded limited quantitative information. Using *in situ* Fluid Cell Atomic Force Microscopy (AFM), we characterized microscopic mechanisms and quantified relationships between solution supersaturation, σ, and step migration rates, v_s. Seeded calcite was grown in a series of Ca-Na-CO_2-Cl-deionized H_2O solutions with supersaturations ranging from σ=0 to 0.65. The mechanism for step nucleation on the $\{10\bar{1}4\}$ faces was sensitive to saturation state with a transition from heterogeneous surface nucleation (spiral growth) to homogeneous surface nucleation at approximately σ=0.4. The rates of step migration and the slopes of growth hillocks were measured to quantify the relationship between crystallography and direction-specific step migration rates. When σ>0.2, v_s was faster along positive directions, $[\bar{4}41]_+$ and $[48\bar{1}]_+$, compared to the negative directions, $[\bar{4}41]_-$ and $[48\bar{1}]_-$. This behavior yielded direction-specific values of the kinetic coefficient (dependence of v_s on σ). At approximately σ=0.2, $v_{s\pm}$ of the two directions became equal and a pseudo-isotropic hillock was formed. Novel observations of an inversion in hillock geometry were made when σ<0.2 as the positive directions assumed slower migration rates. This occurs because the v_{s+} *vs* σ dependence indicates that $v_{s+} = 0$ at σ^* (modified K'_{sp}) and step migration rates along the positive directions acquire a curvilinear dependence upon low values of σ, such that $v_{s+} < v_{s-}$. We propose this behavior is caused by preferential incorporation of an impurity into the positive crystallographic directions. Observations at $\sigma \approx 0$ support our premise by showing that steps along the positive directions show evidence for the existence of pinning points with 'scalloped' edges and imperceptible rates of migration, whereas negative directions maintain straight step edges and measurable rates of movement. Although the identity of the impurity is not known, our observations demonstrate the site-specific nature of impurities in modifying the kinetics of calcite growth and their ability to impact the resultant morphology. Understanding how inorganic and bioorganic solutes modify crystal growth kinetics, gives a fundamental basis for the physical processes governing carbonate mineralization in biogeochemical systems.

CRYSTAL GROWTH OF BARITE: AN *IN-SITU* AFM STUDY

Bosbach D., Pina C.M., Becker U., Risthaus P. and Putnis A. *(Institut für Mineralogie, Universitõt Münster, bosbach@uni-muenster.de)*

Atomic scale observations of crystallization processes are required in order to determine the dominant growth mechanisms. Microtopographic data of barite {001} and {210} surfaces, which are the most common crystal faces have been obtained using Atomic Force Microscopy (AFM) in aqueous solution. On the {001} surface two-dimensional nuclei form with a sector-shaped morphology controlled by monolayer steps parallel to [120], $[1\bar{2}0]$ and a curved step edge in one $BaSO_4$ layer of the barite structure. Since one unit cell consists of two $BaSO_4$ layers crystallographically related by a 2_1 screw diad axis parallel *c*, in the second $BaSO_4$ layer two-dimensional nuclei also have a sector shape morphology but pointing in opposite directions with step edges parallel to $[\bar{1}20]$, $[1\bar{2}0]$ and a curved step edge. The growth of these nuclei is anisotropic with fast growth normal to the curved step edge, whereas growth normal to <120> is extremely slow. Due to the anisotropy in alternating $BaSO_4$ layers, the lateral growth of growth spirals and consequently their further development is self-inhibited. On the {210} surface two-dimensional nuclei occur with a morphology controlled by monolayer steps parallel to <120> and <001>. The spreading of these islands is again highly anisotropic, with needles growing approximately 10 times faster along their length, $[1\bar{2}0]$, than in the opposite $[\bar{1}20]$ direction. Further, their growth in <001> is extremely slow. The high growth anisotropy prevents the development of growth spirals, which have never been observed in the vicinity of screw dislocations. The development of growth spirals on the {001} and {210} surfaces is self-inhibited due to an anisotropy in growth kinetics in alternating layers. Therefore, growth hillocks on the {210} surface cannot be related to growth spirals. The surface site-specific attachment of impurities and the incorporation of trace elements is also affected by the crystallization anisotropy. Sector zoning in barite can only occur via growth of {210} surfaces.

GROWTH MORPHOLOGY AND SECTORAL ZONING OF Cd, Mn, AND Zn DOPED CALCITE CRYSTALS

Temmam M. and Paquette J. *(Dept. of Earth & Planetary Sciences, McGill Univ., jeanne_p@geosci.lan.mcgill.ca)*

The morphology of calcite varies widely in natural inorganic and biological systems. The presence of dissolved divalent metals is known to affect significantly the kinetics of calcite growth but there is little data available on their effect on crystal morphology. This study documents the link between calcite morphology and differential incorporation of three metals, Cd, Mn and Zn, on non-equivalent faces (sector zoning).

The metals were introduced at three concentrations, from ~15 to 92 μM, into unseeded solutions of $CaCl_2$-$NaHCO_3$-NaCl-H_2O with an initial supersaturation index of ~5 with respect to calcite. Experiments were run at a temperature of 25°C, for 5 to 7 days during which pH, $[Ca]_{aq}$ and $[Me]_{aq}$ were monitored. The morphology of calcite single crystals (~40 μm) was examined by SEM. Metal concentrations in calcite were determined for specific growth sectors by EPMA.

The length of the induction period of calcite nucleation followed the trend Zn >> Mn > Cd. The strength of metal inhibition correlates well with the complexing affinities of metals with the "growth units" HCO_3^- and CO_3^{2-}. Calcite grown from metal-free solutions was bounded only by smooth faces of the {10.4} rhombohedron. The presence of Cd, Mn and Zn in solution promoted the appearance of the {10.0} prism, the steep {01.2} rhombohedron and the {0001} pinacoid, respectively. Higher $[Me]_{aq}$ induced an increase of surface roughness and surface area of the new forms at the expense of the rhombohedron {10.4}. In each case, the metals were preferentially incorporated in the new forms relative to the {10.4} rhombohedron. Henderson-Kracek distribution coefficients (D_{Me}) calculated for specific growth sectors (D_{Cd} at {10.0} ~ 70-50 and D_{Cd} at {10.4} = 14; D_{Mn} at {01.2} ~ 10 and D_{Mn} at {10.4} = 2; and D_{Zn} at {0001} ~50) differed substantially from Doerner-Hoskins coefficients derived only from the bulk variation of $[Me]_{aq}$ and $[Ca]_{aq}$ ($D_{Cd} = 30$; $D_{Mn} = 9$; $D_{Zn} = 28$). The increase in surface roughness and surface area of the new forms confirms that the inhibiting effect of these metals on calcite surfaces is site specific. The resulting decrease in growth rate of specific faces may enhance the preferential incorporation.

SECTORAL ZONING (SZ) OF REEs IN FLUORITE: INDICATION OF THE HETEROGENEOUS NATURE AND DISTRIBUTION OF SURFACE PROTOSITES

Rakovan J. *(Dept. of Geology, Miami University, OH)*

Fluorite crystals from several hydrothermal vein deposits show sharp zoning of REEs between coeval portions of symmetrically nonequivalent growth sectors (SZ). Spacially resolved synchrotron X-ray fluorescence microanalysis, conducted at the NSLS, BNL, shows a significant increase in the concentration of individual REEs in the (111) sectors relative to the (100) sectors. Two distinct mechanisms for SZ have been identified; differences in the growth rate of nonequivalent crystal faces, and the presence of distinctly different sites of incorporation (protosites), with different affinities for a given element, on the nonequivalent crystal faces. The internal morphology (concentric zoning and sector shape) of these samples revealed by cathodoluminescence indicates roughly equivalent growth rates on the (111) and (100) crystal faces. Hence, growth rate anisotropy is not the cause of SZ in these samples. REEs substitute for Ca in the fluorite structure. Models of the surface representation of the Ca site on the (111) and (100) faces show distinct topologic differences in both step and kink protosite configurations. Such differences may lead to different partitioning behavior on these two faces during growth, resulting in the differential distribution of REEs in the crystal. If different protosites do exist on a surface then they must be spacially segregated for differential incorporation to lead to zoning. Development of symmetrically nonequivalent crystal faces is one way to attain spacially segregated, structurally different protosites. Distinct protosite differences may also arise on an individual crystal face. These too may become segregated on that face if they occur along straight growth steps of nonequivalent orientation. If differential incorporation occurs between such sites a related phenomenon called intrasectoral zoning (IZ) is produced. Both the (111) and (100) faces of fluorite can grow in such a way that steps of different orientation do occur on a given face. However, the face symmetry of both of these forms precludes differences in protosite geometry between them. Hence, it is predicted that IZ is not possible under these two faces.

"HIDDEN"-PHASE CLUSTERS AND CRYSTAL GROWTH

Askhabov A.M. *(Institute of Geology, Komi SC, RAS; Xmin@geo.komi.ru)*

Groups of atoms and molecules less than a nucleus in size have been established to steadily exist in crystal-forming media (solutions, melts, vapour phase), these are noncrystalline nanoclusters of the "hidden" phase. The clusters are essentially different from crystal seeds dealt with in the classic theory of crystal nucleation. They grow in size alongside with increasing supersaturation in solution or melt's cooling and have a limiting dimension at which they crystallize and form a crystal lattice.

The effective size of "hidden"-phase clusters, adsorbed on crystal surface, increases by adopting the crystal's atoms. As a result, the cluster reaches its limiting dimension and crystallizes. This is the fundamental mechanism of crystal growth accounting for the basic regularities in growth centres' formation on the growing faces, their growth kinetics and morphology, defectiveness and impurities.

Geometrically, "hidden"-phase clusters are finite portions of Delone system and a limiting cluster is a locally regular Delone system. Clusters, exceeding the limiting dimension, display a crystalline structure and are described by Federov (space) groups. An elementary crystal, formed as a result of a limiting "hidden"-phase cluster's crystallization, is built from several to dozens of unit cells. Thus, in epsomite a limiting cluster forms a seed of 7 unit cells, in gypsum -15, calcite - 20, fluorite - 44, quartz - 65.

"Hidden"-phase clusters can form various aggregates and a peculiar cluster phase. Close-packed clusters and their aggregates form solid noncrystalline (amorphous) objects - clusterites. Thus, quartz is silicon dioxide crystals, noble opal -silicon dioxide clusterites. At the nanolevel, many minerals have a crystal-clusterite structure.

The work was supported by RFFI grant # 96-05-66087.

MORPHOLOGY OF SPINEL-TWINNED CRYSTALS OF NATURAL DIAMOND

Ahmadjan A. and Kitamura M. *(Dept. of Geology and Mineralogy, Kyoto Univ., ahmadjan@terra.kueps.kyoto-u.ac.jp)*

Existence of twin boundaries affects the growth forms of a crystal, depending upon the super-saturation conditions. External forms and zonal structures of spinel-twinned diamond crystals from South Africa and Siberia were studied.

Growth forms of the crystals can be divided into three types (A, B, and C), depending upon flatness and the shape at twin boundaries. Type A has the morphology almost similar to that consisting of two regular octahedra and three re-entrant corners. Type A can be explained to be formed under high supersaturation conditions where any sites on {111} surfaces have similar preferences for the incorporation of growth units and no re-entrant corner effect can be expected.

Type B is flattened and has a triangular form with three re-entrant corners. Type C is in a similar triangular form to type B, but has three convex corners or pyramids consisting of four high-index {hhk} faces, instead of re-entrant corners. Flattened morphologies of types B and C suggests the prefer-ential growth at twin boundaries, and can be expected to be formed under relatively lower supersaturation conditions than type A.

Difference between types B and C is resulted from that in the relative rates of the growth layer formation at twin boundaries and the lateral growth from the boundaries. Type B can be expected, when the lateral growth rate is much larger than the formation rate of the layer at the boundaries. In the opposite cases where the formation rate is much larger than the lateral growth rate, the re-entrant corners are filled with growth pyramids and result in a convex shape. The convex shape is naturally expected to consist of {111} faces, while type C has pyramids of high-index faces. Since the crystals have not suffered a severe dissolution process, type C is, therefore, interpreted to be formed in the transient growth stage to the morphology covered fully by convex corners consisting of {111} faces. Type C is probably formed under relatively lower supersaturation conditions than type B.

TEXTURES OF ALPINE SERPENTINITE VEINS CONTAINING ASBESTIFORM MINERALS AS SEEN BY TEM

Belluso E. *(DSMP, Universita' di Torino)*, Baronnet A. *(CRMC2, Marseille, baronnet@crmc2.univ-mrs.fr)* and Ferraris G. *(DSMP, Universita' di Torino)*

A large sampling of asbestiform minerals collected from veins of serpentinized rocks of Western Alps (Piedmont, Aosta Valley and Liguria regions) were examined by TEM. Systematic HRTEM/AEM observations of ion-thinned cross-sections have shown that:

i) [010] fibers of carlosturanite as an axial texture are ubiquitously intergrown with [100] chrysotile, [100] lizardite, and [100] 15-sector and 30-sector polygonal serpentine, and to a lesser extent [010] antigorite. Strict mutual coincidence is observed between these directions and the fiber axis. Antigorite nucleates on carlosturanite polysome defects (prograde alteration) while the other serpentine varieties form at carlosturanite fiber boundaries (retrograde alteration). When carlosturanite is absent serpentine fibers are often made of impressive hexagonal arrays of close-packed chrysotile rolls with constant outer diameter (20 nm),

ii) fibrous diopside is made of parallel fibers with much less preferred orientation thereby suggesting that geometrical selection originated the fibrous texture. Fibers are subdivided into fibrils with matching but rotated outlines. Fibrils themselves, having very few stacking faults, display negative crystals and enlargement of dislocation lines. The interfibril space may be filled by proto-serpentine, polygonal serpentine, and minor chlorite,

iii) fibrous tremolite has [001] close to the fibre axis, very few chain-width errors, and easy parting along {110}. Some small areas in the mosaic show a cataclastic texture.When the texture is open, the grains are idiomorph (regular rhombs). Frequently folded talc and chlorite are present as alteration products of amphibole.

This study shows that vein asbestos fibres i) are often complex mineral composites with topotactic relationships of the mineral species, ii) may have the tightness of the microtexture as the main factor for fiber dispersion in the environment, iii) mostly form by subtle interplay between brittle deformation, dissolution/ crystallization and solution-mediated solid-state transformations.

13. Crystal Morphology, Zoning and Growth

NATURE AND ORIGIN OF THE TWISTED QUARTZ CRYSTALS ("GWINDELS") AND OF QUARTZ WITH WHITE STRIPS ("FADENQUARZ")

Bonev I. K. *(Geological. Inst., Bulgarian Acad. Sci., Sofia, bonev@geology.acad.bg)*

The famous twisted quartz crystals, "Gwindels", known since the last century and exposed in many mineralogical museums, are still an unsolved crystallographic enigma. These bilateral tabular mosaic crystals are developed mainly in the *a* direction. Originating from the Alpine veins in the Swiss Alps and the Subpolar Ural, they always associate with normally shaped crystals. Their most twisted portions form a central zone || (0001) resembling an area of local non-destructive plastic deformation of the brittle quartz.

Morphologically similar are the specific non-distorted crystals with "white strips", "Fadenquarz", known also from the Alpine veins in the Alps, Caucasus and Arkansas. Their narrow milk-white central (0001) Faden-zone contains abundant fluid inclusions. The proposed explanations of their growth mechanism are geologically unrealistic.

In some hydrothermal skarn-ore deposits quartz druses of parallel doubly-terminated crystals were found. Narrow "white strips" trace their central zones. Microscopic, X-ray and microprobe studies established inside them fine relics of seed (0001) calcite plates disintegrated by dissolution. The *a* and *c* axes of both minerals are parallel, clearly indicating epitaxial relationships in the (0001) plane.

The Alpine Fadenquarz shows all features of the same mode of bilateral epitaxic growth on thin (0001) paperspar-calcite seeds, later completely dissolved, with rapid healing of the so-formed notches.

Paperspar can be easily plastically distorted and may act as a seed for twisted quartz, though usually no calcite relics or fluid inclusions are preserved in the dissolved and healed seed area. The numerous slightly divergent quartz nuclei forming the rough mosaic of the distorted central zone, gradually pass into the outer zones of more perfect and undistorted large straight crystals.

MICROSTRUCTURE OF FIBROUS MICAS FROM THE SHUNGA REGION, RUSSIA.

Devouard B. and Buseck P.R. *(Depts. of Geology and Chemistry, Arizona State University, devouard@opgc.univ-bpclermont.fr)*

Minerals of the mica group typically crystallize as stubby platelets fattened along the **c*** direction. A few exceptions are known, including a fibrous variety of dioctahedral mica referred in the literature as gümbelite. Samples from the Shunga region (Karelia, Russia) were found to contain two types of fibrous micas in veinlets, with fibers perpendicular to the vein walls, all within a carbonaceous matrix of "shungite" rock. The first type, which is silvery and asbestos-looking, was identified by X-ray diffraction (XRD) and electron-probe microanalysis (EPMA) as a dominantly dioctahedral mica with a rare $2M_2$ polytype, similar to the previous reports of gümbelite (Drits *et al.*, 1966, *Doklady Akad. Nauk SSSR*, **170**:156-159). Its chemical composition is close to that of phengite. The second type of mica consists of darker, coarser fibrous crystals that were identified by XRD and EPMA as phlogopite.

Sections perpendicular to the fiber axes were ion-milled and observed by transmission electron microscopy (TEM). Low magnification TEM images reveal interlocked textures of laths with their **c*** directions perpendicular to the fiber axes. Individual laths are commonly made of several slabs rotated around their shared **c*** directions, with seemingly random crystallographic orientations of the **a** and **b** axes. High-resolution TEM (HRTEM) images of the phengite shows the $2M_2$ polytype to contain abundant stacking faults. In addition, we observed defects and voids in the mica that we interpret as the possible locations for weakly bound water. A combination of HRTEM and XRD data indicates a mixture of 3T, 1M, and $1M_d$ polytypes for the phlogopite.

Since there is no pronounced preferential orientation of the **a** or **b** axes along the fiber axes, and fibers can occur for very different compositions and micas polytypes, we interpret the observed textures as indications that the fibrous habit is not controlled by the crystallography. Instead, we propose it is caused by the dynamics of the vein opening, which favored the growth of crystals with a fast growth rate perpendicular to the vein walls, *i.e.*, with the **c*** direction perpendicular to the fiber axes.

OSCILLATORY ZONING IN AGATE FROM MONGOLIA

Bryxina N.A. and Ripinen O.I. *(United Institute of Geology, Geophysics and Mineralogy, Siberian Branch of Russian Academy of Sciences, Novosibirsk, Russia, bryxina@uiggm.nsc.ru)*

Agates are tight aggregates of micro-crystalline SiO_2. Impurities in the SiO_2 matrix often make them brightly colored. According to the model proposed by Wang and Merino for crystallization in agates, this self-organization process is quantitatively modeled by a autonomous system of nonlinear differential equations of the first power. The complete qualitative analysis of this system is made in the field of multiplicity of steady states by calculating of the first three Lyapounov coefficients. Various types of behaviors of the system are described by behavior diagrams in terms of four parameters of model. The oscillatory solutions are found for actual parameter values and full list of possible phase portraits is shown. The phase portrait with three limit cycles near one steady state is found for concrete parameter values. Variation in thickness of bands of agate from Mongolia confirms used crystallization model.

COMPLEX ZONATION PATTERNS IN MONAZITE-(Nd) AND MONAZITE-(Ce)

Gieré R. *(Purdue University, IN, giere@purdue-edu)*, Williams C.T. *(Natural History Museum, London)*, Braun M. and Graeser S. *(Universität Basel, Switzerland)*

Two distinct assemblages of rare earth minerals, which include monazite-(Nd) and monazite-(Ce), have recently been discovered in the Monte Giove area in upper Val Formazza (Italy). The assemblages occur in metamorphic rocks, which probably represent a fossil placer horizon incorporated within metasedimentary units of the Penninic Lebendun nappe in the Central Alps.

The older mineral association consists of monazite-(Nd), gadolinite, xenotime, relictic allanite, adularia, quartz, ilmenite, rutile, and siderite. The younger assemblage, found in elongated cavities originating from dissolution of allanite, is characterized by monazite-(Ce), bastnaesite, thorite, adularia, calcite, and hematite. Petrographic investigations show that bastnaesite, calcite and monazite-(Ce) represent breakdown products of allanite, but also that bastnaesite itself exhibits a further stage of dissolution and alteration, with thorite being an apparent breakdown product of bastnaesite.

The two generations of monazite are distinguished by having different body colors, shapes and chemical compositions. The early monazite-(Nd) crystals are pink in color and exhibit a prismatic habit, whereas the yellow colored monazite-(Ce) crystals are tabular; morphological differences of this degree have also been observed for synthetic rare earth orthophosphates. BSE images and element distribution maps of these crystals reveal complex zonation patterns characterized by pronounced sector zoning with a superimposed concentric zonation. Quantitative electron microprobe analyses show that the (021) sector is significantly enriched in Ca, La, and Ce relative to the (011) sector; the inverse is observed for Nd, Sm and Si. Moreover, the concentric zoning in Nd correlates antipathetically with that of Ce, indicating that incorporation of Nd was different from that of Ce and the other REE, suggesting an unusual fractionation mechanism. The compositional variation can be described primarily by substitutions Ca+Th $\rightarrow$ 2REE and Th+Si $\rightarrow$ REE+P. These substitutions, however, are complicated by the antipathetic behavior of Nd and Ce.

13. Crystal Morphology, Zoning and Growth

SPHERICAL GRAPHITE FROM GOODERHAM, ONTARIO, CANADA

Jaszczak J.A. *(Physics Dept. and A.E. Seaman Mineral Museum, Michigan Technological Univ., jaszczak@mtu.edu)* and Robinson G.W. *(A.E. Seaman Mineral Museum)*

We investigate spherical and other unusual aggregates of graphite from an occurrence south of Gooderham, Ontario, Canada. The graphite spheres occur from 0.1 to 10 mm in diameter in coarsely crystalline calcite marble lenses in a highly sheared skarn zone between the Glamorgan gabbro and the adjacent graphitic Grenville marble.

Optical and scanning electron microscopy reveals a variety of surface and internal textures for the spheres, which typically show strong zonation in texture and crystallite grain size in cross section. Many spheres have what appear to be pressure shadows or "wings". Generally, these wings are defined by very finely dispersed graphite crystals or grains, and in some cases, other phases like iron oxide. Some wings seem to show a sense of rotation. Broken graphite spheres are not uncommon and make dramatic shear sense indicators. The broken spheres generally have fractured brittly into two equal halves, and can be separated from each other by several mm, sometimes leaving streak marks on adjacent silicate minerals.

Stable carbon isotope analysis for spherical graphite in three different calcite lenses shows $\Delta^{13}C_{cal\text{-}gr} = 4.3\pm0.6$ ‰ (PDB), while for flake graphite in a mica-rich layer adjacent to a calcite lens $\Delta^{13}C_{cal\text{-}gr} = 10.7$ ‰. Assuming a homogeneous isotope composition throughout the spheres, the calcite-graphite thermometer of Dunn and Valley (1992) suggests peak metamorphic temperatures in the different calcite lenses ranging from 595 to 690°C.

Other unusual aggregates of graphite that appear to be genetically related to the graphite spheres are also present. Preliminary Monte Carlo computer simulations suggest that these aggregates may be a result of relaxation of elastic energy of initially spherical graphite aggregates in the calcite matrix.

EVOLUTION OF A HYDROTHERMAL CAVE ON THE BASIS OF THE RADIOMETRIC DATING OF SPELEOTHEMS

Leél-Őssy Sz. *(Dept. of Physical Geology, Eötvös L. University, Budapest, losz@iris.geobio.elte.hu)*

Under the downtown of Budapest a hydrothermal karst territory of 5-6 square km is hidden. The most typical and in mineral precipitations richest cave of this system is the József Hill Cave. Evolution of the cave has been reconstructed on the basis of the uranium series dating of the mineral precipitations, collected there. Dating was carried out at the University of Bergen, in the laboratory of Dr. S.-E. LAURITZEN.

During the radiometric dating, greater part of the 52 samples, collected at 45 localities in the cave proved to be younger than the 350,000 years limit of the method.

It was proved that solution in the deeper parts and precipitation in the higher passages of the cave occurred contemporaneously.

On the basis of the radiometric data, evolution of the cave system as well as water level change in the cavity system could be dated by different theoretical considerations. According to this, higher passages were dissolved some 450,000 - 600,000 years ago, in the Günzian - Mindelian interglacial. The maximum water level may have spread at 15 m below the today's surface and it decreased in an accelerated rate.

220,000 - 230,000 years ago, water level spread at 70 m below the entrance. At this time, towards the end of the Mindelian glacial, a quick rise in water level commenced. 200,000 years ago, water had got to the surface in the form of springs, and for around 20,000 years it had built a travertine cone, developed in a lake. Afterwards, a quick and already final subsidence of water level started, and for around 150,000 years water has been only at 70 m below the entrance again.

110,000 years ago, precipitation of minerals began in the lowermost passages of the cave, as well. These passages became finally dry around 60,000 years ago. Afterwards, formation of aragonite crystals and botryoid, depending on the existence of thermal water - which spread at a deeper level below the cave and induced vertical air flows in the cave -, went on for 30,000 years. In the last 10,000 years, only the glass ball botryoid, dripstone and gypsum layers have been developed.

TEACHING CRYSTAL GROWTH OF MINERALS

Leonyuk N.I. *(Geological Faculty, Moscow State Univ., leon@geol.msu.ru)*

The crystal growth is taught in many Universities, and the course scope mostly depends on the profile of the department and/or college. The mineralogical aspect of this discipline is a base for understanding of crystallization processes in the nature. Here, the main attention is focused on both fundamentals and laboratory components of the new long-term course concerned with formation of natural and synthetic minerals as an example of a self-consistent curriculum containing lectures, seminars, laboratory practices and research work. This curriculum is combined the educational and research experience of the author in the field of growth and morphology of crystals at the Geological Faculty of Moscow State University (MSU) and his collaboration with other Universities and research institutions during the last three decades.

As a rule, current course topics are as follows. Spatial-temporal factors of "terrestrial" crystallization: characteristics of crystal growth processes in nature as seen from the laboratory. Simulating the natural conditions. Comparative studies of surface and internal morphology of natural and synthetic crystals: deductive analysis of growth and postgrowth histories. Associations of minerals. General characteristic of mineral crystallization: structural aspects of crystal growth in magmas; crystal growth in pegmatite; crystallization under hydrothermal conditions including metasomatic deposits; surficial/sedimentary crystallization; metamorphic crystallization in secondary rocks and during fossilization process. Comparative consideration of crystal growth of most important technological minerals in nature and laboratory: quartz, diamond, calcite, mica, corundum, zeolites, *etc.*

In conclusion, various interdisciplinary aspects of this course will be discussed.

RECRYSTALLIZATION AND THE LUMINESCENCE OF SYNTHETIC CALCITE

Mason R.A. and Miller L.J. *(Dept. of Earth Sciences, Memorial University of Newfoundland, rmason@sparky2.esd.mun.ca)*

Manganese-bearing and Mn,Mg-bearing calcite has been synthesized by rapid precipitation (10 to 30 minutes) and by slow precipitation (7 to 10 days) from solution at room temperature. The calcite was heated hydrothermally at 75 to 400°C and 500 bars. Differences in luminescence signal, grain size and crystallinity before and after heating were monitored as functions of time and temperature using, respectively, cathodoluminescence (CL) spectroscopy, scanning electron microscopy and powder X-ray diffraction (XRD).

Calcite precipitated rapidly forms rhombs or irregularly terminated crystals 0.3 to 4 μm across. Calcite precipitated slowly forms rhombs that are 50 μm to 2 mm across. The former has lower CL intensity (for a given Mn-concentration) and wider XRD reflections than the latter. On heating, the CL signal from rapidly precipitated calcite increases in intensity by up to 16 fold, XRD reflection width decreases by up to half and the crystals coarsen by as much as 15 to 20 fold. The magnitudes of these changes depend on time and temperature. Heating slowly precipitated calcite causes an increase in CL signal by up to 3 fold without significant change in XRD reflection width or grain size.

The magnitude of the change in XRD reflection width and the time scale over which it takes place on heating cannot be explained by the observed coarsening of grain size. It is postulated that the change in reflection width is caused by the coarsening of (sub-micron size) domains formed during crystal growth and that the annihilation of defects at domain boundaries (during their coarsening) is responsible for the increase in the CL signal.

13. Crystal Morphology, Zoning and Growth

THE CRYSTAL SIZE DISTRIBUTION AND GEOCHEMICAL CHARACTERISTICS OF BARITE FROM THE MOTOYAMA KUROKO DEPOSITS, AKITA PREFECTURE, JAPAN

Mizuta T., Miura T. and Ishiyama D. *(Dept. of Applied Earth Sciences, Akita University, Japan, mizutt@ipc.akita-u.ac.jp)*

The Motoyama orebody is the first-discovered Kuroko (Black ore) deposit which had been intensively studied as a model of Kuroko-type ore deposits. Barite is one of the main constituent minerals in massive black ores. It is also observed in black ore fragments in the Uwamuki tuff and in siliceous orebodies in the Motoyama volcanic breccia just below the Kuroko massive orebodies. Barite crystals are also found in marginal low-grade siliceous ores in the Baramori area and in the proximity of the "White Rhyolite" dome. The main purpose of this study is to clarify relationships between crystal size distribution of barite and formation environment of Kuroko deposits.

Quantitative crystal size measurement for area, major and minor axes, and perimeters were carried out. To avoid the preferential arrangement of barite crystals, specimens are cut along 3 diagonal directions. Size frequency distributions for barite crystals for 3 sections are quite similar with log-normal distribution. Those data show the barite crystals in the siliceous ores and black ores are randomly distributed within the specimens. From the analytical results of 38 barite-rich samples, crystals of barite in high-grade siliceous ores just beneath the Kuroko massive orebodies are much larger than those in samples of Kuroko massive ores and in samples of low-grade siliceous ores far apart from the Kuroko mineralization center.

The crystal sizes versus filling temperatures of fluid inclusions in barite and crystal sizes versus salinities both have positive relationships. These observed data reveal that the temperature decease of ascending hydrothermal fluids were not so large with small degree of seawater mixing within siliceous orebodies locating in the main conduit zone of Kuroko mineralization just below the Kuroko massive ores.

Barite in those ores could be precipitated very close to the barite-saturation curve and crystals should be grown slowly and become larger.

THE MULTISTAGE CRYSTALLIZATION PROCESS OF THE SCHELLERHAU GRANITES - A QUARTZ CL STUDY

Müller A., Behr H.-J. *(IGDL Göttingen)* and Seltmann R. *(Potsdam)*

The highly fractionated Variscan Schellerhau Granite Complex belongs to the tin granites of the Eastern Erzgebirge (Germany). It occupies in 1km depth ca. 100km², whereas at the present day surface ca. 15km² of its roof were eroded. It is characterized by the intrusion sequence of porphyritic (G1) to weakly porphyritic monzogranites (G2) and mostly seriate albite granite (G3). The types are interpreted as products of *in-situ* fractionation derived from a common deep-crustal parental magma. G1 and G2 contain two quartz generations of which SEM-CL contrasted growth textures could be correlated. A quantitative model of the crystallization of the Schellerhau granites using its quartz textures, quartz cathodoluminescence and trace element data of quartz has been constructed:

During the 1st crystallization stage the nucleation and undisturbed, red luminescent growth of the euhedral 1st quartz generation (pheno-crysts) took place. The "red" growth was interrupted by rounding (re-sorption) of these crystals. The growth continued (2nd crystallization stage) with blue luminescent quartz and was characterized by periods of undisturbed, self-organized growth (oscillatory zoning) which was periodically disturbed (stepped zoning, resorption surfaces). The euhedral 2nd generation (microphenocrysts) nucleated as a result of a single disturbance. After the G1 melt separation and its uprise the euhedral G2 quartzes continued to grow (volume increase 1st generation: 10-15%; 2nd generation: 100%, resp.). The G1 melt intruded subvolcanic levels and the 3rd generation (matrix quartz), free of growth textures, crystallized (final crystallization). The G2 melt intruded the G1 heated level, thus, the grains of the matrix quartz are less but larger. The idioblastic growth of G3 quartz phenocrysts from a fluid-rich residual melt cannibalized the euhedral quartz generations in the late stages. The melts of G1, G2 and likely G3 already contained 25-30% quartz and feldspar phenocrysts before they indruded the subvolcanic level.

THE SUPERGENE OCCURRENCE OF AN UNUSUAL TETRASILICIC MICA RELATED TO TAENIOLITE

Mordberg L.E. *(Natural History Museum, London & VSEGEI, St.Petersburg, leom@nhm.ac.uk)*, Welch M.D. *(NHM, London, mdw@nhm.ac.uk)* and Lyapitschev, I.G. *(VSEGEI, St. Petersburg)*

An unusual tetrasilicic mica occurs as rims around primary K-feldspar crystals in a Devonian bauxite profile in the Middle Timan, Russia. The average composition (wt%) is K_2O 11.49, MgO 19.68, Al_2O_3 0.97, FeO 0.48, SiO_2 59.49, F 0.05, total 92.16 (microprobe). The Li_2O content is only 0.22 ± 0.2wt% (by ICPMS). The XRD pattern is almost identical to those of natural taeniolite $KLiMg_2Si_4O_{10}F_2$ and the synthetic 2½-mica $KMg_{2.5}Si_4O_{10}(OH)_2$. Calculation to O = 11 gives $K_{1.02}Mg_{2.04}Fe_{0.03}Li_{0.09}Al_{0.08}Si_{4.13}O_{11}$, which does not conform to known mica stoichiometries. In particular, the total charge for octahedral cations is only 4.47 units, rather than the 5-6 units characteristic of micas. We considered the possibility of H replacing Li, with solid solution towards a fictive protonated endmember $KHMg_2Si_4O_{10}(OH)_2$. Calculation to O = 10.5 gives $K_{0.97}Mg_{1.94}Fe_{0.03}Li_{0.09}Al_{0.08}Si_{3.94}O_{10.5}$. Within the small analytical errors, this mica has the ideal composition of the protonated endmember.

The tetrasilicic mica occurs in the lowest and least altered zone of a 100m-thick weathering profile. This zone is composed of corroded feldspars cemented by hematite. Mica forms curved, platy crystals (20-150μm wide, 5 -15μm thick) rimming feldspar. The supergene origin of the mica is unequivocal. Weathering started with the dissolution of carbonates, then the Fe-bearing minerals (aegirine, chlorite, riebeckite, biotite and pyrite). Ca and Mg were removed and Fe formed hematite. The release of K and Si from feldspar began before the total decomposition of dolomite. The weathering solution, saturated in Mg, reacted with K and Si at the feldspar surface to form tetrasilicic mica. The sample characterisation, including micro-Raman spectroscopy, will be described and relations with other micas discussed.

TEM OBSERVATIONS OF THE DISORDERED DOMAIN IN MARCASITE FROM IKEZUKI, JAPAN AND POTOSI, BOLIVIA

Nagase T. and Akizuki M. *(Inst. of Mineral. Petrol. and Econ. Geol., Fac. of Sci., Tohoku Univ., nagase@mail.cc.tohoku.ac.jp)*

Marcasite is a common mineral in the specific low temperature hydrothermal deposits (~150°C). The stability relationship between marcasite and pyrite has been discussed by many previous investigators. Most previous works for formation process of marcasite were concentrated on synthetic experiments, and transmission electron microscopic (TEM) studies of textures within marcasite crystal are quite rare. Objectives of the this study are to described the fine textures of marcasite crystals and to reveal the formation process of marcasite. The analysis of fine texture within a marcasite crystal may provide important and detailed information concerning about the formation process of marcasite.

TEM study was performed on marcasite crystals from Ikezuki in Japan and Potosi, in Bolivia. It is found that marcasite crystals contain a platy-shaped domain associated with numerous (101) twin faults. The thickness of twin lamellae are a few nanometers. The sequence of the disordered stackings does not show a highly order polytype. Detailed analyses of high-resolution TEM image simulations indicate that the composition plane of the (101) twin has a characteristic of an intermediate structure between marcasite-like and pyrite-like twins.

The disordered domain is found at the center of a crystal, and well ordered marcasite overgrew on the disordered domain. A large difference is found in ordering state between the disordered and ordered domains, and the boundary between disordered and ordered domains is coherent and distinct. The difference in chemical composition was not detected between disordered and ordered domains using analytical electron microscopy.

In general, it is considered that randomly stacked structures are attributed to growth process by two-dimensional nuclei. On the contrary, ordered stackings occur when a crystal grows by the spiral-growth process. The internal texture of the marcasite crystals indicates changes in the growth mechanisms, as follows. The examined marcasite crystal initially grew by two-dimensional nuclei in a supersaturated solution. The growth mechanism may be changed from the growth by two-dimensional nuclei to spiral-growth with decreasing degree of supersaturation in solution by precipitation of crystals.

13. Crystal Morphology, Zoning and Growth

CHEMICAL ZONING IN ALKALI FELDSPARS AND ITS RELATIONSHIP TO EXSOLUTION MICROTEXTURES

Parsons I. and Lee M.R. *(Dept. of Geology and Geophysics, Univ. of Edinburgh, ian.parsons@ed.ac.uk)*

Chemical zoning in alkali feldspars from granitic rocks is generally regarded as uncommon because Na-K interdiffusion is so rapid. A form of zoning is often visible which is caused by variation in the coarseness of exsolution microtextures. Sometimes turbid and non-turbid zones alternate, and this can be seen in hand specimen. Complex zoning can also be seen using cathodoluminescence.

We investigated microtextural zoning in phenocrysts from the Shap granite, NW England, using SEM, TEM and EPMA. Featureless zones ≥ 10 μm width can be seen optically, alternating with zones of lamellar microperthite. TEM shows the former to be fully coherent cryptoperthite, of tweed orthoclase with lensoid platelets of albite from 50 to <5 nm thickness and ≤500 nm in length. Microperthites are tweed orthoclase with very flat lenticular lamellae of albite ≤500 nm in thickness and up to ~1 mm in length. Thicker lamellae are semicoherent, and encircled by dislocations. These facilitate deuteric alteration, which produces micropores, while the coherent lamellae remain pristine, and can lead to zoning in turbidity.

EPMA measurements using a rastered beam showed that the average bulk compositions of micro- and cryptoperthite zones differed slightly in An content (micro: 0.7±0.1 mol%, n=49, crypto: 1.0±0.3, n=78) and that the centres of cryptoperthite zones, where the platelets are smallest, were slightly more An-rich. No other systematic variations in composition (Or micro: 68.6±2.2, crypto: 71.8±2.3), including minor elements such as Ba, were observed. It is likely that diffusion rates at low T are very sensitive to subtle variations in An content, because of coupled Ca-Al and Na-Si diffusion, and that this is the main reason that the intergrowths vary in coarseness. The primary zoning in An formed during growth and could have been subject to unknown amounts of homogenisation prior to exsolution.

ZONE CRYSTALS AND DETERMINISTIC CHAOS

Rakin V.I., Kuznetsov S.K., Kodanev I.V. and Lutoev V.P. *(Institute of Geology, Komi Sci. Cent. Ural Div. RAS, rakin@geo.komi.ru)*

Colour zonality observed after γ-irradiation by the dose of 10^7 Ra was analysed in a face pyramid of a big rhombohedron of quartz crystals from the Prepolar Urals. The plates 3 mm thick were sawed out along the 3-fold symmetry axis. Zonality was recorded by a scanning densitometer with 20 μm resolution.

To study zonality we applied methods of the theory of dynamic systems (chaos theory). Optical density of a crystal was taken as a "substantial" parameter for the dynamic hydrothermal crystal-bearing system. Analysis of the fractal dimension of phasal portraits of crystal zonality in pseudophasal embedding spaces (from two- to twenty-dimensional) was carried out according to the method described by P. Grassberger and I.Proccacia (1984) and other investigators. It has been shown that:

- a hydrothermal crystal-bearing system can be described in the first approximation by a few independent parameters (up to 6), and zonality in a quartz rhombohedron pyramid is a determined chaos;

- there is a slight influence of random processes on crystal zonality and an overlapping microzonality, derived from surfacial processes.

The work was support by a grant from RFBR (No. 96-05-66087).

Reference

Grassberger P.and Proccacia I. 1984. Dimensions and entropies of strange attractors from a fluctuating dynamics approach. *Physica*, **13D**,34-54

GOLD MORPHOLOGY FROM Au-Ag ORES OF THE ZARMITAN AND MARZHANBULAK DEPOSITS (UZBEKISTAN)

Gazieva D.G., Possukhova T.V. *(Dept. of Geology, Moscow University, Russia, mineral@geol.msu.ru)*

The morphology of gold was studied by SEM method. It was established that morphology of gold in association with arsenopyrite, quartz, sulphosalts and secondary minerals is different.

In the Zarmitan ores *gold with quartz* has isometric form and smooth surface with rare growth steps. *Gold with arsenopyrite* from the Zarmitan ores has interstitial and wire-like forms and traces of dissolution and leaching on there surfaces. Gold is unhomogeneus, with growth embryos on their surface. It has microblock structure. Gold from the Zarmitan ores in association *with sulphosalts* has complicated form, friable cellular sculpture of surface and inclusions of other minerals.

In the Mardzhanbulak ores gold were investigated from primary and oxidized deposits. The gold *from primary ores* has a lumplucing form, aggregate structure and oolitic texture, which may formed by recrystallization of colloidal solution.

The gold in association *with secondary minerals* was characterized by interstitial forms. On its surface were seen a numerous cube-octahedron embrois of new genegation of gold and cavities and cracks whose origin was probably associated with the oxidation processes. Gold *from upper horizons of oxidizing zone* may be characterized as relict (residual). The gold has a cementation structure. Its small grains are included in complex polimineral ochres.

GROWTH-STEP-SPECIFIC INCORPORATION OF BORATE ANIONS ON THE CALCITE SURFACE

Reeder R.J. *(Geosciences Dept., State Univ. of New York at Stony Brook, rjreeder@ccmail.sunysb.edu)* and Hemming N.G. *(Lamont-Doherty Earth Observatory)*

Studies of growth on the calcite $(10\bar{1}4)$ face from low-temperature aqueous solutions show that borate impurity is incorporated differentially at symmetrically nonequivalent growth steps composing the vicinal faces of spiral growth hillocks. This behavior is similar to the step-selective incorporation of divalent cation impurities at Ca protosites in the same growth steps. Surface-controlled differential incorporation has also been observed for the complex anions sulfate and selenate, but with step preferences exactly opposite that shown by borate. Two types of growth steps are dominant on $\{10\bar{1}4\}$, both parallel to $<\bar{4}41>$; but owing to their orientations relative to surface symmetry elements two sets of steps differ because of their opposite directions of motion during layer growth. Ion microprobe measurements of boron in surface-most layers show enrichment up to a factor of 6 in one set of vicinals (*a'-b'*) relative to the nonequivalent set (*a-b*). Previous work had shown that sulfate and selenate show a preference up to a factor of 2-3 for vicinals *a-b* relative to *a'-b'*, with the likely cause related to differing geometry and nearest-neighbor distances at CO_3 surface sites in nonequivalent steps. The situation for borate is more complex with two species in growth solutions, $B(OH)_3^0$ and $B(OH)_4^-$. Isotopic evidence indicates that the tetrahedral $B(OH)_4^-$ species is preferentially incorporated, yet independent ^{11}B MAS NMR work showed that boron is predominantly in trigonal coordination following incorporation. These observations suggest that a change in primary coordination, from tetrahedral to trigonal, is a necessary step in incorporation. We can speculate that structural differences between incorporation sites within the nonequivalent growth steps are able to influence the coordination change, thereby resulting in the observed step-selective incorporation.

CHEMICAL ZONING IN HIGH-GRADE METAMORPHIC GARNETS: RESULTS OF A MICROPROBE ELEMENT MAPPING STUDY

Reinhardt J. *(Institut für Mineralogie, TU Darmstadt, Germany)*

As the elimination of chemical zoning in minerals by diffusion is largely controlled by temperature and time, even small garnets in high-grade rocks may escape chemical homogenisation if the residence time at high temperatures is relatively short. Such an example is reported here. Garnets from a garnet-sillimanite gneiss exposed in the Saxonian Granulite Massif, eastern Germany, have been examined in detail by using the microprobe element mapping technique as well as line scans.

Despite granulite-facies temperatures at peak metamorphic grade ($T \geq 800°C$ at 8±1 kbar), growth zoning patterns are preserved in extraordinary detail. The Ca distribution in particular reflects multiple growth stages. The transition from the Ca-rich core to the Ca-poor outer parts is accompanied by a change in garnet morphology (rhombic dodecahedron to icositetrahedron). Euhedral growth forms may also be recognized in the Mn, Mg or Fe maps, but changes in concentration are generally more gradual, due to diffusional overprinting. Retrograde zoning is observed at the rims, whereby the penetration depth of Mg, Fe and Mn is of the same order (up to about 300 μm). The change of garnet rim composition is coupled with garnet resorption as biotite, cordierite, hercynite, and formed during decompression and cooling.

Analysis of a large number of garnets revealed that garnets of similar size may not show identical chemical zoning patterns. For example, many of the largest garnets contain no information on the initial growth stage. Furthermore, some of the analyzed garnets have lost their highest-grade record completely due to dissolution of the outer garnet shell and/or retrograde diffusional overprinting of the rim. Using element maps, the extent of garnet resorption can be recognized more easily, and those garnet compositions that are most critical for deriving peak conditions can be much more effectively retrieved than by conventional line scans. This way, garnet rim compositions with pyrope contents in excess of 40 mole% have been recovered despite significant high-temperature retrograde effects.

MORPHOLOGY, GROWTH MODEL AND ITS FRACTAL IMPLICATION OF THE CHRYSANTHEMUM STONE IN QIXIA FM.,SOUTH CHINA

Shanrong Z. *(Faculty of Earth Sciences,China University. of Geosciences, clb@cug.edu.cn)*

The chrysanthemum stone occurring in Qixia Fm., South China is very famous for its beautiful morphology, but the growth mechanics have a theoretical significance which has not been studied before. In this paper, we analyzed the morphology, growth model and its fractal implication. Based on the measure and statistics of the chrysanthemum stone morphs, the characteristic parameters in the morphs have been found: **1**. The petal diameter and the petal interval at the meeting of the core and petal are almost invariable among all chrysanthemum; **2**. the ratio of the petal length to the diameter of core (b) is invariable according to the size of the chrysanthemum but variable according to the occurrence place.

The growth model has also been established. Comparing the model with the real morph, we analyzed the evolution mechanics and speed of the crystallization concentration C and the petal interval H during the growth. The cause of the characteristic parameters in the morphs are: **1**. the invariation of the petal diameter and interval at the meet place of the core and petal is due to the critical point C_o and H_o during the evolution of the C and H, which is not varied by the minor difference in occuring environment condition in the same geological time in south China; **2**. The ratio of the petal length to the core diameter (b) is determined by the evolution speed of C and H. If the speed is slower, then b is smaller. The speed depends on the specific occuring environment, so the b is variable according to the occurence place.

The fractal characteristics of the model is also dicussed. The fractal dimension of the two-dimension model is: $1<Df<2$, that means the chrysanthemum stone is different not only from one-dimensional column, but also from three-dimensional body. The Df has crystallization implication: larger Df indicates more difficult crystallization, more divaricating nucleation to form more petals, *etc*.

TEXTURES AND TRACE ELEMENTS IN PLAGIOCLASE AS EVIDENCE OF MAGMATIC EVOLUTION PROCESSES

Santo A.P. *(Dipartimento di Scienze della Terra, Firenze, Italy. asanto@steno.geo.unifi.it)*

Major and trace element abundances by electron microprobe (EPM) and secondary ion mass spectrometry (SIMS) together with textural features by interference contrast microscopy (NDIC) were obtained from plagioclase (plg) crystals of Nea Kameni dacitic rocks (Santorini volcano, Greece). This island has resulted from several intermittent eruptions from 1570 until the present. Plg crystals display a variety of textures such as fine-scale oscillatory zoning, resorption surfaces, sieved and patchy zones, and a wide variability of Anorthite (An) and trace element content. On the basis of textural and compositional characteristics plg phenocrysts can be divided into two groups: 1) clear crystals displaying a core composition in the range An 40-65%, low Ti, Sr, Y, Ba, and LREE abundance; 2) crystals generally sieved showing a very Ca-rich core (An >75%) and high trace element content. Rims of both plg groups display similar An content but different trace element composition. Correspondence between An zoning and trace element zoning is generally good although in some cases large changes in trace element content accompany only minor changes in An. Changes in trace element composition of the calculated melt generally correspond to changes in plg trace element composition. However, some high Ba_{melt} or Sr_{melt} values are not correspondingly present in the crystals or viceversa.

The combined EPM-SIMS-NDIC data indicate for the studied plg crystals a complex growth history. Composition of group-2 plg cores are too anorthitic, Sr-rich and Ba-poor to have crystallised from an evolved melt thus indicating disequilibrium with the host rocks. The broad range of An and trace element abundance seems to suggest that the plg under investigation experienced a broad spectrum of melt composition and/or chemical-physical condition of crystallisation. Evolutionary processes such as mixing and crystal-liquid mixing are proposed to have played an important role in determining many of the Nea Kameni plg features.

CARBON AND OXYGEN ISOTOPIC COMPOSITION OF CARBONATES FROM THE DEPOSITS OF THE COPPER SANDSTONE FORMATION

Tikhomirova V.D. *(Inst.Geol. Komi Sci.Cent. Ural Div. RASci., Syktyvkar, rmin@geo.komi.ru)*

Objects from copper sandstone formation are widespread on the westen slope of the Polar and Circum-Polar Urals. Carbon and oxygen isotopic composition of carbonates from the largest deposits (Kosyunskoye, Moludvozhskoye and Padyaginskoye) are studied. The copper mineralization on these objects is confined to quartz veins, lens and modified sandstone. Carbonates are present in all deposits and form close associations with ore minerals. Calcite is main carbonate mineral and dolomite is observed in smaller amounts. Isotopic data on carbonates allow to obtain information about the source of the hydrothermal ore-forming fluids.

The average $\delta^{18}O$ values for the carbonates range from 10.5 to 13.8 ‰ in all objects. It indicates an endogenic source for oxygen. The average $\delta^{13}C$ values for the carbonates range from -6.4 to -18.2 ‰. The $\delta^{13}C$ values of deep-seated carbon average from -5 to -7 ‰. Repeated redeposition and re-arrangement of substance during ore deposition leads to a decrease in $\delta^{13}C$ values. Thus, a hydrothermal source is suggested for carbon dioxide in carbonate-forming fluids in the copper sandstones.

13. Crystal Morphology, Zoning and Growth

LASER-INDUCED TIME-RESOLVED LUMINESCENCE SPECTROSCOPY OF MINERALS

Gaft M. *(Dept. of Natural Sciences, The Open University of Israel)* and Panczer G. *(Physico-Chimie des Materiaux Luminescents, University Claude Bernard Lyon 1)*

Luminescent systems in minerals are generally more complex than in synthetic crystals. Minerals are doped simultaneously by many luminescence centers. Thus most of the previously recorded steady-state emission spectra have overlapping features due to several types of luminescence centers. It is our purpose to examine the luminescence of minerals by laser-induced time-resolved spectroscopy which allows to differentiate between centers with similar emission spectra but with different decay times.

The luminescence spectra were investigated under eximer (308 nm), nitrogen (337 nm) and dye (340-600 nm) lasers. The luminescence was analyzed by INSTASPEC equipment enabling time-resolving spectra acquisition: delay times and strobe pulse duration 20 ns - 9 ms, detector type - intensified CCD matrix. It is especially effective in minerals since the studied luminescence centers have decay times ranging from nanoseconds of water-organic complexes and Ce^{3+}, via microseconds of other rare-earths , to milliseconds of transition metals.

We start our study with apatite, scheelite, fluorite, zircon, anhydrite, barite, benitoite, cassiterite, calcite, danburite, datolite which have been extensively studied by steady-state spectroscopy. By applying time-resolved spectroscopy we are able to determine rare-earth elements, luminescence of which has been previously hidden by the stronger bands of water-organic complexes, Ce^{3+}, Eu^{2+}, Mn^{2+}, $(WO_4)^{4-}$, $(MoO_4)^{4-}$ and radiation-induced centers. Luminescence of Pr^{3+}, Tm^{3+}, Ho^{3+}, Yb^{3+} and Er^{3+} have been confidently detected, also in presence of Sm^{3+}, Dy^{3+}, Nd^{3+} and Tb^{3+} with similar emission spectra. Energy migration between UO_2^{2+} and Pr^{3+}, Gd^{3+} and Ce^{3+}, different Eu^{3+}, Sm^{3+} and Sm^{2+} positions inside minerals as well as transitions from different excited levels in Pr^{3+}, Tb^{3+} and Mn^{2+} have been studied.

DIFFUSION OF IMPLANTED EUROPIUM IN APATITE PROBED BY TIME-RESOLVED PHOTOLUMINESCENCE

Panczer G. (LPCML, Universite Lyon 1, panczer@pcml.univ-lyon1.fr), Gaft M. *(The Open University of Israel)*, Martin P. *(IPNL, University Lyon 1)* and Champagnon B. *(LCML, Lyon 1)*

Hydroxyapatite is well known for its adsorption and substitution properties. It is studied for trapped cations and specially actinide ions in the case where apatite minerals will be used as third diffusion barrier in deep geological storage sites for waste material The apatite structure, $Ca_{10}(PO_4)_6(OH)_2$ presents two types of Ca site. In order to simulate the diffusion and fixation of actinides, we used lanthanides, the non radioactive homologues of actinides. The case of europium, the homologue of americium is presented.

Trivalent europium ions are widely used as luminescent probes in the investigation of the crystallographic structure of the activator centers. Synthetic polycrystalline hydroxyapatite samples were implanted with Eu and thermally treated (up to 500°C) to induce the diffusion and fixation inside the apatite lattice. The luminescence was analyzed at each thermal step by equipment enabling time-resolving spectra acquisition. The system is combined with optical microscope allowing spectral acquisition at the micrometer scale.

The emission spectra of the non-heated implanted pellet show very weak luminescent bands. Most of the europium ions are then adsorbed on the surface of the apatite crystallites. The samples heated between 25 and 400°C present emission spectra with specific transitions of Eu^{3+} in Ca(I) sites. This first set of emissions $({}^5D_0 \rightarrow {}^7F_x)$ corresponds to the transitions of Eu^{3+} in the high C_3 symmetry Ca(I) position. At 400°C new bands appear. This second set corresponds to the same transitions of Eu^{3+} but in the low C_s symmetry Ca(II) position.

Such experiments coupled with RBS allow us to calculate the rate of diffusion of Eu^{3+} as well as the precise substituting sites of fixation as a function of time and thermal energy. Similar experiments are being undertaken under radioactive conditions.

14. Mineral Surface Studies

MECHANISM OF Fe(III) TO Fe(II) REDUCTION IN NONTRONITE BY X-RAY DIFFRACTION, POLARIZED EXAFS, AND TEXTURE GONIOMETRY

Manceau A., Lanson B., Drits V.A. *(Univ. of Grenoble, manceau@ujf-grenoble.fr)*, Wu J., Gates W.P., Stucki J.W. *(Univ. of Illinois, jstucki@uiuc.edu)*, Chateigner D. *(Univ. Le Mans, dchat@aviion.univ-lemans.fr)*

The reduction of Fe(III) to Fe(II) is known to profoundly change the physical and chemical properties of clays including their cation exchange capacity, specific surface area, swelling behavior, and ability to fix interlayer cations. Little is known about the structural mechanism of this redox transformation even though it is of key importance to the understanding of a number of environmental processes and to the deliberate modification of clay properties.

The structure of Garfield nontronite in the oxidized and reduced state was investigated by X-ray diffraction (XRD), polarized EXAFS (P-EXAFS), and texture goniometry. XRD showed that oxidized Garfield is trans-vacant, whereas 24 ± 5% of total iron fill trans-octahedral sites in the reduced Garfield. The in-plane and out-of-plane local structure around Fe atoms was probed by angular P-EXAFS measurements on highly oriented self-supporting films. The dispersion of c* axis around the film plane of individual crystallites was 20° FWHM for oxidized and 25° FWHM for the reduced sample. These narrow orientation distributions allowed us to treat the self-supporting films as single crystals during the quantitative analysis of P-EXAFS spectra. Iron(II) atoms were found to form small trioctahedral clusters separated by empty octahedra. The excess of negative layer charge resulting from the Fe reduction is partly compensated by the sorption of Na and H^+ from solution. Na occupies interlayer sites whereas H^+ lowers the negative layer charge by protonating structural OH- groups of empty octahedra in the border of Fe(II)-rich domains, converting them into water molecules, and probably also by hydroxylating external oxygens. The average chemical reaction corresponding to this transformation can be written:

$$Na_{0.93}[Si_{7.12}Al_{0.88}][Fe^{3+}{}_{3.72}Al_{0.19}Mg_{0.11}]\ O_{20}(OH)_4 + 0.2Na + 3.32H^+ \rightarrow Na_{1.33}[Si_{7.12}Al_{0.88}][Fe^{2+}{}_{3.72}Al_{0.19}Mg_{0.11}]\ O_{17.82}(OH)_{5.04} + 1.14\ H_2O$$

This mechanism provides a rationale to explain quantitatively a number of physico-chemical characteristics of reduced smectites.

CRYSTALLISATION OF SOLID SOLUTIONS FROM AQUEOUS SOLUTIONS: GROWTH MECHANISMS AND COMPOSITION RELATIONSHIPS

Pina C.M. and Putnis A. *(Institut für Mineralogie. Univ. Münster, Germany, pina@nwz.uni-muenster.de)*

In many geochemical studies the determination and interpretation of distribution coefficients in solid solution-aqueous solutions (SS-AS) systems is of fundamental importance for inferring physical and chemical conditions in natural environments. However, the ionic partitioning mechanisms during crystal growth, which control the actual distribution coefficients, remain poorly understood. Frequently, approaches based only on thermodynamic considerations are insufficient and recent studies demonstrate that the kinetics of the processes at the solid-fluid interfaces play a crucial role in the chemistry of solid solutions.

The incorporation of substituting ions during the growth of a solid solution is essentially controlled by the interrelation between two factors: (i) the growth mechanisms, operating at a molecular scale on the different faces of the crystal and (ii) the supersaturation of the solution in contact with the growing crystal. In the case of crystallisation of solid solutions, the kinetic of the three classical growth mechanisms (spiral, 2D-nucleation and continuous growth mechanisms) and the transitional supersaturation values between them (β^* and β^{**}) are functions of the solid composition. On the other hand, the supersaturation of a aqueous solution with respect to a solid solution is also a function of the solid composition. In this complex situation it is possible that different compositions of the solid solution can grow according to different growth mechanisms.

In this work supersaturation functions for different carbonate and sulphate aqueous solutions and their relation with growth mechanisms are presented. Experimental data of the crystallisation process are provided by a combined use of Atomic Force Microscopy (AFM) and Time-Of-Flight Secondary Ion Mass Spectrometry (TOF-SIMS). Complementary information about growth behaviour and the chemistry of solid solutions growing on calcite and barite substrates is reported.

DIRECT COMPARISONS OF NATURALLY AND EXPERIMENTALLY WEATHERED FELDSPAR SURFACES BY SCANNING PROBE AND ELECTRON MICROSCOPY

Hodson M.E., Lee M.R. and Parsons I. *(Department of Geology and Geophysics, University of Edinburgh, martin.lee@ed.ac.uk)*

The microtextures and microstructures of perthitic alkali feldspars from soils formed on granites have a major impact on their rates of chemical and mechanical weathering. Their effects are most apparent when etch pits, which have formed by dissolution at edge dislocation outcrops along albite exsolution lamellae, have grown to 0.05 mm in depth and grains disintegrate. These observations are difficult to reconcile with previous laboratory experiments that seem to show that dislocation density has little or no effect on the dissolution rates of silicate minerals. We have sought to account for this discrepancy by performing laboratory experiments on unweathered equivalents of the naturally weathered alkali feldspars previously characterised.

Powdered alkali feldspars from the Lower Devonian Shap Granite, NW England were reacted with pH2 HCl in a flow-through apparatus for 2771 hours. The final dissolution rate was 1×10^{-15} moles cm^{-2} s^{-1}. SPM images of grain surfaces show that albite lamellae and dislocations have dissolved more rapidly than surrounding tweed orthoclase; the lamellae have etched 5 nm deeper than orthoclase and dislocation etch pits at least 8 nm deeper. Thus, intragranular textures and structures *must* have an effect on laboratory dissolution rates, but this effect is clearly too small to quantify from solution chemistry.

We conclude that the laboratory-field discrepancy is due to significant contrasts in saturation states of the ambient solutions. As soil waters are closer to saturation with respect to feldspar than laboratory acids, only those surface sites with a high activation energy for dissolution (dislocation outcrops) will react relatively rapidly in the field, but sites with a wide range of activation energies participate in laboratory dissolution. As a result, hundreds of years of laboratory dissolution will be required for etch pits to grow to a depth of 0.05 mm, at which point the grains start to disintegrate.

SPONTANEOUS MOVEMENT OF IONS IN CALCITE AT ROOM TEMPERATURE AND PRESSURE: ARE THERE IMPLICATIONS FOR FLUID INCLUSION COMPOSITION, ISOTOPE RATIOS AND RELATIVE TRACE METAL DISTRIBUTION?

Stipp S.L.S *(Interface Geochemistry, Geological Institute, Copenhagen University, Denmark. stipp@geo.geol.ku.dk)*

Although a great deal is already understood about calcite composition, structure and solubility, little is known about its surface behaviour. Surface analytical techniques which allow molecular-level observation have provided some rather unexpected results showing that the surface of calcite in contact with air is dynamic, both structurally and chemically. Atomic Force Microscopy (AFM) proves that freshly-cleaved, single crystals of Iceland spar calcite are atomically flat over hundreds of nanometers; chemical maps from Time-of-Flight Secondary Ion Mass Spectrometry (TOF-SIMS) demonstrate that initially, the topmost atomic layers are homogeneous, composed only of $CaCO_3$.

However, during exposure only to air, surface morphology and composition change. Over several months, crystallites form on some of the surfaces; they are composed mostly of Na^+, K^+ and Cl^- and range in size from a few to hundreds of nanometers wide and tall.

Stringent precautions preclude the possibility of external contamination. The shape and distribution of the crystallites are reminiscent of fluid inclusions, and indeed, samples containing abundant inclusions of a size visible by optical microscopy yield aged surfaces with abundant submicrometer scale crystallites, whereas samples without visible inclusions result in aged surfaces where crystallites are absent, in spite of identical preparation and storage. These observations, together with evidence showing movement of divalent ions, Cd^{2+} and Zn^{2+}, into the bulk, leads us to question what other ions might also move in calcite or in other ionic solids such as the halides or phosphates. Ionic mobility may help to explain some data from fluid inclusions, isotope ratios and trace element distribution for calcite samples that is apparently incongruent with general geological relationships. If calcite does not behave as a closed system, caution must be used in selecting samples for studies of petrogenesis, geochronology, paleoclimate or paleogeographic conditions. In environmental systems, movement of ions from or toward calcite surfaces may increase uptake and release capacity for contaminants.

14. Mineral Surface Studies

PHYSICAL CONTROLS ON CALCITE MINERALIZATION

Teng H.[1], De-Yoreo J.J.[2], Dove P.M.[1] and Orme C.[2] *([1]School of Earth and Atmospheric Sciences, Georgia Institute of Technology, Atlanta Georgia 94550; [2]Department of Chemistry and Materials Science, Lawrence Livermore National Laboratory, Livermore, CA 94550)*

The mineralization of $CaCO_3$ is currently the focus of intense research due to its importance in both geological and biological environments. In particular, the possibility of using biorganic molecules as control agents has led to great interest in understanding the mechanisms that underlie biomineralization. Because crystallization is, first and foremost, a phase transition, it is critical to separate the roles of kinetics and equilibrium thermodynamics in controlling crystallization rates and morphologies, and to quantify the energetics associated with growth in both the pure and organically modified systems. To date, our understanding of the fundamental parameters governing calcite crystal growth have been based upon the predictions of classical growth theory. Here we test the theoretical model predictions by directly determining fundamental growth parameters in an in situ AFM investigation of calcite crystallization. Using well-controlled solution conditions with accurately determined saturation states, data were collected with high solution flow rates to ensure that growth was limited only by surface kinetics. By observing the evolution of dislocation-induced growth hillocks, we were able to directly measure the dependence of step speed on step length as well as the dependence of critical step length, step speed, and terrace width over the supersaturation, σ, range of 0.021 to 0.711. The results show that once the critical length, l_c, is reached, the step speed increases to its final value at a length which is short compared to that predicted through free energy considerations. Thus, the Gibbs-Thomson effect is smaller than expected based on classical growth models. Note that this thermodynamic result predicts a growth rate that is faster by a factor of two. As expected from free energy considerations, l_c exhibits the σ^{-1} dependence predicted by growth theories. However, non-equivalent changes in atomic configurations of the positive and negative step directions yield two distinct $l_c(\sigma)$ relationships. For both step directions, the value of l_c goes to zero at finite σ demonstrating that calcite undergoes kinetic roughening (*i.e.* 1D nucleation on step edges becomes dominant) at $\sigma = 1.7$. From this value, we calculate an edge free energy for the 1D nucleus of $\approx$79 erg cm^{-2}. This value is inconsistent with theoretical predictions (slope of l_c *vs.* σ) of 585 and 744 erg cm^{-2} for the two non-equivalent crystallographic directions. These findings lead us to suggest that the classical thermodynamic models used to describe calcite growth may need to be reevaluated.

THEORETICAL STUDIES OF THE REACTIVITY OF ZnS AND HgS SURFACES USING A MOLECULAR APPROACH

Tossell J. A. *(Dept. of Chem. and Biochem., Univ. of Maryland)*

Molecular cluster models are constructed for the surfaces of ZnS and HgS (cinnabar) and the reactivities of these surfaces with various molecules are investigated using Hartree-Fock and density functional quantum chemical techniques. The basic model for the ZnS surface is the tetrahedral species $Zn_4(SH)_6^{-2}$, which occurs as a discrete anion in several inorganic compounds, but both smaller and larger clusters are also considered. Some related species $M_2M'_2(SH)_6^{-n}$, where M,M'=Al, Fe, Cu, Zn, which serve as models for more reactive minerals like $CuFeS_2$, are also studied. The small molecules adsorbed to these surface models are CO, Cl^-, OH^-, SH^- and H_2O. Calculated structures and energetics compare well with experiment, where available.

Cinnabar is modeled using a $Hg_3S_2(SH)_2$ cluster, which accurately reproduces the experimental geometry. We consider the reaction of the cinnabar surface model with H_2O, H_2S, SH^- and various halide ions, to model the dissociation process in sulfidic aqueous solution and adsorption processes relevant to the removal of radioactive iodide.

THE ROLE OF SURFACES IN THE REDUCTION OF OLIVINE

Lemelle L.P. *(LMCP, Paris, France; lemelle@lmcp.jussieu.fr)*, Fuchs Y. *(LMCP, Paris, France)*, Leroux H *(LSPEA, Lille, France)*, Libourel G. *(CRPG, Nancy, France)*, Guyot F *(LMCP and IPGP, Paris, France).*

The evolution of olivine under reducing conditions is important for understanding solar-nebula processes, physics and chemistry of meteorite parent bodies, and early Earth differentiation. In order to study the mechanisms and kinetics of metal extraction from olivine, relevant to such conditions, San Carlos olivine single crystals and powders have been annealed at 1100°C and 1350°C at 1bar under reducing oxygen fugacities buffered by C/CO, for run durations ranging between 30 minutes and 72 hours. The recovered samples were studied by Scanning Electron Microscopy (SEM), Analytical Electron Microscopy (ATEM) on transverse cuts and planar views, Atomic Force Microscopy (AFM), and Mössbauer spectroscopy (MS). The observed reduction reactions can be summarized as:

$$CO_g + Fe_2SiO_{4crystal} = 2Fe_{crystal} + SiO_{2amorphous} + 3/2CO_{2g} \quad (1)$$

$$CO_g + Fe_2SiO_{4crystal} = 2Fe_{crystal} + SiO_g + 2\,CO_{2g} \quad (2)$$

At T=1100°C, metal precipitation occurs exclusively on the surface, and no significant volatilization is evidenced, *i.e.* reaction (2) is negligible. The development of metal precipitation is coupled to a reorganization of the olivine surface, characterized by the migration of steps oriented along [001] in (010). Extraction of Fe-metal also induces Fe-Mg interdiffusion in the bulk crystal. The zero-order kinetics measured by MS suggest that adsorption of CO at the surface, as well as surface reorganization, are the limiting steps of the kinetics of metal extraction.

At T=1350°C, metal precipitation is an internal reaction coupled with significant volatilization, resulting in the development of a reduction reaction front and a surface porosity progressing inside the crystal. Behind the front, chemical fractionation due to volatilization is coupled to metal precipitation at internal surfaces of pores. The importance for internal solar nebula processes of a coupling between surface reduction phenomena and volatilization will be discussed.

SULPHUR AND IRON SURFACE SPECIES ON FRACTURED PYRITE SURFACES

Nesbitt H.W., Bancroft G.M., Pratt A.R. and Scaini M. *(Dept. of Earth Sciences, Univ. of Western Ontario, dopban@julian.uwo.ca)*

Pyrite, unlike most other minerals of rocksalt structure, typically fractures conchoidally, thus parting surfaces are not constrained to specific crystallographic planes. Analysis of Fe-S and S- S bond energies indicates that the latter is weaker, impling that at least some S-S bonds are ruptured when pyrite is fractured. Two mononuclear sulphur species (formally S^{1-}) are consequently produced, one bound to each fracture surface. This surface "sulphur radical" is reduced to S^{2-} (monosulphide) during relaxation through oxidation of surface Fe^{2+} ions to Fe^{3+}. The auto-redox reaction explains the surface states observed in S(2p) and Fe($2p_{3/2}$) X-ray photoelectron spectra (XPS) of pyrite.

Bulk disulfide contributions at 162.6 eV and two surface state contributions at 162.0 and 161.3 eV are evident in the S(2p) XPS spectrum. The 161.3 eV emission is identical to that of S^{2-} of pyrrhotite and is interpreted as monosulphide (S^{2-}). The 162 eV peak is interpreted to result from the surface-most sulfur atom of surface disulfide ions.

The Fe($2p_{3/2}$) XPS spectrum includes a bulk Fe^{2+} emission near 707 eV and two emissions from surface Fe species located at higher binding energies. One surface emission is interpreted as Fe^{2+} surface ions in lower coordination than bulk Fe (square pyramidal after fracture). Consequent stabilization of the Fe d_{z2} antibonding orbital (a result of lowered metal ion coordination) yields unpaired electrons in the valence band, hence surface Fe^{2+} ions display multiplet peaks in the Fe($2p_{3/2}$) spectrum centred at 708 eV. Each surface Fe^{3+} ion has lost a non-bonding 3d electron due to auto-reduction, thus it contains unpaired 3d electrons which causes multiplet splitting of its Fe($2p_{3/2}$) signal. The Fe^{3+} multiplet peaks extend over the energy range 708.75 to 712 eV. The two surface contributions produce the characteristic high energy tail observed in the Fe($2p_{3/2}$) spectrum of pyrite.

GOLD DEPOSITION ONTO ARSENOPYRITE SURFACES

Möller P. *(GeoForschungsZentrum Potsdam, pemoe@gfz-potsdam.de)*

p- and *n*-type conductivity of arsenopyrite (Aspy) is characterised by As/S ratios higher and lower than unity, respectively. The gold grains embedded in Aspy are surrounded by As/S molar ratios varying from < 0.80 to >1.15. In contacts of Aspy with *p*- and *n*-type conductivity, so-called *pn*-junctions, domains with As/S > 1 act as a cathode onto which Au is precipitated, whereas those with As/S<1 act as an anode. If gold is precipitated, the surface of the cathode is sealed from the fluid and acts, henceforth, as a gold electrode, the potential of which is controlled by the underlying Aspy. If the *p*-type Aspy exposed well-developed mineral faces, these are preserved by the gold coverage. Reactions at the anode leads to oxidative dissolution of sulphides by which space for further gold deposition is generated. Broken crystals of chemically zoned Aspy offer numerous *pn*-junctions, *i.e.* tiny galvanic cells, that start to accumulate dissolved gold from fluids. It is the great number of these arrangements that act so efficiently in collecting dissolved gold from fluids and finally form gold deposits.

The concept of electrochemical gold deposition has some advantage over chemical precipitation in the tiny electrolytic cells, Au is accumulated due to the reduced activation energy for nucleation by the negative potential of the cathode. In contrast, the chemical precipitation of gold necessitates 10-times higher gold concentration in fluids. Thus, the established microenvironment favours gold deposition, because supersaturation and nucleation are more easily achieved.

The visible gold in sulphides is formed later than the processes due to which the *pn*-junctions formed, *i.e.* sulphidisation of arsenopyrite or arsenification of pyrite. The well known association of native gold results from the fact that As is probably the most important element controlling the type of conductivity of semiconducting sulphides in general. The role of As as a pathfinder element for hidden gold mineralizations finds a simple explanation.

DYNAMIC SIMULATION OF CRYSTAL GROWTH AT THE MOLECULAR SCALE

Becker U., Bosbach D. and Pina C. *(Universität Münster, Institut für Mineralogie, Germany, udo@pmin37.uni-muenster.de)*

In order to understand the mechanisms of crystal growth at different conditions (*e.g.* supersaturation, pH), for different minerals and in the presence of different growth inhibitors/chelators, it is necessary to measure growth in situ at molecular resolution and to be able to model these processes by using molecular modelling.

As an example for such an approach, we chose the isostructural series $BaSO_4$, $SrSO_4$, $PbSO_4$. The experimental results by using atomic force microscopy (AFM) show growth islands of different shapes and a strong anisotropy, that is these islands grow predominantly in one crystallographic direction. The anisotropy and shape of the islands is strongly dependent on the structure of the mineral and can only be explained by using molecular modelling techniques. We chose two different approaches. A deterministic model can explain the shape of the growth islands by evaluating the attachment energies as a function of the structure. In a second step, this approach was combined with a semistatistical Monte-Carlo approach which allows to calculate growth rates in different directions and to simulate the relative importance of processes such as dynamic attachment and dissolution, surface diffusion, relaxation of the surface structure and migration of ions in the near-surface region. The same structural properties that lead to the growth anisotropy are responsible for the structure-induced self-inhibition of spiral growth as observed by using the AFM. The difference between the different minerals ($BaSO_4$, $SrSO_4$, $PbSO_4$) then only arises from applying the respective sets of ionic potentials

Once crystal growth in pure water is calculated, we introduced the presence of different organic growth inhibitors and chelators as an additional parameter. These play a crucial role in nature and for geotechnical applications. Molecular modelling techniques can be applied to calculate the surface sites to which the organic molecules will be bonded.

OXIDATION OF CHROMIUM AT BIRNESSITE SURFACES AND CONSTRAINTS ON REACTION MECHANISM

Banerjee D. and Nesbitt H.W. *(Dept. of Earth Sciences, Univ. of Western Ontario, dopban@julian.uwo.ca)*

X-ray Photoelectron Spectroscopy (XPS) was used to investigate oxidation of aqueous Cr(III) at the surface of synthetic birnessite [$MnO_{1.75}(OH)_{0.25}$]. Special emphasis was placed on detection of intermediate oxidation states of chromium due to their critical environmental significance. No previous studies have been able to identify these intermediate oxidation states of chromium (namely, Cr[IV] and Cr[V]) on mineral surfaces or in natural solutions.

$Mn(2p_{3/2})$, $Cr(2p_{3/2})$ and O(1s) spectra of the reacted surfaces reveal that Mn(IV) of synthetic birnessite undergoes reductive dissolution in one-electron-transfer steps. Mn(IV) was reduced to Mn(III), while Cr(III) is oxidized stepwise from Cr(III) to Cr(IV) and to Cr(V). Mn(III), Cr(V) and probably Cr(IV) were identified by XPS spectral analyses. A consecutive, competitive reaction scheme (exclusive of sorption reactions) is required to describe the oxidation of Cr(III) on birnessite. Most importantly, these reactions proceed as a combination of one-electron-transfer steps as well as substitution reactions with the formation of all accessible intermediate oxidation states for both metals.

Similarity in XPS binding energy values of Cr(III) and Cr(IV) as well as that of Cr(V) and Cr(VI) preclude separate identification of Cr(III) and Cr(VI) on the near-surface of the solid. Cr(IV):Cr(V) ratio increases with reaction time on the birnessite surface, and may be ascribed to either precipitation of CrO_2 on the surface or to inhibition of Cr(V) production due to consumption of reactive surface sites.

ORGANIC / INORGANIC INTERACTIONS DURING CRYSTALLIZATION AND DISSOLUTION REACTIONS: A MICROSCOPIC PERSPECTIVE

Bosbach D. and Putnis A. *(Institut für Mineralogie, Universität Münster, bosbach@uni-muenster.de)*

Crystal growth and dissolution in natural processes (*e.g.* weathering, biomineralization) and in technical applications (*e.g.* scale inhibitors, settings retarders) are affected by the presence of organic additives. Both naturally occuring organic molecules and synthetic commercial additives contain the same functional groups, *e.g.* carboxylic acid (-COOH) and phosphonic acid ($-PO_3H_2$). The presence of organic additives with such functional groups may inhibit crystallization of inorganic minerals or promote dissolution reactions. However, a fundamental understanding of the interactions between organic molecules and specific surface sites at a molecular scale is still lacking.

In-situ crystallization and dissolution experiments on barite (001) and (210) and calcite ($10\bar{1}4$) surfaces in the presence of carboxylic acids (maleic acid, aspartic acid) and phosphonic acids (1-hydroxyethylidene-1,1-diphosphonic acid, HEDP, nitrilotri (methylene phosphonic acid, NTMP) at different pH levels have been imaged using atomic force microscopy (AFM). Computer calculations (molecular dynamics, MD) have been used to explain the structure and the physical-chemical properties of Ca^{2+} / Ba^{2+} ligand complexes in aqueous solutions and at certain surface sites that were previously observed in our AFM experiments.

AFM *in-situ* experiments reveal the etch pit formation rate, the retreat of monolayer steps, and the morphology of etch pits at atomic scales compared to additive-free environments. In supersaturated solutions, we observe the nucleation rate of two-dimensional nuclei, the advancement of monolayer steps, and the local monolayer step edge morphology as a function of additive type and concentration.

14. Mineral Surface Studies

STRUCTURES OF $FeTiO_3$ (0001) SURFACES OBSERVED BY SCANNING TUNNELING MICROSCOPY.

Fellows R. A. *(Dept. of Earth Sciences, Univ. of Manchester., Rfellows@fs1.ge.man.ac.uk)*, Lennie A. R. *(Dept. of Earth Sciences, Univ. of Manchester.)*, Munz A. *(Dept. of Chemical Physics, Fritz-Haber Institute.)*, Vaughan D. J. *(Dept. of Earth Sciences, Univ. of Manchester.)* and Thornton G. *(Dept. of Chemistry, Univ. of Manchester.)*

Scanning tunneling microscopy (STM) has been used to investigate the structure of the $FeTiO_3$ (0001) surface, following argon-ion sputtering and annealing in O_2. Low Energy Electron Diffraction (LEED) of the $FeTiO_3$ (0001) surface shows two different diffraction patterns which are dependent on preparation. The first (hexagonal) pattern is interpreted as a (1x1) bulk termination. The second pattern is consistent with an inverse spinel type (111) surface termination.

Wide scale STM images of the (1x1) bulk termination show two distinct co-existing areas, large atomically rough terraces (designated X) with small, smoother, areas within them (designated Y). The observed single step height of 2.2±0.3Å (and double this value which is also found) plus data from the surface orientation implies that two termination types are seen on the (0001) surface after initial stages of preparation, and that these are either cation-terminated surface planes (Fe^{2+} or Ti^{4+}) or close packed oxygen terminations.

Atomic resolution STM images of the Y areas show features arranged in a hexagonal array, with a separation of 4.8±0.2Å. A model is proposed which identifies this termination as an unreconstructed (0001) termination of $FeTiO_3$ that exposes half a layer of either Fe^{2+} or Ti^{4+} cations over a close packed O layer, with each feature arising from a trimer of O atoms capped by a single cation (Fe^{2+} or Ti^{4+}).

NANOMETER SCALE MORPHOLOGY OF FRANCKEITE OBTAINED BY SCANNING TUNNELING MICROSCOPY (STM)

Henriksen R.B., Nissen C., Makovicky E., Stipp S.L.S. *(Geological Institute, Copenhagen University, Denmark.)* and Eggleston C. *(Dept. of Geology and Geophysics, University of Wyoming, Laramie, USA.)*

Franckeite is a complex sulphide of Pb, Ag, Sn, Fe and Sb, with a non-commensurate (misfit) layer structure of alternating pseudohexagonal and pseudotetragonal layers, stacked HQQHQQ. In the pseudotetragonal layers, the stacking direction *a* has periodicity of 17.3Å, *b* of 5.84Å and *c* of 5.90Å, whereas in the pseudohexagonal layer unit cell parameters are *a* = 17.3Å, *b* = 3.68Å and *c* = 6.32Å. Layer mismatch causes a modulation in the structure, which can be observed using HRTEM of ion etched sections. With STM we can make three dimensional images of the franckeite surface at atomic resolution. Our purpose was to observe variations in the wavelength and orientation of the modulation, with respect to atomic structure on a local scale.

Freshly cleaved franckeite was investigated in air, with scanned areas ranging from 120 nm × 120 nm to 12 nm × 12 nm. The modulation is continuous and parallel; bending have not been observed. The shape appears sinusoidal, and detailed investigations are underway. The wavelengths range from 3.46 nm to 5.20 nm. Amplitude varies more, results ranging from 0.023 nm to 0.166 nm. The match of $Q_{subcell}/H_{subcell}$ was calculated to be of 12/11 for 3.46 nm, 13/12 for 3.76 nm, 14/13 for 4.05 nm and 15/14 for 4.38 nm. This implies we may be able to interpret local variation in chemical composition, possibly increasing Pb/Sn ratio with increasing wavelengths. Measured wavelengths of about 5.2 nm are of particular interest, such a distance suggests modulation oriented diagonally to the unit cell, whereas in most cases, wavelengths are aligned orthogonally. This may imply significant differences in local response to lattice mismatch.

HIGH-RESOLUTION STM AND AFM INVESTIGATION OF SHUNGITES.

Golubev Ye.A. *(Institute of Geology, Russian Academy of Sciences, Ural Division, Syktyvkar, Russia, rmin@geo.komi.ru)*

Study of the structure of non-crystalline solid carbon, which is responsible for the most essential properties of shungite rocks (shungite occurrences in the north-western part of the lake Onega, Karelia), is of interest because of a number of its physico-chemical properties underlying its many perspective applications.

Weak structural organization of carbon in shungite and its roentgenoamorphity account for the fact that high-resolution methods of direct observation are the most perspective for shungite study. Among these methods are scanning tunneling microscopy (STM) and atomic force microscopy (AFM). They allow to obtain microphotographic portrays of the surface with atomic resolution.

STM and AFM were applied to study highly-carbonaceous (to 98%) vein shungite from various deposits (Shunga, Tchebolaksha, Maxovo, Zazhogino). We relied on the obtained images of the surface, which is a combination of hills with a tendency of similar orientation, to perform statistical analysis of linear dimensions of the elements of shungite structure. The nanostructures observed on the surface were interpreted in terms of V.V.Kovalevsky's model on fullerene-like supermolecular formations in shungite known as globules.

THE DISSOLUTION KINETICS OF AMORPHOUS SILICA: STRUCTURAL CONTROLS ON REACTIVITY

Icenhower J. and Dove P.M. *(School of Earth and Atmospheric Sciences, Georgia Institute of Technology, Atlanta, GA 30332, jicenhow@eas.gatech.edu)*

Amorphous silica, SiO_2(am), is an abundant constituent in natural terrestrial and marine environments as well as an important industrial material. This has motivated investigations of SiO_2(am) reactivity, but clear relationships between the kinetics of dissolution and solution chemistry (pH, ionic strength, *etc.*) have not been established. To date, the behavior of SiO_2(am) is largely inferred from studies of the better known crystalline polymorphs (*e.g.* α-quartz). In this experimental investigation, the dissolution kinetics of SiO_2(am) was determined in solutions over the pH range of 4 to 10 containing 0.0 (deionized water, DIW) to 0.10 M NaCl at 60° to 220°C. Measurements of rates show important differences between the corrosion behavior of SiO_2(am) and quartz. We find that the experimental energy of activation, $E_{a,xp}$, for the dissolution of SiO_2(am) is 65 kJ mol^{-1} in DIW. The introduction of up to 0.05 M NaCl yields similar $E_{a,xp}$ values of 65±5 kJ mol^{-1}. These values are consistent with previous estimates of $E_{a,xp}$ for SiO_2(am) but are ≈10 kJ mol^{-1} lower than reported values of $E_{a,xp}$ for quartz. This lower $E_{a,xp}$ is probably because SiO_2(am) has a fraction of Si-O-Si bonds (angles up to 180°) that have a greater ionic character, and are therefore more reactive than quartz (mean angle of 152°). Measurements of SiO_2(am) dissolution rates *vs.* NaCl concentrations at 200°C yield a novel result: Electrolytes enhance rates by a factor of only 5X compared to rates measured in DIW. This contrasts sharply with the ≈100X increase reported for α-quartz under identical experimental conditions. An explanation for the absence of a substantial salt effect on SiO_2(am) reactivity compared to α-quartz appears to be due to their respective dielectric constants (e). We propose that the smaller ε of SiO_2(am) (3.8) compared to α-quartz (4.3) yields a less favorable ΔG_{sorb} for the Na^+ ion at the SiO_2-H_2O interface. Seemingly small differences in e may impact ΔG_{sorb} by changing solvation and coulombic free energy terms. Results of this study suggest that the role of physical (structural) properties in governing reactivity is significant and illustrate the need to use caution when inferring reactivity trends amongst the SiO_2 polymorphs. Our findings also indicate that Na^+, the most common solute in natural waters, does not significantly enhance the dissolution rate of amorphous silica in low temperature weathering environments or hydrothermal systems.

ELECTROCHEMICAL MECHANISM OF PYRRHOTITE REDUCING Cr(VI) INTO Cr(III)

Jia J.Y.[1] Pan Z.L.[2] Xie X.D.[1] Wu D.Q.[1] Lan B.M.[3] *([1]Guangzhou Institute of Geochemistry, Chinese Academy of Sciences. [2]China University of Geosciences. [3]Xi'an Engineering University)*

We think that the reduction-oxidation reaction of sulfide minerals reducing Cr(VI) into Cr(III) on the interface of sulfide with Cr(VI) solution should have relation to sulfide solubility according to relevant theory. One $Fe_{1-x}S$-Cr(VI) primary element in this paper has been designed and made in order to obtain the experimental evidences, and our judgement has been proved by the measured data of the electric potentials (E), the absorption values (A) of $Cr_2O_7^{2-}$ absorbing visible light (λ) at different time (t), and the relation curves of t-E and λ-A. Because two kinds of oxidation reaction take place on negative pole, the primary element symbol should be the following formulas:

(-)graphite | SO_4^{2-}, S^{2-} || $K_2Cr_2O_7$, Cr(III) | graphite(+)

(-)graphite | Fe^{3+}, Fe^{2+} || $K_2Cr_2O_7$, Cr(III) | graphite(+)

1. Electric potentials fall continuously with the reaction going on, because the electrode potentials of $Cr_2O_7^{2-}$ / Cr(III) fall slowly whereas the electrode potentials of SO_4^{2-}/S^{2-} and Fe^{3+}/Fe^{2+} go up.

2. The absorption values (A) and their λ-A relation curves show that the concentration of $Cr_2O_7^{2-}$ changes decreasingly, but Cr(III) increasingly, because pyrrhotite reduces Cr(VI) into Cr(III) as a reducing reagent.

3. The experiment testifies that the reduction reaction taking place on positive pole is the following formula: $Cr_2O_7^{2-} + 14H^+ + 6e^- \rightarrow 2Cr(III) + 7H_2O$, and the oxidation reactions taking place on the negative pole can be expressed by; $S^{2-} + 4H_2O - 8e^- \rightarrow SO_4^{2-} + 8H^+$, and $Fe^{2+} - e^- \rightarrow Fe^{3+}$.

4. The element reaction can go on unceasingly, because pyrrhotite dissolves continuously.

So the electrochemical mechanism should be summarized like this: Pyrrhotite dissolving → Ion reaction (reduction-oxidation) → Adsorbing Cr(III), not that pyrrhotite adsorbs $Cr_2O_7^{2-}$ first, followed by reduction-oxidation. The reaction between $Cr_2O_7^{2-}$ and $Fe_{1-x}S$, in fact, is an ion reaction, and mineral solubility is one of the most important factors for it, including, of course, sulfide minerals. So, as a kind of common hard dissoluble minerals, the affection of sulfide solubility shouldn't be neglected.

SURFACE MAGNETISM OF FINE DISPERSIONAL MINERALS

Kotova O.B. *(Institute of Geology, RAS Ural Division, Russia, Syktyvkar, common@geo.komi.ru)*

I want to draw your attention to one of the difficult problems of today: surface magnetism on example of magnetite, elmenite and gematite. Magnetism is a quantum-mechanical phenomenon, which complexly depends on electron-electronic interaction in solid bodies. First of all such value, which determine this phenomenon, is insideatomic energy of Coulombis interaction U and energy of insideatomic changing interaction J. So the atom surround of the surface and atom surround of volume are difference, that is why it would be possible, that magnetic properties of surface and volume would be difference.

The dependence of permeability and size of mineral was obtain when the size of mineral particle decrease, the value of permeability are decreased. The researching samples has "real surface" (T=300K, P≈10^5Pa). Clean degree controlled by infrared-spectrometer.

We try to influence on the value M_s with the help of absorption of different nature gas (O_2, H_2, CO, CO_2).

Obtaining result really show about influence of surface state on value of magnetization M (sum magnetic moments of volume unit) and are interesting because absorption can influence only on surface compound of magnetization M, practically do not touch the value compound. So we have $M = M_v + M_s$. Our research shown, that volume magnetic properties of magnetite, elmenite and gematite are different from surface magnetic properties and have complex character of correlation, besides when the number absorbing molecular of gas phase (independently from absorbate nture) are increased, the tendency of decrease are observed for value $M = M_v + M_s$ Surface state influence practically only on surface compound of magnetic properties.

REDUCED COMPOSITIONS OF IMPACT MINERALS

Miura Y., Fukuyama S. and Kobayashi H.*(Dept. of Earth Sciences, Yamaguchi Univ., Yamaguchi 753-8512, Japan; yasmiura@po.cc.yamaguchi-u.ac.jp)*

Compositions of rocks at impact sites reflect mixtures of elements derived from both projectile and target materials under melt and vapour conditions. Fe-rich compositions in smaller impact craters can be explained by passage of the projectile materials through a vapour state. However, this cannot explain how elements derived from the target rocks may occur in pure (reduced) elemental forms[1,2,3]. The present study is to explain how pure Fe or C can be formed in multiple impacts.

In the present context the term 'multiple impacts' refers to progressive impacts by many projectiles (on Earth and on the airless Moon), whereas 'multi-impact' means impact-induced reactions under reduced conditions within the larger impact crater. Multiple impacts produce fine-grained breccias with homogeneous composition (Fe or C) from target rock with reduction state[2,3] as follows:

f(impact vapour-solid)= f(pure element from target rock)

Examples of multi-impact include the shocked graphite derived from limestone target rocks of the Barringer Crater, Arizona, U.S.A., and features in impact cratering experiments. This graphite, stable even at high temperature, is considered to be formed under vapour conditions. The Fe-rich impact materials are produced by the two different processes, (a) Fe from projectile of iron meteoroids found as fine-grained materials after breakdown of Ni-Fe precursor phases, and (b) reduced Fe from FeO-rich target rock under multiple impacts in vapour conditions[2-4]. In summary,

(1) Multiple impacts generate reducing conditions, and thus characteristic compositions originating from the target rock.

(2) Pure carbon can be obtained from limestone target rocks by multiple impacts under reducing conditions.

(3) Pure Fe spherules in lunar agglutinates can be obtained from FeO-rich basaltic rock in multi-impact events on the airless Moon.

References

1. Y.Miura and R.A.Graham (1994): *Shock Waves*, **3**, 293-298.
2. Y.Miura et al. (1995): *Shock Waves Proc.*, **19**, 399-410.
3. Y.Miura (1991): *Shock Waves*, **1**, 35-41.
4. R.M.Housley *et al.* (1973): *Proc. Lunar Sci. Conf.***4**, 2737-2749

EFFECT OF DISSOLVED OXYGEN ON PENTLANDITE AND PYRRHOTITE OXIDATION UNDER FLOTATION RELATED CONDITIONS

Legrand D.L., Nesbitt H.W. and Bancroft G.M. *(Dept. of Chemistry, University of Western Ontario)*

The effect of dissolved oxygen on the surfaces of Voisey's Bay pentlandite, $(Fe,Ni)_9S_8$, and pyrrhotite, $Fe_{1-x}S$, was investigated using X-ray photoelectron spectroscopy (XPS).

Polished cubes containing both mineral phases were reacted in solutions of pH 9.3 (adjusted with lime) containing 50 ppm potassium amyl xanthate (PAX).

At the highest dissolved oxygen content, both mineral surfaces were heavily altered. A thin overlayer consisting of mainly iron oxyhydroxides (FeOOH) formed on the pyrrhotite surface, as evidenced by the presence of Fe $2p_{3/2}$ XPS peaks near 711 eV. The pentlandite surface was covered with both FeOOH and nickel-bearing alteration products which are described below. Both minerals, however, remained relatively unaltered when the dissolved oxygen was lowest, with the XPS peaks for the Fe $2p_{3/2}$ and Ni $2p_{3/2}$ lines arising at 706.8 and 852.8 eV respectively.

The most notable effect was observed when the sample was exposed to solutions in which intermediate dissolved oxygen content was present. The pyrrhotite surface was highly oxidized, with the presence of FeOOH at the surface (Fe $2p_{3/2}$ XPS peak near 711 eV). The pentlandite surface, however, remained mainly unaltered. The notable differences between the pentlandite and pyrrhotite surfaces, under these conditions, may provide an avenue for improved flotation separation.

As mentioned above, altered pentlandite surfaces contain Ni-bearing alteration products at the mineral surface. These consist mainly of hydroxy and sulphoxy nickel species. These species give rise to XPS peaks from the Ni $2p_{3/2}$ line near 856 eV compared with the peak at 852.8 eV which arises from unaltered pentlandite.

ATOMIC-SCALE SURFACE FEATURES OF FRANCKEITE INVESTIGATED BY SCANNING TUNNELING MICROSCOPY (STM)

Nissen C., Henriksen R.B., Stipp S.L.S., Makovicky E. *(Geological Institute, Copenhagen University, Denmark)* and Eggleston C.M. *(Dept. of Geology and Geophysics, University of Wyoming, Laramie, WY, USA)*

Scanning Tunneling Microscopy provides us with a powerful tool to investigate mineral surfaces on an atomic scale. We have used STM to investigate the complex sulfide mineral, franckeite, and have directly measured atomic spacings and surface structures. Franckeite ($FeSn_3Pb_5Sb_2S_{14}$) consists of pseudohexagonal (H) and pseudotetragonal (Q) layers which alternate along the a-axis forming a non-commensurate stacking sequence of HQQHQQ. The unit cell parameters for the pseudohexagonal substructure are: a=17.3 Å, b=3.68 Å, c=6.32 Å, and for the pseudotetragonal substructure a=17.3 Å, b=5.84 Å, c=5.90 Å. Our samples were cleaved perpendicular to the stacking direction in an attempt to image and identify the two distinct kinds of layers. Imaging was performed in air directly after sample cleavage. Investigations to date indicate that imaging of randomly chosen cleavage surfaces shows a dominance of images where hexagonal layers are observed. The cleaved surfaces seem to have reconfigured resulting in a pseudohexagonal superstructure with unit dimensions of 6.32 Å and 11.04 Å rotated 30° to the true subcell. This superlattice corresponds to a pseudohexagonal pattern where 1/3 of the expected metal atoms are visible in the STM image. The dimensional mismatch of the non-commensurate H and Q layers results in a sinusoidal modulation of bulk structure. We have observed small deviations of 2-3° between modulation fronts and (001) planes of the pseudohexagonal layer and deviations of row directions of approximately 13° across some images. The latter angle is consistent with the offset between pseudohexagonal and pseudotetragonal atomic rows and indicates that we are able to observe both layers at the same time and in close proximity.

CHARACTERIZATION OF PENTLANDITE AND PYRRHOTITE ALTERATION PRODUCTS BY X-RAY PHOTOELECTRON SPECTROSCOPY

Scaini M.J., Bancroft G.M. and Nesbitt H.W. *(Dept. of Chemistry, University of Western Ontario)*

Pentlandite (Pn) and Pyrrhotite (Po) powders from South mine, Sudbury have been reacted with potassium amyl xanthate (PAX) and diethylenetriamine (DETA) at pH=9.3, and the surface modification has been monitored by X-ray photoelectron spectroscopy (XPS).

The presence of nickel hydroxide as well as nickel sulphate is observed. The iron speciation is dominated by the presence of iron oxyhydroxide (FeOOH) but in some cases the presence of Fe(III)-S species are observed. Both PAX and DETA reduce the degree of oxidation present on the surface when compared to the samples reacted without either agent on Pn.

The oxidation of Po results in a surface dominated by FeOOH and Fe(III)-S species with little of the parent mineral being observed. The Po iron oxidizes more rapidly than the Pn iron under similar conditions.

CHEMICAL SHIFTS OF SILICON X-RAY PHOTOELECTRON SPECTRA ON VARIOUS SILICATE MINERALS

Okada K., Kameshima Y. and Yasumori A. *(Department of Inorganic Materials, Faculty of Engineering, Tokyo Institute of Technology; kokada@ceram.titech.ac.jp)*

The binding energies of Si 2p X-ray photoelectron spectroscopy (XPS) and the kinetic energies of Si(KLL) X-ray excited Auger electron spectroscopy(XAES) were measured for silicates with SiO_4 tetrahedra of various polymerization types, i.e. monomeric structure (forsterite and merwinite), dimeric structure (akermanite), chain structure (enstatite and wollastonite), sheet structure (kaolinite and talc) and framework structure (cristobalite and quartz) to elucidate relationship between silicate structure and XPS data. The resulting Si 2p XPS binding energies varied from 101.31(3) eV in merwinite to 103.35(14) eV in cristobalite while the resulting Si(KLL) XAES kinetic energies varied from 1608.14(15) eV in cristobalite to 1610.79(10) eV in merwinite. A clear chemical shift relation was observed, relating the polymerization structures of SiO_4 tetrahedra to the plots of their Si 2p XPS binding energy versus the kinetic energy of their Si(KLL) XAES spectra. The Si 2p XPS binding energies in those minerals showed good correlation with average electrostatic force of Si-O bonds. The structural state of the surface silicates in various substances can thus be deduced from this chemical shift relationship.

A MOLECULAR ORBITAL RESEARCH FOR THE REACTION OR ADSORPTION BETWEEN SILICA (H_4SiO_4) AND FLUIDS (H_2O, HF AND HCl)

Tamada O. and Tanimoto M. *(Graduate School of Human and Environmental Studies, Kyoto University, tamada@helios.jinkan.kyoto-u.ac.jp)*

Molecular orbital calculations have been done on silica modeled by H_4SiO_4 and fluids of water (H_2O), hydrofluoric acid (HF) and hydrochloric acid (HCl) to investigate the reaction or adsorption on the surface of silica. The Gaussian94 program was used in the study of the Hartree Fock level calculations under the STO-3g basis. Each of the fluids approached to the silica molecule changing the distance between Si and O, F and Cl, monitoring the total energy and atomic configuration. At each of the frozen distance the calculation was energetically optimized changing the atomic coordinates. Some calculations are fully optimized to find an energy minimum configuration and transition state.

In the course of fluid approach the hydrogen atom is attracted by an oxygen of H_4SiO_4 molecule, and then the fluid begins to rotate to have a contact to hydrogen of another Si-O-H branch of H_4SiO_4. In all three cases of fluids the energy is minimized at the configuration in which a hydrogen atom of fluid is connected to an oxygen and the main atom (O, F and Cl) connected to a hydrogen atom of Si-O-H branch. Three fluids take minimum configurations at the distance from Si atom of 3.213Å for water, 3.093Å for HF and 3.870Å for HCl. In the case of HF the minimum shows a clear V-valley, but in HCl it shows a flat U-valley from about 3.1Å to 4.1Å. In the case of water the molecule shows a different motion from other two. The fluid further rotates to have a connection between a second hydrogen of H_2O and a third branch of Si-O-H. and takes an another energy minimum at the distance of 2.245Å. The difference of two energy minimums is extremely small, 0.7 Kcal/mol.. It is concluded that all of three fluids have a characteristic energy curve, V-valley, U-valley and double valleys.

In the course of fluid approaches up to 1.7 or 1.8Å the Si-O bond keeps its short length less than 1.7Å and shows no clear evidence of weakening.

STUDIES OF PYRITE (111) AND (001) SURFACES BY SCANNING TUNNELING MICROSCOPY

Lennie A.R., Vaughan D.J. *(Dept. of Earth Sciences, Univ. of Manchester, alennie@fs1.ge.man.ac.uk)*, Munz A.W. *(Dept. of Chemical Physics, Fritz Haber Institute)*, Bertrams T. *(IRC for Surface Science, Univ. of Liverpool)* and Thornton G. *(Dept. of Chemistry, Univ. of Manchester)*

We present the results of an experimental study of (111) and (100) pyrite surfaces utilising ultra-high vacuum techniques.

Samples of pyrite were prepared from natural growth faces of FeS_2 (111) and (100), and following sputtering with neon or argon ions, were annealed (in UHV) at ~ 300°C for periods of up to an hour. Surfaces were examined using Low Energy Electron Diffraction, Auger Spectroscopy and Scanning Tunneling Microscopy.

Consistent with the LEED pattern, STM images of (111) surfaces show close-packed features ordered in an hexagonal (2×2) array. The feature-feature separation is 3.8 Å. The (001) surface also exhibits features separated by 3.8 Å which can be arranged as a centred square with surface unit-cell dimensions of 5.4 Å, matching the pyrite unit-cell dimension. The orientation and separation distances of these imaged features are consistent with the locations of Fe in bulk terminations of the pyrite structure at (111) and (100) surfaces respectively.

From a consideration of Tasker's three types of ionic surface, a bulk termination of the (001) surface of pyrite would be expected to form a stable crystal face. In contrast, the (111) surface might be expected to undergo reconstruction, or significant relaxation, in order to reduce surface energy. Models of the pyrite (111) surface are presented in order to illustrate the requirements for surface stabilisation at this face, and are compared with the experimental data from this study.

15. Recent Advances in the Crystal Chemistry of Rock Forming Minerals

NEW DEVELOPMENTS IN CRYSTAL CHEMISTRY AND GEOCHEMISTRY OF ALKALI FELSPARS FROM RARE-ELEMENT GRANITIC PEGMATITES

Teertstra D.K., Černý P. and Hawthorne F.C. *(Dept. of Geological Sciences, Univ. of Manitoba)*

Recent studies of alkali feldspars from rare-element granitic pegmatites have led to recognition of very extensive subsolidus modifications of the primary magmatic phases, and of inconspicuous but widespread occurrences of adularia-type K-feldspar in several paragenetic and compositional modes. Mutual interdependences among P content, $\square Si_4O_8$ substitution, *M*-site "deficiency", ordering and exsolution rates also are suggested. - (i) Adularia replaces blocky microcline-perthite and pollucite, coprecipitates with Rb-dominant feldspar after breakdown of early K-feldspar, and coats crystals of K-feldspar in cavities. - (ii) Low but widespread substitution $\square Si(KAl)_{-1}$ was unambiguously proved in end-member Or compositions, and for the first time in highly ordered microcline. *M*-site vacancies should promote cation migration; they also may host water molecules capable of internal catalyzing of Al-Si ordering. - (iii) Apparent *M*-site deficiency in K-feldspar is most probably caused by substitution of light elements (Li, H, H_3O^+). This is observed in adularia and in microcline, particularly in P-rich samples. - (iv) Phosphorus enters alkali feldspars exclusively by the berlinite substitution $AlPSi_{-2}$. Low-temperature fluid action affects albitic feldspar to a greater extent than potassic phases, generating microporosity and secondary apatite at the expense of feldspar-hosted P. - (v) Rubicline, the Rb analog of microcline, was described, and the existence of Rb analog of sanidine is strongly suspected. Microscopic but widespread Rb-rich to -dominant feldspars form by exsolution and by solution-reprecipitation from Rb-bearing primary feldspar, and by replacement of pollucite. Coexistence with Or_{100} adularia indicates a Kfs-Rbfs solvus cresting below 400°C. - (vi) Totally disordered Or_{100} adularia yields cell parameters for unstrained structural and compositional end-member high sanidine *a* 8.591(1), *b* 13.047(2), *c* 7.170(1) Å, β 115.95(1)°.

CRYSTAL CHEMISTRY OF PEROVSKITE GROUP MINERALS AND THEIR SYNTHETIC ANALOGUES.

Mitchell R.H. and Chakhmouradian A.R. *(Dept. of Geology, Lakehead Univ., rmitchel@gale.lakeheadu.ca)*

Perovskite group minerals are important rock forming minerals in alkaline rocks. In carbonatites and nepheline syenites they are represented principally by solid solutions between perovskite, loparite and lueshite. Some carbonatites are characterized by solid solutions between perovskite, latrappite, lueshite and $Ca_2Nb_2O_7$. Potassic alkaline rocks commonly contain loparite-tausonite solid solutions. The crystal structures of most naturally-occurring perovskite group minerals, apart from $CaTiO_3$-perovskite, are poorly-characterized due to complex twinning coupled with extensive small-scale compositional variation. The structure of latrappite as determined by Rietveld methods is found to be similar to that of $CaTiO_3$-perovskite but characterized by greater tilting of the $(Nb,Ti,Fe)O_6$ polyhedra. The crystal structures of synthetic analogues of natural solid solutions have been determined by Rietveld refinement techniques in order to understand those of the naturally-occurring perovskites and their limits of compositional variation.

Structural data are presented for the binary solid solution series: (1) $CaTiO_3$ - $CaFe_{1/2}Nb_{1/2}O_3$, orthorhombic (*Pbnm*) to monoclinic ($P2_1/n$) with short range B-site cation ordering arising from charge differences; (2) $Na_{1/2}La_{1/2}TiO_3$ - $Na_{2/3}Th_{1/3}TiO_3$, orthorhombic (*Pbnm*) to tetragonal (*P4/mmm*) with partial A-site ordering and Ti displacement from the center of the TiO_6 polyhedron due to the strong electrostatic repulsion effects of Th and La at the A-sites; (3) $Na_{1/2}La_{1/2}TiO_3$-$SrTiO_3$, orthorhombic (*Pbnm*) to cubic (*Pm3m*) via a tetragonal intermediate (*I4/mcm*) with no ordering. Synthetic analogues ($Na_{1/2}Ce_{1/2}TiO_3$; $Na_{1/2}La_{1/2}TiO_3$; $Na_{1/2}Nd_{1/2}TiO_3$) of loparite-(Ce), are orthorhombic (*Pbnm*) and it considered that natural loparite-(Ce) has this space group.

VOLUMES AND VOLUMES OF MIXING IN THE GARNET SYSTEM $(Ca, Mg, Fe^{2+}, Mn^{2+})_3Al_2Si_3O_{12}$

Geiger C.A. *(Mineralogisch-Petrographisches Institut der Universität Kiel, Germany, NMP46@rz.uni-kiel.de)*

The molar volumes of synthetic end-member garnets (almandine, pyrope, grossular and spessartine) and the six binaries in the system $(Ca,Mg,Fe^{2+},Mn^{2+})_3Al_2Si_3O_{12}$ have been determined using precise powder x-ray diffraction methods. The molar volumes depend to a small, but measurable degree on the presence of additional components like Fe^{3+}, Mn^{3+} and OH^-. They act to expand slightly the volume of garnet. A plot of the molar volumes of the end-members versus the X-site cation ionic radius is nonlinear.

The volumes of mixing of the six binaries in the system range from ideal (Al-Py) to distinctly nonideal (Py-Gr). It can be shown that the structural state (short-range order of the X-cations) influences the volumes. This effect could account for much of the differences between the volume determinations given in the literature. A linear relationship exists between the excess volumes of mixing, expressed using a regular solution model, and the difference in magnitude between the volumes of the two end-members. This suggests that strain is largely responsible for causing the volumes to depart from ideality.

X-O bond lengths in garnet solid solutions have traditionally been interpreted using the virtual-crystal approximation, which may not be applicable for many solid solutions. Based on IR, Raman and ^{57}Fe Mössbauer results, the element specific X-O bonds may retain to a large degree their lengths in the solid solutions as they have in their respective end-members. This should lead to lattice strains in solid-solution compositions near the smaller volume garnet end-member component.

The degree of tetrahedral rotation is proposed to play an important role in mediating strain and, hence, the volumes of mixing.

SHORT-RANGE ORDER IN ROCK-FORMING MINERALS

Hawthorne F.C. *(Dept. of Geological Sciences, Univ. of Manitoba, frank_hawthorne@umanitoba.ca)*

Short-range order (SRO) describes the tendency of some local arrangements of atoms to be more frequent than a random distribution would predict. Information on SRO is quite difficult to extract from diffraction data. However, SRO may be examined theoretically using bond-valence theory and the valence-sum rule.

Application of these ideas to the amphiboles show that, for each end-member composition, there is one set of SRO patterns that agrees quite well with the valence-sum rule, and all other sets of patterns show significant deviations from the valence-sum rule. For some end-members, there is no close agreement with the valence-sum rule; compositions close to these end-members (*e.g.* tschermakite) are non-existent. These patterns of local order should give rise to specific bands in the principal OH-stretching region of the infrared spectra of amphiboles, and spectra of complex amphibole solid-solutions can be quantitatively interpreted on this basis.

Application of these ideas to tourmaline shows that there are major sterochemical constraints associated with variation of Si, B and (OH+F). Thus the occurrence of a trivalent cation at the T(1) site (occupied primarily by Si) must be locally associated with trivalent cations at the neighbouring Y- and Z-sites, and possibly with Ca at the neighbouring X-site. The occurrence of O_2^- at O(1) (usually occupied by OH+F) must be locally associated with three trivalent or two trivalent and one divalent cations at the neighbouring Y-sites. These requirements provide stringent constraints on the possible substitution schemes whereby additional O_2^- (*i.e.* a deficiency in OH+F) is incorporated into the tourmaline structure.

15. Recent Advances in the Crystal Chemistry of Rock Forming Minerals

TOURMALINE: NEW VIEWS OF A GARBAGE CAN MINERAL

Henry D.J. and Dutrow B.L. *(Dept. of Geology and Geophysics, Louisiana State Univ., glhenr@unix1.sncc.lsu.edu)*

Over the last 10 years knowledge of the crystal chemistry, crystallography and disparate natural occurrences of tourmaline (*tur*) has exploded. Crystal structure refinement, spectroscopic and crystal chemical investigations have clarified site occupancies and likely site substitution schemes. Consequently, a general *tur* chemical formula can be written as $XY_3Z_6[T_6O_{18}][BO_3]_3V_3W$, with the most common site occupancy as: **X** = Na, Ca, □ (vacancy), K; **Y** = Mg, Fe^{2+}, Li, Al, Mn^{2+}, Fe^{3+}, Cr^{3+}, V^{3+}, Ti^{4+}; **Z** = Al, Mg, Fe^{3+}, V^{3+}, Cr^{3+}; T = Si, Al, (B); **B** =B, (□); **V** =OH, O and **W** =OH, F, O. Some of the more significant recent findings include (1) two distinct "OH" sites (W and V), the sum of these sites is commonly <4 OH apfu, (2) F substitutes only on the W site, (3) ordering of Mg on the Z site, which appears to stabilize the structure and (4) the common occurrence of ^{X}□-dominant tourmalines. These features lead to a reevaluation of classification schemes for *tur*.

Crystal chemical "peculiarities" of *tur* continue to expand. Several additional elements (*e.g.* Cu, Bi, Ni, Zn, K) have joined the panoply of those known to be significant constituents in *tur*. In addition, compositions of natural Li-bearing *tur* have been found to span the range between dravite and elbaite end members, a region previously considered as a compositional gap. Dramatic sector zoning has been noted in low temperature *tur* with compositional differences up to 10 wt%. Also, compositional polarity, development of different *tur* compositions along c-axis pole in time-equivalent growth zones, has been found to diminish as a function of temperature, and disappear at medium grade metamorphic conditions. This latter feature has significant effects on Mg-Fe partitioning with coexisting minerals.

Tur has been found over an expanded range of conditions; from near-surface conditions (*e.g.* cap rock of salt domes) to ultra-high pressure conditions (>37 kbar) to high temperature conditions (>800°C). *Tur* is also a common gangue mineral in many types of metallic ore deposits such as Ag, Au, Sn, W, Mo, Cu and U. *Tur* continues to expand its role as a petrogenetic indicator mineral.

ATOMIC DISPLACEMENTS IN CARBONATE APATITE

Chakoumakos B.C. *(Solid State Division, Oak Ridge National Lab., kou@ornl.gov)*, Leventouri Th. *(Dept. of Physics & Alloy Research Center, Florida Atlantic Univ.)* and Perdikatsis V. *(Institute of Geology & Mineral Exploration, Athens)*

To elucidate the details of carbonate substitution in the apatites, we report Rietveld structural refinements of neutron diffraction data of a highly crystalline, single-phase natural carbonate apatite, francolite of Epirus, Greece. Electron microprobe analysis gives the composition $Ca_{9.56}Na_{0.38}Mg_{0.08}(PO_4)_{4.82}(CO_3)_{0.946}(SO_4)_{0.2}F_{2.34}$. Neutron diffraction is ideal for determining the oxygen mean-square displacement amplitudes because of its sensitivity to oxygen atoms. Data for the native francolite as a function of temperature between 296K and 10K were refined after the material had been heated at 800K to drive off adsorbed water. The *c*-axis contraction is about twice as great as that in the *a*-axis. Analysis of the temperature dependence of the anisotropic displacement parameters can reveal the contribution from the temperature independent static positional disorder. Difference displacement parameters evaluated along various bonding directions are being used to describe the mechanics and dynamics of the carbonate for phosphate substitution. The neutron diffraction data were collected using a wavelength 1.0912 Å on the HB4 high resolution powder diffractometer at the High Flux Isotope Reactor at Oak Ridge National Laboratory.

Supported by the Division of Materials Sciences, U.S. D.O.E. (contract DE-AC05-96OR22464 with Lockheed Martin Energy Research Corporation).

STRUCTURAL CONTROL OF THE OH → F EXCHANGE IN ROCK-FORMING HYDROUS SILICATES: A REVIEW BASED ON EXPERIMENTAL AND SPECTROSCOPIC DATA

Robert J.-L.[1], Della Ventura G.[2], Delbove F[1], Diaz M.[1], Gourdant J.-P.[1], Papin A.[1] and Sergent J.[1] *([1]CRSCM-CNRS, Orléans, France, jlrobert@cnrs-orleans.fr; [2]Univ. Roma Tre, Italy)*

In the major hydrous rock-forming silicates: clay minerals, micas, amphiboles, tourmalines,..., F is able to replace OH groups. The OH → F replacement is controlled by non-dimensional crystal-chemical factors, *i.e.* the nature of neighbouring cations and the consequently local charge balances: cations bonded to the OH group (charge, electronegativity), tetrahedral site occupancy (tetrasilicic, trisilicic, disilicic, and nature of substituting cations, *e.g.* Be^{2+}); presence or absence, and charge of a cation facing the OH dipole.

These constraints can be summarized by a single variable: the OH-stretching wavenumber, which reflects the intensity of the H-bond between the OH proton and nearby oxygens, and, consequently the O-H bond strength. High OH-stretching wavenumbers, >3650 cm^{-1}, allow an easy OH → F replacement: talc (and presumably pyrophyllite), tetrasilicic and trisilicic lepidolites, richterites and pargasites, inner OH-site of Na-tourmalines. By contrast, when the hydroxyl proton is involved in OH···O bond(s), which leads to ν_{OH} <3600 cm^{-1}, the OH → F replacement is difficult or impossible.

This allows to explain:

1) the partition of F in favour of biotite in two-mica assemblages, and in favour of trioctahedral sites in triocta-dioctahedral layer-silicates,

2) the partition of F in favour of Mg_3 associations, rather than Mg_2Al ones, in micas, amphiboles and tourmalines,

3) the deviation of pargasite composition towards edenite as the F content increases in bulk systems (loss of Al owing to Al-F repulsion),

4) the Ba-F and K-OH orders along the phlogopite-kinoshitalite join,

5) the upper fluorine solubility limit ($X_F \approx 0.25$), in Na-bearing tourmalines, since only the inner OH-sites comply with the required H-bond criterion, and its absence in Na-free ones,

6) the well known Fe-F avoidance in all hydrous silicate families.

VECTOR DERIVATION OF A COMPOSITION SPACE FOR SKARN GARNETS

Burt D.M. *(Deptartment of Geology, Arizona State University, dmburt@asu.edu)*

Calcic garnet is the dominant mineral in some skarns and is common in many other rock types. Its composition space can be represented in terms of any three non-coplanar exchange (or substitution) vectors, starting from the composition of, *e.g.* grossular, $Ca_3Al_2Si_3O_{12}$. Three suitable linearly independent exchange vectors are $FeCa_{-1}$, $FeAl_{-1}$, and $MnFe_{-1}$. This last vector is complex in its effects, inasmuch as it represents both $Fe^{2+}(Mn^{2+})_{-1}$ and $Fe^{3+}(Mn^{3+})_{-1}$. An interesting result that is the compositions of the three garnet end-members "blythite," $Mn_3Mn_2Si_3O_{12}$, calderite, $Mn_3Fe_2Si_3O_{12}$, and "skiagite" $Fe_3Fe_2Si_3O_{12}$, lie on the same straight line. The ultimate chemical limits of the garnet composition $M_5Si_3O_{12}$ (where M = Ca,Mn,Fe,Al) define a tetrahedron with apices for M = Ca (unstable), Mn ("blythite"), Fe ("skiagite"), and Al (unstable). More reasonable "crystal-chemical" (that is, valence-satisfying) limits, corresponding to the more restricted garnet formula $(Ca,Mn,Fe)_3(Al,Mn,Fe)_2Si_3O_{12}$, define a modified (truncated) tetrahedron with the Ca and Al apices beveled off to yield triangular faces. The resulting polyhedron (now an irregular hexahedron) is bounded by two triangles that share the grossular composition. The larger triangle, three units to a side, near $Al_5Si_3O_{12}$, is for $(Fe^{3+},Mn^{3+}) = 0$ and Al = 2. Its apices, other than grossular, include spessartine and almandine. The smaller triangle, two units to a side, near $Ca_5Si_3O_{12}$, is for $(Fe^{2+},Mn^{2+}) = 0$ and Ca = 3. Its apices, other than grossular, include andradite and "MAA" ("manganic andradite analog"). The remaining four faces are quadrilaterals for the faces Al = 0, Ca = 0, Mn = 0, and Fe = 0, and don't contain any end-members not mentioned above. The conventional garnet end-members lie inside this irregular hexahedron, and their apices define a tetragonal pyramid. The base of this pyramid is a reciprocal rectangle with grossular, andradite, calderite, and spessartine at its corners (and is defined by the orthogonal vectors $FeAl_{-1}$ and $MnCa_{-1}$, starting from the grossular composition); the composition of almandine lies above this plane (and is derived from grossular by the vector $FeCa_{-1}$).

15. Recent Advances in the Crystal Chemistry of Rock Forming Minerals

NEUTRON DIFFRACTION STUDY OF THE LOW- TEMPERATURE PHASE TRANSITIONS IN LAWSONITE

Lager G.A. *(Dept. of Geography and Geosciences, Univ. of Louisville, galage01@homer.louisville.edu)*, Libowitzky E. *(Inst. für Mineralogie und Kristallographie, Univ. Wien)* and Schultz A.J. *(IPNS Division, Argonne National Laboratory)*

Recent X-ray crystallographic studies of lawsonite [$CaAl_2(Si_2O_7)(OH)_2 \cdot H_2O$] at low temperatures have revealed the existence of two, reversible, order-disorder type phase transitions at 273 and 155 K [*Cmcm* (298 K) → *Pmcn* (< 273 K) → $P2_1cn$ (< 155 K)] (Libowitzky and Armbruster, *Am. Mineral.*, **80**, 1277-1285, 1995) which are related to the development of strong H bonding. In order to model the H-atom displacements in lawsonite as a function of temperature and provide further insights into the mechanism of these transitions, the crystal structure of a natural sample from Tiburon Peninsula, California was refined at temperatures of 295, 110 and 20 K using single-crystal, time-of-flight neutron diffraction methods. The root-mean-square (rms) displacements determined for the Hh atom (OH group) at 295 K revealed a strong anisotropy along [001] which is consistent with the libration of the H atom around O4 atoms. The Hw-atom (water molecule) displacements were also strongly anisotropic with the maximum displacement oriented in the direction of H positions in the low-temperature structures. The two shortest H...O bond distances at 295 K are 2.107(4) Å (Hh), and 1.860(5) Å (Hw). At 110 K, there are four, rather than two unique H atoms due to the ordering of H atoms, and the loss of the --m and m-- mirror planes in space group *Cmcm*. Of these four H atoms, the two atoms (Hha and Hwa) that form weak H bonds are each statistically distributed between two sites which have about the same occupancy. The stronger H bonds involving Hh (1.764(4) Å) and Hw (1.664(4) Å) are significantly shorter than H bonds observed in the 295 K structure. The rms displacements for the weakly bonded Hha and Hwa atoms become more anisotropic at 20 K as Hh...O (1.698(4) Å) and Hw...O (1.618(4) Å) bonding is enhanced.

DAC MÖSSBAUER SPECTROSCOPY OF SYNTHETIC OLIVINES AT ELEVATED TEMPERATURES AND PRESSURES

Annersten H. and Hålenius E. *(Dept. of Earth Sciences, Uppsala University, hans.annersten@geo.uu.se)*

Synthetic Mg-Fe olivines of the composition 40%, 50%, 65% and 100% fayalite have been examined by *in situ* Mössbauer spectroscopy at elevated temperatures and high pressures using diamond anvil cell techniques. Our aim with this study has been to estimate pressure and temperature dependent cation distribution among the available M1 and M2 site in olivine in the temperature range 250 to 600°C and pressures up to 10 GPa.

A regular decrease of the Mössbauer parameter centre shift (CS) is observed due to the SOD (-7.3×10^{-4} $mms^{-1}deg^{-1}$) and a pressure induced change (-0.002 to -0.007 $mms^{-1}GPa^{-1}$) depending of the Fe/Mg ratio. The latter change suggests that a compression of the coordination polyhedra M1 and M2 occurs at increasing pressure. The temperature dependence of the quadrupole splitting is -0.002 $mms^{-1}deg^{-1}$. In addition an observed pressure effect is shown to be compositionally dependent.

Ferrous iron Mössbauer absorption lines indicate an almost statistical distribution of iron in olivine with a small preference of Fe^{2+} for the M1 site (51 %). No statistically significant change in the site occupancy was observed within the temperature and pressure ranges studied.

Experiments above 5 GPa were performed in the stability range of both the α and γ phase. However, the transition was only observed for the iron end member at 10 GPa and 290°C. Slow kinetics at this temperature are the reason for the transition to the γ - phase in the Mg -containing system.

Si/Al DISTRIBUTION AND SITE DISTORTION IN Di-CaTs CLINOPYROXENES, USING ^{29}Si AND ^{27}Al MAS NMR.

Millard R.L., Luth R.W. *(Dept. of Earth and Atmospheric Sciences, University of Alberta, roberta.millard@ualberta.ca)* and Sherriff B.L. *(Dept. of Geological Sciences, University of Manitoba)*

Aluminous pyroxenes are important petrological pressure indicators. Adding aluminum to both tetrahedral and octahedral sites, however, complicates their structure and related stability. Compositions along the diopside-Ca-Tschermak (Di-CaTs) solid solution, containing 0, 25, 50, 75 and 100% CaTs, have been synthesized from anhydrous glasses at 2 GPa and 1400°C in a piston cylinder apparatus, and characterized by ^{29}Si and ^{27}Al MAS NMR and Rietveld refinement of X-ray diffraction data.

^{29}Si MAS NMR (59.6 MHz) spectra exhibit as many as four peaks for intermediate members of the solid solution. Only three unique environments are possible however, if only the effects of tetrahedral NNN cations in single chain pyroxenes are considered (*i.e.* $^2Q(0Al)$, $^2Q(1Al)$ and $^2Q(2Al)$). These NMR spectra can be interpreted by considering the effects of octahedral as well as tetrahedral cation substitution. ^{29}Si peak positions in these pyroxenes are influenced by the NNN octahedral cations (M1 and M2), as well as the bridging NNN tetrahedral cations. Because all M2 sites in Di-CaTs are filled with Ca, six unique combinations of four cations around Si produce six unique local environments, represented by general notation $^2Q(n^{[4]}Al, m^{[6]}Al)$. Substitution of Al for Mg at M1 causes the ^{29}Si chemical shift to be shielded by about the same magnitude as the deshielding caused by substitution of Al for Si in adjacent tetrahedra, causing some of the six unique local environments to have overlapping chemical shifts.

^{27}Al MAS NMR spectra (130.3 MHz) exhibit a very broad tetrahedral peak and broad octahedral peak. The octahedral peak exhibits increased broadening and quadrupolar lineshape with increased CaTs component, correlated to increased distortion at the octahedral site (quadratic elongation (QE) increases from 1.0048 in diopside to 1.0148 in CaTs). Tetrahedral peak broadening decreases with increased CaTs component, although tetrahedral site distortion increases slightly across the solid solution (QE increases from 1.0061 in diopside to 1.0082 in CaTs).

RAADEITE, $Mg_7(PO_4)_2(OH)_8$: TOWARD A HUMITE-TYPE SERIES IN Mg-PHOSPHATES?

Chopin C., Brunet F. *(E.N.S. Paris, chopin@euclase.ens.fr)*, Ferraris G., Prencipe M. *(Dept. Sci. Mineral. Petrol., Univ. Torino)* and Medenbach O. *(Ruhr-Universität Bochum)*

The new mineral raadeite honours Dr. G. Raade, curator of the Mineralogy Museum in Oslo, for his contribution to the study of Mg-phosphates, both natural and synthetic. It occurs in nodules of apatite + Mg-phosphates within one of the serpentinite bodies of the Modum district, S. Norway, from which althausite, holtedahlite and heneuite have been described. Raadeite occurs as veinlets, a few tens of μm wide, crosscutting althausite crystals; as rare, up to 150 μm large anhedral inclusions in holtedahlite; and with apatite, althausite and magnesite in fibrous coronae replacing heneuite. It is colourless, transparent, biaxial (-); for λ = 589 nm, n_x 1.5945(5), n_y 1.6069(5), n_z 1.6088(5), $2V_{meas}$ 45.6(1)°, $2V_{calc}$ 43°; strong dispersion r >v, $n_y \parallel b$. The infrared spectrum shows prominent absorption bands at 3375, 3475, 3540 and 3560 cm^{-1}. Electron-microprobe analyses indicate near-end-member composition, with less than 1 wt% As_2O_5 and 0.5 wt% FeO and MnO. Raadeite is monoclinic, space group $P2_1/n$, a=5.252(1), b=11.642(2), c=9.656(2)Å, β =95.94(3)°, Z = 2. Single-crystal structure refinement (R = 0.02) shows raadeite to be isostructural with the Mn-arsenate allactite. Noteworthy is the presence of face-sharing Mg octahedra, as in the high-pressure Mg-phosphates holtedahlite and phosphoellenbergerite.

Raadeite could be synthesized from 3 to 15 kbar, 500°C, along with the alternative assemblage brucite + β-Mg_2PO_4OH (hydroxyl analogue of wagnerite). At higher T (from 600°C, 3.5 kbar to 850°C, 15 kbar.) raadeite is replaced in this assemblage by a new phase [*cf.* arsenoclasite, $Mn_5(AsO_4)_2(OH)_4$??], These results suggest that a H_2O-conserving reaction of the type

$$m\ Mg_2PO_4OH + n\ Mg(OH)_2 = Mg_{2m+n}(PO_4)_m(OH)_{m+2n}$$

(with a large negative DV in the case of raadeite) may lead to a series of compounds with staggered P-T stability fields, very much like the humite family but which may or may not form a polysomatic series.

15. Recent Advances in the Crystal Chemistry of Rock Forming Minerals

CRYSTAL CHEMISTRY OF AXINITES

Andreozzi G.B., Lucchesi S. and Graziani G. *(Department of Earth Sciences, University of Rome "La Sapienza", graziani@axrma.uniroma1.it)*

Crystal chemistry of axinite group minerals was investigated by electron and ion (SIMS) microprobes (for H and B), single-crystal X-ray diffraction and Mössbauer spectroscopy to clarify correct cation distribution and the correspondent site deformation alongside isomorphic series manganaxinite-ferroaxinite-magnesioaxinite.

Seventeen natural crystals, chemically distributed in the field of the series and including the almost pure Mn, Mg and Fe^{2+} end-members, were structurally refined. The increase in Mn content (up to 1.92(2) apfu), ordered in the octahedral Y-site, results in increase of cell volume (up to 573.60(5) Å^3), **a** cell edge and Y-site volume. Such a deformation of Y site involves the distortion of edge-sharing Z(1) octahedron, the increase of Si-O-B average angle and the decrease of Si-O-Si angle. The increase in Mg content (up to 1.96(1) apfu), also ordered in Y site, results in strong decrease of cell volume (up to 565.21(4) Å^3), **b** cell edge, and Y-site volume. This deformation of Y site corresponds to a regularisation of the octahedron, as the two longest cation-oxygen bonds are reduced proportionally more than the shortest four. Iron is strongly ordered in Y site as Fe^{2+} in ferroaxinite (up to 1.61(2) apfu), while it was proved to be ordered in Z(1) site as Fe^{3+} in manganaxinite (up to 0.23(6) apfu). The presence of Fe^{3+} in Z(1) octahedron, usually filled by Al, may be a response to supergenic conditions in which manganaxinite usually crystallises and is also favoured by the Z(1)-site enlargement connected to Mn increase. According to SIMS measurements, B content is sometimes slightly deficient (up to 1.88(17) apfu), and for the same samples Si is in excess (up to 8.10(2) apfu). The good inverse correlation between B content and B-site volume suggested a partial Si occupancy of the B-deficient tetrahedral site, and lowered the uncertainty of quantitative determination of B by SIMS to 3% of the measured value.

A revised crystal-chemical formula of the axinite group minerals was compiled, containing the observed cation partition mechanisms:

$^{VI}[Ca_2(Ca_{1-x},Mn_x)_2(Mn,Fe^{2+},Mg,Al_y)_2(Al_{1-z},Fe^{3+}_z)_2Al_2]^{IV}[(B_{1-v},Si_v)_2Si_8]O_{30}(OH_{1-w},O_w)_2$

where VI and IV are C.N., and $0 \le x \le 1$, $y < 1$, $0 \le z \le 1$, $v < 1$, $w = y + v$.

CONTRIBUTION TO THE CRYSTAL CHEMISTRY OF GLAUCONITE

Weiszburg T.G. *(Dept. of Mineralogy, Eötvös L. University, Budapest, weiszburg@ludens.elte.hu)*, Pop D. *(Dept. of Mineralogy and Petrometallogeny, Babeş-Bolyai University, Cluj)*, Klencsár Z., Nagy S. and Kuzmann E. *(Dept. of Nuclear Chemistry, Eötvös L. University, Budapest)*

Crystal chemistry of glauconitic minerals is too complex to be characterized by only one analytical method. The structure models of glauconite are frequently tested by combined application of X-ray powder diffraction, Mössbauer spectroscopy and FTIR spectroscopy.

In our previous works we demonstrated the existence of a microenvironment in the glauconite structure characterized by quadrupole splitting (QS) values of 1.2-1.3 mm/s in the Mössbauer spectra of samples from Carpathian region. This observation was supported by all the different evaluation techniques we applied, e.g. parallel fitting of linear temperature dependence of the line shift of every subcomponent and determination of the quadrupole splitting distribution by using different software (Mosswinn of Klencsár, resp. Mossmod of Rancourt).

Based on their bulk chemistry, the samples studied are of dioctahedral character. According to the prediction of Drits *et al.* (1997) the effect of the second neighbours of octahedral Fe^{3+} in glauconite should not cause QS > 1.05 mm/s.

These results open the way for a combined crystal chemical interpretation of the glauconite structure, where besides the dominating Fe^{3+} and subordinate Fe^{2+} in cis positions both Fe^{3+} and Fe^{2+} occupy a part of the trans positions, producing a mixed (simultaneously trans and cis) vacant configuration. In the samples studied the trans:cis distribution of Fe^{3+} was around 1:10. We also tested the trans/cis vacant X-ray powder discrimination criteria proposed by Tsipursky and Drits (1984). They are not sensible enough for detecting the effect.

The model helps to interpret the Mössbauer spectrum of glauconite, where both the effect of the second neighbours and that of the cis and trans positions should be taken into account.

This work was sponsored by the grants #OTKA T025873 and #MKM FKFP 0111/1997.

MAGNESIOSTAUROLITE IN UHP ROCKS: A HP PHASE WITH SOME UNCOMMON FEATURES

Simon G. *(Dept. of Geosciences, Univ. of Potsdam, simon@geo.uni-potsdam.de)*, Chopin C. *(Dept. of Geology, Ecole normale supérieure, Paris, chopin@cristal.ens.fr)* and Czank M. *(Dept. of Mineralogy, Univ. of Kiel, czank@min.uni-kiel.de)*

Magnesiostaurolite is the Mg-dominant member of the staurolite group and is known from several occurrences. Near-end-member Mg-staurolite occurs exclusively as inclusions in pyrope megablasts from the coesite-bearing terrain in the Dora-Maira massif, Italian Alps.

Prograde magnesiostaurolites have X_{Mg} = Mg/(Mg+Fe) in the range 0.77-0.955, which are consistently lower than those of the coexisting garnet (X_{Mg} = 0.86 and 0.958, respectively). Their crystal-chemistry is characterized by the absence of tetrahedral Al, and about 25% occupancy by Mg in the normally vacant M(4) octahedra against only 70% occupancy in the T(2) tetrahedra (by Mg, Li and Fe) (Hawthorne *et al.* 1993; *Can. Mineral.*, **31**, 551-582). Li contents are quite variable but commonly low, in the range 250 to 390 ppm.

Some of these staurolites show domains remiscent of 'cross-hatched' twinning. Universal-stage measurements revealed one or two 'lamellar' systems, one of which is almost perpendicular to n_β and the other is rotated by 80-92° with respect to the first one.

TEM investigations show lamellae parallel (001) which are a few unit-cells thick and irregularly distributed. The clear presence of otherwise pseudoextinct 00*l* (*l* = 2n+1) diffraction spots indicates a different cation distribution within the lamellae. Other lamellae are parallel (100) and have various thicknesses (10 nm - 0.3 μm). They are in 'twin relation' with the matrix, however additional spots parallel a* indicate a new structural variant of staurolite with a superstructure having $\mathbf{a} = 2\mathbf{a}_{St}$. Interestingly, all these lamellae disappear under exposure to the electron beam, suggesting that proton ordering may be one of the reasons for the formation of these lamellae.

LOW SYMMETRY IN GARNETS: CAUSED BY ITS "WATER" COMPONENT ?

Andrut M. *(Inst. of Min. & Cryst., Univ. Vienna, Austria; a8601uaa@rs6000.univie.ac.at)*, Zeiske Th. *(Inst. of Min. & Cryst., Univ. Tübingen)*, Schulz R. *(GeoForschungsZentrum Potsdam)* and Krane H.-G. *(DESY, Hamburg)*

Garnets from Saranow/Ural Mountains are up to 1 mm in size with {110} shape. In thin section, crystals show strong birefringence with domains aligned according to crystal faces belonging to the form {110}. Microprobe analyses yielded a composition of $Uw_{75}Gross_{25}$ with only traces of titanium and iron. Element mapping showed a homogenous element distribution. HRTEM investigations gave no evidence of a deviation from cubic symmetry *Ia3d*.

In contrast, polarized Micro-Raman spectra recorded in the range 2000 to 100 cm^{-1} showed a polarization dependence of Raman modes parallel $[001]_{cub}$ in different domains. Polarized IR-spectra of one domain oriented parallel to (110) were measured in the OH vibrational region 3800 - 3400 cm^{-1}. Fourteen bands were detected. The linear extinction coefficients ranged up to 150 cm^{-1} and most of them show a strong dependence from the polarization direction. Temperature- dependent measurements at liquid nitrogen temperature show no further splitting of bands and only a slight energy shift. An X-ray data set was collected at the synchrotron source Hasylab/DESY at Hamburg using the Huber 4-circle diffractometer. The results show a monoclinic distortion of the lattice with equidistant lattice vectors equal *a*=11.9697 (12)Å but with β=90.139 (4)°.

Unlike previous investigations of hydrogrossular spectra the present results indicate that the hydrogarnet substitution is not the only possible mechanism of incorporating OH^-.

15. Recent Advances in the Crystal Chemistry of Rock Forming Minerals

CRYSTAL CHEMISTRY OF Li-BEARING MICAS FROM THE PIKES PEAK BATHOLITH, CENTRAL COLORADO

Brigatti M.F., Lugli C, Poppi L. *(Dept. of Earth Sciences, Univ. of Modena, Italy, brigatti@unimo.it)*, Foord E.E. and Kile D.E. *(U.S. Geological Survey, Denver Federal Center, USA, dekile@usgs.gov)*

Crystal structure refinements were performed on 14 1M micas showing wide chemical variations in octahedral sites ($0.34 \leq Li \leq .93$, $1.03 \leq Fe_{total} \leq 3.55 \leq$, $0.98 \leq {}^{[6]}Al \leq 2.04$ apfu, calculated on the basis of $O_{20}(OH)_4$). The crystals can be classified as zinnwaldite, Li-biotite and Fe-lepidolite. The samples occur in miarolitic pegmatites that formed within host granitic rocks of the Precambrian, anorogenic Pikes Peak batholith in central Colorado; they are associated with amazonite and smoky quartz for which the region is famous.

All crystals were studied by single crystal X-ray methods, and the refinements carried out in the space group *C*2 gave R_{obs} values between 2.72 and 3.82%. Results showed ordering of cations in octahedral cis sites, which leads to a lowering in the layer symmetry from the ideal *C*2/*m* to *C*2 space group. The ordering scheme of octahedral cations is meso-octahedral (*i.e.* one of the three sites is greater than the other two) or hetero-octahedral (*i.e.* all octahedra are different). In crystals where the Li content ranges from 1.22 and 2.41 apfu (zinnwaldite), the ordering scheme of octahedral cation is meso-octahedral, with M1≅M3>M2. Meso-octahedral ordering can be observed also for lepidolite (Li=2.93 apfu) in which M1≅M2>M3. Li-biotite, in which the Li content is low, display an hetero-octahedral order, with M1>M3>>M2, or a meso-octahedral pattern with M1≅M3>M2. In the last case, the mean <M2-O> bond length is greater (1.915 Å) than those observed for zinnwaldite crystals (<M2-O> ranges from 1.882 to 1.896Å). Furthermore, for all crystals analyzed, the two non-equivalent tetrahedra differ slightly in size (mean <T1-O> = 1.643Å, <T11-O>=1.639Å); this difference increases in hetero-octahedral biotites (<T1-O>=1.658Å, <T11-O>=1.637Å).

INTERLABORATORY COMPARISON OF TOURMALINE ANALYSES: MAJOR ELEMENTS INCLUDING B, Li, AND FE

Dyar M.D. *(Dept. of Geology and Astronomy, West Chester University, mddyar@amherst.edu)*, Guidotti C.V., Grew E.S., Yates M. *(Dept. of Geological Sciences, University of Maine)*, Delaney J.S. *(Dept. of Geological Sciences, Rutgers University)*, McGee J.J. *(Dept. of Geological Sciences, University of South Carolina)*, McGuire A.V. *(Dept. of Geosciences, University of Houston)*, Paul R.L. *(Nuclear Methods Group, N.I.S.T.)*, Robertson J.D, Cross L. *(Dept. of Chemistry, University of Kentucky)*, Sisson V.M. *(Dept. of Geology and Geophysics, Rice University)*, Wiedenbeck M.W. and Fowler G. *(Advanced Materials Lab, Univ. of New Mexico)*.

A suite of 22 optically homogeneous, naturally-occurring tour maline grains was analyzed for major elements including B using electron microprobe (EMPA) at four different labs, for B and Li by secondary ion mass spectrometry at UNM, and for $Fe^{3+}/\Sigma Fe$ synchrotron micro-XANES (NSLS, Brookhaven Natl. Lab). Splits of bulk sample were also prepared for B and Li analyses by proton-induced gamma-ray emission at UK; B by thermal neutron capture prompt gamma-ray activation analysis at NIST; H by uranium extraction; and $Fe^{3+}/\Sigma Fe$ by Mössbauer spectroscopy.

Results of up to 54 analyses per grain show average standard deviations (σ) of 0.59 wt% SiO_2, 0.71 wt% Al_2O_3, 0.13 wt% TiO_2, 0.61 wt% FeO, 0.05 wt% MgO, 0.02 wt% Cr_2O_3, 0.13 wt% CaO, 0.18 wt% Na_2O, 0.04 wt% K_2O, 0.12 wt% F, and 0.03 wt% ZnO. Zoning was observed in only a few samples. For wt% B_2O_3, σ values were 0.20 wt% for SIMS but varied from 0.20-0.74 wt% at the four different EMPA facilities. Agreement between the two methods for $Fe^{3+}/\Sigma Fe$ was excellent within the ±5-10% error estimated for both techniques. Poor agreement was observed among the methods for B analysis, suggesting a need for better standards, specialized analytical conditions, and, perhaps, revised matrix corrections for B. Until these problems are resolved, caution should be used in interpreting the details of any tourmaline analysis!

GEOCHEMISTRY OF AMPHIBOLE FROM HYBRID GRANITOID ROCKS OF RIO ESPINHARAS-PB PLUTON, NORTHEASTERN BRAZIL

Campos T.F.C. and Neiva A.M.R. *(Dept. of Geology of UFRN-Brazil, tcampos@geologia.ufrn.br and Dept. of Earth Sciences, Univ. of Coimbra -Portugal, neiva@gemini.ci.uc.PT)*

The Rio Espinharas-PB pluton consists of shoshonitic metaluminous diorite, hornblende-biotite quartz-monzodiorite, quartz-monzonites, quartz-syenite and peraluminous biotite granite, 606±33 Ma old, which have diffuse and interpenetrated contacts. Most of them are hybrid rocks, which resulted from different degrees of mixing of biotite granite magma with a dioritic magma as indicated by modelling of major and trace elements. The analysed amphiboles are magmatic. Most of the crystals are heterogeneous and their crystallographic orientations and chemical compositions are not related. They are mainly of magnesiohornblende, ferrohornblende, ferro-edenite, edenite and hastingsite. However some crystals have core either of ferrohornblende, magnesio- hornblende or of edenite and a rim of actinolite. A few crystals are mainly of actinolite with a thin rim of magnesiohornblende. Edenite-type and tschermakite-type substitutions were important. Some linear variations were found *e.g.* total Al, total Fe, K, Mg and Mg/(Mg+Fe) from hastingsite to actinolite versus Si. There is a general linear decrease in Cl, V, Nb and Li of amphibole versus increase in SiO_2 of rocks, showing a relationship between the evolutions of chemical compositions of amphibole and rocks. These amphiboles crystallised at 825-760°C and 6.8-5.8 kb.

HRTEM EVIDENCE FOR RETROGRADE EXSOLUTION IN PHENGITE-3*T* FROM THE DORA-MAIRA MASSIF (ITALIAN WESTERN ALPS)

Ferraris C. *(Inst. Mineral. Petr., Univ. Fribourg, Switzerland)* and Chopin C. *(E.N.S. Paris, chopin@euclase.ens.fr)*

Purely magnesian phengite-3*T* $(K_{0.94}Na_{0.02})(Al_{1.39}Mg_{0.60}Ti_{0.01})[Al_{0.4}Si_{3.6}]O_{10}(OH_{1.93}F_{0.07})$ occurs in the ultrahigh-pressure (30 ± 3 kbar, T = 750 ± 30°C) continental unit of the Dora-Maira massif (Western Alps), at Parigi near Martiniana Po. The outcrop is characterized by an assemblage of nearly pure pyrope garnet with kyanite, large phengite flakes and talc in a quartz matrix, in which coesite occurs as inclusions in garnet and kyanite and is partly inverted to quartz.

A systematic HRTEM and AEM study of phengite-3*T* samples was carried out in order to explain the presence of quartz and talc peaks in the mica X-ray powder diffraction patterns and of Mg anomalies in electron-microprobe WDS analyses. HRTEM images seen along [uv0] directions show the presence, at a nanometric scale, of quartz domains associated with talc layers in close proximity. The quartz domains show tabular forms parallel to the cleavage direction of mica, with rounded edges and no preferred crystal orientation. The talc interlayers are present as continuous domains about 19 Å thick (double layers). This occurrence can be correlated with optical observations which show the presence of late, small talc lamellae growing on the prismatic faces of phengite crystals. The absence of deformation in the phengite layers around the quartz inclusions, the direct contact between quartz and phengite and the contemporary presence of talc all suggest an exsolution origin from a more Si- and Mg-rich phengite (Ph1). A semiquantitative estimate from HRTEM images of the molar ratio between the phengite present in the sample (with the composition Ph2), quartz (Qz) and talc (Tc) is in agreement with the hypothesis of a destabilization of Si-Mg-rich phengite (Ph1) during decompression, in the α-quartz stability field, according to a reaction approximately of the type:

$$6\ Ph1 \rightarrow 4\ Ph2 + 1\ Tc + 5\ Qz + 2\ KOH$$

CATION ORDERING AND THERMAL EXPANSION IN $2M_1$ AND 3*T* MICAS BY NEUTRON DIFFRACTION - ROLE OF THE *TOT* LAYER STRUCTURAL DETAILS

Pavese A. *(Dip. Scienze Terra, Univ. Milano)*, Ferraris G., Ivaldi G., Pischedda V. *(Dip. Scienze Mineralogiche e Petrologiche, Univ. Torino, ferraris@dsmp.unito.it)* and Nespolo M. *(Min. Inst., Grad. Sch. Sci., Univ. Tokyo)*

It is often overlooked that the symmetry of the *TOT* layer in micas is not constant. Taking as basic structure the layer of the 1*M* polytype [*C*12/m(1) layer symmetry; s.g.*C2/m*; *M2* ≡ *M3*, *T1* ≡ *T2*], a *TOT* building layer with *C12(1)* real symmetry occurs in *3T* (s.g. $P3_112$; *M2, M3, T1* and *T2* independent sites). $2M_1$ polytype has s.g. *C2/c*, in which two independent T sites exist: the single layer real symmetry is C1. Besides, the effective coordination of the interlayer cation largely depends on the trigonal distortion and the O-H orientation is quite variable.

Temperature dependent powder neutron diffraction data collected from Mg-pure *3T* (Dora-Maira massif) and Fe-rich $2M_1$ (Valle Passiria) phengites, on HRPD (ISIS) and D2B (ILL) diffractometers, have been analyzed by the GSAS software package obtaining:

(i) 3*T* shows Al/Si/Mg cation order in the *M2/M3* and *T1/T2* sites throughout the 293 - 873K explored range of temperature. Orientation of O-H and chemical composition must also be considered.

(ii) $2M_1$ shows Al/Si order in *T1* and *T2* only at high temperature.

The present results imply different energetics for the independent *M* and *T* sites. On the basis of ours and others' previous results, it turns out that, while the bulk thermal expansion is left invariant through different polytypes, anisotropy varies considerably. Taking into account (1) the above mentioned symmetry, (2) anisotropy and (3) structural details, it descends that to attriibute differences between the so-called "basic mica polytypes" (1*M*, $2M_1$, 3*T*, and perhaps $2M_2$) to stacking only can be a misleading oversimplification, being these differences originated by causes rooted into energetics. In this context, it is sound that, *e.g.*, different phengite structures are *P/T* dependent.

CRYSTAL CHEMISTRY OF LANTHANIDE- AND ACTINIDE-RICH ACESSORIES FROM PERALUMINOUS GRANITES

Förster H.-J., Rhede D. and Tischendorf G. *(GeoForschungsZentrum Potsdam, Germany, forhj@gfz-potsdam.de)*

Compositionally heterogeneous Variscan granites of the German Erzgebirge contain a complex suite of REE-Y-Th-U-bearing accessory minerals (monazite, xenotime, uraninite, actinide orthosilicates, allanite, zircon, apatite *etc.*) which display extreme ranges in crystal chemistry at a variety of scales. These rocks, which comprise granites of transitional I-S-, S- and A-type affinity, are ideally suited to study the accessory mineral chemistry in peraluminous granites in general. *In situ* WDS-electron microprobe analyses document mineral compositions not previously reported from granitic rocks.

Monazite is the most compositionally diverse phase in terms of the lanthanides and actinides and their ratios. For example, even at the thin section scale, the brabantite mole fraction may vary over a range of more than 60%. Compositional data are consistent with complete miscibility in the monazite-(Ce) - brabantite solid solution series. Xenotime chemistry is strongly dependent on the type of host granite. Granites of S-type affinity contain xenotime with $(Gd\text{-}Ho)PO_4/(Er\text{-}Lu)PO_4$ close to 5, whereas those of A-type affinity may contain xenotime with ratios as low as 0.5, and a proportion of $HREE\text{-}PO_4$ approaching 45 mol%. Thorite accepts important substitutions (in mol%) of coffinite (up to 30), zircon (up to 50) and xenotime (up to 30) as well as brabantite, which reaches 30 mol% at a maximum. Uraninite may incorporate Th, Y, and the REE in total amounts between 1 and 29 mol%. However, its composition typically does not change significantly at the pluton scale. Important concentrations of lanthanide and actinide elements in a range of several wt% may be present in metamict zircons in more fractionated intrusions.

Mass-balance calculations imply that accessory minerals constitute the main contributors to the whole-rock lanthanide and actinide contents. However, the proportion of the whole-rock budget of these elements, which is contained in the individual minerals, is strongly dependent on the type of host rock and the degree of differentiation which a given granite has reached.

EPMA DETERMINATION OF TRACE ELEMENTS: REE AND METALS IN AMPHIBOLES AND CLINOPYROXENES. A RECORD OF METASOMATIC EFFECTS IN THE MANTLE.

Wagner C. *(CNRS-UPRESA 7058, UPMC, Paris cw@ccr.jussieu.fr)* and Fialin M. *(Centre CAMPARIS, Paris 6)*

Informations related to geochemical processes are retained at the scale of individual phases. Microanalytical techniques have thus become essential tools to perform major and trace element analyses on single grains.

A new electron-probe microanalysis (EPMA) procedure has been developed for trace element determination at concentration levels of about a few tenths of ppm in glasses and minerals. The improvment consists both in the acquisition and the processing of the data, with high excitation conditions, fractional counting time, careful background modelling and data statistical filtering.

We present EPMA data for LREE, Y and Zr in amphiboles and clinopyroxenes from metasomatic mantle nodules.

Amphiboles have been analyzed in a spinel lherzolite from the French Massif Central. The "composite nodule" shows a partial hornblendite selvage with pervading veins of amphibole + relict spinel within the peridotite. The major element composition of amphiboles varies in a regular fashion from the hornblendite to the peridotite. We have found similar variations in the trace element contents: La 39 ppm, Ce 86 ppm, Nd 53 ppm, Y 22 ppm, Zr 190 ppm in the hornblendite towards La 59 ppm, Ce 61 ppm, Nd 35 ppm, Y 16 ppm, Zr 24 ppm in the veins. Precision is 20-30% (2σ) and accumulated counting times of 4000s on 4 points per crystal. The progressive chemical variations could record some metasomatic effects of alkaline magmas on the mantle underlying the Massif Central.

Clinopyroxenes from alkali pyroxenites from North Morocco shows complex zoning both in major and trace elements. Traverse profiles (one point every 6-8 μm) in zoned crystals reveal a sharp compositional limit between the colorless diopside core and the pink Mg-richer diopside mantling zone. The latter is enriched in La (64/34 ppm), Ce (100/42 ppm), Nd (104/40 ppm), Y (29/12 ppm) and Zr (600/62 ppm), but shows a progressive decrease in these elements La, Ce, Nd (28, 36 and 57 ppm), Y (12 ppm) and Zr (377 ppm) towards its outer salitic rim. Such a zoning may record complex interactions between silicate (carbonate ?) fluid or melt within the mantle.

AN UNUSUAL CLINOPYROXENE - EARLY MINERAL OF THE ACHTARANDITE ROCKS FROM THE WILUY RIVER (YAKUTIA)

Galuskina I., Galuskin E. *(Dept. of Earth Sciences, Univ. of Silesia, galuskin@us.edu.pl)* and Winiarski A. *(Inst.of Physics, Univ.of Silesia)*

Al-rich diopside was discovered as a relic metacrystals in the hydrogarnet-serpentine rocks and as inclusions in vesuvianite and grossular metacrystals and in achtarandite. The Al-rich diopside and melilite paragenetic with it are indicators of high-temperature and low-pressure skarn process of primary achtarandite rocks formation. The Al-rich diopside is represented by short-prismatic, pseudopyramidal, light-green, whitish crystals up to 4 mm in size. Its main simple forms developed on the crystals are: {131}, {110}, {$\bar{2}$21} with the subordinate forms: {$\bar{2}$11} and {$\bar{4}$41}. According to the EMPA data we can distinguish two types of the subsilicic aluminian diopsides (Al_2O_3 up to 15.5 wt. %): 1 - with increased Ti^{4+} content - $Ca(Mg_{0.60}Al_{0.21}Fe^{3+}_{0.12}Ti^{4+}_{0.07})(Si_{1.53}Al_{0.47})O_6$ - inner part of crystal and 2 - with low Ti^{4+} content - $Ca(Mg_{0.59}Al_{0.24}Fe^{3+}_{0.16}Ti^{4+}_{0.01})(Si_{1.58}Al_{0.42})O_6$ - outer part of crystal. The later Al-Fe-poor diopside are substituted for the Al-rich diopside and also forms epitaxial growths on it. The diopside growing epitaxially is represented by clear diopside with the formula: $Ca(Mg_{0.98}Fe^{3+}_{0.02})(Si_{1.98}Al_{0.02})O_6$, whereas pseudomorphic diopside shows intermediate compositions. More fresh diopside from inclusions in vesuvianite is a mixture of two phases (C2/*c*) with following unit-cell parameters: 1) *a* = 9.716±0.004Å, *b* = 8.859±0.005Å, *c* = 5.277±0.002Å, β = 105.90±0.03°; 2) *a* = 9.75±0.01Å, *b* =8.89±0.01Å, *c* =5.294±0.006Å, β = 106.17±0.08°. Aluminium in the diopside is bound in three components: $CaAlAlSiO_6$, $CaFe^{3+}AlSiO_6$, $CaMg_{0.5}Ti^{4+}_{0.5}AlSiO_6$, sum of which often exceeds 40 mol.%. On the Wo-En-Fs diagram they plot in the area of pyroxenes having untypical composition.

15. Recent Advances in the Crystal Chemistry of Rock Forming Minerals

SUBSTITUTION OF VARIOUS CATIONS ON THE A- AND M4-SITE IN AMPHIBOLES

Gottschalk M., Melzer S., Andrut M., Najorka J. *(GeoForschungs Zentrum, Potsdam, gottschalk@gfz-potsdam.de)*

Cations covering a large range of ion radii can be incorporated into the A- and M4-sites in amphibole. Usually the A-site is either empty or occupied by alkali metals, the M4-site is filled with alkaline-earth metals, ferrous iron or by sodium in the case of richterite.

To study the structural and thermodynamic properties due to substitution of different cations on the A- and M4-sites systematically, amphiboles in equilibrium with various aqueous chloride solutions containing Na, K, Rb, Mg, Ca and Sr were synthesized. The obtained amphiboles, having the M123-sites always occupied by Mg, were solid solutions of the endmembers tremolite, cummingtonite, Sr-tremolite, richterite, K-richterite, Rb-richterite, described by $(\square,Na,K,Rb)^{A}(Mg,Ca,Sr,Na)_2{}^{M4}Mg_5{}^{M123}[Si_8O_{22}/(OH)_2]$.

The experiments were performed in more limited subsystems, however. Due to the size of the obtained crystals (width $\perp c$ >5μm), the compositions could determined precisely by electron microprobe analysis. The results showed that even amphiboles intended to be on a binary of two endmembers are mixtures of at least three components.

HRTEM investigations showed that the amphiboles were mostly free from chain multiplicity faults. The lattice constants are a linear combination of those from the endmembers and Vegards rule is obeyed. IR investigations showed that the OH-stretching band, which is a single band for endmembers, is split up for solid solutions studied here. As for M123-sites also specific configurations of the next neighbor A- and M4-site occupancies lead to different band positions. Two band systems can be distinguished, one for vacancies and one for alkalies on the A-site. Band positions corresponding to the configurations $Ca^{M4}\square^{A}Ca^{M4}$, $Ca^{M4}\square^{A}Mg^{M4}$, $Ca^{M4}\square^{A}Sr^{M4}$, $Sr^{M4}\square^{A}Sr^{M4}$, $Ca^{M4}Na^{A}Na^{M4}$, $Ca^{M4}Na^{A}Ca^{M4}$, $Ca^{M4}K^{A}Na^{M4}$ and $Ca^{M4}Rb^{A}Na^{M4}$ could be clearly identified. Within each band system the intensities are proportional to the probability of each configuration. Integral intensities of such bands can be used for the quantification of A- and M4-site occupancies. The results also imply that, at least for synthetic amphiboles, the $\square^{A}Ca^{M4} \leftrightarrow Na^{A}Na^{M4}$ exchange is decoupled, *i.e.* the replacement of Ca^{2+} by Na^{+} on M4 is not necessarily charge balanced by a Na^{+} on A in the next vicinity which has important implications for the mixing entropy. Because the compositions of the coexisting fluids were also measured, it was possible to determine thermodynamic properties for the A- and M4-site mixing.

Mn^{3+}-BEARING GARNETS AND HYDROGARNETS

Holtstam D. and Hålenius U. *(Dept. of Mineralogy, Swedish Museum of Natural History, dan.holtstam@nrm.se)*

The crystal chemistry of natural Mn-bearing garnets and hydro-garnets from high-$f(O_2)$ parageneses has been studied with chemical and spectroscopic (optical absorption, FTIR, Mössbauer) methods.

The anhydrous garnets (<0.1 wt.% H_2O) investigated, essentially spessartine-grossular-andradite in composition, are optically isotropic and show spectral characteristics in the visible and near infrared ranges that are related to variable amounts of Mn^{3+} located at the octahedral Y site of the garnet structure. Three Gaussian bands centred at 20800-19300, 18600-17100 and 9000-7000 cm^{-1} are ascribed to electronic *d-d* transitions. The pattern is incompatible with the formal symmetry of the Y site (C_{3i}); the deviation is most likely an effect of static or dynamic changes in the electronic structure of the Mn^{3+}-ion. Δ_O is calculated to around 15000 cm^{-1} for andradite and 15500 cm^{-1} for aluminous garnets (assuming D_{4h} point symmetry), which results in CFSE values in the range 151-166 kJ/mol.

The tetragonal hydrogarnets essentially belong to the hibschite-henritermierite series (31-77 mol.% $Ca_3Mn_2(SiO_4)_2(OH)_4$). Their spectra are characterized by four Gaussian bands present in both principal vibration directions at 23000, 21300, 19600 and 12200 cm^{-1}, consistent with the transitions expected for $Mn^{3+}O_4(OH)_2$-octahedra (site symmetry C_{2v}). Calculated values for Δ_O and CFSE are 15200 cm^{-1} and 182 kJ/mol, respectively. The gradual appearance of a broad OH-band in the IR spectrum at 3475 cm^{-1} is related to the Al-Mn^{3+} substitution.

The average integrated molar extinction coefficient for absorption due to Mn^{3+} in the visible spectral range of the cubic garnets is 7.9×10^4 $l.mol^{-1}.cm^{-2}$. The corresponding values for the hydrogarnets are 1.2×10^5 (E||O) and 1.9×10^5 $l.mol^{-1}.cm^{-2}$ (E||E).

THE SIGNIFICANCE OF ALUMINUM SUBSTITUTION FOR SILICON INTETRAHEDRAL SITES, GIVING RISE TO DEFECTS AND COLOR CENTERS IN SILICATE MINERALS

Greenidge D.C. *(Slippery Rock University)*

There are various reasons for color in minerals, such as impurity transition metal ions, missing ions and charge transfer. It is theorized that the purple color of amethyst is due to Charge transfer between interstitial Fe and trapped holes on oxygens in the structure of quartz, and that the smoky color is due to those trapped holes on the oxygens in the structure that are related to Al substituting for silicon in tetrahedral sites while there exists a deficiency of impurity Fe atoms. It can be stressed that these occurences reflect changes that occur in other silicate minerals due to the fact that there exists significant substitution of Al for Si in the tetrahedral sites. Due to this substitution, the likelihood of defects in the bonding of the surrounding oxygens caused by natural or artificial radiation is greater, thus giving rise to particular optical absorption band energies. Depending upon the atoms in the environment of the Al Substitution, different colors may arise in different minerals, but all may be related to the trapped holes at this Al tetrahedron. Upon heating of such minerals, surrounding trapped electrons may quench these sites, as may electrons provided by particular transition metals. This may result in an additional and permanent color change as in the case for topaz. Such conditions can be shown to be true for the minerals sillimanite, where Al substitutes for Si by as much as 50%, for kyanite, and beryl.

CRYSTAL FIELD STUDY OF Mn^{3+} IN DIASPORE

Hålenius U. *(Dept. of Mineralogy, Swedish Museum of natural History, ulf.halenius@nrm.se)*

As a consequence of strong Jahn-Teller effects trivalent manganese is stabilized in structures containing distorted cation sites. As a part of an ongoing crystal chemical study of Mn-bearing silicate and oxide minerals, room-temperature polarized optical absorption spectra of single crystals of Mn^{3+}-substituted diaspore (0.3 - 0. 5 wt.% Mn_2O_3) from Postmasburg, RSA, were recorded in the spectral range 333-2000 nm.

The spectra are characterised by four absorption bands (22650, 20600, 18400 and 6650 cm^{-1}) caused by spin-allowed electronic d-d transitions in Mn^{3+} at the six-coordinated M-site. The absorption bands are strongly polarised and the calculated molar extinction coefficients of these *d-d* bands attain values of up to 230 $l{\cdot}mole^{-1}{\cdot}cm^{-1}$. The calculated *10Dq*-value for Mn^{3+} in disapore, 17225 cm^{-1}, is considerably lower than in corundum, 19470 cm^{-1}, which is attributed to a decrease in effective ligand charge at the Mn-site. Furthermore, the appearance of the low-energy *d-d* band in the NIR spectral region reflects the decrease in symmetry of the Mn-centered site from C_3 in corundum to C_s in diaspore in combination with an increase in distances for the two longest Mn-O and Mn-OH bonds.

CRYSTAL STRUCTURE DATA OF BERLINITE, $AlPO_4$, AND MOLECULAR DYNAMICS SIMULATION

Kihara K. *(Dept. of Earth Sciences, Kanazawa Univ., Japan)* and Matsui M. *(Dept. of Earth and Planetary Sciences, Kyusyu Univ.)*

Berlinite ($AlPO_4$) has a trigonal (α)↔hexagonal (β) structure transition as in quartz. An intermediate phase has been also found. The α-phase structure has been well established, especially at room temperature. With increasing temperature, atomic equilibrium positions (α_1-position) move toward the midpoints (β-positions) of the lines joined to their Dauphiné twin positions (α_2). On the other hand, the "order-or-disorder" problem has still remained unsettled for the β-phase structures of quartz and berlinite. Our main objective of this study is to obtain an atomic view of the β-phase structure, using molecular dynamics simulation (MDS).

We performed the calculations for an NPT ensemble at different temperatures from 300 to 1500K using potential energy parameters in literature. The MDS cell includes 10800 atoms of the 300 orthohexa-gonal (600 hexagonal) cells. The results of MDS were compared with the X-ray structural data such as anisotropic temperature factors and coordinates parameters.

The positions of atom κ at time τ is expressed using the displace-ments, $\delta(\kappa,\tau)$, from its β-position. Then $\delta(\kappa,\tau)$ is divided by the room temperature value of the time average of $\delta(\kappa,\tau)$ to give a normalized displacement, $\eta(\kappa,\tau)$. The time averages of $\delta(\kappa,\tau)$ and $\eta(\kappa,\tau)$ are denoted as $\delta(\kappa)$ and $\eta(\kappa)$, respectively.

In the α phase, even far below the transition point, the histograms with $\eta(\kappa,\tau)$ as abscissas show two local maxima near ±1 of $\eta(\kappa,\tau)$ and a minimum at 0. On the other hand, the histograms for $\eta(\kappa,\tau)$ show narrow single peaks positioned at h between 0 and +1. With temperature approaching the transition, the second peaks begin to appear in the negative region of $\eta(\kappa,\tau)$, whereas the heights change from run to run. In the β-phase, the $\eta(\kappa)$ histograms show stable double peaks. Through all the cases treated here, the minima appeared at $\eta \approx 0$.

In summary, atoms stay for longer time around the room temperature positions or their α_2 positions than around the β-positions, even in the β-phase. No atom in the MD cell appear to prefers to stay at the β-position. We presume for the β-phase structure that atoms are grouped into two sets, which reside mainly in the α_1-sites and α_2-sites, respectively, each contributing one of the two peaks in the histograms. Analysis of the variables is underway to relate the individual atomic behaviors to phonon spectrum data.

CRYSTAL CHEMISTRY OF SYNTHETIC HIGH-PRESSURE STAUROLITE

Koch-Müller M. *(GFZ-Potsdam, mkoch@gfz-potsdam.de)*, Abs-Wurmbach I., Bubenik W. *(Inst. für Angew. Geowissenschaften I; TU Berlin)*, Gottschalk M. and Wirth R. *(GFZ-Potsdam)*

Staurolite (st) is a common rockforming mineral occurring in medium but also in high grade metamorphosed pelitic rocks. Mostly, st is Fe-rich and is grown at low to medium pressures. The average chemical composition for this st (coexisting with garnet) is best approximated by the formula: $[Fe^{2+}_{2.4}Mg_{0.8}Al_{0.4}\square_{0.4}]^{T2}$ $[Fe^{2+}_{0.2}\square_{3.8}]^{M4}[Al_{17.2}Mg_{0.4}Fe_{0.4}]^{M1-3}$ $[Si_{7.6}Al_{0.4}]^{T1}O_{48}H_3$. Mg-rich st only occurs in high-pressure regimes and its crystal chemistry differs from that of the Fe-rich low-pressure st primarily in a higher occupancy of M4 and a lower occupancy of T2. It is generally assumed that the increase in octahedrally coordinated two-valent cations in Mg- rich st is caused by the high-pressure condition of its formation. The aim of this crystal chemical study was to check this assumption.

Therefore, the structure and crystal chemistry of Fe-Mg st, synthesized at 20 - 25 kbar, have been investigated by microprobe analyses high-resolution transmission electron microscopy, X-ray powder diffraction in combination with Rietveld analyses, Mössbauer-spectroscopy and ^{27}Al-NMR spectroscopy.

The occupancies of the T2, M4 and M1-M3 sites of perfectly grown Fe- and Mg-st endmembers synthesized at high pressures have been determined as: $[Fe^{2+}_{2.9}Al_{0.6}\square_{0.5}]^{T2}[Fe^{2+}_{0.25}\square_{3.75}]^{M4}$ $[Al_{17.5}Fe^{2+}_{0.5}]^{M1-3}$ and $[Mg_{2.2}Al_{0.1}\square_{1.7}]^{T2}$ $[Mg_{0.9}\square_{3.1}]^{M4}[Al_{17.6}Mg_{0.6}]^{M1-3}$. Thus, Fe-st shows no increasing occupancy of the octahedral sites with pressure. Within the whole Fe-Mg st solid solution series there is a continuous substitution of Fe by Mg at the T2, M1 and M2 sites. But with increasing Mg-content 1 Fe plus 2 vacancies at M4 are replaced by 3 Mg in combination with a decrease of Al at T2.

PYROANION LINKAGE MODELS FOR FELDSPAR AND SILICA MINERALS

Kimata M., Nishida N., Shimizu M., Saito S. and Matsui T. *(Inst. of Geosci., Univ. of Tsukuba, kimata@arsia.geo.tsukuba.ac.jp)*

As a modern aspect of structural mineralogy, the concept of Pyroanion (Si_2O_7) Linkage Model (PLM) has been extended more generally for cleavage or habit in framework structures built from the linkage of coordination polyhedra. The availability of PLM analysis provides opportunities for tailoring the framework structures of silicates with feldspar chemistry. Incorporation of an eclipsed Si_2O_7 into the structure induces the more extensive range of its solid solution than that of a staggered one. An eclipsed Si_2O_7 always offers a potential for the framework silicates with more polymorphs or isotypes than a staggered configuration. Incorporation of the staggered Si_2O_7 pyroanions into the silica framework leads to difficulty in developing the cleavage or habit vertical to the Si-Obr-Si direction. On the contrary, the eclipsed Si_2O_7 pyroanions function as the basic parameter to yield the cleavage or habit with comparative ease. The evidence that by reference to the stable Si-O bond in quartz the eclipsed configuration has more unstable Si-Obr bond than does the staggered one is provided by chemical shift of X-ray SiKβ peaks detected by EPMA for several silicates. This is one material reason why appearance of the cleavage or habit occurs in minerals with framework-silicate structures. The new PLM work spans a significant portion of the breadth of mineralogy.

STRUCTURAL STATE OF K-FELDSPARS OCCURRING IN S-HUNGARIAN AND S-BOHEMIAN (AUSTRIA) GRANITOIDS

Lovas Gy.A., Buda Gy. and Háden S. *(Dept. of Mineralogy, Eötvös L. University, lovas@ludens.elte.hu)*

The Si/Al occupancy of the tetrahedral positions in the K-feldspars can be related to the genesis of the host rock. A possible approach to assess the structural state is via the accurate determination of the unit cell dimensions, since the related crystallographic measures are functions of the actual occupancy of the T_1o and T_1m sites. Symmetry changes are also reflected by optical properties (optical orientation, $2V_x$) and their actual values are also good measures of these changes.

Unit cell parameters determined by Rietveld analysis, derived site occupancies, n_{Or} ratios and $2V_x$ measurements are presented on feldspars from two geochemically similar Variscan granitoid areas that once formed a continuous belt of the Moldanubicum, but were later separated by plate motions; **1**. S-Hungary (Tisza Megaunit; Mecsek- Mts.), and **2**. Austria (S-Bohemian Pluton; Rastenberg, Weinsberg).

Granitoid of the first occurrence contains intermediate microcline in the groundmass. Megacrysts from the more basic variety of the rock, and at the rim of the granitoid body also show medium ordered structure, while the majority of the samples are maximum microclines. Zoned megacrysts of the Rastenberg-area are intermediate microcline with a slightly higher order at their rims relative to their cores, suggesting a gradually decreasing crystallization temperature. K-feldspars of the Weinsberg-type were found to be maximum microclines. The medium ordered structure of the K-feldspars in the ground mass, as well as in the megacrysts of the basic variety of the rocks suggests a higher crystallization temperature. The lower Si/Al order of the megacrysts occurring at the margin of the granitic body is likely due to a faster cooling rate. The ordered structure of the majority of the megacrysts suggests late crystallization at a lower temperature. The individual Rietveld treatment of feldspars provides true structure sensitive phase quantification for granitoids making the procedure superior to any traditional modal analysis.

Financial support of this research by HNRF (OTKA) projects T014969 and T023762 are greatly acknowledged.

15. Recent Advances in the Crystal Chemistry of Rock Forming Minerals

STRUCTURAL POSITION AND GEOLOGICAL SPECIFICITY OF SUBSTITUTIONAL V^{4+} IONS IN WAVELLITE

Lutoev V.P. *(Inst. Geol., Komi Sci. Centre, Ural Div., RAS, Syktyvkar, Russia, lutoev@geo.komi.su)*

Wavellite ($Al(PO_4)_2(OH)_3 \cdot 5H_2O$, *Pcmn*) is a widespread product of hypergenic low-temperature transformations of black shales, bauxites and other alumo-phosphate-bearing rocks. The mineral is characterized by a variable crystal structure, which essentially depends on the states of crystal water and hydroxyl groups. Paramagnetic ions may serve as indicators of such transformation and bear information on peculiarities of the mineralization process.

We identified two types of VO^{2+}-complexes in natural wavellite by the ESR technique. They arise as a result of substitution of Al-ions in two unequivalent sites of the wavellite structure. The double V=O bond of the first centre corresponds to the short Al-OH bond, parallel to the chains of [Al: 2·(H_2O)-2·(OH)-2·O]-octahedra. Direction of the double V=O bond of the second centre is similar to Al-H_2O direction in the equatorial plane of [Al: H_2O-2·(OH)-3·O]-octahedra. $VO^{2+}(1)$ and $VO^{2+}(2)$ behave differently under ionizing radiation and annealing, the former being more stable. Both centres disappear and a new $VO^{2+}(3)$-complex arises when the mineral loses water at heating. The spectroscopic parameters of the $VO^{2+}(3)$-complex vary at progressing annealing, reflecting the process of transformation of the wavellite structure.

The distribution of $VO^{2+}(1)$- and $VO^{2+}(2)$-complexes was studied on example of a Pai-Khoy (Russia) wavellite deposit, located in black shales and vein quartz. Concentration ratios of $VO^{2+}(1)$- and $VO^{2+}(2)$-complexes were found to strongly differ in some cases from the ideal ratio, 1:2. This ratio and the VO^{2+} concentration in general considerably increase away from the central zone of crystallization. These tendencies are attributed to the geological position of the wavellite zone and pH conditions at its formation.

EVIDENCE FOR A LOW-P-T ORIGIN OF COOKEITE POLYTYPES IN PELITES OF THE IBERIAN RANGE (SPAIN): A TEM STUDY

Mata P.[1], López-Aguayo F.[2] and Peacor D.R.[1] *([1]Dept. of Geological Sciences, University of Michigan, [2]Dept. of Mineralogy and Petrology. University of Cádiz, Spain)*

Occurrences of ordered polytypes of the dioctahedral Li-chlorite, cookeite, have previously been ascribed to a high-pressure origin on the basis of studies of natural material. Polytypism has been viewed by many investigators as a questionable indicator of stability relations, however. We found that cookeite is an important mineral in low-grade metapelites of the Cameros Basin, in northern portions of the Iberian Range, and we have therefore carried out a detailed study using SEM and TEM to determine its conditions of formation.

Cookeite occurs primarily as thin coatings on the surface of porphyroblastic pyrite crystals and intergrown with other phyllosilicates in the matrix of phyllites of epizonal grade. TEM images show that cookeite occurs as large (up to 1-2 μm thick) crystals relatively free of defects. Twinning by layer rotation commonly occurs every 50 to 300 layers. Strain in the form of bent, kinked and rotated packets giving rise to high-angle boundaries is common. Cookeite can also be found intergrown with *ca.* 70-nm thick packets of kaolinite, single 1-nm layers of paragonite and pyrophyllite, and packets of chamosite and berthierine. The relations are consistent with formation via hydrothermal fluids in a syn- to late-regional metamorphic environment. SAED patterns of cookeite display a wide range of stacking order-disorder, varying with streaking parallel to c* in k≠3n reflections to sharply defined reflections having one-, two- and >two-layer periodicities. Well-ordered polytypes up to 0.1 μm-thick occur, of the Ia type as determined by XRD. Chamosite likewise displays a range of order in polytypism from complete disorder to the well-ordered IIb polytype, typical of low-grade metamorphism. Pyrophyllite occurs as well-ordered polytypes.

Contrary to assertions that ordering in cookeite and chamosite are indicators of high-pressure metamorphism, the occurrence of both ordered and disordered polytypes in the same sample is compatible with the generally accepted notion that free energy differences between polytypes are too small to be indicators of conditions of stable equilibrium. The occurrence of well-ordered polytypes in this low-P environment is direct evidence that although ordered cookeite may occur in high-P environments, it is equally indicative of low-P environments, and so can not be used as an indicator of high pressure.

A NONSTOICHIOMETRIC PYROXENE SYNTHESIZED UNDER AMBIENT PRESSURE

Okui M. and Marumo F. *(Dept. of Geosystem Sciences, Nihon Univ., marumo@chs.nihon-u.ac.jp)*

Clinopyroxenes were synthesized from a silicate glass with the chemical composition 23 mol% $CaMgSi_2O_6$, 53 mol% $CaFeAlSiO_6$ and 24 mol% $CaAl_2Si_2O_8$ in the air under ambient pressure.The glass was pulverized and shared into platinum envelopes. The respective raw materials were heated with an electric furnace and kept at the prescribed temperatures for 90 h. Then, the products were quenched by dropping into ice-water. The crystals obtained after heating at 1350°C were stoichiometric ferrian aluminian diopside, to which chemical analysis with EPMA gave the composition $Ca_{1.00}Fe_{0.48}Al_{0.30}Mg_{0.19}(Si_{1.78}Al_{0.22})O_6$. On the other hand, the crystals grown at 1300°C and 1250°C were nonstoichiometric clinopyroxenes poor in Fe and Mg, having approximate compositions $Ca_{0.75}Fe_{0.15}Al_{0.87}Mg_{0.02}(Si_{1.55}Al_{0.45})O_6$ and $Ca_{0.75}Fe_{0.17}Al_{0.84}Mg_{.02}(Si_{1.58}Al_{0.42})O_6$, respectively.

Structure refinement of the nonstoichiometric clinopyroxene was carried out by utilizing a single-crystal obtained by slow cooling of a melt of the glass from 1400°C to 1000°C. The crystal is a C-clinopyroxene with the cell dimensions a=9.719(1), b=8.814(1), c=5.305(1)Å, and β=106.04(1)°. The least-squares iteration converged to give the weighted R value of 0.045 for 2678 reflection data. The chemical formula derived from the atomic populations at respective sites is $(Ca_{0.742}Fe_{0.087}\square_{0.171})(Al_{0.888}Fe_{0.075}Mg_{0.016}\square_{0.021})(Si_{1.500}Al_{0.500})O_6$. The amount of vacancy is quite large in the present crystal compared with those of previously reported nonstoichiometric pyroxenes.

Nonstoichiometric pyroxenes have been found exclusively from kimberlite to date, and were supposed to be a stable phase under high pressures. Actually, Wood and Henderson synthesized nonstoichio-metric clinopyroxenes from glasses with compositions on the joins $CaAl_2SiO_6$ - SiO_2 and $[(CaAl_2SiO_6)_{0.7}\ (CaMgSi_2O_6)_{0.3}]$ - SiO_2. Although nonstoichiometric clinopyroxenes reported in literatures have smaller cell volumes compared with those of stoichiometric clinopyroxenes with similar chemical compositions in conformity with their crystallization under high pressures, the present crystals have cell volumes comparable to that of diopside.

COMPOSITIONAL AND XRD CHARACTERISTICS OF GLAUCONITES FROM TRANSYLVANIA, ROMANIA

Pop D. *(Dept. of Mineralogy and Petrometallogeny, Babeş-Bolyai University, Cluj; danapop@hera.ubbcluj.ro)*, Weiszburg T.G. *(Dept. of Mineralogy, Eötvös L. University, Budapest)* and Bedelean I. *(Dept. of Mineralogy and Petrometallogeny, Babeş-Bolyai University, Cluj)*

Eight representative, thoroughly separated glauconite samples from Cretaceous, Eocene, Oligocene and Miocene green grain containing beds of Transylvania were submitted to wet chemical analysis and powder XRD. The d_{060} values (>1.510) and the calculated chemical formulae show that our samples are glauconites, as defined by AIPEA (Bailey, 1980); according to the K_2O content (6.1-8.5 %) they represent all the structural types: 1M, 1Md and interstratified glauconite-smectite (Odom, 1984). The almost ideal dioctahedral character is indicated by octahedral occupancy values between 1.97-2.06. According to the values of the Fe^{3+}/Al ratio, the studied samples could be classified in three groups: low-Fe^{3+} (<2), intermediate (~3-5) and low-Al (>9). These values slightly differ from those indicated in previous works (Goilo *et al.*, 1993) but are more suitable for defining distinctive chemical groups among our samples, certified also by chemical and structural-chemical plots.

Unit cell parameters do not show good correlation with the main cations contents. This feature is true even for parameter b, which is different from previous observations (Odom, 1976; Buckley *et al.*, 1978). OD parameters of glauconites (Sakharov *et al.*, 1990; Goilo *et al.*, 1993; Drits *et al.*, 1997), calculated from XRD patterns, oscillate and do not allow unequivocal characterization of the vacancy behavior (trans/cis) of the octahedral layers.

These characteristics were used for interpreting particular and general crystal chemical respectively mineralogical aspects of glauconite formation.

This work and its presentation were sponsored by: the Ph.D. grant and World Bank grant 87/1997 of the Ministry of National Education, Romania; OTKA #T025873; FKFP #0111/1997, Hungary.

15. Recent Advances in the Crystal Chemistry of Rock Forming Minerals

CATHODOLUMINESCENCE OF APATITES: NEW DATA ON POTENTIAL ACTIVATORS AND INHIBITORS AND THEIR BEARING ON GEOCHEMICAL INTERPRETATIONS

Blanc Ph. *(CNRS-ESA 7073)*, Perseil E. A. *(CNRS-ESA 7058, MNHN)*, Roger G. and Wagner C. *(CNRS-ESA 7058, UPMC, cw@ccr.jussieu.fr)*

CL images and spectra coupled with quantitative EPMA data are presented for natural F-apatites from various parageneses (granitic, hydrothermal and metamorphic) of Portugal (P) and Italy (I) in order to focus on the complexity of the CL interpretation. CL imagery was performed with a Technosyn MarkII device and a JEOL JSM 840A SEM. CL spectra were collected from 200-900 nm and processed with the Spectramax software.

Activators: Mn^{2+} and REE were found as main activators. The intensity of the CL emission can be correlated with the concentration of a given activator: apatites (P) from Sb-Au quartz vein show a gradual variation from grey to bright yellow color correlated with an increase in the MnO content up to 0.5 wt%. Similarly, apatites (P) from metamorphic phosphate-rich layer show a positive correlation between increasing intensity (x3) of the CL emission bands and higher Nd, Sm, Gd and Dy contents (up to 530 ppm). However, in apatites (P) from aplite, CL decreases and varies from yellow to brown when MnO+FeO contents are higher than 3 wt%, without any evident relation to FeO content alone or FeO/MnO ratio. The "well-known" inhibition role of Fe has to be further examined.

Inhibitors: We evidenced for the first time the role of As (replacing P) as a CL inhibitor in apatites (I): As decreases gradually the Mn^{2+}-induced CL, which is suppressed for 1 wt% As_2O_5. Some highly fractured apatite crystals with the highest As content (up to 9 wt%) are not luminescent. The fractures may record preferential paths for As-rich fluid circulation.

Co-activation and co-inhibition: ? Apatites (P, I) contain variable amount of Sr (up to 2 SrO wt%) which may be correlated with the CL color. The eventuality of Sr activation has to be tested. Apatites (P) from the Sb-Au quartz vein contain 230-410 ppm of Er, Tm, Pr. The CL spectrum do not reveal their presence, whereas it has been shown that these REE are individual activators.

Clearly the interpretation of apatite CL requires the investigations of synthetic multi-element doped apatites, which are in progress.

THE PROBLEM OF ORDERING IN THE VESUVIANITE STRUCTURE EVIDENCED BY VIBRATIONAL SPECTROSCOPY

Paluszkiewicz C. and Zabinski W. *(Academy of Mining and Metallurgy, Cracow, Poland, zabinski@geol.agh.edu.pl)*

Vibrational spectroscopy methods, *i.e.* FT-NIR, MIR and Raman spectroscopy, were used to confirm the existence of two structural forms of vesuvianite, differing in the state of ordering. This phenomenon concerns principally the arrangement of cations and vacancies occupying partially filled B and C positions on the four-fold axes and enables the distinguishing of high-temperature (above *ca.* 400°C), disordered structural variety and low-temperature ordered one. First reported on the basis of more sophisticated single-crystal X-ray investigations, it was previously observed also by the present authors when studying FTIR absorption spectra in the OH-stretching region, thermal decomposition of these mineral varieties and their EPR spectra. The existence of two above mentioned structural forms of vesuvianite was confirmed experimentally. After heating the sample of low-temperature vesuvianite (800°C, 20 hrs) both IR and EPR spectra changed distinctly towards those typical of high-temperature ones.

In this paper, the FT Raman and NIR spectra of several vesuvianites, reflecting also well the existence of above mentioned structural forms of vesuvianites, are presented. A Bio-Rad FTS 6000 spectrometer was used, with Nd-YAG laser system in the case of recording Raman spectra.

In the NIR region (4000-7500 cm^{-1}) two distinct groups of spectra can be distinguished, differing in the position of overtones and/or combination bands, corresponding to high- and low-temperature vesuvianites. Raman spectra of these two structural groups, recorded in the region 200-1200 cm^{-1}, differ in their quality (signal/noise ratio is distinctly lower in the case of high-temperature samples). The possible influence of some chemical components (first of all of fluorine) of vesuvianites on their vibrational spectra is discussed taking into account also the results of investigations of other authors.

This study was supported by KBN (Poland) grant # 6 P04D 019 11.

CRYSTAL CHEMISTRY OF ZEOLITES OF THE MERLINOITE FAMILY

Yakubovich O.V.*, Massa W.**, Kucherinenko Y.V.* and Pekov I.V.* *(*Dept. of Geology, Moscow Lomonosov State Univ., Russia, **Dept. of Chemistry, Philipp-Univ. of Marburg, Germany)*

The crystal structure of the rare zeolite merlinoite had been studied twice before. Our new attempt was caused by the high *R* factor values that characterized the previous works, on one hand and by the different chemical composition of the new found samples from the Kola Peninsula, Russia, on the other hand.

The orthorombic crystal structure of merlinoite is strongly pseudotetragonal: a = 14.084(3), b = 14.264(3), c = 10.112(2)Å. It is built by double eight member circles of Si,Al - tetrahedra to form the three dimensional open framework. Alkali cations (together with alkaline earths in some cases) and water molecules are the interstitial components.

Here we present the experimental results of X-ray crystal structure investigation of the pure alkali variety of merlinoite $(K,Na)_3Al_3Si_5O_{16}.6H_2O$: a=13.840(3), b=14.104(2), c=10.040(3)Å, sp.gr. *Immm*, Z=4, STOE IPDS diffractometer, λMoK_α radiation, R = 0.0406, σ=1.055 (1467 reflections with $F_o \geq 4\sigma$ (F_o)), T = 120K. The structure refinement was done with the supposition of pseudotetragonal twinning of our crystal.

Four independent interstitial positions were found for K^+ cations in the structure, three - for Na^+ cations and ten - for the water molecules. Only two of these positions in the framework cavities are ordered. The others are statistically occupied by the atoms.

The comparative crystal chemical analysis of the interstitial component distribution for different merlinoite varieties is presented.

This work was financially supported by the Russian Fund for Fundamental Investigations.

MULTIVARIATE ANALYSIS OF NATURAL GARNETS USING IR REFLECTANCE SPECTRA.

Zecchini P., Mérigoux H., Yamni K. *(Université de Franche-Comté, laboratoire de Cristallographie et Chimie Minérale, route de Gray, 25030 Besançon cedex France)*, Aurisicchio C. *(Centre di Studio per gli Equilibri Sperimentali in Minerali e Rocce, Consiglio Nazionale delle Richerche, Ple A. Moro, 5, 00185 Roma Italia)* and Grubessi O. *(Universitá La Sapienza, Laboratorio de Mineralogia, Ple A. Moro, 5, 00185 Roma Italia)*

Three different non destructive techniques are first applied to a selected set of cut natural garnets in order to determine their specie, their chemical composition and their lattice parameter. These techniques are the reflectance IR spectrometry, the microprobe analysis and X-ray diffraction. After that, a multivariate calibration can be applied. Two steps in the multivariate analysis are used: first, by applying the principal component analysis (PCA) method to the IR reflectance spectra of the calibration set, it is possible to dispatch the samples into their six normal species, pyrope, almandine, spessartine, uvarovite, grossular and andradite. By adding the other corresponding variables- the chemical analysis results and the value of the lattice parameter- to the IR data, and then, by using multivariate linear regressions (MLR), a model of natural garnet can be created. This created model and only the reflectance spectrum allow to determine the specie, the end member partition and the lattice parameter of unknown garnets.

PCA and MLR analyses do not need the pure end member of each class to create the model. For application of IR spectrometry, no particular preparation is necessary. Another advantage of this analytical method is that each new analyzed sample can be introduced as a complementary sample in the calibration sample set, so that, more samples are measured, more the calibration is reliable and more accurate analyses and lattice parameters can be obtained.

STUDY ON THE CONVERGENT-BEAM ELECTRON DIFFRACTION TO DISLOCATION OF QUARTZ

Zhao W.X. and Liu X.W. *(Center for Analysis of Mineral and Rock, China University of Geosciences, wxzhao@dns.cug.edu.cn)*

This paper introduces a method determining the Burgers vector $\bar{b}$ of dislocation in minerals by transmission electron microscope. The Burgers vector $\bar{b}$ of dislocation in minerals may indicate its conditions deformed. It provides the quantitative evidence for studying of the tectonic deformation.

The TEM is the unique method determining the Burgers vector $\bar{b}$ in minerals. Generally, two-beam method is applied for determination of the disappearance of dislocation line. By this method at least over 3 pieces of electron diffraction patterns are needed to determine the Burgers vector $\bar{b}$ of one dislocation.

The convergent-beam electron diffraction (CBED) is a technique developed recently in electron microscopy. It contains more information than the general electron diffraction. It is of unique advantages on studying of the micro-defect in crystal. When we determine the Burgers vector $\bar{b}$ of one dislocation we just need one piece of electron diffraction pattern. It provides the convenience for us to collect a vast amount of statistical data of dislocation in minerals.

In this paper the Burgers vector $\bar{b}$ of the dislocation in quartz has been determined with this method. The CBED pattern was indexed by the computer simulation figure of corresponding zone. The result shows quartz in this sample possesses two kinds of dislocation, $\bar{b}$ =1/6[1 $\bar{2}$ 10] and $\bar{b}$ =1/6[1 $\bar{2}$ 13]. According to the experimental result in quartz, these two kinds of dislocation were formed in high temperature ($\approx$ 700°C) and low strain rate (=$10^{-5}s^{-1}$) during the deformation process. This result agrees with the result by the general electron diffraction, and other evidence about deformed conditions.

As compared with the two-beam electron diffraction, this method is more convenient and useful.

16. Mineralogy of Alkaline Rocks

MINERALOGY OF HYPERALKALINE ROCKS: ADVANCES AND PROSPECTS

Khomyakov A. P. *(Inst. Miner. Rare Elem., Moscow)*

Nepheline syenite complexes with hyperalkaline (hyperagpaitic) pegmatites and hydrothermalites are superior in mineral diversity to all other rock associations. Their most striking examples are found in the Kola (Khibina and Lovozero), Gardar (Ilimaussaq), and Monteregian (Mont Saint-Hilaire) provinces. Between 1967 and 1997, these complexes yielded some 150 IMA-approved new minerals. The all-time list of new minerals discovered there includes about 200 entries. These discoveries have substantially extended our views on mineral diversity in alkaline rocks and the earth's crust as a whole, stimulating the development of many fields in theoretical and applied mineralogy.

The majority of these minerals represent previously unknown structural types and are dominated by complex, mostly persodic compounds. Their extraordinary diversity is largely controlled by the special ability of Na atoms to be distributed over many structural sites and form shape- and size-variable polyhedra with a unique range in coordination numbers, from 4 to 12. Another striking feature of these minerals is a prevalence of low-symmetry structures and a considerable predominance of triclinic species over cubic ones (tric/cub = 3.2). This is due mainly to the properties of alkali- and volatile-rich low-viscosity residual melts/solutions, which promote the formation of long-range ordering in boundary courts of crystals, lower the temperature, and markedly extend the temperature/time range of crystallization.

In addition to the approved minerals, hyperagpaites have been the source of dozens potentially new minerals, which are currently under study. These unique rocks will undoubtedly continue to make a growing contribution to the overall mineral system. It is also clear that, regardless of the source of new species, they will be increasingly dominated by microminerals, most of which crystallize after macrominerals at lower temperatures, thus being generally of lower symmetry. The change in the tric/cub ratio over the years speaks for itself: in 1891 (era of large crystals), it equalled 0.3, in 1966 0.6, in 1991 0.9, and is now steadily approaching 1.0. Based on correlation diagrams (number of species vs. time), it can be predicted that the overall number of known minerals will approach 11 000 by the year 2050, with the proportion of triclinic minerals increasing from the present 9.1 to 14.5% and the share of cubic minerals decreasing from 10 to 5%. The cubo-triclinic inversion of the mineral system is expected near 2005.

CRYSTAL CHEMICAL CHARACTERISTICS OF THE EUDIALYTE GROUP

Johnsen O. *(Geological Museum, University of Copenhagen, Denmark)* and Grice J.D. *(Research Division, Canadian Museum of Nature, Ottawa, Canada)*

Single-crystal structure refinements of twenty crystals representing the chemical variation of the eudialyte group are carried out in $R\bar{3}m$, $R3m$ or $R3$. The object of the study is to determine proper structural formulae based on site populations consistent with refined scattering values, mean bond-lengths and local bond-valence requirements.

The basic part of the eudialyte structure consisting of three-membered and nine-membered rings of SiO_4 tetrahedra cross-linked by octahedrally coordinated Zr is essentially uniform in composition. Al is almost non-present and Zr is only seldomly substituted by other cations, at the most up to 10% Ti. The M1 octahedra constituting six-membered rings by edge-sharing are mainly occupied by Ca. The major replacing elements are Mn and REE. In one case up to 70% of Ca is replaced by these elements in an ordered manner resulting in a loss of the mirror planes and thus reducing the symmetry to $R3$. The M2 site, horizontally combining the six-folded rings of M1 octahedra, accommodates four-folded Fe in the eudialyte end-members and five-folded Mn in the kentbrooksite end-members. In most eudialytes the M2 split sites are present simultaneously with a combined scattering power roughly corresponding to one fully occupied site with Fe/Mn. The M3 and M4 sites are located on the three-fold axes in the centers or nearby the centers of the nine-fold rings of SiO_4 tetrahedra. They are distinct sites in $R3m$ and $R3$ and symmetrically related in $R\bar{3}m$. M3 is designated the octahedrally coordinated site occupied by Nb as seen in kentbrooksite, while M4 designates a tetrahedrally coordinated site occupied by Si. The previously shown Nb ↔ Si correlation can in stereochemical terms be rewritten as M3M4 ↔ M4M4. The eudialyte structure is filled with Na in four-fold to eleven-fold coordination, adding up to 15 apfu. One Na site, Na4, appears to be especially well suited for accommodating heavier elements such as REE, Sr, K, Y and Ca. O19 is a key site as the fifth ligand in $^{[5]}$M2, the ligand completing the M3 octahedron and as part of the coordination of the Na4 site. The sof of O19 varies from < 0.2 to 1 and serves as a measure of the non-centrosymmetry of the eudialyte structure.

CARBONATE MINERALOGY, MONT SAINT-HILAIRE, QUEBEC, CANADA

Grice J.D. *(Research Division, Canadian Museum of Nature, Ottawa)*

At Mont Saint-Hilaire, Quebec, 56 carbonate minerals have been identified, as well as several unknowns. The crystal chemistry of these minerals gives an introspective into the crystallization history of this alkaline complex. Of the carbonates identified, 28 contain Na as an essential element, 17 others contain alkaline earths and 20 contain rare-earths. The more volatile components H and F are essential in 20 and 10 of the carbonate minerals respectively. In general the carbonate minerals at MSH have complex chemistries and crystal structures. The following 13 new carbonate mineral species described from MSH attest to the complexities of this intrusion; abenakiite-(Ce), calcioburbankite, caresite, charmarite, donnayite-(Y), horváthite-(Y), lukechangite-(Ce), petersenite-(Ce), quintinite, reederite-(Y), rouvilleite, sheldrickite, and thomasclarkite-(Y).

During crystallization of nepheline syenite rocks the alkali and water concentrations increase. The alkali increase is exemplified by increasing amounts of Na silicates, Na carbonates and light REE minerals. At Mont Saint-Hilaire the late stages of crystallization would be in the pegmatite/altered pegmatite rocks, miarolitic cavities, breccia in-filling and sodalite xenoliths. It is in these occurrences that natrite, natron, trona, and thermonatrite are found often coexisting with REE- and fluoro-carbonates. These minerals certainly correspond to the maximum alkalinity stage observed in the Khibina and Lovozero massifs, Kola Peninsula. The final acidic phase of the Kola massifs is not as clearly defined at Mont Saint-Hilaire. Although zeolites and highly-hydrated Y carbonates of Mont Saint-Hilaire, indicative of the final acidic phase, are certainly very late in the crystallization sequence, being most commonly found in the pegmatite/altered pegmatite rocks, they are still associated with Ce carbonates and the basic Na carbonates which are considered more indicative of the maximum alkalinity stage.

THE CRYSTAL CHEMISTRY OF ASTROPHYLLITE-GROUP MINERALS FROM MONT SAINT-HILAIRE, QUEBEC.

Piilonen P.C., Lalonde A.E. *(Ottawa-Carleton Geoscience Centre, Dept. of Geology, Univ. of Ottawa)* and McDonald A.M. *(Dept. of Earth Sciences, Laurentian University, Sudbury).*

The crystal chemistry of 35 specimens of astrophyllite-group minerals from the peralkaline East Hill Suite at Mont Saint-Hilaire, Québec were studied by *EMPA* and Mössbauer spectroscopic methods. Samples show complex zoning, wide variations in chemistry, and significant departures from ideal stoichiometry ($A_3B_7C_2D_8X_{31}$), a reflection of the highly heterogeneous conditions which prevailed at the time of crystallization and the ability of this group of minerals to incorporate a wide range of cations. Two distinct solid-solution series are observed: (1) between astrophyllite (sensu stricto) and a potentially new Fe-dominant zircophyllite species characterized by the dominance of Fe^{2+} in the *B*-site, enrichments in K, Ca, Sr, Mg, and Al, and complete substitution of Zr for Ti in C; and (2) between kupletskite and a second potentially new species, Mn-dominant niobophyllite, characterized by the dominance of Mn within the octahedrally-coordinated B-site, enrichments in Na, Rb, Ce, Zn, F, and Si, and complete substitution of Nb for Ti in C. Preliminary Mössbauer spectroscopic studies indicate lower Fe^{2+}/Fe^{3+} ratios within the kupletskite - Mn-niobophyllite series, with both Fe^{2+} and Fe^{3+} in octahedral coordination. Concentric zoning in individual crystals indicates compositional changes from astrophyllite or kupletskite proper towards the Zr and Nb end-members with progressive fractionation. Substitution schemes for both series are proposed with an emphasis on the crystal chemical effects of Ti-Zr-Nb partitioning between the two solid-solution series.

16. Mineralogy of Alkaline Rocks

THE CRYSTAL STRUCTURE OF UK92, A POTENTIALLY NEW SILICOBORATE FROM MONT SAINT-HILAIRE, QUEBEC, WITH COMMENTS ON LAYERED ALKALI SILICATES OF THE REYERITE MESOTYPE SERIES

McDonald A.M. *(Dept. of Earth Sciences, Laurentian University, amcdonal@nickel.laurentian.ca)*

UK92 is an extremely rare, paragenetically late-stage mineral discovered in sodalite syenite xenoliths at Mont Saint-Hilaire (MSH), Quebec, in association with eudialyte, villiaumite, erdite and lovozerite-group minerals. It occurs in lavender to colorless pseudohexagonal plates up to 50 μm across and less than 10 μm thick with a perfect {010} cleavage. Its structure has been solved by direct methods using single-crystal X-ray diffraction data, and refined to $R = 6.0\%$ and $wR^2 = 14.6\%$. Results from the structural analysis confirm the mineral is triclinic, probable space group $P\bar{1}$, and when combined with data obtained from *EMPA* methods, suggest the ideal chemical formula, $(Ca,Na)_6(Na,Ca)_7(Si,S)_{14}B_2O_{38}(OH,F,Cl)\cdot 6H_2O$.

The mineral is layered parallel to (010). Its structure is dominated by a tetrahedral layer, S_1, composed of six-membered rings of SiO_4 tetrahedra cross-linked along (100) and (001) by SiO_4 and BO_4 tetrahedra. Two centrosymmetrically related S layers (S_1,$\bar{S}_1$) are indirectly linked along (010) through a closest-packed octahedral layer (O) composed of edge-sharing CaO_6 and NaO_6 polyhedra. The S_1-O-$\bar{S}_1$ composite units are weakly joined along (010) *via* an interlayer sheet (X) containing $NaΦ_5$ (Φ = unspecified ligand) and H_2O groups.

The structural scheme for UK92 may be described as $OS_1X\bar{S}_1O$. UK92 is a member of the polysomatic-like series termed the *reyerite mesotype series*, which includes the layered alkali silicates, gyrolite, fedorite, truscottite, UK57 (another potentially new mineral from MSH), and reyerite. The structures of these minerals are all based on the reyerite module ($S_1OS_2\bar{S}_2\bar{O}S_1$), which can be modified to include an interlayer module (X), various alkalis/ alkaline earths (K,Na,Ca) in O, and single or double tetrahedral sheets, these modifications being a function of the geochemical conditions of formation.

MODULARITY IN MINERALS OF THE HYPERALKALINE ROCKS: JUST CLASSIFICATION CATEGORIES OR GENETIC MECHANISMS?

Ferraris G. *(Dept. Sci. Mineral. Petrol. Univ. Torino, Italy, ferraris@dsmp.unito.it)*

The role of complex structural modules in some title minerals shall be discussed also on the basis of the contributions presented at the Session *Mineralogy of Alkaline Rocks*. The unique geological environment which characterizes the hyperalkaline rocks is the ultimate reason for the impressive occurrence of several hundreds of species in a handful of outcrops of these rocks (about 200 species are peculiar of them); however it is of general interest to investigate the role of crystal-chemical mechanisms which materialize into species the peculiar geochemical and geophysical processes.

Besides classical crystallochemical tools (as isomorphous replacement, flexibility in coordination of the alkaline cations, polymerization of coordination polyhedra), the application of the concepts of modular crystallography [*cf.* Merlino S. (ed.): *Modular aspects of minerals*. Eötvös Univ. Press, Budapest 1997] shows that some complex structural modules repeatedly occur in different minerals and generate species through mechanisms as:

1. isomorphism within the same module;
2. filling cavities, channels and interlayer space by different fragments (merotypic series);
3. combination and polymerization of modules (polysomatic and homologous series, polytypism);
4. variable connections of the same module(s) (plesiotypic series);
5. "polymorphism" and/or change of details of a basic module;
6. combination of the previous mechanisms.

As in the classical classification of the silicates, groups, chains, nets and frameworks are not simply crystallochemical labels but often they may be connected with the genetic environment, the same is becoming clear for the complex modules mentioned above.

ALKALINE - PHOSPHATE BLOCKS IN THE CRYSTAL SRUCTURES OF MINERALS OCCURRING IN THE HYPERALKALINE ROCKS OF KOLA PENINSULA

Sokolova E.V. *(Fac. of Geology, Moscow State Univ.)*, Ferraris G. *(Univ. of Torino)* and Khomyakov A.P. *(Inst. Miner. Rare Elem.)*

Residual fluids supersaturated with alkalis and volatiles give rise to a number of minerals where phosphate-alkaline blocks play an important role stabilizing the crystal structure. In recent years, a number of titanosilicate-phosphates with two types of blocks or modules (titanosilicate and phosphate) have been described in the hyperalkaline rocks of Kola Peninsula. Several phosphate mineral structures are based on the same type of module.

Nacaphite $Na_2Ca[PO_4]F$ is an alkaline phosphate from the Khibina massif: $a=10.654(4)$, $b=24.443(6)$, $c=7.102(2)$Å, $\alpha=89.99(2)$, $\beta=90.01(2)$, $\gamma=90.01(2)°$, sp.gr. $C1$, $z=16$. In the nacaphite structure, (Na,Ca)-polyhedra and $[PO_4]$-tetrahedra constitute a framework. Two types of modules have been identified in the nacaphite structure. Module I of nacaphite (NI) has pseudoorthorhombic symmetry and dimensions of about 7.1 × 5.3 × 6Å. The titanosilicate members of a merotype series seidozerite-nacaphite (18 minerals), contain the same seidozerite module, whereas corresponding to NI interlayer contents are either absent or represented by alkalis and/or alkaline earths plus/or H_2O, SO_4 or PO_4. Nacaphite module II (NII) has pseudo-hexagonal symmetry and dimensions of 7.1 × 7.1 × 5.3Å. It occurs in the crystal structure of a synthetic nacaphite dimorph $(Na,Ca)_4(Ca,Na)[PO_4]_5F_5$ ($a=7.0179(1)$, $c=40.5653(4)$Å, sp.gr. $R3m$, $z=3$) together with NIII module. NII and NIII modules have been established in the arctite $(Na_5Ca)Ca_6Ba(PO_4)_6F_3$ (sp.gr. $R\bar{3}m$, $z=1$) structure. Possible discovery of natural nacaphite dimorph is discussed.

Phosphate block has been playing an important role of protostructure for transformation minerals, which form on hydration of high temperature titanosilicate-phosphates: lomonosovite → murmanite.

CL AND TEM INVESTIGATION OF ZIRCONOSILICATES IN THE SUBSOLVUS GRANITE OF THE STRANGE LAKE PERALKALINE COMPLEX, QUEBEC-LABRADOR, CANADA.

Roelofsen J.N. and Veblen D.R. *(Dept. Earth and Planetary Sciences, Johns Hopkins Univ.)*

The origin, whether primary (magmatic) or secondary (Ca-metasomatic after elpidite $[Na_2ZrSi_6O_{15}\cdot 3H_2O]$), of the Ca-rich zirconosilicates armstrongite ($CaZrSi_6O_{15}\cdot 3H_2O$) and gittinsite ($CaZrSi_2O_7$) in the subsolvus granite of the Strange Lake peralkaline complex on the Quebec-Labrador border in Canada has been a well-debated topic. These zirconosilicates, along with zircon, account for much of the Zr in the associated ore deposit (50 million tonnes of 2.93% ZrO_2, 0.54% REE, 0.31% Y_2O_3, 0.38% Nb_2O_5, and 0.08% BeO). Cathodoluminescence (CL) examination and transmission electron microscopy (TEM) have been used to shed light on the relationships among and origin of these zirconosilicates. Optical and CL observations indicate that elpidite is replaced by armstrongite and, subsequently, by gittinsite. This gittinsite is generally associated with quartz and variable amounts of hematite. TEM results suggest the bulk replacement of elpidite by poorly crystalline armstrongite, followed by gittinsite and quartz, or zircon and quartz. Inclusion of minute amounts of these Ca-rich zirconosilicates in elpidite increases its apparent Ca content, as determined from electron microprobe analysis. Moreover, the enrichment of gittinsite in Mn and some of the armstrongite in Y, as determined by analytical electron microscopy, correlates with the presence of these elements in the Ca-metasomatic fluid. In conclusion, the primary, magmatic elpidite is replaced by armstrongite and, subsequently, gittinsite and quartz during Ca-metasomatism of the complex.

16. Mineralogy of Alkaline Rocks

CRYSTAL-CHEMISTRY OF 10 NATURAL *C2/c* PYROXENE PHENOCRYSTS FROM KAMAFUGITIC ROCKS OF KATWE-KIKORONGO (SW-UGANDA, AFRICA)

Princivalle F., Greblo S., Piccirillo E.M. *(University of Trieste, princiva@univ.trieste.it)*, and Cundari A. *(University of Napoli)*

C2/c pyroxene phenocrysts from perowskite-bearing kamafugitic rocks from Katwe-Kikorongo (SW Uganda, Africa) were studied by means of single-crystal X-ray diffraction and microprobe analyses.

The clinopyroxenes correspond to diopsides and are characterised by Si+Al deficiency in the tetrahedral site, whose complete occupancy was ensured by Ti. Ti entry in T site, in addition to Si+Al, is quite common in *C2/c* pyroxenes crystallised from potassic magmas.

The investigated clinopyroxenes typically show the lengthening of both T-O bridging and <M2-O3> bond lengths, with respect to cpx crystallised from sodic alkaline melts. It should be noted that the M2-O3C2 bond lengths are, in spite of the very high Ca content, close to those of the synthetic diopside.

Using the barometer of Nimis (1995), which compares the cell and M1 volumes, the studied cpx fall in a pressure field corresponding to a crystallisation regime lower than 5 Kb., even for cpx core megacrysts, sometimes believed crystallised at mantle pressure.

Finally, it is remarkable that considering cpx crystallised from strongly potassic melts, the studied cpx show the presence of Ti in T site and a structural configuration like to pure diopside.

UNUSUAL Zr- AND Sn-RICH TITANITE IN ASSOCIATION WITH BARATOVITE AND ZIRCON FROM THE DARA-I-PIOZ COMPLEX, TAJIKISTAN

Reguir E.P., Chakhmouradian A.R. *(Department of Geology, Lakehead University, Thunder Bay, Ontario)* and Evdokimov M.D. *(Department of Mineralogy, St. Petersburg State University, St. Petersburg, Russia)*

The Dara-i-Pioz complex comprises a variety of granitic and syenitic rocks emplaced in carbonate sedimentary rocks and shales of Middle-to-Late Paleozoic age. The youngest igneous lithologies at Dara-i-Pioz are alkaline pegmatites and albite metasomatic rocks hosting a broad spectrum of rare Ti-, Zr-, B- and Li-bearing minerals.

Titanite of unusual composition was found in association with baratovite, zircon, datolite, albite, fluorite, microcline and quartz in an albite rock, possibly developed after alkaline syenitic pegmatite. Titanite, zircon and datolite fill fractures within the early minerals, including baratovite. Crystals of titanite are zoned, with relatively uniform Zr- and Sn-depleted cores $[Ca_{1.00}(Ti_{0.87}Sn_{0.01}Fe_{0.06}Al_{0.04})\ (Si_{0.97}Al_{0.03})O_{5.00}]$, and oscillatory-zoned Zr- and Sn-rich rims $[Ca_{0.99}(Ti_{0.80}Sn_{0.11}Zr_{0.04}Fe_{0.03}Nb_{0.02})(Si_{0.98}Fe_{0.02})O_{5.00}]$. From the core toward the rim, there is a negative correlation between (Sn, Zr)O_2 and $(Al,Fe)_2O_3$. Baratovite is characterized by Ca-depletion coupled with enrichment in Li, similar to baratovite ("katayamalite") from Iwagi Islet, Japan. The structural formula of baratovite is $(K_{0.87}Na_{0.13})Li_{2.94}(Ca_{6.84}Na_{0.06}Mn_{0.03}Zr_{0.07})(Ti_{1.93}Fe_{0.05}Zr_{0.03})Si_{12}O_{37}(F,OH)$. Zircon, datolite and other minerals occuring in the paragenesis with titanite, are close to their ideal compositions.

The combination of high Zr and Sn in the composition of titanite reflects an unusual geochemical specialization of parental alkaline magma at Dara-i-Pioz. The crystallization of titanite plus zircon in intimate paragenesis with datolite suggests a dissociation of R^{4+}-borate complexes at the late stages of albitization.

RE-FREE AND RE-POOR BURBANKITE FROM PECTOLITE METASOMATITES: CHEMICAL COMPOSITION AND CRYSTAL STRUCTURE REFINEMENT

Belovitskaya J.V., Pekov I.V., and Kabalov Yu.K. *(Dept. of Geology, Moscow State University, mineral@geol.msu.ru)*

RE-free and RE-poor burbankite specimens from pectolite metasomatites of two alkaline massifs: Murun (Yakutia) and Khibiny (Kola peninsula) were examined. Their composition: $(Na_{1.96}Ca_{0.99}Y_{0.02})_{2.97}(Sr_{2.52}Ca_{0.37}Ba_{0.11})_{3.00}(CO_3)_5$ (Murun; associates with charoite); $(Na_{1.82}Ca_{1.02}Y_{0.02})_{2.86}(Sr_{2.32}Ba_{0.43}Ca_{0.17}La_{0.06}Ce_{0.02})_{3.00}(CO_3)_5$ (Khibiny; associates with fluorite, biotite, and sphalerite). Burbankite from Murun is the REE-free end-member $(Na_2Ca)R^{2+}_3(CO_3)_5$, R^{2+}=Sr, Ba, Ca, first discovered in nature.

X-ray powder patterns of the burbankite with such composition contain pairs of reflections (hkl: 011 & 110; 012 & (121+030); 112 & 031; 132 & (231+140); 033, 231 & 051; 242 & 060; 341 & 250 *etc.*) which are not distinguished in the X-ray diagrams of ordinary burbankite. The crystal structure of burbankite was refined by the Rietveld Method for sample from Niorkpakhk Mt., Khibiny (R_{wp}=4.49%, anisotropic; a=10.5263(1), c=6.5392(1)Å). Burbankite with more typical composition $(Na_{2.22}Ca_{0.65}Y_{0.03})_{2.90}(Sr_{2.10}Ba_{0.33}Ce_{0.23}Ca_{0.15}La_{0.12}Nd_{0.05}Pr_{0.02})_{3.00}(CO_3)_5$ from hyperalkaline hydrothermalite (Kukisvumchorr Mt., Khibiny) was studied for comparison (R_{wp}=3.23%, a=10.5313(1), c=6.4829(1)Å). The space group $P63mc$ is confirmed for both samples. Thus the "splitting" of reflections can be explained only with unit cell parameters ratios (c/a).

EVOLUTION OF THE ACCESSORY Sr-LREE AND Ti-Nb MINERALIZATION IN NEPHELINE SYENITE AT PEGMATITE PEAK, MONTANA

Chakhmouradian A.R. and Mitchell R.H. *(Department of Geology, Lakehead University, Thunder Bay, Ontario)*

The nepheline syenite at Pegmatite Peak (Montana) is a medium-to-coarse-grained mesocratic rock with panidiomorphic texture. The rock consists of large (up to 5 cm) crystals of microcline and altered nepheline set in aegirine. Nepheline is replaced by a fine-grained assemblage of muscovite, analcite and phillipsite. Nepheline, microcline, biotite plus accessory zircon, magnetite, and rutile represent the early miaskitic assemblage in the pegmatite. Primary repositories for Sr, *LREE* and Nb are Ce-Th-pyrochlore and loparite. Ce-Th-pyrochlore occurs as inclusions in loparite. The latter compositionally evolves from strontian calcian (15-20 wt.% SrO, 2-4 wt.% CaO) to niobian loparite (16-18 wt.% Nb_2O_5). Other important *LILE*-bearing phases are crichtonite and Ba-"hollandite" developed as discrete crystals or reaction rims on rutile. The crystallization of aegirine corresponds to the agpaitic stage. Fine-grained fibrous and radial aegirine is commonly intergrown with platy lamprophyllite. This assemblage also includes $(Fe,Mn)TiO_3$ phases, titanite and strontio-chevkinite. Strontio-chevkinite and titanite are found mostly in fractures within loparite. Titanite is zoned towards Na-, Nb- and *LREE*-enriched compositions (up to 2 wt.% Na_2O, 6 wt.% Nb_2O_5 and 4 wt.% $LREE_2O_3$). Strontio-chevkinite (up to 20 wt.% SrO and 37 wt.% $LREE_2O_3$) evolves by depletion in Sr and enrichment in LREE.

The youngest mineral assemblage includes ancylite-(Ce) and Sr-apatite (up to 17.2 wt.% SrO) occurring interstitially. These minerals precipitated from residual fluids enriched in Sr and *LREE*. The following three stages can be distinguished in the evolution of Sr-*LREE* and Ti-Nb mineralization in the nepheline syenite: (i) primary (oxides); (ii) agpaitic (silicates), and (iii) hydrothermal (carbonates and phosphates).

16. Mineralogy of Alkaline Rocks

MICROHETEROGENEITY AND STRUCTURE ORDERING IN APATITE GROUP MINERALS: IR SPECTROSCOPIC INVESTIGATION

Chukanov N.V. *(Institute of Chemical Physics in Chernogolovka, Russia, adpomog@icp.ac.ru)* and Pekov I.V. *(Dept. of Geology, Moscow State University)*

Two series of apatite group minerals have been studied: RE-bearing and OH-enriched.

One can distinguish two subgroups among RE-bearing apatite-like minerals: RE-dominant members - belovite-(Ce), belovite-(La) (Pekov e.a., 1996), and deloneite-(Ce) (Khomyakov e.a., 1996) and minerals with lower REE content - fluorcaphite (Khomyakov e.a., 1997) and RE-varieties of fluorapatite. According to the data of IR spectral contour analysis, the second subgroup includes several types of "RE-apatites." 1. "Saamite" from Lovozero alkaline massif, Kola peninsula (Na_2O 0.8, SrO 9.5, REE_2O_3 4.1% wt.), is fluorapatite containing microclusters (<0.n mm) of belovite-(Ce). 2. Sr-poor "NaRE-apatite" from Ilimaussaq alkaline complex, South Greenland (Na_2O 3.1, SrO<0.1, REE_2O_3 16.7%) (Roensbo, 1989), is fluorapatite containing clusters with belovite-like structure, perhaps "calciobelovite," $Ca_3NaREE(PO_4)_3F$. 3. Fluorcaphite from Khibiny alkaline massif, Kola peninsula (Na_2O 1.6-1.9, SrO 19-21, REE_2O_3 9.3-13.5%), seems to be homogeneous.

Splitting of the band of O-H-stretching vibrations (the region 3500-3600 cm^{-1}) in IR-spectra of OH-bearing apatite-like minerals is appeared when OH-group content exceeds 1 per unit cell. This effect was observed for hydroxylapatite, hydroxylellestadite, and johnbaumite. This (OH)-band splittering can be explained by existence of non-equivalent positions of OH-groups in apatite-like structures. It is very likely that symmetry lowering for some OH-rich apatite-like minerals is the reason of such splitting.

GENTHELVITE FROM ITAPITANGUI, SÃO PAULO, BRASIL

Coutinho J.M.V. and Oliveira M.C.B. *(Inst. Pesq. Tecn. S.P. IPT/SP)*, Atencio D. and Carvalho F.M.S. *(IG-USP)*

Genthelvite, $Be_3Zn_4(SiO_4)_3S$, cubic, is a rare mineral of the helvite group, which also includes helvite $Be_3Mn_4(SiO_4)_3S$ and danalite, $Be_3Fe_4(SiO_4)_3S$. Genthelvite forms solid solution with danalite, but not with helvite (Dunn, 1976). Natural occurrences of genthelvite are restricted to highly fractionated alkaline to peralkaline granites and syenites or to their associated pegmatites, and also in greisens and skarns. The extremely high "chalcophilicity" of Zn explains, in part, why genthelvite is such a rare mineral (Burt, 1988). The first Brazilian occurrence of genthelvite was first described in 1988. A new occurrence of genthelvite in Brazil is here described from a peralkaline granitic body, in Itapitangui, southern São Paulo state. Only two millimetric genthelvite crystals were found, in riebeckite- mesopertite- quartz granite. The macroscopic color is intense pink, similar to typical rhodonite and rhodochrosite, but with yellowish- brown spots of intemperic manganese oxide. The luster is vitreous and the hardness is between 6 and 7. One crystal displayed a striated face, possibly tetrahedral, and another vicinal face with intense luster. Some weak reflections seem to indicate a poor octahedral cleavage. The tetrahedral habit may also be deduced from the triangular shapes seen in thin section.

Refractive index measured with checked Cargille immersion liquids in white light, by the method of the Becke line was 1.741(1). The determination of specific gravity was impeded by the small crystal dimensions and association with manganese oxide. The best obtained value was 3.55. EDS analysis showed the expected presence of S, Si, Zn, Fe and Mn. Secondary electron images exhibited homogeneous distribution of Zn and Fe with maximum concentration of Zn. The cell parameter a=8.131(2), calculated from X-ray powder diffraction data, together with the refractive index was used in the diagrams of Vlasov to estimate the approximate composition: genthelvite 78%, danalite 14%, helvite 14%.

RHABDOPHANE GROUP MINERALS IN PSEUDOMORPHS AFTER STEENSTRUPINE-(Ce) FROM LOVOZERO ALKALINE COMPLEX, KOLA PENINSULA.

Ekimenkova I.A., Pekov I.V. and Kononkova N.N. *(Dept. of Geology, Moscow State University, mineral@geol.msu.ru)*

The rhabdophane group minerals are typical product of low-alkaline steenstrupine-(Ce) alteration.

In many pegmatites of the Lovozero complex there are pseudomorphs after belovite-(Ce) and vitusite-(Ce) composed of silicon-free rhabdophane-(Ce). Whereas all examined rhabdophane group minerals composing pseudomorphs after steenstrupine from the same pegmatites contain admixture of silicon prevailing over phosphorus in the samples from the Natrolite Stock pegmatite. Its formula is $(Ce_{0.4}La_{0.2}Ca_{0.15}Th_{0.15}Nd_{0.1})_{1.0}(Si_{0.6}P_{0.5})_{1.1}O_4*H_2O$, therefore it is not correct to name this phase as rhabdophane proper. Thus we propose the term "siliceous rhabdophane" like (but not identical) to that of E.I.Semenov's (1959) "Th-Si rhabdophane". This mineral is clearly shown by stoichiometry of this compound, X-ray powder data, and IR spectra to be a Si-dominant RE-member of the rhabdophane group.

An interesting case of Ce separation from other lanthanoids was discovered in alterated steenstrupine-(Ce) from weathered ussingite pegmatite at the Karnasurt Mt. Oxides of Ce^{4+} and Mn^{4+} yield aggregate, occurring as fine grained (less than 0.1 mm) heterogeneous weak-crystalline mass enriched in Ce (about 30% CeO_2, 6% La_2O_3, 2,5% Nd_2O_3). All other lanthanoids were concentrated in Ce-poor rhabdophane-(La) with composition $(La_{0.59}Nd_{0.17}Th_{0.14}Ca_{0.07}Ce_{0.03}Y_{0.02})_{1.02}(P_{0.93}Si_{0.06})_{0.99}O_4*H_2O$. It consists of monomineralic balls about 0.05 mm, which consist of tiny long-prismatic crystals. Diagnostics of this phase is confirmed by X-ray powder data and IR-spectra. This fractionation of REE is caused by oxidation of Ce^{3+} to Ce^{4+} under hypergene alteration of steenstrupine. This is the first find of rhabdophane-(La) in the Khibiny-Lovozero alkaline complex.

RECENT CONTRIBUTINOS TO THE MINERALOGY OF POCOS DE CALDAS ALKALINE MASSIF, MINAS GERAIS, BRAZIL

Matioli P.A., Atencio D., Tsugawa J.K. *(Inst. Geociencias, Univ. Sao Paulo, datencio@usp.br)*

The Mesozoic Poços de Caldas alkaline complex is circular-shaped with a mean diameter of about 33 km. It comprises a suite of alkaline volcanic and plutonic rocks (mainly phonolites and nepheline syenites). Recent contributions to its mineralogy includes gaidonnayite, barium-free burbankite, hilairite, taeniolite, narsarsukite, quartz, tuppersuatsiaite and some unidentified minerals associated to hainite. Gaidonnayite and barium-free burbankite occur as a latest interstitial filling mineral in the nepheline sienite from Pedreira da Prefeitura ("City Hall Quarry"), Poços de Caldas, Minas Gerais, Brazil. Associated minerals in the fracture are hilairite, calcite, fluorite, natrolite, analcite, pyrite, manganoan ilmenite, strontianite, ankerite, kutnahorite, and chamosite. Quartz, aegirine, fluorite and pectolite were recorded in vugs in the nepheline sienite from Pedreira da Prefeitura. Narsarsukite, aegirine, quartz, riebeckite and taeniolite were recorded in association to potassic feldspar in a rock from the Bortolan quarry. The vug filling crystals of hainite of the subvolcanic phonolite from Bortolan quarry are associated to some unidentified minerals. Mineral (A), displaying rectangular contours and maximum dimensions of 8 × 0.2 μm develops along fracture surfaces of hainite crystals. EDS analyses indicated a Sr, Ce, Ca, La and Na silicate-phosphate, with F and Cl. A second unidentified mineral (B), grows around the same hainite grain. It is anhedral, its area measures about 10 × 10 μm, and is a Ba, Na, Nb, Ti and Ca silicate. In another sample, hainite is associated to manganoan pectolite, one other mineral similar to tuperssuatsiaite and a third unidentified mineral (C). The latter is a Ti, Na, Mn, Fe, Ca, K and Al silicate with rectangular contours and maximum dimensions of 120 × 15 μm.

16. Mineralogy of Alkaline Rocks

IMPLICATION OF CALCIUM DISTRIBUTION PATTERNS IN SYENITE ALKALI FELDSPARS

Nakano S. *(Department of Natural Sciences, Shiga University. Japan, nakano@sue.shiga-u.ac.jp)*

The textural features of three syenite alkali feldspars from Oki-Dozen and Cape Ashizuri (Nakano *et al.*, 1997), Japan, and from Chile (Patagonia) are similar to those of the Klokken syenite feldspars (Brown and Parsons, 1994). Pristine feldspars are preserved around the cores, whose compositions are around $Or_{33}Ab_{64}An_3$ (two Japanese syenites) and around $Or_{40}Ab_{59}An_1$ (Chilean syenite). Compositional variation patterns in these feldspars have been observed in detail by EPMA mapping.

The compositional maps clearly show that rims are very poor in Ca and the interiors are relatively rich in Ca. The compositional variations are too irregular to be assigned to a magmatic origin alone. Reactions of the feldspars with fluid or solution are considered to have played an important role in producing such patterns. The presence of Ca-poor microperthite in the cores and Ca-poor, Or-rich-veins traversing feldspar grains support this idea.

The cooling model proposed from the studies of the Klokken syenite alkali feldspars advocates the importance of fluid-feldspar interactions in microperthite formation at the hydrothermal stage. The present study may provide new insight on the model.

LANTHANUM-RICH MINERALS IN HIGH-ALKALINE PEGMATITES AND HYDROTHERMALITES OF KHIBINY MASSIF, KOLA PENINSULA

Pekov I.V. *(Dept. of Geology, Moscow State University, pekov@minmuz.msk.su)*

Strong fractionating of light lanthanoids (LREE = La-Sm) have been observed in RE-minerals of high-alkaline pegmatites and hydrothermalites of Khibiny massif, Kola peninsula. La^{3+} is the largest ion of REE^{3+}; fractionating processes influence on it to the greatest degree and give a stable positive La-anomaly in late minerals. Six La-dominant RE-minerals were found in Khibiny: nordite-(La), belovite-(La), ancylite-(La); La-dominant analogues of kukharenkoite-(Ce), petersenite-(Ce), and vitusite-(Ce) are potentially new mineral species. La-maximum is also typical for RE-bearing minerals here: burbankite, strontium-apatite, isolueshite. Ancylite-(Ce), belovite-(Ce), phosinaite-(Ce), tundrite-(Ce), loparite-(Ce), donnayite-(Y), late apatite and goetzenite from Khibiny are La-enriched in comparison to same minerals from other objects. One can distinguish three main mechanisms of LREE fractionating giving this La-anomaly: 1. Joint crystallization (mainly in hydrothermalites) of two or more RE-minerals with different crystal chemical features: growths of kukharenkoite (La/Nd = 16.0, La/Ce = 1.2) and ewaldite (Nd/La = 14.3, Nd/Ce = 3.6), a bright example of "antagonism" of La and Nd; paragenesis of La-dominant petersenite, vitusite-(Ce), rinkite, and sazykinaite-(Y). 2. La enrichment of minerals in pegmatites related to rinkite- and titanite-bearing nepheline syenites: belovite-(La), nordite-(La), ancylite-(La), etc.; rinkite and titanite characterized by low La-content (Nd>La) are main LREE minerals of such rocks. "Unclaimed" La is concentrated in pegmatite minerals. 3. Isomorphism REE-Sr in Sr-minerals: Sr^{2+} radius exceeds REE^{3+} radii and La^{3+} has preference in this isomorph scheme (La-maximum in strontium-apatite, burbankite; La>other Ln in donnayite-(Y)). Apparently La-mineralization in Khibiny is a result of combination of three factors: wide distribution of rinkite and titanite in rocks, Sr-enrichment, and strong hydrothermal activity.

PHLOGOPITES FROM LAMPROPHYRES, SEMI-LAMPROPHYRES AND SOME ALKALINE BASALTS FROM SERBIA, YUGOSLAVIA

Prelević D., Pantó Gy., Nagy G. and Jovanović M. *(Hungarian Acad.Sci., Budapest, panto@sparc.core.hu)*

Fifty electron microprobe analyses for major elements, twenty AAS analyses for trace elements and ferrous and ferric iron by wet-chemical analysis for most samples, are given for phlogopites from lamprophyres, alkaline basalt and xenolites from leucite-basalt, from Serbia, comprising 9 semilamprophyres (leukominette), 6 minettes, 1 kersantite and 2 alkaline basalts. Investigated rocks come from different geographic regions, but all belong to Tertiary magmatism of the Balkan Peninsula.

Results show different, but mostly very primitive character of phlogopites. That statement is confirmed by high Mg# (atomic Mg/Mg+TFe) and very high Cr and Ni content of investigated minerals.

Phlogopites from semilamprophyres are always in coexistence with macrocrysts of biotite, quartz and feldspare of xenocrystic origin. In these rocks, two generations of phlogopites are recognized, according to their major and trace element chemistry: cores and major parts of macrocrystals have higher content of Mg, Cr, F, Ni, Rb, V, but lower TFe_2O_3, Fe^{2+}/Fe^{3+} ratio, TiO_2, Al_2O_3, Na_2O and Ba, compared to the rims of phlogopite macrocrystals, groundmass grains and phlogopitic rims of biotites. Phlogopites from lamprophyres, xenolite and alkali basalt show similar compositional trend.

Thermobarometer calculations exhibit narrow temperature range (1056 - 1179°C) and much wider range for pressure of crystallization (8-26 Kbar) evidencing different history of lavas from which phlogopites originated and very wide range of thermodynamic conditions in which crystallization of phlogopite has taken place. Considering distribution coefficients for investigated trace elements, high content of Cr, Ni and Co refers to very primitive (mantle) nature of liquid from which phlogopite crystallized, but high content of Cs and Rb, implies source which is enriched by LILE.

RECENT CONTRIBUTION TO STRUCTURAL MINERALOGY OF OXIDES AND CARBONATES OF ALKALINE ROCKS

Pushcharovsky D.Yu., Rastsvetaeva R.K., Vinogradova S.A. *(Dept. of Geology, Moscow State Univ, dmitp@dgeo.phys.msu.su)*

This work summarizes the recent results of XRD studies of oxides and carbonates discovered in alkaline massifs. Their structural topology, comparative crystal chemistry and petrogenetic significance are reported.

Two complex oxides - tazheranite, $CaZr_3TiO_9$, and chemically related calzirtite, $Ca_2Zr_5Ti_2O_{16}$, were found in nepheline syenites of Eastern Syberia. The structures of both minerals belong to fluorite-like structural type. The specific feature of tazheranite as compared with all structurally studied calzirtites is connected with the complete disorder of the same cations in their only position which leads to the change of tetragonal symmetry of cazirtite for cubic symmetry of tazheranite. These structural pecularities of both minerals correlate with the P,T-parameters of their crystallization: tazheranite was formed in hypabisal skarns in the conditions of rapid cooling. The stucturally studied order-ed calzirtite was found in low temperature rodingites (South Ural).

The new mineral from alkaline mafic massif Jacupiranga (Brasil), originally identified as manasseite $Al_2Mg_6(OH)_{16}CO_34H_2O$, was studied by XRD ($P\bar{6}2m$, a 5.283(3), c 15.150(9), R 0.039 for 52 reflections). Its chemical formula, $Al_2Mg_4(OH)_{12}CO_33H_2O$, corresponds to that for the mineral, recently approved by IMA (N 92-028). Inside hydrotalcite-manasseite family this structure represents the first example of the ordering between Mg and Al in brucite-like octahedral layers as well as between CO_3- and H_2O-interlayers. The variety of chemically related minerals is considered in terms of polytypism, the atomic order in the structure, of sublattices and isomorphous substitutions.

The rare earth sodium carbonate, shomiokite-(Y), $Na_3Y(CO_3)_33H_2O$, was discovered in hyperagpaitic pegmatites of Lovozero massif. Its structure contains isolated mixed complexes, formed by YO_9 polyhedra, which share their 3 edges with CO_3 groups. The mixed complexes are considered as relicts of corrugated polyhedral layers, revealed in tengerite, kimuraite and lokkaite.

16. Mineralogy of Alkaline Rocks

Si-BEARING ILMENITE FROM TUFF PIPES OF OLENYOK UPLIFT, N.-E. OF SIBERIAN PLATFORM (RUSSIA)

Shamshina E.A. and Zayakina N.V. *(Institute of Geosciences SB RAS, Yakutsk, geo.@yacc.yakutia.su)*

This mineral was found in the K-alkalic volcanites of the Khorbusuonka river basin on the Olenyok right bank. Paragenesis of the Si-bearing ilmenite: sanidines, chromespinelides, clinopyroxenes, forsterites, picro-ilmenites, and single grains of Cr-pyropes. Size of its grains is up to 2 mm. The grains are isometric, oval or of spheric form; color is black with red-brownish shining through. The electron microprobe analyses gave (wt.%) following chemical composition of the mineral : SiO_2 8-30; TiO_2 30-53; Al_2O_3 1.6 - 6.3; FeO 5.1 - 13.0; MnO 6.4 - 15.5; MgO 2.1 - 4.4; CaO 3.8 - 15.7; Na_2O 0 - 1.4; K_2O 0 - 4.0; Cr_2O_3 0.1 - 0.3.

Contents of SiO_2 and TiO_2 are inversely proportional, the contents of K_2O and Al_2O_3 are directly proportional. The microprobe profiles for Si, Ti, Fe, Mn, Ca, Al have shown similar distribution of these elements on the surface of the grain polish section. Reflection of this mineral in the visible spectrum varies from 8.2% to 13.2% and depends on the contents of SiO_2 in its composition : the less SiO_2 the greater the reflectance value.

The X-ray diffraction patterns show that the most grains of the studied mineral have a structure type of ilmenite- geikielite, though some grains are amorphous in X-ray. The strongest lines of the powder pattern are: 2.778 (10); 2.556 (7); 2.553 (3); 1.881 (5); 1.738 (7) ; 1.480 (5)Å.

Discussion : Structure of ilmenite - geikielite type consists of two kinds of octahedrons and therefore all cations in this mineral occupy in octahedral voids. But Si can occupy an octahedral position in the mineral structure mainly in conditions of high P and T. This means that Si-bearing ilmenite can be formed in high P - T conditions and it is a protomineral of extreme depths. It is an unusual mineral and it can be expected as a mineral of diamond association together with Cr-rich spinelide and Cr - pyrope. The tuffs of the Olenyok uplift can be considered as potentially diamondiferous rocks since they contain Cr-rich spinelides and Si-bearing ilmenites.

GEOCHEMISTRY OF GARNETS IN ACID VOLCANICS: INFLUENCE BY SUBDUCTION-RELATED MAGMAS

Togawa Y., Kimata M., Nakano T. *(Inst. of Geosci., Univ. of Tsukuba, kimata@arsia.geo.tsukuba.ac.jp)*, Kato A. and Matsubara S. 2: National Museum)

For many years there has been an ongoing controversy about the origin of garnets in acid volcanics (Miyashiro, 1955; Green & Ringwood, 1968; Birch & Gleadow, 1974; Green, 1992; Filatova *et al.*, 1996). XRF, ICP, EPMA and Sr-isotopic analyses have focused on geochemistry of garnets in acid volcanics, Central Japan. Their occurrences in the fore-arc and back-arc regions are along tectonic lines of a great significance to island arc magmatism, linked to subduction of Pacific and Philippine Sea plates and opening of the Japan Sea. Common features of all the present volcanics rich in phenocrystal garnets are of a peraluminous type following the petrochemistry of calc-alkaline rock series. All the present garnets are abundant in almandine content, and identified as a pyralspite series commonly occurring in acid volcanics. The diagram of CaO versus MnO for garnets of a magmatic origin discloses that crystallization pressures for garnets occurring in fore-arc regions are about 5 kbar and some 3 kbar, while those in the volcanic front and the back-arc region are probably in excess of 5-7 kbar. Apatite inclusions, garnet and the host volcanics which are arranged in order of decreasing $^{87}Sr/^{86}Sr$ ratios in the fore-arc region subducted by the Pacific plate have a potential for contributing the subducted slab to the parent magma to a considerable degree. However, the order of increasing $^{87}Sr/^{86}Sr$ ratios in the back-arc side has an implication for mixing of the primary magma generated by partial melting of the lower crust or mantle wedge, with volatile species derived from the oceanic crust. The content of large ion lithophile elements (LILE) in the acid magma has proved to be a parting of the ways in yielding either garnet-bearing or -free volcanics: depletion of LILE relative to high field strength elements (HFSE) is characteristic of the magma producing the former. The origin of calc-alkaline magma generating the garnetiferous acid volcanics

ORIGIN OF MEGACRYSTS IN THE ALKALINE VOLCANIC ROCKS OF WEST EIFEL, GERMANY

Shaw C.S.J. *(Bayerisches Geoinstitut, Universität Bayreuth)*

In the West Eifel volcanic field, phlogopite, pargasite and clinopyroxene megacrysts occur with a variety of mantle xenoliths including anhydrous and phlogopite- and/or pargasite- bearing peridotite, peridotite cut by hornblendite veins and Al-Ti-rich augite clinopyroxenites.

Phlogopite and pargasite megacryst compositions overlap with those in hornblendite veins in peridotite and with intercumulus phlogopite and pargasite in Mg-rich clinopyroxenites.

Four distinct types of clinopyroxene megacryst are present.

1) Cr-diopside megacrysts identical to those in peridotite xenoliths.

2) Moderately Cr-rich diopsides similar in composition to those from anhydrous, high-temperature pyroxenite veins in peridotite.

3) Al-rich augites that show a linear compositional trend that overlaps with clinopyroxene from hydrous veins in peridotite and with Mg-rich clinopyroxenites. This trend is due to fractionation and extends to include iron-rich Al-augite clinopyroxenites.

4) Fe-rich, Ti-poor augite similar in composition to the partially resorbed cores of phenocrysts in the host lavas and to Fe-rich, Ti-poor clinopyroxenites.

All the megacrysts have characteristics consistent with crystallization at high pressure. Phlogopite, pargasite and type 3 clinopyroxene megacrysts represent fragments of pargasite- phlogopite and Mg-rich clinopyroxenite veins that cut the peridotitic West Eifel mantle. The size of the megacrysts (up to 10 cm) suggests that these veins may be much larger than those preserved in composite xenoliths at the surface. If this interpretation is correct, it indicates that the sub-Eifel mantle may be more extensively altered and veined than was previously thought.

COMPOSITIONAL VARIATION IN CUMULUS AND INTERCUMULUS MINERALS FROM THE LOVOZERO ALKALINE COMPLEX, RUSSIA

Kogarko L.N. *(Vernadskiy Institute, Moscow, Russia)*, Williams C.T. and Woolley A.R. *(Dept. of Mineralogy, NHM, London, UK)*

Few alkaline intrusions show well-developed igneous layering. The only such intrusion studied in detail is Ilimaussaq in Greenland, which is relatively small and in which the liquid changed little throughout the layered series. In contrast, the Lovozero intrusion in the Kola Peninsula, Russia is the second largest such intrusion in the world, is strongly layered and the liquid evolved from miaskitic to agpaitic. The chemistry of the extensive suite of cumulus and intercumulus minerals, and their constituent rare elements, have not previously been studied in detail using modern analytical techniques.

Here, we report microprobe analyses from two of the rare earth-bearing minerals occurring throughout the intrusion, loparite-(Ce) and eudialyte, both of which display compositional changes that can be correlated with depth within the layered intrusion. In the deepest part of the intrusion intrusion, loparite is interstitial and its composition here reflects crystallisation from evolved trapped liquid. Above this depth, loparite is a cumulus phase and its composition changes systematically towards the top of the intrusion, with increases in Na, Sr, Nb, Th. The total RE_2O_3 and La:Nd ratio also change systematically with depth, with cumulus loparite becoming relatively heavy-REE enriched towards the top of the intrusion. Thus, the mineral chemistry of loparite, as a cumulus phase, reflects changes in the magma composition during its evolution and crystallisation.

Eudialyte does not show much variation in the lower differentiated complex where it occurs as an interstitial phase, and its compositional variation reflects crystallisation within localised trapped magma environments, rather than the large-scale magmatic evolution that influenced the composition of loparite. In the later intrusive phase (intrusion III of the Lovozero Massif), eudialyte becomes a cumulus mineral and here does display some degree of systematic compositional variation, particularly for REE, Mn and Fe.

16. Mineralogy of Alkaline Rocks

DIVERSITY OF AMPHIBOLES OF ILMENOGORSKY MASSIF OF NEPHELINE SYENITES (THE SOUTH URAL, RUSSIA)

Bazhenov A.G. *(Institute of Mineralogy, Russian Academy of Science, mak@imin.urc.ac.ru)*

Various amphiboles are widespread in the rocks of Ilmenogorsky massif and its contact aureole. Amphibole compositions are changed widely and reflect rock compositions.

Within nepheline syenites (miaskites) magnesiohastingsites are changed by taramites from the roots of massif towards its apical parts. The leucocratic aluminous alkali-syenites and fenites so as apoamphibolitic melanocratic fenites are characterized by magnesiohastingsites. Exotic amphiboles, sadanagaite and its ferri- analogue, occur in the plagiosyenites. Amphiboles of the series of richterite- magnesiokataphorite are peculiar to leucocratic peralcaline fenites, syenites, granosyenites. Richterites, fluorrichterites or edenites combine apometaultrabasitic fenites.

Fluorrichterites and fluormagnesioarfvedsonite are inherent in fenites closed to its composition to lamproites. Late veins of alpine type are encrusted by acicular and fibrous amphiboles of the series of actinolite-ferriwinchite-magnesioribekite.

NEW DATA ON THE MINERALS OF THE LABUNTSOVITE - NENADKEVICHITE FAMILY AND THEIR SYSTEMATIZATION

Rastsvetaeva R.K., Chukanov N.V. and Pekov I.V. *(Institute of Crystallography RAS, Moscow, Russia)*

Crystal structures of six new members of labuntsovite-nenadkevichite family from pegmatites and hydrothermalites of alkaline Kola Peninsula massifs are studied. The general formula for monoclinic members of the family on the basis of chemical and microprobe analyses for 43 samples (among them 24 new ones) is suggested (Z=1):$A^{I}_{4}A^{II}_{4}A^{III}_{4-2x}[M^{I}(O,OH)]_{8}[M^{II}_{x}(H_2O)_{2x}][Si_4O_{12}]_4 \cdot nH_2O$ where x=0-2; A^{I}=Na, Ca, ; A^{II}=K, Na, H_3O, ; A^{III}=K, Ba, Sr, H_3O, ; M^{I}=Ti, Nb; M^{II}=Mn, Fe, Mg, Zn, ; n=8. The crystal structure of these minerals consists of M^{I} octahedra columns linked by tetrahedral four-membered rings and additional M^{II} octahedra. Alkaline and alkaline-earth atoms occupy the zeolite like cavities of this framework together with H_2O molecules. The main feature of this structural type is in a relationship between A^{III} and M^{II} positions which are occupied according to alternative mechanism: $2(K,Ba,Sr) + \square \leftrightarrow 2H_2O + (Mn,Fe,Mg)$. The established correlation between chemical composition, crystal structure, and IR spectral parameters allowed us to divide the minerals of the family into three groups. 1) Minerals with vacant M^{II} position. Their general formula is simplified to $A^{I}_{4}A^{II}_{4}A^{III}_{4}[M(O,OH)]_{8}[Si_4O_{12}]_4.nH_2O$. So called "monoclinic nenadkevichites" represent this group. We have studied two minerals - vuoriyarvite and its Ti dominant analogue M69. 2) Minerals with predominance of vacancies in M^{II} octahedra; A^{III} positions are consequently occupied by large cations more than 50%. Most part of labuntsovites are in this group. We have investigated three of them - Ba and two K-rich ones. 3) Minerals with predominance of cations in M^{II} octahedra and more than 50% occupancy of A^{III} position by H_2O molecules respectively. This group involves some labuntsovite-like minerals, which may be considered as Mn dominant, Mg dominant, Zn dominant *etc*. Nenadkevichite itself is characterized by orthorhombic symmetry and individual chemically and structurally. We have refined its Ti dominant analogue structure. Though it may be formally considered as a mineral of the first group we actually don't include it into this systematization.

17. Mineral Synthesis

SYNTHESIS AND CHARACTERIZATION OF PYROPIC GARNETS

Geiger C.A. and Stahl A. *(Mineralogisch-Petrographisches Institut der Universität Kiel, Germany, NMP46@rz.uni-kiel.de)*

Pyrope garnet has been synthesized at high pressure and temperature using different starting materials and fluxes. Single crystals of end-member pyrope and pyrope-rich compositions doped with different transition metals (Cr^{3+}, Ni^{2+}, Ti^{4+}, $V^{3+/4+}$, Co^{2+}) up to 2 mm size have been grown in the presence of an H_2O flux. The introduction of certain high-valence cations (*i.e.* Ti^{4+} , $V^{3+/4+}$) in either the dodecahedral and octahedral position often results in more complicated IR spectra around 3600 cm^{-1} compared to the spectra of pyrope with divalent cations, which is indicative of OH^- substitutions other than the hydrogarnet type. Multiband OH^- stretching vibrations can be observed in their single-crystal FT-IR spectra.

Isotopically enriched pyrope containing ^{26}Mg was grown for single-crystal Raman measurements and aided in the assignment of low frequency vibrational modes. The growth of large millimeter size single crystals with ^{29}Si should also be possible.

Polycrystalline pyrope has been synthesized dry with Yb^{3+} and characterized by X-ray absorption spectroscopy at the ESRF synchrotron (Quartieri et al., submitted). Measurements on the L_{III} edge show that Yb^{3+} is incorporated in the dodeca-hedral site. These results are of importance for geochemical trace element studies, as it was shown how rare-earth elements in small concentrations can be structurally incorporated in silicate garnet.

We have also begun to experiment with the growth of single crystals using different oxide fluxes [*e.g.* $Pb_2B_2O_5$, PbO-PbF_2, $(Na,Li)_2B_2O_4$] at high P and T in a piston-cylinder device. Large euhedral single crystals have been obtained with the PbO-based fluxes and with less success using alkali-borate fluxes. These crystals show no OH stretching bands in their IR spectra.

MÖSSBAUER STUDY OF SYNTHETIC $Mg_{0.2}Fe_{0.8}SiO_3$ CLINOPYROXENE

Eeckhout S.G., De Grave E. *(Dept. of Subatomic and Radiation Physics, Univ. of Gent, Belgium, sigrid.eeckhout@rug.ac.be)* and McCammon C. *(Bayerisches Geoinstitut, Univ. of Bayreuth, Germany)*

Low-pressure $Mg_{0.2}Fe_{0.8}SiO_3$ clinopyroxene (space group $P2_1/c$) was synthesized in a multi-anvil press (at the Bayerisches Geoinstitut) at 10 GPa and 1200°C using a mixture of fayalite, MgO and SiO_2. Transmission Mössbauer spectra (MS) were collected in a broad temperature range of 4.2 to 773 K. The paramagnetic spectra were fitted with symmetric, Lorentzian-shaped doublets. A small amount of Fe^{3+} was detected, but, the weak doublet (~ 2 %) could only be fitted by constraining some of its Mössbauer parameters. It is believed that the presence of Fe^{3+} does not significantly affect the ferrous Mössbauer parameters for the M1 and M2 sites. At 26 K, development of magnetic ordering was observed, but, even at 4.2 K saturation has not been reached. The temperature dependencies of the Fe^{2+} centre shifts δ at the M1 and the M2 site are analysed using the Debye model for the lattice vibrations to calculate the second-order Doppler shift. The lattice temperature for the M1 site was found to be somewhat smaller than that for the M2 site. The variations of the M1 and M2 ferrous quadrupole splittings ΔE_Q are consistent with the stronger deformation of the M2 octahedra. The crystal-field model is used to estimate from the $\Delta E_Q(T)$ the energy gaps of the first excited electronic state within the ^5D orbital term. In an attempt to determine the sign of the principal component V_{zz} of the electric field gradient for both sites and to estimate the magnitude of their respective asymmetry parameters η, an external-field MS (6 T) was recorded at 180 K. For both sites, V_{zz} is most likely positive. The η values are probably small, however, cannot be determined with reasonable precision.

HYDROGEN EXCHANGE KINETICS IN CLINOPYROXENE

Skogby H. *(Dept. of Mineralogy, Swedish Museum of Natural History, Stockholm, Sweden, henrik.skogby@nrm.se)*

Several nominally anhydrous minerals of upper mantle origin have been reported to contain small amounts of hydrogen, bonded as OH^- ions in the crystal structures. For some minerals, *e.g.* pyroxenes, concentrations ranging up to 500-1000 wt.-ppm H_2O have been measured, and it has been suggested that these minerals may provide a water storage mechanism in the upper mantle. However, an important question is whether the measured concentrations represent true mantle conditions, or if hydrogen may have been exchanged with the environment during the ascent process from the upper mantle.

To answer this question, there is a need for kinetic data for the possible hydrogen exchange reactions in these minerals. An important hydrogen exchange reaction has been shown to involve changes in the oxidation state of Fe according to the reversible reaction $Fe^{3+} + O^{2-} + \frac{1}{2}H_2 = Fe^{2+} + OH^-$. Iron probably also plays a role for the hydrogen transport mechanism in the structure.

In this work, the kinetics of hydrogen exchange in clinopyroxene have been studied, with emphasis on the effect of the Fe content. A series of synthetic single-crystal samples, essentially along the diopside-aegirine join, with Fe contents ranging from 0.00 to 0.39 atoms per formula unit has been subjected to hydrogen incorporation experiments. Oriented sections of these crystals were heat-treated in hydrogen atmosphere at temperatures between 600 and 800°C in consecutive time steps. The concentration of hydrogen was determined by polarized infrared spectroscopy between each step.

For the Fe-containing samples, the results show a considerable increase in reaction rates with increasing iron content, up to a certain limit around 0.10 Fe atoms per formula unit. For compositions above this limit the kinetics of the hydrogen incorporation is uniform, with diffusion coefficients close to $\log(D) = -12.5$ m^2/s at 700°C.

Also the Fe-free samples take up hydrogen, but show a different behaviour with distinctly faster kinetics. The charge-balance mechanism for the hydrogen exchange is in this case unknown, but probably connected with some type of defects.

HYDROTHERMAL SYNTHESIS OF PUMPELLYITE-OKHOTSKITE SERIES MINERALS

Akasaka M., Suzuki Y. *(Dept. of Geoscience, Shimane Univ., akasaka@riko.shimane-u.ac.jp)* and Watanabe H. *(Dept. of Earth Science, Kanazawa University. Japan)*

Mn-pumpellyites of pumpellyite-okhotskite series have been synthesized at 200, 300 and 400 MPa Pfluid and 250-400°C by using cold-seal pressure vessels and solid oxygen buffering techniques. Starting materials are (1) Ca_4MgAl_2-$Mn^{3+}{}_3Si_6O_{24.5}$-oxide mixture + H_2O and (2) synthetic Ca_2Al_2-$MnSi_3O_{12}(OH)$-piemontite + H_2O. From the charge (1), Mn-pumpellyites (Mn-pum) crystallized at temperatures of 300 and 400°C and pressures of 200, 300 and 400 MPa. At 200 MPa and 300°C, hausmannite (Ha), wollastonite (Wo), clinopyroxene (Cpx), braunite (Br), alleghanyite (All) and macfallite (Mac)? are associated, whereas, at 400°C, piemontite (Pie) and garnet (Gt) crystallized in addition to above minerals. At 300 MPa and 300-400°C, the assemblages of Mn-pum + Pie + Wo + Cpx + All + Ha + Mac? ± Gt ± Br were given. The amount of piemontite in the run products at 400°C is larger than that at 300°C. At 400 MPa and 300°C, the assemblage similar to that at 300 MPa was given. Mn-pumpellyite occurs as rounded aggregates or platy crystals up to 5 microns. Chemical compositions are variable and range between pumpellyite- (Mn^{2+}) and okhotskite; 31-36 SiO_2, 9-21 Al_2O_3, 12-27 total Mn_2O_3, 0.6-4 MgO and 20-24 wt.% CaO. From the starting material (2), Mn-pumpellyites were synthesized at 300 MPa and temperatures of 250, 300 and 400°C. Garnet, wollastonite, alleghanyite and macfallite? are associated minerals. The chemical compositions of Mn-pumpellyites are 32-37 SiO_2, 19-27 Al_2O_3, 4-18 total Mn_2O_3, 20-25 wt.% CaO. It has been confirmed that the Mn-pumpellyite is stable at lower temperatures than piemontite.

17. Mineral Synthesis

A NEW METHOD OF SYNTHESIS OF BOLTWOODITE AND RELATED MINERALS.

Vochten R. *(Dept. of Chemistry, University of Antwerp, Belgium, revo@ruca.ua.ac.be)* and Blaton N. *(Lab. of Analytical Chemistry, FFW, University of Leuven, Belgium, Norbert.Blaton @farm.kuleuven.ac.be)*

Boltwoodite has been synthesized at elevated temperature and pressure from quartz, KCl and uranylnitrate. The related minerals Na-boltwoodite, uranophane, sklodowskite and kasolite were obtained from boltwoodite. Chemical analysis in combination with infrared spectroscopy lead to the formula of boltwoodite: $K(UO_2)(SiO_3OH).H_2O$.

XRD measurements show that boltwoodite is monoclinic with space group $P2_1$ and refined lattice parameters: a = 7.0316(8); b=7.0668(2); c=6.6633(2)Å and β =105.862(6)°. Sodium-boltwoodite seems to be unstable, after 40 days at 185°C in a teflon lined bomb. The product was fully transformed to a F-containing product: $Na_2(UO_2)_2SiO_4F_2$ which is structuraly related to soddyite. The results of these experiments must be a warning that in case of synthesis experiments performed in teflon lined bomb, fluorine can be incorporated.

This compound crystallizes in the tetragonal space group $I4_1/amd$. The powder pattern was refined resulting in the lattice parameters: a=6.9872(9) c=18.334(2)Å.

The crystal structure has been determined.

ON THE PROGRESS OF ORDERING IN THE SYNTHETIC AIKINITE - BISMUTHINITE SERIES

Bente K., Doering T., Wagner G. *(Institut fur Mineralogie, Kristallographie und Materialwissenschaft, Universitat Leipzig, Germany)* Bernardini G.P., Borrini D. and Danti C. *(Dpt of Earth Sciences, University of Florence, Italy)*

Numerous investigations have established the minerals of aikinite-bismuthinite series to have correlated structures based on the ordered link of structural units (ribbons) of aikinite ($CuPbBiS_3$) and krupkaite ($CuPbBi_3S_6$) or krupkaite and bismuthinite (Bi_2S_3), depending on the chemical composition. The synthetic analogues showing disordered structures are, on the contrary, members of a complete solid solution. The transformation from disordered to ordered structures was assumed by Pring (1995) to occur in four steps controlled by the intracrystalline Cu^+ diffusion at a temperature of above 300°C.

The members of the aikinite-bismuthinite series were synthesised using as starting materials the pseudoternary end-members (Cu_2S-PbS-Bi_2S_3) at 500°C and aikinite + krupkaite or krupkaite + bismuthinite at 300°, 450° and 550°C. The synthetic products were investigated by electron microprobe, X ray powder diffraction and HRTEM observations. Distinctive structural aspects and compositional associations were detected.

X ray diffraction spectra and HRTEM images of the synthetic products and those simulated for different ordering steps have been compared. Partially ordered synthetic members were detected

Preliminary results point to an ordering process, for the 300°C synthetic products, starting from aikinite + krupkaite and krupkaite + bismuthinite, supporting the ordering mechanism proposed by Pring (1995).

Additionally the "AC" and "AG" phases, as reported by Mariolacos (1979) and Bente (1987), were identified associated with some of the synthetic members of the aikinite-bismuthinite series.

STRUCTURAL CONTROL OF SOLID SOLUTION LIMITS AND IONIC DISTRIBUTIONS IN SYNTHETIC TOURMALINES

Gourdant J.-P. and Robert J.-L. *(CRSCM-CNRS, Orléans, France, gourdant@cnrs-orleans.fr)*

Synthetic tourmalines have been prepared (600°C, 1 kbar PH_2O, under NNO buffering conditions) to understand solid solutions extends and ionic distributions. Structural similarities between Y and Z sites, and ubiquity of Al raise many crystal-chemical problems.

For the Y and Z sites occupancies, Al^{3+} (0.54 Å) has been replaced by the larger Ga^{3+} (0.62 Å); Mg^{2+} (0.72 Å) by the smaller Ni^{2+} (0.69 Å) and by the larger Mn^{2+} (0.83 Å). The Si (0.26 Å) → Ge (0.39 Å) substitution in tetrahedra was also studied. XRD was used for phase identification and cell parameter measurements, and FTIR absorption spectrometry to characterize the environments of OH-groups, and quantify their proportion.

The tourmaline structure is divided in two areas with separate behaviors: the core-zone, made of the X, Y, T and 'B' sites, and the outer zone, made of Z-sites.

It is difficult to enlarge the central entity, which therefore incorporates small cations. The tetrahedral ring, occupied by Si, being too small to fit with large nearby Y-sites. Thus, Ni^{2+} easily replaces Mg^{2+} at Y-sites. Complete solid solutions exist between dravite and Ni-dravite, Mg-foitite and Ni-foitite, and Ni-dravite and Ni-foitite. At the opposite, the large Ge cannot quantitatively replace Si. The behavior of this central zone can be a structural explanation to the unstability of some compositions, as the incorporation of large cations at these sites is limited. For example, a Ga-tourmaline is stable only with Na at X-site, *i.e.* with Y-sites occupied by Mg, whereas the Na-free end-member, which needs one-third Ga at Y-sites, is not stable. The second zone serves as "concrete" to bind the island-core entities together. In this case, it is possible to incorporate large cations, like Ga instead of Al, and to increase extremely the cell parameters (+ 1.36% for a, + 2.51% for c), compared to the usual variations due to natural substitutions.

NATURAL AND EXPERIMENTAL ZEOLITIZATION OF PHONOLITIC GLASS: A COMPARISON

Bernhard F. and Barth-Wirsching U. *(Institut für Technische Geologie, TU Graz, bernhard@egam.tu-graz.ac.at)*

The phonolitic pyroclastic flow deposits of the Laach volcanic area, Germany, are zeolitized in three, up to 10 m thick layers. These layers are intercalated by fresh ashes. The fine-grained, vitreous ash particles of the matrix are altered to analcime + K-feldspar in the lowermost zeolitized layer, whereas the matrix of the middle and uppermost layer consist of analcime + phillipsite + chabazite. Coarse pumice clasts within the matrix are predominantly altered to chabazite with only subordinate amounts of phillipsite and analcime, despite the same glass chemistry. The contacts between totally altered and fresh matrix are sharp, whereas the alteration of pumice clasts decreases gradually towards the fresh matrix. The chemistry of zeolites in the different layers is quite similar. Si/Al ratios vary between 2.2 and 2.6 and are similar to those of the fresh glass (2.2-2.3). Chabazite is very poor in Na and shows a Ca/K ratio of about 1, analcime is dominated by Na and phillipsite by K, respectively. Zeolitization is assumed to be due to diagenetic reactions with groundwater.

Experiments (0.5, 1 or 2 g of ground, fresh pumice as starting material, 25 ml H_2O, 0.01n NaOH, KOH, NaCl and mixtures as reacting solutions, 150-200°C, 8-200 days reaction time, unstirred system) showed that chabazite and phillipsite represent transition phases with respect to analcime and K-feldspar under all conditions. Therefore, the two upper zeolitized layers represent a less advanced alteration stage than the lowermost layer. Predominantly chabazite, as in pumice clasts, forms experimentally only with at least a slight K^+-input from the solution. These chabazites are extremely poor in Ca and have a Na/K ratio of about 1, the Si/Al ratio is 2.2-2.4. However, cation exchange experiments with $CaCl_2$ solution show that only Na is exchangeable by Ca, leaving K nearly unaffected, thereby approaching the natural chabazites in composition. The different alteration of matrix and pumice clasts is probably kinetically controlled.

17. Mineral Synthesis

SYNTHETIC RUBY WITH UNUSUAL Cr^{3+} CONCENTRATION

Leonyuk N.I., Klimanova Yu.V., Lyutin A.V. *(Geological Fac. Moscow State Univ., leon@geol.msu.ru)*, Barilo S.N., Bychkov G.L. and Kurnevich L.A. *(Inst. of Phys. of Solids and Semicond., Minsk)*

The interest in ruby crystals for gemology applications has led to a demand for crystals of colour, real structure and habit like natural red corundum. For this reason, attempts have been made to grow these crystals by flux method or under hydrothermal conditions. However, most of these are impracticable for the commercial production of isometric crystals because the synthetic corundum with usual cromium concentration tends to grow as a plate-like crystal. Only, a few authors could obtain the isometric crystals from high-temperature solutions, but the influence of the type of solvent, impurities, and temperature on the corundum habit is yet to be understood precisely.

Here, this paper concerns experimental results on the growth conditions, composition and morphology of ruby crystals grown by flux method using Li_2O-MoO_3 (I), Li_2O-WO_3 (II), Na_2O-WO_3 (III) and PbO-V_2O_5-WO_3 (IV) as fluxes. The crystals have been obtained in the temperature intervals of 1250-1100°C and 1150-900°C. Details of growth conditions will be presented for each flux and temperature range.

The distribution coefficients of impurities depend on the flux type and crystallization temperature. As a matter of fact, the concentration of Mo, W, Pb admixtures is not more then 0.01 wt.%, but the amount of Cr and V impurities depend on the crystal growth conditions. In the case of IV flux, the ruby crystals contain up to 6.38 at.% of Cr. All these factors affect the growth rate of the crystal faces. The ruby crystals grown at the temperatures 1150-900°C (with I and II fluxes) have a plate-like habit with a strongly developed pinacoid. The ruby obtained in the temperature interval 1250-1100°C (with II and IV fluxes) have more equidimensional crystal shape. The {0001} faces rarely develop.

Correlation between the crystal morphology, crystal structure and growth conditions will be demonstrated. The crystallo-chemical interpretation will be given to understand the influence of solvent type and complexes in the fluxed melts on crystal morphology.

THERMAL BEHAVIOUR OF SYNTHETIC ALKALI- BIRNESSITES

Rziha T. *(Inst. für Mineralogie, Ruhr-Universität Bochum, Germany)*

Birnessite, a common Mn mineral in soils, belongs to the family of layered hydrous manganese oxides. The layers are built up of edge-shared MnO_6 octahedra. In alkali-birnessite, the interlayer space between adjacent layers is occupied by alkali cations and H_2O molecules.

With the exception of Na-birnessite, previous thermal studies of alkali-birnessites have been carried out using natural samples or cation-exchanged birnessites. The materials for the present thermal study are directly synthesized Li-, Na-, K-, Rb-, and Cs-birnessites. Thus, the problem of mixed cation birnessites due to incomplete exchange could be avoided.

The thermal behaviour of alkali-birnessites in the temperature range from 20°C to 800°C is essentially characterized by two main processes. At about 200°C water is released, resulting in a continuous decrease of the interlayer distance. At about 500°C, the various alkali-birnessites show a phase transformation involving the release of oxygen. Li-birnessite changes to a spinel-type structure, whereas Na-birnessite transforms to a tunnel-like structure. All other alkali-birnessites show topotactic transformations to tunnel structures. K- and Rb-birnessites form a hollandite structure with a 2×2 tunnel, and the phase transformation of Cs-birnessite results in a 2×4 tunnel structure termed "RUB-7" (Rziha, 1996).

The topotactic phase transformation from the layer to the tunnel structure can be explained by breaking either every second or fourth of the shared edges of the MnO_6 layers in a zig-zag-like manner, and connecting these zig-zags on each side via corner-sharing of MnO_6 octahedra to a tunnel framework. The alkali cations are located inside the tunnels.

SYNTHESIS OF IRON CONTAINING DIOCTAHEDRAL SMECTITES

Nagase T., Iwasaki T., Ebina T., Hayasi H., Onodera Y., Chatterjee M. and Torii K. *(Tohoku National Indust. Res. Inst., nagase@tniri.go.jp)*

Novel method for synthesizing iron containing dioctahedral smectites which are useful as adsorbents for nuclear wastes and rheological additives was developed. This method can be characterized by low temperature and short duration of hydrothermal treatment suitable for industrial production.

Samples were obtained by hydrothermal treatment of Si-Fe-(Mg, Al) hydrous oxides. The solubility curves of smectite, hematite and kaolinite which are expected to be formed by the treatment were calculated thermodynamically to anticipate the phase relationships between them in advance. It was found that factors such as composition of solution, reaction temperature and pH intensely affect the purity of the smectite; the condition in which ferric ion is supplied slowly to the solution is suitable for the formation of the smectite. For the achivement of such condition, the hydrous oxide was prepared by mixing an acidic sodium silicate solution and metal chloride solutions to make the atomic ratio to be Si-Fe-Mg = 4: 1.7: 0.3 or Si-Fe-Al = 4: 1.7: 0.3. After washing with distiled water, the hydrous oxide was dispersed in water and the pH was adjusted with a NaOH solution to be a value between 6.5-14. Then, the slurry was sealed in the teflon container and hydrothermally treated at 175°C or 200°C for 24 hrs. Results of the experiments were almost in accordance with the expectation from the calculation.When the pH was lower than 12, liquid or amorphous phase was formed. When the pH was higher than 12.5, ferric oxide or acmite was precipitated. In the pH range of 12-12.5, smectite was obtained as transparent yellowish brown gel without impurities.

The products obtained under the pH condition of 12.0-12.5 were characterized by XRD, TEM, XPS and IR. From the XRD patterns, d(001) spacings were found to be 12.8-9Å and d(06) spacings 1.52-1.53Å. After treatment with ethylene glycol, d(001) spacings were expanded to *ca.* 17-19Å. These values coincide with those of dioctahedral smectites. By TEM observation, the particle size of the smectites was larger than 500Å. The chemical compositions of the samples measured by TEM-EDS were Si-Fe-Mg = 4-1.9-0.05 and Si-Fe-Al = 3.8-2.0-0.2 in atomic ratios, which correspond to iron-montmorillonite and nontronite, respectively.

Ti IN SYNTHETIC CLINOAMPHIBOLES: INFLUENCE OF BULK COMPOSITION, TEMPERATURE AND Fe CONTENT ON Ti SOLUBILITY AND SUBSTITUTIONAL MECHANISMS

Sergent J., Robert J.-L. *(CRSCM-CNRS, Orléans, France, sergent@cnrs-orleans.fr)* and Della Ventura G. *(Univ. Roma Tre, Italy)*

Titanium can enter the amphibole structure both at tetrahedral and octahedral sites. The tetrahedral coordination is restricted to Al-free or Al-poor compositions, typically richterites, whereas octahedral Ti is typical of hornblendes lato sensu (*e.g.* kaersutites).

Temperature favours the incorporation of Ti in amphiboles, as it is also well known in other ferro-magnesian silicates (*i.e.* micas). The favourable temperature effect can be understood by considering the differential thermal expansions of polyhedra: for example, high tetrahedral Ti contents, up to ≈ 0.8 Ti apfu at T ≥ 800°C, 1 kbar, in Mg-richterite improve fitting between the tetrahedral double-chain (Ti larger than Si) and the thermally expanded octahedral beam. The Ti-solubility limit is only 0.2 apfu, at 600°C, 1 kbar. A similar dimensional effect is produced by the replacement of Mg by divalent Fe in octahedra, and the same upper Ti solubility limit (≈ 0.8 Ti apfu) is reached at only 700°C, 1 kbar in ferrous systems, provided that fO_2 conditions are sufficiently low (MW buffer).

In Al-amphiboles [pargasite: $NaCa_2(Mg_4Al)(Si_6Al_2)O_{22}(OH)_2$], similar dimensional considerations can explain the behaviour of Ti, but the substitutional mechanisms are more complicated. Ti replaces octahedral Al, and the charge imbalance can be compensated according to two schemes: the Ti-Tschermak substitution which leads to $[NaCa_2(Mg_4Ti)(Si_5Al_3)O_{22}(OH)_2]$ (1), and a deprotonation process which leads to $[NaCa_2(Mg_4Ti)(Si_6Al_2)O_{23}(OH)]$ (2). Experiments performed at 900°C, 3 kbar PH_2O show a large solid solution range, up to >70 mol %, between pargasite and (1), and up to >60 mol%, between pargasite and (2). Under lower temperatures (700°C), the solubility limits of Ti are about two times smaller.

MULTISTAGE LEAD SULFOSALTS FROM ZIMAPÁN, HIDALGO, MEXICO.

Villaseñor-Cabral M.G., Gómez-Caballero J.A. *(Instituto de Geología UNAM, mgvc@sevidor.unam.mx)* and Petersen E.U. *(Dept. of Geology & Geophysics, University of Utah)*

Zimapán is a Pb-Zn-Ag ore deposit that belongs to the peculiar limestone replacing deposits known as of "Mexican type". At Zimapán, lead sulfosalts are common ore minerals, boulangerite and jamesonite being the most abundant and accounting, sometimes, for 5% approximately of the total ore.

X-ray diffraction, reflected-light microscopy, scanning electron microscopy and microprobe analyses were used to identify these minerals in order to establish their paragenesis and try to obtain information useful to the understanding of the metallogenic processes at Zimapán.

The mineralogy of the ore bodies is complex and includes a large number of species including: sphalerite, galena, pyrite, pyrrhotite, chalcopyrite, tetrahedrite-tennantite, freibergite, boulangerite, jamesonite, meneghinite, as well as unnamed minerals of Bi, Te and Sn, among others. The textures of these minerals are very interesting, particularly the replacement textures and they show that the processes which produced Zimapán were diverse. Variation in the Bi and As content of boulangerite is ascribed to variation in the composition of the mineralising fluids, and high temperature bismuth minerals, which cut across earlier minerals, reveal the influence of an intrusive event. These facts, together with varied crystal habits, show clearly that the deposit was mineralized in several stages. Preliminary fluid inclusion data confirm this observation.

UNUSUAL CONCENTRATIONS of TETRAHEDRITE AND TENNANTITE IN THE VMS OF NEVES-CORVO DEPOSIT

Gaspar O.C.(IGM, Portugal); Bowles J. (Mineral Sciences, UK), Ferreira J.(IGM), Ferreira A. and Nelson P. *(SOMINCOR, Portugal)*

The volcanogenic massive sulfide ore deposit of Neves-Corvo lies in the Portuguese sector of the Iberian Pyrite Belt. It is well known not only for its large tonnage (>300 Mt.) but also for its substantial content of Cu (4 Mt.) and Sn (105 $\times 10^3$ t). Discrete ore lenses consisting mainly of tetrahedrite/tennantite + sphalerite occur at different levels in the massive copper-rich ores (6.25% Cu) of the Graþa and Corvo orebodies. Ore microscopic studies were carried out on 150 samples from these lenses. Stannite, kesterite, stannoidite and mawsonite along with minor quantities of arsenopyrite, galena, bournonite and enargite were observed. The ore textures show complex mineral intergrowths and replacements mostly of sphalerite by tetrahedrite/tennantite and/or chalcopyrite.

These tetrahedrite/tennantite + sphalerite ore lenses are characterised by their anomalous contents of Hg and Ag. Electron probe analysis has been carried out on 60 samples showing the following distribution of Hg and Ag in the most common ore minerals:

MINERALS	*Hg, ppm (average)*	*Ag, ppm (average)*
Sphalerite	170 to 100 0, (630)	below the detection limit
Tetrahedrite	328 to 2660, (1140)	1020 to 52500
Stannite	660 to 1340, (1000)	below the detection limit
Kesterite	630 to 740, (690)	below the detection limit
Stannoidite	420 to 600, (510)	low Ag values
Mawsonite	180	below the detection limit
Galena	420 to 700, (550)	up to 650
Bournonite	580 to 990, (790)	up to 1600
Enargite	280 to 300, (790)	up to 2300

A MICROPROBE STUDY OF COMPLEX Ag-Sn ORES FROM PIRQUITAS, JUJUY PROVINCE, ARGENTINE

Paar W.H. *(Dept. of Mineralogy, University of Salzburg, Austria, Werner.Paar@sbg.ac.at)*, de Brodtkorb M.K. *(CONICET- INREMI, Univ. Nac. de la Plata, Arg.)*, Sureda R.J. *(Catedra de Min., Univ. Nac. de Salta, Arg.)* and Topa D. *(Dept. of Geology, Univ. of Salzburg, Austria)*

The Pirquitas district is located 135 km W of Abra Pampa, in the Province of Jujuy, NW-Argentine. Primary Ag-Sn ores as well as Sn and Au placer deposits were exploited intermittently from 1936 to 1990. An extensive drilling program was performed during 1996-97.

Pirquitas is a porphyry tin deposit associated with a later vein system, and is located in the southern continuation of the Bolivian tin belt. The host rocks are Ordovician sediments. The vein-type polymetallic silver-tin mineralisation was precipitated in several pulses. Colloform banding and crustification are abundant. Very fine-grained intergrowths and micro-penetration of the minerals could be a major problem for the beneficiacion of the ores.

An early stage is typified by the ubiquitous presence of pyrite, marcasite, arsenopyrite, cassiterite and ferberite, either followed by a complex assemblage of pavonite type minerals, gustavite (6wt.% Sb), Te-canfieldite, matildite, tetradymite and bismuthinite or sphalerite/wurtzite, associated with franckeite, cylindrite, potosiite and two new mineral species belonging to the Pb-Sn-S and Pb-Sn-As-S systems, resp. Important carriers for Ag and/or Sn in all veins are members of the hocartite-pirquitasite and rhodostannite-toyohaite series, aramayoite, canfieldite as well as stannite-kesterite and ferrokesterite. Ag sulfosalts, such as pyrargyrite (As, Bi : 4, 0.6 wt.%), miargyrite (As, Bi : 3.1, 2.3 wt.%), freibergite, members of the diaphorite s.s. series (Bi 17.2 wt.%) and andorite-fizelyite-ramdohrite are more enriched in the upper parts of the veins.

Sphalerite is the host of In-bearing minerals such as petrukite and sakuraiite (In : 1.6 and 23.2 wt.%, resp.). Thallium occurs as constituent of a possibly new mineral, chemically $TlAsAg_3S_4$.

PECULIARITIES OF COMPOSITION OF GERMANITE SUBFAMILY MINERALS

Nenasheva S.N. *(Fersman Mineralogical Museum RAS, Moscow)*

According to the systematic classification (structural and chemical) of minerals of A.A.Godovikov, germanite and renierite belong to the germanite subfamily, of the chalcopyrite family. It is generally thought that the unit cell of renierite contains 33 atoms - $Cu_{10}(Zn_{1-x}Cu)Ge_{2-x}As_xFe_4S_{16}$ (where $0<x<1$), and the germanite unit cell, 66 atoms - $Cu_{26}Ge_4Fe_4S_{32}$. Both structures are derived from the structure of sphalerite. Examination of the published electron microprobe analyses of renierite and germanite from various kinds of ore deposits shows, however, that it is impossible to fit all of these analyses to the foregoing formulae. From 86 electron microprobe analyses of renierite investigated, only 63 fit a formula with 33 atoms; 9 fit a 32 atom cell and 14 a formula with 34 atoms. Similarly, from the 40 analyses of germanite investigated, only 26 correspond to a formula with 66 atoms, 9 to 64 atoms and 14 analyses to a formula with 68 atoms. Such result cannot be accidental.

Let us draw a parallel between renierite, germanite and chalcopyrite, and that of the other members of the chalcopyrite family - talnakhite, mooihoekite and chalcopyrite which are compositionally and structurally similar. Differences in their structural formulae result from differences in the tetrahedral packing of metal atoms. Sixteen of these tetrahedrons in chalcopyrite are empty, in talnakhite one is packed by Cu or Fe and in mooihoekite two of them are packed by Fe. There are 32, 33 and 34 atoms in the formulae of chalcopyrite, talnakhite and mooihoekite respectively. The analyses of renierite and germanite may also be recalculated to unit cells with 32, 33, 34 atoms. We suggest, therefore, that it is possible that three different renierites and three different germanites may exist.

18. Ore Mineralogy

A NEW PHASE DIAGRAM FOR THE BORNITE-DIGENITE JOIN: RESULTS FROM *IN SITU* NEUTRON DIFFRACTION AND DSC EXPERIMENTS.

Grguric B. *(Dept. Earth Sciences, Univ. Cambridge, England)*, Harrison R. and Putnis A. *(Institut für Mineralogie, Univ. Münster, Germany, putnis@nwz.uni-muenster.de)*

Intermediate compositions along the bornite-digenite join were synthesized in sealed quartz capsules from component elements, water-quenched from 600°C and analysed using high-resolution neutron powder diffraction (HRPD) at the ISIS Spallation Source. The very high resolution of this instrument ($\Delta d/d = 8 \times 10^{-4}$ over the entire TOF range) showed conclusively that all quenched samples were completely exsolved to bornite plus low digenite (*5a* superlatttice) during quenching. Samples annealed for longer times below the solvus temperature showed typical 'basket-weave' exsolution textures in reflected light, but their neutron diffraction patterns were essentially identical to the quenched samples, indicating that annealing merely coarsens the existing phases.

The rapid kinetics of exsolution in this system enables in situ equilibrium experiments to be carried out using high temperature neutron diffraction and differential scanning calorimetry (DSC) techniques. In the neutron diffraction experiments the formation of the high temperature solid solution could be observed as a function of temperature and starting bulk composition of the samples. Changes in lattice parameters of coexisting phases were also measured as a function of temperature. DSC measurements of samples with bulk compositons at intervals of 5 mol.% bornite were used to monitor the structural changes as a function of temperature. By correlating the DSC and the neutron diffraction results a new phase diagram for the bornite-digenite join was determined.

The new phase diagram differs substantially from that previously published by Kullerud (1960) and Morimoto and Kullerud (1966). For example, at bulk compositions of 50 and 75 mol.% bornite the solvus lies at 140° and 190°C respectively, compared with published temperatures of over 300°C for both compositions.

The rapid kinetics of exsolution in this system at geologically low temperatures explains the lack of authenticated natural occurrences of intermediate compositions in the solid solution in nature and the limited degree of stoichiometric variation observed in end-members.

NATURAL SPHEROIDS OF MINERALS IN THE GOLD OCCURRENCE

Gamyanin G.N. and Zhdanov Yu.Ya. *(Inst. of Geosciences SB RAS, Yakutsk, geo@yacc.yakutia.su)*

Different-colored ideal-shaped spheroids were first revealed in ore crushed samples from shatter zones of gold occurrence of the Indigirka river basin (northeastern Russia). They are different in composition, complex in relationships between various mineral phases, their microstructures being specific. Heavy fraction contains 3 to 5% of spheroids up to 2 mm in size. Black magnetic spheroids with a bright or dull surface are most abundant. They are generally composed of magnetite having ilmenite exsolution structure. Sometimes, there are pyrrhotite spheroids. Golden-colored spheroids with an ideal bright or slightly shagreen surface predominate in a nonmagnetic fraction. Sometimes, they occur in quartz cavities and contain semispheroidal dark-colored excrescences. Spheroids are abundant in Au and contain 10 to 40% Ag, concentration being the same as in the shapeless ore gold from the occurrence. Polished gold spheroids contain intergranular phases of native arsenic and Au(AsSb) and Au_7Sb_3 intermetallides as well as small circular cavities. Dark-brown spheroids are composed of hematite and galenite. Galenite contains boulangerite and antimonite forming the ice-flower dendrite-like structure. Cross sections of these spheroids always contain different-sized circular gold inclusions. In this gold, the ratios of Au, As, Sb, and Pb components are often different in the intermetallide phases. Of them, Pb_2SbAu phase is most stable. Exsolution structures of gold and eutectoid-type intermetallides occur. All the brown spheroids contain a great number of gas cavities and relics of quartz, pyrite, arsenopyrite, and shapeless gold. Transparent and cherry-colored spheroids are composed of Pb oxide compounds containing 2 to 4% As and S. Framboidal or zonal internal structure is typical of pyrite spheroids. Data on the morphology, internal structure, successive formation of spheroids (from native intermetallides to oxides through sulfides)as well as the presence of gas cavities in them indicate their natural origin. Spheroids are assumed to be formed as a result of gas-jet ore metamorphism.

GEOCHEMICAL PROSPECTING AND GENETIC STUDY OF GOLD MINERALIZATION AT THE FAWAKHIR GOLD MINE AREA, EASTERN DESERT, EGYPT

El-Bouseily A.M., Arslan A.I. and Khalil K.I. *(Geol. Dept., Alexandria University, Egypt)*

Geochemical survey at the El Sid-Fawakhir gold mine area has shown anomalous patterns of Cu, Pb, Zn, As, Sn, Be, Co, Ni, Ag, and Hg in vicinity of previously-known Au-mineralizations as well as in localities of as-yet-undiscovered mineralization. Mercury anomalies are clearly indicated over the mineralized zones, but the highest values are mostly observed in proximity to structural features such as faults and contact zones. Chloritization, sericitization, carbonatization, sulphidization and silicification are the main hydrothermal alterations in the study mine area. Sulphidization is the most important process. The distribution of the sulphide minerals reflects different generations and various parageneses. Based on geological, mineralogical and chemical investigations, the following genetic model can be advocated:

1. Within the rock types in the mine area, the predominant oxide is ilmenite in basic rocks, and magnetite in acidic varieties.

2. The rocks underwent metamorphism; replacement of ilmenite by rutile is an important mineralogical feature of this period.

3. Along shear zones, post-metamorphic hydrothermal alteration activities occurred, and four stages can be distinguished:-

(a) Alteration minerals such as chlorite, sericite, epidote, calcite.

(b) Development of the main sulphides such as pyrrhotite, pyrite, arsenopyrite, marcasite, and the first generation of chalcopyrite and gold. Pyrite and marcasite were also formed as a result of increase of sulphur fugacity which caused pyritization of pre-existing pyrrhotite and probably chalcopyrite. The gold was previously contained in the pyrrhotite lattice, probably due to its non- stoichiometric character. The pyrite formed at the expense of pyrrhotite is gold-bearing.

(c) Formation of fracture-filling sulphides and second generations of chalcopyrite and gold.

(d) Silicification and formation of quartz veining where all of the previous stages were affected by the silicification process.

4. Finally, supergene minerals such as limonite, malachite, leucoxene and covellite were formed.

TELLURIUM-BEARING PHASES IN BLACK SMOKER CHIMNEY FRAGMENTS FROM THE SILURIAN YAMAN KASY MASSIVE SULPHIDE OREBODY, SOUTHERN URALS, RUSSIA

Herrington R.J.[1], Maslennikov V.V.[2], Stanley C.J.[1] and Buslaev F.[3] *([1]Natural History Museum, London; [2]Institute of Mineralogy Uralian Branch of RAN, Miass 456301, Chelyabinsk district, Russia; [3]Institute of Geology and Geochemistry Uralian Branch of RAN, Ekaterinburg, Russia)*

Silurian volcanogenic massive sulphide ores of the Yaman Kasy deposit in the southern Urals show evidence of exceptional preservation of primary mineral assemblages. Of particular note are features of seafloor exhalative activity which include sulphide-replaced vent fauna and fragments of black smoker chimneys.

The chimney fragments can be sub-divided into four types based on paragenetic associations. These are: 1) pyrite-isocubanite-pyrrhotite; 2) pyrite-chalcopyrite; 3) pyrite-marcasite-sphalerite-chalcopyrite; and, finally, 4) marcasite-barite-galena-sphalerite-chalcopyrite. These broad mineralogical zonations are comparable with the zonation seen in modern black smoker chimney material. The Yaman Kasy sulphide ores have unusually high tellurium contents, which are reflected in the development of complex tellurium-bearing mineral assemblages in specific zones within the chimney structures.

In type 1 and 2 chimney fragments tellurobismuthite is the only telluride developed. In type 3 chimney fragments, a more complex telluride assemblage is marked by goldfieldite, sylvanite, hessite-stutzite, coloradoite, volynskite, altaite (often replaced by benleonardite), cervellite, and unresolved (Au,Ag,Pb) (Te,As,S) sulphosalts. In the same zone, galena, native gold and tellurium are sometimes developed. In the type 4 chimneys, altaite, Ag-tellurium sulphosalts, galena, native tellurium and gold are found.

The tellurium mineralisation is generally found at a distinctive mineralogical boundary within the chimney, at the transition between an outer Fe-sulphide dominated zone, which forms the outer wall of the chimney and an inner Cu-rich, higher temperature conduit lining. The broad sulphide zonation and specific location of tellurium-bearing phases can be interpreted in terms of extreme gradients of temperature, oxygen and sulphur fugacity across the vent chimney walls and the interaction between high-temperature hydrothermal fluid in the central conduit of the chimney and cold seawater outside the external wall.

A REMARKABLE OCCURRENCE OF Pd-Pt-Au-Ag-Cu-Se MINERALIZATION IN WESTERN AUSTRALIA

Nickel E.H. *(Division of Exploration & Mining, CSIRO, Australia, e.nickel@per.dem.csiro.au)*

A vein containing Pd and Pt selenides and oxides, Cu selenides, and gold and silver minerals in a malachite-quartz matrix has been discovered in the East Pilbara region of Western Australia. The primary minerals include oosterboschite [$(Pd,Cu)_7Se_5$], naumannite [Ag_2Se], an unnamed Ag_2CuSe_2 mineral, berzelianite [Cu_2Se], klockmannite [CuSe], and native gold and silver. The Pd and Pt minerals have been extensively oxidized to a number of finely intergrown oxides and hydroxides, and the native silver has been partially replaced by bromian chlorargyrite.

The PGE minerals, gold and silver occur in botryoidal malachite-quartz nodules that comprise a portion of the mineralized vein. The PGE minerals exhibit a variety of remarkable textures, including concentric layering, "starbursts", dendritic forms, arborescent efflorescences, and fern-like fronds. The abundant inclusions, both microscopic and submicroscopic, of PGE minerals make the malachite nodules black and opaque, in contrast to green malachite of supergene origin that is also present in the vein.

The textural features exhibited by the PGE minerals in the malachite-quartz nodules are interpreted as evidence for codeposition of the PGE minerals, malachite and quartz, and possibly also the gold. The native silver may have been introduced later. A postulated origin for the mineralization involves a saline, low-pH hydrothermal fluid containing Pd, Pt, Au, Ag, Cu, Se and Si encountering dolomitic rock, thereby causing the minerals of economic interest to be precipitated with malachite formed by the reaction of the Cu-bearing solutions with the carbonate wallrock.

SUBSTITUTION MECHANISMS IN SOROSITE, Cu(Sn,Sb)

Barkov A.Y., Laajoki K.V.O. *(Dept. of Geology, Univ. of Oulu, Finland, barkov@sveka.oulu.fi)*, Gornostaev S.S. *(National Mining Univ. of Ukraine, Dnepropetrovsk, Ukraine)* and Taikina-aho O. *(Inst. Electron Optics, Univ. of Oulu, Finland)*

Sorosite, Cu(Sn,Sb), is a new ore mineral from Baimka, Russian Far East (Barkov et al., in press). It occurs as inclusions in Sb-bearing native tin and is associated with stistaite (SnSb), herzenbergite (SnS), native lead and trace cassiterite. Here we provide a preliminary report on a zoned sorosite; these results may be important for better understanding of substitutions in the mineral. A total of 115 wavelength-dispersion electron-microprobe analyses was carried out (JEOL-733 electron microprobe) on several subhedral to euhedral crystals (0.1-0.3 mm), including core-to-rim traverses. The analyses show that the central zones are relatively enriched in Fe (up to 3.23 wt.%; 0.11 atoms per formula unit, apfu, Fe), Ni (up to 1.31 wt.%; 0.04 apfu Ni) and Sb (up to 8.02 wt.%; 0.12 apfu Sb), and correspondingly are depleted in Cu and Sn; Co only was detected in the central zones (up to 0.14 wt.%; 0.004 apfu Co). The content of Fe displays a very strong negative correlation with Cu (R= -0.97), a very strong positive correlation with Sb (R= 0.99), and a moderately strong positive correlation with Ni (R= 0.68). The 100 Ni/(Ni + Fe) (atom.%) ratio is distinctly decreased toward the center, indicating that Fe is partitioned into the central zones more strongly than Ni. The results indicate that Cu is replaced by Fe, and Sn is replaced by Sb in the sorosite structure. The existence of a solid solution between sorosite (CuSn), FeSb, and NiSb is clearly implied. This is favored by structural similarities between sorosite and hexagonal ε-FeSb (PDF-34-1053) and NiSb (breithauptite), which both are crystallized with NiAs type structure. Thus, more extensive solid solution in the system CuSn-FeSb-NiSb is possible. Two principal substitutions are consistent with the compositional data, and are tentatively suggested to occur in sorosite: $Fe^{2+}+Sb^{3+} \leftrightarrow Cu^{+}+Sn^{4+}$, and $Ni^{2+}+Sb^{3+} \leftrightarrow Cu^{+}+Sn^{4+}$.

PETROMAGNETIC PROPERTIES AND OPAQUE MINERALOGY OF HOST ROCKS AND MAGNETITE-APATITE ORE FROM CERRO DE MERCADO, MEXICO

Alva-Valdivia L.M., Cruz Ocampo J.C. *(Instituto de Geofisica, Universidad Nacional Autonoma de Mexico, 04510 Mexico D. F., MEXICO, lalva@tonatiuh.igeofcu.unam.mx)* and Vivallo W. *(Servicio Nacional de Geologia y Mineria, Chile)*

We report results from a petromagnetic and microscopic study from the host rocks and Fe-mineralization in the Cerro de Mercado, Durango, Mexico. The microscopy of the analyzed phases of the system TiO_2 -FeO-Fe_2O_3 show that the magnetic oxide minerals are abundant, with trellis, sandwich and composite textures. Grain sizes range from a few microns to >100 μm, and possible magnetic state from simple to multi-domain, which have been affected by slow cooling and deuteric oxidation from low to high degree, respectively. Oxides mainly include titanomagnetites, with notable amounts of minerals from the ilmenite-hematite series, and goethite-limonite resulting from alteration processes. The NRM polarities for most of the lithologic units range from normal to reverse, possibly reflecting the postmineralization alteration processes. Scattering of NRM directions for Fe-ore is lower than that for the other units, possibly because the mineralization process happened in a short period. The polarity and scatter are directly affected by oxidation, metamorphism and hydrothermal alteration processes. Rock magnetic properties of Fe-ore are mainly of titanomagnetite with single to multi-domain magnetic state. Magnetic susceptibility of intrusive bodies is relatively low, belonging to the I-type granites. Thermal spectra, vector plots, and IRM acquisition show a direct association with microscopic observations, suggesting a predominance of titanomagnetites with variable content of magnetite and ulvospinel. The effect of few magnetic or nonmagnetic minerals (paramagnetic and diamagnetic) is well distinguishable. There are secondary magnetic components associated mainly to metamorphism and hydrothermal alteration processes assessed by reflected and transmitted light studies. These secondary components also can be the effect of VRM and/or IRM. Data on bulk susceptibility and remanent intensity provide important constraints for modeling of the magnetometric anomalies, *i.e.*, by quantifying the relative contributions of induced and remanent magnetization components thus allowing a better control of the geometry of source bodies.

BEAVERITE-OSARISAVAITE SERIES FROM OXIDATION ZONE OF ALEXANDRINKA MASSIVE SULPHIDE DEPOSIT (SOUTH URAL, RUSSIA)

Belogub E.V. *(Institute of Mineralogy Urals Branch of Russian Academy of science, bel@imin.urc.ac.ru)*

The Alexandrinka massive sulfide deposit which is in Devonian volcanic-sedimentary rocks is hidden by a zone of supergene alteration. The structure of this zone, from ore to surface consists of: oxidized ores with secondarily enriched sulfides, followed by pyrite-barite-quartz sand (leached in part), then jarosite ochres and limonite. Supergene alunitization of the host rocks was also observed. The full series of alteration from jarosite to beaverite to osarizawaite was observed at Alexandrinka. Pb- and Cu-bearing members of jarosite subgroup were found as: 1) massive ochre (beaverite) formed by xenomorphous, roundish crystals; 2) replacement of galena-bearing ores in zonal oxidation products (beaverite) as pseudomorphs; 3) crystals on walls of cavities in limonite (osarizawaite-beaverite). The morphology of the last formed minerals of this group depends of their composition, e.g., iron-rich members have the best crystal shape. According to X-ray, optical, infrared and chemical analysis the jarosite-alunite minerals form a completely continuous series. Their Pb-Cu enrichment is a characteristic feature of the Alexandrinka deposit as compared with other massive sulphide deposits.

18. Ore Mineralogy

CONTRASTING MINERALOGY OF SILURIAN AND CARBONIFEROUS SEDEX DEPOSITS, SW CATALONIA

Canet C. and Melgarejo J.C. *(Dept. Crist. Min. Dip. Min., Univ. Barcelona, joanc@natura.geo.ub.es)*

The Silurian and Carboniferous sedex deposits in the SW region of Catalonia display many mineralogical similarities. These deposits have been affected by the Hercynian deformation and regional metamorphism in low grade. Late Hercynian granitoids produced a contact aureola, that affect the deposits in different grade.

The Silurian series are composed by 200 m of black shales, interbedded with quartzites and sedex deposits at the bottom. The ore deposits consist of an interbedding of almost monomineralic beds composed by fine-grained minerals: albite, anorthite, K-feldspar, apatite, pyrrhotite, V-biotite, V-tremolite and goldmanite. The feldspar-rich beds also contain disseminated grains of armenite, V-titanite, allanite, uraninite, vuorelainenite, chromite, monazite, xenotime and scheelite. Minor quantities of minerals of gold and PGE are also disseminated in lesser amounts: Pd-löllingite, sperrylite, native palladium, as well as chalcopyrite, sphalerite, galena, arsenopyrite and several selenides and tellurides of Bi, Pb and Ag. Titanium minerals are widespread, as rutile in metapelitic beds and as titanite in the feldpar beds.

The Carboniferous series have 10 m of chert at the bottom (Tournaisian), and consist of more than 2000 m of turbiditic series (Visean to Upper Namurian). The ore deposits occur embedded in sediments formed in low energy sedimentary media (pelitic units). They also consist of an interbedding of almost monominerallic, decimeter-thick beds: sulphide-rich (pyrrhotite, pyrite, galena, sphalerite, or chalcopyrite), feldspar-rich (albite, anorthite, K-feldspar), quartz, chlorite, epidote and tremolite. The feldspar- and chlorite- rich beds contain disseminations of REE minerals (monazite and xenotime), Ti minerals (titanite in feldspar beds, rutile or ilmenite in the rest), thorianite, scheelite, cassiterite or stannite, Bi minerals (native bismuth, bismuthinite and bismuth tellurides), hessite, apatite and zircon.

THE COPPER QUEEN DOME NORTHERN ZIMBABWE

Dunlevey J.N. *(Dept. Geology, Univ. Durban-Westville, South Africa)* and Duane M.J. *(Dept. Geology, Univ. Kuwait, Kuwait)*

The Copper Queen Dome mineralization in the Sanyati District of norther Zimbabwe was initially discovered by indigenous people. Although ore reserve in the 'J-Lines Deposits' alone are calculated as being in excess of 15 million tonnes, with some 7% metal, metallurgical problems have severely limited attempts to develop these deposits.

The early Proterozoic Deweras, Lomagundi and Piriwiri Groups (Magondi Supergroup) are composed mostly of metasediments, with minor mafic and intermediate to felsic intrusions, were metamorphosed and deformed by the Magoni Orogeny (2.0 - 1.8 Ga). The mineralisation displays characteristics of both syngenetic and epigenetic phases. The stratiform (Zn-Pb-Cu-Fe-Ag) massive sulphide deposits (Copper Queen, J Lines and Copper King) in the Piriwiri Group appear to have a sedimentary exhalative origin, overprinted and modified by later tectonic and intrusive events to produce ores that display many complex textures. The mineralization is associated with bands of amphibolite and dolomitic marble in a phyllite, schist and quartzite sequence. Chalcopyrite, pyrite, pyrrhotite, arsenopyrite, sphalerite, galena and some cassiterite are the main ore minerals with amphibole, garnet, and carbonate gangue. The minerals are intimately associated, with complex intergrowths on the micron scale; a feature which is believed to have caused the spurious identification of sub-microscopic intergrowths as exotic mineral phases.

SEM and EDS studies of samples from the Copper Queen Dome area have revealed evidence of at least three phases of overprinting on the original stratabound ores. This complexity in the orebody suggests that the presently accepted origin as a skarn deposit (associated with the phase of gneiss and granite intrusion late in the Magondi Orogeny) is an over-simplification, and that an initially 'Beshi' model (SEDEX) with later remobilisation-coupled and tectonic disruption is more applicable.

Stable isotope data for the ore zone carbonates are interpreted to indicate that fluidization coupled with contact metamorphism produced a skarn association not the products of the Magondi Orogeny.

PHOTOACOUSTIC AND SOME OPTICAL PROPERTIES OF MINERAL MARMATITE (ZnS+Fe)

Nikolić P.M.[1], Đurić S.[2],Todorović D.M.[1], Blagojević V.[3], Uroević D.[4], Mihajlović P.[1], Bojičić A.I.[1], Radulović K.T.[1], Vasiljević-Radović D.G.[1] and Dimitrijević M.[1] *([1]Joint Laboratory for Advanced Materials of SASA, [2]Faculty of Mining and Geology, [3]Electrotechnical Faculty, [4]Mathematical Institute of SASA)*

Thermal diffusivity and some electron transport properties of semiconducting ore mineral marmatite (ZnS+Fe) from the Trepča mine, were determined using a modern photoacoustic method with a transmission detection configuration. Thermal diffusivity (for single crystal (index SC) $D_{TSC}=0.2 \times 10^{-5} m^2/s$ and polycrystalline small grain size (index PC) $D_{TPC}=0.86 \times 10^{-6} m^2/s$), coefficient of the carrier diffusion ($D_{SC}=0.108 \times 10^{-2} m^2/s$ and $D_{PC}=0.5 \times 10^{-3} m^2/s$), the excess carrier life time ($\tau_{SC}=130\mu s$ and $\tau_{PC}=5\mu s$) and the rear and front surface recombination velocities ($s_{bSC}=0.33 m/s$, $s_{gSC}=45 m/s$ and $s_{bPC}=133 m/s$, $s_{gPC}=51 m/s$, respectively) were calculated by fitting experimental spectra and theoretical photoacoustic amplitude and phase signals. The results obtained by optical transmission and reflectivity measurements were also used to compare the determined values of the optical absorption coefficient using photoacoustic (PA) and optical methods. The value of minority free carrier holes of single crystal marmatite was calculated for the first time as $\mu_p \sim 428 cm^2/Vs$.

MINERALOGICAL AND GEOCHEMICAL CHARACTERISTICS OF STANNIFEROUS QUARTZ VEINS AT ERVEDOSA, NORTHERN PORTUGAL

Gomes M.E.P. *(Dept. of Geology, Univ. of Trás-os-Montes and Alto Douro, Portugal, mgomes@utad.pt)* and Neiva A.M.R. *(Dept. of Earth Sciences, Univ. of Coimbra, Portugal)*

The hypothermal stanniferous quartz veins at Ervedosa cut Silurian mica-schists and a Sn-bearing muscovite granite (327±9 Ma). They resulted from a hydrothermal system related to this late highly fractionated granite of a granitic fractionation suite. These veins fill faults related to the Hercynian movements along a dextral N30°W shear zone. They were exploited for cassiterite. The primary minerals, some showing recurrences, belong to three paragenetic stages separated by faulting. Euhedral to subhedral cassiterite crystals are generally less than 10 mm across, but they are locally associated in round masses with a diameter of 10 cm. The cassiterite shows sequences of alternating parallel darker and lighter zones. The darker zones are strongly pleochroic and have more Fe, Nb and Ta than the lighter zones, which are nearly pure SnO_2. They show exsolved columbite-tantalite, titanian ixiolite, rare wolframo-ixiolite and locally wolframite and ilmenite, which mainly occur in the darker zones. Arsenopyrite is the most abundant sulphide. The earliest euhedral to subhedral arsenopyrite has inclusions of pyrrhotite, the most common subhedral arsenopyrite crystallized at 440°C and the last anhedral arsenopyrite contains inclusions of bismuth, bismuthinite and matildite, but it is replaced by pyrite, chalcopyrite and stannite. Monoclinic pyrrhotite may have been formed by inversion of hexagonal pyrrhotite at about 248°C. The crystallization temperature of an earlier generation of sphalerite was estimated as 280-240°C and of a later sphalerite poorer in Fe as 109°C. Anhedral stannite occurs with quartz and chalcopyrite in veinlets cutting other sulphides or filling fractures in arsenopyrite.

18. Ore Mineralogy

CATIONIC COMPOSITION OF SULPHIDE, SELENIDE AND TELLURIDE MINERALS

Gorchakova O.E. and Smirnova N.L. *(Dept. of Chemistry, All-Russian Inst. of Scientific and Technical Information, Moscow, goe@viniti.msk.su)*

Minerals belonging to the sulphide class are considered. The set of sulphide minerals can be divided in three subsets: sulphides, selenides and tellurides. Besides pure S, Se and Te mixed anions are also possible: SeS, TeS, $S{\cdot}H_2O$ (for example: $NaFeS_2{\cdot}2H_2O$ - erdite). Qualitative formulae of these minerals are being considered. An ideal qualitative formula consists of main (species forming) chemical elements without isomorphic impurities, coefficients and charges of atoms. The cationic composition of sulphides, selenides and tellurides was established. 439 S-containing, 46 Se-containing and 55 Te-containing minerals were analysed. The total number of cations in sulphide minerals is 939, in selenide minerals-65, in telluride minerals-72. All cations of selenide and telluride minerals were found in sulphide minerals, but some cations were met only in sulphides: Na (7 minerals), K(6), Cs(1), Be(3), Mg(4), Ca(3), Ba(1), Ti(1), V(8), Nb(1), Cr(7), W(2), Mn(6), Ru(2), Os(2), Ir(7), Al(2), Ga(1), In(3). Each of these cations has frequency not more, than 5% of Cu maximal frequency. Cation frequency correlation was defined only for common cations of all three subsets.

Based on the difference (Δ) between the frequency of sulphide, selenide and telluride cations it was established that minerals containing Cu, Pb, Sb, Fe, Ag, As, Bi are leaders for sulphides, Ni, Cu, Ag minerals - for selenides, Pd, Ag, Sb, Bi - for tellurides. The frequency of Pd minerals in tellurides is three times more than in sulphides. Fe, As, Sn and Co cations in tellurides are 56, 56, 25 and 8% correspondingly of maximal frequency of Cu(144) cations in sulphides. Rare cations are Mo, Cd, Ge for selenides, and Fe, Co, Rh, Sn, As - for tellurides, among these cations only Rh is rare for sulphide minerals. Analysis of qualitative formulae is an important characteristic of ore deposits.

SOLID STATE GROWTH OF ARGENTOPENTLANDITE AND MACKINAWITE IN CHALCOPYRITE

Kerestedjian T. *(Geol. Inst., Bulg. Acad. Sci., thomas@geology.acad.bg)*, Mladenova V. *(Sofia University)*, Petrov P. and Neykova E. *(Earth and Man Museum, Sofia)*

The scarce mineral argentopentlandite, first found in Sudbury, Canada at 1940 and recognized by the IMA new minerals commission in 1977, is currently known from less than 10 occurrences in the world.

All the available descriptions of the mineral agree in one point: argentopentlandite is always found as fine euhedral to semieuhedral inclusions in chalcopyrite, together with mackinawite and sometimes with cubanite. The last finding in the Rhodope Mts., Bulgaria, revealed also regular crystallographic relationships between the three minerals, which may be considered as a strong clue to a common genetic mechanism, producing the whole observed assemblage during a solid state transformation of an ISS. Similar in crystallochemical respect is the possibility for a thermal and chemical influence of later solutions on solid chalcopyrite.

The crystal structures of the three minerals were analyzed and found to be comparable both in topological and metrical respect. Even belonging to different crystal classes, with the small compromise to take unconventional cell choices, they can all be represented based on one and the same anion sublattice. Then, the transformation: ISS-chalcopyrite-argentopentlandite-mackinawite is easily explained in terms of energy driven cation repositioning. The chemical differentiation of the three minerals follows the zero electronic charge rule. Regular twinning relations between the minerals are determined by the similarities in their specific net parameters.

MOOIHOEKITE AND TALNAKHITE STUDIED BY MÖSSBAUER SPECTROSCOPY AND OTHER METHODS

Kalinowski M.P. and Ericsson T. *(Department of Earth Sciences, University of Uppsala, Villavägen 16, SE-752 36 Uppsala, Sweden)*

Natural mooihoekite ($Cu_9Fe_9S_{16}$) and talnakhite ($Cu_9Fe_8S_{16}$), identified using powder XRD and electron microprobe (EMP), have been analysed using Mössbauer spectroscopy.

The sulphides with Me/S >1 in the central part of Cu-Fe-S system have structures similar to that of chalcopyrite with additional cations at interstitial positions, forming superstructures.

Observed Mössbauer spectra are complex, with magnetic and paramagnetic signals. The spectra consist of one doublet with low quadrupole splitting (QS) = 0.2 - 0.6 mm/s and centroid shift (CS) = 0.3 - 0.5 mm/s, one sextet with hyperfine field (B) = 34 tesla, QS close to 0.0 mm/s and CS $\approx$ 0.3 mm/s, corresponding to the sextet observed in chalcopyrite and at least two additional sextets with lower hyperfine fields (B = 26 - 30 tesla). The observed doublet is assumed not to be caused by superparamagnetism as the natural material is of coarse-grained character.

Natural mooihoekite and synthetically produced samples give similar Mössbauer spectra. However, in the synthetic phase the sextet characteristic for iron in the chalcopyrite structure is reduced in intensity.

The intensity of the paramagnetic signal is not proportional to the number of interstitial cations. The lack of magnetic coupling between iron atoms seems neither to be caused by long range disorder. A high temperature cubic phase with a cell dimension a = 5.30 Å, produced by heating natural talnakhite to 300°C - 600°C followed by quenching, gives paramagnetic signals with intensities comparable with those given by untreated samples (14 - 17 %).

HYDROTHERMAL ALTERATION OF GRANITOID ROCKS IN THE DUBRAVA Sb-Au DEPOSIT, WESTERN CARPATHIANS

Majzlan J. *(Univ. of California at Davis, USA, jmajzlan@ucdavis.edu)*, Orvošová M. *(Slovak Museum of Nature Protection and Speleology, Liptovsk Mikuláš, Slovakia)* and Chovan M. *(Comenius Univ., Bratislava, Slovakia)*

Dúbrava Sb-Au deposit is located in Nízke Tatry Mts, Slovakia. It is hosted by Variscan I-type granodiorites and granites with xenoliths of migmatite and amphibolite gneisses.

Three alteration zones were recognized at the Dúbrava Sb-Au deposit, Nízke Tatry Mts: I. chlorite zone (outermost), II. muscovite zone, III. illite-carbonate zone (innermost).

Increasing degree of alteration results in decomposition of plagioclase and K-feldspar. Biotite is progressively replaced by chlorite, muscovite and illite. Primary magmatic minerals and textures are completely erased in the most internal alteration zone.

The collected data indicate a temperature decrease from the outermost chlorite zone (≈320°C, chlorite thermometry) toward the inner zone rich in illite and carbonates (180-200°C, crystallinity index). The initial stages of alteration bore pervasive character, altering mostly biotite in large volumes of rocks within the ore field. Muscovite and illite-carbonate zones are superimposed on the most external chlorite zone. They are a product of action of lower temperature fluids whose circulation was restricted to open tectonic structures and channelways. Gradual sealing of the walls of the veins and temperature decrease led to isolation of external chlorite zone and preservation of its mineral assemblage.

In the course of alteration, the rocks were enriched in K_2O, H_2O, CO_2, Sb, S and depleted in CaO, Na_2O, MgO and Fe_2O_3. Local redistribution and/or variation in the chemical composition of the magmatic precursor caused small changes in Al_2O_3 and SiO_2 content. Zr, TiO_2 and Sc seem to be the least mobile elements, although rutile appears in pyrite-arsenopyrite assemblage of the ore veins

TWO NEW RARE EARTH MINERALS IN AN UNUSUAL MINERALIZATION OF THE NISI BAUXITE DEPOSIT, GREECE

Pantó Gy. *(Hungarian Acad.Sci, Budapest, panto@sparc.core.hu)* and Maksimović Z. *(Serbian Acad.Sci.Arts, Belgrade, zmaks@eunet.yu)*

The Nisi bauxite deposit, in the Lokris area of Greece, represent a transitional deposit between the karst bauxites and karstic nickel deposits. It is characterized by high enrichment of the rare earth elements (REE) and Ni at the base of the deposit. It was the result of strong leaching of these elements in karstic environment during the formation of the deposit. As a result, the authigenic RE minerals and a Ni clay-like mineral have been formed. Contact between footwall limestone and the ore is marked by a zone 0.3-0.5 m thick, containing a greenish clay-like mineral and blackish Mn concentrations. XRD and microprobe study of these materials revealed an unusual association of takovite, halloysite, gibbsite, lithiophorite, birnessite, bastnäsite and two new RE minerals: hydroxylcarbonate-(Nd) and hydroxylcarbonate-(La).

RE minerals occur as irregular segregations, micropore and space fillings and microveins. Larger grains up to 70 x 100 μm in diameter are rare. The XRD of some samples show the reflections of bastnäsite. In most of the samples, however, only the strongest d_{122} reflection appeared, with changeable values from d =2.875 Å to d =2.930 Å. The reflection with the highest d_{122} value appeared in samples where fluorine was absent. The substitution of the OH^{1-} for F^{1-} in the structure of bastnäsite resulted in the increase of the unit cell volume.

The microprobe analyses gave the following formulas of the RE minerals, including a hydroxylbastnäsite-(La), on the basis of 4(O,OH,F):

$(La_{.34}Pr_{.12}Nd_{.42}Sm_{.05}Eu_{.01}Gd_{.02}Ca_{.01})\ CO_3\ OH$,

$(La_{.48}Pr_{.10}Nd_{.37}Sm_{.03}Eu_{.01}Gd_{.02})\ CO_3\ OH$, and

$(La_{.38}Pr_{.08}Nd_{.36}Sm_{.05}Eu_{.01}Gd_{.03}Dy_{.01}Y_{.04}Ca_{.06})\ CO_3\ OH_{.32}F_{.46}$

It is interesting to note an absence of cerium in all analyses.

According to the XRD and microprobe analyses the two new RE minerals are the end members of the series $(La,Nd)CO_3F$ - $(La,Nd)CO_3OH$, belonging to the bastnäsite group.

TETRAHEDRITE-TENNANTITE FROM CAPILLITAS MINE, A HIGH-SULFIDATION EPITHERMAL-TYPE DEPOSIT FROM NORTHWESTERN ARGENTINA

Marquez-Zavalia M.F. *(IANIGLA, CRICYT-CONICET, C.C.330, 5.500-Mendoza, Argentina)* and Craig J. R. *(Virginia Tech, 4044 Derring Hall, Blacksburg, VA 24061, USA)*

Capillitas mine (27°27'S, 66°30'W) is a high-sulfidation epithermal-type deposit related to volcanism with shoshonitic affinities in the inner Miocene-Recent magmatic arc of northwestern Argentina. The vein type mineralization is hosted by volcanic and granitic rocks, and is emplaced in and around a diatreme which cuts a lower Paleozoic granite of the Pampean Ranges. Seven stages of ore mineralization occur, separated by episodes of fracturing.

Tetrahedrite-tennantite group minerals have been observed during the 3rd and 4th stages of mineralization, in 12 of the 19 veins of the deposit. Rhodochrosite is the dominant gangue, with subordinate quartz and alunite. Tetrahedrite-tennantite occurs as coarse grain masses or as tetrahedrons (< 5 mm) in small cavities with quartz, enargite, and hübnerite. They are associated especially with enargite, sphalerite, pyrite and galena, and usually host several inclusions of sulfosalts, tellurides and gold. The chemical composition displays considerable variability among veins, as well as within veins and single grains. Composition ranges are: Cu 33.91-50.60, Fe 0.00-7.96, Zn 0.00-10.35, S 23.81-28.47, As 0.38-22.75, and Sb 0.00-29.73 wt.%. The analyses span almost the entire tetrahedrite -tennantite series in terms of Sb-As, and Fe-Zn contents. Where tellurides and Au were found, the content of Ag in tetrahedrite-tennantite is lower (average 0.20 wt.%) than in other areas (average 0.49 wt.%). The veins with the most Ag-rich tetrahedrite-tennantite are La Grande (up to 6.30 wt.%), and 25 de Mayo (2.60 wt.%). Ag seems to have more affinity with tetrahedrite-tennantite than with gold (average fineness 920). Silver substitutes copper in various quantities, and correlates with the Sb content of the tetrahedrite-tennantite. There were also found some Pb-rich (up to 3.15 wt.%) and Bi-rich (up to 8.37 wt.%) tetrahedrite-tennantites.

THE BREAKDOWN OF BRAUNITE + QUARTZ ASSEMBLAGES THROUGH SYNTECTONIC VEINING IN MANGANESE ORES OF EASTERN LIGURIA (ITALY)

Marescotti P., Cabella R. and Lucchetti G. *(Dept. of Earth Sciences, Univ. of Genova, marescot@dister.unige.it)*

In Eastern Liguria manganese ores occur as stratiform layers (0.01-0.1 m thick) or massive lenses (5-20 m thick) near the base of the chert sequences ("Diaspri di Monte Alpe" Formation) overlaying Jurassic ophiolites. The stratiform ores originated as a consequence of Mn and Fe fractionation during turbiditic re-sedimentation of hydrothermal metalliferous siliceous muds; they consist of rhythmic interlayering of braunite-bearing levels and hematite-rich cherts. Tectono-metamorphic re-equilibration (80 Ma), under prehnite-pumpellyite facies conditions (T = 275 ± 25°C; P = 2.5 ± 0.5 kbars), affected ophiolites and their sedimentary covers inducing mobilizations and thickening of stratiform ores at the fold hinges where massive lenses, up to some tens of meters, formed. A complex network of sygmoidal veins formed during these stages, due to the strong competence contrast between the Mn-mineralized lenses and the surrounding cherts or to volume expansion at the fold hinges. Braunite + quartz is the stable assemblage formed during the diagenetic stage and the effect of the following tectono-metamorphic evolution is reflected only in structural and textural re-arrangements. Textures evolve from an intimate intergrowth of anhedral cryptocrystalline braunite and quartz to microcrystalline aggregates of equant braunite and interstitial quartz. The chemistry of braunite is faintly modified during this evolution and the variations are reflected in the progressive decreasing of the Ca, Al and Fe content. In contrast to the weak effects induced by the thermo-baric evolution, the interaction between the massive Mn-mineralization and the fluids circulating in the syntectonic veins induced the complete breakdown of the braunite + quartz assemblages close to these vein systems. Braunite + quartz assemblages were replaced by Mn-silicates (bementite, johannsenite, parsettensite and rhodonite) and carbonates (Mn-calcite and rhodochrosite) distributed with a concentric zonation from the massive mineralization to the vein wall. This mineralogical and textural evidence together with the microchemical and microthermometric analyses on primary fluid inclusions in quartz, suggest a syn-metamorphic interaction between the massive mineralization and an H_2O-CO_2 fluid with high water activity. Fluid-rock interaction caused water consumption and an increase of the CO_2 content in the residual fluid.

EPITHERMAL ALTERATION OF THE W. YEMEN RIFT-RELATED VOLCANICS AND THEIR GOLD POTENTIAL

Mattash M.A. *(Mineral Resources and Geological Survey Corporation, P.O. 5822, maalla-Aden, Yemen, Fax: 967-2-241-765)*, Diner J.A. and Strachan D.G. *(Odyssey Resources Ltd., Toronto)*

Rift formation is a key element of global tectonics. Yemen is associated with the Gulf of Aden- Red Sea- Afar triple junction. Continental extension generated large volumes of effusive rocks (2,000 m thick) in the late Oligocene- early Miocene. Basalts plot on mildly alkaline- transitional trends, whereas a majority of rhyolites show peralkaline character, (A/CNK)<1. Areas of epithermal alteration in the bimodal volcanic suite are relatively large, providing an exploration target. We have identified various styles of epithermal alteration. There are numerous propylitic areas, mostly pyrite-poor. The argillic alteration assemblage indicates low-pH solutions that converted feldspars to clays. Most argillic anomalies are hypogene, but some supergene clays may be derived from hypogene argillic zones. Epithermal clay minerals pass from smectites and illites to kaolinite, and often to dickite and pyrophyllite, with increasing degrees of acid leaching. Advanced argillic assemblages were observed in some localities indicating acidic conditions, probably in the upper levels of a quartz-adularia epithermal system. Such alteration is represented by kaolinite and alunite (jarosite). Silicification occurs as silica flooding (neutral to alkaline) or replacements (low-pH fluids). Adularia was not observed. Higher-T potassic alteration forms secondary biotite. No acid-sulfate systems were recognized. Shallow intrusions may develop hydrothermal circulation systems with the best potential for forming Au deposits in Yemen.

Mineralization is mostly pyritic or limonitic (after pyrite). Gangue is quartz (veins, stockwork, or epithermal breccia matrix), calcite or clay. Opaline silica or opalite indicates near-surface conditions. Opalite is sometimes pyritic or limonitic, but very low in gold. Quartz veins with chalcedonic banding and quartz-replaced lamellar calcite are often Au-anomalous. Most quartz-sulfide breccias carry anomalous Au and trace elements. Au in some areas correlates moderately with Ag and As, not with other analysed elements. The most prospective area (Utmah) is enriched in all analysed trace elements except Zn. The observations indicate the potential for epithermal Au discoveries in Yemen.

18. Ore Mineralogy

MINERALOGY OF THE EL MOLAR METAMORPHIZED DEPOSIT OF Mn, CATALONIA

Escusa A. and Melgarejo J.C. *(Dept. Cristal·lografia, Mineralogia i Dipòsits Minerals, Univ. of Barcelona, joanc@natura.geo.ub.es)*

The Carboniferous series in the southernmost part of the Catalonian Coastal Ranges (NE Spain) unconformably lies on a Precambrian basement. The Carboniferous series consists of 10 m of cherts (Tournaisian), unconformably covered by 2000 m of turbiditic series (Visean-Upper Namurian). These sediments were affected by the Hercynian deformation and low-grade regional metamorphism. Late-Hercynian granitoids produced a contact aureola.

The Tournaisian chert is rich in radiolarians, and contains the Mn deposits. In the El Molar mine, a meter-thick bed of Mn silicates occurs close to the contact with the basement. The Visean series contains angulous blocks of cherts and Mn sediments.

The Mn mineralization consists of banded and fine grained Mn silicates (a mm-thick interbedding of amphibole-spessartine beds, tephroite beds and pyroxmangite beds), crosscut by irregular veins with coarse pyroxmangite. These associations formed during prograde metamorphism of a protore composed by Mn carbonates, clays and quartz. The random arrangement of most of these minerals suggests that they formed during the contact metamorphism. Retrograde metamorphism produced replacement of tephroite by friedelite.

Accompanying minerals occur disseminated, are fine-grained (20-100 μm), and comprise Ni-Co arsenides (niccolite, skutterudite), galena, sphalerite, chalcopyrite, pyrite, molybdenite, chalcostibite, melonite, hessite, breithauptite, scheelite, apatite, monazite, geikielite and manganochromite. The primary association indicates low S activity in the ore forming fluids, but the niccolite grains are partly replaced by gersdorffite, indicating a late sulphidation.

The geological context of these deposits (deep sediments, absence of contemporaneous volcanism, stratiform mineralization), and their complex mineralogy suggest that they formed by sedimentary-exhalative processes.

PETROMETALLOGENY AND PETROMETALLITES

Marza I. *(University of Cluj, Romania, imarza@bioge.ubbcluj.ro)*

This study approaches in detail the relationship between Petrometallogeny (the process) and petrometallite (the mineralised rock or the result of petrometallogenetic process). Petrometallogeny is a highly general concept reflecting the phenomena which cogenetically comprises the petrogenesis and metallogenesis of the endogenic and exogenic environments including the tectonic setting as a manifestation framework.

We consider the Petrometallogenetic phenomenon as an unique process which is developed in various geological hypostases and we distinguish: Global Petrometallogeny or Geospheres Petrometallogeny (consisting of processes related to the Geospheres of the Earth), Plate Geopetrometallogeny or Geomegastructural Petrometallogeny (referring to the megastructures of the Earth, i.e. to the lithospheric plates and the contact between them), Petrometallogeny Proper (regarding the geochemical-mineralogical environment of the unitary synprocessual and quasi-synprocessual rock and ore formation), which concerns the magmatic field (magmatic petrometallogeny), the metamorphic field (metamorphic petrometallogeny) and the exogenic field (exogenic petrometallogeny).

Considering ores as geological entities, without taking into account their relationship with the genetically associated rocks, means to ignore the causative link and the interdependence which exists between them.

The concrete product of Petrometallogeny is the petrometallite (mineralized-metalized rock); the mineralogical composition of which as well as its structure and texture reflect the nature of the process - that is the geochemical conditions and the thermodynamics of the forming environment - and consists of orthopetrometallite (*i.e.* chromiferous peridotite), of postmagmatic petrometallite (greisen skarn petrometallite *etc.*), of metamorphic petrometallite (metaoxypetrometallite, *e.g.* magnetite - hematite - quartzite), exogenous petrometallite (exopetrometallite, *e.g.* gold conglomerates).

REVISION OF SULFOSALT NOMENCLATURE AND DEFINITION: 1998th SITUATION

Moëlo Y. *(Lab. of Solid Chemistry, Univ. of Nantes, moelo@cnrs-imn.fr)*, Mozgova N.N. *(IGEM-Acad. of Sci., Moscow)* and the members of the Sulfosalt Sub-Committee of the COM/IMA

Sulfosalts form an heterogeneous group of about 190 complex sulfides (together with minor selenides and tellurides), which correspond to the general chemical formula:

$$(Me_1,Me_2...)^{n+}_x[(Bi,Sb,As)^{3+},Te^{4+}]_y[(S,Se,Te)^{2-},Cl\text{-}O^{2-}]_z$$

Many new mineral species have been discovered in the last thirty years. The crystal structures of most of them have been solved, and various classification schemes based on their crystal chemistry developped. Intensive reexamination of data on the sulfosalts, particularly in the 1980s, revealed problems in definition and nomenclature that needed to be solved.

This poster reviews the problems, taking as a basis the general modular classification of Makovicky (1989). Individual groups are presented and discussed (with those minerals which represent a series shown in brackets): galena 3D- and 2D-derivatives (freieslebenite, lillianite, pavonite, matildite, jordanite); SnS 3D- and 2D-derivatives (miargyrite, meneghinite) ; composite PbS/SnS 2D-derivatives (cylindrite, galenobismutite); PbS/SnS 1D-derivatives (boulangerite, zinkenite, aikinite, plagionite, sartorite); specific Tl- and Hg-sulfosalts (hatchite, routhierite); Ag-rich sulfosalts (pyrargyrite, polybasite); Cu-rich sulfosalts (bournonite, tetrahedrite); other Cu sulfosalts (muckeite).

Of the *c.*190 known sulfosalts, different questions of definition and nomenclature remain for about 30, *e.g.*, are they species or varieties; are they pure compounds, or mixtures; are they two names for a single species... ? To solve these questions will, in most cases, require further detailed study, especially the acquisition of crystal structure data on type specimens. The best way to do this involves ore mineralogists and crystallographers working as a team.

Reference

Makovicky, E. (1989) - *N. Jb. Miner. Abh.* **160**, 269-297.

$\delta^{34}S$ SYSTEMATICS IN POLYMETALLIC ORE DEPOSITS IN THE CARPATHIAN CONTINENTAL VOLCANIC ARC

Pantó Gy., Demény A., Nagy B. *(Lab. for Geochem. Res, Hung. Acad. Sci., panto@sparc.core.hu)*, Krouse R. *(University of Calgary)* and Vytik M. *(Virginia Polytechnic Institute and State University)*

The ore deposits studied in this paper belong to the Cenozoic Inner Carpathian volcanic arc that consists mainly of subduction-related andesitic rocks with subordinate amounts of dacite and rhyolite. The main ore minerals are pyrite, galena, sphalerite, chalcopyrite, marcasite, wurtzite, antimonite in the Mátra deposit and pyrrhotite, sphalerite, chalcopyrite and pyrite in the Börzsöny deposit. Formation temperatures are ~200-250°C. In this work S isotope compositions of sulfide minerals and whole rocks have been measured to refine the models of fluid origin. The data are scattered from -20.7 to 18.1 ‰ (relative to CDT). The average whole rock composition is +3.2 ±1.5 ‰ that can represent the magmatic composition. This composition is significantly higher than the primary mantle value of ~0 ‰ and would indicate significant crustal contamination in accordance with earlier O, Sr, Nd, Pb isotope studies. The sulfide minerals that belong to the early ore generations have $\delta^{34}S$ values close to the presumed magmatic compositions, whereas the gel pyrite formed in the latest generation have the very negative and positive values. Such large variations can be attributed to mobilization of sedimentary material, which is supported by the fact that these late-stage dikes are situated close to coal-bearing country rocks. The comparison of the $\delta^{34}S$ values with earlier H, C, O isotope data suggests that magmatic water carrying magmatic sulfur was mixed with fluids originating from the country rocks. These formation waters were of meteoric origin and contained dissolved sedimentary carbon and organic-derived CO_2. Fractionations between sulfide minerals indicate disequilibrium due to the combined effects of contamination by mobilized sedimentary sulfur and fractionation during mineral precititation.

PHOTOLUMINESCENT MINERAL HALOES AROUND KIMBERLITE PIPES

Bushev A.G., Portnov A.M., Rogozhin A.A., Gorobets B.S. and Tiulenev V.M. *(VIMS, Moscow)*

Photoluminescent (PL) mineral haloes around veins, orebodies, mineral occurrences for various types of mineral deposits were studied. Particularly, kimberlite pipes of Arkhangelsk region proved to be surrounded by huge haloes formed by pathfinder PL mineral scatterings. Grains of calcite with blue or reddish PL, of apatite with violet or yellow PL, of zircon with yellow PL were systematically found in halo zones of the pipes, these zones stretching up to as far as 1.5 km from exocontacts. In the horizontal plan the surface of the haloes surpasses many times this one of the pipes themselves. A special index of contents of PL minerals was induced as a number of PL grains per 1 cm^2 of the surface of rock pieces to be looked through under UV-lamp. The highest index proved to be for the minerals in the halo coaxial zones stretching up to about 350 metres from the exocontact, there the index is up to 110 grains/cm^2 for calcite having red PL (due to Mn^{2+}) and 280 for calcite having blue PL (intrinsic centers); it is about 0,7 for apatite with yellow PL (Mn^{2+}) and about 1,1 for apatite with violet PL (Ce^{3+}). The index is up to 2,5 for zircon with yellow PL. The contents of the PL minerals in the halo zones surpass background values for the same minerals in the country rocks evaluated at the distances more then about 1500 m from kimberlite exocontacts: for calcite by 40 times, for apatite by 20 times, for zircon by 140 times (!). The observed effect is supposed to be due to heating and recrystallisation of the country rocks by means of abyssal fluids. Heating stimulated entering of Mn^{2+} ions either calcite crystal lattice, or the apatite one, the last of these minerals having been formed due to mantle phosphorus. Thus the PL haloes studies can help in local prospecting for kimberlite as PL of minerals can be an indicator of exocontact action on the country rocks by mineral forming fluids.

STRUCTURAL PATTERNS AND THEIR ROLE IN THE FORMATION OF ALTERATION AND MINERALIZATION IN THE WESTERN YEMEN RIFT-RELATED VOLCANICS

Shawki M.N. and Mattash M.A. *(Department of Geological Sciences, University of Ta'iz, Yemen, P.O. No. 6803, Fax: 967-4-222-871)*

All the structural patterns display in the rift-related volcanic area are associated with major tectonic components of the Red Sea and less commonly with the Gulf of Aden. Faults which belong to the Cenozoic volcanics frequently have WNW (290-300°) trend. In the southwestern-most region such faults are considered as feeders for volcanic activity. Most of the volcanic dikes follow the same trend of faulting (WNW). Some other faults strike N-NW (330-350°) characterize those structures which are more or less parallel to the main Red Sea trend. The Majority of these structures are normal faults. NE trending faults in the volcanic area follow the transform system in the Red Sea trough. East-west structures, and less commonly north-south faults have very important role in controlling mineralization. The central (Dhamar) and southern (Ad Dhala) regions formed the Tertiary (probably early Miocene) and are consistent with the graben formation, which became a troughs of the relatively younger volcanic activity. Calderas are also significant in this respect as they are considered to be the source structures of huge pyroclastics found at the upper part of the volcanic stratigraphy.

The magnetic map reveals large magnetic domains trending northwest, west-northwest, and east-west, which exert influence over the distribution of hydrothermal systems. Hydrothermally altered areas are relatively large and widely distributed and probably related to preexisting basement structures.

Tertiary intrusions have risen preferentially to high crustal levels throughout the basement structures and groundwater has penetrated to great depth along fractures and fault systems producing alteration haloes. This suggest that Tertiary structures are shallow and don't cut to deep structural levels, comparing with some other extensional areas.

The shallow intrusions tend to develop hydrothermal circulation cells with the best potential for generating gold deposits in Yemen.

Ag-Cu ISOMORPHISM IN MINERALS FROM SILVER DEPOSITS OF YAKUTIA.

Samusikov V.P., Gamyanin G.N. and Pavlova L.A. *(Inst. of Geosciences, SB RAS, Yakutsk, geo @ yacc. yakutia. su)*

Ag and Cu ionic radii differ significantly from each other (Cu^+ - 0.96 Å, Ag^+ - 1.26 Å), so isomorphism is difficult between them. The available data show they can substitute for each other forming isomorphous series when generating minerals under the near-surface conditions. Ag and Cu minerals such as native Ag, acanthite, polybasite, pearceite, pyrargyrite, miargyrite, tetrahedrite-freibergite, chalcopyrite, chalcocite, and others were revealed in near-surface silver-base metal and silver deposits of Eastern Yakutia. From the above minerals, in accordance with reference data, limited Ag-Cu isomorphism was established in polybasite (to 10% Cu) and pearceite (to 18% Cu). Their complete intersubstitution was only established in the tetrahedrite-freibergite series. According to our data, there are other isomorphous series of these elements too. In 1994, the Commission on New Minerals has affirmed a new mineral - lenaite ($AgFeS_2$) comparable with chalcopyrite in structure. The authors have got information about composition of mineral segregations intermediate between chalcopyrite and lenaite with different Ag/Cu ratios. The analyses are well calculated for a formula $(AgCu)FeS_2$. It allows us to consider chalcopyrite and lenaite to be the end members of a single isomorphous series. From the N.Suhr's experimental data (*Econ. Geol.*, 1955, **50**, 247), Ag-Cu isomorphism in the Ag_2S-Cu_2S system is insignificant. Reference books show that admixture of Cu in acanthite and Ag in chalcocite is no more than 1%. We have determined the whole of spectrum of intermediate mineral compositions in the acanthite-chalcocite series. Taking into account that both minerals are from the monoclinic system we can conclude that there is a complete isomorphous series for Ag and Cu. We have also determined Cu substitution for Ag in miargyrite up to 19%. This is the intermediate composition between miargyrite ($AgSbS_2$) and chalcostibite ($CuSbS_2$). It is possible there is a complete Ag-Cu intersubstitution though these minerals differ in structure.

A PRELIMINARY STUDY OF O, Si, S, AND Pb ISOTOPIC COMPOSITIONS FOR THE BESSHI-TYPE Cu-Zn DEPOSIT AT FAZIBA, SE GANSU, NW CHINA

Song X., Guo Y., Xu Q. *(Institute of Mineral Deposits, CAGS, imdcags@public3.bta.net.cn)*, Li S. and Qiao L. *(Geological Brigade No. 1, Gansu Bureau of Geology and Mineral Resources)*

The Faziba Cu-Zn deposit is the first example of the Besshi-type deposits in China at present. The Cu-Zn deposit occurs in the Yangba Formation which is composed of low- and medium-grade metamorphic rocks(chlorite schist, epidote-chlorite schist, quartz-albite-epidote-chlorite schist, chlorite-sercite schist, sercite-quartz schist, quartzite, chlorite quartzite and magnetite quartzite) and belongs to the the Bikou Group of the Middle and Upper Proterozoic Erathem. In the Faziba district, massive sulphide ores mainly occur at the contact between magnetite quartzite and chlorite schist of the Yangba Formation. Ore minerals of the Besshi-type Cu-Zn deposit are chalcopyrite, pyrite, sphalerite and magnetite. Gangue minerals include quartz, chlorite, sericite and carbonates.

Average (15.08 ‰) of $\delta^{18}O$ values, ranging from 14.2 to 15.7 ‰, for quartz separates of magnetite quartzite and quartz vein from the Faziba deposit is very similar to that (15.23 ‰) for quartz separates of sericite-quartz schist and magnetite quartzite from the Yangba Cu-(Co) deposit which is situated in the same Yangba-Bikou Metallogenic Belt, SE Gansu.

$\delta^{30}Si$ values for magnetite quartzite (0.0-0.4 ‰) and quartz vein (0.1‰) in massive chalcopyrite-pyrite ore from Faziba are similar to those for the quartzite (0.0 ‰) of the Middle Proterozoic Erathem in Beijing area, the Bayan Obo quartzite (0.0-0.1 ‰) of Pt_2 and the Bajiazi quartzite (0.1 ‰) of Pt_2, N. China.

$\delta^{34}S$ values for pyrite separates from the massive Cu-Zn ores at Faziba range from -1.7 to +1.0 ‰. This implies that sulphur of the Faziba sulphide ores was derived from a mantle source.

Lead isotopic ratios of pyrite separates from Faziba have been determined. $^{206}Pb/^{204}Pb$, $^{207}Pb/^{204}Pb$ and $^{208}Pb/^{204}Pb$ ratios of Faziba pyrite range 17.977-18.612, 15.479-16.039 and 37.850-39.131, respectively. On $^{207}Pb/^{204}Pb$-$^{206}Pb/^{204}Pb$ and $^{208}Pb/^{204}Pb$-$^{206}Pb/^{204}Pb$ diagrams, the data define a linear trend extending from the mantle field to the lower crust field of Zartman and Doe (1981). This isotopic trend is interpreted as resulting from the mixing of lead from a mantle source with that from a lower crust source. The scatter of the Pb isotopic data for the Faziba deposit may be due to the addition of radiogenic lead to the pyrite during a post-oreforming event.

NEW DATA ON THE MINERALOGY OF SULPHOSALTS FROM THE FELBERTAL SCHEELITE DEPOSIT, AUSTRIA

Topa D. and Paar W.H. *(Dept. of Mineralogy, Univ. of Salzburg, Dan.Topa@sbg.ac.at)*

The Felbertal scheelite deposit is the fourth largest producer of tungsten in the world. It is located in the Felbertal, Salzburg Province of Austria, hosted by amphibolites and hornblendites, and is mined underground from different ore bodies. Sulphides and sulphosalts are frequently associated with scheelite and occur in quartz veins and irregular quartz masses. Uneconomic grades of Ag and Au have been recognized with this type of ore.

No study of the sulphosalts has been performed since 1984. As part of a PhD project a systematic investigation of the sulphosalts has recently begun. The following associations of sulphosalts were analysed by microprobe, image and X-ray techniques:

1) galenobismutite (gb) -bismuthinite derivatives (bd) - members of the lillianite homologous series (LHS) -cannizzarite -tetradymite -native Bi, 2) gb-eclarite, 3) eclarite-cosalite, 4) cosalite - galena ss-members of LHS, 5) gb-bd members of the pavonite homologous series (PHS)- members of LHS, 6) bd- hodrushite- wittichenite.

Members of the lillianite homologous series are Cu-free, contain up to 2 wt.% Cd, present no exsolution textures and can be grouped as follows: $^{\sim 4}Lill_{1-70}$, $^{\sim 5.5}Lill_{4-47}$, $^{\sim 6}Lill_{7}$, $^{\sim 7}Lill_{2-52}$. The bismuthinite derivatives almost continuously cover the composition field of the bismuthinite - aikinite series. Several gaps exist between pekoite and gladite. Exsolution pairs are rare and appear between phases defined by the following N_A: 11-30, 14-35, 39-42 , 38-48 and 38-42-49.

Members of the pavonite homologous series can be divided into two groups:1) Cu-free, high-Cd (2.5-6.7 wt.%) makovickyite (x=0.4-0.6) and pavonite (x=0.4-0.8), 2) Cu(2.9-3.9 wt.%), low-Pb (~2 wt.%) and low-Cd (0.2-0.9 wt.%) makovickyite.

The cannizzarite-like mineral shows a continuous increase of Ag (from 0-1.7 wt.%) and Bi, and decrease of Pb, suggesting a possible substitution mechanism of the type: $2Pb^{+2} \rightarrow Ag^{+1} + Bi^{+3}$.

BONCHEVITE AND KIRKIITE: TWO RARE SULFOSALTS FROM VULCANO (AEOLIAN ISLANDS, ITALY)

Garavelli A., Vurro F. *(Geomineralogical Dept., Univ. of Bari, vurro@lgxserver.uniba.it)*, Borodaev Y.S. *(Dept. of Geol. Univ. Of Moscow)* and Mozgova N.N. *(IGEM RAS, Moscow, nad@igem.msk.su)*

Since 1990, a deposition of Pb-Bi sulfide and sulfosalt assemblage was recorded in the crateric fumarolized area of the "La Fossa" cone of Vulcano (Aeolian Islands, Italy). Among the collected phases two rare mineralogical species were collected : bonchevite, $PbBi_4S_7$, and kirkiite, $Pb_{10}(Bi,As)_6(S,Se)_{19}$. Bonchevite (admixed with bismuthinite, galeno-bismutite, cannizzarite and lillianite), was collected from a high temperature (607°C) fumarolic vent. Results of electron-microprobe analyses and X-ray powder diffraction data agree closely with those of the synthetic phase V-2. A distinguishing feature of the mineral composition is an admixture of Se (0.64-2.23 wt.%). The data obtained support bonchevite as a valid mineral species which can be used as indicator of high temperature environments. Se-kirkiite, sporadically admixed with sphalerite and cannizzarite, occurs at Vulcano, as aggregate of pseudo-hexagonal short-prismatic crystals (up to 100μm) covering breached altered rock. Optical properties, X-ray powder diffraction data and the results of electron-microprobe analyses are close with those of kirkiite. The mineral contains as much as 0.73 -1.16 wt % Se to distinguish it from type samples. As and Bi concentrations range from 6.49 to 7.98 wt % and from 14.32 to 16.84 wt %, respectively, with a negative correlation between As and Bi contents. The composition field of kirkiite from Vulcano is described by formula $Pb_{10}(As_{6-x}Bi_x)_6(S_{19-y}Se_y)_{19}$ where $2.3 \leq x \leq 2.8$, $0.3 \leq y \leq 0.5$. The average formula is $Pb_{9.97}(As_{3.35}Bi_{2.61})_{5.96}(S_{18.65}Se_{0.42})_{19.07}$, close to ideal $Pb_{10}(As,Bi)_6(S,Se)_{19}$. Kirkiite assemblage in Vulcano is caused by high fugacity of sulfur and rather high temperature (470°C). This temperature is in agreement with that known for synthetic analogue.

20. Breakthroughs in Synchrotron Radiation in Mineralogy

SURFACE STUDIES OF MINERALS WITH XPS AND XANES USING SYNCHROTRON RADIATION

Bancroft G.M.* *(Dept. of Chemistry, University of Western Ontario, London, Ontario)*

Monochromatized synchrotron radiation has recently made it possible to obtain much more detailed analysis of mineral surfaces using X-ray photoelectron spectroscopy (XPS), X-ray absorption near edge structure (XANES), and XANES microscopy. Better spectroscopic resolution can be obtained with synchrotron-based XPS (SXPS); but the major advantage to date of SXPS has been the dramatic improvement in surface sensitivity. The advantage of SXPS will be illustrated with recent studies of the reactivity of pyrite (FeS_2) surfaces using S 2p SXPS spectra. Future prospects for narrower linewidths (with better chemical resolution) will be discussed.

XANES spectroscopy often offers much improved chemical resolution over XPS (or present SXPS) especially on non-conductors; but the surface sensitivity is not as good as SXPS. The analysis depth can be varied by detecting Auger electrons, total electrons (TEY), or fluorescence photons (FY). The advantages of XANES will be illustrated with the B 1s spectra of borates and the P 2p spectra of phosphates.

Finally, microscopic techniques with high spatial resolution (<1μm) and excellent energy resolution are being developed now using synchrotron radiation. The power of one of these techniques (XANES microscopy) will be illustrated using phosphate and oxidized sulphide surfaces.

* *I would like to acknowledge my coworkers: A. G. Schaufuss, H.W. Nesbitt, R. Szargan; M. Kasrai, M.E. Fleet, D. Li; M. J. Scaini, G.W. Canning, D.L. Legrand and G. Destasio.*

APPLICATIONS OF SOFT X-RAY XANES SPECTROSCOPY TO MINERALOGY AND GEOCHEMISTRY

Fleet M.E., Muthupari S., Kasrai M. and Farrell S.P. *(Depts. of Earth Sciences and Chemistry, Univ. of Western Ontario, mfleet@julian.uwo.ca)*

Soft X-ray region K-edge XANES collected by fluorescence yield (FY) is now used routinely to obtain information on nearest-neighbour coordination, chemical state and bonding of light elements in amorphous and uncharacterised crystalline materials and thin films. Typical edge shifts are +5 eV for $^{[3]}B$ to $^{[4]}B$, +2 eV for $^{[4]}Si$ to $^{[6]}Si$, and +11 eV for S^{2-} to S^{6+}. Spectra collected by total electron yield (TEY) are sensitive to near-surface structure, and have been used to characterise ubiquitous near-surface damage of borates and borosilicates involving conversion of $^{[4]}B$ to $^{[3]}B$, and tarnish on copper sulfides. The technique is non-destructive and requires minimal sample preparation and small sample size (*e.g.* <5 mg). XANES results for Si and B are in good agreement with ^{29}Si and ^{11}B NMR, respectively. The proportion of $^{[6]}Si$ is 50-60 % in 1 bar alkali and alkali-CaO silicophosphate ($2SiO_2.3P_2O_5$) glasses, and is largely independent of quench conditions. $^{[6]}Si$ varies from 0 to 49 % in ternary MoO_3-SiO_2-P_2O_5 glasses with molar (MoO_3 + SiO_2) > P_2O_5; our results reveal that the glass structure is comprised of separate molybdophosphate and silicophosphate entities. Surprisingly, pressures up to 20 kbar result in a decrease in $^{[6]}Si$ in glasses of SiP_2O_7 composition. Unlike the PEELS method for exciting B K-edge spectra, B K-edge XANES is not affected by beam damage. B K-edge XANES have been collected for a variety of borate and borosilicate minerals of known structure and used to predict that priceite has 80 % $^{[4]}B$. Study of alkali borosilicate glasses reveals that addition of alkali (particularly K2O) at 50 % SiO_2 first converts $^{[3]}B$ to $^{[4]}B$ then depolymerises silicate entities. S K-edge XANES reflect the contribution of metal 3d electrons to metal-S bonds, and are useful for chemical state of S in silicate glasses and coals. All spectra were collected on Aladdin-CSRF DCM and grasshopper beamlines.

SYNCHROTRON STUDIES OF INTERACTIONS AT THE SURFACES OF IRON OXIDE AND IRON SULFIDE MINERALS—PROBING THE REDOX BOUNDARY

Vaughan D.J. *(Dept.of Earth Sciences, Univ. of Manchester, David.Vaughan@man.ac.uk)*, Charnock J.M. *(Depts of Earth Sciences and Chemistry,Univ. of Manchester)*, Livens, F.R. *(Dept. of Chemistry, Univ. of Manchester)*, Parkman R. H. and Pattrick R.A.D. *(Dept. of Earth Sciences, Univ. of Manchester)*

The (hydroxy)oxide and sulfide minerals of iron span a key redox boundary in the natural environment and play an important role in the large scale geochemical cycling of the elements; they are also important phases in the wastes from mining and related industrial activities.

These extremely fine particle materials are difficult to characterise and highly reactive, having large surface areas. Techniques employing synchrotron radiation, and in particular X-ray absorption spectroscopy (XAS), offer one of the few methods of characterisation and of studying the reactions between these phases and other species, notably metals, in solution. Our recent work in measuring the uptake of a range of metals (Cu, Cd, As, La, U, Tc) by bulk chemical analysis, and in detecting their mode of uptake using XAS, shows a rich variety of behaviour, including chemisorption and redox and replacement processes of particular relevance to the geochemical cycling of the metals.

X-RAY ABSORPTION SPECTROSCOPY AS A TOOL FOR THE DETERMINATION OF CRYSTALLOGRAPHIC AND ELECTRONIC STRUCTURES OF MINERALS

Sainctavit Ph., Cabaret D., Ildefonse Ph. and Deudon C. *(Lab. de Minéralogie-Cristallographie de Paris, sainctavit@lmcp.jussieu.fr)*

X-ray Absorption Spectroscopy (XAS) in the soft x-ray range provides original answers in the determination of electronic or crystallographic structures of minerals. One needs to record high quality experimental data with excellent spectral resolution and take advantage of all the possible dichroisms: natural or magnetic, linear or circular dichroisms. The data cannot usually be interpreted by EXAFS (Single Scattering) theory, and state of the art theoretical methods of XAS are required to yield valuable information.

For the K-edges of low Z cations, as Al or Mg, Full Multiple Scattering (FMS) calculations coupled with band structures are essential. In the case of Al in tetrahedral or octahedral coordination, the combination of experiment and calculations allows to characterize the nature of the valence bands and relate spectral features to the nature of the Al-O chemical bond. This can be corroborated by band structure calculations whose density of states can be compared to XAS spectra. Natural dichroism helps to determine the medium range nature of features generally attributed to the coordination shell. At the Mg K-edges in pyroxenes, it is possible to separate the M1 and M2 contributions by a comparison between enstatite and diopside. The analysis is confirmed by FMS calculations where the medium range nature of the features of the edge region can be well demonstrated. Moreover the very powerful finger-print approach can receive through a comparison with calculations a theoretical confirmation, as shown by a series of Al K-edges in phyllosilicates.

For the $L_{2,3}$ edges of 3d transition elements, the usually appropriate method to interpret the data is the Ligand Field Multiplet theory. This theory is mainly well suited in compounds where the chemical bond plays an important role. In the case of copper based spinel and thiospinel, it is possible to assign a formal valence to Cu ions and clearly identify the local (tetrahedral vs octahedral) environment of copper. X-ray Magnetic Circular Dichroism helps to go further and show clear evidence for the magnetic coupling between the ions. In some magnetic chromite and thiochromite, we have unambiguously determined the spin orientation of the sub-networks and separated the orbital and spin contributions to the magnetic moments.

20. Breakthroughs in Synchrotron Radiation in Mineralogy

X-RAY PHOTO-EMISSION ELECTRON MICROSCOPY (XPEEM): APPLICATION TO VALENCE-STATE IMAGING AND MICRO-AREA SPECTROSCOPY OF MINERAL INTER-GROWTHS

Cressey G., Schofield P.F. *(Dept. of Mineralogy, Natural History Museum, London, g.cressey@nhm.ac.uk)*, Cressey B.A. *(Dept. of Geology, Univ. of Southampton)* and Smith A.D. *(Daresbury Laboratory)*

Recent advances in soft X-ray absorption spectroscopy show that $2p(L_{2,3})$ spectra provide a sensitive fingerprint of the electronic states of 3d metals, and that calculated spectra facilitate the interpretation of valence states, site symmetries and crystal field parameters. However, area-selectivity is not possible with the standard technique. Hence, if impurity phases are intergrown on a micro-scale, these cannot be excluded from contributing to the spectrum from a powdered sample measured by conventional total electron yield methods. We are developing X-ray stimulated Photo-emission Electron Microscopy (XPEEM) for use on the undulator beamline at the Daresbury SRS in order to obtain valence-state images and L-edge X-ray absorption near-edge structure (XANES) spectra from individual component phases in multi-phase micro-intergrowths in a non-destructive manner.

Secondary electrons (stimulated by the primary X-ray absorption) emitted from the polished surface of the specimen are focused into an image by electrostatic objective and projector lenses. As the X-ray energy is scanned across an edge of interest, XPEEM images are recorded at each 0.1 eV step. Selected area XANES spectra can subsequently be extracted from chosen pixel areas of the resulting image set by plotting image intensity against incident X-ray energy.

We demonstrate that single-phase spectra can be extracted from fine-scale intergrowths of magnetite, hematite and goethite using XPEEM. Our investigations of Mn-Fe spinel (jacobsite), show that Mn^{2+}, Mn^{3+}, Fe^{2+} and Fe^{3+} are present, but a Mn^{4+} signature (present in the powdered sample) is predominantly from 10μm-wide veins and patchy intergrowths of Ba-Mn oxide (hollandite).

CHEMICAL FORMS OF HEAVY METALS IN SOILS: CONTAMINATED FIELDS VS. GEOCHEMICAL ANOMALIES

Juillot F., Morin G., Ildefonse P., Calas G. *(Lab. Min. Crist., Paris, calas@lmcp.jussieu.fr)*, Buatier M. *(Lab. Sédiment. Géodyn., Lille)*, Chevallier P., Populus P. *(LURE, Orsay)*, Brown G.E.Jr., Trainor T. and Ostergren J. *(Dept. Geol. Env. Sci., Stanford)*

More than 100 years of lead and zinc processing in Western-Europe gave rise to important contamination of agricultural fields by smelter emissions. Laboratory field sites, where lead and zinc levels exceed 200 ppm in soils throughout a several tenth km² area, have been chosen, in order to determine the long term mobility and bioavailability of these contaminants. Comparing the speciation of these metals in smelter-contaminated soils with that in natural geochemical anomalies, may help to better predict their ultimate fate. These parameters are essentially controlled by molecular-scale mechanisms involving surface/solution interactions with soils components, and can then be directly assessed by in-situ analyses, as EXAFS spectroscopy, coupled with trace elements mapping (μSXRF) as well as with micro- and nano-scale analyses (AEM, TEM).

In the smelter-impacted fields, μSXRF mapping on top soil thin-sections evidences that dark silty dusts related to eolian transfers from the smelter and tailings constitute important sources of both Pb and Zn in the soils. Besides, Zn and, at a lesser extent, Pb are always detected in the clayey matrix. In these finely-divided materials, TEM analyses show that Zn is intimately associated with phyllosilicate minerals and iron oxides while Pb is locally concentrated in Pb and P rich phases. Pb-Pb contributions in Pb-L_{III} edge EXAFS data strongly support these latter observations, while Zn-K edge EXAFS data suggest the occurence Zn-rich surface precipitates. In the natural analogue studied, μSXRF and AEM observations evidence that Pb, released from galena weathering, is sinked in secondary crystalline phases and associated with hydrous metallic oxides. Eventually, with the help of selective chemical extractions, quantitative data on exchangeable and more tightly bonded species will be presented.

APPLICATIONS OF SOFT X-RAY SPECTROMICROSCOPY TO ENVIRONMENTAL GEOCHEMISTRY AND MINERALOGY

Myneni S.C.B. *(Earth Sciences Division, Lawrence Berkeley National Laboratory, smyneni@lbl.gov)*, Warwick A., Hussain Z. *(Advanced Light Source, Lawrence Berkeley National Laboratory)* and Meyer-Ilse W. *(Center for X-ray Optics, Lawrence Berkeley National Laboratory)*

Synchrotron based soft X-ray spectromicroscopy technique is a new emerging technique in environmental geochemistry. This technique enables the examination of absorption spectra of K-edges of lighter elements, and the L-, and higher edges of high atomic number elements in a wide variety of matrices. High resolution element-, or functional-group specific images (currently the resolution is better than 50 nm) of samples can be obtained in wet environment. NEXAFS spectra and information on the coordination environment of different elements can also be obtained from regions as small as 70nm size in a sample. Using this technique, we examined the *in-situ* aggregate structures of mineral and organic colloids collected from aquatic and soil systems. The morphology of the aggregates, internal structures and their chemistry have been examined as a function of solution pH, ionic strength, and other chemical parameters. A brief discussion of these results will be presented. Some preliminary results of the soft X-ray spectroscopic studies of mineral-water interfacial reactions, and organic coatings on mineral surfaces will also be presented.

TRACE-ELEMENT CHARACTERIZATION OF EARTH MATERIALS USING THE SYNCHROTRON X-RAY FLUORESCENCE MICROPROBE

Sutton S.R. *(Dept. of Geophysical Sciences and CARS, The University of Chicago, sutton@cars.uchicago.edu)*

High energy synchrotrons are valuable sources of highly collimated, intense x-ray radiation for use in x-ray microprobe analysis of trace elements and chemical state quantification and mapping. The undulators at third generation synchrotrons (e.g., the Advanced Photon Source, Argonne, IL, the European Synchrotron Radiation Facility, Grenoble, France) are excellent sources for x-ray microprobes because of the extremely high brilliance. A variety of techniques allow the production of x-ray microbeams including microfocusing mirrors, zone plates, and tapered capillaries. Each of these devices has advantages and disadvantages in terms of working distance, achievable beam size, gain, achromaticity, expense and ease of use. Kirkpatrick-Baez mirrors are highly versatile in being achromatic so that all energies are focused to the same spot, providing gains near 10^4, and offering long working distances (centimeters) to accommodate an array of ancillary instruments (microscopes, detectors, *etc.*). Capillaries can produce sub-micrometer beam sizes but working distance is limited (sub-millimeter).

Microprobes based on these techniques are capable of determining trace element microdistributions with <10 μm resolution and <1 ppm sensitivity. Chemical state maps can be produced with <100 μm resolution and <100 ppm sensitivity. Samples in any form (solid, liquid, gas) can be analyzed and the technique is particularly well suited for studies of wet materials because no vacuum chamber is required. In practice, most samples consist of individual particles mounted on thin plastic films or conventional thin sections with pure silica as the substrate.

These capabilities have wide applicability in geochemistry and cosmochemistry to problems such as oxygen fugacity quantification in natural systems, chemical state of hydrothermal fluid inclusions, toxic metal and radioisotope speciation in contaminated sediments, redox chemistry of metals at the root-soil interface and its role in agriculturally-relevant plant diseases, and origins and histories of interplanetary dust particles and other extraterrestrial materials.

SYNCHROTRON INFRARED SPECTROSCOPY OF EARTH AND PLANETARY MATERIALS

Hemley R.J., Goncharov A.F., Lu R. and Mao H.K. *(Geophysical Laboratory and Center for High-Pressure Research Carnegie Institution of Washington, Washington, D.C. 20015).*

Synchrotron infrared spectroscopy has been used to characterize a growing number of Earth and planetary materials at low to very high pressures. We give an overview of activity at the U2 synchrotron IR beam line of the National Synchrotron Light Source (NSLS). The beam line has up to ~10^3 times the flux of a conventional thermal source (*e.g.*, globar) and improved spatial resolution approaching diffraction limits for microspectroscopy. The facility utilizes a commercial FT-IR instrument together with custom-built microscope optics designed for a variety diamond-anvil cell experiments, including low- and high-temperature studies, and contains an integrated laser optical/grating spectrometer for concurrent optical experiments. Recent efforts have focused on the high-pressure behavior of hydrous silicates and oxides. Studies of the OH bands as a function of pressure are important for identifying mechanisms for hydrogen incorporation in these materials. The synchrotron measurements revealed that $MgSiO_3$ perovskite and coesite can accommodate a surprising amount of hydrogen in the form of OH. The high sensitivity and spatial resolution of the technique has been exploited for phase identification and for determination of hydrogen content and speciation in multiphase samples quenched from high P-T to ambient conditions. Examples include measurements on run products from the $(Mg,Fe)_2SiO_4$ system. Studies of natural diamonds at ambient pressure have also been performed: measurements reveal the detailed distribution of minerals within single inclusions of Sao Luiz diamonds, which have been proposed to have originated from the lower mantle; and measurements on aggregated cuboid diamonds reveal the presence of H_2O ice. The facility has also been used extensively in studies of planetary gases and ices to very high pressure (*e.g.*, to above 200 GPa). It has been played a major role in the discovery of new phenomena in dense molecular hydrogen. Measurements on H_2O ice have revealed the transition to the symmetric hydrogen-bonded (*i.e.*, non-molecular) phase. New transitions in high-pressure van der Waals compounds such as CH_4H_2 have also been discovered with the technique. A new integrated facility having higher IR brightness and allowing a broader range of optical and IR measurements will be discussed.

EFFECT OF PRESSURE AND WATER ON THE LOCAL ENVIRONMENT OF NI IN SILICATE GLASSES

Farges F., Siewert S. *(Lab. des Géomatériaux, Université de Marne-la-Vallée, France, farges@univ-mlv.fr)*, Büttner H. *(Mineralogisch-Petrologisches Institut, Göttingen Universität)* and Brown G.E. Jr *(Dept. of Geological and Environmental Sciences, Stanford University, and SSRL, CA 94305-2115, USA)*

The structural environment of Ni in albite and sodium trisilicate glasses containing 200 ppm to 3 % Ni has been examined using x-ray absorption near edge structure (XANES) spectroscopy. Glasses have been exposed to pressures up to 7 kbars. They contain from 0 to 5 wt.% water. High-resolution XANES data has been also collected for Ni(II)-model compounds in various coordination environments (4-, 5- and 6-coordinated, regular to highly distorted).

In model compounds, the pre-edge intensity and position change as a function of the Ni-coordination with systematic trends that are similar to other transition elements such as Ti and Mo. For 4-coordinated Ni(II), the pre-edge is more intense and located 0.55 eV lower in energy as compared to that for 6-coordinated Ni(II). The pre-edge feature increases in intensity with decreasing Ni-coordination and centrosymmetry. With this method, the influence of coordination and centrosymmetry on the pre-edge intensity can be separated.

In the glasses synthesized at ambient pressure, Ni(II) has a pre-edge intensity that is exactly similar to that measured for $KNiPO_4$ in which Ni is 5-coordinated or that for a ≈ 50:50 mixture of 4- and 6-coordinated Ni. As compared to an highly distorted octahedral site, the pre-edge for the glasses is shifted by -0.25(5) eV suggesting that distorted 6-coordinated sites cannot be the dominant coordination environment in these glasses.

In the glasses synthesized at higher pressures, a positive shift in the pre-edge position is observed, suggesting the presence of 6-coordinated environments around Ni(II), consistent with the lighter color of these glasses. In the glasses the richest in water, regular octahedral environments are detected, consistent with their crystal field spectra.

The results show that the average Ni-coordination ranges from ≈ 5 in sodic glasses synthesized at ambient pressure to ≈6 in water-bearing high pressure glasses.

TITANITE AND MALAYAITE: STRUCTURAL INVESTIGATIONS AND THE 500 K ANOMALY

Bismayer U., Meyer H.-W. *(Mineralogisch-Petrologisches Inst., Univ. of Hamburg, FRG, ubis@mineralogie.uni-hamburg.de)*, Zhang M. *(Dept. of Earth Sciences, Univ.of Cambridge, UK)*, Groat L.A. *(UBC, Canada)*, Nistor L. *(Nat. Insti. for Mat. Science, Bucharest, Romania)* and G. Van Tendeloo *(EMAT-Univ. Antwerpen, Belgium)*

Titanite, $CaTiSiO_5$, and malayaite, $CaSnSiO_5$, are isostructural. Both minerals exhibit a thermal anomaly near 500 K but diffuse reflections only occur in titanite. Synthetic titanite and natural titanite crystals from Rauris, Austria (Fe 1.8%, Al 3.8%) were studied using synchrotron X-ray diffraction, IR spectroscopy and high-resolution transmission electron microscopy (HRTEM) [1, 2, 3]. In the pure material near 500 K a structural transformation $P2_1/a$ - $A2/a$ leads to the disappearance of the gaussian contribution of the A-centering reflections. Anisotropic diffuse intensities with lorentzian profile remain visible up to *ca.* 825 K where the excess specific heat disappears. In the natural samples the phase transformation near 500 K is suppressed by impurities and the diffuse scattering occurs at room-temperature. Defect induced renormalization phenomena alter the critical behaviour. *No* antiphase boundaries were found in natural titanite.

High-temperature X-ray diffraction and IR spectroscopy were used to study the thermal anomaly of a malayaite sample from northern British Columbia. Structure determinations at different temperatures reveal a non-linear evolution of the unit cell volume and the anisotropic Debye-Waller factors of the Ca atoms near 500K. At this point IR spectra show a break in the temperature dependence of the intensity of the 533 cm^{-1} mode and the peak positions of the 499 cm^{-1} mode and the Si-O stretching mode near 908 cm^{-1}.

References

1. Kek S., M. Aroyo, U. Bismayer, C. Schmidt, K. Eichhorn and H. G. Krane. 1997. *Z. Kristallogr.* **212**, 9-19.
2. Groat L.A., S. Kek, U. Bismayer, C. Schmidt, H.G. Krane, H.W. Meyer, L. Nistor and G. Van Tendeloo. 1996. *American Mineralogist* **81**, 595-602.
3. Zhang M., E.K.H. Salje and U. Bismayer. 1997. *American Mineralogist* **82**, 30-35.

HIGH RESOLUTION Fe K- PRE-EDGE SPECTROSCOPIC STUDY IN MINERALS AND GLASSES

Galoisy L. and Calas G. *(Laboratoire de Minéralogie-Cristallographie, Universities of Paris 6/7 and IPGP, case 115 - 4 place jussieu, 75005, Paris, France, galoisy or calas@lmcp.jussieu.fr)*

Iron is a major component of most minerals and magmatic liquids. The determination of the sites occupied by ferrous and ferric cations in volcanic glasses gives information on cooling conditions as well as on the influence of fluids on the glass/melt structure. However, the sites occupied by ferrous and ferric cations in glasses are still poorly understood due to the complex structure of amorphous materials.

High resolution XANES spectra have been recorded at the Fe K-edge. A pre-edge peak is observed on the low energy side of the main edge and is usually assigned to $1s \rightarrow 3d$ like levels transitions. The shape, position and relative intensity of the various components of the pre-edge depend on Fe- coordination number and oxidation states. High resolution XANES spectra have been systematically recorded in several minerals in order to determine the modification of pre-edges as a function of Fe crystal chemistry. The influence of oxidation state, coordination number, site distortion, nature of ligands, on the position and relative intensity of the various pre-edge features has been evaluated. This set of data can be used to discuss the oxidation state and local surrounding of Fe in volcanic glasses. The glasses investigated include basaltic compositions, andesitic and more differentiated silicic glasses of rhyolitic and pantelleritic compositions.

INCORPORATION OF Yb IN SYNTHETIC PYROPE AND GROSSULAR GARNETS: XAFS/XRD STUDY AND MULTIPLE SCATTERING CALCULATIONS

Quartieri S. *(Dip. di Scienze della Terra, via S.Eufemia 19, 41100 Modena, Italy, quartieri@unimo.it)*, Antonioli G. *(Dip. di Fisica, INFM, Viale delle Scienze, 43100 Parma, Italy)*, Geiger C.A. *(Mineral.-Petrograph. Inst., Olshausenstr. 40, 24098 Kiel, Germany)*, Chaboy J. *(Inst. de Ciencia de Materiales de Aragon and Dep. de Fis. Mat. Cond., Plaza S. Francisco s/n. 50009 Zaragoza, Spain)* and Artioli G. *(Dip. Scienze della Terra, via Botticelli 23, 20133, Milano, Italy)*

Garnets of lower crust mafic and ultramafic rocks usually contain rare earth elements (REE) in trace amounts (a few tens of ppm). Although REE diffusion coefficients among garnets and coexisting phases are widely used as petrological parameters to interpret the crystallization and metamorphic history of crustal rocks, there is as yet no direct crystal-chemical characterization, due to the difficulty of obtaining structural information on trace and minor species.

In this work, the incorporation and the site preference of minor levels of Yb^{3+} (about 1.0 wt.%) in synthetic pyrope and grossular garnets have been studied by a combined approach, based on X-ray powder diffraction, XAFS spectroscopy and multiple-scattering calculations of XANES spectra. The Yb L_I- and L_{III}-edge XAFS spectra were collected in fluorescence mode at different temperatures ranging from 77 to 343 K at the GILDA beamline (ESRF, Grenoble, France). The EXAFS data analysis has been performed using FEFFIT and FEFF6 software, to simulate the most important single and multiple scattering paths of the photoelectron. The computation of the XANES spectra was carried out using the CONTINUUM code, based on the one-electron full multiple- scattering theory. Different scattering potentials and atomic cluster sizes have been tested.

Both experimental and theoretical results indicate that Yb^{3+} enters the garnet structure and is located in the X dodecahedral site in both pyrope and grossular samples. Moreover, Yb^{3+} is able to modify the local geometry of the X site. This is particularly evident in Yb-grossular: here the large X site, characteristic of Ca, contracts to be more suitable for the smaller ionic radius of Yb^{3+}.Similar structural relaxation effects have been found by Galoisy *et al.* in Ni-bearing olivines.

AN ATTEMPT TO ESTIMATE THE AGE OF OBSIDIANS USING POSITRON ANNIHILATION SPECTROSCOPY

Sachanbiński M. *(Inst. of Geological Sciences, Univ. of Wroclaw)* and Chojcan J. *(Inst. of Experimental Physics, Univ. of Wroclaw)*

Our several years of study into the microporosity of obsidians with positron annihilation spectroscopy has shown that the natural ageing process of obsidians is accompanied by an increase of a micropore concentration "seen" by positronium atoms (Ps) and this can be used to estimate the age of volcanic rocks.

It is known that a certain system can be used as a measurer of time if it changes with time. Moreover, one should know a time dependence for a proper characteristic of the system. From our studies it follows that such a useful characteristic for natural glasses (including obsidians) is intensity I_3' of the long-lived ortho-Ps component in a positron lifetime spectrum which is related to the micropore concentration "observed" by Ps. Next the dependence of I_3' on time can be obtained by measuring the positron lifetime spectra for obsidians with age known from other studies, for example radiometric research. Selected results for several obsidians are presented below.

Locality	Age[Ma]	I_3'[%]
Teneryfa, Minas de San Jose	1	0.5
Tuff, Jemez Mountains	6.7-6.8	2.7
Canovas Canyon Rhyolite, Jemez Mount.	8-11	5.9
Trzebusz, Northern Poland	276(autunion)	8.8

The lifetime spectra for the materials studied were collected by using a conventional fast-timing apparatus with BaF_2 scintillators, constant fraction differential discriminators (Ortec 583 Model), a time-to-pulse-height converter (Ortec 457 Model) and a multichannel analyzer data buffer (Ortec 919 Model). The full width at half maximum (FWHM) of the time resolution function of the spectrometer is about 350 ps. The obtained data was analysed in terms of a three-component model with the computer programs RESOLUTION and POSITRONFIT.

QUANTITATIVE ANALYSIS OF Sr-REE-Ba-DAUGHTER MINERALS IN FLUID INCLUSIONS BY COMBINED SYNCHROTRON MICRO-XRF AND SEM-EDX TECHNIQUES

Rankin A.H. *(Kingston University, UK, a.rankin@kingston.ac.uk)*, Bühn B. *(Univ Giessen, Germany, and Kingston Univ, UK, Bernhard.Buehn@geo.uni-giessen.de)*, Haller M. *(DESY Hamburg, Germany)* and Radtke M *(Lab Nac de Luz Sincrotron, Brazil)*

This study focusses on the identification and comprehensive geochemical characterization of Sr, REE, Ba-daughter minerals in natural fluid inclusions in quartz related to carbonatite metasomatism, Namibia. Burbankite $(Na,Ca)_3(Sr,REE,Ba)_3(CO_3)_5$ is a rare mineral mostly confined to highly alkaline igneous rocks. The broad spectrum of elements (from Na over LIL elements to the heavy REE) present in the burbankites can be analysed by combining Synchrotron-XRF microprobe and SEM/EDX techniques.

Quantitative and semi-quantitative SEM/EDX analyses yield SrO between 5 and 26 wt%, ΣLREE between 8 and 17 wt% and BaO between 2 and 5.5 wt% for burbankite daughter crystals. For Synchrotron-XRF analysis long-time measurements were taken on the spots with the highest count rates for Sr, REE and Ba. The quantification via fundamental parameter analysis uses Ba an internal standard, since it displays a narrow compositional range as indicated by EDX analyses, and because it is a close neighbour to the REE group of elements with respect to atomic weight. The very similar results for the REE quantification by Synchrotron-XRF and EDX analyses, respectively, indicate that the quantification procedures for both techniques yield reliable results. The Synchrotron-XRF-derived chondrite-normalized REE patterns display a negative slope of 2 to 3 orders of magnitude from La to Yb, reflecting a LREE enrichment typical of solid rock carbonatites. The Th/U ratios of burbankites are between 4 and 6 and Y/Ho ratios are very low (<5). The mere presence of REE-carbonates as large daughter minerals in these fluids shows the capability of such H_2O-CO_2-F-Cl fluids in dissolving and transporting high field strength elements in large quantities.

FRACTURED PYRITE SURFACES: EVIDENCE OF SITE SPECIFIC REACTIVITY USING SYNCHROTRON RADIATION

Schaufuss A.G., Nesbitt H.W. and Szargan R. *(Dept. of Earth Sciences, Univ. of Western Ontario, dopban@julian.uwo.ca)*

Synchrotron radiation excited photoelectron spectroscopy (SXPS) has been used to study the reactivity of pyrite surfaces in air and during adsorption of two sulfur containing surfactants, heterocycles 2-Mercaptobenzothiazole (MBT) and 2-Mercaptobenzoxazole (MBO). Unlike conventional XPS techniques, synchrotron radiation with tunable radiation source yields exceptional surface sensitivity. The use of an excitation energy of 210 eV for S2p spectra improves the contribution of the first monolayer by about one order of magnitude. Individual surface species consequently can be identified and their reactivity documented.

Air oxidation of pyrite proceeds initially by oxidation of two surface sulphur sites, S^{2-} and the surface-most S atom of surface disulphide species. The S^{2-} species undergoes oxidation to sulfate whereas bulk sulfur mainly forms polysulphide. There are also to Fe surface species, Fe(II) and Fe(III). The surface Fe(II) species is highly reactive forming FeOOH while Fe(III) sites are largely unreacted. Based on these results an oxidation mechanism is proposed which includes Fe(II)/Fe(III) redox cycling at the pyrite surface mediating the electron transfer between pyrite and molecular oxygen.

MBT sorbed to pyrite surfaces (10^{-4} M MBT solutions) is oxidized to 2,2=-Dithiobis(benzothiazole) (BBTD). This surface reaction involves reduction of pyrite. S2p spectra obtained with different excitation energies show conclusively that BBTD forms as an overlayer on the adsorbed MBT.

Although MBO and MBT are structurally similar, oxidation of MBO by pyrite is not observed. Nevertheless, the slight differences in the electronic structure seem to be responsible for this behavior.

STRUCTURAL ENVIRONMENT AND OXIDATION STATE OF MANGANESE IN GOETHITE-GROUTITE SOLID-SOLUTIONS: A RIETVELD, EXAFS, XANES, AND DRS STUDY

Scheinost A.C. *(University of Delaware, scheinos@udel.edu)*, Stanjek H. *(TU München, Germany)*, Schulze D.G. *(Purdue University)*, Gasser U. *(College of Engineering ISW, Switzerland)* and Sparks D.L. *(University of Delaware)*

We investigated the goethite-groutite solid solution, $Mn_xFe_{1-x}OOH$, using synthetic samples with x from 0 to 0.47, grown from Mn^{2+} and Mn^{3+} systems. The long-range order studied by X-ray diffraction (XRD) and Rietveld refinement confirmed that the linear increase of the unit-cell length in a-direction (UCL_a) and the linear decrease of UCL_b and UCL_c, when x increases, is caused by an increasing elongation of the basic metal octahedra, in line with the Jahn-Teller effect of Mn^{3+}. Because Mn and Fe cannot be discriminated by XRD, Mn was separately investigated by extended X-ray absorption fine structure (EXAFS) spectroscopy. While at low x the environment of Mn was very similar to that of Fe in pure goethite, increasing x led to an increasing distortion of the oxygen cage around Mn. This indicates, that at low x Mn did not cluster, but was preferentially surrounded by Fe. Only when x increased, the neighborhood of additional Mn cations allowed for a stronger distortion. This trend was confirmed by an increasing structuring of the crest in the X-ray near-edge structure (XANES) spectra, and by an increasing splitting of the cubic e_g level revealed by diffuse reflectance spectroscopy (DRS). In spite of the increasing Jahn-Teller stabilization, the crystal field splitting energy (10Dq) decreased from 13500 to 12000 cm^{-1}. The decrease of 10Dq was not counterbalanced by the increase in Jahn-Teller-stabilization, so that the overall crystal field stabilization energy (CFSE) decreased from 142 to 133 kJ mol^{-1}. The low absolute level of CFSE and its decreasing tendency with increasing x may be the key factor explaining the low stability of Mn substituted goethite in natural environments and, in turn, the rareness of $Mn_xFe_{1-x}OOH$ in soils.

GOLD COMPLEXATION BY CHLORIDE BEARING FLUIDS

Schofield P.F. *(Mineralogy, Natural History Museum, UK pfs@nhm.ac.uk)*, Bailey E.H. *(Environmental Science, University of Nottingham, UK)* and Mosselmans J.F.W. *(CLRC Daresbury Laboratory, UK)*

Gold chloride complexation has been studied for a variety of technological and geochemical reasons for over 100 years. While it is generally thought that Au is transported in sulphidic solution under hydrothermal conditions, the dominant species being $[Au(HS)_2]^-$, the importance of chloride or mixed chlorohydroxide complexes is likely to be during weathering processes.

We have monitored gold-chloride complexation up to 175°C from *in situ* XAS measurements using a specifically developed cell and furnace. Solutions of 0.1 m and 0.01 m Au were prepared from $KAuCl_4 \cdot 2H_2O$ at a range of solution pHs (pH 0.4 - 8.6). The pH adjustment was carried out by the addition of NaOH and HCl.

EXAFS spectra were collected in transmission mode at 25°C temperature intervals between 25°C and 175°C. Analysis of the absorption-edge position and the XANES structure indicates no reduction in oxidation state from Au(III) to Au(I) with increasing temperature, pH or chloride concentration.

Speciation changes were observed with increasing pH and temperature. At low pH (<4) and high chloride concentrations the square-planar $[AuCl_4]^-$ complex predominates with a bond length of ~2.28 Å. No variation is observed as a function of temperature. At pH 6 OH^- enters the first co-ordination sphere and by pH 8.6 the first co-ordination sphere appears to be dominated by OH^- at 1.98Å. While the basic square-planar geometry of these Au(III) species remains, the symmetry of the $[AuCl_4]^-$ complex is lost. Increasing the temperature for the solution at pH 6 causes the removal of the OH- ligand and the predominance of the $[AuCl_4]^-$ complex. At the higher pH however, increased temperature induces the replacement of the Cl^- ligand by OH^- ligands.

21. Ore Mineralogy of Modern Sea Floor Hydrothermal Systems

SETTING, MINERALOGY AND GEOCHEMISTRY OF THE MIDDLE VALLEY SULFIDE DEPOSITS: ODP LEG 169

Peter J.M., Goodfellow W.D. *(Geol. Survey of Canada, Ottawa, jpeter@nrcan.gc.ca)* and Leg 169 Shipboard Scientific Party

Middle Valley, northern Juan de Fuca Ridge, is a hydrothermally active rift covered by a thick sequence of turbiditic and hemipelagic sediments. The Bent Hill and ODP massive Zn-Cu sulfide mounds (BH and ODP, respectively) have been drilled during two Ocean Drilling Program Legs (139 and 169) and subsequently revisited by ROV and submersible. The mounds occur about 9 km from the axis of the rift in sediments overlying ≈300,000 year old basaltic crust. Micropaleontology suggests the deposits started to form >125 ky ago.

The N-S alignment of the deposits and the occurrence of faults that truncate the western margin of an adjacent sediment hill indicate control by extensional faults. The surface expression of BH is ≈100m across by 35 m high; ODP is 350 m to the south, consists of two peaks, and is about 150 m long by 12 m high. Drilling indicates that BH has a 104 m-thick massive sulfide accumulation that is 200 m wide E-W and which extends ≈100 m south of its summit. ODP comprises three stacked lenses of massive sulfide extending 170 m in the subsurface. The major sulfide minerals are pyrite, marcasite, pyrrhotite, sphalerite, chalcopyrite, and isocubanite. Non-sulfide minerals include carbonates, quartz, chlorite, clays and anhydrite. Mineral textures are diverse and reflect sulfide infilling and zone refining. The estimated combined tonnage of the two mounds is 15 to 20 Mt. Exceptional grades of >20 wt% Zn occur over 50 m in the lowest lens of ODP.

Both BH and ODP have well-developed sulfide feeder zones composed of impregnations and subvertical, anastomosing pyrrhotite-isocubanite-chalcopyrite-pyrite veins of variable thickness that cut hydrothermally altered sediment. At the base of the BH feeder system is a 13 m-thick, stratabound zone of isocubanite- pyrrhotite-quartz-clay ("Deep Copper Zone") containing up to 16 wt% Cu which has been deposited from high-temperature (up to 366°C) fluids which have preferentially replaced a sandstone layer in finer grained sediments. Sediments away from the mounds are altered or infilled by chlorite, quartz, smectite, carbonate and anhydrite, and are depleted in alkalis and enriched in Mg, Fe, and S.

Several of the drilled holes are now venting hydrothermal fluids. These sampled fluids, and those from anhydrite chimneys, are metal-poor and have lower temperatures (145-275°C) than measured in fluid inclusions in the massive sulfides and feeder zones (up to 354°C); therefore, they are not likely to be representative of fluids which formed these deposits.

THE THIRD DIMENSION OF A PRESENTLY FORMING CYPRUS-TYPE VMS DEPOSIT: TAG HYDROTHERMAL MOUND, MID-ATLANTIC RIDGE, 26°N

Petersen S., Herzig P.M. *(Freiberg University of Mining and Tech-nology)* and Hannington M.D. *(Geological Survey of Canada)*

ODP drilling of the active TAG hydrothermal mound in 1994 provided the first insights into the third dimension of volcanic-hosted massive sulfide deposits on a sediment-free mid-ocean ridge.

Sulfide precipitation at this site, located at 26°N on the slow-spreading Mid-Atlantic Ridge, started 50,000-20,000 years ago and resulted in the formation of a distinctly circular, 200-m-diameter pyritic mound with minor copper (2.4 wt%) and zinc (0.4 wt%) mineralisation and very low trace element concentrations when compared to other mid-ocean ridge deposits.

The episodic release of high-temperature hydrothermal fluids at TAG with intermittant periods of hydrothermal quietness is the dominant feature of this deposit. The complex assemblage of sulfide-anhydrite-quartz breccias, as well as prominent zone refining, resulting in the strong enrichment of Au, Zn and other trace elements near the top of the deposit, can be related to this processes. Mass wasting and oxidation of sulfides are widespread at TAG because of the maturity of the deposit.

The sulfur isotopic composition of bulk sulfides ($\delta^{34}S$ +4.4 to +8.2 ‰; average +6.5 ‰) implies an introduction of heavy sulfur originating from reduced seawater to the hydrothermal fluid. The distribution of sulfur isotope ratios within the deposit indicates a deep seated as well as a shallow source for the introduced seawater.

Vertical and horizontal zonations are also evident from fluid inclusion studies, providing evidence for changes in the flow regime of the hydrothermal fluids underneath the deposit between hydrothermal cycles.

HYDROTHERMAL PHYLLOSILICATE FORMATION AT SEDIMENTED RIDGES: A COMPARISON BETWEEN AXIS AND OFF-AXIS SYSTEMS (JUAN DE FUCA RIDGE)

Buatier M.D. *(Univ. Lille 1, Lab. de Sédimentologie, Martine.Buatier@univ-lille1.fr)*, Früh-Green G. *(ETH Zurich, gretli@eurasia.ethz.ch)*, Monnin C. *(Univ. Toulouse, monnin@lucid.ups-tlse.fr)* and Karpoff A.M. *(EOST-CGS Strasbourg, amk@illite.u-strasbg.fr*

Hydrothermal fluid compositions and the type of authigenic phases in marine hydrothermal systems greatly depend on a number of factors; e.g. distance from ridge axes, the presence of a sedimentary cover; heat flow, and fluid circulation patterns. In this study we discuss controls on phyllosilicate formation and their relation to ore mineralisation at the ridge axis and flank of the sedimented Juan de Fuca Ridge (JF). The presence of sediments is important for mineralizations because they limit heat and mass transfer between the crust and the open ocean and provide chemical elements for authigenic phases.

At Middle Valley (northern JF Ridge), a sequence of Mg- and Fe-rich phyllosilicates are associated with the production of extensive massive sulphide deposits in an area of high heat flow and active fluid venting. In the discharge area, saponite, corrensite and chlorite associated with authigenic quartz and pyrite form pure hydrothermal layers in the detrital sedimentary cover. Highly altered fluids of about 270°C circulating upward and laterally through the sedimentary column permit the precipitation of these authigenic phases. Reactions in both the basaltic basement and the sediments control silicate and sulphide mineral chemistries. In contrast, phyllosilicate (and rare sulphide) formation at the Eastern flank of the JF Ridge is controlled by the circulation of weakly altered seawater at low temperature (about 70°C) and is limited to the interface between sedimentary cover and the cooling basaltic crust. Zones of fluid discharge are restricted to topographic highs where the sedimentary cover is thin. Fe-Mg rich smectite sometimes associated with Ca-Na zeolites precipitates in the coccolithe rich sediments located at less than one meter from the basaltic crust. These data indicate that hydrothermal circulation in sedimented ridge environments remains active far from the ridge axis. Interactions between hydrothermal fluids and the sedimentary cover at Middle valley is very strong and allow fluid discharge through the sedimentary cover; whereas in the flank, sediments constitute an impermeable barrier which restricts circulation and fluid-sediment interaction to the most permeable layers just above the oceanic crust.

FOSSIL HYDROTHERMAL VENT COMMUNITIES AND ASSOCIATED FEATURES FROM EXCEPTIONALLY PRESERVED MASSIVE SULPHIDES IN THE GEOLOGICAL RECORD

Herrington R.J., Little C.T.S. *(Natural History Museum, London)* and Spiro B. *(NERC Isotope Facility, Keyworth, UK)*

Exceptionally well preserved volcanogenic massive sulphide ores at 19 massive sulphide deposits ranging in age from the Silurian to the Eocene are host to assemblages of fossils preserved by pyrite and other sulphides. In addition, a number of these deposits also contains fragments of black smoker chimney spires.

The Palaeozoic massive sulphide belt of the southern Urals has 9 fossiliferous deposits. Three of these also have vent chimney fragments which we have studied in some detail. The oldest assemblages are from the Silurian Yaman Kasy deposit and two other deposits of the same age. At Yaman Kasy, zoned vent chimney material occurs together with fossils of vestimentiferan and polychaete tube worms, molluscs (monoplacophorans, gastropods and bivalves), lingulate brachipods and probable microbial structures. The Devonian aged giant Sibay deposit has yielded fossils of two types of tube worm and a modiomorphid bivalve, whilst at Safyanovka, worm tubes and zoned chimney material have been recovered. Other Devonian deposits in the southern Urals only contain fossil worm tubes.

In the Mesozoic, fossil vent assemblages have been found in the Cretaceous deposits from Oman (Bayda) and Cyprus, and the recently discovered Jurassic Figueroa deposit from the San Rafael Mountains, California. Recent work in Cyprus has turned up fossil tube worms and gastropods in a number of the deposits together with new zoned chimney material. The Figueroa deposit contains fossils of vestimentiferan tube worms, gastropods and rhynchonellid brachiopods and together with at least one fragment of vent chimney material. In this deposit pervasive silicification of the sulphides has preserved many of the original textures including filamentous microfossils.

Tertiary sulphide deposits at Bayda in the Philippines and Azema in New Caledonia also yield some poorly preserved worm tubes.

Study of these deposits with well-preserved fossil assemblages allows us insights into the mineralogical preservation and evolution of fossil vent communities as well as the associated processes of seafloor sulphide formation through geological time. Preliminary evidence indicates that while the conditions of sulphide deposit formation have remained fairly constant, fossil assemblages have changed substantially through geological time.

21. Ore Mineralogy of Modern Sea Floor Hydrothermal Systems

FORMATION OF Fe-OXIDES AND Fe-SILICATES ON BACTERIAL SURFACES IN HYDROTHERMAL DEPOSITS COLLECTED NEAR THE SOUTHERN EXPLORER RIDGE IN THE NORTHEAST PACIFIC OCEAN

Fortin D. *(Dept. Geology, University of Ottawa)* and Ferris F.G. *(Dept. Geology, University of Toronto)*

Hydrothermal deposits, collected in low-temperature waters at the Southern Explorer ridge in the northeast Pacific ocean, were largely composed of very fine mineral particles closely associated with bacteria. X-ray diffraction indicated the presence of poorly ordered Fe-oxides, such as ferrihydrite, and smectite-like minerals, possibly nontronite. TEM/EDS analyses showed a wide range of morphology and chemical composition for oxides and silicates formed in association with bacteria and their associated exopolymers. Fine precipitates occurred as amorphous material, nodules, fine needles, sheets and filaments. According to EDS analyses, Fe-oxides were mixed with very fine Mn-oxides and contained variable amounts of Si. Mineral nucleation in the presence of bacterial surfaces was likely the result of the interactions between soluble metal species (such as Fe and Mn) and reactive binding sites (such as carboxyl, phosphate and hydroxyl groups) present within the cell wall components. Bacteria served as passive substrates for metal binding and subsequent mineral nucleation in hydrothermal environments, where hydrothermal solutions were saturated with respect to various mineral phases.

MINERAL AND METAL COMPOSITION OF MODERN MASSIVE SULFIDES FROM DIFFERENT SUBMARINE GEOLOGICAL ENVIRONMENTS

Muench U., Pracejus B. and Halbach P. *(Dept. of Geology, University of Berlin, Germany; umuench@zedat.fu-berlin.de)*

Samples from the JADE hydrothermal field (Central Okinawa Trough) and from the MESO zone (Central Indian Ridge) were compared mineralogically and geochemically. The observed differences strongly reflect the nature of the leached source rocks: a) the MESO zone is a mature mineral deposit located close to the top of a neovolcanic ridge at a water depth of 2850 m, and its geologic environment is dominated by basalts; b) the JADE deposit, in contrast, is an active vent field situated at a water depth of about 1500 m on the flank of a caldera-like depression in a back-arc environment; the area is governed by felsic differentiates (rhyolites) and andesites/dacites (in the vicinity) partially covered by sediments.

The sulfides from the Indian Ocean are highly enriched in copper, as indicated by large amounts of chalcopyrite, whereas the Okinawa Trough material has concentrated sphalerite, galena, and a number of low-temperature sulfides, such as orpiment, realgar or stibnite (which do not occur at the Indian Ocean site), some of these ores are very silver-rich.

The Cu-Fe ratios of primary ore minerals have been used to attribute the respective suites of copper-iron-minerals to the geologic situation, and it shows that the mineralogy of the samples indeed focuses around two regression lines with different slopes. The mineral association at the MESO zone comprises pyrite, chalcopyrite, bornite, and digenite, while the mineral suite at JADE shows pyrite, pyrrhotite, isocubanite, chalcopyrite (here the regression lines meet), idaite, and covellite.

Formation and replacement processes, which caused the different mineral associations will be discussed based on mineral textures and the related enrichment of metals.

MINERALOGY AND GEOCHEMISTRY OF HYDROTHERMAL PLUMES ON THE FAST-SPREADING SOUTHERN EPR

Marumo K. *(Mineral and Energy Resource Dept., Geological Survey of Japan,marumo@gsj.go.jp)*

During the R/V Melville RidgeFlux cruise in 1994, we observed the Fe-enriched (S/Fe molar ratio <1) hydrothermal plumes at S13°50' to S16°35' and S-enriched (S/Fe molar ratio >1) hydrothermal plumes at S17°30' to S18°40' of EPR.

The Fe-enriched plumes (Fe<730nmol/l) are rich in Cu (<35nmol/l), and Zn (<36nmol/l). They are dominated by iron oxyhydroxide particles and contain significant amount of metal sulfide. The iron oxyhydroxide particles are <0.1mm in size and scavenge Si (Si/Fe molar ratios 0.17 to 0.25), P (P/Fe molar ratios 0.19 to 0.21), and Ca (Ca/Fe molar ratios 0.01 to 0.09) from seawater. Amorphous Al-Si particles (allophane?) dominate in the upper part of some Fe-enriched plumes, suggesting precipitation of Al postdatas Fe precipitation.

The S-enriched plumes (S<490nmol/l) are characterized by high S/Fe molar ratios (<14.5) and are dominated by elemental sulfur. Kaolin (kaolinite and halloysite) and Al-rich chlorite (Mg/Al=0.16, sudoite?) also occur in these S-enriched plumes. The Al-rich chlorite contains significant Cr (Cr/Si=0.10) and Ni (Ni/Si=0.06) and is assumed to be a major Cr- and Ni-bearing phase in the plumes. The presence of kaolin and native sulfur indicate that the intensive hydrogen metasomatism, akin to those of subaerial hydrothermal system which formed native sulfur deposit, occur at EPR.

Room temperature Mossbauer spectra of the Fe oxyhydroxide in the plume particles from S13°50', extremely rich in Fe (2,290 nmol/l), Cu (34.9 nmol/l), and Zn (35.8 nmol/l), show a paramagnetic doublet that can be fitted by two Lorentzian doublets with isomer shifts 0.359, 0.377 and 0.352 mm/s and quadrupole splitting of 1.315, 0.863 and 0.500 mm/s, assuming that all ferric iron occurs in octahedral coordination sites. These isomer shifts and quadrupole splitting values are similar to those of ferrihydrite.

The IR spectra of Fe-oxyhydroxides are very similar to those of ferrihydrite and consist of broad banded patterns around 3450 to 3400, 1650, 1040, and 515 to 490 cm^{-1}. The strong absorption band around 1040 cm^{-1} suggests a large amorphous silica component in the sample. High-resolution bright field image of a Fe oxyhydroxide shows 0.25nm lattice fringes of ferrihydrite. Electron diffraction patterns of the Fe oxyhydroxide show sharp spots at 0.25, 0.21, 0.19, 0.18, 0.15nm and diffuse rings around 0.21 and 0.15nm.

MINERALOGY AND GEOCHEMISTRY OF INDIUM IN SEAFLOOR HYDROTHERMAL SYSTEMS

Schwarz-Schampera U. and Herzig P.M. *(Freiberg University of Mining & Technology, Germany, schwarz@mineral.tu-freiberg.de)*

Indium generally occurs in different types of magma-affiliated ore deposits. Many polymetallic VMS deposits also contain significant indium mineralization. Hydrothermal precipitates from seafloor hydrothermal systems have been studied in order to determine the mineralogical and geochemical characteristics of indium in actively formed massive sulfides. The highest indium contents were detected in mature copper-rich sulfide precipitates of hydrothermal vent fields associated with intraoceanic back-arc spreading centers. Indium-bearing assemblages are dominated by chalcopyrite, tennantite, and sphalerite. Microanalytical and microthermometric studies indicate coprecipitation of indium with Cu and Fe in chalcopyrite, likely representing primary indium enrichment. Increasing pH, $a(H_2S)$, and decreasing temperature and a(Cl-) will favour increasing indium saturation of the fluid or precipitation of indium-rich chalcopyrite. Conductive cooling is likely to be more effective than fluid-seawater mixing, producing small-scale local precipitation of metals from trapped pore fluids at low seawater/hydrothermal fluid ratios. Secondary indium enrichment in more complex, polymetallic ores is related to high-temperature replacement of 2Zn(II) by Cu(I) and In(III) by diffusion processes and coupled substitution in Fe-rich sphalerites of active smokers. SEM studies indicate a strong mineralogical control of zonal indium substitution in sphalerite representing binary roquesite-sphalerite solid solution series. No discrete indium minerals have been found. Strong affiliation of indium to magmatic tin-base metal, skarn, and epithermal deposits, a close geochemical association of indium with Sn, Bi, Ni, and Mo, and typical sulfur and helium isotope ratios in indium-rich deposits may furthermore suggest a contribution of magmatic volatiles to the hydrothermal fluids. This may point to indium as a possible indicator for the presence of magmatic volatiles in volcanogenic massive sulfide deposits.

21. Ore Mineralogy of Modern Sea Floor Hydrothermal Systems

SPECIFIC FEATURES OF ORE MINERALOGY OF MODERN SEA FLOOR HYDROTHERMAL SYSTEMS

Mozgova N.N. *(Institut of Geology of Ore Deposits, Petrology, Mineralogy and Geochemistry, Russian Academy of Sciences. mail@igem.msk.su)*

Modern oceanic sulfides differ from old land massive sulfides by the following main pecularities:

1) The abundance of some minerals (isicubanite, wurtzite) which are very rare in continental environments.

2) The occurrence of some new sulfide compounds unknown in land sulfide deposits and not synthesized under equilibrium conditions.

3) Unusual high contents of admixtures of some isimorphic elements in sulfides (e.g. Cu in ZnS) not corresponding to equilibrium conditions.

4) Wide distribution of exsolution textures (breakdown of isocubanite, bornite and idaite solid solutions).

5) Very contradictory relations between minerals which often create difficulties in its interpretation.

These features obviously reflect non-equilibrium conditions of formation of ore substance on the ocean floor and various transformations of minerals, partly under the action of cool marine water.

Typomorphic mineral assamblages,typomorphic minerals and typomorphic pecularities of its chemical compositions take place in modern oceanic sulfides as well as in old land deposits. Most of these features are related with underlaying rocks and provide reasons to discuss source of metals.

LEAD IN SULFIDE AND SULFATE-RICH CHIMNEYS FROM GUAYMAS BASIN, GULF OF CALIFORNIA, AND THE PACMANUS DEPOSIT, EASTERN MANUS BASIN

Loon C.E., Scott S.D. *(Marine Geology Research Laboratory, Department of Geology, University of Toronto)* and Rucklidge J.C. *(Department of Geology, University of Toronto)*

The occurrence of lead in hydrothermal deposits and its global recycling is not well understood, partly due to the paucity of reliable lead analyses. This study examines the concentration and distribution of lead in hydrothermal chimneys from two contrasting tectonic environments - the PACMANUS site, a Cu-Zn-Pb-Ag-Au sediment-poor deposit hosted by felsic volcanics in a back-arc basin, and Guaymas Basin, an Fe-Cu-Zn-Pb deposit located at a sediment-rich rift zone.

Samples required complete dissolution in order to obtain accurate determinations of bulk lead by ICP-OES. A HNO_3-HF-$HClO_4$ digestion was followed by the isolation of insoluble sulfates [(Ba,Pb)SO_4], which were then digested by microwave, in a Na_2CO_3 solution. Microwave-assisted digestion has reduced the time of sulfate digestion by Na_2CO_3 from several hours to less than one hour.

Preliminary results show Pb concentrations in the range of 0.43-1.55 wt% across a large sulfide-rich chimney from PACMANUS. Smaller carbonate-sulfate-rich chimneys from Guaymas Basin show concentrations of up to 4420 ppm.

Pb, As and Sb elemental maps were collected by electron microprobe, and processed using VISILOG image analysis software. Pb-Sb scatterplots showed no correlation in either PACMANUS or Guaymas chimneys. Pb-As scatterplots indicated the existence of at least two Pb-As-(Ag?) phases in the PACMANUS chimney outer wall. These lead sulfosalts line open cavities, indicating a late, low-temperature formation. By contrast, galena is the primary Pb-rich phase at Guaymas, and is found mainly in the inner walls of both high and low temperature sulfate-carbonate chimneys.

Chimney assemblages are characterized as sulfate-carbonate, sulfide-sulfate, and massive-sulfide. Differences in chimney mineralogy correspond with distinct groups on Pb *vs* Au and Pb *vs* Ag binary plots. Independent of vent site location, mineralogy is an important factor in the correlation between Pb and precious metal concentrations.

MODERN SEA FLOOR SULFIDE MINERALIZATION: MINERALOGICAL AND ISOTOPIC CONTRASTS

Bortnikov N.S. *(IGEM, Russian Acad Sci, bortnikov@igem.msk.su)*

A study of hydrothermal fields at mid-ocean ridges (EPR 18-20S, Middle Valley. TAG, Snakepit, Broken Spur, and MAR), and in back-arc tectonic settings (Manus and Lau basins), reveals mineralogical and isotopic contrasts. In both environments, high-temperature vents precipitate chalcopyrite, isocubanite, (?bornite) pyrrhotite, pyrite (?marcasite), and sphalerite. Low- temperature edifices consist of marcasite, pyrite, sphalerite, barite, and subordinate chalcopyrite (pyrrhotite and isocubanite are absent). An individual hydrothermal field contains a minor characteristic mineral (*e.g.* galena in EPR, galena and silver sulfosalts in Manus). Variations from fine-grained concentric colloform and dentritic to coarse-grained euhedral aggregates over a few mm were observed.

FeS contents in the Zn sulfides vary considerably in the most hydrothermal fields. A characteristic trace-element geochemistry is a prominent feature of an individual deposit (*e.g.* high contents of Ag, Sb, and Pb in Manus, high a Co content in MAR, the Au and Ag contents in the TAG field, *etc.*).

Sulphur-isotope ratios vary considerably in minerals. The most common values of $\delta^{34}S$ lie within +2.0 to +5.0 ‰ (CDT). Negative values occur at the EPR (-11 ‰) and Snakepit (-4 ‰). Significant temporal variation in $\delta^{34}S$ within individual samples or zones (more than 3 ‰) were found.

A main conclusion may be drawn that mineral-forming processes beneath sea floor are not everywhere the same and are controlled by the temperature-pressure-pH-fO_2 evolution paths of a fluid. The evolution are controlled by the rate of mixing a hydrothermal fluid and the phase separation which are related to the local tectonic and magmatic environments.

This study was supported RFBR (project No 97-05-64804).

GEOCHEMISTRY AND MINERALOGY OF SILVER IN HYDROTHERMAL PRECIPITATES ON THE MODERN SEAFLOOR.

Moss R. and Scott S.D. *(Dept. of Geology, Univ. of Toronto, roger@quartz.geology.utoronto.ca)*

Currently forming volcanogenic massive sulphide (VMS) deposits on the seafloor are variably enriched in silver, and thus afford the opportunity of studying primary controls on silver distribution. The most silver - enriched samples (average >200 ppm) occur in the back arc basins of the west Pacific, and range up to 1.1% Ag for a sample from the Jade hydrothermal site in the Okinawa trough. Enrichment of silver in the hydrothermal system is dependent on effective transport of the metal, precipitation as silver minerals or in solid solution in more abundant sulphide phases, and preservation of the precipitates. Post-depositional modification can also play an important role in upgrading the silver content.

At temperatures greater than about 250°C, and under acidic and slightly oxidising conditions, silver is most likely transported as a chloride complex. Such conditions are characteristic of many seafloor vent sites. High silver values associated with zinc-rich chimneys at 21°N and 13°N on the East Pacific Rise (EPR), are independent of the iron-content of sphalerite, indicating little control by bisulphide complexing. Silver is also stongly enriched in zinc-rich chimneys from the PACMANUS hydrothermal field in the Manus Basin.

Although silver minerals (e.g. acanthite) and silver-containing minerals (*e.g.* tennantite) have been reported from various seafloor deposits, they are generally present in minor to trace amounts. It is, therefore, the silver contained in the more abundant galena, chalcopyrite and even sphalerite and pyrite that contributes the most to the overall silver content of the precipitates.

Evidence from 21°N and 13°N, EPR indicates that deposits become progressively enriched in silver as they mature. The silver content ranges from an average of 4 ppm in anhydrite-rich chimneys to an average of 182 ppm in the basal mounds at 21°N, EPR.

22. Ore Minerals in Hot Water

MINERALS IN HOT WATER AND HOT FLUIDS IN MINERALS: VISUAL OBSERVATIONS AND *IN-SITU* CHARACTERIZATION OF SAMPLES THROUGH DIAMOND WINDOWS

Chou I-Ming *(U.S. Geological Survey, imchou@usgs.gov)* and Bassett W.A. *(Department of Geological Sciences, Cornell University, bassett@geology.geo.cornell.edu.)*

Recent development of the hydrothermal diamond-anvil cell (HDAC) allows direct visual observations and in-situ characterization of samples through diamond windows under well- controlled temperature (*T*) and water pressure (*P*) conditions. The applicable *T's* range from -190 to 1200°C at *P's* up to 2.5 GPa. Visual observations were made under a microscope, and images of the samples, together with T and time information, were recorded continuously on VCR tapes.

Important observations made to date for mineral-water systems in the HDAC include nucleation, phase transition, dissolution, dehydration, melting, and critical phenomena. Advanced spectro- scopic techniques used for in-situ sample characterizations include Raman spectroscopy, luminescence, infrared absorption, and x-ray diffraction, and x-ray absorption using synchrotron radiation. The behavior of the following minerals in hot water has been studied: quartz, cristobalite, albite, calcite, muscovite, portlandite, petalite, and Na-, Mg-, and Ca-montmorillonite.

The HDAC has also been used to impose external pressures for fluid inclusion samples in minerals during microthermometric analysis, such that stretching and decrepitation of the samples can be prevented. This application is especially useful for soft host minerals, such as calcite or fluorite, and also for inclusions rich in volatiles, such as CO_2 or CH_4.

The advantages of the HDAC are its (1) large applicable P-T region; (2) simple construction; (3) inexpensiveness when compared with other types of high P-T facilities; (4) safety; (5) amenability to visual observations and VCR documentation; and (6) amenability to *in-situ* sample characterizations.

SPECTROSCOPIC STUDIES OF HYDROTHERMAL SOLUTIONS

Seward T.M. *(Institute for Mineralogy and Petrology, Swiss Federal Institute of Technology, ETH Zentrum, 8092 Zürich, Switzerland)*

Aqueous solutions occur ubiquitously throughout the earth's crust over a wide range of temperatures and pressures and are intimately involved with metamorphism, magmatic processes, ore formation and tectonism. In addition, hydrothermal fluids comprise an important transport medium by which the upper mantle and crust communicate with the earth's surface by discharge of both heat and chemical components into the oceans and atmosphere. Understanding of how all these various processes operate is fundamentally premised on a knowledge of the physical inorganic chemistry of hydrothermal solutions. Direct insight into many aspects of the molecular chemistry of hydrothermal solutions may be obtained from electronic and vibrational spectroscopy as well as X-ray absorption spectroscopy using suitably designed autoclaves containing windows of silica, sapphire or diamond.

Uv-vis spectroscopic studies of metal complex equilibria and weak acid/base equilibria are being studied up to 400°C and 1000 bar. The stepwise complex formation of metal chloride complexes [*e.g.* Sn(II), Mn(II), Cu(I), Pd(II)] is currently being studied. In the case of Mn(II)chloride complexes, for example, uv-spectroscopic data demonstrate the increasing importance of the dichloridomanganese(II) species in hydrothermal solutions with increasing temperature.

High temperature-high pressure extended X-ray absorption fine structure (EXAFS) spectroscopy measurements on hydrothermal solutions also provide fundamental data on ion solvation, complexing and cluster molecule formation. It has been shown recently for example that cation-oxygen(water) distances contract with increasing temperature up to 350°C. This has important implications for our understanding of many chemical processes such as stable (oxygen and hydrogen) isotope fractionation in high temperature aqueous systems.

THE SOLUBILITY OF SIDEROPHILE ELEMENTS (Pt, Pd, Os AND Re) IN HYDROTHERMAL SOLUTIONS

Wood S.A. *(Dept. of Geology and Geological Engineering, Univ. of Idaho, swood@uidaho.edu)*

Measurements of the solubility of Pt and Pd phases in hydrothermal solutions show that, at temperatures up to 400°C, significant concentrations of these metals (*i.e.* 1 μg/kg or greater) can be transported as chloride complexes only in fluids that are oxidizing (hematite stable) and acidic (kaolinite stable). The solubility of Pt and Pd in bisulfide solutions has been determined by Gammons & Bloom (1993) and Pan & Wood (1994). Comparable Pt and Pd concentrations were measured in these studies, but the predominant species were determined to be $Pd(HS)_3^-$ and $Pt(HS)_3^-$ in the former, but $Pd(HS)_2^0$ and $Pt(HS)_2^0$ in the latter. Both studies conclude that bisulfide complexes are likely to be the predominant complexes of these metals in most hydrothermal environments at T < 400°C (pyrite, pyrrhotite or magnetite stable, slightly acidic to neutral pH).

Solubilities of ReO_2 and Os have been measured in hydrothermal KCl solutions in equilibrium with K-feldspar + muscovite + quartz and various oxygen buffers (Re-ReO_2, Ni-NiO, Co-CoO, MnO-Mn_3O_4). The solubility of ReO_2 in 1.0 m KCl solutions at 410°- 500° C is 20 to 80 mg/kg Re and is relatively insensitive to temperature and f_{O2}. The insensitivity to f_{O2} indicates that the predominant oxidation state is Re(IV). Solubility depends on KCl concentration, indicating that the predominant species may contain chloride. The solubility of Os at 500°C and 800 bars is dependent on both f_{O2} and KCl concentration, ranging from approximately 2 mg/kg in 1.5 m KCl solutions (Re-ReO_2) down to 20μg/kg in 1.0 m KCl solutions (Ni-NiO). Thus, an Os-chloride complex may be the predominant species. Our results indicate that Os, and especially Re, can be mobilized by Cl-rich, oxidized hydrothermal fluids. Experiments are in progress to elucidate the predominant species and to investigate the effect of reduced sulfur on Re and Os mobility.

MINERAL/WATER INTERACTION STUDIES WITH *IN SITU* pH MONITORING TO 300°C

Wesolowski D.J., Palmer D.A., Bénézeth P. *(Oak Ridge National Laboratory, dqw@ornl.gov)* and Machesky M.L. *(Illinois State Water Survey, machesky@sun.sws.uiuc.edu)*

Multivalent elements undergo hydrolysis reactions in water, such as

$$Al^{3+} + yH_2O \Leftrightarrow Al(OH)_y^{3-y} + yH^+ \qquad (y = 1,2,3,4)$$

$$WO_4^{2-} + yH_2O \Leftrightarrow H_y(WO_4)^{y-2} + yOH^- \qquad (y = 1,2),$$

which impart a strong pH dependence to the solubilities of their oxides, sulfides, silicates, tungstates, carbonates, sulfates, etc. Over the last 30 years, hydrogen-electrode concentration cells have been used at ORNL to study such homogeneous reactions at temperatures of 0-300°C in dilute to concentrated brines. The cells employ platinum-hydrogen electrodes to measure the difference in pH between a test and a reference solution of known pH. However, many multivalent metals form polymetallic ions, even at sub-millimolal concentrations, or precipitate as oxyhydroxides during pH titration, thus hampering determination of their hydrolysis constants.

Recently, we have coupled *in situ* pH monitoring during acid/base titrations with periodic sampling to establish the solubility profiles of minerals (brucite, boehmite, zincite) in hydrothermal brines. The low solubilities of the minerals prevent the formation of polynuclear species, and the total solubility can be modeled as a function of pH to extract the stepwise aqueous hydrolysis constants. Monitoring pH also permits real-time observation of the rate of approach of heterogeneous reactions to equilibrium from both under- and super-saturation. Addition of complexing ligands enhances the total solubility at a given pH, permitting determination of complex formation constants for ligands such as Na^+, Cl^-, SO_4^{2-}, acetate, *etc.* Finally, mineral surface charge, which affects ion adsorption and dissolution-precipitation rates at elevated temperatures, can be determined by titrating mineral surfaces with acid or base while monitoring the pH (rutile, zincite, magnetite to date).

MINERAL SOLUBILITY CONSTRAINTS ON METAL MOBILITY IN SUBSEAFLOOR HYDROTHERMAL SYSTEMS.

Seyfried W.E.,Jr., Ding K., Allen D.E. and Berndt M.E. *(Department of Geology and Geophysics, University of Minnesota, Minneapolis, MN. 55455, wes@tc.umn.edu).*

A series of mineral solubility experiments were conducted at 400-425°C, 300-500 bars to assess the role of redox, temperature, pressure and dissolved Cl on metal mobility (Fe, Cu, Zn) and hydrothermal alteration processes in subseafloor reaction zones at mid-ocean ridges. In general, dissolved metal concentrations increase with increasing temperature and dissolved Cl and decrease with increasing pressure. These data, combined with phase equilibria constraints, place limits on physical and chemical conditions needed to account for the chemistry of hot spring vent fluids. For example, in comparison with experimental and theoretical data, dissolved H_2 concentrations, together with dissolved Fe, Cu and mFe/mCu ratios of hot spring vent fluids from most localities suggest moderately oxidizing conditions and near neutral pH ($pH_{in\text{-}situ}$). Oxidizing conditions likely result from ingress of seawater derived sulfate, leading to anhydrite formation. Relatively high dissolved Ca concentrations from metastable plagioclase (An_{70})-fluid equilibria enhance further the likelihood of anhydrite formation at reaction zone conditions. Thus, the following assemblage of minerals appears to play a particularly important role in buffering key aspects of the chemistry of hot spring vent fluids at mid-ocean ridges: plagioclase ($An_{60\text{-}80}$), epidote, quartz, magnetite, anhydrite, pyrite, and chalcopyrite. To account for the conspicuously low mFe/mCu ratios and dissolved H_2S concentrations of some vent fluids, in particular, TAG, on the Mid-Atlantic ridge, however, relatively high fluid/rock ratios are likely, which may cause more extreme oxidative effects, such as loss of pyrite from the mineral buffer assemblage.

Cl variability of hot spring fluids results from supercritical phase separation of seawater. Mixing of brine and vapor components with seawater in subseafloor reaction zones, together with mineral-fluid equilibria at temperatures and pressures of 400°C and 500 bars, accounts well for metal concentrations in hot spring vent fluids. Equilibrium phase relations are confirmed by experimental and theoretical data.

Future experimental studies making use of *in-situ* chemical sensors are needed to better constrain experimental and theoretical models and subseafloor hydrothermal processes.

23. Mineralogical Museums Serving Science and Society

INTERDISCIPLINARY USES OF MINERAL COLLECTIONS

DeMouthe J.F. *(Geology Section, California Academy of Sciences, San Francisco, California USA, jdemouthe@calacademy.org)*

Non-traditional use of mineral collections held by natural history museums and universities has increased dramatically in recent years. As technology in all fields of science has improved, the potentials for using natural inorganic compounds in research has expanded beyond the fields of geology, mineralogy, and crystallography. Researchers in fields such as medicine, chemistry, physics, astronomy, archaeology, and botany are now using minerals in a variety of ways.

Research and teaching opportunities arise for mineralogists as a result of these alternative uses of collections; collaborative efforts among scientists, students, and teachers involving more than one field of science. Multi-disciplinary use of collections are mutually advantageous to all involved. There may also be financial and administrative reasons to seek out non-traditional users for a collection. In these days of tight budgets and restricted staff time, it is often necessary to explain and justify the existence of collections. By demonstrating multi-disciplinary uses of specimens, the worth of a collection may be reinforced in the minds of administrators and other decision-makers.

INSTALLATION OF A 6 X 8 FOOT RHODOCHROSITE POCKET IN THE DENVER MUSEUM OF NATURAL HISTORY COORS MINERAL HALL

Murphy J. *(Denver Museum of Natural History, Geology Department)* and Hurlbut J. F. *(Denver Museum of Natural History, Geology Department)*

This paper will present a description of the two year program to mine and remove a 6 x 8 foot rhodochrosite pocket from the Sweet Home Mine at Alma, Colorado. Its reconstruction was performed in the Collectors Edge shop in Golden, Colorado while the construction of a replica mine tunnel was built in the newly renovated Coors Mineral Hall at the Denver Museum of Natural History. Photographs will be used to describe all of the detailed steps involved to produce a realistic display for public viewing depicting how the pocket existed in the mine.

This two year program was the result of close cooperation between the mine operator Bryan Lees and personnel of the Geology Department at the Museum and was underwritten by the Aldoph Coors Foundation. This exhibit was opened in September 1997.

SCIENCE AND SERVICE, THE NEW MEXICO BUREAU OF MINES AND MINERAL RESOURCES MINERAL MUSEUM, SOCORRO, NEW MEXICO, USA

Lueth V.W. and Eveleth R.W. *(NMBMMR, vwlueth@nmt.edu)*

"Science and Service", the motto of the New Mexico Bureau of Mines and Mineral Resources, requires the Mineral Museum to be one of the most important educational outreach programs of the Bureau. In addition, staff at the museum conduct and publish geological, historical, and mineralogical research.

The museum was established essentially at the same time as the NM School of Mines in 1889. The collection has grown to over 12,000 pieces, much of which is mineralogical material from New Mexico. The New Mexico Bureau of Mines & Mineral Resources (NMBMMR) assumed responsibility for the collections in 1961 and built a museum facility. A newly remodeled facility includes a large display gallery, education/ demonstration room, clean and dirty preparation labs, and a secure warehouse. Minerals are electronically cataloged and completely accessible.

Educational programs for the public include museum tours, lectures both on and offsite, exhibitions at major mineral shows and sponsorship of the New Mexico Mineral Symposium (now in its 19th year). The museum has an annual attendance of over 10,000. There is no charge for admission. Educational tours for groups ranging in age from preschoolers to senior citizens are routinely conducted and generally number over 25 per year totaling some 1000 visitors.

Mineralogic materials are available for researchers worldwide with over 20 requests processed in the past five years. Museum staff members also conduct research projects on a wide variety of topics. The museum is home to the type material of santafeite and native selenium in addition to a large amount of material from New Mexico type localities.

IS IT REAL? THE IMPORTANCE OF MINERALS IN EDUCATION AND RESEARCH TODAY

Eriksson S.C. *(Dept. of Geological Science and Museum of Natural History, Virginia Tech, serikssn@vt.edu)*

In a technological age in which virtual museum tours, internet access to collections and data, and compact discs holding images of specimens worth tens of thousands of dollars are the modus operandi, is there a place for small, regional mineral collections? At Virginia Tech, a small museum with minimal budget and collection of only 13,000 specimens serves the University's mission of research, education and outreach and it illustrates how traditional museum objects are relevant in today's society.

Inquiry of mineral specimens in museum tours provides the opportunity to use many of the basic science skills (observation, comparison, analysis, evaluation, description) advocated in state and national science standards of learning. At 'higher' levels of education in univeristy classes and research lectures, real objects illustrate or reflect complex scientific principles. Surveys of college freshman in laboratory experiences in the museum as well as children in elementary schools visiting the museum share the same first question, "Is it real"?

The connection of theory to the real object is increasingly important during the late twentieth century in which people have, in general, little direct experience with the natural world.

Examples of strategies for using minerals to enhance education include 1) using selected research specimens for educational programs and classes, 2) expanding the content area of researchers and educators using minerals, and 3) making extraneous materials available through loans. Public relations and intimate knowledge of current educational theory facilitate increased use of our real objects.

23. Mineralogical Museums Serving Science and Society

THE EARTH GALLERIES: NATURAL HISTORY MUSEUM, LONDON, UK.

Stanley C.J. *(Department of Mineralogy, Natural History Museum, London, United Kingdom, cjs@nhm.ac.uk)*

The new Earth Galleries at the Natural History Museum are complete and the whole of our community can now assess whether they succeed in the aim of communicating our science to society as a whole. Developed to replace the old systematic displays of economic materials (ores, industrial minerals, dimension stones, etc.) and regional geology, and the more recent displays of North Sea Oil, Story of the Earth, Treasures of the Earth and Gemstones, there are now five major new exhibitions set around the spectacular atrium space with revolving Globe, escalator and icons. In the old exhibition very few people ventured to the two upper floors and the exhibition designers made the escalator a central attraction to draw customers to the top of the building and leave them to filter down and around the exhibitions.

"The Power Within" deals with processes within the Earth's crust and mantle introducing plate tectonics, earthquakes, and volcanoes with an earthquake experience in a "Kobe supermarket" as the grand finale.

"The Restless Surface" covers surface processes involving gravity, wind, rain, frost, sunlight and heat, wave action, sedimentation processes, mechanical and chemical weathering of rocks and ends with a large specimen illustrating open cavity infill of Pb-Zn-celestite mineralization and brecciation in karstic limestone.

On the next level down the first exhibition is "From our beginnings" which looks at Earth history and the evolution of life through to the present day. This leads naturally into the next exhibition "Earth's Treasury" which is a specimen-rich display of minerals, gemstones, ores, rocks, building stones, construction materials, etc. illustrating the usefulness of the minerals that we extract from the Earth.

The final exhibit on the ground floor "Earth Today and Tomorrow" tackles issues of environment, recycling and sustainability, looking at food, water, manufactured goods, and energy.

HISTORY OF MINERALOGY THROUGH EUROPEAN MINERALOGY MUSEUMS, THE GOAL OF EUROMIN

Touret L. *(Min. Museum, School of Mines, Paris, touret@musee.ensmp.fr)*
and Participants of the Euromin Project*

The history of mineralogy is intimately related to the history of mineralogical museums in Europe, as these have been the first and oldest museums in the world. As a discipline, the beginning of scientific mineralogy, which dates back to the 18th century, the "Siècle des Lumières" was directly linked and sometimes even preceeded the development of other fields of knowledge such as physics, chemistry and technology. For instance, when the emperor Napoléon requested a "Traité de Physique" for his newly established system of secondary education, the asked for author the best mineralogist of this time, the abbey René-Just Haüy. Besides a purely scientific interest - cristallography, the science of crystals, started shortly before the French Revolution, ultimately led to the theories of atoms a century later-, mineralogy had a very practical application: to find the natural resources needed for the industrial explosion. For a long time, this has been done in a rather simple way: collecting in some places some reference materials (gold, silver, copper-bearing minerals, *etc.*), showing them to students, who later should try to find them all over the world. Mineralogical collections, nowadays very much considered as examples of natural art, can afford more than spectacular show. They also witness the development of modern science. Until now, the historical aspects of mineralogy have been studied and published by historians of sciences, in publications reserved for a very specialized audience. Famous places in Europe (France, Germany, Austria, United Kingdom, *etc.*) contain a lot of written and non written sources of information, which for a large part have escaped to the attention of professional historians.

Through a common work, 8 European museums, which host the most important collections in respectively, Austria, Belgium, France, Germany, Italy, Spain, have decided to bring together their patrimony, archives, actual experiences from the very beginning when mineralogy was a curiosity up to nowadays, since it became a science involved in modern technologies.

*Cipriani C. (Firenze), Curto-Mila C. (Barcelona), Damaschun F. (Berlin), Deliens M. (Brussels), Fabries J. (MNHN, Paris), Grubessi O. (Rome), Kurat G. (Vienna), Mahl R. (Paris)

THE NATURE OF DIAMONDS: AN EXHIBITION INTEGRATING SCIENCE, HISTORY, CULTURE, AND TECHNOLOGY.

Harlow G.E. *(Amer. Museum of Nat. Hist., New York, NY, USA, gharlow@amnh.org)*

Diamond-mineral, myth, mantle messenger, cosmic carbon, superabrasive, portable fortune, technological wonder, and brilliant gem-provides an excellent subject for creating an informative and dazzling exhibition that communicates science, culture, history, technology and their connections. By most accounts, *The Nature of Diamonds* has accomplished these goals successfully. Here are some of the factors important in the way the exhibition was developed.

First, diamond has rich connotation, recognition, and appeal that can connect science to history, culture, and even fashion. Thus, many links can be made between the substance diamond and its historic meaning and modern utilization. Likewise, the diversity of content provides every visitor with something of interest and some new information or perspective.

Second, connections between the scientific and cultural or historic issues are recurring themes, so that the context of science is made explicit and relevant. The diamond indicator minerals-garnets, Cr-diopside, and ilmenite-are shown in rocks, as inclusions in diamonds, as concentrate, and as the pointers in exploration for new diamond pipes. The history of diamond jewelry is shown as a combination of the evolution of cutting technology and the availability of diamonds, dependent on discoveries, that transform a dark rare stone into brilliant paved jewels.

Third, the project was organized and executed by the Museum and its employees. Everyone was on one team with one set of loyalties and accountabilities. It was an in-house team effort that worked well. Finally, content was controlled by the curator/scientist (me), who worked with the team of editors and designers to make the prose intelligible and approachable. Three levels of text content were used to allow visitors to browse topics or explore them more thoroughly. Graphics were placed with text on panels to make each section more inviting.

Surveys show that visitors stay, on average, an hour, 3 times longer than is ordinary, and leave appreciating new facts and concepts. *The Nature of Diamonds* demonstrates that the combination of good subjects, serious content and interesting objects succeeds in informal education.

ENGAGING MUSEUM VISITORS IN MINERALOGY: THE BIRTHSTONE EXHIBIT AT THE HARVARD MINERALOGIAL MUSEUM

Monaghan S. N. *(Exhibit Designer, Harvard Mineralogical Museum)*

Display collections of minerals, especially systematic displays, are daunting experiences for most museum visitors. In order for visitors to engage in meaning-making, they are required either to have special knowledge of the subject, or be able make connections to their existing knowledge frameworks and their own life experiences. As most visitors are non-specialists, they find it difficult to relate their lives and personal experiences to minerals. The exhibit forms an overwhelming assault on the visitors' visual senses, leaving them with little comprehension of minerals, mineralogy and related natural history.

How can we facilitate visitor engagement, not only with display objects, but with the associated natural history and science? The Harvard Mineralogical Museum has considered this question for many years, as the museum has maintained a dual role as a teaching/research collection and public display since its inception in the late 1700s. The staff has dealt with this difficulty through a series of temporary thematic exhibits that not only relate to the large systematic display, but also explore areas of natural history and science. The current exhibit is "Birthstones".

The choice of Birthstones has proved to be an excellent medium for engaging visitors in natural history, science, and cultural history. Since most visitors are aware that they have a birthstone, even if they are unsure of the particular gem, they can draw an immediate, personal connection to the gems (and subsequent mineral species) and be encouraged to learn something about "their stone" in the exhibit.

Four sub-themes were created to reinforce the educational goals of the exhibit: occurrences of gems- the natural history of gem material; the science of color mechanisms; the cultural history of birthstones- development of astronomy, lunar/solar calendars, precession of the equinox, medieval lapidaries; and the influence of the marketplace. Evaluation has indicated that the exhibit encourages social interaction among visitor groups, and that visitors leave with a very positive attitude towards gems, minerals, and mineralogy. This exhibit has proved to be the most visitor-engaging temporary exhibit produced by the museum.

23. Mineralogical Museums Serving Science and Society

THE NEW GEOLOGY, GEMS AND MINERALS EXHIBITION AT THE SMITHSONIAN INSTITUTION

Post J.E. *(Dept. of Mineral Sciences, Smithsonian Institution)*

The new 20,000-square-foot Janet Annenberg Hooker Hall of Geology, Gems and Minerals opened to the public on September 20th, 1997. Nearly ten years in the making, the hall showcases the SmithsonianÆs collections of gems, minerals, rocks and meteorites. It is divided into seven major galleries: The Harry Winston Gallery, featuring the Hope Diamond; the National Gem Collection; Minerals and Gems; The Mine; Rocks; Plate Tectonics, including volcanoes and earthquakes; and Moon, Meteorites and Solar System. The major stories and concepts are introduced by the more than 3500 specimens and accompanying label text, with computer interactives, dioramas, models, and videos serving in supporting roles. The exhibit was designed to be interesting to a broad range of visitors, and one of the approaches used to accomplish this was to design two pathways through the exhibit complex. The ôfast trackö features the most spectacular specimens and provides brief introductions into basic concepts. Study alcoves adjacent to the fast track offer many more specimens, and explore concepts in greater detail. In a major departure from the old exhibit, the minerals are not arranged, in general, according to the Dana system. Instead the gallery is divided into topical areas: crystals, pegmatites, diversity, color, crystal growth, etc. Each topical area is introduced by a group of fast-track cases and has an accompanying study alcove. In addition to an overview of the exhibition and discussion of its major goals, results of preliminary postopening visitor surveys and evaluations will be presented.

MINSPEC- MINERALOGICAL DATABASE INFORMATION SYSTEM FOR MUSEUM COLLECTION MANAGEMENT AND MINERAL SPECIES FAST DIAGNOSTIC.

Belakovskiy D.I. and Fiveyskiy D.M. *(Fersman Mineralogical Museum, RAS, Moscow, Russia; dmz@minmuz.msk.su)*

MINSPEC consists of two groups of related databases. First one carries information for mineral species (>4000) and their attributes, variety and synonyms of minerals, uncertain and nonmineral natural compounds like bitumen, glasses *etc.*,(>10000). The program application allows to execute fast context search for any combination of data in databases including names, any parts of chemical formulas (with subscript), crystal systems and space groups, type localities of mineral species, colors, luster, optical properties for both ore and transparent minerals, d-spaces, density, hardness *etc.* Related information such as occurrence, place of type specimen deposit, references, and any kind text data can be viewed inputted and edited in a special window. The program allows to edit any data, to add new entries and to fill pre-existing empty fields with user's information for existing entries as well. Second group of databases for collection services. It includes data about 135000 items belongs to the systematic, crystal, locality, gem and pseudomorph collections of the Fersman Museum and 60000 items in mineral collection of State Geological Museum, Moscow. It's allows to get information about specimens in museum storage or expositions by their names (or mineral species names), inventory numbers, localities, years and sources of acquisitions, place of storage (in any combinations). The test information (description, comments, analytical data *etc.*) is stored in memo fields and available for editing or inputting data. It is also possible to get an image of particular specimen or scientific information related to it. The program allows to attach new database (collection) or change one for another. While all data in museums databases are easy editable the original information remains in special file and always available for comparison.

The project is supported by the Russian Fund for Basic Research.

CATALOGUE OF TYPE SPECIMENS IN THE HARVARD UNIVERSITY MINERAL COLLECTION

Francis C. A. *(Mineralogical Museum, Harvard Univ., francis@eps.harvard.edu)*

A catalogue of type specimens archived in the Harvard Mineralogical Museum has been compiled as a contribution to the Catalogue of Type Mineral Specimens (CTMS), an ongoing project of the IMA Commission on Museums. Specimens representing about 250 recognized species and 40 obsolete mineral names were accepted for this catalogue following careful scrutiny of their labels, the catalogues, and the published literature, including comparisons with type specimen catalogues of other museums. Many of the specimens listed are the product of in-house investigations. They are designated as *holotype*, *cotype*, *neotype*, *pleisotype* or *metatype* where warranted. The purposefully ambiguous status type is used to denote significant specimens that cannot confidently be assigned more specific type status. Many other specimens in the collection whose labels are annotated "type" or "type material" were not accepted for the catalogue because their pedigrees are not adequately documented. Publication of the CTMS, envisioned as a truly comprehensive worldwide directory of type specimens, will permit comparisons among the holdings of many institutions and hopefully eliminate the need to include specimens of inferior or questionable pedigree.

COMPUTER DATABASE DESIGN FOR EFFECTIVE MINERAL COLLECTION MANAGEMENT

Kampf A.R. *(Los Angeles County Museum of Natural History)*

To be effective, a computer database system for collection management must be easy to use, permit relatively rapid data entry, encourage a high level of accuracy and consistency, and accommodate the documentation and tracking of all pertinent information related to the collection. Most systems currently in use fail in one or more of these areas, but in particular, most fail to adequately address the last of these requirements.

At the Los Angeles County Museum of Natural History, we have redesigned a system first developed by Joe Nagel (Kustos) and now in use in several other major institutions. The hybrid system provides, within a single integrated database application, a remarkably effective means for comprehensively documenting and tracking virtually all specimen data and transactional activity. Our system facilitates essentially "paperless" information handling, although it also accommodates the production of hardcopy for specimen labels and institutionally required documentation.

Our design follows a multi-tiered relational database approach. The most innovative feature is the ability to interactively record and access data on all current and past collection activity including, but not limited to, acquisitions (donation, purchase, exchange, field trip, etc.), loans (both to and from the museum), and internal usage (display, education, research, appraisal, etc.). Our design is implemented using Superbase (for Windows) software, which provides a very effective visual programming environment for relation database development, but it could be implemented using any full-featured relational database management software.

23. Mineralogical Museums Serving Science and Society

SAMPLE DATABASE AND REFERENCE SAMPLES FOR SCIENCE AND SOCIETY : AN ATTEMPT OF GEOLOGICAL MUSEUM, GS JAPAN

Okuyama-Kusunose Y., Kusunose K., Togashi S., Imai N., Haruna M, Cho A. *(Geological Survey of Japan)*, Yanagitani T. and Kawakata H. *(Kyoto University. Japan)*

Geological Museum of the Geological Survey of Japan (GSJ) was founded in 1980, aiming to demonstrate scientific activities in GSJ through displays in the exhibition rooms, and to store and manage geologic samples collected through the research activities in GSJ over 110 years of its history. The total numbers of samples registered to the museum are 33,372 for minerals, 65,969 for rocks and 15,100 for fossils, by the end of 1997. The disclosure of collection data as well as the extended scientific utilization have been becoming an important subject of the museum in these years.

For the first subject, we are on a way to open our sample database on internet-base to visitors of the museum as well as anyone outside the museum. The database has its basis on the computer-aided sample management system that has been constructed in these fifteen years.

We also began preparation and distribution of reference samples with various kinds of reference data. The sources of material are our Imayoshi Mineral Collection and 108 rock samples described in a book entitled "An Illustrated Guide to Rocks and Minerals of Japan". Minerals and rocks in the two collections furnish a lot of duplicate samples. For 108 rock samples described in the book, a set of reference data has been obtained in exchange with providing the samples, under an agreement to be used as a reference. We are extending the plan to prepare CD-ROMs in which the reference data are combined with image data of samples for further scientific analyses.

SPECIAL EXHIBITIONS: A TOOL FOR CONNECTING SCIENCE AND SOCIETY?

Schuermann K.U. *(Mineralogical Museum, Univ. of Marburg, schuerma@mailer.uni-marburg.de)*

More or less permanent exhibitions are common for museums and collections serving the broad field of geosciences. A lot of them are specialized in regional features or certain main topics like palaeontology, mineralogy, or gemmology. It should be the aim of each institution open to public to involve a great amount of visitors into its scientific fields. Moreover needs each museum from time to time special highlights to recreate former visitors and to create groups of new visitors. Common and well established methods are special exhibitions at various themes. There should be a broad variety of topics in relation to the basic exhibition.

At the Mineralogical Museum Marburg mainly minerals and in addition gems, meteorites, rocks, and ores are presented on an area of about 600 sqm. Since 10 years we got the opportunity to have a special area of about 50 sqm with 6 or 7 show cases and poster facilities to present special exhibitions (regular twice a year - about 22 up to now in total). Some had connections to health as for example "Minerals used as Medicaments". Some had technological aspects ("From Mineral to High-Tech Ceramics"). We also presented some more general geoscientific aspects as "Volcanoes and their Products" or "Meteorites - Primary Rocks from the Solar System". There have been gemmological exhibitions on special groups of gems and mineralogical exhibitions with regional main focuses or exhibitions presenting special minerals in their whole variety.

To exhibit something means always to select exponates and to present them in an extraordinary way. But there are some distinct difficulties between keeping a strong scientific background and serving a clear and easily understood presentation. These difficulties will be also discussed in the given contribution.

CATALOGUE OF TYPE MINERAL SPECIMENS - CTMS

Stalder H.A. *(Natural History Museum, Dept. of Mineralogy, Bern)*

CTMS is a project of the IMA-Commission on Museums (CM), started in 1979 by H.J. Rösler of Freiberg. The first edition of the catalogue, prepared in Freiberg, has been distributed 1991 to all members of the CM. But at the CM-meeting 1992 in Toronto it was, for different reasons, decided to establish a CTMS on a new basis. In 1994 the first outprint of the CTMS for the minerals first described from Italy has been presented at the IMA-meeting in Pisa. This part of the catalogue is stored - as all the following parts - in the computer database of A.R. Hölzel.

Type mineral specimens are first reference samples for the definition of mineral species, and secondly historical documents. - After the description of a new mineral species it is common to designate the type specimen. This is the specimen on which the chemical, crystallographic and physical properties of the new mineral species were originally determined. Since the determinative analysis may have been destructive, the material which remains as the type specimen(s) may not be identical of the original sample, but it is that which is most closely related. - For historical and scientific reasons the authors who describe a new mineral species must deposit the corresponding type specimen(s) in a museum or scientific institute. Only where a safe conservation is most probable a unique document may be attainable. This procedure was once simply recommended but today it is strictly demanded.

In the last years, initiated once by the CM, a lot of work has been done to enlarge the CTMS. For many countries curators made lists of the minerals first described in their own country together with the list of the respective type specimens. Since 1987 a new formal definition of the different type specimens exists. But the designation of a mineral species as a type specimen is sometimes still a problem - and the older a specimen, the more serious the problem is.

Some examples, which do not represent the änormalô case of the designation of holo- or cotype will be discussed: such as types not distinguishable between holo-, co- and metatype (the last term in use until 1986), neotypes, plesiotypes (term in use until 1986) *etc.*

24. Mineralogy of Large and Superlarge Ore Deposits

ARE THERE MINERALOGICAL CRITERIA OF LARGE AND SUPERLARGE MINERAL DEPOSITS?

Rundqvist D.V. *(Geological Museum, Moscow, dvr@sgm.ru)*

Since 1995 the Project 354 IGCP "Economic Superaccumulations of Metals in the Lithosphere" (Leader - Prof. Pei Rongfu, Co-leaders - Prof. J. Kutina, Prof. P. Laznicka, *et al.*) has been carried out. The main goals of the Project are to create database of the large and superlarge mineral deposits (LSMD), to define geological factors of their development, distribution, and petrologic-mineralogical criteria. The research allows us to define that LSMD are characterized by:

- Restricting to the structures with deep mantle roots (plums, hot spots, mantle magmatism in nodes of lineament intersections, etc.) and mixing of fluids and metals from mantle and crust sources;

- Development during long multistage geological process on the background of geodynamic-system evolution with a duration preliminary period - forming of favorable environments to ore bearing (metal sources, structural-geochemical barrier).

Generalization of data on LSMD mineralogy of the Former Soviet Union shows that different deposits (Au, PGE, Sn - W, W - Mo, Nb - Ta, U) have following common typical features:

1) wide variety of mineral paragenesises different in the origin time, temperature, alkalinity-acidity, oxidation-reduction potential, and progressive-regressive trend;

2) complicated chemical ore composition, sometimes with "anomalous" element associations;

3) alternation of short periods of intensive mineralization, intraore magmatism, and long "rest" periods;

4) existence of telescoped, multi-level ore bodies with signs of repeated rejuvenation;

5) ore minerals are represented by many species, generations, polimorphic modifications, native elements;

6) nonmetalloferrous minerals (fluorite, mica, feldspar, etc.) often have increased impurity of rare alkali elements and high-level REE fractionation;

7) isotopic evidence show that at the early stages fluids were predominantly reductant, from the mantle, and at the late ones from the upper crust.

Thus, mineralogical criteria may be of great significance and used to define LSMD together with regional geological data.

THE CRYSTAL CHEMISTRY OF AMPHIBOLES IN THE FOOTWALL BRECCIA, AT THE FRASER MINE, SUDBURY, ONT.

McCormick K. A. and McDonald A. M. *(Mineral Exploration Research Center and Dept. of Earth Sciences, Laurentian Univ., kmccormick@nickel.laurentian.ca)*

Amphiboles from two cores drilled through the footwall breccia between the Sudbury Igneous Complex and the footwall Levack Gneiss at Fraser mine in the North Range of the Sudbury Basin were analyzed by EMPA, SEM, and optical microscopy techniques in an effort to determine their paragenetic relationship with Ni-Cu sulfide mineralization in the area. The amphiboles in the breccia matrix are typically euhedral to subhedral, reach > 200 μm in width, and have a pale green to green pleochroism. These amphiboles often have rims (<40 μm thick) of an amphibole having a distinctive, moderate to deep blue-green pleochroism. The rimmed amphiboles commonly occur intimately intergrown with or adjacent to sulfides (pyrrhotite with minor pentlandite and chalcopyrite).

Compositionally, these amphiboles are quite variable. Both halogen-poor and halogen-bearing phases are present within the breccia matrix. The halogen-poor amphiboles, which dominate the mineral assemblage, are actinolite to magnesiohornblende in composition. The rims on actinolite and magnesiohornblende are an Fe-rich amphibole that is frequently enriched in Cl (0.7 - 4.0 wt.%). The Cl-poor, Fe-rich rims range in compositions from ferroactinolite to ferrohornblende, whereas the Cl-bearing, Fe-rich rims are always hastingsite. Strong correlations are present between Cl, K, Fe, Al, and Si. The more magnesian amphiboles are Cl-poor, but can be enriched in F. There is a concomitant increase in Fe, K, and Al with Cl, but a decrease in Si.

Cl-bearing amphiboles are associated with sulfides, but are erratically distributed through the ore zone; reaching a maximum of > 1.10, but usually < 0.2 vol.% in a sample. Cl-bearing phases are not unique to Sudbury. Cl-apatite, Cl-amphibole and Cl-biotite are found associated with ores in other geologic settings. The presence of these Cl-bearing phases suggest that they crystallized from a Cl-Fe-rich fluid that, at least spatially, is related to mineralization.

MINERALOGY OF THE VOISEY'S BAY NI-CU DEPOSIT, LABRADOR

Naldrett A.J., Singh J. and Krstic S. *(University of Toronto, ajn@quartz.geology.utoronto.ca)*

The Voisey's Bay Ni-Cu deposit is one of the most significant discoveries made in Canada in the last 30 years. Reserves plus indicated and inferred resources amount to 98.5×10^6 tonnes at 1.85 wt.% Ni. The deposit can be described in terms of four geological settings; the "Eastern Deeps" consisting of massive and disseminated sulfide along the line of intersection of a feeder sheet with the base of a troctolite intrusion; the "Ovoid" , a 600 m long by 350 m wide by 110 m deep lens of massive sulfide underlain by a feeder sheet; the "Discovery Zone" which comprises a series of swellings containing disseminated and massive sulfides in the troctolite feeder; and the Reid Brook zone which is where the feeder sheet opens out into a deeper level intrusion.

The principal minerals are hexagonal pyrrhotite, troilite, pentlandite, chalcopyrite, cubanite and magnetite. Troilite is restricted to the Reid Brook, Discovery and Ovoid zones, where it occurs as exsolution lamellae in hexagonal pyrrhotite. The texture of pentlandite varies with the presence of troilite in coexisting pyrrhotite; where troilite is present pentlandite occurs as equant masses, up to several cm across; where troilite is absent; it occurs around pyrrhotite grain margins and as lamellae in a pyrrhohtite host. The Ni content of hexagonal pyrrhotite averages 0.28 wt.% in troilite-bearing zones and 0.51 wt.% in troilite-absent zones. Cubanite is restricted to troilite-bearing zones.

The presence of troilite indicates a metal-rich high temperature hexagonal pyrrhotite from which pentlandite will exsolve at higher temperature than from more sulfur-rich pyrrhotite, thus developing as larger masses; cubanite can exist with metal-rich pyrrhotite, but not with sulfur-rich pyrrhotite. Metal-rich pyrrhotite indicates an original metal-rich sulfide melt, which, in turn, indicates a low oxygen fugacity in the silicate magma within which the sulfides have formed; this is thought to be due to the presence of graphite in the region where the magma extracted sulfide from surrounding gneisses.

MINERALOGY OF THE SUPERLARGE LINGLONG GOLD DEPOSIT IN SHANDONG PROVINCE, N. CHINA

Chen G.Y., Sun D.S. Shao W. *(China Univ. of Geosciences)* and Chen Y. *(Okanagan Univ. College)*

The mining history of the superlarge Linglong Gold Deposit can be dated back to 1007 AD in Song Dynasty. Its gold production from a few quartz lode veins had already totalled over 200t before 1949. Its hosting rocks are four generations of the sheared Mesozoic regenerated granitoids, cut by 543 auriferous quartz veins and veinlet-disseminated hydrothermal alteration zones, out of which at least 387 have already been proved to be industrially valuable. The maximum length for the former and the latter is over 5000m and up to 4500m respectively. Its mineralogical characteristics are as follows.

1. Multiple mineralization stages totalled 9 including the final hydrothermal monomineral native-gold stage.

2. Multiple mineralization substages totalled 5 for the quartz-pyrite stage and totalled 3 for the polymetallic stage.

3. Multiple mineral associations up to 22.

4. Multiple mineral species up to 50.

5. Multiple mineral generations including 10 for quartz, 10 for pyrite, 7 for native gold-electrum, 5 for chalcopyrite, 4 for sphalerite, 3 for galena, 2 for native silver, 5 for calcite and 2 for siderite.

6. Multiple modes of occurrence like native gold-electrum including inclusions in host minerals, intergranular fillings between other minerals, crack-fillings in broken minerals, grided filaments like spider web in drusy cavities, discontinuous veinlets several meters in length cutting quartz-carbonate veins and thin film-like veinlets cutting into altered country rocks over ½ m2 in extension.

7. Large to superlarge euhedral crystals as reprcsented by pyrite up to 2cm, 3cm and 5-6cm for its cubic edge from pyrite-quartz stage, quartz-pyrite stage and muscovite-quartz stage respectively; and also by sphalerite up to 5-6 cm for its tetrahedral edge from the pyrite-quartz stage.

8. Large to superlarge mineral aggregates of quartz of the pyrite-quartz stage, forming quartz vein several tens of meters in width with quartz crystallite germinations on its cleavage planes.

9. P-conduction-type pyrites up to 78.2%, 87.1% to 97.1% from west to east and lower to upper part of the deposit respectively.

24. Mineralogy of Large and Superlarge Ore Deposits

MINERALOGICAL TYPES OF URANIUM ORES OF RUSSIA AND CONTIGUOUS TO COUNTRIES, MINERALOGICAL TYPES OF LARGE AND SUPERLARGE DEPOSITS

Chernikov A.A. *(Fersman Mineralogical Museum RAS, Moscow)*

The large diversity of the ore forming mineral associations have been revealed: 1. The brannerite type with native gold and (or) molybdenite in the kalifeldspathic metasomatite zones of the long-living fractures of the Elkon horst, Aldan and the uraninite-coffinite-pitchblende-brannerite type in the albite long-living fractures of the Kirovograd fault block of the Ukrainian shield. 2. The coffinite-brannerite type in chlorite-carbonate-albite metasomatites and brannerite-uraninite type in beresites and carbonate-albite zones of the North Kazakhstan province. 3. The coffinite-nenadkevite- uraninite- brannerite- pitchblende type in the magnetite-albite-carbonate metasomatites of Krivoj Rog's basin, Ukraine. 4. The coffinite-pitchblende type in the chromphengite- phlogopite-roscoelite metasomatites of the Lake Onega region, Karelia with the complex (V, Pd, Pt, Au, U) ores. 5. The uranium-containing apatite in the weathered rock of the Ordovician carbonate phosphorite and in the bone fragments of pyrite oligocene clay of Kazakhstan. 6. The pitchblende type, in which it is possible to find the carbonate-pitchblende, quartz-pitchblende, and other paragenetic mineral subtypes in Russia, eastern Germany and other countries. 7. The sooty pitchblende as a major uranium constituent of the ore. Pitchblende, coffinite and phosphates, containing quadrivalent uranium are present in the ores. There are five subtypes of deposits of this type in Uzbekistan, Kazakhstan and other countries.There are other types. Among them there are original ore associations, for example, beta-uranophane-zeolite, gold-brannerite, molybdenite-brannerite and other, which are not known in other place over the word. Gold-brannerite, molybdenite-brannerite, pitchblende-molybdenite ores made up large and giant deposits. In the complex (V, Pd, Pt, Au, U) deposits the reserves of the noble and other metals are not appraised and possibilities of their increase are grand.

This work is supported by RFFI. Project N 96-05-65732.

THE JIAODONG GOLD PROVINCE OF CHINA: ALTERATION AND ORE MINERALOGY

Chen Y. *(Dept. of Earth & Environ. Sci., Okanagan Univ. College)*, Zang W. *(Geologist)*, Fyfe W.S. *(Univ. of Western Ontario)*, Chen G.Y. and Sun D.S. *(China Univ. of Geosci.)*

The Jiaodong gold province is situated in the southeast margin of the Sino-Korean Platform. The basement rocks are Archean and Proterozoic metamorphic rocks. The Archean rocks are mainly composed of gneisses, (plagioclase) amphibolite and biotite schists. The Proterozoic rocks include granulites, schists, marbles and iron formation (conglomerate?). Mesozoic sedimentary and volcanic rocks occur within extensional basins. Mesozoic granitoid intruded the basement. The structures are an E-W-trending anticlinorium in the basement complex, and large-scale NE-SW- and NNE-SSW-trending fault zones of Mesozoic age.

The gold mineralization is mainly associated with the Mesozoic faults and related secondary fractures in the granitoid or granitoid-basement contacts. The mineralization types are gold-quartz veins and altered fracture zones, namely quartz-vein type and wall-rock alteration type. Large gold deposits of both types were discovered in west part of the gold province. In the east part, only quartz-vein type deposits were discovered. Wall-rock alteration is very well developed around the ore zones. Alteration minerals include quartz, sericite (and fuchsite), pyrite, calcite, chlorite, hematite, rutile, graphite, *etc*. Ore assemblage is quiet uniform in all deposits, including pyrite, chalcopyrite, galena, sphalerite, pyrrhotite, arsenopyrite, gold, electrum, hessite, petzite, *etc*. The fineness of gold is different between the west part (700-900) and the east part (400-600). Another characteristic feature is that hessite, petzite and other Ag-bearing minerals are common in the east part of the province.

Mesozoic collision between the South China and North China continental blocks contributed to formation of the granitoid intrusions. The granitic magma was derived from partial melting of the Precambrian complex through underplating processes. Gold was remobilised from basement rocks and deposited in fracture zones by the high temperature fluids associated with these processes.

GENESIS OF THE LARGE TUNGSTEN DEPOSIT VOSTOK-2 (PRIMORIE, RUSSIA): Sm-Nd AND Rb-Sr ISOTOPE CONSTRAINTS

Krymsky R.S. and Belyatsky B.V. *(IPGG RAS, St.Petersburg, Russia, robert@RK2258.spb.edu)*

The large Vostok-2 scheelite greisen-skarn deposit situated in the central part of the Sikhote-Alin region (Far East, Russia). The ore deposit is spatially associated with the granodiorite stock which cuts Permian sandstone-carbonate units. The sequence of mineral formation at the ore-deposit is: skarn-, greisen- formation, and Sch-Ap-Qu, sulfide and Qu-Carb veins. The time of granodiorite and ore formation was restricted by the narrow age limits at 100-103 Ma ago. For deciphering of genetic relationships all different kinds of rock types (magmatic, sedimentary rocks, ores and minerals) presented in this deposit were studied by using Sm-Nd and Rb-Sr isotope methods. All data-points form single trend in $^{87}Sr/^{86}Sr$-ε_{Nd} space in the following order from the mantle component: basalt dykes, quartz diorite of neighboring batholith, diorite dyke, granodiorite of hosted stock, marble, ore and greisen. This trend could be explained in the frame of existence of single magmatic source evolved during time. The formation of this source was undertaken on the crust level by means of intruding depleted mantle melts. Further diversities of isotope parameters of studied granitoids were connected with contamination of granitic magmas by host sandstone during emplacement of granitic bodies. The isotope compositions of scheelite-apatite ores and ore greisens suppose a share of the mantle component amounts 55-60 % in the source of ore fluid, without any significant contamination by host rocks. On the contrary, intrusive rocks and dykes show a different degree of host rock contamination: low in the dykes and high in the granitoids. This difference of contamination degree between magmatic rocks and ores could be explained by different time of melts and fluids interaction with host sedimentary rocks.

MINERALOGICAL PECULIARITIES OF LARGE GOLD AND PLATINUM DEPOSITS

Kulish E.A. and Komov I.L. *(State Sci. Centre of Envir.Radiogeochem. Kiev, CENTER@radgeo.freenet.kiev.ua)*

Two enlarged groups of gold deposits were picked out. The first group includes deposits connecting with the Precambrian greenstone belts and containing gold-bearing conglomerates. The most favourable conditions for large gold deposit formations were being created under the following conditions: 1. within zones enriched by sulphides, carboniferous formations and ferriferous materials; 2. under repeated rock transformation that is being manifested in various mineral composition of gold ores zones. Gold more often associates with phyrrotine, chalcopyrite, pyrite, tellurides, arsenopyrite, antimonite, quartz, ankerite, scheelite, molibdenite, sphalerite, galenite, tetrahedrite *etc*. The rocks of greenstone belts were the sources of ore matter for conglomerates with that large gold deposits are associated. The gold-bearing conglomerates unique is connected with the many stages of their formation that is reflected in multiformity of minerals (more than 100 units) containing in them and in high gold standard (>1000). The deposits of the second group, containing large units associated with metamorphic and terrigenic series containing carbonate and graphitic rocks. The major gold concentrators are sulphides and bioorganic matter. The As, Sb, Zn, Pb, Bi, Ag, U, Th, Mo, Ba, Corg, Te, Hg minerals predominate. Hypergenic processes with the development of areal and lineal crusts of weathering had important significance within the regions where the deposits of second groups were localized.

The mineral forms of platinum group elements within large deposits are exceptionally various. They are unregulated hard solutions and intermetallic compounds (aurides, stannites, plumbites, bismuthites, antimonides, tellurides, arsenides), sulphides. Platinum metals are in ores in forms of Pd and Rt mineral individuals and also in diffused condition. Pt minerals associating with chalcopyrite predominate among major minerals of large deposits, but Pd minerals predominate in more poor deposits. Rhodium is concentrated in pyrrhotite ores.

MINERALOGY OF CARBONATES FROM LARGE-SUPERLARGE GOLD DEPOSITS IN SHANDONG PENINSULA, N. CHINA

Sun D.S., Chen G.Y., Shao W. *(China University of Geosciences)* and Li G.Y. *(Henan Building Material Research Institute)*

The mineralogy of carbonates from nine large superlarge gold deposits in Shandong Peninsula is described below.

1. Wide-spread in gold deposits, occurring more that 100m away from the orebody both in the overlying and in the underlying wall rocks, especially in the latter where they are found more than 180m away.

2. Multiple species, including calcite, dolomite, ankerite and siderite, but no pure calcite, dolomite, ankerite and siderite are found. Ca, Mg, Fe, Mn isomorphous mixtures very common. Calcite contains MnO, FeO, MgO up to 4.64 wt%, 3.80 wt% and 2.58 wt% respectively. Content of FeO in Ferrous dolomite-ankerite are 6.13-20.19 wt% with the content of MnO up to 4.42 wt%. Siderite contains CaO, MgO, MnO up to 1.88 wt%, 3.91 wt% and 12.07 wt% respectively.

4. Presence of metallogenic chalcophylic elements Zn, Cd frequently found as isomorphous mixtures and Au, Ag as mechanical mixtures. Contents of ZnO in calcite, ferrous dolomite-ankerite and siderite are up to 0.36, 0.22 and 4.7 wt% respectively. CdO contents in ferrous dolomite is 0.14 - 0.30 wt%. Contents of Au in calcite, ferrous dolomite-ankerite and siderite are up to 4.1ppm, 16.7ppm and 1.6ppm respectively. Those of Ag in calcite, ferrous dolomite-ankerite and siderite are 1.8, 1.4 and 2.2ppm respectively.

5. Very distinct spatial zonation with respect to the orebody. They are in distal altered wall rocks disseminated, in proximal altered wall rocks veinlet-disseminated, but in orebodies mainly in veinlets. Calcite presents over all in both distal and proximal altered wall rocks and also in orebodies, but ferrous dolomite only in proximal altered wall rocks, while manganiferous siderite and ankerite are found only in orebodies.

6. Temporal distribution is also characteristic. Calcite occurs from the early stage of wallrock alteration to the late stage of ore-mineralization. Ferrous dolomite occurs mainly in the late stage of wall alteration while ankerite and siderite are present only in the main ore-mineralization stage.

In summary carbonates in large-superlarge gold deposits are characterized by multiple species, complex composition with large amount of isomorphous mixtures of both lithophylic and chalcophylic components as well as gold and silver mechanical mixtures, and also by spatial zonation and multiple temporal stages.

25. Granite Pegmatites: Nature versus Experiment

NATURE *VS* EXPERIMENT IN GRANITIC PEGMATITES: WHAT WORKS AND WHAT DOES NOT

Černý P. *(Dept. of Geological Sciences, Univ. of Manitoba)*

Experimental studies have always played a significant role in interpreting overall petrologic evolution of granitic pegmatites, conditions of their crystallization, and geochemical history. (i) The Jahns-Burnham model of pegmatite consolidation, based on experiments apparently indicative of crystallization from coexisting melt and fluid, was universally accepted for three decades. London's recent work demonstrated extensive solubility of water in highly fractionated pegmatite-forming melts, which remain homogeneous till very late stages of solidification. - (ii) The lithium-aluminosilicate P-T diagram is a widely used petrological tool today; however, effects of stress on petalite, and of incorporation of Fe into spodumene, are not quantitatively elucidated. Stability of chrysoberyl relative to beryl is well established, as are the limits on incorporation of Be into cordierite. However, stabilities of Ca,Fe,Mn-phosphate minerals are difficult to investigate, and experimental evidence of their formation is missing. Similarly, many gaps mark experimental understanding of Nb,Ta-oxide minerals, such as the columbite-tapiolite immiscibility, order-disorder in columbite-tantalite, and (meta)stability of complex phases such as ixiolite. - (iii) Breakdown of primary Na,H_2O-bearing pollucite into end-member pollucite ± albite or analcime was suspected to be an exsolution effect, but experimental work points to metastability of the primary phase with non-integral stoichiometry. In contrast, sluggish reaction rates hinder experimental simulation of the diverse origins of Rb-dominant feldspar ± coexisting end-member K-feldspar. - (iv) Relative to the above lines of study, genetic significance of textural patterns (graphic, dendritic, layered *etc.*) of mineral assemblages started attracting attention only recently. - (v) In contrast, recent studies of elemental concentrations require to stabilize accessory minerals such as tourmaline or beryl are quite advanced, and they emphasize the significant difference between compositions of solidified pegmatites and their parent melts.

PEGMATITIC AND RELATED TEXTURES IN COMPOSITIONALLY SIMPLE GRANITIC ROCKS

Candela P., Piccoli P. *(Laboratory for Mineral Deposits Research, Department of Geology, University of Maryland, candela@geol.umd.edu)*

We have mapped two dike complexes in the Tuolumne Intrusive Suite (California). Dikes exhibit internal textural variability; many are aplites, pegmatites, or related textural variants, and are mineralogically simple. Field relations suggest that some dikes are locally derived, with diking occurring within a partly molten crystallization interval.

We suggest that changes in dike texture along strike are a function of changes in host crystallinity and temperature during diking. In some cases, individual dikes can be followed along strike (for 10s of meters) from areas where the dike is wider, has faint or undulose borders, and has a texture similar to the groundmass of the host granodiorite, to areas farther along strike where the dike is thinner, contacts are sharp, and the dike texture does not resemble the host texture. In the direction of decreasing dike width and increasing brittleness of the dike wall (increasing undercooling), the dikes exhibit: 1) Fe-poor CP groundmass-like granite (internally nucleated), 2) a texture with euhedral to anhedral quartz "eyes", 3) poorly-developed graphic texture, 4) well-developed graphic texture, 5) pegmatitic texture (externally nucleated), and 6) in places, aplitic (*i.e.* fine-grained) borders. Our observations of changing physical and textural character within dikes are consistent with intrusion into a partially molten crystallization interval with varying degree of undercooling along dike length, indicating the importance of undercooling in the development of aplitic, pegmatic, graphic and quartz "eye" textures. Dike solidification can be modeled as a function of the Avrami number, $Av = I(U^3)([x^2]/k)^4$, the ratio of the time scale for heat flow to the time scale for crystal growth (each raised to the fourth power). I, U, x, k are the max. rates of crystal nucleation and growth, the half-with of the dike, and thermal diffusivity.

According to Spohn *et al.* (*JGR*, **93**, p 4880), kinetic effects dominate crystallization for $Av < 10^6$; devitrification occurs for $Av < 10^4$.

Some fine-grained dikes may be the result of devitrification.

EXPERIMENTAL SIMULATION OF PEGMATITE TEXTURE

London D. *(Geol. & Geophys., Univ. Oklahoma, dlondon@ou.edu)*

Experimentalists have known for nearly a century that silicate melts, especially siliceous ones, tend to persist metastably when cooled below their liquidus (measured as ΔT). Because the emphasis of experimental petrology has been on the application and derivation of equilibrium properties, experiments with undercooled magmas have been sparse. When they have been done, they have produced textures that are pegmatitic (albeit microscopic). The textures of undercooled experiments have been likened to replication of the pegmatite-forming process, and specific textures of experiments have been deemed directly analogous to natural ones (*e.g.*, graphic granite). Recent work in our lab has subjected simple and complex granitic bulk compositions to liquidus undercoolings of 100° - 150°C over time frames of 1-3 months at 200 MPa (above and below H_2O saturation), conditions comparable to cooling in natural pegmatite dikes. All aspects of pegmatite texture and textural variation, and mineralogical and chemical zoning found in pegmatites, have been reproduced. These features are derived from the intrinsic properties of melts as a function of ΔT, which determine the nucleation response, orientation and habit, composition, and sequence of the crystalline phases. With increasing ΔT, fabric becomes more oriented and zoned from the sidewall of the charge. For most granitic compositions, undercooling of this magnitude induces oscillations in the chemistry (*e.g.*, Na/K) and proportions (*e.g.*, feldspar/quartz) of crystalline phases. Oscillations in feldspar/quartz produce "aplitic line-rock", blocky feldspar interiors, and pure quartz cores. Even with large undercooling, however, alkali feldspars tend to evolve (as they would following equilibrium) from single-phase ternary compositions to exsolved solvus pairs. Some experiments capture the development of a highly fluxed boundary layer of melt. In most cases, melt inclusions trapped in crystals are from the boundary layer and are not representative of the bulk melt composition.

DIFFUSION IN PEGMATITE MELTS AND THE SIZE OF COMPOSITIONAL GRADIENTS IN FRONT OF GROWING CRYSTALS

Baker D.R. *(Earth and Planetary Sciences, McGill University, Canada)* and Freda C. *(CNR, Centro di Studio per gli Equilibri Sperimentali in Minerali e Rocce, Scienze della Terra, Università degli Studi "La Sapienza", Italia)*

The distinctive compositional and textural heterogeneity of pegmatites has recently been attributed to disequilibrium processes. Supercooling followed by rapid crystal growth can form a zone of depletion in the melt in front of growing crystals for components with partition coefficients (D) > 1 and of enrichment for those with D < 1. Eventually the melt could become undersaturated in the growing crystal and supersaturated with another, causing crystallization of the newly supersaturated phase. Diffusion of cations in pegmatitic melts was measured or estimated to model the effects of rapid crystal growth on the possible formation of heterogeneities in pegmatites. Na-K chemical interdiffusion between granitic composition melts with 6 wt % H_2O has been measured: $D = 2.49 (+1.9,-1.1) \times 10^{-6} \exp(-111.0 \pm 6.4/RT)$; D is the diffusivity in m^2s^{-1}, the activation energy is in kJ mol^{-1}, R is the gas constant and T is in K. Interdiffusion of Si and Al in pegmatite melts + 6 wt. % H_2O at 500 to 700°C can be estimated by: $D = 6.7 \times 10^{-9} \exp(-142/RT)$. Combining these data with feldspar growth rates, 10^{-8} to 10^{-10} ms^{-1}, and models for solute redistribution in melt, the width of affected melt zones be calculated for realistic growth times. The affected zone for Al_2O_3 and SiO_2 is microns in length and independent of growth rate. The affected zone for Na_2O and K_2O is strongly dependent upon growth rate. At 10^{-8} ms^{-1}, micron-scale zones extremely enriched in one or the other alkali are created. Growth rates of 10^{-10} ms^{-1} produce cm-scale affected zones with less enrichment. These results demonstrate that diffusion in the melt cannot account for the m-scale heterogeneities in pegmatites, but may be responsible for the formation of "line rock" with cm-scale heterogeneity.

25. Granite Pegmatites: Nature versus Experiment

KINETICS OF OSCILLATORY CRYSTALLIZATION IN GRANITIC MELTS: INTERNAL VERSUS EXTERNAL FORCING

Dewers T. *(School of Geology and Geophysics, University of Oklahoma, tdewers@ou.edu)*

Observations of banded or oscillatory mineralogical zonation in granite rocks (orbicules or line rock associated with pegmatites) pose the question as to origin. Do the textures arise from such external forcing such as periodic extrusive events, or may they form as an example of self-organization, in which a cooling crystallizing melt undergoes an instability leading to oscillatory crystallization? Self-organization can occur in systems driven far from chemical or thermal equilibrium, and require positive feedback. We examine potential for oscillatory mineralization at an advancing solidification front. We review potential feedback mechanisms proposed for igneous systems. One feedback mechanism arises if excluded melt species or components somehow enhance the growth and/or nucleation rate of the melt-solid interface. Such species can enhance rates directly by surface catalysis, or indirectly by influencing speciation at the melt-solid interface. Another feedback involves the famous Ostwald-Prager supersaturation-nucleation-depletion cycle.

To evaluate these mechanisms, we develop a mathematical model coupling equations for crystal growth and nucleation to melt diffusion and advection, in the front-fixed reference frame. We restrict our treatment to Qz-Ab-H_2O and Qz-Or-H_2O psuedo-binaries. All thermodynamic relationships, growth, and diffusion laws, kinetic constants, and P-T-X dependencies of melt viscosity used in the model are parameterized from the literature. Numerical simulations of crystallization show that a H_2O-undersaturated melt becomes unstable to the formation of spatially alternating quartz and feldspar crystallized regions at intermediate undercooling greater than 100°C, and less than 300°C and over narrow compositional ranges. At these undercoolings, growth rates exhibit a mixed interfacial/diffusion kinetic control and peak in magnitude, and nucleation rates are inhibited by increasing H_2O.

WATER-RICH SILICIC MELT VISCOSITIES: INFLUENCE OF THE ALKALI/ALUMINUM RATIO AND IMPLICATIONS FOR MAGMATIC DEGASSING

Dingwell D.B., Hess K.-U. *(Bayerisches Geoinstitut, Bayreuth, don.dingwell@uni-bayreuth.de)* and Romano C. *(Terza Universitá, Roma)*

The viscosities of a series of water-bearing peralkaline and peraluminous rhyolitic melts have been experimentally determined. The dry melt compostions are composed of a series of additions of Na_2O and Al_2O_3 to a metaluminous base composition. The melts, initially been hydrated at high pressures and quenched isobarically, have been prepared by cutting and polishing, then reheated across the glass transition at 1 atm where they are annealed to a relaxed metastable state and then investigated dilatometrically using micropenetration methods. The measurements have been performed in the viscosity range of $10^{8.5}$ to $10^{11.5}$ Pa which corresponds to temperatures in the range of 675 to 220°C for these compositions.

The hydrous peraluminous melt viscosity data agree well with calculational model of Hess and Dingwell (1996) which was based on and designed for metaluminous melt viscosities. That model is capable of describing the viscosities of hydrous peraluminous granitic melts within the uncertainties stated for its application in metaluminous melts.

The viscosities of peralkaline rhyolitic melts also decrease strongly and non-linearly with the addition of water. The resulting viscosity-temperature relationships for water-bearing peralkaline rhyolitic melts are shifted to much lower temperatures such that glass transition temperatures for moderate cooling rates correspond to extraordinarily low temperatures. A model is presented for the calculation of melt viscosities in the range of $10^{8.5}$ to $10^{11.5}$ Pa for peralkaline rhyolites with up to 7 wt.% H_2O. The very fluid nature of the peralkaline melts over a wide range of water contents may facilitate very efficient degassing in peralkaline melts in nature.

CRYSTALLIZATION IN GRANITIC PEGMATITES: INSIGHTS FROM MY PLATE COLLECTION

Martin R.F. *(Department of Earth and Planetary Sciences, McGill University, bob_m@geosci.lan.mcgill.ca)*

One topic of debate concerning granitic pegmatites addresses the role of the orthomagmatic fluid in promoting the formation of the pegmatitic texture. Was such a fluid phase essential or not in achieving the spectacular growth of giant tapering crystals from the walls inward? According to some, growth must have taken place in a H_2O-saturated magma. That it did reach fluid saturation is not difficult to imagine in view of the massive crystallization of anhydrous minerals. A "film" of aqueous fluid between growing crystal and residual magma assures the efficient transfer of nutrients, and molecules of H_2O play the role of "little red wagons" in this respect. Others claim, on the contrary, that saturation in H_2O, although expected at some stage, occurs later rather than sooner, and largely after the formation of the bulk of the zoned body. The long tapering crystals thus are considered largely to grow inward from the walls into a melt that has not yet achieved saturation. The claim rests on experimental duplication on a reduced scale of textures seen in nature, but here achieved in geochemically evolved H_2O-undersaturated systems undergoing normal crystallization.

Most potters work hard to prevent crystallization in the glaze that they apply to their creations; a rarefied number of these choose to cool their plates or bowls from a high temperature (1060°C) slowly enough (30°C/hr) specifically to induce crystallization. The glaze used by the artists I know has willemite on the liquidus; the boron-fluxed system also contains impurities of Cu, Co or Mn, which partition into the residual liquid. The crystals of willemite form in the interval 1060-775°C. They typically grow in 2-D fan-like and spherulitic arrays. The tapering crystals widen outward into the melt, and "face" other tapering crystals that have nucleated along a wall zone. Between the two fronts of crystallization is the rest-liquid, which, to judge from its color, holds high concentrations of the pigment. These patterns duplicate in many respects those found in zoned granitic pegmatites. Yet H_2O is not present. These 1-atm "experiments" show that H_2O is not needed to achieve centimetric crystals in these planar "pegmatites". In nature, the role of H_2O is likely crucial as a component, but not as a phase. As a component, it will be a principal contributor to a decrease in the viscosity of the melt. As a free phase, it likely will be incidental to the growth taking place.

COOLING RATES AND CRYSTALLIZATION DYNAMICS OF SHALLOW LEVEL PEGMATITES, CALIF., USA

Webber K.L., Simmons Wm. B. and Falster A.U. *(Dept. of Geology, Univ. of New Orleans, klwgg@uno.edu)*

Pegmatites of the Pala and Mesa Grande District, San Diego County, California are typically thin, sheet-like composite pegmatite-aplite dikes. Aplitic portions of many dikes display pronounced mineralogical layering referred to as line rock. This rhythmic layering is characterized by fine-grained, garnet-rich bands alternating with albite-quartz-muscovite-rich bands. Line rock textures are not consistent with formation by settling or plastic flow. The George Ashley Block (GAB), Pala District, has been examined in detail and serves as a model for the crystallization dynamics and cooling rates of San Diego County pegmatites. Based on a melt emplacement temperature (ET) of 650°C into 150°C fractured, gabbroic country rock (CRT) at a depth of 5 km (1.5 kbar), and with an estimated 3% initial H_2O content, the calculated crystal-free magma viscosity for the GAB melt is $10^{6.2}$ Pa s. Calculated average magma density is 2.31 gm cm^{-3}. Using Stokes Law and a measured average crystal size of 0.5 mm, the calculated settling velocity for garnet is 0.51 cm yr^{-1}. Crystal size distribution (CSD) studies of garnet in line rock suggest growth rates of ~10^{-7} cm s^{-1}. Overall, no consistent whole rock chemical fractionation trends are observed from the dike margins to the center, nor are there any consistent changes in Mn and Fe abundance in garnets from the line rock portion of the dike. Observed textures and calculated magmatic parameters suggest that mineralogical layering in the GAB results from an in situ diffusion controlled process of rapid, heterogeneous, oscillatory nucleation and crystallization with a layer of excluded components developing in front of the crystallization front.

Using conductive cooling equations, the 8 m thick GAB dike cools to below 550°C in ~100 days. Using the same ET and CRT, the nearby 25 m wide Stewart Lithia dike cools to below 550°C in ~1000 days. The 1 m wide Himalaya dike, Mesa Grande district, contains abundant tourmaline, up to 9 cm in length in the wall zone and up to 15 cm in length in miarolitic cavities. Using the same ET and CRT, the Himalaya dike cools to 400°C in ~5 days. Using a CRT of 300°C, the Himalaya dike will still cool to 400°C in ~14 days. Thus, the thermal modeling strongly suggests that despite the variable and sometimes large crystal size exhibited by the dikes, they cooled very quickly with rapid crystallization and high growth rates.

25. Granite Pegmatites: Nature versus Experiment

WHAT CAN WE LEARN FROM MELT INCLUSIONS IN GRANITE PEGMATITES?

Thomas R. *(GeoForschungsZentrum Potsdam, Germany D-14473 thomas@gfz-potsdam.de)*

Crystallization and the postmagmatic alteration of igneous rocks eliminate the extreme chemical variations that are produced during the melt fractionation. The best way to preserve the extreme chemical variations is for samples of these melts to become trapped within rock-forming minerals as melt inclusions - the encapsulating crystals prohibit such alterations and give us the opportunity to study magmatic processes during growth of the host and trapping of the inclusions.

The considerable body of work on melt inclusions indicates that late-stage liquids can release significant quantities of P, F, Cl and Al to fluids immediately connected with the magmatic-pegmatitic processes. This information is also preserved in syngenetic fluid inclusions, which are sometimes arranged in the same growth zones in the studied quartz crystals.

From these results important questions arise: **Where did these fluxing components go? How did they move? How were they transported?** And: **Which information can we obtain for the transport and speciation of ore-forming elements?**

Moreover, besides obtaining data on the composition of pegmatitic liquids, we directly obtain other important and unique information on solidus temperature, pressure, oxygen fugacity, melt density, viscosity and others from the study of melt inclusions. We also obtain insights about the course of the very complicated natural processes of crystallization and element enrichment, and impressions about the transition of a magmatic system to a hydrothermal one.

Finally, the study of a large number of melt inclusions show us directly that **"the whole is more than the sum of his parts"**.

GEOCHEMISTRY AND CRYSTAL CHEMISTRY OF NB-TA OXIDES FROM "FONTE DEL PRETE" DIKE (ELBA ISLAND, ITALY)

Aurisicchio C., De Vito C., Ferrini V. *(C.S. Equilibri Sperimentali in Minerali e Rocce, C.N.R., Roma)* and Orlandi P. *(Dip. Scienze della Terra, Università di Pisa, Italia)*

Following the undertaken researches to characterise and classify the pegmatite dikes in the south-west area of the granodioritic pluton outcropping in the Elba island, are here given the results of a study developed on the Nb-Ta oxides found along the "Fonte del Prete" dike near the S. Piero in Campo's village. It shows asymmetric, complex zoning, with a massive texture from the wall to the intermediate zone, primitive pockets in the core and evolved ones in the peripheral zone. Nb and Ta like the other rare elements in the melt, migrate towards the surface as chemical complexes whose complexing agents are F, Cl, B and P. The environmental conditions (P-T and pH-fO2) affect the complexes stability and namely their fractionation. EMPA, and X-Ray results show the presence of phases belonging to ilmenrutile-struverite, euxenite-polycrase, columbite-tantalite, pyrochlore-microlite, wodginite and ixiolite groups. Nb/Ta, Fe/Mn, Ca/U, LREE/HREE+Y, HREE+Y/U+Bi are the main identified differentiation processes driving the paragenetic sequence. Joining field observations, and data analysis it is possible to mark two kind of pockets: the primitive ones show a paragenesis formed by Qz, Kf, Ab, Bi, Schorl and between the accessory terms ilmenrutile, euxenite, polycrase, (Fe, Mn)columbite, titanowodginite, polycrase-Y, uranpolycrase and microlite. Qz, polychrome tourmalines, Kf, Ab, petalite, pollucite, microlite, uranmicrolite, manganotantalite, W-ixiolite and hubnerite, crystallise in the evolved late cavities.The low amounts and the pattern type of rare elements fractionating mainly during pockets formation let us think that the "Fonte del Prete" dike could be considered belonging to a new class between those of the rare elements and that of miarolitic pegmatites (Cerny, 1990). The variations of the chemical composition shown by some accessory minerals occurring in the different pockets confirm our hypothesis.

TANTALUM-NIOBIUM OXIDE MINERALS AND PEGMATITE GENESIS

Ercit T.S. *(Canadian Museum of Nature, Ottawa, Canada)*

Oxide minerals of tantalum and niobium are typical accessory phases of a number of types and subtypes of granite and granitic pegmatite. The state of affairs a decade ago was such that only columbite- and pyrochlore-group minerals could be applied to problems in pegmatite petrology. Furthermore, applications were limited to moderate- to exceptionally fractionated members of the rare-element class of granitic pegmatite. The possibilities today are numerous, and the limitations relatively few, as the following examples illustrate.

Mineral Typomorphism – Some mineral species or assemblages of species are indicative of specific conditions of formation. Simpsonite, alumotantite and rankamaite-sosedkoite are indicative of extreme degrees of transition-metal fractionation in granitic pegmatites. The assemblage stibiocolumbite – manganocolumbite - microlite often typifies oxide assemblages in the elbaite and lepidolite subtypes of granitic pegmatite.

Mineral Chemistry – Decreases in Fe/Mn and Nb/Ta in columbite-group minerals have long been known to correspond to increases in melt differentiation. Work has progressed to a point where even exotic REE-Ta-Nb minerals of pegmatites emplaced at deep crustal levels can be used to study pegmatite genesis. Variations in Nb/Ta can be correlated with similar variations in Th/U and REE/Y, resulting in a variety of methods for assessing the relative degrees of fractionation and genesis of these pegmatites.

Experimentation and Natural Systems – Recent experimental studies of the geochemistry of Ta and Nb have shown that simple crystal-melt fractionation can be invoked to explain much of the behaviour of Ta and Nb in granitic melts (*e.g.*, Linnen & Keppler 1996). Comparison with data on natural systems provides insights on the behaviour of other phases.

Structural studies – Cation ordering in Ta-Nb minerals with α-PbO_2 derived structures (ixiolite, columbite, wolframite and wodginite structure types) is still poorly understood, but trends are emerging. Broader study and a better understanding of cation-ordering styles are needed before the causes of these variations can be determined.

EXPERIMENTAL CONSTRAINTS ON THE ASSOCIATION OF Li WITH Ta IN GRANITIC PEGMATITES

Linnen R.L., *(Dept. Earth Sci., Univ. of Waterloo, rlinnen@uwaterloo.ca)*

Tantalum mineralization invariably is associated with lithium in pegmatites and granites. One explanation for this relationship is that extreme fractionation is required for a granitic melt to attain saturation in either Ta or Li minerals. Another possibility is that the presence of Li in granitic liquids changes the solubility of Ta, similar to the effect of F. Experiments at 750° to 1035°C and 2 kbar were therefore conducted to measure the effect of lithium on columbite-tantalite solubility in water-saturated granitic melts. Experiments were also conducted to determine whether the effect of Li and F on tantalite solubility are additive.

Starting materials consist of synthetic fully ordered $MnNb_2O_6$ and $MnTa_2O_6$ and glasses with 0.0, 0.5, 1.0, 2.0 and 3.8 wt% Li_2O. Lithium was added to the 2 kbar water-saturated haplogranite minimum composition such that the mole% Si was constant and the (Na+K+Li)/Al ratio remained at one.

Columbite and tantalite solubilities in the granitic liquids increase by a factor of ~2 to 3 with the addition of 2 wt% Li_2O to water-saturated haplogranite at 750° to 1035°C and 2 kbar. The solubility data were extrapolated to 600°C, more reasonable for columbite-tantalite crystallization, then compared to compositions representative of evolved liquids from which rare-metal granites and pegmatites crystallize. It is estimated that at 600°C these melt compositions could be saturated in columbite, but not tantalite (a melt with 0.05 % MnO and 1 to 2% Li_2O requires 2000-4000 ppm Ta for tantalite saturation at 600°C). However, tantalite saturation is predicted if the effect of Fe is taken into account and the melts contained less Li. Therefore, the genesis of tantalum mineralization is potentially explained by Ta being retained in the melt because of high Li-F concentrations. Tantalite crystallization is delayed until a Li±F±P mineral crystallizes, which lowers tantalite solubility, and results in a general association of Ta with Li.

25. Granite Pegmatites: Nature versus Experiment

CHEMICAL AND PARAGENETIC DATA ON GADOLINITE GROUP MINERALS FROM BAVENO AND CUASSO AL MONTE, SOUTHERN ALPS, ITALY.

Pezzotta F., Guastoni A. *(Natural History Museum of Milan)*, Diella V. *(C.N.R., Centro Studio Geodinamica alpina e quaternaria, Milan)*, Gramaccioli C.M. *(Dept. Earth Sciences, Univ. of Milan)* and Demartin F. *(Dept. Structural and Stereochemical Inorganic Chemistry, Univ. of Milan).*

The Hercynian miarolitic Baveno granites and Cuasso al Monte granophyres are characterised by abundant pegmatitic cavities rich in rare accessory phases. For instance, the gadolinite group minerals are present as euhedral crystals included in feldspars close to the pockets, or in cavities as well formed crystals with different colour and habit.

A set of 6 samples from Baveno have been selected for chemical and X-ray structural analysis: a) two gadolinite crystals included in feldspar from the peripheral pegmatitic zone of large cavities from different portions of the pluton; b) a group of cm-sized crystals from the aplitic portion of a zoned aplitic-pegmatitic dike outcropping in the upper part of the pluton; c) two strongly zoned crystals from two different pockets; d) one datolite crystal from a pocket. Furthermore, 2 gadolinites from pockets at Cuasso al Monte corresponding to early (e) and late (f) formation were also examined.

Our results indicate that the more primitive minerals from Baveno (a, b) are homogeneous to zoned gadolinite-(Y) with the Y/REE ratio increasing from the core to the rim. Gadolinites (c) have a partially altered core, are deeply zoned, and from the core to the rim show an increase of the Y/REE ratio and of Ca, and a marked decrease of Fe, leading to hingganite-(Y) in solid solution with datolite. From Cuasso al Monte, (e) shows a compositional trend similar to (a, b). The crystal (f) displays a hingganite-(Y) rim with a lower Ca content than for hingganite-(Y) from Baveno. The more primitive gadolinites are mainly metamict.

In particular, such effects can be ascribed to the evolving paragenesis and the presence of complexing factors such as fluorides in the pegmatitic or hydrothermal medium.

THE ANALYSIS OF CHEMICAL COMPOSITION OF MELT INCLUSION OF BERYL IN PEGMATITE AND DISCOVERY OF ZINC SPINEL BY ELECTRONIC PROBE*

Li Z.L.[1,2], Zhang W.L.[2] and Yang R.Y.[1] *([1]Dept. of Earth Sciences, Zhongshan University, [2]LRMD,Nanjing University)*

The compositions of melt inclusions in beryls from pegmatites in Xinjiang, Hunan and Yunnan,China, have been successfully analyzed by the electronic probe by the authors. Minerals such as beryl,zinc spinel, mica, quartz, magnetite, hematite, siderite, sphalerite and silicate melt have been determined from 120 analysis points in the melt inclusions. The daughter mineral beryl in melt inclusions shaped like granular and irregular ranges from 10×5 to 40×8 μm. Its composition ratio of SiO_2/Al_2O_3 varies from 3.57 to 3.83, which is similar to that of host mineral beryl. In addition, the daughter mineral beryl contains minor components of Fe,Ca, K, Na, Mg, Nb and Ta *etc*. The zinc spinel, which appears as solid inclusion or daughter mineral in melt inclusion of beryl, was first discovered in melt inclusions of beryls from Xinjiang and Hunan pegmatites in China. Zinc spinel shaped like hexagon and long strip ranges from 15×7 to 60×30μm and is commonly associated with quartz and mica. The contents of Al_2O_3, ZnO and FeO are in the range of 53.83-58.58%, 31.68-41.71% and 8.98-2.94, respectively. The minor components of zinc spinels are Mg, Mn, Si, Al, Nb and Ta *etc*. Mica shaped like longstrip contains high content of K and Fe, and its composition ratio of SiO_2/Al_2O_3 varies from 1.313 to 1.741. Fe-enriched and aluminosilicate-enriched melts are extensively distributed in inclusions. Compared with host mineral and daughter mineral beryl, the compositions of silicate melt are enriched in Fe, Mg, Zn, Ca, P, Ti, Nb. Quartz is widely scatted in inclusion, and its SiO_2 content ranges from 79.28 to 100%. The FeO content of magnetite, hematite and siderite in inclusions ranges from 42.26 to 95.14%. The sphalerite-quartz association only appears in psudo-secondary inclusion, and the contents of Zn and S range from 65.11 to 63.42% and from 35.41 to 35.36% respectively.

**The Project is supported by National Science Foundation (41673189) and the foundation of LRMD,NJU*

BERYL FROM THE GRANITIC PEGMATITE AT NAMIVO, ALTO LIGONHA, MOZAMBIQUE

Neiva A.M.R., Neiva J.M.C. *(Dept. of Earth Sciences, Univ. of Coimbra, Portugal NEIVA@GEMINI.CI.UC.PT)* and Esson J. *(Dept. of Earth Sciences, Univ. of Manchester, U.K.)*

Beryl occurs in 3 out of 4 zones of the elongated concentric zoned granitic pegmatite of Namivo, but it is more abundant in the earliest intermediate zone and quartz core. It occurs in: 1) quartz + albite + biotite intermediate zone, as long pyramidal green, bluish green and rarely white crystals; 2) lepidolite + clevelandite unit, an extension at depth of the albite + perthite intermediate zone, as small tabular pink crystals; 3) quartz core, as abundant enormous white, light green, blue and light pinkish crystals (up to 5 × 4 m in size), but at depth the core passes to a quartz + spodumene unit with small tabular pink crystals.

The analyzed beryls from association 1) are green, bluish green and rarely white, while those from the other associations are pink, but a blue crystal from the quartz core was also studied. They are sodic-lithian beryls with the alkali contents ranging between 0.70 and 3.48 wt %. The pink and blue crystals have higher a_0 and are richer in $\sum R_2O$, Al, Li, Cs, Rb, Tl, Ge, Se, In and are poorer in Fe^{3+}, $Fe^{2+}+Fe^{3+}$ and Mg than the other analyzed beryls. Several diagrams (*e.g.* a_0 vs Mg, a_0 vs Li, a_0 vs Na+K+Li+Cs+Rb, Mg vs Al, $Fe^{3+}+Fe^{2+}$ vs Al, Li vs Mg, Cs vs Ge, Rb vs Tl, Na/Li vs Cs, Mg/Al vs Li and $(Fe^{3+}+Fe^{2+})$-Mg-Li) show the evolution of beryl composition from the early intermediate zone to the younger zones and suggest a common origin for all types of beryl. Chondrite normalized rare-earth elements patterns show strong positive Sm anomaly and negative Eu anomaly. Fractionation within HREE is more pronounced than within LREE. There is increase in ∑REE and LREE from beryls of the early intermediate zone to those of the quartz core.

A bluish green crystal is zoned with a white core which has higher $\sum R_2O$, Al, Li, K, F, Zn, Ga, Nb, Rb, Tl, Cs, Ge, Ta, W, U, and lower Fe^{3+}, $Fe^{3+}+Fe^{2+}$, Mg, Ca, Cr, Sc, Y and Th contents than the bluish green rim.

TRACE ELEMENT DISTRIBUTION IN PEGMATITIC QUARTZ: PETROGENETIC APPLICATIONS TO GRANITE PEGMATITES IN SOUTH-NORWAY

Larsen R.B. *(Geological Survey of Norway)* and Polvé M. *(Laboratoire de Géochimie, Université Paul Sabatier, France)*

Traditionally, studies of rare minerals provide the main body of constraints to granite pegmatite genesis. An alternative approach may be to determine the trace element chemistry of pegmatitic quartz. Quartz features an exceptionally stable crystal lattice and may be considered "inert" and, hence, does not fractionate between most trace elements of widely different ionic radii and oxidation states. Accordingly, quartz provide an unbiased imprint of the chemistry of the igneous fluids from which it crystallised. To demonstrate this model, fluid inclusion studies and solution ICP-MS analysis of quartz was combined with XRF analysis of feldspar and mica separates from the intermediate and core zones of Late Proterozoic granite pegmatites in South-Norway. The total concentration of structurally bound trace elements in quartz increases from ~ 45 ppm to 100 ppm over a N to S distance of 30 kilometres parallel with a systematic increase in FeO/MgO and Rb/Sr ratios of quartz. Co-existent potassic feldspar and plagioclase display N to S decrease in the anorthite component and increase in the Rb/Sr ratio whereas biotite show a gradual decrease of the MgO/FeO ratio. Primary fluid inclusions in quartz contain 6.4-17.4 wt% NaCl and 5 mol% CO_2 and belong to the H_2O-CO_2-NaCl-($\pm N_2$) system. In correlation with mineral compositions, total fluid salinities follow a crude declining trend from N to S. Given these constraints, the trace element distribution in quartz imply that pegmatites formed from progressively more differentiated granitic melts towards the south. Compositional changes of fluid inclusions, feldspar and biotite conform to this model, and it can be concluded that trace element analysis of quartz may provide an important tool in understanding pegmatite forming processes. Results of complimentary *in situ* laser ablation HR-ICP-MS analysis of REE in quartz are in progress.

25. Granite Pegmatites: Nature versus Experiment

COMPOSITIONAL EVOLUTION OF TOURMALINE IN PETALITE-SUBTYPE PEGMATITES

Selway J.B., Černý P., Hawthorne F.C. *(Dept. of Geological Sciences, University of Manitoba, umselway@cc.umanitoba.ca)* and Breaks F.W. *(Ontario Geological Survey)*

Petalite-subtype pegmatites are defined as pegmatites with petalite as the dominant Li-bearing mineral.Tourmaline from four petalite-subtype pegmatites was examined : (1) Pegmatite #5, and (2) Marko's Pegmatite, both from Separation Rapids pegmatite field, northwestern Ontario, (3) Tanco, southeastern Manitoba, and (4) Utö, Sweden.

The general compositional evolution of tourmaline in petalite-subtype pegmatites is ± black Mg-rich schorl, foitite-schorl and schorl-foitite to black or brown schorl-elbaite to green elbaite-schorl to green or blue Fe-rich schorl to pink elbaite-rossmanite to ± pink rossmanite-elbaite. In Pegmatite #5, the tourmaline compositions are the most primitive, with black Mg-rich schorl in the border, wall and blocky K-feldspar zones, and brown schorl-elbaite in the petalite-bearing core. In the outermost zone of the Utö pegmatite, black schorl-elbaite is particularly Fe-enriched due to contamination of the melt by the magnetite-rich host rock. The petalite-bearing zones in Utö and Tanco pegmatites contain pink Ca-bearing elbaite-rossmanite and pink rossmanite-elbaite.

This general compositional trend indicates that the tourmaline is initially Mg- and Fe-rich in the border and wall zones; Fe-rich in the intermediate zones, and Al- and Li-rich in the inner petalite-bearing zones. The majority of the tourmaline is Na-rich and Ca-poor, except for that in the late-stage petalite zones which is slightly Ca-enriched and Na-poor. In several respects, tourmaline from petalite-subtype pegmatites shows slight, up to distinct, differenes relative to tourmaline crystallized in lepidolite- and elbaite-subtype pegmatites.

PHOSPHATES FROM THE CAP DE CREUS GRANITE PEGMATITE FIELD, EASTERN PYRENEES, CATALONIA

Alfonso P., Melgarejo J.C. *(Dept. Crist. Min. Dip. Min., Univ. Barcelona, joanc@natura.geo.ub.es)*, Fontan F. *(Laboratoire de Minéralogie, Univ. Paul Sabatier, Toulouse)*

More than 200 pegmatite dykes occur in the Cap de Creus field. They are arranged according to the zones of regional metamorphism: barren (type I) and beryl-columbite subtype (type II) pegmatites occur in the sillimanite-K-feldspar and sillimanite zones; beryl-columbite-phosphate (type III) and albite pegmatites (type IV), in the cordierite-andalusite zone. The exceptional outcropping conditions allow a good sampling of all the pegmatite types and all the zones of a single pegmatite. Therefore, the aim of this contribution is to describe the mineralogical and chemical variations in P minerals along the pegmatite field and during the crystallization of a single pegmatite.

Phosphates occur as accessory minerals in all these pegmatites, and their abundance increases from the type I to IV. P is also present in some silicate structures, substituting Si. The rate of this substitution also increases from type I to IV. Hence, the total P amount of these pegmatites is high, increasing from type I to IV.

Phosphates are present in almost all the pegmatite zones of each pegmatite type. In addition, the phosphates formed during the early crystallization stages were affected by the latest processes of pegmatite formation. As a result, many metasomatic and meteoric phosphates were produced.

Primary phosphates are good indicators of the evolution degree of a pegmatite. Phosphates in type II pegmatites are Ca-Mg-Fe phosphates, Li-Fe-Ca-Be in type III, and Li-Al-Fe-(Mn)-Ca in type IV.

Some phosphates occur in several pegmatite types, and their chemical composition (particularly the Mn/Fe ratio) is a good tracer of the evolution degree of a pegmatite: this ratio increases in these phosphates from type I to type IV.

LINE ROCK FORMATION IN THE ORLOVKA AND ETYKA TANTALUM DEPOSITS, EASTERN TRANSBAIKALIA

Seltmann R. *(GFZ Potsdam)*, Taylor B. *(GSC Ottawa)*, Aksyuk A., Fedkin A., Reyf F., Shatov V., Zaraisky G. *(IEM Chernogolovka)*

Chemical and petrogenetic modeling of the Orlovka and Etyka tantalum deposits, Eastern Transbaikalia, has been carried out as prerequisites for experimental simulation of line rock formation.

According to the geological, petrological, and geochemical data of the district, the following rock groups can be distinguished:

1) barren bt and bt-ms granite massifs (Khangilay and Oldanda);

2) highly-evolved ms-ab and amz granite stocks (Orlovka and Etyka);

3) layered pegmatites-aplites, with locally- developed "line rock", within the mineralized apical parts.

The less-evolved Khangilay (for Orlovka) and Oldanda granitic plutons (for Etyka) are characterized by high values of Zr/Hf (25-32) and Nb/Ta (2.5-6.1), whereas low values are common for more evolved granites and "line rocks" of the deposits (~ 0.5-2.2 and 0.1-0.4, respectively). Greisens situated within the layered complex are enriched in Li (up to 8000 ppm), F (1.5-6.2 wt.%), and Ta (up to 700 ppm). The less-evolved granites of the deposits show intermediate values for these elements fitting the obvious evolution trend from the parental granites to the layered complex. The fractionation trend for the Orlovka region begins with bt-ms and subsequent bt granites of the Khangilay massif. More fractionated bt-ms-lith granites develop into ms-ab high Li-F granites, related line rocks and greisens. In case of Etyka, the Oldanda bt-ms granites are followed by highly fractionated amz granites, amz-ab granites, and finally by the layered complex, whereas greisens are untypically and only rarely developed.

Oxygen isotope ratios of some samples (~ 7.5 - 9.8 ‰) are consistent with a single fractionation trend from parental granites to the layered complex and "line rocks". Other samples have oxygen isotope ratios (-0.3 to 4.4 ‰), and most have hydrogen isotope ratios (< -130 ‰) due to sub-solidus, variable W/R alteration by isotopically light meteoric waters.

CHARACTERISTICS OF SOME VARISCAN GRANITOIDS IN CENTRAL EUROPE

Buda Gy. *(Dept. of Mineralogy, Eötvös L. University, Budapest, buda@ludens.elte.hu)*

Geological and geochemical comparisons have been carried out on the Variscan granitoids of the southern part of Central Bohemian Pluton (SCBP), South Bohemian Pluton (SBP), West Carpathians (WCA), South Hungary (SH), Balaton-Velence (BV) tectonic line, and South Alps (SA).

SCBP and SH Variscan granitoids have similar features. They contain approximately equal amounts of peraluminous and metaluminous granitoids. Rare pyroxene, actinolitic hornblende, actinolite, calc-alkaline-type Mg-biotite, microcline, allanite, zircon are characteristic minerals. Chromite occurs rarely in the basic part. They are K-calc-alkaline granitoids (Na/K=O.9), mostly I-type ($\delta^{18}O$=8.84 ‰), the $^{87}Sr/^{86}Sr$ ratios (0.7073-0.7108) suggest continental crustal contamination. They formed in the continent/continent collision zones and crystallized from a melt originating from the lower crust, but mantle contribution is also possible (mixed origin). Majority of SBP is peraluminous, postcollisional, S-type with only few small metaluminous granitoid bodies (*e.g.* Rastenberg). Consequently they have mainly a continental crustal origin. The more basic-type has K-calc-alkaline characteristic which have old (620 m.y.) and young ages (360 m.y. Klötzli 1995), like the SH granitoids. The WCA granitoids are mainly peraluminous granodiorite, tonalite (Na/K=1.7-3.4). Fe- and Mg-biotite, allanite as well as monazite occur. They are mixed, subduction related rocks. The younger (280 m.y.) SA and BV granitoids are peraluminous, S-type, postcollisional, hypabyssal instrusions.

It is suggested that the SCBP, eastern part of SBP and SH granitoids formed in a continent/continent collisional belt in the Moldanubicum zone of the Variscan orogenetic range producing mixed I/S granitoids. Later, the South Hungarian crystalline plate was disconnected by the eastward movement of the microplate of South Alps (Pelso unit) containing post-collisional, S-type granitoids and moved in a southeast direction.

Project was financed by HNRF No 023762.

25. Granite Pegmatites: Nature versus Experiment

SOLUBILITY OF BERYL IN HAPLOGRANITE MELTS

Evensen J.M., London D. *(Geol. & Geophys., Univ. of Oklahoma, jeven@hoth.gcn.ou.edu)* and Wendlandt R.F. *(Geol. & Geol. Eng., Colo. School of Mines)*

The BeO content of haplogranite melts at beryl saturation was investigated at 200 MPa (H_2O) and in the temperature range of 650°-850°C. Saturation of melt in beryl was approached by forward and reverse experiments using (1) beryl and (2) a compositionally equivalent reactive mixture of phenakite + Al_2O_3 + quartz added to metaluminous (ASI = 1.00) and peraluminous (ASI = 1.21) haplogranite minimum melt compositions. In peraluminous systems, chrysoberyl becomes stable (chrysoberyl + beryl + quartz) with granitic melt via the reaction

$$\text{beryl} + 2\ Al_2SiO_5 = 3\ \text{chrysoberyl} + 8\ \text{quartz}$$

BeO contents of glass (measured using IMPA-SIMS) increase from 0.05-0.31 wt% over the temperature range of 700°-850°C in metaluminous haplogranite melt, and from 0.03-0.13 wt% BeO in peraluminous haplogranite melt. The solubility of beryl is an activity product, $[a_{BeO}]^3[a_{Al2O3}][a_{SiO2}]^6$. Consequently, the increased a_{Al2O3} in peraluminous granitic melts lowers the observed BeO content required for beryl saturation. This relationship explains the common occurrence of beryl in peraluminous granitic rocks, which are typical of the less evolved classes of rare-element pegmatites.

The BeO content of melt projects to 0 wt% at the solidi of the metaluminous and peraluminous haplogranite systems (~675°C). Thus it is not surprising that pegmatite-forming melts, which crystallize at low temperature, are so commonly beryl-saturated. The insignificant amount of BeO in melt at beryl saturation produces negligible effects on liquidus phase relations. The freezing points of the simple haplogranite systems are depressed ≤5°C with beryl saturation, and a small (3.5 norm wt%) shift of the liquidus minimum toward Qtz is observed in the Be-bearing systems. This effect is consistent with a network-forming role for tetrahedrally coordinated beryllium in silicate melt.

ORIGIN, EMPLACEMENT AND MINERALIZATION OF RARE-ELEMENT PEGMATITES, CENTRAL DAMARA PROVINCE, NAMIBIA

Keller P. *(Inst. f. Mineralogie & Kristallchemie, Univ. Stuttgart, paul.keller@po.uni-stuttgart.de)*

The late Pan-African Damara pegmatites (about 500 m.y. old) constitute several belts. In contrast to other belts, the origin and mode of emplacement have been virtually unknown for the economically important pegmatites of the Karibib belt. Those pegmatites will be discussed by preliminary results from field observations and studies of aerial photographs as well as by recent data of pegmatite mineralization and geochemical characteristics.

In the Karibib belt, deep stratigraphic levels of Damara meta-sediments were exposed, which were floored by a granite-gneiss basement, the Abbabis inlier (about 1900 m.y. old). The pegmatites occur in a high-temperature-low-pressure zone that is characterised by (i) sillimanite-cordierite metamorphic assemblages, (ii) numerous granitic plutons and (iii) dome structures. The latter have evidently controlled the distribution and emplacement of pegmatites in the Karibib belt. Only few pegmatites have intruded into the basement or granite bodies, but mainly into folded Damara metasediments, preferentially dolomitic marbles. These pegmatites are usually steeply dipping dykes, more or less concordant to the host rock foliation. The pegmatites are unmetamorphosed and thus post-tectonic.

Significant fractionational trends can be determined by individual pegmatite mineralization. Around the exposures of basement, for instance on Okatjimukuju farm, exist clear successions with increasing distances from barren to highly fractionated pegmatites. Geochemical data gave similar pictures. The Fe/(Fe+Mn) ratio of phosphates has been proved true, like the well-known K/Rb ratio of K-feldspar, as indicator for the degree of fractionation.

The conclusion of all recent results is, that the parent granite bodies are evidently not widely exposed, but stuck mostly in the Abbabis basement. Consequently, the rare-element pegmatites of the Karibib belt do not originate from two widely distributed granite types ("Salem" and "Donkerhoek") in the area under discussion.

COMPLEX Ti, Ta, Nb OXIDES FROM BAVENO, ELBA ISLAND AND VAL VIGEZZO (NORTH OF ITALY).

Aurisicchio C., De Vito C., Ferrini V. *(IC.S. Equilibri Sperimentali in Minerali e Rocce, C.N.R., Roma)* and Orlandi P. *(Dip. Scienze della Terra, Università di Pisa, Italia)*

A correlation between complex oxides of Nb, Ti, Ta, coming from pegmatites developed in magmatic events of different geodynamic environments, is given here. 1) Baveno area: around the pink granitic pluton have been found big pockets carrying Qz, Pl, Kf and accessory minerals. 2) Elba island: were collect samples from a dike near the S. Piero in Campo village. 3) Val Vigezzo: have been collect samples from dikes filling tectonic faults. The studied samples belong to the group euxenite-polycrase, except those from Baveno which are aeschynites, polymorphs of low temperature of the euxenite. X-ray analyses show the metamictic state of these phases at room temperature, even if usually they develop an own habit. The increase of T (°C), promotes lattice ordering. The terms Y-rich show a complete re-ordering at about 750°C, while those Ce-rich need a higher temperature (900°C). EMPA allow to discriminate the three sampling areas on the basis of the cations occupying A and B sites. The Baveno's samples show a sharp trend from LREE+Ca to HREE+Y in the A site, while Ti, Nb prevail in the B site. Sometimes W reach a noteworthy activity. The complex Elban oxides have a trend from HREE+Y to U+Bi terms in the A site. The strong Ti activity is confirmed by the abundant presence of polycrases. The Val Vigezzo samples are yet polycrases showing a prevailing content of HREE.These compositional trends, obtained from the three localities, confirm the variation of the chemistry of the parent magmas.

MINERALOGY AND CHEMICAL COMPOSITION OF GRANITIC PEGMATITES IN DIFFERENT METAMORPHIC ZONES, SEINÄJOKI REGION, FINLAND

Mäkitie H., Lahti S.I., Kärkkäinen N. and Alviola R. *(Geological Survey of Finland; seppo.lahti@gsf.fi)*

Numerous pegmatite granite bodies, barren and rare -element pegmatite dykes are characteristic in the Paleoproterozoic Svecofennian schists and plutonic rocks of the Seinäjoki region, W-Finland. The rare element pegmatites can be classified to beryl-columbite, beryl-columbite-phosphate, spodumene, lepidolite and amblygonite pegmatites. The age of the pegmatite dykes (about 1.80 Ga) is younger than that of the peak of the regional metamorphism (1.88-1.90 Ga).

The rare-element pegmatites are concentrated to the lower- to medium-grade amphibolite facies rocks, especially to andalusite mica schists that form an east-west trending zone in the Seinäjoki region. The grade of metamorphism increases northwards and southwards reaching finally the granulite facies conditions. The rare minerals disappear in the pegmatites, when the metamorphic grade of the host rock reaches the Sil-Kfs isograd. Narrow anatectic biotite pegmatite bodies with accessory almandine and cordierite only occur in Crd-Kfs and Grt-Crd-Kfs zones.

The concentrations of Na_2O, P_2O_5, Ta, Li, Cs, Sn and B characterictic in the LCT-type of pegmatites are increased, K/Rb and Sr/Rb decreased in the dykes of the And and Sil-Ms zones, although there are locally large compositional variation due to the different degree of fractionation of the pegmatite magma. Concentrations of Li, Cs and Ta typical elements in complex pegmatites begin to increase, when the Sr/Rb ratio reaches a value of 0.2.

FT-IR MICRO SPECTRA OF PEGMATITE ALKALI FELSPAR FROM HANAZONO, JAPAN

Nakano S., Eriguchi T. *(Department of Natural Sciences, Shiga University. Japan, nakano@sue.shiga-u.ac.jp)* and Makino K. *(Shinshu University)*

Alkali felspar ($Or_{66}Ab_{33}An_{0.6}$) in Granite pegmatite from Hanazono, Kosei Town, Shiga Prefecture< southwest Japan, consists of two parts: one is non-colored and transparent, and the other is pinkish and opaque to the naked eye. The transparent part is clear, cryptoperthitic and almost free of micropores, and the opaque part is turbid, vein microperthitic and with many micropores under a microscope.

Fourier-transform infrared micro spectroscopy was applied to this alkali felspar. Absorbance spectra between 2500 and 4000 cm^{-1} were obtained and resolved to several constituent peaks for both the clear and the turbid parts. The data show that the water content of the turbid part is relatively higher than that of the clear part. This difference is probably due to the differences of quantities of mainly H_2O inclusions in micropores and subordinately structural OH molecules in each part. These differences in water allocation are consistent with the cooling history of the Hanazono alkali felspar, which is estimated based on the well known Klokken model (Parsons and Brown, 1984; Brown and Parsons, 1994).

MINERALOGY OF A LATE SVECOFENNIAN GRANITIC PEGMATITE, NORRSKOGEN, UPPLAND, SWEDEN.

Nysten P.N. *(Insti. of Earth Sci., Uppsala Univ.)* and Jonsson E. *(Dept.. of Geol. and Geochem. Univ. of Stockholm)*

Rare-element granitic pegmatites of LCT-affiliation cut early orogenic (≈1.9 G.a.) Svecofennian granodiorite associated with antophyllite and cordierite-bearing schists at Arlanda (N59°38′, E17°57′). The most fractionated dike contains abundant FeMn-, MnAl-, LiAl-, and Al-phosphates, löllingite, beryl, schorl and muscovite as well as minor cassiterite, Nb-Ta-(U)-oxides, bertrandite, Be-phosphates and zircon. Lenticular Al-phosphate pods display a complex zonation with augelite and eosphorite in the core followed outwards by scorzalite and alluaudite. The margin is composed of fine-grained arrojadite, triplite-zwieselite and sceletal corundum reminiscent of a breakdown texture. Similar margins also surround amblygonite pods whereas triphylite shows alteration to vivianite, heterosite and alluaudite. The pods are always surrounded by fine-grained muscovite and chlorite. Rough tapering yellow beryls, often showing secondary alteration to bertrandite, coexist with schorl from the wallzone whereas sharp beryls, intergrown with blocky K-feldspar, 'cleavelandite' and triphylite, are greenish white which indicates a compositional fractionation towards the interior of the dike. Fine-grained replacement-stage mica pods carries disseminated tapiolite and uraninite with secondary U-phases concentrated along fractures. The dike narrows in width northwards displaying a much less fractionated assemblage.

GEOCHEMICAL STUDY OF THE MUELHA TIN SPECIALIZED GRANITE, EASTERN DESERT, EGYPT

Morsy M.A. and Mohamed F.H. *(Geology Dept., Fac. of Science, Univ. of Alexandria, Egypt)*

The Muelha post orogenic granite is located at the intersection of major structural weaknesses that dissected the Eastern Desert of Egypt. The common rock type is a muscovitized biotite granite. However an albitized variety is common particularly at the SW part of the pluton. This granite is a plumasitic specialized type as reflected from the relatively high levels of Si, Na+K, Sn, Rb, Zn, Pb, Ga and Y compensated by extremely low contents of Ca, Mg, Ti, Ba and Sr, as well as strongly negative Eu anomalies and HREE enrichment. The remarkable low values of some elemental ratios like K/Rb and Al/Ga and the high values of Rb/Sr are additional indication for such geochemical specialization.

The calculation of mass transfer reveals that albitization is reflected by significant addition of Al, Na, Rb, Sn, Ga, Nb and La, and remarkable loss of Si, K, Fe, Ca, Zn, Zr, Ce and Pb. These chemical alterations of the original rock to a metasomatically albitized granite are concomitant with mineralogical changes.

A genetic model illustrates the involvement of both crustal rocks and subcontinental mantle sources in the granite genesis. Fluorine was an important complexing anion during the magmatic crystallization history to yield a volatile-rich residual melt enriched in highly charged cations like Sn, Nb and HREE. This resulted in the emplacement of the Sn specialized Muelha granite along reactivated deep-seated tectonic zone.

THE EL MUERTO MINE, OAXACA, MEXICO: AN EXAMPLE OF THE ALLANITE-SUBTYPE PEGMATITES

Melgarejo J.C. *(Dept. Crist. Min. Dip. Min., Univ. Barcelona, joanc@natura.geo.ub.es)*, Prol-Ledesma R.M., Sandoval-Miranda M.A. and Morales-Alvarado M. *(Inst. Geofísica, UNAM)*

El Muerto pegmatite is located in the Oaxaca Precambrian metamorphic complex. The complex is formed by granulites, gneisses, charnockites, meta-anorthosites, marbles and pegmatites.

El Muerto pegmatite is a vertical lens-shaped zoned body, up to 20 m wide and 100 m length, and was emplaced after the main metamorphic episode in amphibolitic gneiss. The pegmatite zones are:

1.-Wall zone: with fine-grain texture, consisting biotite and K-feldspar. The contact with the host rock is irregular at small scale and displays replacement textures.

2.-Border Zone: is fine-grained and contains mainly allanite - plagioclase ± muscovite. Allanite crystals are subhedral to euhedral in shape, and their crystals have 1-2 cm. There are minor amounts of magnetite, ilmenite, zircon, apatite and titanite. This unit can also be found riming the fragments of host rock included in the pegmatite.

3.-Intermediate Zone I: consists of andesine-microcline ± muscovite ± allanite ± magnetite ± quartz ± biotite. Allanite crystals are decimeter-size, euhedral, prismatic, concentrically zoned. These crystals grow perpendicularly to the contact with the enclosed host rock fragments. Primary allanite crystals altered to a second syntaxial allanite generation. Weathering produces bastnäsite along the grain borders.

4.-Intermediate Zone II: microcline-biotite-quartz±magnetite.
5.-Intermediate Zone III: consists of oligoclase, biotite and quartz, with lesser amounts of microcline. All crystals are meter-size.

6.-Core Zone: It consists of fractured massive quartz. This quartz contains small inclusions of allanite, zircon and apatite.

Textural patterns suggest that the allanite crystals formed by reaction between the pegmatite magma and the host rock, which provided Ca and Fe for the allanite formation.

25. Granite Pegmatites: Nature versus Experiment

COLQUIRIITE, CARLHINTZEITE, RALSTONITE AND PACHNOLITE FROM SERRA BRANCA-PEGMATITE/ BRAZIL

Wegner R., Pöllmann H., Witzke Th. and Schuckmann W. *(Dept. of Mineralogy, University of Halle /S., Germany, poellmann@geologie.uni-halle.de)*

The Serra Branca pegmatite, about 10 km SW of Pedra Lavrada, Paraiba, Brazil is characterized by two different phosphate parageneses. The main constituents of this granitic pegmatite are quartz, potassium feldspar, muscovite and amblygonite. Minor minerals are uranium - columbite, apatite, black tourmaline, sparse blue tourmalines, beryl and uraninite/gummite.

Besides this mineralogical bulk assemblage two different phosphate mineralizations occur, one originating from triphylite, the other from triplite as primary phosphates. Triphylite and triplite, each with complex secondary mineralizations, occur as isolated pods up to several tons each in the innermost part of the pegmatite.

The Serra Branca pegmatite of Brazilian age strikes 85 and is intruded almost vertically into biotite-schist. Distinctive zoning could not be observed. Quartz occurs as isolated massive blocks in the central pegmatite part, not as a massive quartz core. The outcrop of the pegmatite is incomplete, a hillside relict, yet the diameter of the body can estimated at 20-25 m.

It is very unusual that iron and manganese separated from these two phosphate mineralizations; triphylite and its secondary minerals like hureaulite, tavorite and barbosalite (among others) are very rich in iron and poor in manganese, whereas triplite and its secondary minerals are very rich in Mn and poor in Fe, thus representing almost in each case the pure end-members of iso-structural assemblages. This is significantly different to Hagendorf or Mangualde phosphate parageneses with their iron/manganese mixture and makes the Serra Branca phosphates distinctive .

Besides the phosphates some fluor-bearing parageneses of minerals, such as colquiriite, carlhinzeite, ralstonite and pachnolite occur within the same pegmatite, all of them derived from triplite. Idiomorphic, perfect crystals of colquiriite up to 1 mm in size have never before been reported, and it is remarkable that they are different in shape.

TRIOCTAEDRICAL MICAS FROM THE INTERNAL CONTACT ZONE OF TWO PEGMATITES FROM MINAS GERAIS, BRAZIL, AS INDICATORS OF REFLUX FLUIDS

Quéméneur J. *(Dept. of Geology, Fed. Univ. of Belo Horizonte, Brazil, jokarfun@igc.ufmg.br)*

The studied pegmatites, Urubu and José de Linto, belong to the cambrian pegmatite field of Araçuaí-Itinga (Jequitinhonha Valley), in the northeastern Minas Gerais State. Both are lithiferous pegmatites of the lepidolite complex-type with normal zonation.

In the upper border zone of these pegmatites occur bodies of small trioctaedrical micas. These minerals, with compositions varying from lepidolite to zinnwaldite, are very different from the lepidolite of the central part of the pegmatites. They are characterized by high content in Cs, F, Mg and Fe.

In the Urubu pegmatite the lepidolite of the central zone contains 2.56% Rb_2O, 0.88% Cs_2O and is very poor in Fe and Mn. The trioctaedrical micas of the border zone contain 1.21% Rb_2O, 0.6% Cs_2O, 2.32% FeO and 2.0% MgO. The lepidolites of the José de Linto central zone possess 1.85% Rb_2O, 0.27% Cs_2O, 5.43% F and the micas of the contact pockets contain 0.69% Rb_2O, 0.82% Cs_2O and 6.66% F.

These compositional differences suggest that the trioctaedrical micas of the border zone were crystallized from solutions originated from the pegmatite center. Such solutions are very rich in F, depleted in Rb and enriched in Cs, since pollucite did not crystallize.

This scheme explains the exotic composition of the trioctaedral micas of the pegmatites. In the José de Linto pegmatite the micas of the border zone are three times richer in Cs than the lepidolites of the center. In the Urubu pegmatite the content in Cs is slightly inferior than in the central lepidolites. It can be explained by the presence of pollucite. The high content of Mg and Fe in the micas of the border zone could result from metasomatism near the wall rocks, due to the reflux of solutions from the center of the pegmatite body.

GEOCHEMISTRY OF BIOTITES FROM MICROGRANULAR ENCLAVES AND HOST GRANITES FROM OPORTO-GAIA, NORTHERN PORTUGAL

Silva M.M.V.G. and Neiva A.M.R. *(Dept. of Earth Sciences, Univ. of Coimbra, Portugal, NEIVA@GEMINI. CI.UC.PT)*

The Hercynian metaluminous medium- to coarse- grained porphyritic biotite granite from Lavadores (314±11 Ma) and the metaluminous to peraluminous medium- to fine-grained porphyritic biotite granite from Maninho have microgranular enclaves which were originated by mingling and mixing of a basic magma with the host granite magma. At Lavadores they have dimensions up to 2 m in diameter, compositions of diorite, quartz-diorite, tonalite, granodiorite, monzodiorite, quartz-monzodiorite, quartz-syenite and quartz syenite with alkali feldspars, and most have characteristics similar to those of shoshonitic rocks, but some are ultrapotassic rocks and similar to vaugnerites. They contain biotite, amphibole and rare pyroxene. At Maninho quartz-diorite, tonalite and granodiorite enclaves have up to 20 cm diameter and are calc-alkaline rocks. Biotite is the only mafic mineral.

They are Mg-biotites, but at Lavadores they have compositions similar to those of biotite from sub-alkaline rock series, while at Maninho their compositions are similar to those of biotite of calc-alkaline rock series. The variation diagrams of biotites suggest that the two granites were originated from two distinct pulses of granitic magma. At Lavadores and Maninho, the biotites of such a large variety of microgranular enclaves have contents of major and trace elements similar to those of biotite of the respective host granite, suggesting equilibrium conditions during biotite crystallization. The fluorine content of melt calculated from biotite compositions is similar for enclaves and host granite.

THE ELATIA GRANITIC PLUTON (NORTH GREECE): MINERALOGY, PETROLOGY, GEOCHEMISTRY

Soldatos T. K. *(Dept. of Mineralogy-Petrology-Economic Geology, Aristotle University of Thessaloniki, soldatos@geo.auth.gr)*

The Elatia granitic pluton is the largest pluton in Greece (430 km^2). It is emplaced in the Hellenic Rhodope Massif that is a polymetamorphic terrain consisting mainly of gneisses, amphibolites, mica-schists, and marbles.

The pluton's main rock-types are (hornblende)- biotite granodiorite and two-mica granite. Granitic, aplitic and pegmatitic dykes cross-cut these rocks. Contact metamorphism phenomena are very limited. The main rock-forming minerals are plagioclase, microcline, quartz and biotite, with subordinate hornblende and muscovite. Accessory minerals are epidote (both primary and secondary), titanite, allanite, apatite, zircon, and opaques.

Geochemically the Elatia pluton is calc-alkaline to high-K calc-alkaline, and metaluminous to slightly peraluminous.

Rb-Sr isotopes on whole rock-mica pairs give a cooling age of at least 47 Ma and Sr initial ratios of 0.7061-0.7079. The increase in the Sr initial ratio coupled with the strong decrease in Sr is consistent with an AFC process with assimilation/crystallization ratio r = 0.2 and Sr bulk distribution coefficient D_{Sr} = 1.8. Oxygen isotope values range between 7.9 - 10.8‰.

K-feldspar-plagioclase equilibrium temperatures range between 600-790°C. Haematite-ilmenite exsolution intergrowths indicate a solidification temperature of at least 600°C for the granodioritic rocks. Crystallization pressure based on aluminium in hornblende is calculated at 4.6-5.4 (±0.6) kb. Similar crystallization pressure - about 6 kb - is estimated from the Q-Or-Ab-An-H_2O system. This crystallization pressure is supported by the presence of magmatic epidote in the plutonic rocks of Elatia.

PRIMARY PETALITE + SPODUMENE ASSEMBLAGES IN RARE-ELEMENT PEGMATITES OF THE PENINSULAR RANGES BATHOLITH, SOUTHERN CALIFORNIA

Taylor M.C. *(Dept. of Geological Sciences, San Diego State Univ.)* and Wise M.A. *(Dept. of Mineral Sciences, Smithsonian Institution)*

Petalite + spodumene assemblages occur at three localities in the Peninsular Ranges batholith of southern California. In the miarolitic Stewart Lithia pegmatite, Pala District, lath-like crystals of colorless to lilac spodumene occur locally within massive white petalite in the core zone that also contains abundant amblygonite-montebrasite, massive quartz and microcline. Late alteration of petalite and spodumene at relatively low temperatures yields brown fibrous petalite + heulandite including veinlets throught spodumene, while at lower temperatures spodumene alters to a kaolin group clay. Directly beneath the core zone of the miarolitic Clark pegmatite Rincon District, a quartz-rich unit contains unaltered prismatic crystals of white spodumene in intimate association with white, coarse-grained corrugated crystals of petalite along with gray-green mica, apatite, helvite and heulandite. In the non-miarolitic Lithia Queen pegmatite, Banner District, both white, prismatic spodumene and white, coarse-grained corrugated petalite occur in the core zone with abundant amblygonite-montebrasite, massive quartz, albite and microcline.

In all occurrences, the paragenetic sequence is spodumene first, then petalite, contrary to isobaric crystallization pathways for the lithium aluminosilicates. Moreover, the range of pressures and temperatures lie mostly outside of the experimentally determined stability field of petalite. The pressure conditions during emplacement and crystallization for the Lithia Queen pegmatite, for example, are constrained to within a range of 4.5 to 5.9 kbar based on hornblende crystallization pressures of two adjacent granitoids and their cross-cutting relations with local related pegmatites. These aspects of the petalite-bearing pegmatites raise serious doubt as to the effectiveness of the lithium aluminosilicate phase diagram in determining P-T conditions during rare-element pegmatite consolidation.

EXPERIMENTAL STUDY OF TOURMALINE STABILITY IN GRANITIC MAGMAS

Wolf M.B. *(Geology, Augustana College, glwolf@augustana.edu)* and London D. *(Geology&Geophys., Univ. Oklahoma, dlondon@ou.edu)*

Experiments at 750°C, 200 $MPa_{(H2O)}$, $a_{(H2O)}$=1, and fO_2~Ni-NiO established that the equilibrium among tourmaline, biotite, cordierite, and melt (± spinel, aluminosilicate, or corundum) occurs with ~2 wt.% B_2O_3 in strongly peraluminous melt with an aluminosity, measured by the parameter ASI, of >1.2. The experiments demonstrate the relationship of tourmaline stability to the activity product of the tourmaline components boron and aluminum, which are inversely related to one another. Tourmaline is unstable in metaluminous to mildly peraluminous melts (ASI <1.2) at 750°C regardless of their boron content. For a given aluminosity, addition of components such as F requires a greater boron content of melt at this equilibrium. The stability of tourmaline increases with decreasing temperatures below 750°C. At the inception of melting, tourmaline breaks down incongruently to assemblages containing crystalline AFM silicates (biotite, cordierite, garnet, sillimanite), aluminates (spinel, corundum), and B-enriched but Fe-Mg-poor melt.

Granitic melts are likely to be undersaturated in tourmaline from the start of their crystallization, and their initial boron contents will be limited by the abundance of tourmaline in their source rocks. Quartzofeldspathic (gneissic, metapelitic) rocks that reached conditions of the granulite facies and still contain (prograde) tourmaline are rare, and probably have never yielded a partial melt. Most leucogranitic magmas will initially crystallize biotite, cordierite, or garnet, but not tourmaline. With crystallization, the Fe-Mg content of melt decreases and the B_2O_3 content increases until the tourmaline-biotite and/or tourmaline-cordierite (or garnet) equilibria are attained. The B_2O_3 content of melt is buffered as long as these equilibria continue to operate, but low initial Fe-Mg contents of the magmas limit the quantity of boron that can be consumed by these reactions to <1 wt.% B_2O_3. Normally, leucogranitic magmas contain insufficient Fe and Mg to conserve all boron as tourmaline and thus lose a large fraction of magmatic boron to wallrocks. Leucogranites and pegmatites with tourmaline as an early and only AFM silicate mineral probably contained >2 wt.% B_2O_3 in their bulk magmas.

26. Descriptive Mineralogy at the Close of the 20th Century

NATURAL CRYSTALLINE CARBON POLYMORPH FROM MANTLE XENOLITE

Novgorodova M.I. *(Fersman Mineralogical Museum, Moscow, min@minmuz.msk.su)*

Graphite crystals from mantle spinel peridotite xenolites (basalt pipe Tuvish, Gissar Ridge, Tien-Shan, Tajikistan) were investigated. It was observed under SEM in cathodoluminescene light small (up to microns) carbon globules, hollow spheres, ribbons and polyhedral microcrystals which have (visually) cube, and pentagondodehaedron planes, (probably symmetry group 23). They are overgrow pinakoids and prizms planes of graphite crystals. The powder X-ray data were obtained and indexed using the theoretical unit cell parameters for f.c.c. C_{60} by Guo *et al.* (1991). The coincidence of the experimental with the calculated values of diffraction reflections appeared to be good. Thus natural crystalline carbon polymorph composed of fullerene C_{60} determined as pseudocubic tetragonal *P4/mmm* with a=14.22 Å, c=13.56 Å, c/a=0.95, z = 4, ρ =1.745 g/cm^3 (calc.). The model of fullerene epitaxial formation from 30°-dislocation <1$\bar{1}$00> of hexagonal graphite structure was suggested and discussed.

THREE NEW MINERALS FROM TUSCANY, ITALY

Orlandi P. and Merlino S. *(Dip. Scienze della Terra, Università di Pisa, orlandi@dst.unipi.it)*

More than one hundred natural phases have been so far found within the cavities of the marble in the Apuan Alps. Sulfides and sulfosalts are the most frequent species; among them sphalerite, wurtzite, colusite and sulvanite are the most representative. During a systematic study of the hydrothermal alteration products of these primary sulfides, various secondary phases have been identified. Three of these products appeared as new mineral species, as described in the following.

Zaccagnaite $Zn_4Al_2(OH)_{12}(CO_3)\cdot 3H_2O$, already approved as new mineral by CNMMN of IMA, is hexagonal, space group $P6_3/mmc$, a = 3.073, c = 15.114 Å. It is isostructural with sjögrenite, with Zn and Al substituting for Mg and Fe^{3+} respectively. It is associated with hydrozincite and fraipontite and is clearly formed as alteration product of sphalerite.

The second phase, already submitted to CNMMN, has composition $[Ca_3Ge(OH)_6\cdot 12H_2O](SO_4)_{1.35}(CO_3)_{0.65}$. It is hexagonal, space group $P6_3/m$, a = 11.03, c = 10.64 Å, isostructural with thaumasite and jouravskite, with germanium cations substituting for Si^{4+} and Mn^{4+} respectively. It is is associated with azurite and is, most probably, an alteration product of colusite, the only germanium containing mineral in Carrara marble.

The third phase, a zinc, aluminum and antimony hydroxide, space group $P3_12$, a = 5.33, c = 9.79 Å, presents a novel structural arrangement built up by dioctahedral layers.

These three mineral phases are to be added to the various new species already found in the apuan metamorphic complex and in other occurrences from Tuscany.

The description and discussion of the three new natural phases will be followed by an illustration of the new discoveries in the last twenty years.

THE IMHOFITE-JENTSCHITE GROUP OF Tl-As SULFOSALTS, LENGENBACH, SWITZERLAND

Graeser S. *(Natural History Museum/University of Basel graesers@ubaclu.unibas.ch)*

The sulfosalt locality Lengenbach in Binntal, Canton Wallis, Switzerland, has provided mineralogical research with numerous uncommon mineral species for almost 200 years. These minerals formed under hydrothermal conditions in cavities of a slightly metamorphic dolomitic rock of white color. At the present time, Lengenbach is the type locality for almost 30 species which, with one exception, are all sulfide minerals.

The old classical site (operated from 1833 to 1987) provided mainly Pb-Cu-Ag-As-sulfosalts, in particular, Pb-As-sulfosalts. A new site was opened in 1987 at a slightly higher level (about 25-30 meters) above the old quarry, which was abandoned mainly because of technical problems.

The mineral paragenesis at the new site turned out to be significantly different from the old quarry; whereas thallium was a very rare constituent before, thallium-sulfosalts became very important at the new site. Five new species were identified within the past few years, some others are still under investigation. Lengenbach has become one of the most prominent occurrences of Tl-minerals. Among about 25 valid Tl-sulfides known so far, 11 occur in Lengenbach, and for 10 of these Lengenbach is the type locality. Unexpectedly, some of the new sulfosalts show close relationships with respect to their structures, and form a group of their own in mineral systematics (imhofite-jentschite). They all contain Tl and/or Pb and Ag, As and a few Sb, plus sulfur. At the present time, minerals of this group occur exclusively in a very restricted area at the locality Lengenbach.

NEW DATA ON RHODIZITE FROM MADAGASCAR

Pezzota F. *(Museo di Storia Naturale di Milano)*, Falster A.U., Simmons Wm.B. and Webber K.L. *(Dept. of Geology, Univ. of New Orleans, aufgg@uno.edu)*

In a recent field study, rhodizites from the Manandona valley and the Betafo region, central Madagascar, were collected from a range of geochemically evolved pegmatite dikes. The more evolved pegmatites include the Antandrokomby dike, the Besesitra dike, the Ifasina dike, and several unnamed dikes. Less evolved dikes include the Andasy dike, the Fiakarandava dike, as well as several other unnamed dikes. Rhodizite occurs either in the wall zone, close to the contact with the carbonate country rock, or in the inner zones of the pegmatites, at times even in miarolitic cavities. Rhodizite from the more evolved pegmatites is typically associated with red or green tourmaline, whereas in the more primitive dikes, black tourmaline is more commonly associated with rhodizite. Rhodizite forms white to yellow-green crystals up to 3 cm in diameter. Microprobe analyses of representative samples reveal a wide range of K and Cs contents and overall low Rb abundance (Rb_2O ranges from 0.44 to 1.37 wt. %). All analyzed rhodizites exhibit striking heterogeneity under backscattered electron imaging, oscillatory and patchy zonations are common. Cs-enriched portions in rhodizite crystals occur in four main types: as primary growth zoning, as irregular patchy areas, as exsolution-like lamellae, and as late-stage fracture controlled veins. A direct correlation exists between Cs content and the degree of pegmatite evolution. In terms of K-Cs content, rhodizite crystals associated with primitive minerals such as black tourmaline, have a composition close to the K-end member. Rhodizite from the Ifasina dike, has a moderate Cs-content. Rhodizite crystals from the remaining locations have variable K-Cs contents, including some samples with over eight wt. % Cs_2O. In the rhodizites with the highest Cs content, the Cs-occupancy in the X-site is close to 0.50 apfu. In terms of the three major monovalent cations, Cs, K, and Rb, the rhodizite compositions plot in the Cs-dominant ternary field. These results show that a new rhodizite mineral exists and that the nomenclature for rhodizite should be revised to group status and include Cs- and K-end members.

26. Descriptive Mineralogy at the Close of the 20th Century

MINERALOGY AND CHEMISTRY OF DESERT ROSES, AYN DAR AREA, ABQAIQ, EASTERN PROVINCE, SAUDI ARABIA.

Almohandis A.A. *(Dept. of Geology, King Saud University)*

Desert roses are crystals which take the form of rose petals. They have definite crystal shapes, and enclose sand grains. The desert roses were scattered along an area of about 500m² in the Ayn Dar area, near Abqaiq, about 80 km southwest of Ad- Dammam, Eastern Province, Saudi Arabia.

Desert roses are made up of gypsum crystals including sand grains, in the form of rosettes with distinctive petal morphology. Most quartz grains are cemented by gypsum. Most gypsum crystals show a fibrous structure.

The main components of desert roses are SiO_2, CaO and SO_3. Other oxides include Na_2O, K_2O and small amounts of Fe, Al, Ti, Mg, Mn, Cr, Ni and P.

High porosity and permeability in the Ayn Dar area permitted rapid ionic migration to promote the growth of desert roses. Desert rose crystals were grown in loose sand near the surface of the sabkha, and finally concentrated inside the sand as scattered large rose crystals.

The large size of most crystals and the poikilitic inclusion of sand suggest accretion under stable hydrochemical conditions.

AN OVERVIEW ON ZEOLITES FROM ANTARCTICA

Quartieri S. *(quartieri@unimo.it)*, Galli E., Vezzalini G., *(Dip. di Scienze della Terra, Modena, Italy)* and Alberti A. *(Inst. of Mineralogy, C.so Ercole I d'Este 32, 44100 Ferrara, Italy)*

In the course of an extensive investigation into zeolites from Mt. Adamson, northern Victoria Land (Antarctica), a large number of known zeolitic species were identified in the Jurassic Ferrar Dolerites of Mt. Adamson: heulandite, stellerite, stilbite, mordenite, erionite, levyne, cowlesite, phillipsite, chabazite, epistilbite, ferrierite, analcime and, particularly interesting, boggsite and a tschernichite- type mineral. Of great interest is the discovery of three new zeolites: gottardiite, terranovaite and mutinaite. Boggsite from Antarctica - the second occurrence in the world - is morphologically similar to that of the type-locality (Goble, Oregon) and is characterized by a higher Na content. Tschernichite - the third occurrence in the world - is the natural counterpart of the synthetic zeolite beta and it is both morphologically and chemically quite similar to that from the type-locality (Goble, Oregon). It occurs as large steep tetragonal dipyramids very similar to those synthesized for beta zeolite. Some differences in X-ray powder diffraction pattern suggest that Antarctica tschernichite has a different polytypic sequence. Gottardiite - orthorhombic, s.g. *Cmca* - has the same framework topology as the synthetic zeolite NU-87. It occurs as thin pseudo-hexagonal lamellae and is characterized by high Si/Al ratio and Mg content. Terranovaite is orthorhombic, s.g. *C2cm*. Its framework topology is unique both in natural and synthetic zeolites and is characterized by the presence of pentasil chains and a bidimensional channel system delimited by 10-tetrahedra rings. Mutinaite is the natural counterpart of the synthetic zeolite ZSM-5. It occurs as subspherical aggregates of milky-white tiny radiating lath-like fibres. Its crystal habit is very similar to that of ZSM-5. The Si/Al ratio is the highest up to now found in natural zeolites.

The complete characterization of Antarctica zeolites was made very difficult by the extreme paucity of the available rock samples. Notwithstanding this, it is noteworthy the extremely high number of identified zeolitic species. This was made possible, in the first stages of the study, mainly by the morphological characteristics of these minerals.

NOMENCLATURE FOR ZEOLITE MINERALS

Coombs D.S. *(Dept. of Geology, Univ. of Otago, New Zealand, doug.coombs@stonebow.otago.ac.nz)*

The following rules for zeolite nomenclature adopted by CNMMN should be viewed as guidelines rather than as being rigidly prescriptive, with each case to be treated on its merits. Nomenclature should facilitate communication between specialists and non-specialists; needs and practicalities evolve with progress in science.

Rule 1: (a) One or more zeolite minerals having a topologically distinctive framework of tetrahedra and a composition that is distinctive for zeolites having that framework, constitute separate species. (b) Zeolites having the same topologically distinctive framework of tetrahedra constitute a series when they display a substantial range in composition in which differing extra-framework cations may be the most abundant in atomic proportions. Such series consist of two or more species that are distinguished on the basis of the most abundant extra-framework cation.

Rule 2: (a) Differences in space-group symmetry and in order-disorder relationships in zeolite minerals having the same topologically distinctive framework do not in general provide adequate grounds for recognition of separate species, but each case should be treated on its merits. (b) In assessing such cases, other factors, such as relationship to chemical composition, should be taken into consideration.

Rule 3: Zeolite mineral species shall not be distinguished solely on the basis of the framework Si : Al ratio. (An exception is made in the case of heulandite and clinoptilolite).

Rule 4: Dehydration, partial hydration, and over-hydration, whether reversible or irreversible, are not sufficient grounds for the recognition of separate species.

Rule 5: Individual species in a zeolite mineral series with varying extra-framework cations are named by attaching to the series name a suffix with the chemical symbol for the most abundant extra-framework element, *e.g.*, chabazite-Ca.

Rule 6: (a) Space-group variants of zeolite mineral species may be indicated by placing the space-group symbol in parentheses after the species name, *e.g.*, analcime (*Ibca*), heulandite-Ca (*C2/m*). (b) Levels of order may be indicated by appropriate adjectives. Such modifiers are not part of the formal name.

OPTICAL PROPERTIES OF NATURAL AND CATION-EXCHANGED HEULANDITE GROUP ZEOLITES

Palmer J.L. and Gunter M.E. *(Dept. of Geology, Univ. of Idaho, palm1541@novell.uidaho.edu)*

Heulandite group zeolites, with endmembers clinoptilolite and heulandite, $(Na,K)_6(Al_6Si_{30}O_{72})20H_2O$ & $(Na,K)Ca_4(Al_9Si_{27}O_{72})24H_2O$, have dynamic optical properties due to their low birefringence and their cation exchange capabilities. The optical properties of these minerals, specifically refractive index and optical orientation, change with hydration state and variations in framework cations, which in turn causes variations in exchangeable cations. In general, refractive indices increase from clinoptilolite to heulandite and the optical orientation changes from b parallel to Y to b parallel to Z because of an increase in electron density in the channels.

Whereas the overall trends in optical properties are known, the effect of exchangeable cations on optical properties is poorly understood. The optical orientation and principal refractive indices were measured for a series of monovalent and divalent cation-exchanged heulandite samples from Nasik, India by use of the spindle stage and double variation method. For monovalent cations Na, K, Rb, and Cs, the mean refractive indices were 1.4881, 1.4841, 1.4874, and 1.5039 respectively; and for divalent cations Mg, Mn, Cu, Sr, and Cd, the mean refractive indices were 1.4968, 1.5053, 1.4726, 1.5086, and 1.4860 respectively. Lower mean refractive indices correspond to changes in optical orientation from b parallel to Z in the natural sample to b parallel to Y in the K-exchanged sample and b parallel to X in the Cu-exchanged sample.

Relationships between refractive index and ultimately optical orientation and type and amount of exchanged cations in heulandites are complex. Samples exchanged with divalent cations generally have higher channel water content and refractive indices than those exchanged with monovalent cations. For all samples, refractive index increases with cation radius of exchanged cations. As cation radius of the exchangeable cation increases however, channel water content decreases. Consequently, refractive index is affected by two disproportionately related parameters, cation radius and channel water content - water having the highest Gladstone-Dale constant of any constituent in the samples. The Cu- and Cd-exchanged samples do not conform to these trends, as one might expect from their higher charges and moderate cation radii. Full cation exchange did not occur in these samples. Preliminary crystal structure data by other workers indicate that charge balance was obtained by H^+ instead of the exchangeable divalent cations in the channels.

26. Descriptive Mineralogy at the Close of the 20th Century

ON THE FUTURE OF MINERALOGY AND THE CNMMN

Raade G. *(Mineralogical-Geological Museum, University of Oslo, gunnar.raade@toyen.uio.no)*

Mineralogy will always be closely connected with geology although recent developments indicate that the ties between mineralogy and the earth sciences will weaken. Modern mineralogy is more and more connected with solid state physics and chemistry. Descriptive mineralogy, although regarded as bad science by many people, will certainly survive in some form, albeit marginal.

This may have a bearing on the future of the Commission on New Minerals and Mineral Names (CNMMN) and certainly on the definition of a mineral. It is probably only a matter of time before, for example, substances formed in nature on anthropogenic material will be regarded as minerals (as they partly have been in the past). Such substances should by all means be studied by mineralogists, but the crucial point is if they should be given mineral names.

As for the concept of mineral *species*, it is generally accepted that each member of an isostructural group having a predominance of a particular chemical element at a specific structural site would constitute a separate species. It is suggested that by introducing the concept of *subspecies*, there might be at least two exceptions to this rule: the REE minerals and the zeolites.

Whether one or the other of the coherent group of rare earth elements predominates in a REE mineral is more of geochemical than of mineralogical interest. Thus, lanthanite would be a species but lanthanite-(Ce), lanthanite-(La) and lanthanite-(Nd) would be subspecies. Similarly for the zeolites with regard to the exchangeable cations: chabazite would be a species but chabazite-Ca, chabazite-Na and chabazite-K (suggested as species in the new zeolite nomenclature) would be subspecies. It is presupposed that the creation of a subspecies, named according to the Levinson system, does not need the approval of the CNMMN.

ROLE OF THE MODULAR ASPECTS OF MINERALS FOR A CRYSTAL-CHEMICALLY ORIENTED DESCRIPTIVE MINERALOGY

Ferraris G. *(Dpt. Scienze Mineralogiche e Petrologiche, Univ. Torino, Italy)* and Merlino S. *(Dpt. Scienze della Terra, Univ. Pisa, Italy, merlino@mailbox.dst.unipi.it)*

The lectures of the School *Modular Aspects of Minerals*, recently organized by the European Union of Mineralogy (EMU) in Budapest (December 1997), have been collected in a book with the same title (S. Merlino ed., Eötvös Univ. Press, Budapest 1997). School and book have offered a unique occasion for illustrating the impact of a modular approach in fields as (i) interpreting crystal-chemical and crystallographic aspects of minerals, (ii) solving crystal structures, (iii) classifying groups of minerals, (iv) further understanding growth, genesis, transformations and associations of minerals.

Traditionally in the crystal chemistry of minerals, emphasis has been given to 'polyhedra' and the description and classification of the natural phases has been carried on the basis of the kinds of polyhedra in the structural arrangement and on the degree of their connections and polymerization (groups, chains, layers, frameworks).

It was then realized that more complex modules may stack, with different sequences in different structures (polytypes), or may combine, more or less unmodified, with other modules, in different ratios and according different ways, to build wide families of minerals (polysomatic and homologous series). This realization presented one of the most powerful tools for a modern descriptive mineralogy and the various aspects of the structural modularity have been systematized mainly by *OD* theory, polytypism, homologous and polysomatic series.

Some examples of families of minerals grouped together through the modular aspects of their structures shall be illustrated and discussed.

PRESENT AND FUTURE OF IMPACT MINERALOGICAL SCIENCES

Miura Y. *(Department of Earth Sciences, Yamaguchi University, Japan, dfb30@po.yb.cc.yamaguchi-u.ac.jp)*

Minerals on the Earth are formed mostly in endogenous processes such as tectonism, metamorphism and magmatism. However, the planet has many craters formed by the impacts of extraterrestrial bodies, and so in a chemical sense the Earth cannot be considered a closed system. The present purpose is to discuss the new field of impact mineralogy by clarifying the significance of the new terminology, with reference to the more-familiar processes of mineral formation which occur at and beneath the Earth's surface.

Mineralogical processes may be viewed in various dimensions[1-3]; in terms of Time (microseconds to years), Space (localized on one planetary body, or across the whole solar system), Reaction (static and closed, or dynamic and open), Pressure and Temperature conditions (including both magmatic and impact-induced high-P/T events). Impact mineralogy should be extended to planetary mineralogical sciences, by using mathematics, physics, chemistry, biology, earth sciences, and engineering sciences.

The significance of impact-mineralogical science is highlighted by three scenarios of known impact events, *e.g.*, oceanic impacts on Earth (the 'water planet'), new materials formed by impact-induced sedimentation, and effects of collision and shock impact[2-5]. The current state of the art includes the following features;

1) Impact mineralogical sciences open new fields in planetary science, especially with regard to the 'water planet'.
2) Shock-wave impact products lend new ideas to materials science.
3) Data on other solar-system bodies help with unsolved problems of Earth's lands and oceans and life's origin and evolution.
4) Buried deformed impact craters on the Earth.
5) Effects of impacts on the global circulation system.

References.

1. French, B. (1968): *Shock Metamorphism of Natural Materials* **1**
2. Miura, Y. (1992): *Proc. Missions, Technologies and Design of Planetary Mobile Vehicles* (Toulouse, CNES) **1**, 115-124
3. Miura, Y. (1997): (in press)
4. Miura, Y. (1994): *Astron. Soc. Pacific (ASP) Conf. Series* **63**, 259-264
5. Miura, Y. and Kato, T. (1993) *AIP Conf. Proc.* **283**, 488-492

AN ALGEBRAIC METHOD FOR CHOOSING EXCHANGE VECTORS THAT BEST DESCRIBE A MINERAL

Sonnet Ph. *(Lab. de Géologie et Minéralogie, Univ. Catholique de Louvain, Belgium, sonnet@gem.ucl.ac.be)*

Exchange vectors are increasingly used to describe structural formulae when minerals exhibit solid solutions. Any structural formula can be expressed by using an appropriate set of exchange vectors. However, exchange vectors are but algebraic constructs. The only requirement is that they form a basis of the subspace spanned by the structural formulae that one wants to express. There is thus an indefinite number of sets which satisfies this requirement.

The present work focuses on how to find the ôbestö set of exchange vectors to express a series of measured mineral compositions. Desired properties for the set are: the number of exchange vectors in the set should be as small as possible; the exchange vectors should have integer coefficients and should express simple or coupled substitution exchange mechanisms that are supposed to occur in the species; the exchange vectors should allow most of the features of the analyzed minerals to be expressed.

Suppose that a series of mineral analyses are available and that several possible substitution mechanisms can be invoked to account for the observed chemical variations. Two algebraic methods are presented to choose the best set of exchange vectors.

The first one constructs an approximation of lower dimension to the data by singular value decomposition of the data matrix. The best set of exchange vectors is then chosen using principal angles between two linear subspaces: the subspace spanned by the exchange vectors and the subspace filled by the approximation to the data.

The second method considers all the pairs that can be formed by the analyzed compositions. For each pair, there is a vector which connects the mineral formulae at each extremity of the pair. The best set of exchange vectors is found by considering the principal angle between all these vectors and the subspace spanned by the exchange vectors.

26. Descriptive Mineralogy at the Close of the 20th Century

RECENT MINERAL DISCOVERIES AND THE NUMBER OF MINERAL SPECIES: A RECONSIDERATION

Khomyakov A.P. *(Inst. Miner. Rare Elem., Moscow)*

The latter half of the 20th century was marked by a dramatic acceleration of the rate of new mineral discoveries. The mineral species discovered worldwide since 1970 are roughly equal in number to all those recorded throughout the preceding historic time. As a result, the overall mineral system has rapidly increased from 2000 to ~4000 species. This has radically changed our views on the chemical and structural diversity of the mineral world, on the distribution patterns of various elements in rocks and ores and provided a powerful stimulus for further advancement of both mineralogy and allied sciences. This has also initiated a drastic revision of the theories concerning the number of mineral species and the prospects for their further discoveries.

The long-held thesis that there is a finite number of mineral species (A. Fersman, A. Saukov, A. Povarennykh, V. Urusov, etc.) holds only for ordinary types of rocks and ores. However, the new species recorded in recent years have primarily come from unique deposits, which were formed in anomalous geotectonic and geochemical environments. The conditions of formation of such deposits bracket virtually the entire range of physico-chemical parameters (T, P, X, pH, and Eh) that are accessible to modern experimental mineralogy and also involve geologic time and other factors that cannot be realized in an experiment. All this virtually removes any barriers to species diversity and provides the basis for my hypothesis that there is no natural limit to the number of minerals.

A striking example of these deposits are the alkaline massifs of Khibina and Lovozero (Kola Peninsula). Since they began to be systematically studied in the 1890s, these massifs have yielded 120 new species, more than 80 of which have been discovered during the last 30 years. Most of the latter were encountered in the deep zones of the massifs within hyperagpaitic rocks, a special type of pegmatite and hydrothermalite with natrite, natrosilite, and other previously unknown, maximally alkaline minerals – indicators of the hyperalkaline state of natural substances. Remarkably, most of new minerals from Khibina and Lovozero are represented by hitherto unknown structural types. The increasing structural diversity of newly discovered minerals highlights the structural factor as a determinant of the virtually infinite species diversity of the mineral kingdom, which is still largely unexplored.

THE STATE OF DESCRIPTIVE MINERALOGY IN BRAZIL

Atencio D. *(Inst. Geociências, Univ. São Paulo, datencio@usp.br)*

Before the establishment of the Commission on New Minerals and Mineral Names of the International Mineralogical Association (1958) about 80 new mineral names were generated from Brazilian samples. Only about 20 of these have a reputable standing in mineralogy today. After IMA establishment, the descriptions of tantalaeschynite-(Y) (1974), atheneite (1974), isomertieite (1974), bahianite (1976), palladseite (1977), whiteite-(CaFeMg) (1978), whiteite-(MnFeMg) (1978), lanthanite-(Nd) (1980), minasgeraisite-(Y) (1986), parabariomicrolite (1986), arupite (1990), zanazziite (1990), yanomamite (1994) and quintinite-2*H* (1997) were published after IMA approval and remain valid. The mineral staringite (1969) also was published after IMA approval but was officially discredited (1992). The name pseudorutile (1966) was introduced without IMA approval for a mineral from several occurrences including Brazil, but none of the specimens investigated was designated as a type specimen. This name was rejected (1968), but subsequently was officially revalidated (1994) and a neotype specimen was proposed from South Australia. The name zirkelite (1895), introduced for a Brazilian mineral, was redefined (1989) and the new type specimen is from Russia. The minerals chavesite (1958) and ferrazite (1919) were discredited (1994 and 1996, respectively) with IMA approval. The name iridosmine (1827) was officially discarded in favour of osmium (1991) and the type specimen of osmium is from Borneo. The pyrochlore-group minerals rijkeboerite (1963, without IMA approval) and djalmaite (1939) had their names changed officially to bariomicrolite and uranmicrolite, respectively (1977) and the type specimens remain from Brazil. The names tantalaeschynite-(Ce) (1968), ferrohalotrichite (1969), coutinite (1980), coutinhite (1981) and neodymite (1980, 1981) were introduced without adequate justification and also without IMA approval.

MINERALOGY OF THE CARPATHIANS - A LEGEND OF THE PAST-A CHALLENGE TO THE FUTURE

Udubasa G. *(Geological Institute of Romania, Bucharest, udubasa@igr.ro)*, Szakall S. *(Herman Otto Museum, Miskolc, Hungary)*, Duda R. *(East Slovakian Museum,Kosice, Slovakia)* and Kvasnitsa V.M. *(Institute of Geochemistry and Mineralogy, Ukrainian AS Kiev, Ukraine)*

The 1500 km long mountain chain of the Carpathians in Central Europe shows a very long and complex geological history and hosts numerous mineral occurrences of very different genetic types. Some of them are world wide known, especially as type localities of some 30 mineral species, *e.g.* andorite, hodrushite, nagyagite, pilsenite, sylvanite, native tellurium, szomolnokite, *etc.*

The total number of so far described minerals is of about 900, *i.e.* some 25 precent of the valid mineral species. In addition, the so-called Verespatak twin law of beta quartz, several new crystal forms of many minerals, especially of pyrite, were here for the first time described. The celebrated Golden Quadrangle delivered huge amounts of precious metal during some 2000 years of extractive industry as well as unusually rich gold grain morphologies, *e.g.* octahedral crystals, leaves,snake, fibres *etc.*

The space and time distribution of mineral occurrences was governed both by the position of the Carpathians at the junction of there major plates and by quite different lithologies of the subducting and/or colliding plates. This is the support of the existing mineral parageneses diversity and a basis for new mineral discoveries.

A NATURAL MINERALIZATION PROCESS RESULTING FROM *IN SITU* SELF-IGNITION AND BURNING OF COAL

Belakovskiy D.I. *(Fersman Mineralogical Museum RAS, Moscow, Russia dmz@minmuz.msk.su)*

The natural modern mineralization process caused by natural self-ignition and burning of coal beds in situ investigated. The cause of self-ignition is exothermic oxidation of iron sulfides, contained in the coal. Host argillites and alevrolites melted to pseudobasaltic rocks or scorched as a result of coal burning described in Siberia and Central Asia. Most of fires occurred many millenium B.C. Some of the fires still active. The duration of fires is estimated as ranging from dozens years to several thousand years (Ravat, Tajikistan). The process is characterized by remarkably sharp geochemical zonation, specific mineral assemblages, certain stages. A typical hanging wall environment is strongly reductive. It formed by high temperature (up to 800°C) gases, contained Cl, S, NH_4^+ emanating from burning areas. The sal ammoniac gryphons are forming by crystallization from those gases. A number of minerals such as galena, wurtzite, sphalerite, greenockite, hedleyite, native Bi and Se, sulfur (in all polymorph modifications) and many others are crystallizing from the gases inside or outside gryphones. The environment in footwall is strongly oxidizing beacause of oxygen supply and H_2SO_4 activity. Various sulphates (letovicite, mascagnite, alunogen, godovikovite, efremovite, etc.) are forming here together with crystallized and amorphous Mo oxides.

The process has three main stages:

1. The beginning of burning - mostly non-mineral products such as bitumens, pitches *etc.* are generated.

2. Main stage - the maximum temperature (up to 1300°C) - the most part of sublimates are forming and host rock melting.

3. Extinction - some crystallized organic compounds as ravatite, natural naphtalene are forming, sulfates are hydrating and dissolving.

Analogs of those processes (burning dumps *etc.*) have been widely described, but the many phases discovered there are not approved by IMA because of their technogenical origin. At the same time some of those phases ahve been found in similar natural occurrences.

26. Descriptive Mineralogy at the Close of the 20th Century

SOLID SOLUTION IN THE EPIDOTE GROUP OF MINERALS: Pb AND REE-RICH PIEMONTITE FROM NEÄILOVO, MACEDONIA

Bermanec V. *(Department of Mineralogy and Petrology, University of Zagreb, Croatia, vberman@public.srce.hr)*, Armbruster T. *(University of Bern)*, Oberhänsli R. *(University of Potsdam)*, Zebec V. *(Natural History Museum, Zagreb)* and Kniewald G. *(Rudjer Boskovic Institute, Zagreb)*

An unusual Pb- and REE-rich epidote group mineral, related to piemontite was found near Nežilovo, Macedonia, within a micaschist complex in the upper part of the Babuna river, *ca.* 40 km SW of Skopje. The rock contains red mica, quartz, ardennite, gahnite and piemontite was found.

X-ray single crystal structural refinement (a = 8.880(1), b = 5.681(1), c = 10.166(3) Å and β =114.66(2)°, space group $P2_1/m$, Z = 2, **R** =3.35, **Rw** = 3.26 %) and electron microprobe analyses lead to the following crystallochemical formula:

$Ca(Pb_{0.27}Ca_{0.14}Mn_{0.13}La_{0.16}Ce_{0.06}Nd_{0.04}Na_{0.02}vac_{0.18})(Fe^{3+}_{0.49}Al_{0.39}Mg_{0.07}Zn_{0.05})Al_{1.00}(Mn^{3+}_{0.82}Al_{0.12}Fe^{3+}_{0.06})Si_{3.00}O_{12}OH$. The charge balance is obtained by divalent elements on M1 and M3 positions. This mineral appears to be an intermediate member between piemontite, the hypothetical Pb- end member and allanite, with predominantly Mn^{3+} on M3 positions as confirmed by average M3 - O distances (2.08 Å) and the characteristic Jahn-Teller distortion.

The piemontite from Nežilovo is deep red in color, almost black, with an adamantine luster and greyish-pink streak. It is brittle, with an uneven fracture and with no observable cleavage. Following forms were measured - 001, 100, 301, 101, 105, $\bar{1}02$, $\bar{1}01$, $\bar{2}01$, $\bar{3}01$ and 011.

The crystals often show twinning parallel to 100 and in this case display sections of isometric shape. Monocrystals are flattened in 001 and elongated parallel to b. They are optically negative with $2V_x$ *ca.* 60º. Refractive indices are around 1.8 and thus could not be measured precisely. The optical orientation is similar to that of allanite, Y = b, X to c = 23° in acute angle.

REE and Y MINERALS IN AN Fe-Mn DEPOSIT (MARITIME ALPS, ITALY)

Cabella R., Lucchetti G. and Marescotti P. *(Dept. of Earth Sciences, Univ. of Genova, cabella@dister.unige.it)*

Rare and unknown REE- and Y-minerals were found associated with Fe-Mn-ore in upper Jurassic quartz-arenites and quartz-bearing marbles from "Klippen di Deviglia" (Corsaglia Valley, Western Alps). Fe-Mn mineralizations (hematite ± braunite ± hollandite) occur both as boudins and thin massive recrystallized layers in quartz-rich marbles and meta-arenites; apatite, zircon and rutile are present as detrital minerals. Fe and Mn mainly came from the subaerial weathering of Permian (mainly calcalkaline volcanic products) and Triassic (mainly dolostones) rocks. The REE enrichment mechanism is possibly related to precipitation of the Fe-Mn colloids and/or clayey materials which operated as "scavengers" in the relatively shallow seawater. During polyphasic alpine tectonic-metamorphic events these rocks were affected by blueschist facies metamorphism; the observed minerals originated as a consequence of metamorphic mobilization and concentration processes. RE minerals have been found using a SEM with EDS analyzer as small, disseminated aggregates, (up to some tens of microns) interstitial with quartz and white mica in metamorphic veins, especially in hematite-rich meta-arenites. The small dimension and the paucity of materials impeded any XRD identification. Preliminary SEM analyses showed some different compositions: nearly pure As-Y, nearly pure As-La and LREE-As compounds; in many cases the compositions of these RE minerals differ greatly within the same sample; LREE and V contents may vary even at the single grain scale (up to 20-30μm). Microprobe analyses were carried out in WDS mode. The nearly pure As-Y compound shows As and Y amounts consistent with chernovite ($YAsO_4$). All the analyzed compositions arbitrarily calculated on the basis of 4 oxygen atoms show a good agreement with a general formula ABO_4; some compositions agree well with $LaAsO_4$ and could be a "new mineral". Th has been found in some LREE- and Y-rich compounds without any systematic variations (up to 0.15 a.p.f.u.). V replaces As in variable amounts (up to 0.3 a.p.f.u.). The Y-rich terms exhibit a generally low LREE content while HREE, (with the exception of Gd) , are present in low amounts; a wide range of LREE isomorphous substitutions seem to take place in La-rich compounds suggesting the existence of a solid solution series between LREE-rich phases.

DISTRIBUTION OF RARE EARTH ELEMENTS IN SEDIMENTS FROM THE TUZLA SALT MINE, BOSNIA AND HERZEGOVINA

Kniewald G. *(Rudjer Boskovic Institute, Zagreb, Croatia and Research Center Juelich, Juelich, Germany)*, Rossbach M. *(Research Center Juelich, Juelich, Germany)*, Amer H. *(National Center for Nuclear Safety and Radiation Control, Cairo, Egypt and Research Center Juelich, Juelich, Germany)* and Bermanec V. *(Department of Mineralogy and Petrology, University of Zagreb, Croatia, vberman@public.srce.hr)*

The concentration of rare earth elements (REE's) in the mineral tuzlaite (a new mineral, discovered in the evaporite series of the Tuzla salt mine in Bosnia and Hercegovina) and in surrounding marls were determined by instrumental neutron activation analysis (INAA). The crystal structure and crystallochemical characteristics of tuzlaite strongly influence the concentrations and distribution of individual rare earth elements. As a consequence of this, the REE content of the marls is greater than in tuzlaite by a factor of hundred.

The mineral tuzlaite displays a significant Eu and Yb anomaly and a positive Tb anomaly, contrary to the marls which show no pronounced anomalies. The distribution of REE's in the proximal marls shows the same overall pattern as in the distant northupite-containing marl equivalents. The marl that contains tuzlaite also show higher overall concentrations of rare earth elements than the distant marls, indicating a sequential diagenetic loss, probably due to recrystallization. The causes and implications of specific REE distributions are discussed in terms of HREE *vs.* LREE ratios.

A RE-EXAMINATION OF THE COMPOSITIONAL FIELDS OF THE MEMBERS OF THE AIKINITE-BISMUTHINITE SERIES

Cipriani C., Moggi-Cecchi V., Rubechi S. *(Mineralogical Museum, University of Florence, Italy)*, Bernardini G.P. and Danti C. *(Dept. of Earth Sciences, University of Florence, Italy)*

The compositional fields of the different members of the aikinite-bismuthinite series have also recentely been the object of numerous investigations also recently. In spite of this, no definite limits for all the members have been established either because some studies are related only to particular phases or because of the complicated intergrowth between the members of the series. In this work numerous samples, kindly provided by different mineralogical museums all over the world, have been investigated by optical microscope, electron microprobe and HRTEM observations. Owing to the exceedingly small samples, few X ray and electron diffraction spectra have been collected. X ray diffraction patterns confirm the existence of ordered superstructures for the intermediate members of the series but HRTEM observations show that the periodicity may be variable in the same sample. The results of the spectrochemical analyses point to a continous series between aikinite and krupkaite, while at least three different phases have been detected between krupkaite and bismuthinite. Apart from gladite and pekoite (respectively 2.00 and 1.00 Pb atoms for 18 S in formula unit), in fact, another phase, with a composition ranging from 0.27 to 0.57 Pb atoms, has been revealed. This phase, the reflectivity and the microhardness behaviour of which are slightly different from those of bismuthinite, could correspond to some of the supposed ôbismuthinite varietiesö as reported in literature. Unfortunately no single crystals were available for structural determinations, but the indexing of the powder pattern shows some differences with that of bismuthinite. A Rietveld refinement is under way.

26. Descriptive Mineralogy at the Close of the 20th Century

NEW DATA ON COQUIMBITE, PARACOQUIMBITE AND COPIAPITE-GROUP MINERALS FROM HUNGARY

Kovács A., Lovas Gy.A., Weiszburg T.G. *(Dept. of Mineralogy, Eötvös L. University, Budapest; koviatti@ludens.elte.hu)* and Kuzmann E. *(Dept. of Nuclear Chemistry, Eötvös L. University, Budapest)*

Coquimbite ($Fe_2(SO_4)_3 \cdot 9H_2O$) and its polytype modification, paracoquimbite, were found for the first time in Hungary. They occur together with copiapite-group phase(s), hereafter referred as copiapite. The mineral assemblage was studied at two localities: in the enargite-luzonite type mineralization of Lahóca Hill, Recsk, (N-Hungary), and in the coal open pit near Pécsszabolcs (S-Hungary). Coquimbite and copiapite form white and yellow efflorescence, respectively.

In Recsk both coquimbite and copiapite are euhedral. Coquimbite crystals are of a characteristic size of 200-300 μm. The balanced appearance of positive and negative rhombohedra lends a hexagonal holohedral pseudosymmetry to the crystals. Coquimbite could be easily separated for further studies. Thermal behavior of coquimbite (DTA, TG, DTG) was characterized for the first time. The platy crystals (dominating {010}) of the Recsk copiapite are of 50 μm in size. The perfect separation of copiapite from coquimbite was not possible. The X-ray powder diffractogram (XPD) of a sample enriched in copiapite shows the presence of peaks 8.97 Å, 17.95 Å and 18.54 Å, none of them present on the coquimbite XPD. This peak triad (and some additional peaks) can be interpreted either by the presence of two copiapite group minerals (ferricopiapite +another one, based on the low Al and Mg content of the samples, probably copiapite), or, less probable by the presence of a coquimbite-related phase besides copiapite. In the first case the powder data of ferricopiapite (the inconsistent position of the (010) peak in the JCPDS data base) should be revised, in the second case a new polytype (np) of coquimbite (cq) ($c_{np}=3c_{cq}$; $a_{np}=2a_{cq}$) should be taken into consideration.

In the Pécsszabolcs sample only copiapite is euhedral. Besides its platy crystals an earthy mass can only be recognized. This latter proved to be a mixture of coquimbite and paracoquimbite (XPD). Mössbauer data of copiapite were determined for the first time from the sample.

SULFATE MINERALS. THEIR POSSIBLE TECHNOGENE NATURE

Shcherbakova E.P. *(Inst. of Mineralogy, Rus. Acad. Sci., founds@imin.urc.ac.ru)*

The end of XX century is characterized by sharp increase of emission of so-named technogene matter in particular sulfur to the Earth's surface.

Is this fact affected on mineral kingdom? The attempt was made to answer this question in the following way. Four temporal periods, 1801-1900(I), 1901-1950(II), 1951-1980(III), 1981-1995(IV), were distinguished. For every period such characteristics of the major mineral classes were calculated: a) atios of mineral classes; b) indexes of discoveries, $Id_i = N_j/n$, where N_j - total amount of mineral species of j-mineral class ,discovered for i-period, n - duration of i-period, years; c) factors of increase of ID, $F_i = ID_{(i+1)}/ID_i$, where i - period number.

Results of calculations allowed to make next conclusions.

Now sulfates (8.7%) take the 5th place in mineral kingdom, being inferior to silicates(26.5%), phosphates(19.3%), sulfides(16.3%), oxides(12.0%). For the whole century this situation have been retained practically no changes.

ID of most mineral classes (silicates, carbonates, sulfides etc.) change in the same way irrespective of their absolute values. They increase slightly in the second and fourth periods (F=1.05-1.76) and sharp rise in the third (F=3.4-7.9). It seems this leap is the consequence of science-technical revolution and connected with introduction of quite new methods of mineral researches to mineralogical practice.

ID of sulphate change in the another way. They increase slightly in the second period (F=1.16) and almost equally both in the third(F=2.47) and in the forth (F=2,30). It means the increase of sulphate minerals in contrast of the other mineral classes become exponential now. It is very interesting that emission of technogene sulfur to environment changes in the same way. This coincidence isnÆt accidental apparently and may be an evidence of technogene nature of the most sulfates discovered last years.

It seems similar regularities may be established too for the other chemical elements in particular arsenates.

SCAINIITE AND PILLAITE, TWO NEW Pb-Sb SULFOSALTS FROM TUSCANY: DEFINITION AND CRYSTAL STRUCTURES.

Orlandi P. *(Dept. of Earth Sci., University of Pisa, orlandi@dst.unipi.it)*, Meerschaut A., Moëlo Y. and Palvadeau P. *(Lab. of Sol. Chemistry, Univ. of Nantes, moelo@cnrs-imn.fr)*

Scainiite and pillaite (CNMMN proposals n° 96-014 and 97-042, accepted) have been discovered at Buca della Vena Mine (Tuscany, Italy), a small iron and barite deposit (Orlandi & Checchi, 1986). These minerals formed in hydrothermal calcite veins within dolomitic limestone, together with other antimony sulfosalts: boulangerite, robinsonite, zinkenite, tintinaite, bournonite, andorite and tetrahedrite.

Scainiite is monoclinic (space group *C2/m*), with unit cell parameters: a = 52.00(2) Å, b = 8.148(2) Å, c = 24.311(6) Å, β = 104.09(1)°, V = 9991(10) Å^3. The structural formula is $Pb_{14}Sb_{30}S_{54}O_5$ (Z = 4). Scainiite is the first oxysulfide in the lead sulfosalt group. Its crystal structure is an expanded homologue of synthetic hexagonal $Ba_{12}Bi_{24}S_{48}$ (Aurivilius, 1983). This expansion according to a zig-zag surface parallel to **b** creates lozenge-shape rods, which are filled by columns directly derived from the structure of kermesite, Sb_2S_2O.

Pillaite is triclinic (space group $P\bar{1}$), with unit cell parameters: a = 24.829(2) Å, b = 4.1260(3) Å, c = 21.828(1) Å, α = 89.829(6)°, β = 99.594(7)°, γ = 94.780(7)°, V = 2197(1) Å^3. Its structural formula is close to $Pb_9Sb_{9.7}S_{23}Cl$ (Z = 2). Pillaite is the third natural Pb-Sb chlorosulfosalt, together with ardaite and dadsonite. The crystal structure is organized around columns with a pseudo-ternary axis, where are located chlorine atoms. These columns correspond to an higher homologue of the triangular rods of synthetic $Bi(Bi_2S_3)_9I_3$.

These two new Pb-Sb oxy- or chloro-sulfosalts enlarged the group of compounds belonging to the zinkenite homologous series (Makovicky, 1985).

References

Aurivilius, B. (1983) - *Acta Chem. Scand.* **A37**, 399-407.
Makovicky, E. (1985) - *Z. Kristallogr.* **173**, 1-23.
Orlandi, P. and Checchi, F. (1986) - *Min. Record* **17**, 261-268.

PRETULITE, $ScPO_4$, A NEW SCANDIUM MINERAL FROM THE STYRIAN AND LOWER AUSTRIAN LAZULITE OCCURRENCES, AUSTRIA

Taucher J. *(Referat für Mineralogie, LMJ, Graz)*, Bernhard F. *(Institut für Technische Geologie, TU Graz, bernhard@egam.tu-graz.ac.at)*, Walter F. and Ettinger K. *(Institut für Mineralogie-Kristallographie und Petrologie, KFU Graz)*

Pretulite is a new Sc-phosphate from the phyllite-micaschist hosted hydrothermal lazulite-quartz veins in the Lower Austroalpine Grobgneis complex, eastern Austria. The species is the Sc-dominant analogue of xenotime-(Y) and occurs as an ubiquitous accessory mineral at all investigated lazulite occurrences, forming anhedral to euhedral crystals up to 200 μm long with the dominant form {211}. At the type locality Höllkogel, euhedral crystals up to 2.5 mm in length occur. Pretulite is associated with lazulite, fluorapatite, chlorapatite, quartz, muscovite, clinochlore, paragonite, kyanite, pyrophyllite, augelite, wardite, hydroxylherderite, goyazite, florencite-(Ce), xenotime-(Y), bearthite, rutile, pyrite, corundum, and an AlO(OH)-phase. Pretulite is translucent to transparent with an adamantine luster, colorless to pale pink, uniaxial positive with ω =1.790 (5), ε =1.86 (1) and shows a weak orange fluorescence at 254 nm as well as a bright blue cathodoluminescence. Mohs hardness is about 5. The empirical formula of pretulite is $(Sc_{0.98}Y_{0.02})_{1.00}PO_4$. It contains variable amounts of Y with Y/(Y+Sc) = 0.5-3.2 mol% and traces of Yb, Er and Dy. The space group is $I4_1/amd$ with a =6.589 (1) Å, c =5.806 (1) Å, V =252.1 (1) Å^3, d_{calc} = 3.71 g/cm^3, Z = 4. The four strongest lines in the X-ray powder pattern are d_{200} = 3.293(100), d_{112} = 2.4636(42), d_{312} = 1.6927(45), d_{332} = 1.3697(15) Å. Cell parameters and average M-O distances confirm a small amount of Y substituting Sc in the eightfold-coordinated M-position. The formation of pretulite is interpreted to be due to a moderate enrichment of Sc in the lazulite-quartz veins (about 180 ppm) and the inability of the accompanying minerals to incorporate this quantity of Sc in their crystal structures.

CELADONITE-FAMILY MICA IN PYROCLASTIC ROCKS FROM HRVATSKO ZAGORJE (NW CROATIA)

Tibljaš D., Ščavničar S., Bermanec V. *(Inst. Mineralogy and Petrology, Faculty of Science, Univ. of Zagreb, Croatia, Darko.Tibljas@public.srce.hr)* and Slavković R. *(INA-Naftaplin, Laboratory Research Department, Zagreb, Croatia)*

Diagenetically zeolitized pyroclastic rocks which crop out in the NW part of Hrvatsko zagorje are often green due to the presence of celadon green mineral which is concentrated in the fiamme. In thin sections one can see that the mineral occurs in thin veins and inside pumice vesicles.

X-ray powder data revealed that the mineral belongs to the group of 10 Å phyllosilicates *i.e.* to the micas, and that its octahedral sheet is Fe-rich. Widened but still relatively sharp reflections, observed intensities and d_{060} indicate that investigated mineral corresponds rather closely to celadonite than to glauconite. Comparison of the recorded powder pattern of the glycolated sample with calculated ones exclude the possibility of the presence of more than 5% of expandable layers in investigated material.

Microprobe analyses showed that the mineral is interlayer-deficient, dioctahedral with aluminium as dominant cation in the octahedral sheet.

IR spectrum is in the OH stretching region typical for celadonite. Two strong sharp absorption bands indicate that Al is dominant trivalent cation in octahedral sheet. On the other hand the appearance of observed spectrum in the low frequency part is not so characteristic, some bands are absent while some bands can be ascribed to glauconite. Some of these differences could indicate tetrahedral substitution.

In spite of the fact that no investigation method gave unequivocal results, the most probably because of the variable composition and possible micrometer intergrowths of different phyllosilicates, it can be concluded that investigated mineral corresponds mostly to alumininan celadonite.

EVOLUTION OF MINLIB, A MINERALS- ORIENTED BIBLIOGRAPHIC DATABASE.

Wilson G.C. *(Turnstone Geol. Serv. Ltd, Toronto, Ont. and IsoTrace Lab., Univ. of Toronto, gcw@quartz.geology.utoronto.ca)*

The MINLIB database project was initiated in August 1983. With a content of 45,000 records (March 1998), each containing up to 30 lines of keywords and calls to ~80 possible logical fields, MINLIB provides a relatively small, text-rich probe of the Earth Sciences literature. Others in this category include IMMAGE (Institution of Mining and Metallurgy, London) and MinSource (incorporating Mineralogical Abstracts, 1982-, plus Clarke's update of Hey's Mineral Index). MINLIB has a primary focus on aspects of mineral deposits geology, mineralogy and igneous petrology. Developed in a context of both academic and applied research, the orientation of MINLIB has diversified with time, covering thematic specialities such as precious and base metal deposits, meteoritics and mineral analysis, and geographic strengths such as North and South America and the Indian subcontinent. This blend of gradual and episodic evolution is a feature common to literature-scanning databases, library and museum holdings. The largest science bibliographies contain millions of records each; prime examples for geology and mineralogy are GeoRef and GeoSEARCH (with GeoArchive). A key feature of all the above- mentioned databases is an adherence to their own terminology, generally formalized in a thesaurus. This is an important design strength, one which may be weakly developed or entirely absent in generalist library catalogues or (especially) resources accessible on the World Wide Web. These structures contain hierarchical features with arrays of broad and narrow terms for, *e.g.* taxonomies of minerals, rocks and fossils, geographic regions, and stratigraphic sequences. Major databases are available in a range of print, on-line and CD-ROM formats. Subscriptions are generally high, with distribution directed to large libraries and other institutions. The growth of MINLIB is driven both by new publications and by the changing demands of current projects, which account for much of the pre-1983 content. It is hoped to publish MINLIB in illustrated form on CD-ROM, offering enhanced access to and retrievability of the records, while retaining the keyword selection. The plan involves an image bank of `slide shows' with multi-level captions, aiming to broaden the educational appeal of the subjects (regional geology, introductory geology, metallogeny and geochemistry). With a broader audience in mind, 2.5% of MINLIB records are flagged as non-technical.

Author Index

A = Abstract Page P = Programme Page
L = Left R = Right

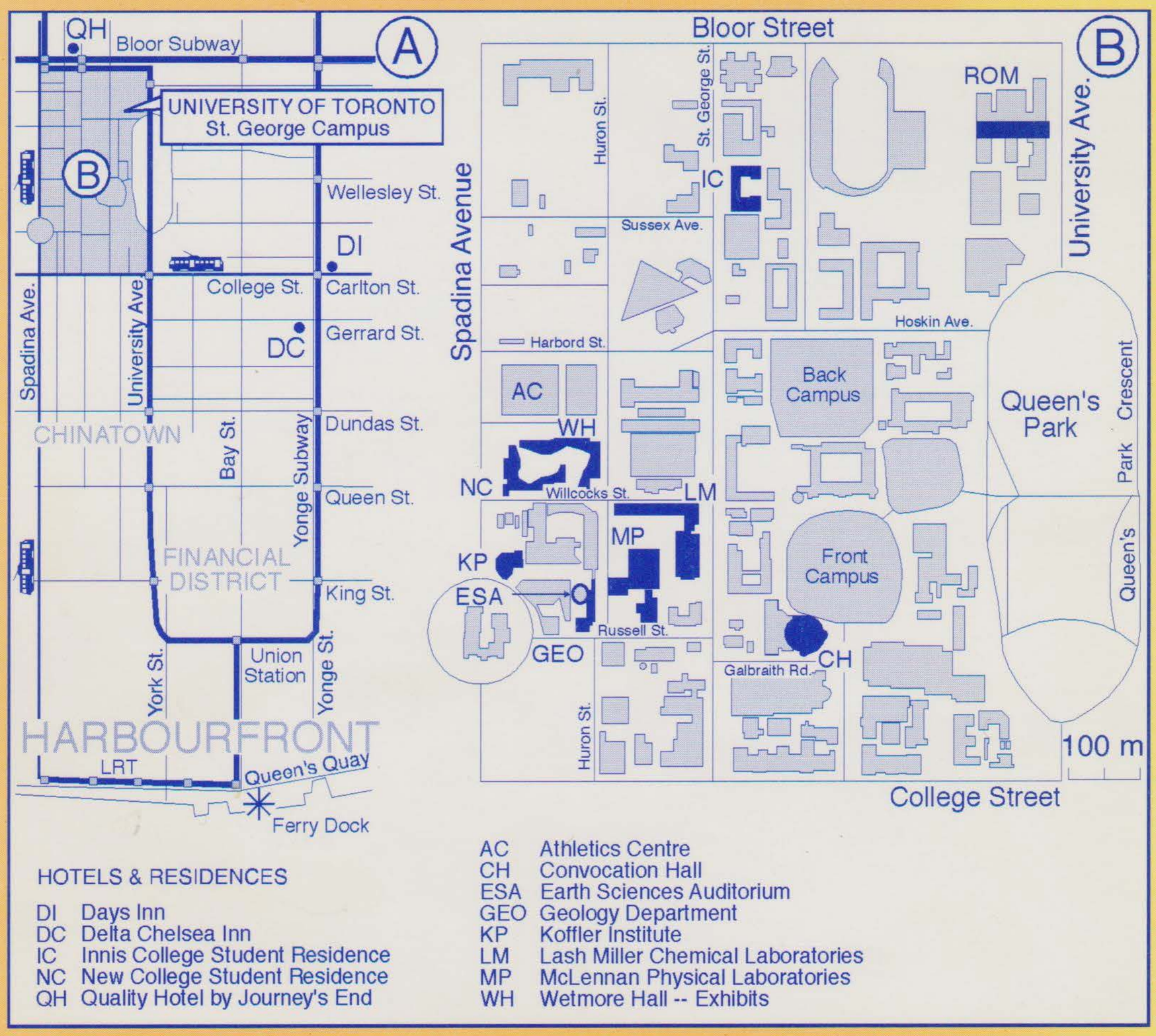

HOTELS & RESIDENCES

DI Days Inn
DC Delta Chelsea Inn
IC Innis College Student Residence
NC New College Student Residence
QH Quality Hotel by Journey's End

AC Athletics Centre
CH Convocation Hall
ESA Earth Sciences Auditorium
GEO Geology Department
KP Koffler Institute
LM Lash Miller Chemical Laboratories
MP McLennan Physical Laboratories
WH Wetmore Hall -- Exhibits

IMA Logo:
Pyrochlore crystals on an aegirine needle from Mont St-Hilaire, Quebec